

Biomechanical Aspects of the Anterior Segment in Human Myopia

HETAL DALPAT PATEL
Doctor of Philosophy

ASTON UNIVERSITY
November 2010

This copy of the thesis has been supplied on condition that anyone who consults it is understood to recognise that its copyright rests with its author and that no quotation from the thesis and no information derived from it may be published without proper acknowledgement.

Aston University
Biomechanical Aspects of the Anterior Segment in Human Myopia

Hetal Dalpat Patel
Doctor of Philosophy
2010

The thesis investigates the relationship between the biomechanical properties of the anterior human sclera and cornea *in vivo* using Schiötz tonometry (ST), rebound tonometry (RBT, *iCare*) and the Ocular Response Analyser (ORA, *Reichert*). Significant differences in properties were found to occur between scleral quadrants. Structural correlates for the differences were examined using Partial Coherent Interferometry (*IOLMaster*, Zeiss), Optical Coherent tomography (*Visante* OCT), rotating Scheimpflug photography (*Pentacam*, Oculus) and 3-D Magnetic Resonance Imaging (MRI). Subject groups were employed that allowed investigation of variation pertaining to ethnicity and refractive error. One hundred thirty-five young adult subjects were drawn from three ethnic groups: British-White (BW), British-South-Asian (BSA) and Hong-Kong-Chinese (HKC) comprising non-myopes and myopes.

Principal observations:

ST demonstrated significant regional variation in scleral resistance a) with lowest levels at quadrant superior-temporal and highest at inferior-nasal; b) with distance from the limbus, anterior locations showing greater resistance.

Variations in resistance using RBT were similar to those found with ST; however the predominantly myopic HKC group had a greater overall mean resistance when compared to the BW-BSA group.

OCT-derived scleral thickness measurements indicated the sclera to be thinner superiorly than inferiorly. Thickness varied with distance from the corneolimbus junction, with a decline from 1 to 2 mm followed by a successive increase from 3 to 7 mm.

ORA data varied with ethnicity and refractive status; whilst axial length (AL) was associated with corneal biometrics for BW-BSA individuals it was associated with IOP in the HKC individuals. Complex interrelationships were found between ORA Additional-Waveform-Parameters and biometric data provided by the *Pentacam*.

OCT indicated ciliary muscle thickness to be greater in myopia and more directly linked to posterior ocular volume (from MRI) than AL.

Temporal surface areas (SAs, from MRI) were significantly smaller than nasal SAs in myopic eyes; globe bulbosity (from MRI) was constant across quadrants.

Key words: sclera; cornea; intraocular pressure; refractive error; biometry

For my mum
without whom none of this would have been possible.

Acknowledgements

I would like to begin by thanking my supervisors Professor Bernard Gilmartin, Dr Nicola Logan and Dr Robert Cubbidge for all their support and guidance throughout the course of this thesis. In particular I consider it an honour and privilege to have worked with Bernard as his untiring commitment, support and guidance has been central to accomplishing this thesis.

Aston University is gratefully acknowledged for supporting the work via the Clinical Demonstratorship. The College of Optometrists (UK) must also be thanked for awarding the student summer scholarships to Elena Dold and Larissa Dorochtchak and for their relative contributions to the data collection. I would also like to extend my gratitude to Manbir Nagra for collecting the MRI and *Pentacam* data.

Thanks to the students and staff at Aston University, in particular Dr Richard Armstrong for his statistical advice. I am also greatly appreciative of the help and support of Dr Andrew Ingham on the agarose biogel experiment and Dr David Webb, Dr Kate Sudgen and Jana Rasakanthan for their assistance on the OCT work. A sincere thanks must also go to Dr Andrew Lam and the staff at the Hong Kong Polytechnic University for the collaborative work described in the thesis.

I am also grateful to Keeler (UK) for their assistance in the work with the *Pulsair EasyEye* and to Professor Sunil Shah for the loan of the Reichert ORA. A huge thanks to Graham Davies, John Hannock and Kim Wooley for their technical help over the course of the thesis.

I am forever indebted to my family and friends, in particular my uncle and aunty who have provided me with so much love and support over the years. This journey would not have been so enjoyable had it not been for my best friend and partner Phillip Buckhurst, who's support and encouragement has been there when I needed it the most.

Finally I would like to dedicate this thesis to my late father, who inspired me to do a PhD and I hope would have been proud of me.

CONTENTS

THESIS SUMMARY	2
DEDICATION	3
ACKNOWLEDGEMENTS	4
LIST OF CONTENTS	5
LIST OF APPENDICES	13
LIST OF TABLES	14
LIST OF FIGURES	18
LIST OF ABBREVIATIONS	21
1.0 OCULAR ANATOMY AND PHYSIOLOGY OF THE ANTERIOR SEGMENT	23
1.1. Introduction.....	23
1.1.1 Gross anatomy of the eye	23
1.2 Anatomy and physiology of the anterior segment	24
1.2.1 The Sclera.....	24
1.2.2 The Cornea	28
1.2.3 Comparison of the structural characteristics of the sclera and cornea.....	29
1.2.4 Aqueous humour	30
1.2.5 Intraocular pressure (IOP).....	30
1.2.6 Iris.....	31
1.2.7 Ciliary body.....	31
1.2.8 Crystalline Lens.....	32
2.0 HUMAN MYOPIA	33
2.1 Introduction.....	33
2.1.1 Refractive error.....	33
2.1.2 Myopia development.....	33
2.1.3 Classification of myopia.....	33
2.1.4 Prevalence of myopia	34
2.1.5 Genetic influence on myopia.....	35
2.1.6 Environmental factors	36
2.2 Animal models.....	36
2.2.1 Retinal image manipulation and refractive error development in animal models.....	36
2.2.2 Recovery in animal models	38
2.2.3 The sclera and myopia.....	38
2.2.4 Application of animal model findings to human myopia	40
3.0 SCLERA AND OCULAR PATHOLOGIES	42
3.1 The role of the sclera in glaucoma.....	42
3.2 The role of the sclera in Age Related Macular degeneration.....	44

4.0 ASSESSING IOP AND BIOMECHANICAL PROPERTIES OF THE OCULAR TISSUES <i>IN VIVO</i>	46
4.1 Introduction.....	46
4.2 The Ocular Pressure-Volume relationship.....	46
4.3 Pressure-Volume relationship in Schiottz tonometry	47
4.3.1 Theory of the Schiottz tonometer and IOP measurement.....	48
4.3.2 Schiottz tonometry and Friedenwald’s rigidity measurement	48
4.4 Goldmann applanation tonometer (GAT).....	51
4.5 Rebound tonometry	52
4.5.1 Technical aspects of rebound tonometry	54
4.5.2 The <i>iCare</i> tonometer instrument	55
4.6 Ocular Response Analyser (ORA).....	57
5.0 AIMS AND OBJECTIVES OF THE THESIS	67
6.0 THE INVESTIGATION OF CORNEAL AND SCLERAL BIOMECHANICS USING SCHIOTZ INDENTATION TONOMETRY – INITIAL CONSIDERATIONS	69
6.1 Introduction.....	69
6.2 Study Objective	70
6.3 Methods	70
6.3.1 Schiottz tonometry.....	71
6.3.2 Ocular biometry and refractive error.....	72
6.4 Statistical analysis.....	74
6.5 Results.....	75
6.5.1 Schiottz Indentation: raw data	75
6.5.2 Friedenwald’s Ko and Ks values.....	76
6.5.3 Comparison of IOP measures using Schiottz tonometry and GAT	77
6.5.4 Intra- and interobserver variability using Schiottz tonometry	78
6.6 Discussion.....	79
6.6.1 Regional variation in scleral resistance	79
6.6.2 Friedenwald’s corneal and scleral rigidity.....	82
6.6.3 Reliability and sources of variation in Schiottz tonometry	84
6.7 Conclusions.....	88
7.0 <i>IN VIVO</i> MEASUREMENT OF SCLERAL THICKNESS IN HUMANS USING ANTERIOR SEGMENT OPTICAL COHERENT TOMOGRAPHY.....	89
7.1 Introduction.....	89
7.1.1 Anterior-Segment Optical Coherent tomography (AS-OCT)	93
7.2 Study objective	95
7.3 Method.....	96

7.3.1 Image acquisition	96
7.3.2 Image processing.....	97
7.3.3 Scleral thickness measurements	97
7.3.4 Intra- and inter-observer reliability of scleral thickness measurement.....	99
7.4 Statistical procedures	100
7.5 Results.....	101
7.5.1 Intraobserver variability	101
7.5.2 Interobserver variability	102
7.5.3 Differences in scleral thickness between meridians and location of measurement	102
7.5.4 The effect of various parameters on scleral thickness	107
7.5.5 Additional ocular biometric parameters	110
7.6 Discussion.....	111
7.6.1 Reliability and reproducibility of measurement of scleral thickness.....	111
7.6.2 Comparison of present results to previous reports of scleral thickness.....	113
7.6.3 Meridional variation in scleral thickness.....	115
7.6.4 The effect of distance from the corneolimbus on the scleral thickness profile..	117
7.6.5 The effect of axial length and refractive error on scleral thickness.....	118
7.6.6 Gender differences in scleral thickness	119
7.6.7 The effect of ethnicity on scleral thickness	119
7.6.8 Corneal and scleral thickness	120
7.7 Conclusion	122
8.0 THE USE OF REBOUND TONOMETRY TO ASSESS INTRAOCULAR PRESSURE AND REGIONAL VARIATIONS IN SCLERAL RESISTANCE.....	123
8.1 Introduction.....	123
8.2 Study Objective	124
8.3 Methods	125
8.3.1 General measurement procedure with the <i>iCare</i> tonometer.....	125
8.3.2 Procedure for the use of the <i>iCare</i> tonometer on the sclera	127
8.3.3 Determining the intra- and inter-observer variation for both corneal and scleral <i>iCare</i> measurements	129
8.3.4 Evaluating the concordance between IOPs measured with the <i>iCare</i> , GAT and the ORA and assessing the relationship between <i>iCare</i> IOPs and the ORA biometrics	130
8.3.5 Investigating the application of <i>iCare</i> tonometry to evaluate regional variation in scleral resistance in mixed British White (BW) and British South Asian (BSA) (UK) subjects.....	130
8.3.6 Evaluating the agreement between the measures of scleral resistance with the <i>iCare</i> and Schiøtz tonometry.....	130
8.3.7 Assessing the relationship between scleral <i>iCare</i> values and scleral thickness measurements	131

8.3.8 Application of the <i>iCare</i> tonometer for scleral measurement in Hong Kong Chinese (HKC) individuals	131
8.3.9 Determination of the influence of ethnicity and refractive error on scleral resistance....	131
8.4 Statistical procedures	131
8.5 Results.....	133
8.5.1 Determining the intra- and inter-observer variation for both corneal and scleral <i>iCare</i> measurements	133
8.5.2 Concordance of <i>iCare</i> tonometry with GAT and the Reichert ORA	134
8.5.3 Application of the <i>iCare</i> tonometer to the sclera	137
8.5.4 Comparison of regional scleral <i>iCare</i> values to Schiottz scleral indentation for the 4 mm location from the limbus.....	139
8.5.5 Scleral <i>iCare</i> values and scleral thickness.....	139
8.5.6 Assessment of regional variation in scleral <i>iCare</i> measurements in HKC subjects.....	139
8.5.7 Comparison of BW-BSA (UK) and HKC (HK) scleral <i>iCare</i> measurements	141
8.6 Discussion.....	144
8.6.1 Reliability and reproducibility of <i>iCare</i> tonometry for the cornea and sclera.....	144
8.6.2 Comparison between <i>iCare</i> , GAT and ORA tonometry	145
8.6.3 Measurement of scleral resistance with <i>iCare</i> tonometry	148
8.6.4 Comparison of present findings to previous studies examining scleral biomechanics....	151
8.6.5 Scleral thickness and resistance.....	153
8.6.6 Scleral curvature and shape	153
8.6.7 Scleral resistance and Age.....	154
8.6.8 Scleral resistance and its relation to myopia and ethnicity.....	155
8.7 Conclusion	159
9.0 CALIBRATION OF MEASUREMENTS OF HUMAN SCLERAL RESISTANCE USING AGAROSE GELS.....	160
9.1 Introduction.....	160
9.2 Materials and Methods	162
9.2.1 Agarose preparation	162
9.2.2 <i>iCare</i> tonometry and agarose gels	163
9.2.3 Hounsfield Tensometer	163
9.2.4 The conversion of force-extension data to stress-strain data.....	165
9.3 Statistical analysis.....	167
9.4 Results.....	167
9.5 Discussion.....	172
9.5.1 Agarose gels	172
9.5.2 Agarose gels and <i>iCare</i> tonometry.....	173
9.5.3 Present findings in relation to scleral biomechanics	175

9.6 Conclusion	177
10.0 <i>IN VIVO</i> VARIATION IN SCLERAL RESISTANCE	180
10.1 Introduction.....	180
10.2 Study objective	181
10.3 Method.....	181
10.4 Statistical analysis.....	182
10.5 Results.....	184
10.5.1 Schiottz scale readings: the effect of distance from limbus and Schiottz weights	184
10.5.2 Schiottz scale readings at 8 mm	184
10.5.3 Schiottz scale readings at 4 mm	187
10.5.4 Corneal indentation	190
10.5.5 Conversion of Schiottz scale readings to Friedenwald's rigidity values	190
10.5.6 Ocular biometry.....	192
10.6 Discussion.....	192
10.6.1 Comparison of current results to findings of Chapter 6	192
10.6.2 Regional variation in scleral resistance	193
10.6.3 Friedenwald's rigidity values	197
10.6.4 Effect of refractive status and axial length on scleral resistance	198
10.6.5 The effect of age on scleral resistance.....	199
10.6.6 Scleral resistance and gender.....	199
10.6.7 Scleral resistance and ethnicity	200
10.7 Conclusion	202
11.0 STRUCTURAL CORRELATES OF CORNEAL BIOMECHANICS.....	203
11.1 Introduction.....	203
11.2 Study Objective	204
11.3 Methods	204
11.4 Statistical Analysis.....	205
11.5 UK Results.....	206
11.5.1 IOP and corneal biometrics (corneal hysteresis (CH) and corneal resistance factor (CRF) for UK subjects	206
11.5.2 Corneal biomechanics and additional ocular biometrics for UK subjects.....	210
11.5.3 ORA Additional Waveform Parameters (AWPs) for UK subjects	212
11.6 HK Results.....	213
11.6.1 IOP and corneal biometrics (CH and CRF) for HKC subjects.....	213
11.6.2 Corneal biomechanics and additional ocular biometrics for HKC subjects	214
11.6.3 ORA Additional Waveform Parameters (AWPs) for HKC subjects.....	216

11.7 Comparison of ORA metrics and ocular biometry between BW - BSA (UK) and HKC individuals.....	216
11.7.1 IOP and corneal biometrics (CH and CRF) for UK and HK subjects	216
11.7.2 ORA Additional Waveform Parameters (AWPs) for UK and HK subjects	217
11.8 Discussion.....	217
11.8.1 Comparison between measures of IOP with the ORA and GAT	218
11.8.2 Structural correlates of corneal biomechanics.....	219
11.8.3 Corneal biomechanics and glaucoma	221
11.8.4 Corneal biomechanics and myopia.....	222
11.8.5 IOP and myopia.....	224
11.8.6 Ocular wall stress and its relation to myopia and glaucoma	225
11.8.7 Ethnicity and corneal biomechanics	227
11.8.8 Age and corneal biomechanics.....	228
11.8.9 Gender and corneal biomechanics.....	228
11.8.10 ORA Additional waveform parameters (AWPs).....	229
11.9 Conclusion	231
12.0 INVESTIGATION OF THE RELATIONSHIP BETWEEN ANTERIOR SEGMENT BIOMETRY AND CORNEAL BIOMECHANICS	232
12.1 Introduction.....	232
12.1.1 The relationship between anterior segment and refractive status.....	232
12.1.2 Evaluation of the anterior segment.....	233
12.1.3 Operational principles of the <i>Pentacam</i>	234
12.2 Study objective	235
12.3 Method.....	235
12.3.1 Image acquisition	235
12.3.2 <i>Pentacam</i> image parameters.....	236
12.4 Statistical analysis.....	237
12.5 Results.....	238
12.5.1 Structural correlates of anterior segment biometry	238
12.5.2 Anterior segment biometry and corneal biomechanics	239
12.6 Discussion.....	240
12.6.1 Corneal biometry and refractive status.....	241
12.6.2 Regional differences in corneal thickness (CT)	242
12.6.3 Anterior and posterior corneal surface curvature	242
12.6.4 Anterior chamber biometry and refractive status	243
12.6.5 Corneal biomechanics and anterior segment biometry.....	243
12.7 Conclusion	244

13.0 STRUCTUAL CORRELATES OF THE HUMAN CILIARY MUSCLE	246
13.1 Introduction.....	246
13.1.1 Functional and structural evaluation of the ciliary body	247
13.1.2 Imaging the ciliary muscle body	248
13.2 Study objective	248
13.3 Method.....	249
13.3.1 Image acquisition	249
13.3.2 Image analysis	249
13.3.3 Calculation of ocular volume using 3-D MRI.....	250
13.4 Statistical analysis.....	251
13.5 Results.....	252
13.5.1 Correlates of ciliary muscle thickness	252
13.5.2 Ocular volume and ciliary muscle thickness	255
13.5.3 Ciliary muscle thickness and scleral thickness.....	257
13.6 Discussion.....	258
13.6.1 Structural correlates of ciliary muscle thickness	258
13.6.2 Thickening of the ciliary muscle in myopia	261
13.6.3 Ciliary muscle thickness and corneal biometry.....	262
13.6.4 Comparison to previous reports of ciliary muscle thickness.....	263
13.7 Conclusion	266
14.0 CONFORMATION OF THE ANTERIOR SEGMENT IN HUMAN MYOPIA.....	267
14.1 Introduction.....	267
14.1.1 Theoretical principles of MR imaging	269
14.2 Study Objectives.....	270
14.3 Method.....	270
14.3.1 Image acquisition	270
14.3.2 Image analysis	271
14.4 Statistical analysis.....	273
14.5 Results.....	274
14.5.1 Surface area	274
14.5.2 Quadrant bulbosity	276
14.6 Discussion.....	277
14.6.1 Quadrant surface areas	277
14.6.2 Quadrant bulbosity	283
14.6.3 Ocular surface characteristic and scleral biomechanics	284
14.7 Conclusion	285
15.0 GENERAL DISCUSSION.....	286

15.1 Introduction.....	286
15.2 The assessment of scleral biomechanics <i>in vivo</i>	286
15.3 Regional variation in scleral biomechanics	287
15.4 Scleral biomechanics and myopia.....	288
15.5 Corneal biomechanics and myopia	290
15.6 Ciliary muscle thickness and myopia	292
15.7 The effect of ethnicity and myopia on scleral and corneal biomechanics	292
15.8 Limitations of present investigations and proposals for future work.....	293
15.8.1 Scleral biomechanics and myopia	293
15.8.2 Regional variation in scleral biomechanics and gaze dependent IOP	293
15.8.3 Rebound tonometry and scleral resistance	294
15.8.4 Scleral biomechanics and conformation of the anterior segment.....	294
15.8.5 Corneal biomechanics and myopia.....	294
15.8.6 Scleral and ciliary muscle thickness and AS-OCT off-axis distortion.....	295
15.8.7 Scleral biomechanics and pulsatile ocular blood flow	295
15.8.8 Biomechanics of the limbus	296
15.9 Conclusion	296
REFERENCES.....	297

LIST OF APPENDICES

APPENDIX 1: ETHICAL APPROVAL	346
APPENDIX 2: SUBJECT GROUPS FOR EACH STUDY	347
APPENDIX 3: STATISTICAL APPENDIX FOR CHAPTER 6	349
APPENDIX 4: STATISTICAL APPENDIX FOR CHAPTER 7	351
APPENDIX 5: HIGH SPEED PHOTOGRAPHY OF REBOUND TONOMETRY ON THE CORNEA AND SCLERA (unbound material; CD)	352
APPENDIX 6: STATISTICAL APPENDIX FOR CHAPTER 8	353
APPENDIX 7: STATISTICAL APPENDIX FOR CHAPTER 10	356
APPENDIX 8: STATISTICAL APPENDIX FOR CHAPTER 11	361
APPENDIX 9: STATISTICAL APPENDIX FOR CHAPTER 12	372
APPENDIX 10: STATISTICAL APPENDIX FOR CHAPTER 13	378
APPENDIX 11: STATISTICAL APPENDIX FOR CHAPTER 14	380
APPENDIX 12: EVALUATION OF OFF-AXIS DISTORTION IN IMAGES PRODUCED BY ANTERIOR SEGMENT OPTICAL COHERENT TOMOGRAPHY (AS-OCT)	381
APPENDIX 13: INVESTIGATING HUMAN LIMBAL BIOMECHANICS USING THE PULSAIR EASYEYE TONOMETER (KEELER, WINDSOR, UK)	383
SUPPORTING PUBLICATIONS	386

LIST OF TABLES

Table 4.1 ORA additional waveform parameters (AWPs)	66
Table 6.1 RE Rigidity values ($\text{mm}^3)^{-1}$ for myopic, non myopic and both groups combined.....	76
Table 6.2 GAT and Schiötz (5.5g and 7.5g) tonometry measures of IOP (mm Hg)	77
Table 6.3 Correlation between GAT and Schiötz (5.5g and 7.5g) tonometry measures of IOP (mm Hg)	77
Table 6.4 Average CoV values for scleral regions	79
Table 6.5 Schiötz rigidity values for humans found in previous studies (mean \pm SD given where available)	83
Table 6.6 Reports of IOP changes with gaze in normal individuals (mean \pm SD given where available)	87
Table 7.1 Previous measures of scleral thickness in humans by various investigators	92
Table 7.2 Intraobserver CoV (%) for the different meridians and distances from the corneolimbus junction	101
Table 7.3. ICC values for scleral thickness values	102
Table 7.4 Measurements of scleral thickness for each meridian and distance from the corneolimbus junction (mean \pm SD (μm))	103
Table 8.1 RE Intraobserver ICC for <i>iCare</i> tonometry on the cornea and sclera	133
Table 8.2 Intraobserver Coefficient of Variance (%) for <i>iCare</i> tonometry for the RE cornea and sclera	133
Table 8.3 Single and average ICC values for <i>iCare</i> tonometry for the RE cornea and sclera	133
Table 8.4 RE measures of IOP (mm Hg) obtained with the <i>iCare</i> , GAT and ORA	135
Table 8.5 Correlations between different measures of RE IOP (mm Hg); mean IOP differences between tonometric tests; 95% LoA.....	135
Table 8.6: RE scleral <i>iCare</i> (mmHg) values for UK data set	138
Table 8.7 RE scleral <i>iCare</i> values (mmHg) for the HKC individuals	140
Table 9.1 A summary of biomechanical terminology commonly used to describe the physical properties of biological materials	161
Table 9.2 <i>iCare</i> readings and E values for each concentration of agarose	168
Table 9.3 RE mean regional <i>iCare</i> values converted to E values for both UK and HK data	171
Table 9.4 Previously reported Young's modulus values for different concentrations of agarose gels. ^a Estimated results from graphical representation of data.	174
Table 9.5 Previously reported values for human and animal sclera, and associated methodologies	178
Table 10.1: RE 8 mm Schiötz indentation scale readings	185
Table 10.2. RE 8 mm Schiötz indentation scale readings for non-myopes and myopes	186

Table 10.3 RE 4 mm Schiötz indentation scale readings	187
Table 10.4 RE 4 mm Schiötz indentation scale readings for non-myopes and myopes	189
Table 10.5 RE Schiötz scale readings converted to Friedenwald’s rigidity values ((mm ³) ⁻¹) for 4 and 8 mm from the limbus	191
Table 11.1 RE IOP (mm Hg) and ORA metrics (mm Hg) for the UK data	207
Table 11.2 Correlations and differences between RE IOP (mm Hg) measurement with GAT and ORA	207
Table 11.3 RE ORA metrics for the HK subjects	213
Table 12.1. Overall mean ± SD and range for the <i>Pentacam</i> parameters.....	238
Table 12.2 Glossary of the <i>Pentacam</i> parameters and their abbreviations.....	245
Table 13.1 RE Ciliary muscle thickness (CMT) (µm)	252
Table 13.2 CMT (µm) for myopes and non-myopes	253
Table 13.3 CMT (µm) between different axial length groups	255
Table 13.4 RE MRI Ocular volumes (mm ³)	257
Table 13.5 Previously reported <i>in vivo</i> thickness measurements of human ciliary body/muscle	265
Table 14.1 RE surface areas of quadrants (mm ²)	274
Table 14.2 RE bulbosity for the different quadrants	276
Table A2.1 Subjects included in each chapter throughout the thesis	347
Table A3.1 RE Scale readings and CoV for observer LD for the 5.5g weight	349
Table A3.2 RE Scale readings and CoV for observer LD for the 7.5g weight	349
Table A3.3 RE Scale readings and CoV for observer HP for the 5.5g weight	349
Table A3.4 RE Scale readings and CoV for observer HP for the 7.5g weight	350
Table A3.5 Schiötz 5.5g single and average ICC	350
Table A3.6 Schiötz 7.5g single and average ICC	350
Table A3.7 Schiötz 5.5g average PE	350
Table A3.8 Schiötz 7.5g average PE	350
Table A6.1 Model summary for outcome variable corneal <i>iCare</i> measurements	353
Table A6.2 Multiple linear regression outcome table for corneal <i>iCare</i> measurements	353
Table A6.3 Pearson’s correlation coefficients for scleral <i>iCare</i> values and Schiötz indentation readings at 4 mm from the limbus. (Note only significant correlations shown)	354
Table A6.4 Pearson’s correlation coefficients for scleral <i>iCare</i> values and scleral thickness along the same meridians at different distances from the limbus. (Note only significant correlations shown).	354
Table A7.1 Multiple two-way repeated measures ANOVAs assessing for the effect of different variables (treatment effect) on regional Schiötz scale values (RSV) at 8 mm	357

Table A7.2 Multiple two-way repeated measures ANOVAs assessing for the effect of different variables (treatment effect) on regional Schiotz scale values (RSV) at 4 mm	358
Table A7.3 Pearson's correlations coefficients for meridional scleral thickness at various distances and regional Schiotz scale readings with different weights at 4 mm from the limbus (Note only significant results shown).	358
Table A7.4 Independent samples <i>t tests</i> assessing for an effect of different variables upon corneal scale values with different weights (only p values given).	359
Table A7.5 ANOVAs on Friedenwald's scleral rigidity (Ks) values at 4 and 8 mm	359
Table A7.6 Independent samples <i>t tests</i> assessing for an effect of different variables upon corneal rigidity values (only p values given)	360
Table A8.1 Correlation matrix for various measures of IOP (mm Hg) and ORA biometrics (mm Hg)	361
Table A8.2 Model summary for outcome variable CH	362
Table A8.3 Multiple linear regression outcome table for CH	362
Table A8.4 Model summary for outcome variable CRF	362
Table A8.5 Multiple linear regression outcome table for CRF	363
Table A8.6 Model summary for outcome variable IOPg	363
Table A8.7 Multiple linear regression outcome table for IOPg	363
Table A8.8 Model summary for outcome variable IOPcc	363
Table A8.9 Multiple linear regression outcome table for IOPcc	364
Table A8.10 Independent <i>t tests</i> assessing the effect of refractive error, gender and age grouping on the ORA and biometric parameters.	364
Table A8.11 Independent <i>t tests</i> assessing the effect of refractive status, gender and age (years) grouping on the AWP (Note: only significant outcomes shown).	365
Table A8.12 Model summary for outcome variable Rx	365
Table A8.13 Multiple linear regression outcome table for Rx	366
Table A8.14 Model summary for outcome variable AL	366
Table A8.15 Multiple linear regression outcome table for AL	366
Table A8.16a Correlations (only r values shown) between ocular biometric data and the AWP for the UK data (p<0.05). AWP from upper 75% of the applanation peak.	367
Table A8.16b Correlations (only r values shown) between ocular biometric data and the AWP for the UK data (p<0.05). AWP from the upper 50% of the applanation peak	367
Table A8.17 Correlation matrix for various measures of ORA biometrics (mm Hg) and ocular variables for the HK subjects	368
Table A8.18 Model summary for outcome variable IOPg	368
Table A8.19 Multiple linear regression outcome table for IOPg	368
Table A8.20 Model summary for outcome variable IOPg	369
Table A8.21 Multiple linear regression outcome table for IOPg	369

Table A8.22 Model summary for outcome variable IOPcc	369
Table A8.23 Multiple linear regression outcome table for IOPcc	369
Table A8.24 Model summary for outcome variable IOPcc	369
Table A8.25 Multiple linear regression outcome table for IOPcc	369
Table A8.26 Independent <i>t tests</i> assessing the influence of refractive status and gender on the ORA and ocular biometry parameters for the HKC subjects	370
Table A8.27 Correlations between ocular biometric data and the AWP (p<0.05)	370
Table A8.28 Independent <i>t tests</i> assessing the effect of data origin (UK or HK) on ORA biometrics	370
Table A9.1 RE Schiottz corneal rigidity (mm ³) ⁻¹ and ORA biometrics (mm Hg)	372
Table A9.2 Significant correlations between <i>Pentacam</i> parameters.	373
Table A9.3 Significant correlations between <i>Pentacam</i> parameters and the main ORA biometrics (CH and CRF)	373
Table A9.4 Significant correlations between <i>Pentacam</i> parameters and the AWP's	374
Table A9.5 Model summary for outcome variable CH	376
Table A9.6 Multiple linear regression outcome table for CH	376
Table A9.7 Model summary for outcome variable CRF	376
Table A9.8 Multiple linear regression outcome table for CRF	376
Table A9.9 Best <i>Pentacam</i> predictor variables for ORA AWP's	376
Table A10.1 Pearson's correlation coefficient matrix for temporal and nasal CMT, age and ocular biometry variables.	378
Table A10.2 Pearson's correlation coefficient matrix for scleral thickness along various meridians/distances from the corneolimbic junction and CMT (temporal and nasal) Note: only significant correlations are shown.	379
Table A11.1 Pearson's correlation coefficient matrix for quadrant SAs and ocular biometry variables	380

LIST OF FIGURES

Figure 4.1 Illustration of the motion parameters of the probe assessed in RBT	53
Figure 4.2 Illustration of the change in the signal voltage (mV) from the solenoid with changes in probe speed and direction	56
Figure 4.3 Diagrammatic representation of the distinct phases the cornea travels through on application of the air pulse and the consequent changes in the intensity of light detected by the ORA	58
Figure 4.4 Diagrammatic representation of an ORA waveform	58
Figure 4.5 (a-m) Diagrammatic illustrations of the additional waveform parameters (AWPs) obtained from the ORA for the upper 75% and 50% of the applanation peaks	61
Figure 6.1 Schiötz tonometry on superior-temporal sclera of the LE	72
Figure 6.2 Scale readings with Schiötz 5.5g (a and b), Schiötz 7.5g (c and d)	76
Figure 6.3 a) RE difference versus mean plot: Schiötz 5.5g:GAT IOP (Bold line denotes mean, dotted line +/- 2SD b) RE difference versus mean plot: Schiötz 7.5g:GAT IOP	77
Figure 7.1 OCT image of temporal sclera and ciliary muscle. Dotted line delineates sclera (A) and ciliary muscle (B).	98
Figure 7.2 OCT image of the superior-temporal sclera; callipers (in red) shown for scleral thickness measurements of 6 mm along at 1 mm intervals.	99
Figure 7.3 (a-h) Scleral thickness mean \pm SD (error bars) from 1-7 mm for meridians SN, S, ST, T, IT, I, IN and N.	104
Figure 7.4. Scleral thickness for all 8 meridians from 1-7 mm.	107
Figure 7.5 Scleral thickness changes in males and females a) with meridian and b) with distance from corneolimbic junction.	108
Figure 7.6 Comparison of present (A) measures of scleral thickness along the temporal meridian at 1-3 mm distance to previous studies; B (Pavlin <i>et al.</i> , 1996), C (Oliveira <i>et al.</i> , 2006), D (Mohammed-Noor <i>et al.</i> , 2009) and E (Yoo <i>et al.</i> , 2010).	114
Figure 8.1 <i>iCare</i> tonometry experimental setup side view. A: Customed-designed housing for the <i>iCare</i> tonometer, B: Graticule for estimating location of scleral measurement, C: <i>iCare</i> tonometer, D: Head rest for subject, E: Examiner ED.	127
Figure 8.2 Scleral measurement with <i>iCare</i> tonometry (graticule omitted for clarity)	129
Figure 8.3 a) RE difference versus mean plot: GAT- <i>iCare</i> IOP, b) RE difference versus mean plot: IOPg- <i>iCare</i> IOP and c) RE difference versus mean plot: IOPcc- <i>iCare</i> IOP (Bold line denotes mean, dotted lines +/- 1.96SD)	135
Figure 8.4 RE mean \pm SD (error bars) scleral <i>iCare</i> values at different regions for the UK data set	138
Figure 8.5 RE Mean \pm SD (error bars) scleral <i>iCare</i> values at different regions for the HKC data set	140

Figure 8.6 RE mean \pm SD (error bars) scleral <i>iCare</i> values for different regions in the UK and HK data set	142
Figure 8.7 RE Mean \pm SD (error bars) scleral <i>iCare</i> values at different regions for the various ethnicities	143
Figure 9.1 Experimental set-up for assessing <i>iCare</i> measurements of agarose gels of varying concentrations. A: clamp/stand, B: vial of agarose, C: <i>iCare</i> tonometer	163
Figure 9.2 Experimental setup showing indentation of the agarose gel A: Vial of agarose B: <i>iCare</i> probe ‘indenter’ C: Screw attachment D: 5N load cell E: Hounsfield tensometer F: Retort stand/clamp	164
Figure 9.3 Average stress-strain curves for the multiple concentrations of agarose.	166
Figure 9.4 Agarose concentration versus mean E values \pm SD (error bars)	169
Figure 9.5 Agarose concentration versus mean <i>iCare</i> readings \pm SD (error bars)	169
Figure 9.6 Agarose E values versus mean <i>iCare</i> readings \pm SD (error bars)	170
Figure 9.7 <i>iCare</i> values versus mean E values \pm SD (error bars)	170
Figure 9.8 RE mean E \pm SD (error bars) for each region for both UK and HK groups.	171
Figure 10.1 Regional mean \pm SD (error bars) Schiotz scale values at 8 mm from the limbus	185
Figure 10.2 Regional mean \pm SD (error bars) Schiotz scale values at 4 mm from the limbus	188
Figure 11.1 RE Bland Altman plots: a) GAT and IOPg difference as a function of their mean IOP, b) GAT and IOPcc difference as a function of their mean IOP and c) IOPg and IOPcc difference as a function of their mean IOP. Horizontal bold line denotes mean difference and dotted lines 95% LoA	208
Figure 11.2 Box and whiskers plot (median and interquartile range) for a) CRF, b) CH, c) IOPg and d) IOPcc for three different intervals of axial length	212
Figure 11.3 Box and whiskers plot (median and interquartile range) for a) CRF, b) CH, c) IOPg and d) IOPcc for three different intervals of axial length	215
Figure 12.1 <i>Pentacam</i> topographical maps and numerical data	236
Figure 13.1 OCT image of the temporal ciliary muscle; callipers (in red) shown for the reference point and ciliary muscle thickness at 1, 2 and 3 mm from the scleral spur.	250
Figure 13.2 a) 3-D MRI depiction of the ocular globe, dotted line delineates the anterior and posterior ocular volume. b) Shading of the MRI images using the mri3dX program to derive ocular volumes (after Gilmartin <i>et al.</i> , 2008).	251
Figures 13.3 (a-f) Box and whiskers plot (median and interquartile range) for temporal and nasal CMT (1, 2, and 3 mm)	254
Figure 14.1 Diagrammatic depiction of the 15%-40% axial length range assessed.	272
Figure A12.1 Experimental setup- A: rotatory table, B: custom designed slide holder, C: silica slide (with femtosecond inscription) D: <i>Visante</i> AS-OCT	382

Figure A13.1 Pressure-response graph from the <i>Pulsair</i> (after Rai, 2007)	383
Figure A13.2 Pulsair waveforms from a) temporal paracentral region b) nasal paracentral region c) central corneal. Subject RC RE +4.00D.	385

LIST OF ABBREVIATIONS

ACD	Anterior chamber depth
AL	Axial length
AMD	Age related macular degeneration
AS-OCT	Anterior segment optical coherent tomography
AWPs	Additional waveform parameters (ORA)
BSA	British South Asian
BSV	Best signal value
BW	British White
CBT	Ciliary body thickness
CCT	Central corneal thickness
CH	Corneal hysteresis
CMT	Ciliary muscle thickness
CoV	Coefficient of variation
CR	Cornea
CRF	Corneal resistance factor
CT	Corneal thickness
ECM	Extracellular matrix
EOM	Extraocular muscles
FVD	Form vision deprivation
GAG	Glycoaminogycans
GAT	Goldmann applanation tonometry
HKC	Hong Kong Chinese
ICC	Intraclass correlation coefficient
IN	Inferior nasal
IOP	Intraocular pressure
IOPcc	Corneal compensated IOP (ORA)
IOPg	Goldmann-correlated IOP (ORA)
IT	Inferior temporal
Ko	Corneal rigidity
Ks	Scleral rigidity
LE	Left eye
LoA	Limits of agreement
MMPs	Matrix metalloproteinase
MRI	Magnetic resonance imaging
MSE	Mean spherical error
NCMT	Nasal ciliary muscle thickness

NTG	Normal tension glaucoma
OH	Ocular hypertension
ONH	Optic nerve head
ORA	Ocular response analyser
PE	Percentage error
POAG	Primary open angle glaucoma
RBT	Rebound tonometry
RE	Right eye
RSV	Regional scale values (Schiotz tonometry)
Rx	Refractive error
SA	Surface area
SN	Superior nasal
ST	Superior temporal
TCMT	Temporal ciliary muscle thickness
TIMPs	Tissue inhibitors of matrix metalloproteinase
UBM	Ultrasound biomicroscopy
α -SMA	Alpha-smooth muscle actin
TGF	Transforming growth factors
FGF	Fibroblast growth factors
FE	Finite element
NCT	Non-contact tonometer
PCI	Partial coherent interferometry
GO	Graves ophthalmopathy
SD	Standard deviation
CI	Confidence intervals
IT AFM	Indentation type atomic force microscopy
LTG	Low tension glaucoma
CXL	Collagen crosslinkage
MD	Maximum distance
NP	Nodal point
OBF	Ocular blood flow
POBF	Pulsatile ocular blood flow

1.0 OCULAR ANATOMY AND PHYSIOLOGY OF THE ANTERIOR SEGMENT

1.1. Introduction

The following section provides a brief outline of the gross ocular anatomy and physiology, with a particular focus on the anterior segment structures that have been implicated in ocular biomechanics.

1.1.1 Gross anatomy of the eye

The ocular globe is composed of three primary coats, the outer fibrous layer comprising the sclera and cornea, the middle vascular coat constituting the choroid, ciliary body and iris and the inner photosensitive retinal layer.

The anterior segment represents the front one-sixth of the globe and encompasses the structures anterior to the vitreous humour: cornea, iris, ciliary body and crystalline lens. Within the anterior segment there are two distinct chambers: the anterior chamber is a fluid filled cavity bound by the corneal endothelium and the iris; the posterior chamber lies between the iris and the anterior vitreous chamber. The crystalline lens is situated behind the iris and is attached to the ciliary body via the zonule fibers. The lens is a transparent biconvex structure that separates the anterior and posterior chambers.

The posterior segment is comprised of the back five-sixths of the globe, and consists of the anterior hyaloid membrane, vitreous humour, retina, choroid and the optic nerve. The vitreous body is attached to the lens, ciliary body and the retina near the optic nerve head. The optic nerve head lies medially to the macula lutea and is the site where the retinal nerve fibers exit the eye via a scleral aperture known as the lamina cribrosa; this is also the point of entry and exit of the central retinal artery and vein.

1.2 Anatomy and physiology of the anterior segment

1.2.1 The Sclera

1.2.1.1 Function

The sclera forms the chief protective layer of the eye; it has multiple functions but of these the most crucial is the protection of the intraocular components from injury and displacement, while resisting the stress of the intraocular pressure (IOP). Further, the sclera provides a rigid base for attachment of the extraocular muscles (EOMs) and accommodative apparatus and acts as a conduit for vascular and neural fibres for anterior and posterior structures. Importantly the sclera permits eye movement with minimal fluctuation in ocular shape or IOP and its opaque characteristics ensure internal light scatter does not degrade the retinal image (Watson and Young, 2004).

The sclera also plays a role in the aqueous humour transportation systems; the first being the conventional route via the Canal of Schlemm, a route formed by the scleral spur and the trabecular meshwork, the second, the uveoscleral outflow, which accounts for 10% of aqueous drainage. The function of the sclera in the uveoscleral pathway is of indirect importance as it ensures retinal integrity via maintenance of the retinal pigment epithelium.

1.2.1.2 Gross anatomy of the sclera

The sclera comprises approximately five-sixths of the outer fibrous layer of the eye and extends from the limbus to the site of the optic nerve head. The sclera and the cornea are linked via the transitional limbal zone; however both tissues have significant differences in composition and physiological parameters.

The anterior sclera has a radius of curvature of 11.6 mm along its inner surface (Watson and Young, 2004). The size of the scleral sphere varies in humans but the average coronal diameter is approximately 22-24 mm (Bron, 1997). The sclera is approximately 1 mm thick posteriorly near the optic nerve head and thins to 0.6 mm at the equator (Foster and Sainz de la Maza, 1994). It is thinnest, at 0.3 mm, in the regions behind the insertion sites of the recti muscles and then progressively thickens to 0.8 mm at the corneoscleral junction (Hogan, 1971).

The insertion sites of the EOMs vary in regards to their distance from the limbus; the medial rectus joins the sclera at 5.5 mm, lateral rectus at 6.9 mm, superior rectus at 7.7 mm and the inferior rectus 6.5 mm. The insertion of the superior oblique and inferior oblique muscles is posterior to the equator.

The sclera has two main perforations, the anterior scleral foramen and the posterior scleral foramen: the former is occupied by the cornea and is the site where the sclera merges with the cornea; the latter is located approximately 3 mm medial to the mid line and 1 mm above the horizontal meridian and creates the opening for the optic nerve head. It is at the optic nerve head that the lamina cribrosa sclera is formed by elastin and collagen fibres traversing over the aperture, consequently forming the weakest site along the scleral surface.

The sclera is also perforated by three groups of smaller channels and these can be divided into anterior, middle and posterior depending on their location. The purpose of these openings is to provide a route of passage for nerves and blood vessels. The anterior apertures are located near the insertion of the recti muscles and are the route for the branches of the anterior ciliary arteries and veins, aqueous veins and ciliary nerves. The middle apertures are located behind the equator of the eye and provide an exit passage for the vortex veins. The posterior apertures are located around the optic nerve head and these form channels for transmission of the long and short ciliary nerves and vessels. The short ciliary nerves supply the posterior scleral regions whilst the long ciliary nerves serve the anterior regions.

The sclera is composed of three layers: episclera, scleral stroma and lamina fusca. The episclera forms the outer layer of the sclera, which is in apposition with the overlying Tenon's capsule and conjunctiva. The episclera has a rich blood supply via the anterior ciliary arteries and is composed of loosely arranged collagen bundles that are thinner than in the scleral stroma (Foster and Sainz de la Maza, 1994). The scleral stroma is composed of irregularly arranged collagen fibrils and elastin fibres (see below) (Komai & Ushiki, 1991). It is this irregularity (compared with the precise organisation of the fibrils in the cornea) that is thought to be the cause of the opaque feature of the sclera (Maurice, 1957). The lamina fusca forms the pigmented tissue between the sclera and the underlying choroid and is attached to the choroid via weak collagen fibres. The lamina fusca

comprises smaller collagen bundles and shows a greater density of elastic fibres than the scleral stroma (Marshall, 1995).

1.2.1.3 Structural organisation of the sclera

The sclera is composed of dense interwoven bundles of collagen, some elastic fibres, few fibroblasts and moderate levels of extracellular matrix (ECM). The human sclera has been reported to contain 50% collagen by weight, consisting predominantly of type I collagen (Keeley *et al.*, 1984) with the total collagen content being greater in the posterior sclera than the equatorial and anterior regions (Avetisov *et al.*, 1983). In addition to type I collagen, the human sclera has also been found to contain collagen types III, IV, V, VI, VIII, XII and XIII (Wessel *et al.*, 1997; Thale and Tillman, 1993; Sandberg-Lall *et al.*, 2000; Foster and Sainz de la Maza, 1993) and distribution of these various collagen types has been shown to demonstrate regional variation (Marshall *et al.*, 1993; Konomi *et al.*, 1983).

In comparison to the cornea, scleral collagen fibrils have a larger range of diameter 25-230 nm and their arrangement within each collagen bundle is more irregular (Komai and Ushiki, 1991). The collagen bundles vary in diameter from 0.5 to 6 μm depending on their location; outer regions are thinner than inner regions (Foster and Sainz de la Maza, 1994). The distribution of these bundles also varies, from a lamellae like organisation in the outer layers, which progressively changes to an irregular pattern in the inner regions (Watson and Young, 2004).

The collagen bundle sizes and distribution also varies with the geographic location on the globe; anteriorly the collagen bundles are smaller and are moderately compact, at the equator they are thinner and densely packed, whilst posteriorly the bundles are medium to large in size and loosely arranged (Curtin, 1969). Further, the orientation of the collagen bundles also shows regional variation; generally the collagen fibres run circularly but in the anterior regions the orientation changes to a meridional and oblique course near the nasal/ temporal limbal areas and the vertical meridian, respectively (Kokott, 1934). Aside from regional variation in the arrangement of the collagen bundles, the collagen fibril organization within each bundle changes with locations on the globe (Thale and Tillmann, 1993; 1996a; 1996b) and between the surface layers, with larger diameter fibrils being found in the outer layers and smaller in the inner layers (Spitznas, 1971).

1.2.1.4 Proteoglycans

Proteoglycans are non-collagen modulators in the ECM which co-ordinate collagen synthesis, orientation and tissue hydration (Oyster, 1999). The concentration of proteoglycans in the sclera is lower than that of the cornea (Krachmer, 2005). Proteoglycans are complex molecules comprising a core protein of varying length, which is covalently bonded to glycoaminoglycan side chains (GAG). GAGs are long-chained, unbranched, linear polysaccharide molecules that are formed of sugar residues such as N-acetylglucosamine, N-acetylgalactosamine, glucuronic acid, and iduronic acid (Rada *et al.*, 2006). At least four types of GAGs have been reported in scleral tissue: dermatan sulfate, chondroitin sulfate, heparan sulfate and hyaluronic acid (Trier *et al.*, 1990). As the GAGs are negatively charged, the proteoglycans have a hydrophilic property and this characteristic governs the hydration and elasticity of the sclera (Rada *et al.*, 2006). The water content of the sclera is approximately 70% (Tier *et al.*, 2005) with the posterior sclera shown to have greater hydration than anterior (Boubriak *et al.*, 2003).

Proteoglycans can be categorised by their size and by the presence of several characteristic regions found within their core proteins; aggrecan is an example of a large proteoglycan whilst decorin, biglycan, fibromodulin and lumican are classified as small leucine-rich proteoglycans (Johnson *et al.*, 2006). The main proteoglycans in the sclera are aggrecan, decorin, and biglycan (Rada *et al.*, 1997). Aggrecan has been found in high concentration posteriorly and may be related to the greater distensibility of the scleral tissue in this region (Rada, *et al.*, 2000).

1.2.1.5 Elastin Fibres

The sclera has a low percentage (2% of dry weight) of elastin (Moses *et al.*, 1978) though this relatively minor structural element is important in the ECM (Foster and Sainz de la Maza, 1994). Elastic fibres are found in greater density in the lamina fusca and the inner stromal layers and along the stress lines of the EOMs (Marshall, 1995). Elastin fibres also show regional variation in distribution with localised concentrations along the equator, limbus and optic disc (Watson and Young, 2004). Elastin may contribute to the viscoelastic properties of the sclera and alter modulus and energy absorption when exposed to stress (Schultz *et al.*, 2008).

1.2.1.6 Scleral Fibroblasts

The scleral fibroblasts are few in number and are located between collagen bundles (Krachmer, 2005). These cells have characteristic long branching processes, which make slight contact with each other (McBrien and Gentle, 2003). The fibroblasts are capable of synthesizing all the components of the ECM, and hence the biosynthetic activity of these cells is vital in supporting the structural and functional role of the scleral connective tissue.

1.2.1.7 Other constituents of the sclera

Other components of note within the sclera that regulate the tissue include glycoprotein and matrix degrading enzymes. The function of these glycoproteins is as binding agents for molecules in the ECM (Foster and Sainz de la Maza, 1994). The matrix metalloproteinase (MMPs) are a group of enzymes that can break down collagen and ECM elements, which are regulated by tissue inhibitors of matrix metalloproteinase (TIMPs) (Di Girolamo *et al.*, 1997).

1.2.2 The Cornea

The cornea is a transparent anterior structure that constitutes approximately one-sixth of the outer fibrous layer. The shape of the cornea is elliptical, with average dimensions of 10.6 mm vertically and 11.7 mm horizontally. The inner and outer surfaces of the cornea differ; anteriorly the central radius of curvature is 7.8 mm and posteriorly 6.5 mm. The cornea is thinnest centrally approximately 0.5-0.6 mm and thicker peripherally 0.7 mm. Anteriorly, the tear film coats the cornea whilst posteriorly it is in contact with the aqueous humour. As the cornea is avascular it receives its oxygen mainly via the tear film and from the peripheral limbal arcades. The cornea is composed of five main layers, each with their very distinct ultrastructural organisation.

The epithelium is the outermost layer of the cornea, which is 50-90 μm thick and composed of 5 layers of cells. The acellular Bowman's layer lies below the epithelium (8-14 μm thick) and consists of interwoven collagen fibrils, which are thinner and more randomly organised than the stroma below it. The stroma is the thickest layer of the cornea (500 μm), containing lamellae of collagen fibrils lying parallel to the surface (Komai and Ushiki, 1991). The direction of the fibrils in a given lamellae is the same but this is perpendicular to the adjacent layers; it is this regularity and the uniform spacing of the

fibrils that is thought to create the transparency of the cornea (Maurice, 1957). The different layers are bound together by lamellae travelling from one layer to another and the collagen fibrils tend to be larger in the inner surface than in the outer (Bron, 1997). The stroma contains mainly collagen type I, with smaller amounts of type III, V, VI (Krachmer, 2005). Beneath the stroma, the Descemet's membrane (3-4 μm thick) is composed of type IV collagen fibrils arranged in a distinct hexagonal pattern. Finally the endothelial layer is characterised by a single layer of flattened cells with distinct polygonal shapes connected by tight junctions.

1.2.3 Comparison of the structural characteristics of the sclera and cornea

In regards to their primary structural components, the sclera and cornea are alike; both tissues are avascular and consist mostly of collagen and have few types of cells. However when comparing their ultrastructures and tissue characteristics significant differences are evident. Of note the collagen fibrils in the cornea demonstrate a uniform diameter in contrast to the large range of diameters found in the sclera. In regards to the collagen fibril arrangement in the corneal and scleral stroma, the corneal fibrils demonstrate even spacing and a regular layer-like organization, whilst in the sclera, although a lamellae-like arrangement is evident, the organisation is not as regular due to the interweaving of the collagen bundles. Thus the difference in the uniformity of the collagen size and distribution results in the cornea being transparent and the sclera being opaque.

Further differences between the cornea and sclera originate from differences in the arrangement of their non-collagen components and composition of the ECM. In particular the fibroblast cells in the cornea are parallel to the corneal surface in between the layers of the collagen fibrils, whilst in the sclera this arrangement is less organised. Additionally the cornea has a greater content of ECM than the sclera and its water content is slightly higher (78%) (Bron, 1997) than that of the sclera (70%) (Tier *et al.*, 2005). In regards to non-collagen modulators in the ECM, the cornea has greater levels of dermatan sulphate and hyaluronic acid than the sclera, however in contrast the sclera has greater keratin sulphate than the cornea. Additionally, the cornea contains greater density of proteoglycans than the sclera.

The cornea and sclera also differ significantly in their gross structural characteristics; the cornea's transparent structure allows it to function as a refracting component, whilst the three-dimensional heterogeneous collagen structure of the sclera makes it a much more resilient tissue and allows it to perform its role as a protective coat and in maintaining ocular shape. Therefore considering the differences in their ultrastructure and their gross morphology, the biomechanical characteristics of the two structures are likely to vary significantly.

1.2.4 Aqueous humour

The aqueous humour is a clear colourless fluid that fills the anterior and posterior chambers, providing nutrients to the avascular components of the anterior segment. The equilibrium between the production and drainage of the aqueous humour maintains the level of IOP within the eye. The formation of the aqueous humour occurs in the ciliary processes of the ciliary body and involves three different mechanisms: diffusion, ultrafiltration and an active transport system (Oyster, 1999). The majority (85-90%) of the aqueous humour drains out of the anterior chamber via the root of the iris, front surface of the ciliary body and the trabecular meshwork. Additionally, a smaller amount (3-20%) leaves the eye via the uveoscleral outflow mechanism, which involves drainage into the anterior uvea through the iris root and the interstitial spaces of the ciliary muscle and into the suprachoroidal space (Forrester, 2008).

1.2.5 Intraocular pressure (IOP)

The intraocular pressure occurs as a result of the constant formation and drainage of the aqueous humour. In order to sustain the normal IOP level, the rate of aqueous humour formation needs to match the rate of drainage of the aqueous humour. Data from population studies follow an almost normal distribution of IOP with a mean value of 16 mm Hg. The distribution curve for IOP is slightly skewed, since IOPs over two standard deviations of the mean (> 21 mm Hg) account for 5-6% of the population instead of the 2.5% predicted by the normal distribution (McAllister, 1986). Normal IOP ranges from 10 to 21 mm Hg. Many factors can affect the IOP; age has been found to be a significant factor as IOP become higher with advancing age (Harvey, 2003) and diurnal fluctuations in IOP are widely documented with IOPs peaking in the morning (Read *et al.*, 2008; Liu *et al.*, 2005; Jaén-Díaz *et al.*, 2007).

1.2.6 Iris

The iris is a circular contractile membrane of approximately 12 mm diameter which has a central perforation; the pupil. The iris is situated in front of the crystalline lens and behind the cornea and is bathed on both surfaces by the aqueous humour.

1.2.7 Ciliary body

The ciliary body is a circumferential tissue in the anterior eye that comprises both the ciliary muscle and ciliary processes along with connective and vascular tissues. When viewed in cross-section, the ciliary body conforms to a triangular like shape with its base at the iris root and its apex at the ora serrata (Bron, 1997). The ciliary body is lined with two layers of neuroepithelial cells: a non-pigment layer internally and a pigment layer externally (Hogan, 1971). The non-pigmented layer is in apposition to the aqueous humour and is involved in the secretion of the aqueous humour (Davson, 1990). Although the ciliary muscle is described as a smooth muscle it demonstrates characteristics of all three muscle types: smooth, striated, and cardiac (Pardue and Sivak, 2000; Tamm and Lütjendrecoll, 1996; Ishikawa, 1962). The ciliary muscle makes up the bulk of the ciliary body and is attached to the crystalline lens by zonular fibers. In turn these zonular fibers are attached to the lens near the equator at three different sites (Rohen, 1979). The ciliary body has three main functions: accommodation, aqueous humour production and the maintenance of vitreous mucopolysaccharides (Snell and Lemp, 1997).

The ciliary body is innervated by the autonomic nervous system and brings about accommodation via the contraction of the ciliary muscles (Croft *et al.*, 2001). In their natural relaxed state the zonules are under tension making the crystalline lens thin allowing the eye to focus for distance objects (Charman, 2008). On contraction the ciliary muscle moves forwards and inwards towards the equator of the lens reducing the tension in the zonule fibers (Helmholtz, 1855; Glasser and Kaufman, 1999). Consequently the crystalline lens becomes more convex and hence increases its dioptric power for near viewing (Croft *et al.*, 2001). Undoubtedly this ability to focus over a range of distances is essential in humans although the facility to accommodate reduces with increasing age, to the point that by the age of 50-55 years the capacity to accommodate is completely lost (Weale, 2003; Strenk *et al.*, 2005). The actual causes for the loss of this mechanism remain obscure.

1.2.8 Crystalline Lens

The crystalline lens is a biconvex, avascular, transparent structure situated between the iris and the vitreous humour. The lens is suspended from the ciliary body by the zonular fibers attached at the equator of the lens. This allows the mechanism of accommodation to occur whereby objects from near to infinity can be focused on the retina. The anterior surface of the lens shows less convexity than the posterior surface; the anterior surface central radius is between 8-14 mm and the posterior surface radius 4.5-7.5 mm (Forrester, 2008). In adults the mean diameter of the lens is approximately 10 mm and the thickness 4 mm.

The lens is made up of three distinct components; an elastic capsule, the lens epithelium and the lens fibers. The elastic capsule encloses the whole lens. The epithelium is only found on the anterior surface of the lens and can be divided into two zones. The equatorial epithelium cells actively divide and differentiate into lens cell fibers, whilst the centrally located epithelial cells are responsible for the transportation of substances from the aqueous humour to the lens interior and in the secretion of the capsular material (Snell and Lemp, 1997). The lens fibers comprise the main body of the lens.

2.0 HUMAN MYOPIA

2.1 Introduction

The following section provides a brief overview of myopia and in particular focuses on the literature pertaining to animal models and the involvement of the sclera in myopia.

2.1.1 Refractive error

Emmetropia describes the refractive state of the human eye where an object at infinity is sharply imaged on the retina with the accommodation relaxed. In order to achieve this visual state, an optimal equilibrium must be attained between the eye's refracting components; radii of curvature of the cornea and the crystalline lens surfaces, the refractive indices of the ocular media, anterior and vitreous chamber depths and lens thickness. The emmetropisation process constitutes a co-ordinated process whereby increase in axial length growth is compensated in part by a progressive equal but opposite change in lens/corneal power. Failure to maintain this co-ordination results in development of a refractive error. Myopia results when the image is formed in front of the retina whilst in hypermetropia the image falls behind the retina.

2.1.2 Myopia development

It is commonly accepted that myopia develops as a consequence of an increased axial length that is not countered by the decrease in optical power of the cornea and crystalline lens. Non-pathological myopia is therefore not a cause of excess axial elongation but instead the failure of the anterior segment to compensate for this growth (Jones *et al.*, 2005; Zadnik *et al.*, 2003), whereas pathological myopia can be caused by excess axial length development (Curtin, 1985).

2.1.3 Classification of myopia

2.1.3.1 Severity

Conventional categorisation of the levels of myopia is based on the spherical equivalent error (SE). Low myopia is considered as -3.00 D or less, medium myopia between -3.00 D and -6.00 D and high myopia as greater than -6.00 D (Weymouth and Hirsch, 1991). High

myopia is linked to ocular pathology such as retinal detachments and/or choroidal degenerations and thus poses greater concerns than the lower levels of myopia (Grossniklaus and Green, 1992; Celorio and Pruett, 1991).

2.1.3.2 Age of Onset

Early onset myopia is a form of myopia that manifests from very early infancy until the age of 6 years (Grosvenor, 1987). This type of myopia progresses rapidly in the early years of development and is associated with an increased risk of ocular pathology (Curtin, 1985). A strong genetic component has been identified in this type of myopia (Morgan and Rose, 2005; Baird *et al.*, 2010) due, in part, to its association with systemic diseases such as Marfan's (Dietz *et al.*, 1991) and Stickler's (Brunner *et al.*, 1994) syndromes.

School myopia accounts for around 70% of myopia; which is characterised by an onset at 9 to 11 years of age with a gradual progression through the teenage years, which stabilises by late teens or early twenties at around 3-4 D of myopia (Gilmartin, 2004).

Adult onset myopia is typically classed as myopia that occurs after the age of 20 and is thought to be more attributable to environmental factors such as near work (Gilmartin, 2004; Mutti and Zadnik, 1996).

2.1.4 Prevalence of myopia

2.1.4.1 Population and ethnicity

The prevalence levels of myopia are generally increasing around the world (Kempen *et al.*, 2004; Vitale *et al.*, 2009) but substantial variations have been observed across different populations (Morgan and Rose, 2005; Weale, 2003). Amongst children and young adolescent prevalence levels of as high as 60-80% have been identified in East Asian countries such as Taiwan, China, Hong Kong and Singapore (Lam *et al.*, 2004; Lin *et al.*, 2004; Saw *et al.*, 2002a; He *et al.*, 2004). Parts of Europe have also shown levels (i.e. 49.7%) approaching those of East Asia (Villarreal *et al.*, 2000) although Australia (Ojami *et al.*, 2005; Ip *et al.*, 2008), and USA (Kleinstejn *et al.*, 2003; Jones *et al.*, 2007b) have reported lower levels in the region of 10-25%. In regards to the severity of myopia, the prevalence levels of high myopia are less than 3% in Western populations (Katz *et al.*, 1997; Wensor *et al.*, 1999), whilst amongst the Asian populations the levels are higher at

10% (Wong *et al.*, 2000; Wu *et al.*, 2001). In addition to population differences in the prevalence of myopia, ethnicity has also demonstrated a significant influence, with some ethnic groups showing greater susceptibility to myopia than others (Kleinstei *et al.*, 2003; Rudnicka *et al.*, 2010; Ip *et al.*, 2008). In particular this susceptibility is notable amongst Chinese children, where higher rates of myopia have been identified in comparison to other ethnicities in studies conducted in and out of China (Cheng *et al.*, 2007; Goh *et al.*, 2005; He *et al.*, 2009).

2.1.4.2 Occupational

Environmental factors such as occupation have also been considered to influence the prevalence levels of myopia (Curtin, 1985). Both Goldschmidt (1968) and Tscherning (1882) reported higher levels of myopia amongst students when compared to individuals in occupations requiring little near vision. More recently Ting *et al.*, (2004) observed clinical microscopists to show higher levels of myopia (87%) when compared to the general population, whilst similarly McBrien and Adams, (1997) reported 45% of eyes of microscopists to develop myopia over 2 years.

2.1.5 Genetic influence on myopia

A genetic component in myopia has long been suggested. High heritability for refractive errors and ocular biometry has been observed in twin studies (Lyhne *et al.*, 2001), with greater levels of concordance being demonstrated in monozygotic twins when compared to dizygotic twins (Hammond *et al.*, 2001; Baird *et al.*, 2010). Additional support for a genetic influence in myopia comes from family aggregation studies where children of myopic parents have been shown to be at significantly higher risk of developing myopia when compared to children of non-myopic parents (Li *et al.*, 2009; Guggenheim *et al.*, 2000; Saw *et al.*, 2001). Genetic mapping has also identified several chromosomal loci for high myopia (Hornbroke and Young, 2009; Baird *et al.*, 2010; Farbrother *et al.*, 2004a). Furthermore recent work by Hysi *et al.*, (2010) identified single nucleotide polymorphisms (SNPs) on the chromosome 15q25 associated with refractive error; that overlaps with the transcription initiation site of RASGRF1, which is highly expressed in neurons and retina and has been implicated in retinal function and memory consolidation. Similarly Solouki *et al.*, (2010) reported refractive error to be significantly associated with chromosome 15q14, with the associated loci being in the vicinity of two genes that are expressed in the retina.

These findings provide further confirmation of a genetic component in myopia, although it is widely accepted that most myopia is polygenic, resulting from a combination of genetic susceptibility and environmental factors (Guggenheim, 2009).

2.1.6 Environmental factors

There is a significant body of literature to suggest that myopia is a multifactorial condition that is influenced by both genetic and environmental factors (Schaeffel *et al.*, 2003). Environmental factors involving near work such as reading or increased levels of education have often been found to be associated with myopia (Rosenfield and Gilmartin, 1998; Saw *et al.*, 2002b). Other environmental factors such as high glycaemic index diets, body mass index (Cordain *et al.*, 2002), early exposure to night lights (Quinn *et al.*, 1999), and parental history of myopia (Mutti *et al.*, 2002) have also been implicated in the risks of developing myopia. In regards to the actual levels of influence of environmental factors in myopia, studies have found these risk factors to explain approximately 12% of the variance in myopia (Saw *et al.*, 2004; Mutti *et al.*, 2002). Environmental factors have also been suggested to have a protective influence in developing myopia; both parental smoking (Stone *et al.*, 2006) and outdoor activity (Rose *et al.*, 2008; Dirani *et al.*, 2009; Jones-Jordan *et al.*, 2010) have been suggested to reduce the risk of developing myopia, although the actual mechanism by which this protection occurs is unknown.

2.2 Animal models

2.2.1 Retinal image manipulation and refractive error development in animal models

Animal models are a vital aspect of myopia research as they enable the *in vivo* assessment of anatomical and physiological changes that occur during refractive error development. Such changes can be assessed in humans during refractive error development but in contrast to the changes that occur in animal models these alterations are less dramatic (Read *et al.*, 2010) and often take longer to develop. Wiesel and Raviola (1977) first introduced these models when observing that retinal image degradation (reduced form vision) produced axial length elongation in monkey eyes. Form vision deprivation (FVD) induced refractive error development has since been demonstrated in various animal species; tree shrew (Gentle *et al.*, 2003; Guggenheim and McBrien, 1996), monkey (Qiao-Grude *et al.*, 2010; Smith *et al.*, 2009), marmoset (Rada *et al.*, 2000), cat (Wilson and

Sherman, 1977), guinea pig (Backhouse and Phillips, 2010) and chick (Rada and Wiechmann, 2009) and have provided essential understanding of the mechanisms by which environmentally determined visual input regulates ocular growth. Myopic growth in such models is usually axial in nature and is generally associated with an increase in vitreous chamber depth (McBrien and Norton, 1992).

Aside from FVD, ocular growth in animal models has also been manipulated in experiments where high spatial frequency information is deprived by producing optical blur with the use of positive and negative lenses (Irving *et al.*, 1992; Siegart and Norton, 2010; Qiao-Grider *et al.*, 2010). Hence the artificial change in the refractive status of the eye promotes a compensatory response from the choroid and sclera which modulate the retina to move towards the image plane (Wildsoet and Wallman, 1995; Nickla and Wallman, 2010); the introduction of negative lenses promotes myopia via axial expansion and conversely on positive lens application axial elongation ceases and hypermetropia develops. Myopic defocus promotes thickening of the choroid and decreased scleral growth (anterior movement of the retina) whilst hyperopic defocus leads to thinning of the choroid and increased scleral growth (posterior movement of the retina). Choroidal thickness changes with optical defocus have been observed in both chicks (Wildsoet and Wallman, 1995) and primates (Troilo *et al.*, 2000).

Moreover, local FVD and lens defocus studies have further demonstrated the plasticity of ocular growth by controlling the visual environment; in animal models involving rhesus monkey and chicks, vision deprivation in only half of the visual field has shown elongation to occur in only the deprived hemi-field (Smith *et al.*, 2009; Wallman *et al.*, 1987; Diether and Schaeffel, 1997). Additionally, animal model have also shown that in some species the visual-feedback co-ordination of ocular growth is localised to mechanisms that reside entirely in the eye. In animal studies pertaining to chicks and tree shrew, where neural signals via the optic nerve were prevented either by pharmacologic blockade or surgical sectioning, the effect of FVD was still evident (Norton *et al.*, 1994; Troilo *et al.*, 1987; Wildsoet and Pettigrew, 1988).

The findings of these animal studies have highlighted that the emmetropization mechanism involves an active feedback system where the scleral growth and choroidal thickness regulates the retinal plane to compensate for out-of-focus images and that local changes in

visual experience can lead to regional changes in ocular growth (Wallman and Winawer, 2004).

2.2.2 Recovery in animal models

Following removal of the FVD device, chick eyes have shown recovery from myopia and to return back to an emmetropic state (Wallman and Adams, 1987; Rada and Wiechmann, 2009). Similarly this mechanism has also been demonstrated in FVD and lens defocus models in mammals although some inconsistencies have been reported (McBrien *et al.*, 2000; 2006; Qiao-Grider *et al.*, 2004; Troilo *et al.*, 2000; Siegwart and Norton, 2010). After removing the FVD device or the optical defocus, the recovery mechanism constitutes the cessation of vitreous chamber growth, whilst the rest of the eye continues to grow normally, until the other ocular components catch up with the deprivation-induced axial elongation (Wallman and Adams, 1987; Siegwart and Norton, 1998). Additionally choroidal thickness also demonstrates significant modulation to compensate for the induced refractive error (Wallman *et al.*, 1995) and has been suggested to be a significant mechanistic component in regulating scleral growth (Nickla and Wallman, 2010).

2.2.3 The sclera and myopia

The sclera is a tough fibrous tissue that has been implicated in the development of myopia. In high myopia the eye is often characterised by posterior scleral thinning and weakening, rendering it vulnerable to the expansive stresses of the IOP (Curtin, 1969; Siegwart and Norton, 1999). Biochemical and histological assessments of *post-mortem* tissues in humans have confirmed scleral changes in myopia (Curtin *et al.*, 1979; Avetisov *et al.*, 1983), although in regards to the mechanism by which scleral remodelling occurs, animal models have provided a clearer understanding of how these biological changes arise. In particular the following discussion will focus on mammalian (tree shrew and rhesus monkey) models of myopia due to their scleral structure being similar to that of humans (McBrien *et al.*, 2001a).

The visual-feedback mechanism demonstrated in animal models suggests that ocular growth in myopia is a consequence of retinal signals that induce changes in the scleral biomechanics (McBrien *et al.*, 2009). Anterior and equatorial regions are known to undergo thinning in high myopia but these alterations are less evident than the changes that

occur at the posterior pole (McBrien and Gentle, 2003). Thinning of the sclera leads to increased tissue elasticity, which is likely to affect the growth of the eye (Phillips and McBrien, 1995). Previously, when comparing the Young's modulus of the myopic and non-myopic sclera no significant differences have been found (Siegwart and Norton, 1999) and on finite element analysis elasticity only accounted for 20% of the ocular size (Phillips and McBrien, 1995). In comparison, changes in biomechanical properties such as scleral creep (i.e. time-dependent mechanical properties that are independent of scleral thickness) have shown a more significant effect on ocular growth than scleral elasticity (Siegwart and Norton, 1999; Phillips *et al.*, 2000). These observations have suggested that material properties such as thickness are less likely to influence myopic growth when compared to other biomechanical properties of the sclera which are under the influence of its ECM and cellular components (McBrien and Gentle, 2003; McBrien *et al.*, 2009).

The scleral remodelling process in mammalian myopia is associated with a reduction in the synthesis of collagen type I and GAGs induced by the scleral fibroblasts (McBrien *et al.*, 2000; Gentle *et al.*, 2003; Norton and Rada, 1995). These metabolic changes are accompanied by increased production of collagen-degrading enzymes such as the active gelatinase MMP-2 and the inhibitors TIMP-1 and TIMP-2 (Guggenheim and McBrien, 1996; McBrien *et al.*, 2001b). The increased levels of TIMP-1 and TIMP-2 have been associated in both the regulation and activation of the latent MMP-2 during myopic growth (McBrien and Gentle, 2003). Further, in longer periods of myopia (>3 months) the gradient of collagen fibril diameter (N.B. outer layers have larger diameter collagen than inner layers) across the layers of the sclera is also lost, with the median diameter fibrils being replaced by smaller diameter collagen fibrils (Funtana and Tokoro, 1990; McBrien *et al.*, 2001a). The lower levels of GAG results in reduced tissue hydration, which when coupled with the lower density of collagen fibres and the loss of the collagen diameter gradient results in the weakening of the mechanical properties of the posterior sclera (Norton and Rada, 1995).

The precise mechanisms that drive these ECM changes in myopic eyes are still uncertain but studies have indicated that the alterations may be a result of growth factors and hormones regulating the matrix components (McBrien *et al.*, 2001a). In particular, transforming growth factors (TGF) and fibroblast growth factors (FGF) have been investigated as determinants of these changes (Rohrer and Stell, 1994). Further, details on the mediators of the active retino-scleral feedback system are also unclear; components

such as retinoic acid have been implicated in the feedback system but inconsistencies between animal species have been noted in regards to this inter-mediatory role (Mertz and Wallman, 2000; McFadden *et al.*, 2004).

In addition to the biochemical instigators of scleral remodelling, contractile cells have also been recently implicated in modulating scleral biomechanics (Poukens *et al.*, 1998; McBrien *et al.*, 2009). In an *in vivo* investigation that assessed axial length changes induced by acute elevation of IOP, Phillips and McBrien (2004) observed tree shrew eyes to initially increase in axial length but then to rapidly shorten in length in less than 1 hour. The rapidity of the response of the eye to stress suggested to the investigators that ECM remodelling was an unlikely explanation for the change in shape, but that scleral contractile cells may have been responsible for the response. Indeed on examination of the scleral tissue the protein alpha-smooth muscle actin (α -SMA) was identified. Since muscle cells involved in response to tissue stress commonly express α -SMA, its presence suggests that a sub-set of scleral cells called myofibroblasts may have an active role in governing the mechanical properties of the tissue (Phillip and McBrien, 2004). Fibroblast cells have been reported to differentiate into myofibroblasts during matrix stress exposure or when introduced to TGF- β (Serini and Gabbiani, 2003; Jobling *et al.*, 2009). Myofibroblasts have the ability to contract the matrix as well as modulate the ECM (Gabbiani, 2003) suggesting that these cells may have an important role in the short- and long-term response to mechanical stresses on the sclera during myopic growth (McBrien *et al.*, 2009).

2.2.4 Application of animal model findings to human myopia

Despite the greater understanding of refractive error development provided by animal models caution must be exercised when applying animal models to humans due to various dissimilarities between animals and humans (Zadnik and Mutti, 1995). In particular the experimental protocols used to induce myopia in animals are often too severe to be encountered by humans during visual development and it is unclear whether the period of animal plasticity in infancy is an appropriate analogue for myopia development in human adolescents (Zadnik and Mutti, 1995). Differences in experimental results within species (Raviola and Wiesel, 1985) and physiological variations between species have further raised doubts about the relevance of animal models to human myopia (Edwards, 1996). Animal sclera has been found to be thin and of equal thickness around its circumference and is often supported by cartilage or bone (Rada *et al.*, 2006). In mammals the sclera has a

less rigid structure, which may facilitate a more even distribution of blood supply to the choroid and retina during extensive voluntary eye movements (Watson and Young, 2004). Furthermore, studies of collagen organisation have indicated differences between animal and human scleral ultrastructure (Curtin, 1969, Kokott, 1938). Additionally variation in the biochemical composition of animal and human scleral tissue has been previously noted; juvenile animal scleral tissue have lower density of non-enzymatic cross-links in comparison to human sclera, which may affect the mechanical behaviour of the tissue (Schultz *et al.*, 2008).

In consideration of the limitations of animal models and their application to human myopia, more recently Read *et al.*, (2010) demonstrated short term monocular defocus to lead to significant axial length changes in humans, consistent with the changes that occur in animal models during optical defocus. These findings support the supposition that the human visual system is also driven by localised visual input, which consequently causes axial length changes to move the retina closer to the image plane via modulation of the choroidal thickness and subsequent changes in scleral growth (Nickla and Wallman, 2010). Despite these findings inconsistencies in regards to optical defocus driven ocular growth changes between animals and humans have been observed; in animal models myopic defocus appears to have a significant inhibitory effect on axial elongation (Smith and Hung, 1999; Wildsoet, 1997), whilst in humans, studies examining myopic defocus in children have failed to show reduced myopic growth (Adler and Millodot, 2006) but in fact demonstrated a more rapid progression of myopia and axial elongation (Chung *et al.*, 2002). Therefore these contrasting findings again question the applicability of animal models to humans and suggest that in humans, myopia could be caused by a failure to detect the direction of defocus (Chung *et al.*, 2002).

3.0 SCLERA AND OCULAR PATHOLOGIES

3.1 The role of the sclera in glaucoma

Glaucoma is the collective name for a group of progressive optic neuropathies, where retinal ganglion cell damage causes loss of visual function. There are two main types of glaucoma; open-angle glaucoma and closed-angle glaucoma and this categorisation is primarily based on the patency of the anterior chamber angle. These two subsets of glaucoma are then further sub-divided by the underlying cause of the change in the aqueous humour dynamics. Of interest to the present discussion are primary open angle glaucoma (POAG), normal tension glaucoma (NTG) and ocular hypertension (OH). The pathogenesis of glaucoma is still unclear although it is widely considered to be multifactorial in nature. Considering the close embryological origins of the lamina cribrosa and its geographic and structural association with the sclera, several studies have suggested the biomechanical properties of the sclera to influence the more pliable lamina cribrosa (Ethier, 2006; Eilaghi *et al.*, 2010a). Since increased IOP is a significant risk factor in the development of glaucoma, the mechanical stress imposed on the sclera from the IOP may translate to stress on the optic nerve head (ONH) and in particular the weaker lamina cribrosa; these stress-strains even at low IOP levels may contribute towards the retinal ganglion cell loss in glaucoma (Burgoyne *et al.*, 2005).

Therefore the posterior sclera is likely to play an important role in the aetiology of glaucoma and an accurate assessment of its biomechanical features is necessary to understand its influence on the ONH (Girard *et al.*, 2009a). The biomechanics of the ONH are complex due to the presence and interactions of various tissues that are mechanically different (Bron, 1997), characteristics which when coupled with the inaccessibility of the ONH, poses a challenge to evaluate. In order to address this difficulty a number of investigators have evaluated the ONH and posterior scleral biomechanics using finite element (FE) modelling (Roberts, *et al.*, 2010; Eilaghi *et al.*, 2010a; Sigal *et al.*, 2005a; Bellezza *et al.*, 2000). These FE models have indicated scleral canal size, shape, scleral thickness and stiffness to be significant factors in the level of IOP-induced stress on the ONH (Bellezza *et al.*, 2000; Sigal *et al.*, 2004; 2005b; 2009; Girard *et al.*, 2008). Additionally some FE studies have also observed that geometric factors such as globe radius may play a determinant role in the ONH biomechanics (Sigal *et al.*, 2005b).

implying that glaucoma susceptibility is dependent on various structural and mechanical properties of the sclera and their respective interactions.

Animal studies investigating experimental glaucoma have found viscoelastic properties of monkey peripapillary scleral tissue to be altered following chronic periods of elevated IOP (Downs *et al.*, 2005). In particular changes were observed in the long-term elastic properties of the tissue, causing speculation that localised changes in the lamina cribrosa ECM may lead to changes in tissue response to IOP (Downs *et al.*, 2005). Furthermore the posterior sclera has been found to be stiffer in older monkeys when compared to young monkeys and therefore subjected to higher stresses but lower strains at all levels of IOP; these findings may explain the greater susceptibility to glaucoma with increasing age (Girard *et al.*, 2009b).

Histologically the collagen fibrils in the region of the lamina cribrosa are arranged circularly around the points of passage of axons and blood vessels (Thale and Tillmann, 1993). In glaucoma this characteristic arrangement is absent and instead the collagen fibrils are found to be arranged in coarse bundles with no specific alignment (Thale *et al.*, 1996a; 1996b). Furthermore the collagen content and composition have also been found to differ in glaucomatous eyes (Tengroth and Ammitzbøll, 1984). In regards to ECM changes in glaucoma, investigators have previously observed increased secretion of ECM in the region of the lamina cribrosa, which may lead to axon strangulation and subsequent nerve damage (Albon *et al.*, 2000, Thale *et al.*, 1996b). Other studies examining ageing of the lamina cribrosa tissue have revealed increased cross-linkage and reduced concentration of collagen type III possibly implying increased levels of rigidity (Albon *et al.*, 1995; 2000).

More recently *in vivo* clinical studies have also provided evidence for altered scleral biomechanics in glaucoma (Ebner *et al.*, 2009; Hommer *et al.*, 2008). In a study examining axial length changes after lowering IOP with acetazolamide, Ebner *et al.*, (2009) reported axial length shortening to be more pronounced in healthy individuals when compared to glaucomatous (POAG) eyes, suggesting that ocular rigidity increases in glaucoma. These findings would also imply that the greater levels of rigidity in glaucoma would make the eye less resistant to fluctuations in IOP due to the lack of elasticity in the ocular walls (Ebner *et al.*, 2009). Similarly in a study employing pulse amplitude and fundus pulsation to determine ocular biomechanics Hommer *et al.*, (2008) also demonstrated increased ocular rigidity in POAG eyes. Furthermore, in a study

implementing Schiøtz indentation tonometry to assess anterior scleral resistance, Sullivan-Mee *et al.*, IOVS 2010, 51: ARVO E-Abstract 5548, reported increased anterior scleral rigidity in glaucomatous (POAG, OH, suspect glaucoma) eyes when compared to healthy eyes, suggesting that the anterior scleral biomechanics may also be liable to changes in glaucoma.

3.2 The role of the sclera in Age Related Macular degeneration

Age-related macular degeneration (AMD) is the leading cause of visual impairment in individuals over the age of 55 years in developed countries (Congdon *et al.*, 2004). The pathogenesis of the disease is still unclear, however it is often associated with pigmentary abnormalities of the macula region (Coleman *et al.*, 2008). AMD can be classified as nonexudative AMD, which is characterised by large drusen and retinal pigment epithelial changes that can lead to geography atrophy, and exudative (neovascular) AMD which is an advanced form of AMD and is associated with choroidal neovascularisation (CNV).

The vascular theory proposed by Friedman, (1997; 2000; 2004) suggests that the pathogenesis of AMD is related to atherosclerotic changes affecting the eye. This model proposes that lipid deposition in the sclera and in Bruch's membrane causes an increase in scleral stiffness, which leads to resistance in the choroidal vasculature. These changes subsequently produce an elevation in the choriocapillary pressure resulting in reduced choroidal blood flow. Aside from affecting the retinal vascular system the lipid deposits in Bruch's membrane also cause degenerative changes in the elastin and collagen fibrils, leading to the characteristic retinal atrophy seen in AMD.

In support of this theory, biochemical assessment of Bruch's membrane and its collagen have shown a significant decline with age in the solubility of collagen present in the macular and peripheral regions, from close to 100% in the first decade of life to 40-45% in the ninth decade (Karwatowski *et al.*, 1991; 1995). Non-collagen proteins have also been shown to increase with age in the macular region but not at the peripheral sites, suggesting that changes in the collagen composition at the macula may contribute to the accumulation of debris in Bruch's membrane with age and thus consequently interfere with the function of the retinal pigment epithelium (Karwatowski *et al.*, 1995).

Clinical evidence for reduced or altered choroidal and pulsatile ocular blood flow in AMD provides further support for the vascular theory (Grunwald *et al.*, 1998; Chen *et al.*, 2001; Ciulla *et al.*, 2001). Moreover, clinical studies have also reported findings of increased ocular rigidity in AMD patients (Friedman *et al.*, 1989; Pallikaris *et al.*, 2006). Utilising the Schiottz indentation tonometer Friedman *et al.*, (1989) observed increased scleral rigidity in AMD patients when compared to age-matched healthy individuals. More recently, in a pressure-volume experiment (see Chapter 4), Pallikaris *et al.*, (2006) reported increased ocular rigidity in neovascular AMD patients who had been treated with photodynamic therapy when compared to non-neovascular AMD patients and healthy individuals. However the investigators of the Pallikaris *et al.*, (2006) study were unable to determine conclusively whether the increased ocular rigidity was a secondary effect of neovascular AMD or due to independent primary pathological factors.

4.0 ASSESSING IOP AND BIOMECHANICAL PROPERTIES OF THE OCULAR TISSUES *IN VIVO*

4.1 Introduction

It is evident from the overview give afore that the structural organization and biochemical composition of the cornea and sclera differ significantly and hence when evaluating their biomechanical attributes both should be assessed independently. The difficulties posed in investigating such properties *in vivo*, means there is a paucity of research on human scleral biomechanics. A theoretical analysis of the mechanical features of the scleral shell indicates that IOP, scleral curvature and thickness all contribute to the level of stress imposed on the ocular walls (Friedman, 1966). Previous experimental examination of the biomechanical features of the sclera has been mainly via two modes; extensimetry (i.e. assessing change in length of strips of sclera following application of a predetermined force) and by evaluation of the pressure-volume relationship of the ocular globe (i.e. increasing the volume of the eyes by known amounts and measuring the induced curvature, thickness and pressure changes). Such studies have contributed significantly to our current understanding of ocular tissue biomechanics, despite their limitations (see Chapter 9). This section provides a review of the concepts and techniques used to investigate the biomechanical characteristics of the cornea and sclera *in vivo*, which are implemented in various studies throughout the thesis.

4.2 The Ocular Pressure-Volume relationship

Historically the ocular pressure-volume relationship has been widely studied to gain an insight into IOP and the biophysical properties of the ocular coats (Friedenwald, 1937, Gloster and Perkins, 1957, Pallikaris *et al.*, 2005; 2006, Perkins, 1981, Ytteborg, 1960b). The assessment of this relationship can be performed both *in vivo* (Pallikaris *et al.*, 2005, Ytteborg, 1960b) or *in-vitro* (Gloster and Perkins, 1957, Perkins, 1981) and involves the manipulation of IOP via the addition or removal of known volumes of fluid to/from the anterior chamber; this procedure is also termed manometry. In order to undertake an engineering analysis of the pressure-volume relationship within the eye, certain assumptions need to be made. These include assuming the eye is a spherical vessel, with a uniform thickness that is small in comparison to the radius (Greene, 1985). Furthermore, to simplify the models all viscoelastic properties are ignored and the tissue is assumed to be isotropic and homogenous (Purslow and Karwatowski, 1996).

In early work, various investigators (Clark, 1932, Gloster and Perkins, 1957, Ridley, 1930), ((Koster, 1895, Schulten, 1884) cited in Friedenwald, (1937)) attempted to explain the pressure-volume relationship using empirical studies. Using the data from such studies, Jonas Friedenwald demonstrated in 1937 a linear relationship above 5 mm Hg between the incremental increase in volume and the logarithm (to the base 10) of the IOP. Friedenwald also noted that the gradient of this relationship varied with the distensibility of the eye, with a steeper gradient indicating a more rigid eye. These findings have since been corroborated by more recent investigations that have utilised the manometric method to calculate ocular rigidity, noting a linear pressure-volume relationship within the IOP range of 10-35 mm Hg (Pallikaris *et al.*, 2006; 2005).

From his findings, Friedenwald, (1937) was able to calculate the well documented formula:

$$\text{Log (Pt/Po)} = K_o (\Delta V) \qquad \text{Eq 4.1}$$

Where Po is the initial pressure in the undisturbed eye, Pt is the final pressure after the volume change, ΔV is the volume change and Ko is a constant termed the co-efficient of rigidity. The unit of measurement for Ko is reciprocal cubic millimetres (mm³)⁻¹ (Greene, 1985). Ko is defined as the resistance offered by the ocular coats to distending forces and has since been commonly used as a measure of corneal rigidity (Friedenwald, 1937). Ko in Eq 4.1 includes the total ocular volume, which is assumed to be constant in all eyes because it is large in relation to the actual volume change, thus Ko incorporates the variation in ocular size that occurs across the population (Friedenwald, 1937).

4.3 Pressure-Volume relationship in Schiøtz tonometry

The Schiøtz tonometer has been widely used since Hjalmar August Schiøtz devised it in 1905 (Schiøtz, 1905). When measuring IOPs, the Schiøtz tonometer has long been replaced by Goldmann applanation tonometry (Jackson, 1965); however when evaluating corneal and scleral rigidity it still remains the technique of choice (Schmid *et al.*, 2003; Lam *et al.*, 2003a).

4.3.1 Theory of the Schiötz tonometer and IOP measurement

The Schiötz tonometer is an indentation tonometer. The design of the instrument features a hand-held style support, which incorporates a free-floating plunger within an outer collar. This outer collar forms a footplate, which has a concave bearing surface of 15 mm radius (Schiötz, 1905). The footplate rests on the central cornea while the central plunger indents the tissue beneath it. The total weight of the tonometer with the standard plunger (5.5g) is 16.5g, although the plunger weight can be altered by adding additional weights of 7.5g, 10g or 15g (Draeger, 1966); due to the constant tonometer weight (11g), conventionally their combined weight is signified by the weight placed upon the plunger (Friedenwald, 1957). The principle of Schiötz tonometry involves the evaluation of the plunger's depth of indentation when applied to the eye (Schiötz, 1905). The level of indentation is indicated by the scale readings on the instrument, which read from zero to 20 units (Draeger, 1966). This indentation measurement has a lever ratio of 1:20; hence the downward movement of the plunger is magnified 20 times by the Schiötz lever assembly so that each millimetre division of the scale corresponds to an indentation of 1/20 mm of the cornea (Schiötz, 1905; Chiara, 1989). The scale reading is then converted to an IOP (mm Hg) value with the aid of the Friedenwald's conversion tables (Friedenwald, 1957). By utilizing the different weights a larger range of IOP can be assessed, as lighter weights are used for low IOPs and conversely heavier ones for higher IOPs (Edwards, 1988). The Schiötz technique is based on the assumption that the eye has an average ocular rigidity of 0.0215, thus if this assumption cannot be met the IOP results obtained will be erroneous (Ytteborg, 1960c).

4.3.2 Schiötz tonometry and Friedenwald's rigidity measurement

The pressure-volume relationship described earlier can also be applied to the indentation tonometer (Friedenwald, 1937). During indentation tonometry the plunger increases the intraocular volume by buckling the cornea inwards (Schiötz, 1920; Moses, 1971). This consequently increases the pressure in the anterior chamber to cause the lens to move backwards and increase the posterior segment volume by expansion of the scleral walls (Greene, 1985). The tension in the scleral wall is raised and the IOP increases until equilibrium is reached between the tonometer weight and the IOP (Ytteborg, 1960a). However it is evident that, besides measuring IOP, there are other factors that determine the level of indentation, in particular the resistance offered by the cornea and sclera (Friedenwald, 1937). Therefore if the corneal rigidity is low the indentation level will be

deeper and consequently the IOP reading will be erroneously indicated as low (Schmidt, 1960). Similarly if the rigidity is high the walls do not have to stretch as much (thus low indentation) and therefore the IOP will be shown to be incorrectly higher (Schmidt, 1960). Due to these sources of error it was evident that the rigidity had to be accounted for in IOP determination and therefore much of the work on ocular rigidity was designed with the aim of accounting for this source of error to obtain more accurate measures of IOP.

Friedenwald, (1937) suggested that ocular rigidity could be assessed by taking Schiötz tonometry readings with two weights. By using the same equation derived from the pressure-volume experiments (Eq 4.1), Friedenwald, (1937) was able to apply this to the tonometric method:

$$P_o = \text{Log } P_t - K_o V_c \quad \text{Eq 4.2}$$

Where P_o is the IOP before tonometry, P_t is the pressure after the change in volume, V_c is the volume change or depth of indentation indicated by the Schiötz scale reading and K_o is the rigidity of the eye.

Assuming a constant K_o value, the greater the value of K_o the larger the difference between P_o and P_t for a given change in volume V_c . Friedenwald, (1937) proposed that by performing Schiötz tonometry with paired weights, K_o could be calculated for any pair of plunger weights as follows:

$$\text{Log } P_o(5.5g) = \text{Log } P_t(5.5g) - K_o V_c(5.5g) \quad \text{Eq 4.3}$$

$$\text{Log } P_o(7.5g) = \text{Log } P_t(7.5g) - K_o V_c(7.5g) \quad \text{Eq 4.4}$$

In his investigations Friedenwald, (1937) performed paired tonometry on 500 subjects and found an average K_o value of 0.0215. Later V_c was determined experimentally by assessing the amount of fluid displaced on indentation for all plunger weights and scale readings (Friedenwald, 1947). Hence from this data it was possible to construct tables for P_o (IOP) for all scale readings and weights while assuming an average K_o value (Friedenwald, 1957). Furthermore, using this information Friedenwald, (1957) devised a nomogram for indentation tonometry that could be used to calculate the ocular rigidity to enhance the accuracy of IOP measurements.

The principle behind the nomogram involves the use of the Schiøtz tonometer with two different weights, one without any additional weight, thus the 5.5g weight of the tonometer on its own (Edwards 1988); then an additional second reading is taken with either the 7.5g or 10g weights (Edwards 1988). If the ocular rigidity is within normal levels then both readings will give similar IOP readings (Friedenwald, 1937). Conversely if the ocular rigidity is higher or lower than the average K_0 value then the readings will be different. If the heavier weight gives a higher IOP reading than the initial lighter weight, the ocular rigidity is higher than that assumed; if the heavier weight gives a lower IOP reading than the initial lighter weight, the rigidity is lower than assumed and it is then deduced that there is greater elasticity in the ocular coats. Additionally, Friedenwald, (1937) appreciated that K_0 determination may vary with corneal curvature and thus devised separate nomograms for a range of corneal radii of 6-9 mm (Allen and Wertheim, 1964).

Much of Friedenwald's work was based on pressure-volume data obtained from enucleated cadaver eyes and research since on *in vivo* and enucleated human eyes has shown the assumed average ocular rigidity of $0.0215 \text{ (mm}^3\text{)}^{-1}$ to be an overestimation (Eisenlohr *et al.*, 1962). In indentation tonometry the increased IOP as a result of change in intraocular volume will result in the expulsion of a volume (i.e. bolus) of blood (Ytteborg, 1960c). Therefore if ocular blood volume is of significance it is likely that a difference will be observed between enucleated and *in vivo* eyes since in enucleated eyes the blood will not be able to leave the eye and hence the pressure change will be greater thus resulting in higher levels of rigidity (Ebner *et al.*, 2009). Blood volume may also produce a source of error *in vivo*, as the outflow mechanism may differ between individuals and hence lead to large variations in rigidity (Ytteborg, 1960c). Friedenwald, (1937) based his K_0 determination on data from Clark, (1932) and Ridley, (1930); both studies found no significant difference between *in vivo* and enucleated eyes although variation in their methodology has since been criticised (Saeteren, 1960). Additionally subsequent work by Eisenlohr *et al.*, (1962) and other investigators (Hetland-Eriksen, 1966; Goodside, 1959) has shown that the pressure volume relationship varies with IOP, such that ocular rigidity decreases with higher IOPs, which was not noted by Friedenwald. The revision of the conversion tables by Friedenwald, (1957) and the failure to account for the differences in biomechanics between *in vivo* and *in vitro* eyes highlight the limitations created by the transformation of scale readings to K_0 values based on empirical data. Hence these inconclusive results from previous studies cast some doubt on the validity of applying Friedenwald's work to living eyes.

4.4 Goldmann applanation tonometer (GAT)

Goldmann and Schmidt invented the GAT to overcome the problems of Ko encountered in Schiotz tonometry when determining IOP (Schmidt, 1957). GAT is based on the principle of measuring the force required to applanate the cornea to a diameter 3.06 mm to assess the IOP; this diameter overcomes the effect of surface tension caused by the tear film and the difference between the internal and external surface area applanated (Schmidt, 1957). In addition when corneal applanation is 3.06 mm, an applied force of 1g corresponds to an IOP of 10 mm Hg, allowing ease of conversion (Edwards, 1988). The instrument is based on the Imbert-Fick law which states that the diameter flattened is proportional to the force applied assuming that the eye is a spherical vessel with a membrane which is infinitely thin, dry and flexible (Draeger, 1966); assumptions that are not met by the human eye. Therefore pressure (P) is equal to the force (W) necessary to flatten an area divided by the area of flattening (A) (Schmidt, 1959). Thus:

$$P = W \text{ (g)} / A \text{ (mm}^2\text{)} \quad \text{Eq 4.5}$$

The tonometer probe has a flattened tip incorporating a doubling prism, which splits a full circle into semi-circles when viewed through the oculars of a slit lamp after instillation of fluorescein. The tonometer houses a spring-loaded lever to which an applanating head is linked. In order to use this tonometer it has to be attached to a slit lamp for viewing of the applanated area and for manoeuvring the tonometer head onto the cornea. When the tonometer head makes contact with the cornea the pressure via the spring-loaded lever is adjusted until the applanation area is 3.06 mm (Schmidt, 1959). It is this pressure that is taken as the IOP reading.

The original work by Goldmann and Schmidt, (1957) indicates that the GAT measurements are only accurate for central corneal thickness (CCT) of approximately 500 μm . Therefore if the cornea is thicker than this assumed value, then greater force is required to deform it, thus creating an artificially higher IOP reading and conversely if the cornea is thin, an erroneously lower IOP is obtained (Whitacre and Stein, 1993). This is a major drawback of the GAT, since studies have shown CCT to vary significantly between populations and ethnicities (Aghaian *et al.*, 2004) and to be influenced by gender (Hanna *et al.*, 2004), refractive error (Nomura *et al.*, 2004) and surgical procedures (Kirwan and O'Keefe, 2008).

GAT has also been coupled with the Schiøtz tonometer to assess K_o ; a method known as the Schmidt technique (Saeteren, 1960, Schmidt, 1960). As the volume displaced with applanation tonometry is approximately 0.56 mm^3 , it is minimally affected by K_o (Schmidt, 1960). Therefore the IOP results derived via GAT are assumed to be P_o (i.e. IOP in the undisturbed eye) in Friedenwald's equation (Eq 4.2) (Ytteborg, 1960a), whilst the values of P_t and V_c are obtained via Schiøtz tonometry.

4.5 Rebound tonometry

Presently the GAT is considered the 'gold standard' technique for assessing IOP (ElMallah and Asrani, 2008). Despite its continued popularity there is a significant body of evidence to indicate that ocular variables such as corneal thickness, curvature, rigidity and axial length may cause large inaccuracies in IOP measurements with this instrument (Goldmann and Schmidt, 1957; Whitacre and Stein, 1993; Whitacre *et al.*, 1993; Herndon *et al.*, 1997, 2006; Shah, 2000; Liu and Roberts, 2005). Moreover the technique entails ocular contact, which subsequently necessitates appropriate disinfection of probes and the use of topical anaesthetics. GAT also requires a slit lamp setup and although commonly used in ophthalmology practice, it has limited use in uncooperative and bedridden individuals. A prerequisite of the technique is that the examiner must have sufficient experience of GAT to determine IOP accurately, which is often difficult in busy clinical settings. Due to the various limitations of GAT, there is an impetus to develop an accurate non-invasive technique of measuring IOP that addresses the above shortfalls.

Rebound or dynamic tonometry (RBT) is a method of measuring IOP *in vivo* that assesses the ballastic properties of a probe when it rebounds from the eye (Dekking and Coster, 1967; Kontiola, 2000). The procedure is similar in concept to vibration tonometry (Krakau, 1971) and was first described by Obink (1931) and then further developed by Dekking and Coster, (1967). The principle of the technique is based upon the projection of a light-weight probe of known mass and velocity which impacts with the ocular surface where it momentarily makes contact and then recoils back to the instrument housing (see Appendix 5) (Kontiola, 1997). The tonometer software subsequently assesses the time-velocity relationship of this event and evaluates various physical characteristics of the probe's motion from the event. In particular it assesses the probe velocity pre- and post-impact, impact duration and deceleration from which biomechanical information such as IOP is

derived (Kontiola, 2000). The motion parameter changes of the probe during the event can be divided into three distinct phases, which are depicted in Figure 4.1 and discussed below.

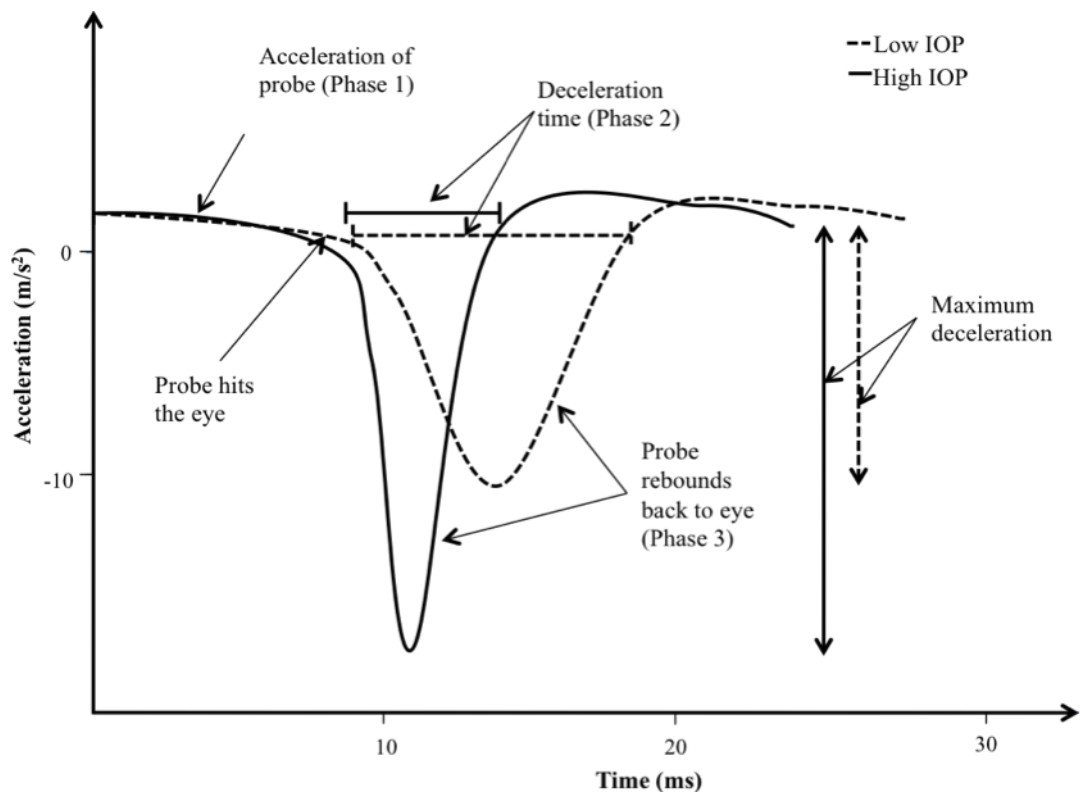


Figure 4.1 Illustration of the motion parameters of the probe assessed in RBT (adapted from Kontiola, 1997).

Phase 1: is the initial phase where the probe has built up momentum and then travels at a constant speed towards the ocular surface; the length of this phase is dependent on the initial eye-probe distance.

Phase 2: The probe impacts with the ocular surface and begins to decelerate; also known as the impact/contact/deceleration time. The properties of the ocular surface material dictate the length of time the probe is in contact with the eye (Dekking and Coster, 1967). If the eye is relatively rigid then the impact time will be short and there will be a steep deceleration curve (bold curve). Conversely if the surface is soft then the impact time will be longer and the deceleration curve will be much more gradual (dotted curve).

Phase 3: is the rebound phase, where the probe changes its direction of travel following impact with the eye and moves back towards the instrument. Maximum deceleration is calculated as the difference in acceleration between the point of contact with the eye to the moment when the probe recoils from the eye.

The RBT was initially developed as a method of assessing IOP in animal models of glaucoma, in particular to address the difficulties in determining accurate IOP in the smaller mice eyes (Danas *et al.*, 2003; Goldblum *et al.*, 2002; Kontiola *et al.*, 2001; Yu *et al.*, 2009). Clinical studies with prototypes of the RBT have demonstrated the technique to produce high levels of correlation with IOP determined manometrically (Goldblum *et al.*, 2002; Kontiola, 2000), via GAT (Kontiola, 1996; 2000) and other portable tonometers (Kontiola and Puska, 2004). Moreover a significant advantage of the procedure is that it does not require topical anaesthesia, as the speed of the probe is relatively low yet faster than the corneal reflex, thus causing minimum discomfort for patients (Kontiola, 2000; Wang *et al.*, 2005).

Therefore as the prototype RBT instrument was found to provide highly accurate determination of IOP and was well tolerated by patients (Kontiola, 1997; Kontiola and Puska, 2004), it was commercially released as the *iCare* rebound tonometer (Tiolat-Oy, Helsinki, Finland) in 2003 for clinical use in humans. The RBT has also been released for animal use as the *TonoVet* and *TonoLab* (Tiolat-Oy, Helsinki, Finland).

4.5.1 Technical aspects of rebound tonometry

The commercially available *iCare* tonometer (RBT; *iCare*, TA01, Tiolat-Oy, Helsinki, Finland) is an induction-based impact device founded upon the principles of rebound tonometry discussed afore. The design and software of the instrument is largely based on various preliminary studies performed on animals and humans using a prototype version of the instrument (Kontiola, 1997, 2000, 2001; Kontiola and Puska, 2004; Danas *et al.*, 2003; Goldblum *et al.*, 2002). During these early studies an evaluation of the various motion parameters of the probe during rebound revealed that the inverse of the deceleration time showed the highest correlation with IOP determined manometrically and via GAT (Kontiola, 1997; 2000; Kontiola *et al.*, 2001; Danas *et al.*, 2003). These studies also indicated that in comparison to deceleration time, maximum deceleration was more vulnerable to the effects of probe-eye distance and instrument tilt (Kontiola, 1997). Maximum deceleration is calculated as the difference between the acceleration before and after impact, hence the larger the probe-eye distance the greater the loss in speed and consequently the smaller the end difference in deceleration. Therefore to overcome this variability Kontiola, (1997) recommended that utilising both maximum deceleration and deceleration time provided an improved measure of IOP, which has subsequently been

implemented in the *iCare* tonometer. Therefore in reference to Figure 4.1 the *iCare* tonometer assesses the combination of phases 2 and 3 to evaluate the IOP.

4.5.2 The *iCare* tonometer instrument

The *iCare* tonometer is a compact handheld battery operated device measuring 23 x 8 x 3 cm (van der Jagt and Jansonius, 2005) and weighing 250g (Detry-Morel *et al.*, 2006). The instrument uses a disposable lightweight probe (11mg) that is composed of a PMMA spherical head of 1.7 mm diameter, which is attached to a 24 mm long 1 mm diameter stainless steel tube. The tube of the probe contains a magnet 20 mm long made from ten 2 mm long magnets at one end and the plastic probe at the other end (Kontiola, 2000). The instrument houses a solenoid 20 mm long with a 2.5 mm opening with *teflon* bearings within it for the probe to move on. A ferrite rod 7 mm long and 3.5 mm diameter is situated behind the solenoid (Kontiola, 2000). The probe movement is initiated by a current pulse (30 milliseconds) to the solenoid coil which creates a magnetic field that repels the permanent magnets in the probe thus making it move. The intensity of this current pulse governs the speed at which the probe is propelled towards the eye. The movement of the probe and its magnets generates a subsequent voltage at the two ends of the solenoid that is proportional to the speed of the probe (Goldblum *et al.*, 2002; Kontiola *et al.*, 2001). The solenoid performs a dual purpose by conducting the initial current pulse but also assesses the signal changes in voltage as a result of the magnetic field. As the probe progresses and collides with the eye the voltage changes direction due to the altered speed/magnetic field (Kontiola *et al.*, 2001). The voltage is amplified and processed by a microprocessor. The analog voltage is converted to digital signals by an analog-to-digital converter, which allows analysis of the results as time vs. voltage graphs (Kontiola, 1996). These graphs provide an inferred measure of probe velocity, impact time and change in direction, which are used to determine the IOP (Figure 4.2).

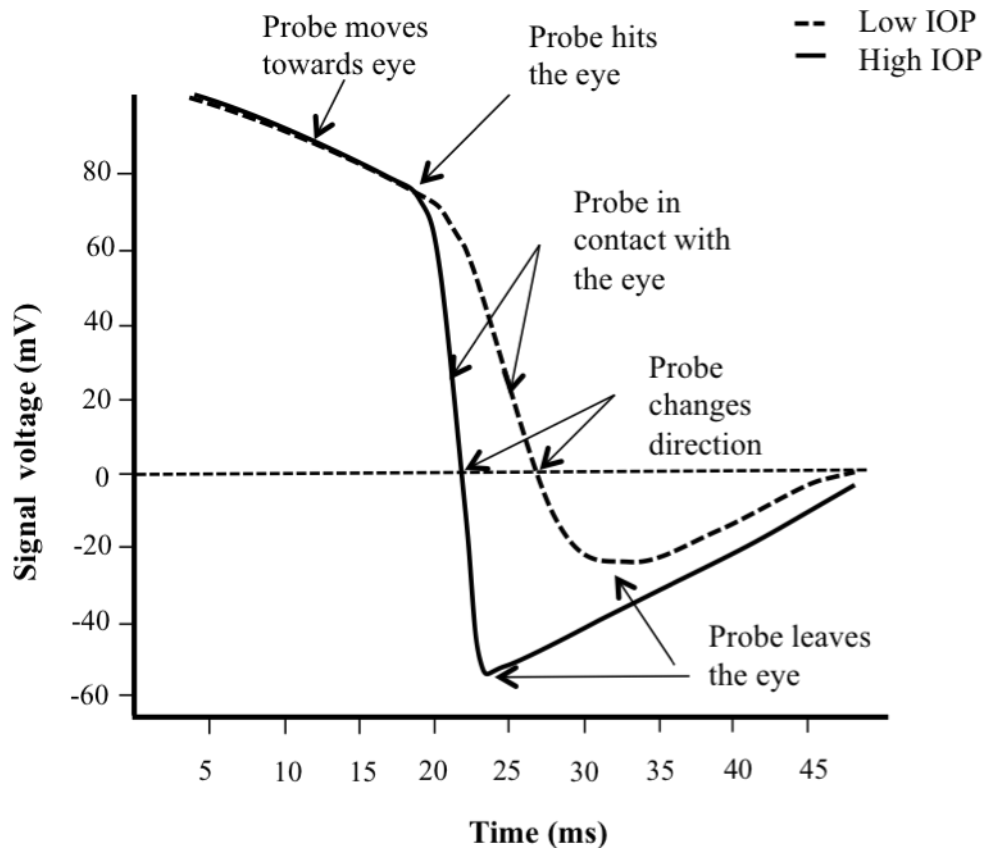


Figure 4.2 Illustration of the change in the signal voltage (mV) from the solenoid with changes in probe speed and direction (adapted from Kontiola, 2000).

A key advantage of the *iCare* tonometer is the avoidance of topical anaesthesia usually required in most contact tonometry. Topical anaesthetics are potentially a significant constraint in contact tonometry, as various studies have reported these to cause a reduction in IOP (Baudouin and Gastaud, 1994; Almubrad and Ogbuehi, 2007). In regards to the rebound mechanism, in order to obtain reliable IOP measurements while minimising both ocular discomfort and the effects of ocular rigidity, consideration of the size and speed of the probe is imperative. As discussed by Dekking and Coster (1967) in their original work on RBT the effect of ocular rigidity can be reduced by minimising the displacement of fluid on contact by decreasing both the weight and speed of the probe. However, if the speed of the probe were too low this would evoke a blink reflex even before the probe touches the eye. Additionally, altering the weight of the probe would affect the motion parameters since a light probe would result in a quicker deceleration and shorter impact duration, leading to an overestimation of IOP. Reducing the weight of the probe could also make its rebound behaviour less predictable as it may be more susceptible to influences from unrelated magnetic fields (Dantias *et al.*, 2003).

Therefore to address these issues the *iCare* tonometer has implemented a lightweight probe (11 mg) (Martinez-de-la-Casa *et al.*, 2005) and low velocity (0.25-0.35 m/s) (Iliev *et al.*, 2006), which however is still faster than the corneal reflex (Kontiola, 2000). Additionally the use of a rounded probe reduces the risk of ocular surface damage and the small probe size (i.e. 1.7 mm diameter) (Briesen *et al.*, 2009) is advantageous as it is minimally affected by corneal irregularities (Cervino, 2006). This is particularly useful when conventional applanation and non-contact tonometers (NCTs) cannot be used on eyes following refractive surgery or on corneas with scarring or pathology (González-Méijome *et al.*, 2006; Moreno-Montañés *et al.*, 2007). Furthermore the probes are disposable thus removing the need for disinfection (Walia and Chronister, 2001).

4.6 Ocular Response Analyser (ORA)

The ORA (Reichert Inc, Buffalo, NY) is a non-contact device that utilizes the principles of non-contact tonometry to derive additional information on the biomechanical characteristics of the cornea (Luce, 2005b). The technique involves the application of a pulse of air of known force to the ocular surface resulting in the deformation of the central cornea. Unlike conventional NCTs, the ORA not only exploits the force-displacement event to derive IOP information but also uses it to provide an additional assessment of the material properties of the cornea (Luce, 2005a; 2005b).

On application of the pulse of air the corneal response is partitioned into various distinct phases, which are monitored by an electro-optical collimation detector system - Figure 4.3 (Luce, 2005b). The cornea initially moves inwards from its normal convex shape to a flat surface (i.e. the first applanation), from where it continues to travel to assume a slightly concave shape. Following the first inwards applanation the air pump generating the air pulse shuts down and the pressure applied to the eye decreases linearly with time and at the same rate as it increased (Luce, 2005a). As the pressure reduces, the eye passes through a second flat surface point (i.e. the second applanation) before it returns back to its normal convex shape.

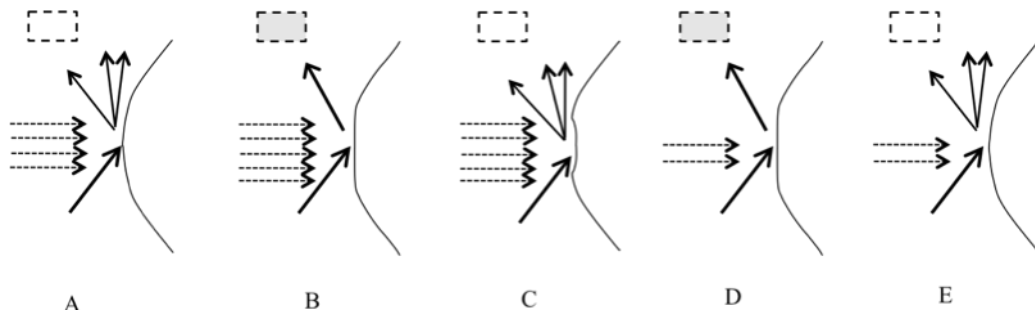


Figure 4.3 Diagrammatic representation of the distinct phases the cornea travels through on application of the air pulse and the consequent changes in the intensity of light detected by the ORA (adapted from Montard *et al.*, 2007).

The optical system detects the increased reflectance of light at each applanation point and displays these via a filtered graphical signal with two well-defined peaks (Figure 4.4). These two measurements are taken within 20 milliseconds thus minimizing the potential effects of eye movement and the ocular pulse (Luce, 2005b). The corresponding time to reach each peak is matched to the pressure of an internal air supply plenum at each particular time. On the graphical output these two pressures (P1 and P2) are determined respectively as the mid point of the intersection between the applanation curve and the plenum pressure curve.

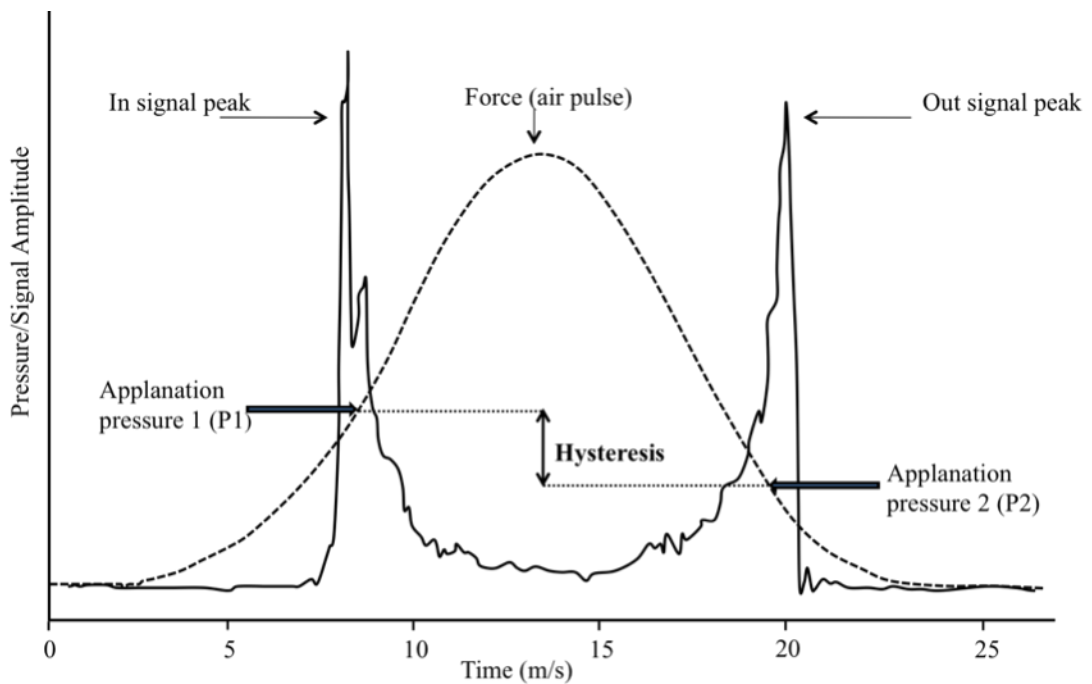


Figure 4.4 Diagrammatic representation of an ORA waveform (adapted from Luce, 2005b).

Due to its viscoelastic nature the corneal tissue not only resists the deformation from the pulse of air but also absorbs and dissipates the energy. Therefore this subsequently causes the plenum pressure to differ between the two appplanation points, with the first pressure being greater than the second (Luce and Taylor, 2006). It is this difference that is termed corneal hysteresis (CH) and allows the differentiation to be made between IOP and the response of the corneal tissue to deformation (Shah *et al.*, 2006). It is conjectured that CH is a composite characteristic of the cornea that encompasses the effects of its thickness, hydration and rigidity (Luce, 2005b). In engineering terms hysteresis is a measure of the energy absorption that takes place during the loading-unloading stress-strain cycle of viscoelastic materials (Kotecha *et al.*, 2006). Viscoelasticity is a combination of two mechanical characteristics: 1) an elastic capacity and 2) energy damping behaviour. The greater the difference between the material's loading and unloading response, the greater the extensibility or hysteresis of the tissue (Dupps, 2007; Curtin, 1969). Therefore in regards to the ORA, the longer the cornea takes to return from concavity to the second appplanation state, the greater the difference in air pressure and hence the larger the hysteresis value (Broman *et al.*, 2007). Lower hysteresis indicates a more deformable cornea in comparison to high hysteresis.

The ORA also provides an additional measure of the tissue biomechanics, termed the corneal resistance factor (CRF), which is thought to measure the overall resistance of the cornea (Luce and Taylor, 2006). The CRF is calculated using Eq 4.6 where P1 and P2 are the two appplanation pressures seen on the ORA waveform (see Figure 4.4).

$$\text{CRF} = (P1 - (0.7 \times P2)) \quad \text{Eq 4.6}$$

Eq 4.6 is based on prior empirical data and a proprietary algorithm formulated by Reichert Inc (Lam *et al.*, 2007; Ortiz *et al.*, 2007). It has been hypothesised that the CH may reflect mainly the viscosity of the cornea whilst CRF (a linear function of P1 and P2) may indicate its elastic characteristics (Luce and Taylor, 2006; Pepose *et al.*, 2007).

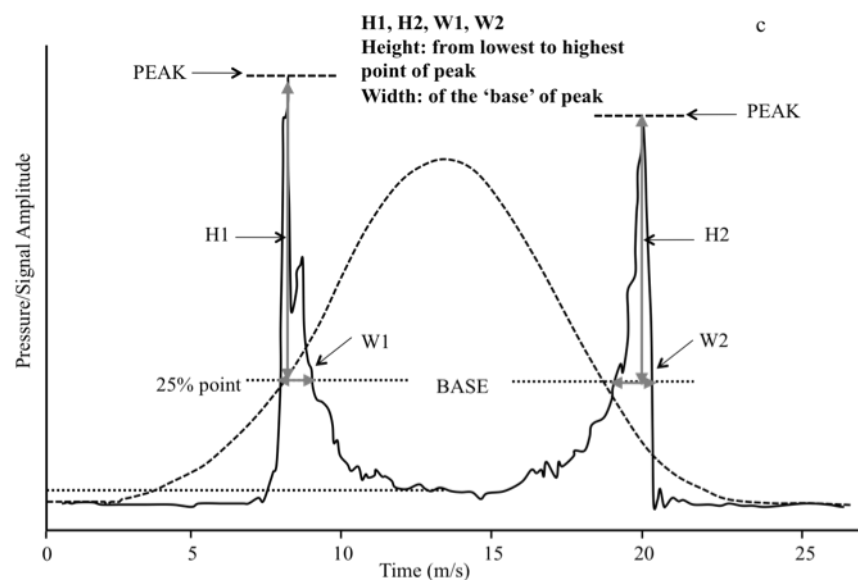
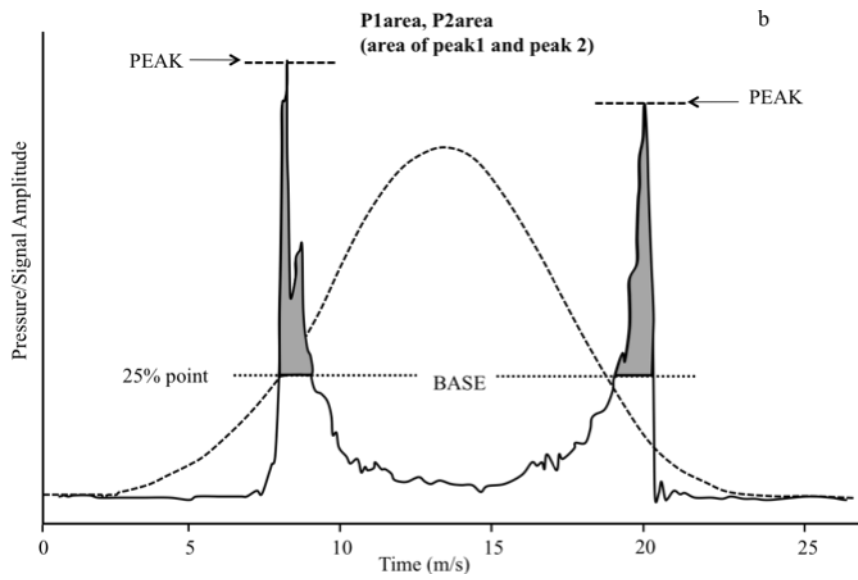
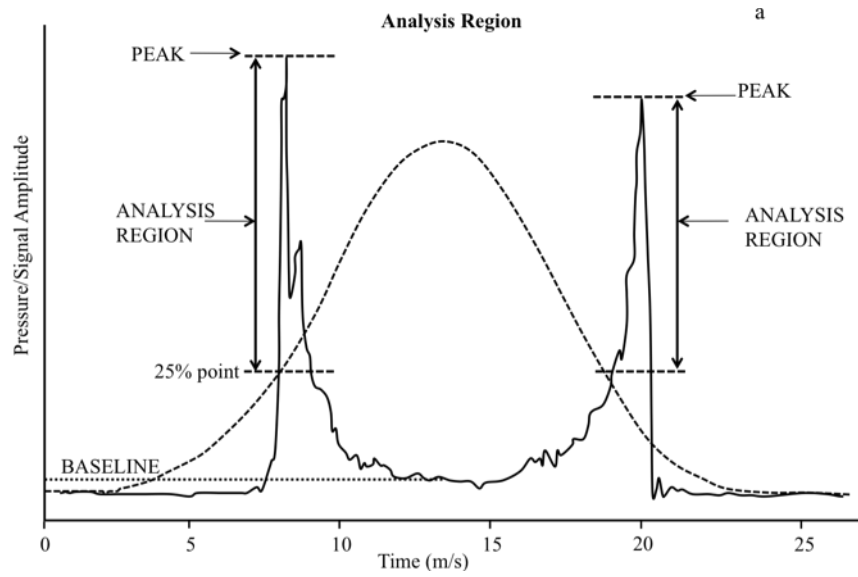
In addition to the corneal biomechanical metrics, the ORA also provides two measures of IOP (i.e. IOPg and IOPcc). IOPg provides a Goldmann-correlated IOP, which is a mean of the two IOP appplanation pressures P1 and P2 (Ortiz *et al.*, 2007). IOPcc is known as the corneal compensated IOP, which is less affected by corneal properties than other methods of tonometry (Medeiros and Weinreb, 2006). IOPcc is calculated as:

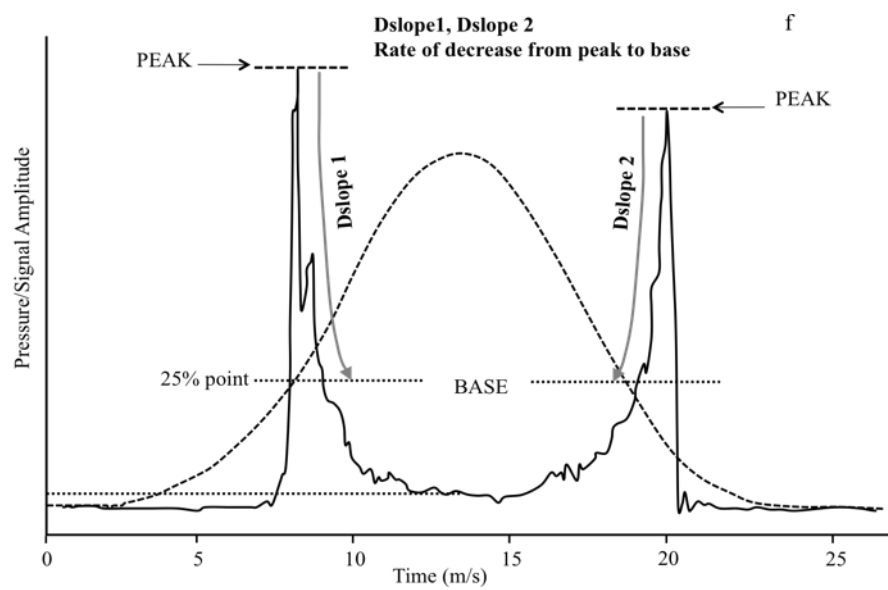
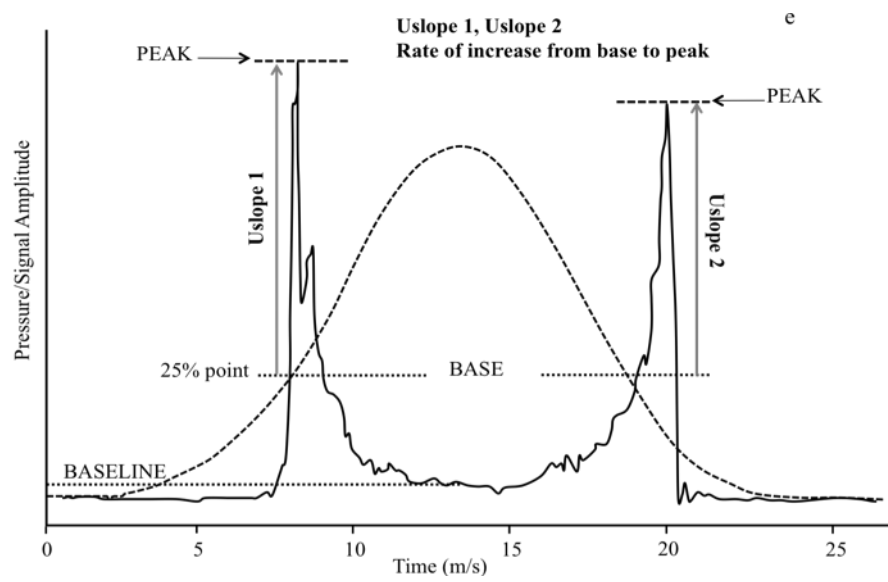
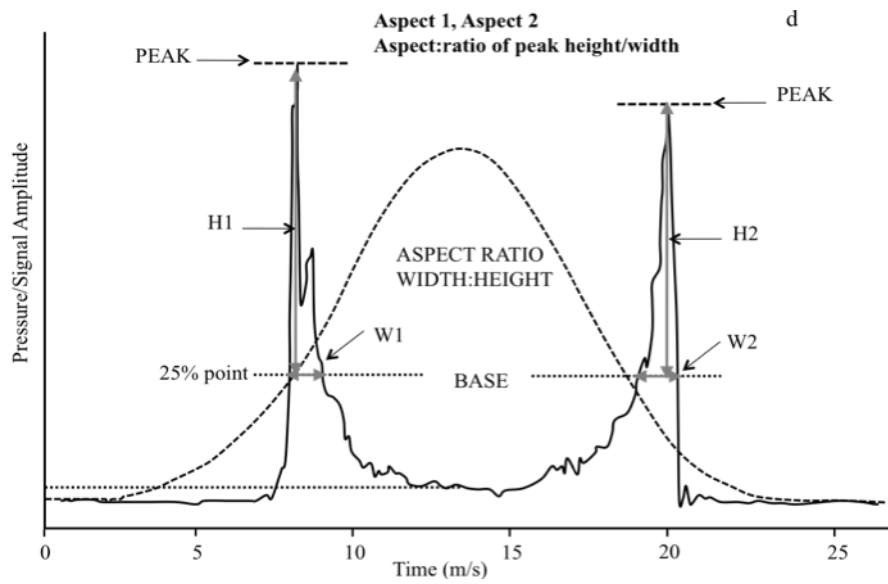
$P1-kP2$

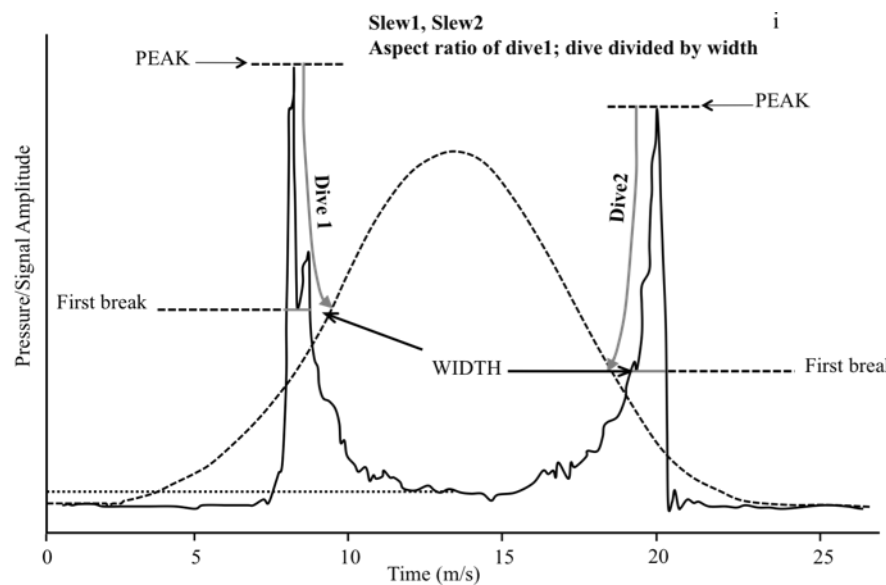
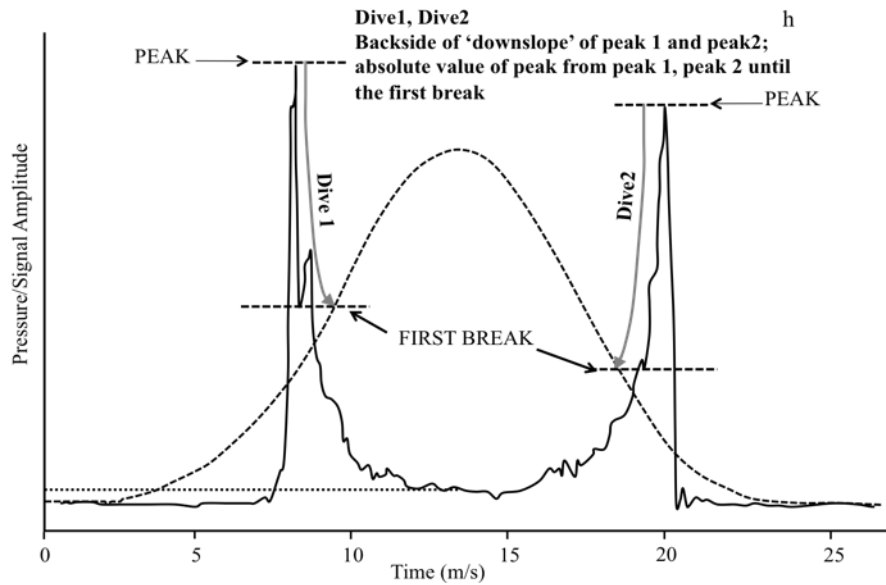
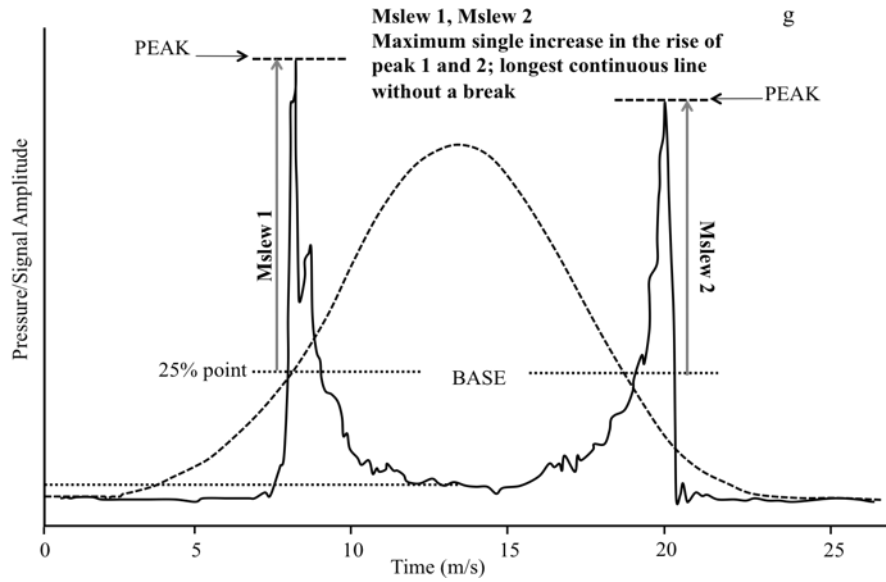
Eq 4.7

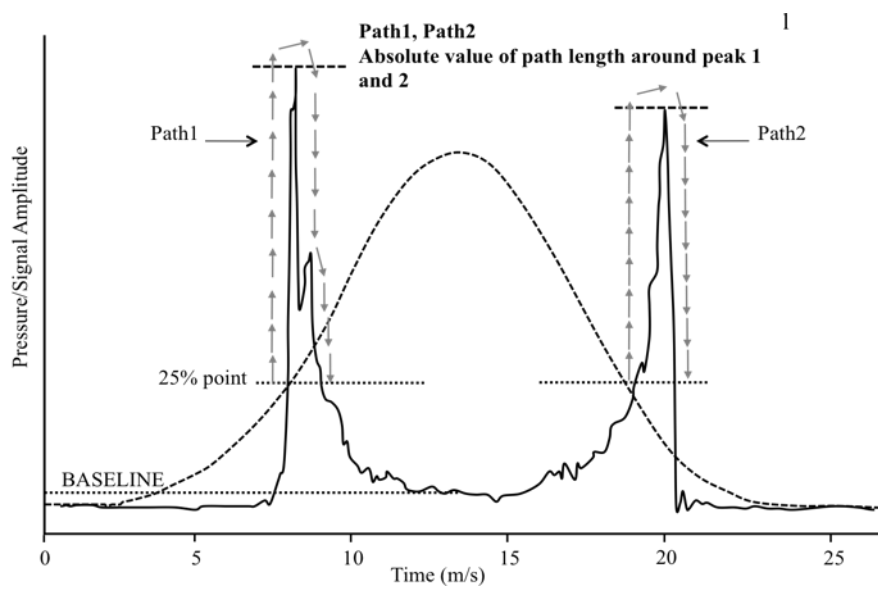
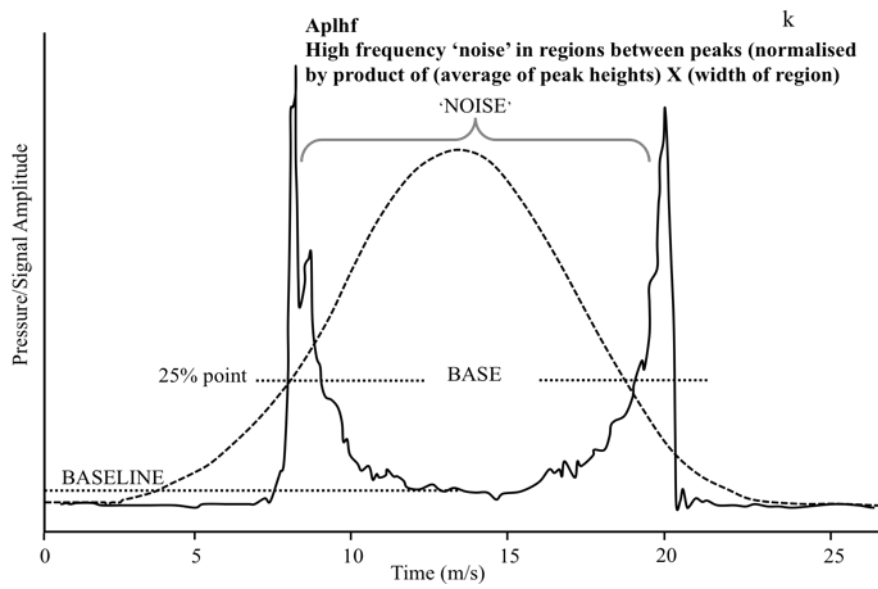
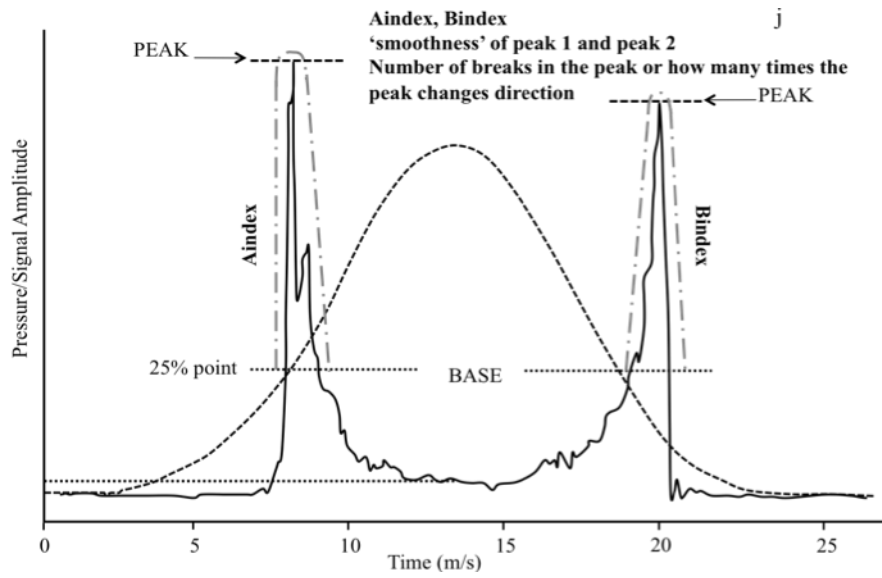
where k is a constant value of 0.43, which was empirically calculated by Reichert Inc in an experimental study that assessed IOP before and after LASIK surgery (Luce IOVS 2006, 47: ARVO E- abstract 2266). $P1$ and $P2$ are the applanation pressures mentioned afore.

It has been suggested that the waveform signal produced by the ORA is a ‘unique morphological signature’ that may provide additional biomechanical information supplementary to the CH and CRF values (Luce and Taylor, 2006). Recently in 2009 Reichert launched a new version of the ORA software (i.e. version 2.04) that analyses a variety of additional features of the signal waveform such as peak amplitude, area of peak and length of peak (see table 4.1 and Figure 4.5 (a-m) for more details). It is envisaged by the manufacturers that this additional analysis will allow further investigations into numerous aspects of the corneal response to deformation in various ocular conditions such as, for example, keratoconus, Fuch’s dystrophy and post-refractive surgery complications.









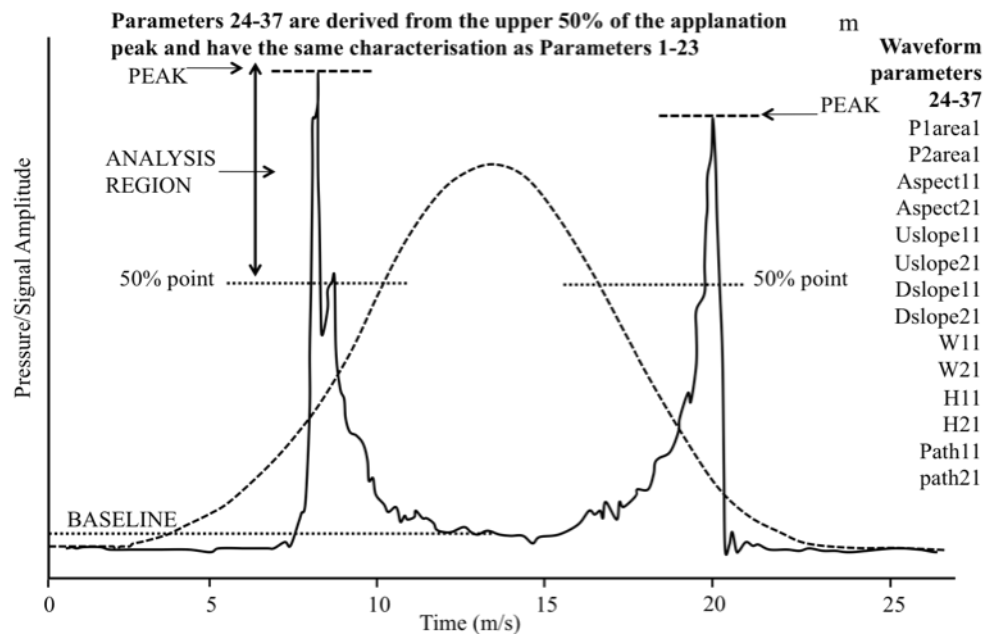


Figure 4.5 (a-m) Diagrammatic illustrations of the additional waveform parameters (AWPs) obtained from the ORA for the upper 75% and 50% of the appplanation peaks. (adapted from ORA website and ORA manual).

Parameter name		Description	Parameter name		Description
From 75% of applanation peak*	From 50% of applanation peak**		From 75% of applanation peak*	From 50% of applanation peak**	
1. Aindex		“smoothness” or degree of “non-monotonicity” or number of breaks when peak changes direction in peak 1	13. H1	34. H11	height (from lowest to highest value) of peak 1
2. Bindex		“smoothness” or degree of “non-monotonicity” or number of breaks when peak changes direction in peak 2	14. H2	35. H21	height (from lowest to highest value) of peak 2
3. P1area	24. P1area1	area under the curve of peak 1 (sum of values)	15. Dive1		absolute value of monotonic decrease on downslope part of peak 1 starting at the peak value
4. P2area	25. P2area2	area under the curve of peak 2 (sum of values)	16. Dive2***		absolute value of monotonic decrease on downslope part of peak 2 starting at the peak value
5. Aspect1	26. Aspect11	aspect ratio (height/width) of peak 1	17. Path1	36. Path11	absolute value of path length around peak 1
6. Aspect2	27. Aspect21	aspect ratio (height/width) of peak 2	18. Path2	37. Path21	absolute value of path length around peak 2
7. Uslope1	28. Uslope11	rate of increase from base to peak value of peak 1	19. Mslew1		maximum single step increase in rise of peak 1 (longest continuous line without a break)
8. Uslope2***	29.Uslope21** *	rate of increase from base to peak value of peak 2 (downslope in real time of peak 2) ***	20. Mslew2***		maximum single step increase in rise of peak 2
9. Dslope1	30. Dslope11	rate of decrease from peak to base value of peak 1	21. Slew1		aspect ratio of dive1 (value of dive divided by width of dive region)
10. Dslope2***	31.Dslope21** *	rate of decrease from peak to base value of peak 2 (upslope in real time of peak 2) ***	22. Slew2***		aspect ratio of dive2 (value of dive divided by width of dive region)
11. W1	32. W11	width of peak 1 at “base” of peak 1 region	23. Alphf		high frequency “noise” in region between peaks (normalized by product of average of peak heights times width of region)
12. W2	33. W21	width of peak 2 at “base” of peak 2 region			

Table 4.1 ORA additional waveform parameters (AWPs) (adapted from ORA website, Hongyok *et al.*, (2010) and ORA manual). *Data are analyzed from upper 75% of the applanation peak. **Data are analyzed from upper 50% of the applanation peak. *** The data from the second applanation were analyzed in time-reversed fashion.

5.0 AIMS AND OBJECTIVES OF THE THESIS

There is now a significant body of literature that implicates scleral biomechanics in the aetiology of myopia, glaucoma and AMD. Whereas animal models have substantially extended our understanding of the role of the sclera in experimental myopia, there is a dearth of literature concerning its properties *in vivo* in human myopia. Historically, corneal rigidity has invariably been used as a surrogate measure of scleral rigidity, despite the significant differences between the corneal and scleral structures. The paucity of literature on human scleral biomechanics, in part, reflects the lack of suitable and accessible *in vivo* techniques to determine ocular tissue biomechanics. Therefore the principal objective of the thesis was to address this deficit in the literature and to investigate the biomechanical properties of the anterior sclera and cornea *in vivo*, in the context of their possible association with myopia.

The thesis aims to assess existing and new *in vivo* methods of inferring the properties of scleral material. The Schiøtz tonometer has been widely utilised to determine corneal rigidity but it has also been applied to assess scleral biomechanics (Schmid *et al.*, 2003). The thesis evaluates the utility of the Schiøtz tonometer to measure corneal and scleral rigidity and assesses its ability to provide an inferred measure of scleral resistance. Furthermore the relatively recent introduction of the ballistic rebound tonometer (RBT) provides a unique method of determining IOP by evaluating the motion parameters of a probe on rebound from the eye. The thesis assesses and validates the novel application of the RBT to the sclera to obtain a surrogate measure of scleral biomechanics.

The literature is equivocal regarding the role of the cornea in myopia. Therefore using Schiøtz tonometry and the Reichert Ocular Response Analyser the thesis aims to examine corneal biomechanics in relation to refractive status. It may be presumed that the biomechanical properties of the sclera and cornea are likely to be influenced by their structural and biometric characteristics. With the implementation of *in vivo* imaging techniques such as anterior segment optical coherent tomography (AS-OCT) and 3-Dimensional magnetic resonance imaging the thesis examines structural correlates of scleral biomechanics such as scleral thickness and anterior segment area and bulbosity. Similarly implementation of 3-Dimensional Scheimpflug imaging via the *Pentacam* provides an in depth evaluation of the anterior segment biometry which is assessed in context of corneal biomechanics.

Aside from the sclera and cornea, other anterior segment structures such as the ciliary muscle have also been implicated in the aetiology of myopia. Using AS-OCT the thesis aims to examine the morphological characteristics of the ciliary muscle in relation to scleral biomechanics and ocular conformation.

Racial differences in prevalence levels of myopia have been widely reported in literature. The thesis examines three racial groups, British White, British South Asian and Hong Kong Chinese to ascertain variation between them in regards to scleral and corneal biomechanics. Furthermore the influences of age and gender on ocular biomechanics are also explored.

6.0 THE INVESTIGATION OF CORNEAL AND SCLERAL BIOMECHANICS USING SCHIOTZ INDENTATION TONOMETRY – INITIAL CONSIDERATIONS

6.1 Introduction

Recently *in vivo* studies have examined ocular rigidity via conventional manometric pressure-volume methods (Pallikaris *et al.*, 2006; Dastiridou *et al.*, 2009), Schiotz tonometry (Schmid *et al.*, 2003), assessment of pulse amplitude and fundus pulsation (Hommer *et al.*, 2008) and by measuring axial length changes following pharmacologically-induced changes in IOP (Ebeneter *et al.*, 2009). Whereas such studies have increased our knowledge of corneal (Ko) and scleral (Ks) rigidity, they suffer from their inability to assess separately the differences in response to stress of the cornea and the sclera, assessing instead the composite eye response. As the structural characteristics of the sclera and the cornea differ significantly, so will their respective biomechanical parameters. Therefore it is imperative that, when assessing biomechanics, the two structures are investigated separately and independently. Furthermore, retrobulbar anaesthesia and the nature of the invasive procedures employed in previous reports are likely to alter biomechanical characteristics of the cornea and sclera possibly confounding the measures of ocular rigidity (Pallikaris *et al.*, 2006; Dastiridou *et al.*, 2009). As a non-invasive method, Schiotz tonometry is still the conventional approach to assessing Ko and Ks although assessment of the latter parameter is limited as the transformation algorithms taken from Friedenwald's tables (Friedenwald, 1937; 1957) are solely based on empirical data taken from the cornea.

In contrast to measures of Ko, there is a paucity of literature on the use of the Schiotz tonometer to determine Ks (Schmid *et al.*, 2003). Scleral measurements have been used for estimating IOP, but owing to its relative accessibility the Schiotz tonometer has only been applied to the superior lateral region (Allen and Wertheim, 1963a; 1964; Schulman, 1963; Schiotz, 1905). In these cases the 5.5 g weight was used as it was less dependent on assumed scleral/corneal rigidity (Allen and Wertheim, 1963b). The scale readings were converted to IOPs using a nomogram that took into account corneal radius within a range of 6-9 mm (Allen and Wertheim, 1963b) although these additional corneal radii nomograms would not encompass the flatter radius of the sclera (i.e. ~12 mm) (Kobayashi *et al.*, 1971).

A significant body of literature indicates an important role of the biomechanical properties of the sclera in the aetiology of myopia (Rada *et al.*, 2006; Siegwart and Norton, 1999), glaucoma (Eilaghi *et al.*, 2010a; Sigal *et al.*, 2005b) and AMD (Friedman, 2004, Pallikaris *et al.*, 2006). These findings have signified the need for an effective non-invasive method of assessing scleral biomechanical properties *in vivo*. With the advent of instruments such as the ORA it is now possible to assess the corneal biomechanics *in vivo* and without contact; however the facility to assess scleral biomechanics is still generally limited to *in vivo* Schiötz tonometry (Schmid *et al.*, 2003) or manometric methods (Dastiridou *et al.*, 2009).

6.2 Study Objective

The objective of the present study was to investigate whether regional variations in tissue resistance exist between different scleral quadrants in humans by assessing *in vivo* both Schiötz tonometry indentation readings and Friedenwald transformed rigidity values for Ks (Patel *et al.*, IOVS 2009, 50: ARVO E-Abstract 3947). Ko was also estimated for comparison purposes. Variation in Ks and Ko is compared between myopic and non-myopic subjects. The reliability of the data is examined with reference to the intra- and inter-observer variation in Schiötz scale readings and the concordance between IOP data obtained by Schiötz tonometry and GAT.

6.3 Methods

The present study employed 26 healthy individuals (52 eyes; 10 males and 16 females) aged between 18-40 years (mean 29.48 ± 5.9). For all investigations in the thesis, ethical approval was obtained from Aston University Ethics Committee and the studies were performed according to the tenets of the Declaration of Helsinki. Informed consent was obtained from each subject prior to commencement of the studies. Subjects were required to complete a short questionnaire that detailed exclusion/inclusion criteria. Ocular tissue biomechanics and IOP have previously been shown to be affected by various eye diseases and conditions, thus the exclusion criteria included previous history of ocular surgery, trauma or pathology, ocular medication and astigmatism >1.75 D. Additionally, individuals suffering from connective tissue related disorders were also excluded due to their putative affect on collagen composition and hence scleral biomechanics (Kaiser-

Kupfer *et al.*, 1985). All investigations in the thesis adhered to these exclusion/inclusion criteria.

6.3.1 Schiottz tonometry

Corneal anaesthesia was induced with one drop of 0.5% proxymetacaine HCl (*Minims*®, Bausch & Lomb, Kingston-Upon-Thames, UK) instilled into both eyes. An inclined scale Schiottz tonometer was used which was calibrated by the manufacturer (Biro Ophthalmic Instruments, Germany) at the beginning of the study. The Schiottz tonometer was sterilized by submersion in 2% sodium hypochlorite solution in compliance with recommended procedures for re-usable ocular devices (College of Optometrists, 2009). Calibration was checked before each measurement session using the manufacturer's calibration block. The order of measurements taken by the two observers (i.e. author HP and assistant LD (details below)) was randomised. Schiottz tonometry was performed according to the technique described by Allen and Wertheim, (1963c) with the subject in the supine position (Schiottz, 1905). Fixation targets were appropriately positioned to aid fixation of 4 selected cardinal positions (i.e. dextrolevation, dextrodepression, levoelevation and levodepression) and to maximise surface exposure of the sclera. Using the Schiottz footplate (diameter 10 mm) as a reference gauge, measurements were taken from each quadrant at approximately 8 mm from the corneolimbic junction (Figure 6.1) to avoid close proximity of the muscle insertion points (Thale and Tillman, 1993; Greene, 1980).

Two plunger weights (5.5 g and 7.5 g) were employed for the cornea (in primary gaze) and for four quadrants: superior temporal (ST), superior nasal (SN), inferior temporal (IT), inferior nasal (IN). The choice of plunger weights was based on the assumption that the subjects being assessed would have IOP within the normal range for healthy individuals. The scale reading recorded was that estimated to be central to the range of pointer oscillation at measurement end point (Chiara *et al.*, 1989). The order of quadrants and eye measured were randomised for each subject. The 5.5 g weight always preceded the 7.5 g in order to minimise any massaging effect on the IOP.

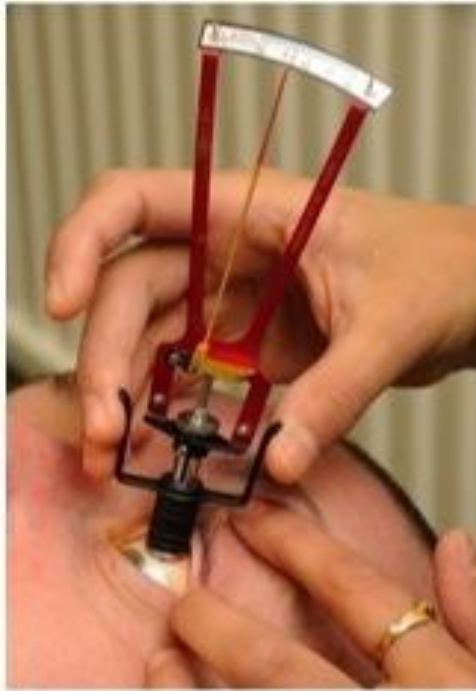


Figure 6.1 Schiottz tonometry on superior-temporal sclera of the LE.

Furthermore a 10 minute interval between each measurement period was designated as sufficient recovery time to pre-measurement IOP (Rosa *et al.*, 2008; Krakau and Wilke, 1971). Each subject was assessed twice on different days separated by a minimum of one day and a maximum of one week and measured at the same time of day to minimise the influence of diurnal variation on IOP (Read *et al.*, 2008).

GAT was performed on each subject on a different day at the same time to ensure that the effect on IOP of the Schiottz indentation procedure and reclined position would not affect the GAT results. Intraobserver variation was assessed for HP and LD by performing Schiottz tonometry on one individual 5 times while controlling for diurnal variation (Read *et al.*, 2008).

6.3.2 Ocular biometry and refractive error

6.3.2.1 Zeiss IOLMaster

The Zeiss *IOLMaster* is a non-contact instrument based on partial coherence interferometry (PCI) that was employed to measure ocular biometry parameters, such as axial length, corneal curvature and anterior chamber depth (ACD) in the present investigation and in various studies throughout the thesis. The theoretical principle behind PCI involves an infrared laser beam ($\lambda = 780$ nm) of coherent length being split by two

mirrors and a beam splitter. On entering the eye the two light beams are reflected back by two interfaces; cornea and the retina, giving a total of 4 beams, which are recorded by a photodetector. By moving one mirror at a constant speed and measuring interference fringes between reflected beams until a particular interference condition is met, a determination of optical length can be obtained (Hitzenberger, 1991); this is then converted to geometric length by using the eye's mean refractive index of 1.3549 (Lam *et al.*, 2001).

The light processed by the *IOLMaster* is reflected from the retinal pigment epithelial layer as opposed to the internal limiting membrane in ultrasound. A conversion factor has been allowed to account for this discrepancy. The *IOLMaster* has been found to measure axial length and ACD at a significantly higher resolution ($\sim\pm 0.01$ mm) compared to that determined by ultrasound ($\sim\pm 0.15$ mm), and has a major advantage in that it is a non-contact device unlike ultrasound biometry techniques (Santodomingo-Rubido *et al.*, 2002). The instrument is table mounted and simple to use with various targets utilised for assessing the axial length, corneal curvature and ACD. The examiner adjusts the focus of the targets with reference to a viewing screen and acquires readings by depressing the joystick button. In this manner 5 axial length, 3 corneal radius measurements and 5 ACD readings were obtained for each eye. The use of the *IOLMaster* facilitates investigation of the relationship between axial length, keratometry, ACD and biomechanical characteristics of the anterior segment.

6.3.2.2 Shin Nippon Autorefractor

The Shin-Nippon autorefractor (SRW-5000, Ryusyo Industrial Co. Ltd, Osaka, Japan) is a binocular open view, infra-red, non-contact autorefractor that can measure refractive error between ± 22 DS and ± 10 D cylinder in 0.125 D steps. The instrument has been found to be reliable in comparison to subjective refraction in adults, in the refractive range of +6.50 D to -15.00 D (Mallen *et al.*, 2001). The Shin Nippon was employed in the present study but is also widely utilised in various sections of the thesis to obtain refractive error data. The SRW-5000 calculates refractive error in two stages. The first stage consists of imaging an infrared ring of light after reflection from the retina. This ring is brought into approximate focus by a moveable lens within the machine. The second stage involves digitally analyzing this image in multiple meridians to derive a sphero-cylindrical refraction (Mallen *et al.*, 2001).

The operation procedure is simple, with the subject fixating a distant target through a clear semi-silvered mirror, while the examiner aligns the eye with reference to a viewing screen. On optimal alignment the subject observes a brief flash of a red ring of light as the examiner presses the joystick button to take a measurement. The protocol implemented throughout the various investigations when determining the refractive error included the use of 1 drop of tropicamide HCl 1% (*Minims*®, Bausch & Lomb, Kingston-Upon-Thames, UK) in both eyes to induce cycloplegia. Cycloplegia was designated as sufficient when the amplitude of accommodation was lower than 2 D. An objective measure of the refractive error was determined with the Shin-Nippon with 5 measurements taken from both eyes, which were averaged and converted to mean spherical error (MSE) (sphere power + 0.5 x cylinder power).

6.4 Statistical analysis

Statistical analysis was performed using *SPSS* Version 15 (*SPSS*, Inc., Chicago IL). The raw scale readings were converted to Ks and Ko using Friedenwald's equations (i.e. Eq 4.3 and 4.4) and the associated tables as described in Section 4.3.3 (Friedenwald, 1937; 1957). Tablecurve 2 D software (*Systat* Software Inc, Chicago, IL) was used to obtain best-fit curves for Friedenwald's empirical data for Pt and Vc for the 5.5 g and 7.5 g weights to avoid any inaccuracies that may occur when using the Friedenwald nomogram, as the nomogram requires manual plotting of results on a graph and extrapolation of rigidity values. These values were then examined statistically using two-way mixed repeated measures ANOVA, with regional rigidity values as the within-subject factor and refractive status as the between-subject factor. Similarly, the same ANOVA model was also applied to the raw scale readings to test for regional variation and for an influence of refractive status. When significant differences were found, a Bonferroni *post hoc* test was performed to determine pair-wise differences. For all statistical tests a p-value of <0.05 was taken as the criterion for statistical significance.

Intra-observer repeatability was assessed by calculating the Coefficient of Variation (CoV) and percentage error (PE) for each region and plunger weight. CoV is the ratio of within-subject standard deviation (SD) to mean values of Schiötz scale readings for one subject. PE was calculated as the difference between each result and the remaining results, i.e. each subject was assessed 5 times, thus the difference between reading 1 and 2, 1 and 3, 1 and 4 etc was calculated, hence 10 readings of differences were obtained. Each difference was

then divided by the mean of the 5 readings to give the PE value. The mean scale reading was taken to be the reference reading for each region. The absolute values of PE were then taken for further assessment.

To assess interobserver reliability for each region and plunger weight, PE was calculated in a similar manner to the intraobserver data and intraclass correlation coefficient (ICC) was also calculated. ICC was calculated using a two-way mixed ANOVA model, with a 95% confidence interval. *SPSS* calculates ICC as both single (i.e. only one examiner) and average (i.e. multiple examiners) values. Average ICC assesses reliability as the mean results of all examiners; therefore as two examiners (HP and LD) collected the data for the investigation, this was the preferred measure of overall reliability and repeatability. Additionally the ICC calculations can also be based on either absolute agreement or on a consistency measurement. Unlike absolute agreement, consistency measures of ICC do not take into account the systematic variability between examiners. In the present study the systematic variability was irrelevant and hence the consistency measure was used. Furthermore, concordance between IOP determined by GAT and by Schiötz tonometry was determined by producing difference *versus* mean plots.

6.5 Results

6.5.1 Schiötz Indentation: raw data

The data were analysed for non-myopic and myopic individuals [MSE (D) 14 non-myopes (≥ -0.50) $+0.48 \pm 1.22$, range (-0.50 to +4.38); 12 myopes (< -0.50) -4.44 ± 3.35 , range (-0.75 to -10.56)]. No significant correlations were found between either raw indentation data or converted rigidity values and *IOLMaster* measures of axial length, ACD and corneal curvature.

Mean refractive group differences were insignificant for scale reading data. Mean scale readings (RE) for 5.5 g were: cornea (CR) 5.93 ± 1.14 , ST 8.05 ± 1.58 , IT 7.03 ± 1.86 , SN 6.25 ± 1.10 , IN 6.02 ± 1.49 ; for 7.5 g: CR 9.26 ± 1.27 , ST 11.56 ± 1.65 , IT 10.31 ± 1.74 , SN 9.91 ± 1.20 , IN 9.50 ± 1.56 (Figure 6.2). There were significant differences for both 5.5 g ($F(4, 96) = 18.444$ ($p < 0.001$)) and 7.5 g ($F(4, 96) = 17.575$ ($p < 0.001$)) weights between mean scale readings for the cornea and ST; ST and SN; ST and IT; ST and IN. These differences were concordant with the LE data and thus only RE data are examined.

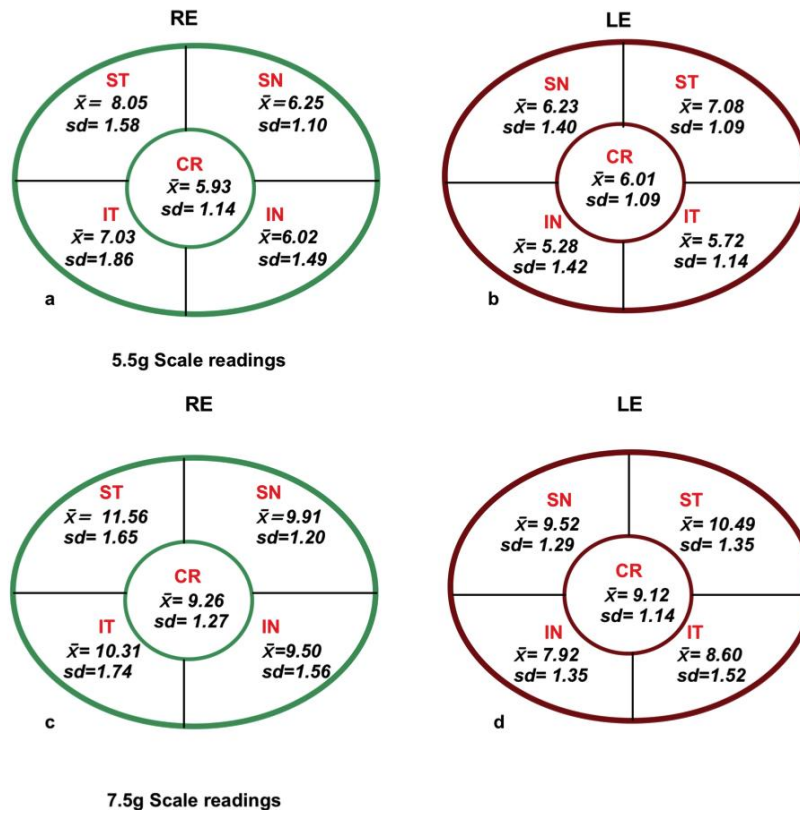


Figure 6.2 Scale readings with Schiotz 5.5 g (a and b), Schiotz 7.5 g (c and d).

6.5.2 Friedenwald's Ko and Ks values

No significant difference in rigidity values was found between refractive groups. In both myopic and non-myopic groups no significant difference was found between Ko and Ks, nor between values for Ks across quadrants (Table 6.1).

Region	Rigidity values for non-myopic group		Rigidity values for myopic group		Mean rigidity measures (myopic and non-myopic groups combined)	
	Mean	SD	Mean	SD	Mean	SD
Ko CR	0.0101	0.0078	0.0093	0.0091	0.0101	0.0082
Ks ST	0.0087	0.0054	0.0082	0.0080	0.0085	0.0067
Ks SN	0.0088	0.0043	0.0096	0.0097	0.0091	0.0070
Ks IT	0.0097	0.0071	0.0083	0.0106	0.0092	0.0084
Ks IN	0.0080	0.0088	0.0204	0.0364	0.0134	0.0252

Table 6.1 RE Rigidity values (mm^3)⁻¹ for myopic, non myopic and both groups combined.

6.5.3 Comparison of IOP measures using Schiottz tonometry and GAT

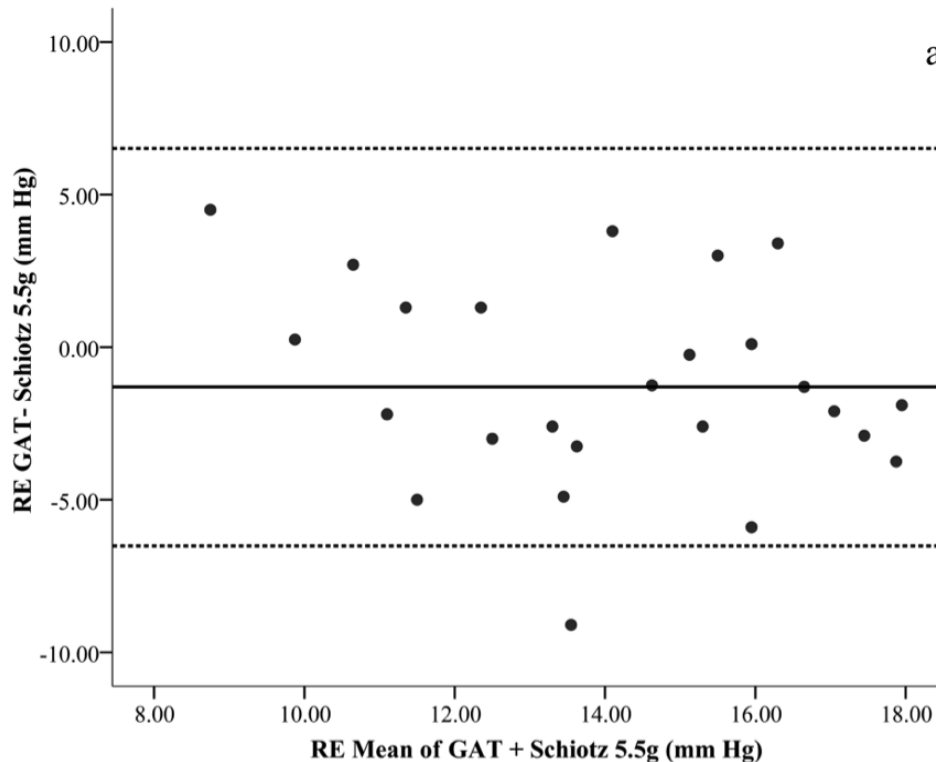
The Friedenwald 1955 Conversion scale, which assumes a constant ocular rigidity value of 0.0215, was used to convert scale values to IOPs (mm Hg). Table 6.2 shows the IOP data obtained with both GAT and Schiottz tonometry and Figure 6.3 (a and b) respective difference versus mean plots (Bland and Altman, 1986). A statistically significant correlation was found between GAT IOP and the 5.5 g readings (Table 6.3).

Method	Min	Max	Mean \pm SD
RE GAT	9.00	18.00	13.36 \pm 2.71
RE Schiottz 5.5 g	6.50	19.75	14.52 \pm 3.26
RE Schiottz 7.5 g	7.50	18.50	12.85 \pm 2.98

Table 6.2 GAT and Schiottz (5.5 g and 7.5 g) tonometry measures of IOP (mm Hg).

Comparison	Pearson Correlation Coefficient
RE 5.5 g vs. GAT	r=0.446 p=0.022
RE 7.5 g vs. GAT	r=0.237 p=0.244
RE 5.5 g vs. 7.5 g	r=0.823 p<0.001

Table 6.3 Correlation between GAT and Schiottz (5.5 g and 7.5 g) tonometry measures of IOP (mm Hg).



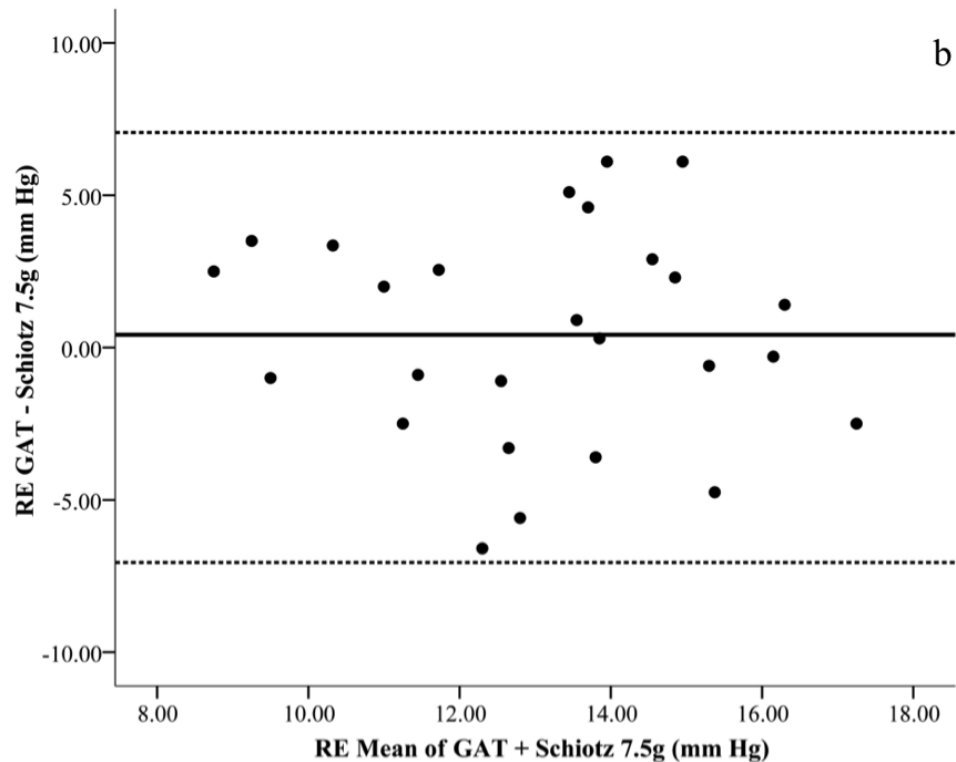


Figure 6.3 a) RE difference versus mean plot: Schiottz 5.5 g:GAT IOP (Bold line denotes mean, dotted line +/- 2SD **b)** RE difference versus mean plot: Schiottz 7.5 g:GAT IOP (Bold line denotes mean, dotted line +/- 2SD).

6.5.4 Intra- and interobserver variability using Schiottz tonometry

The CoV and PE were calculated for each observer (i.e. investigators HP and LD). No significant difference was found between observers for both eyes, thus only RE and average results will be examined for both CoV and PE. Average CoV values for both observers indicated that repeatability varied with site of measurement, with highest repeatability for the cornea (i.e. 5.5 g: 9.37%; 7.5g: 12.63%) and lowest for IT (i.e. 5.5 g: 30.2%) and IN (7.5 g: 28.4%); no significant differences were found between regions. PE of all regions showed no significant differences for 5.5g, however 7.5 g data indicated a significant difference between the cornea and IN region ($p=0.009$). The 5.5 g and 7.5 g data showed the cornea to have the lowest PE (5.5 g: $20.39 \pm 22.32\%$, 7.5 g: $14.92 \pm 10.53\%$). The mean difference in PE between the cornea and scleral quadrants did not reach statistical significance.

Region	Average CoV % 5.5 g	Average CoV% 7.5 g
CR	9.37	12.63
ST	27.43	24.70
SN	20.98	22.05
IT	30.20	23.10
IN	25.25	28.40

Table 6.4 Average CoV values for scleral regions.

Interobserver concordance showed 5.5 g to have the highest ICC (0.682) for the cornea and lowest ICC (0.342) for IN, whereas 7.5 g had lower values of ICC (0.388) for cornea and IN (0.187). Interobserver PE showed no significant difference between plunger weights and a non-significant difference was found between eyes for both weights. No significant difference was found for PE between quadrants; however lowest values were obtained for the cornea (5.5 g: $16.86 \pm 10\%$; 7.5 g: $14.33 \pm 12.27\%$) and highest values for IT (5.5 g: $29.71 \pm 22.86\%$; 7.5 g: $25.26 \pm 18.64\%$). For further details on the results and statistical outcomes see Appendix 3.

6.6 Discussion

The present investigation demonstrated that despite relatively high levels of intra- and inter-observer variation,, measurements of indentation using the Schiötz tonometer are sufficiently robust to measure reliably regional variations in scleral resistance. The study examined raw Schiötz scale readings to investigate regional differences in indentation values. The results showed significant differences in mechanical resistance between the cornea and the sclera but also significant variation across scleral quadrants. Schiötz scale readings converted to Friedenwald's corneal and scleral rigidity failed to show any significant difference between refractive groups. IOP measures with the Schiötz were consistent with IOPs determined with GAT.

6.6.1 Regional variation in scleral resistance

The assessment of the Schiötz scale values consistently showed the greatest level of indentation for quadrant ST and least for IN. The results also showed significant differences for both weights between means for the cornea and ST; ST and SN; ST and IT; ST and IN. As the IOP and tissue compliance modulate the level of indentation produced by the Schiötz tonometer, explanation for such differences may be attributed to regional

differences in collagen infrastructure and possible variations in scleral biomechanics due to localized geometric differences e.g. shape, curvature and thickness (see Chapters 7 and 14).

In support of the proposal that arrangement of collagen fibrils produce an effect on regional variation, studies have previously reported collagen arrangement to vary with different geographic locations on the globe (Curtin, 1969; Thale and Tillmann, 1993). These studies have noted the collagen fibrils at the lamina cribrosa to be arranged circularly around the points of passage of axons and vessels whereas, in contrast, at the sites of the muscle insertions the parallel tendon fibres intersect the scleral collagen fibrils at right angles (Thale and Tillmann, 1993; Watson and Young, 2004). Additionally, scleral collagen fibre bundles are mainly orientated in the circumferential direction and are thus more resistant to variation in globe circumference than changes in radial thickness (Battagliolo and Kamm, 1984).

Shape and size have also been found to influence the results of indentation tonometry with increased rigidity being observed with smaller radii of curvature (Phillips and Shaw, 1970). Friedman, (1966) suggested that eye wall stress and hence tissue resistance may be affected by scleral curvature with flatter curvatures exhibiting greater levels of stress resulting in localised differences in strain for a constant IOP. Moreover, reports of significant variation in the conformation of the internal aspects of the anterior segment (Werner *et al.*, 2008; Rondeau *et al.*, 2004) further support the present findings of regional variation in the biomechanical properties of the overlying sclera.

In contrast to measures of corneal rigidity, there is little literature on the use of the Schiøtz tonometer to determine scleral biomechanics (Schmid *et al.*, 2003; Sullivan-Mee *et al.*, IOVS 2010, 51: ARVO E-Abstract 5548). Additionally few studies have assessed scleral biomechanics *in vivo*, presumably due to the complex inter-relationships between ocular tissues and the difficulties of measuring these tissue properties in different locations in the living eye. Hence many investigators have attempted to quantify the biomechanical properties of the sclera *in vitro* (see table 9.5 in Chapter 9) using extensimetry (Eilaghi *et al.*, 2010b; Elsheikh *et al.*, 2010; Downs *et al.*, 2003; Curtin, 1969, Friberg and Lace, 1988) or pressure-volume studies (Bisplinghoff *et al.*, 2009; Mattson *et al.*, 2010) on human and animal scleral tissue. In contrast to pressure-volume experiments, a key advantage of extensimetry studies (as discussed in Chapter 9) is the ability to assess

variation in the biomechanical properties of the sclera in different locations of the globe and in different orientations (Curtin, 1969; Eilaghi *et al.*, 2010b; Elsheikh *et al.*, 2010).

Using extensimetry, numerous investigators have reported regional (i.e. anterior, equatorial and posterior) differences in scleral biomechanics with the anterior sclera showing greater stiffness than the posterior sclera (Curtin, 1969; Elsheikh *et al.*, 2010; Friberg and Lace, 1988). Of particular note, Smolek, (1988) reported the superalateral region of the posterior globe to distend relatively more than the inframedial and median locations. In spite of these differences being at the posterior globe, it is suggested that these variations may continue forward to the anterior segment and support the present findings of increased distensibility in the ST region when compared to the IN region. Additional support for a stiffer inferior sclera comes from Downs *et al.*, (2003), who reported the inferior peripapillary scleral region in rabbits to show the greatest rigidity.

Several investigators have also attempted to investigate regional scleral biomechanics using pressure-volume (Bisplinghoff *et al.*, 2009; 2008) and deformation testing (Avetisov *et al.*, 1978). Such studies have provided further evidence of anisotropy of the scleral tissue (Avetisov *et al.*, 1978) with significant differences in biomechanics being observed between the equatorial and meridional directions (Bisplinghoff *et al.*, 2009; 2008). ***If Schiotz scale readings are taken as a surrogate measure of biomechanical resistance, then the present results indicate the temporal regions to display lower rigidity than nasal regions.*** Interestingly, in support of a weaker temporal scleral, the posterior temporal sclera has been found to show consistently initial rupturing in pressure-volume tests (Greene and McMahon, 1979) and is often the site of myopic staphyloma (Curtin, 1985).

Further support for regional variation in scleral biomechanics stems from reports of significant variation in thickness of different regions (see Chapter 7; Elsheikh *et al.*, 2010; Guthoff *et al.*, 1987; Schmid *et al.*, 2003; Olsen *et al.*, 1998; 2002; Norman *et al.*, 2009). A number of studies have reported scleral thickness to be greatest at the posterior pole and equatorial regions to be the thinnest (Olsen *et al.*, 1998; Elsheikh *et al.*, 2010). A recent *in vitro* study by Norman *et al.*, (2009) indicated regional variation in scleral thickness across the four quadrants examined (i.e. nasal, temporal, inferior and superior) but due to large inter- and intra-individual differences and a small sample size the investigators could not demonstrate statistically significant differences between quadrants. On inspection of their data, for the 8 mm location evaluated in the present study the inferior quadrant showed the

greatest thickness followed by the nasal, superior and temporal regions. ***These results support the incremental increase in scleral resistance from ST to IN found in the current study.*** Evidence of variation in posterior regional scleral thickness has also been noted in rhesus monkeys (*Macaca mulatta*), where for the midperipheral peripapillary sclera the nasal region was shown to be the thinnest followed by superior, temporal and inferior regions (Downs *et al.*, 2002). Interestingly, several investigators assessing scleral biomechanics and thickness have noted significant inter-individual differences in scleral properties (Elsheikh *et al.*, 2010; Eilaghi *et al.*, 2010b; Norman *et al.*, 2009; Olsen *et al.*, 1998), which may account for the variability of scleral resistance found in the present study.

6.6.2 Friedenwald's corneal and scleral rigidity

The conversion of the scale readings to Ko and Ks indicated no significant differences in rigidity between myopes and non-myopes nor significant regional variations within each group. In regards to Ko and refractive error, a number of investigators have reported reduced Ko with myopic refraction (Drance, 1959; Goodside, 1959; Castrén and Pohjola, 1961b; Draeger, 1959). Furthermore, some studies have also noted significant variation in Ko values amongst myopes (Castrén and Pohjola, 1961b) and levels of myopia; Jain and Singh (1967) reported a general trend for reducing Ko in myopes but observed increased Ko between -9 D to -12 D; similarly Castrén and Pohjola, (1962) failed to show reduced Ko below -3 D but noted a reduction beyond this level of myopia up to -18 D from which point Ko showed an increase. Reduced Ko has also been found to be associated with increasing axial length (Luyckx, 1967) and ocular volume (Rivara and Zingirian, 1968). Contrary to these findings Zolog *et al.*, (1969) and Wong *et al.*, (1991) failed to show any significant influence of myopia on Ko. Such disparity amongst the present findings and those reported in the literature may be a result of differences in study protocols. In particular cohort differences such as age (Lam *et al.*, 2003a; Goodside, 1959; Friedenwald, 1937) and ethnicity (Wong *et al.*, 1991; Jain and Singh, 1967) have been implicated as sources of variability in Ko.

The high variability found in the present results may be due to the relatively high observer variation and the large range of refractive errors assessed. The results obtained for Ko (i.e. mean 0.0101 ± 0.0082 , range 0.0019-0.0304) matched approximately the range of results previously reported (Table 6.5) (Friedenwald, 1937; Lam *et al.*, 2003a; Pallikaris *et al.*,

2005; Schmid *et al.*, 2003). The present sample comprised 46% myopes, which together with its relatively low overall mean age may have biased Ko in a negative direction (Lam *et al.*, 2003a). When assessing the utility of Ks, account has to be taken of the fact that its computation is based on empirical data taken from the cornea and collated by Friedenwald (1937; 1957), which inevitably would restrict its application when evaluating scleral biomechanics.

Investigation	Technique used to determine Ko	Mean / Range of Ko values (mm ³) ⁻¹
Friedenwald, (1937)	Friedenwald's paired tonometry 5.5 g and 10 g	Range 0.002 - 0.550 Mean 0.0215
Schmidt, (1957)	GAT and Schiötz 5.5 g	Range 0.0060 - 0.0136 Mean 0.0203
Heinzen <i>et al.</i> , (1958)	GAT and Schiötz 10 g	Hyperopic: 0.0233 Emmetropic: 0.0220
Draeger, (1959)	GAT and Schiötz 5.5 g	Hyperopic 0.0211 - 0.0220 Emmetropic 0.0199 Myopic 0.0144 - 0.0165
Leydhecker, (1959)	Friedenwald's paired tonometry 5.5 g and 10 g	Mean 0.0240
Goodside, (1959)	Friedenwald's paired tonometry 5.5 g and 10 g	Plano to +5D 0.0187 -0.25D to -6D 0.0157
Drance, (1960)	GAT and Schiötz 10 g	Range 0.0070 - 0.0451 Mean 0.0217
Ytteborg, (1960a)	GAT and Schiötz 5.5 g	Mean 0.0232
Castrén and Pohjola, (1961b)	GAT and Schiötz 10 g	Hyperopia 0.0189 ± 0.0003 Emmetropia 0.0184 ± 0.0002 Myopia 0.0162 ± 0.0005 Mean 0.01829
Jain and Singh, (1967)	Friedenwald's paired tonometry 5.5 g and 10 g	-6D to -8D 0.0154 -9D to -12D 0.0169 -13D to -15D 0.0154 -16D to 21D 0.0140
Singh <i>et al.</i> , (1970)	Friedenwald's paired tonometry 5.5 g and 10 g	Mean 0.0227
Wong, (1991)	Friedenwald's paired tonometry 5.5 g and 10 g	Mean 0.0156 SD 0.0065
Schmid <i>et al.</i> , (2003)	Friedenwald's paired tonometry 5.5 g and 10 g	Myopic 0.0224 Non myopic 0.0224
Lam <i>et al.</i> , (2003a)	Friedenwald's paired tonometry 5.5 g and 7.5 g	<30 years 0.012 - 0.009 30–39 years 0.020 - 0.018 40–49 years 0.025 - 0.022 50–59 years 0.023 - 0.018 ≥ 60 years 0.025 - 0.021

Table 6.5 Schiötz rigidity values for humans found in previous studies (mean ± SD given where available).

6.6.3 Reliability and sources of variation in Schiottz tonometry

Despite relatively high levels of intra- and inter-observer variation, measurements of indentation using the Schiottz tonometer were found to be sufficiently robust to measure reliably regional variations in scleral resistance. Observer differences were insignificant for both CoV and PE. Average intra-observer CoV varied with site of measurement with the highest repeatability found for the cornea and lowest for IT (5.5 g) and IN (7.5 g). Similarly, high levels of repeatability for the cornea were found with both 5.5 g and 7.5 g weights showing the cornea to have the least PE, yet non-significant differences were found between corneal and scleral PE values. Interobserver concordance with the 5.5 g weight showed the highest ICC for the cornea and lowest ICC for IN. In contrast 7.5 g had reduced values of ICC for cornea and lowest ICC for IN. These findings indicate that, in comparison to the sclera, the cornea provides the most reliable and repeatable measurements.

The high concordance between GAT and Schiottz IOP readings with the 5.5 g weight indicates that the Schiottz can be used to obtain robust data. Such findings have been previously noted in literature (Chiara *et al.*, 1989; Pervite *et al.*, 1974). The 5.5 g weight has been recommended as the weight of choice as it minimises the affect of rigidity when used for the sole purpose of assessing IOPs (Rosa *et al.*, 2008; Allen and Wertheim, 1963b); however in the present study this weight had the greatest variability. The Schiottz has been found to give lower readings than GAT in some comparison studies (Chiara *et al.*, 1989; Anderson and Grant, 1970; Roberts and Rogers, 1964) and it has been speculated that differences in posture are the reason for the discrepancy (Anderson and Grant, 1970).

In addition to the intra- and inter-observer variability of the procedure, the Schiottz tonometry technique has inherent errors, which may have further contributed to the inconsistency of the results (Gensler, 1967). All Schiottz tonometers are calibrated and constructed according to the standards laid down by the American Academy of Ophthalmology and Otolaryngology; however errors of up to ± 3 mm Hg in mean tonometric measurements may still exist between instruments used on the same eye (Edwards, 1988). In addition scale readings are susceptible to error due to parallax of the pointer at measurement end point and as a result of the close juxtaposition of scale markings (Harrington and Parsons, 1941; Jackson, 1965).

Further sources of errors originate from the curvature of the tonometer footplate not matching closely that of the sclera. This lack of conformation between the footplate and the tissue surface, especially if the conjunctival surface is uneven, may affect the angle of the footplate on the scleral surface, which may in turn produce misleading results (Allen and Wertheim, 1963b; Eberly, 1967). Previous studies have indicated that the lowest scale reading is usually the most accurate and indicates optimal apposition of the plate and the tissue (Allen and Wertheim, 1963b). This recommendation was taken into account by both observers when performing Schiotz tonometry in the present study. In addition, variability between subjects associated with blepharospasm and lid tonus may also have affected the results by artificially increasing IOP readings (Goodside, 1959; Eberly, 1967). In the present study the occurrence of individuals with significant blepharospasm was rare; although when encountered such individuals were removed from the study. Further explanation for the variance in the Schiotz data could be attributable to the approximation of the site of measurement, which may have introduced inconsistency on repeated testing.

Furthermore a number of studies have previously reported a ‘massaging’ effect on the IOP with Schiotz tonometry, where successively lower IOP readings are observed with multiple readings (Hine, 1916, Kronfeld, 1959). This effect is thought to be a consequence of an increased rate of aqueous outflow as result of the ocular volume change following indentation tonometry (Armaly, 1959; Chiara *et al.*, 1989). The study protocol presently adopted controlled in part for this source of error as intervals were allowed between procedures for each observer. However a stabilization period was not allowed between different plunger readings. This omission may have caused reduced IOP readings with the 7.5g and in turn produced lower rigidity values.

The procedures used in the study were unable to control for the possibility of differential extraocular muscle traction on the globe for the different directions of gaze (Greene, 1980). The mechanical stresses induced by the oblique muscles may affect the posterior sclera (Greene, 1980) although the affects of the extraocular muscles on the anterior sclera are unknown. Versional eye movement with consequent strain on the sclera may affect IOP and the subsequent determination of rigidity. Associated effects have been reported in patients with dysthyroid ophthalmopathy (Graves ophthalmopathy (GO)) where, on elevated gaze, IOP rises due to the pressure exerted by the rectus muscles (Fishman and Benes, 1991; Gamblin *et al.*, 1983; Gomi *et al.*, 2007). It is generally assumed that the change in IOP in versional gazes in normal individuals is lower than those with GO or in

individuals with restricted ocular motility (Helveston *et al.*, 1980; Nardi *et al.*, 1988; Zappia *et al.*, 1971). In healthy individuals the literature is equivocal in regards to levels of changes in IOP in different gazes (Table 6.6). Such divergence in the range of IOP changes may be a consequence of the methodology implemented to assess the IOPs in the various gazes. On performing gaze-dependent tonometry, GAT is usually applied to the peripheral cornea or the sclera and is thus likely to provide misleading measures of IOP (Herzog *et al.*, 2008). Interestingly, in a recent study using an inclining chin rest, Herzog *et al.*, (2008) reported no significant change in IOP on 20° up gaze in healthy individuals. In consideration of the present findings of regional differences in scleral resistance, it is unlikely that the putative effect of extraocular muscle traction on the sclera and IOP would confound data for the healthy eyes evaluated in the present study.

An additional source of variability may have been introduced by differential accommodative responses in the various gazes, which may have had a secondary effect on IOP (Hine, 1916). Accommodation has been previously shown to lower IOP (Mauger *et al.*, 1984) although significant inter-subject variability has been reported in regards to this response (Rai *et al.*, IOVS 2006, 47: ARVO E-Abstract 5859). Furthermore in the present study the fixation targets for the various gaze locations were situated >1.5 meters and hence it is unlikely that the accommodation response would be sufficient to confound the findings of regional variation in scleral resistance (Bullimore *et al.*, 1992; Krantz *et al.*, 2010).

Investigators	Method	IOP mean ± SD (mm Hg)
Zappia <i>et al.</i> , (1971)	GAT in primary gaze and 15° up and down gaze on normal individuals and in patients with adhesive muscle syndromes	Change in IOPs (normal individuals): up gaze 0.38±0.8 and down gaze -0.34±0.9
Saunders <i>et al.</i> , (1981)	Non-contact tonometry in extreme horizontal and vertical gazes	6.8 up gaze and 3.9 down gaze
Moses <i>et al.</i> , (1982)	GAT in horizontal gazes (temporally (T) and nasally (N)) at 10°, 30° and 50° on normal individuals	IOPs: 50°T 17.09, 30°T 15.18, 10°T 13.84 50°N 13.96, 30°N 14.61, 10°N 15.75
Reader, (1982)	GAT in primary and vertical gazes +20° up and -20° down at 5° intervals in normal individuals	Lowest IOP at -5°; mean rise of 2.75 through 25° on up gaze and 1.5 through 15° of down gaze from the lowest -5° point.
Nardi <i>et al.</i> , (1988)	GAT in primary and infra- and supra- adduction and abduction at 22° in normal and eyes with disorders of restrictive ocular motility	Differences in IOP (normal individuals): Primary-supraduction +0.77±0.8 Primary-adduction -0.19±0.7 Primary-infraduction -0.52±0.8 Primary-abduction -0.25±0.7 Infra-supraduction +1.29±1.1 Adduction-abduction -0.07±0.7
Spieler and Eisenstein, (1991)	GAT in primary gaze and 25° up gaze in normal and GO patients	Change in IOPs (normal individuals): 0-4 change from primary to up gaze
Herzog <i>et al.</i> , (2009)	GAT in primary and vertical up gaze 20° with a non-inclining and inclining chin rest in normal and GO patients	IOPs (normal individuals) Primary position 16.2±3.0 Non-inclining chin rest up gaze 19.1±3.3 Inclining chin rest 16.6±2.8

Table 6.6 Reports of IOP changes with gaze in normal individuals (mean ± SD given where available).

6.7 Conclusions

Key findings of the study:

- Schiotz tonometry provides a robust non-invasive technique to measure regional variation in scleral resistance *in vivo*.
- Converted Friedenwald's scleral rigidity values failed to show regional variation in scleral biomechanics and are considered to be of limited value as a result of the transformation algorithms based solely on corneal empirical data.
- The use of Schiotz scale readings as a surrogate for assessing scleral resistance demonstrated significant regional variation in tissue resistance, with quadrant ST showing the least resistance and quadrant IN showing the most resistance to mechanical deformation.

Acknowledgements

College of Optometrist's Summer Scholarship (2008) for Larissa Dorochtchak- Technical Assistant in the above study.

7.0 *IN VIVO* MEASUREMENT OF SCLERAL THICKNESS IN HUMANS USING ANTERIOR SEGMENT OPTICAL COHERENT TOMOGRAPHY

7.1 Introduction

The properties of scleral material are of significant interest physiologically, surgically and for their potential role in pharmacokinetics. In contrast to the cornea the sclera covers 90% of the human globe, but despite this greater proportional coverage, there is a significant dearth of literature on this multifunctional ocular tissue (Oliveira *et al.*, 2006). The sclera offers substantial mechanical strength and thus plays a vital role in the protection of the vulnerable components within the eye, while also withstanding the expansive stress of the IOP (Meek and Fullwood, 2001). As such it is the main load bearing tissue of the eye and hence variation in its biomechanical properties are likely to affect the response of the tissue to the constant stress of the IOP (Norman *et al.*, 2009).

With an increasing body of literature implicating scleral biomechanics in the aetiology of myopia (McBrien *et al.*, 2009; Guggenheim and McBrien, 1996; Rada *et al.*, 2006), glaucoma (Eilaghi *et al.*, 2010a; Mortazavi *et al.*, 2009) and AMD (Friedman, 2000; Pallikaris *et al.*, 2006) there is added impetus to attain a comprehensive understanding of the properties of the scleral material. Due to experimental limitations in assessing the characteristics of scleral tissue such as rigidity, thickness and curvature *in vivo*, numerical simulation models have often been explored (Eilaghi *et al.*, 2010a; Sigal *et al.*, 2009). These models are able to provide an invaluable insight into the complex inter-relationships between the various ocular tissues but are constrained by the lack of information (e.g. variation in thickness) on the scleral material thus questioning their accuracy and reliability (Elsheikh *et al.*, 2010). Therefore, before a composite understanding of the biomechanics of the sclera can be gained, experimental studies must provide a greater knowledge of its primary material properties.

The thickness of the eye's outer tunic is an important biometric measure that may govern the mechanical properties of its tissues (Asejczyk-Widlicka *et al.*, 2008b). In particular central corneal thickness (CCT) in primary open angle glaucoma (POAG), normal tension glaucoma (NTG) and ocular hypertension (OHT) patients has been widely investigated over recent years (Herndon *et al.*, 1997; Copt *et al.*, 1999; Shah *et al.*, 1999). Many such

investigations have demonstrated OHT patients to show greater CCT and NTG patients to have thinner CCT than normal individuals (Herman *et al.*, 2001; Brandt, 2004, Mohamed-Noor *et al.*, 2009; Yoo *et al.*, 2010). As a result of the substantial evidence relating CCT to glaucoma, the Ocular Hypertension treatment study implicated a thin cornea in OHT eyes to be a significant risk factor for POAG development (Gordon *et al.*, 2002). When combined with reports of reduced corneal hysteresis in glaucomatous eyes (Congdon *et al.*, 2006; Shah *et al.*, 2008; see Chapter 11) these findings have led to the conjecture that corneal biomechanics may be related to the biomechanics of the sclera and the lamina cribrosa, suggesting that a weak cornea may constitute a greater propensity to glaucomatous changes (Oliveira *et al.*, 2006).

Furthermore, support for a possible relationship between corneal biomechanics and globe conformation stems from the findings of Chapter 11 where axial length was found to modulate corneal hysteresis and corneal resistance factor in the UK subjects examined. Such an association between the cornea and ocular structural changes is likely to include the sclera, and in particular the thickness of the sclera may play a crucial role in ocular biomechanics and refractive error development. Despite the increasing evidence that the sclera is involved in the pathogenesis of myopia there is little literature on the changes in scleral thickness with myopia *in vivo* (Guthoff *et al.*, 1987; Schmid *et al.*, 2003).

Aside from its physiological role, the sclera may also provide an important alternative for topical drug transmission to the posterior globe when compared to conventional means of drug delivery such as intraocular injections, systemic delivery, implantable devices, and topical eye drops (Olsen *et al.*, 1998). Transscleral drug delivery has been found to be dependent upon scleral permeability, which is related to surface area and thickness (Olsen *et al.*, 1998). In fact the sclera has been found to be permeable to different hydrophilic compounds of varying molecular size *in vitro* (Olsen *et al.*, 1995; Ambati *et al.*, 2000; Lee *et al.*, 2004) but further knowledge of scleral thickness may aid in deciding optimal sites for *in vivo* drug delivery.

Moreover, knowledge of scleral dimensions is also important in ophthalmic surgery. During surgical procedures such as scleral buckling and in correction of strabismus, lamellar dissection of the sclera is performed and sutures applied through various levels of the scleral stroma. Precise knowledge of scleral thickness is important in these procedures to avoid risk of scleral perforation (Olsen *et al.*, 1998). The introduction of anti-vascular

endothelial growth factor (i.e. anti-VEGF) treatment in age related macular degeneration requires multiple injections into the sclera. Current practice is for the injection to be applied through the inferior temporal sclera mainly due to ease of access but there is no consensus as to the most suitable choice of location (Royal College of Ophthalmologists, 2009). It is envisaged that greater understanding of the anterior scleral anatomy will provide details on regional thickness profiles and may aid avoidance of areas of thinnest sclera that would be most vulnerable to perforation.

Until relatively recently, few studies had investigated scleral thickness in humans (see Table 7.1) presumably as a result of technological limitations in imaging the sclera *in vivo*. Early *in vitro* studies attempted to evaluate scleral thickness using techniques such as light scattering with intensity detecting photo-diodes (Perkins, 1981), microscopic measurement of scleral strips (Curtin, 1969) and by assessing photographic slides of cross-sectional profiles of scleral sections (Olsen *et al.*, 1998). In an attempt to assess posterior scleral thickness *in vivo*, Guthoff *et al.*, (1987) employed a combination of A- and B-scan ultrasonography to determine scleral thickness changes with axial length. In regards to *in vivo* anterior scleral thickness Pavlin *et al.*, (1992) first demonstrated the utility of ultrasound biometry (UBM) for measuring various anterior segment structures such as scleral and ciliary muscle thickness. Following this, a number of studies utilised the UBM technique to assess anterior scleral thickness in the vicinity of the scleral spur but noted some variability in their findings (Lam *et al.*, 2005; Oliveira *et al.*, 2006; Mohamed-Noor *et al.*, 2009). Other investigators have utilised ultrasound pachymetry *in vitro* (Elsheikh *et al.*, 2010; Stewart *et al.*, 2009) and *in vivo* (Schmid *et al.*, 2003) and more recently MRI scanning has also been applied *in vitro* (Norman *et al.*, 2009) and *in vivo* to assess scleral thickness (Cheng *et al.*, 1992; Lam *et al.*, 2005; Atchinson *et al.*, 2005). With current advances in ocular imaging technology, anterior segment optical coherent tomography (AS-OCT) has been utilised to assess scleral thickness *in vitro* in porcine eyes (Asejczyk-Widlicka *et al.*, 2008b) and *in vivo* in human eyes (Wirbelauer *et al.*, 2003; Yoo *et al.*, 2010; Taban *et al.*, 2010). Unlike the contact UBM procedure, which limits scleral thickness measurements usually to one meridian (Oliveira *et al.*, 2006; Mohamed-Noor *et al.*, 2009), AS-OCT offers a non-contact method of assessing scleral thickness in all meridians.

Investigators	Technique and location of measurement	Scleral thickness (μm) Mean \pm SD /Range
Pavlin <i>et al.</i> , (1992)	<i>In vivo</i> UBM used to measure scleral thickness at the scleral spur in the temporal meridian	938 \pm 58
Cheng <i>et al.</i> , (1992 ^a)	<i>In vivo</i> MRI in emmetropic, hypermetropic and myopic individuals; measuring scleral thickness along the anterior-posterior (axial), vertical and horizontal (equatorial) planes	Emmetropes: Axial 600 \pm 200 Vertical 400 \pm 100 Equatorial 400 \pm 100 Hypermetropes: Axial 800 \pm 400 Vertical 400 \pm 100 Equatorial 400 \pm 100 Myopes: Axial 400 \pm 200 Vertical 400 \pm 200 Equatorial 400 \pm 200
Olsen <i>et al.</i> , (1998)	Photographic slides of <i>in vitro</i> human scleral cross sectional profiles	Limbal 530 \pm 140 Equator 390 \pm 170 Near optic nerve, range 900-1000
Schmid <i>et al.</i> , (2003)	<i>In vivo</i> ultrasound pachymetry in myopic and non-myopic children; measured scleral thickness approximately 12 mm from centre of pupil in the temporal meridian	Myopes: 1870 \pm 120 Non-myopes: 1960 \pm 120
Wirbelauer <i>et al.</i> , (2003 ^b)	<i>In vivo</i> OCT in a case study patient with scleral expansion bands; measured scleral thickness at the scleral spur	831 \pm 84 range (751-952)
Atchison <i>et al.</i> , (2005 ^a)	<i>In vivo</i> MRI in emmetropic and myopic individuals; measuring scleral thickness at the nasal, temporal, superior and inferior equatorial regions and the fovea	Emmetropes: Nasal + Temporal 750 \pm 140 Superior + Inferior 710 \pm 100 Fovea 730 \pm 270 Myopes: Nasal + Temporal 870 \pm 240 Superior + Inferior 670 \pm 210 Fovea 630 \pm 210
Lam <i>et al.</i> , (2005)	<i>In vivo</i> UBM in humans at 2 and 3 mm from the scleral spur in four meridians 12, 3, 6 and 9 o'clock	560 \pm 50 at 2 mm 550 \pm 60 at 3 mm mean 550 \pm 50
Jackson <i>et al.</i> , (2006)	<i>In vitro</i> light microscopy on scleral strips from human donor eyes between 8-14 mm posterior from the limbus	509 \pm 115
Oliveira <i>et al.</i> , (2006)	<i>In vivo</i> UBM in humans at scleral spur, 2 mm and 3 mm in the temporal meridian	699 \pm 65 range (567-840) at 1 mm 510.5 \pm 62 range (306.5-712) at 2 mm 506.5 \pm 65 range (314.5-660) at 3 mm
Norman <i>et al.</i> , (2009)	<i>In vitro</i> MRI on normal and ostensibly glaucomatous eyes; measured scleral	Corneoscleral junction 588 \pm 63

	thickness in 4 quadrants (superior, inferior, temporal and nasal)	Equator 491 ± 91 Posterior 996 ± 181
Mohamed-Noor <i>et al.</i> , (2009)	<i>In vivo</i> UBM in humans at 2 mm posterior to scleral spur in the temporal meridian	724.45 ± 73.27 (604-864)
Elsheikh <i>et al.</i> , (2010)	<i>In vitro</i> ultrasound pachymetry in humans eyes; measured scleral thickness in 8 meridians from the limbal edge to the posterior pole (PP)	Mean of 8 meridians PP 1062 ± 6.6 18-20 mm from PP 716 ± 68 Limbal edge 767 ± 34.9
Taban <i>et al.</i> , (2010)	<i>In vivo</i> OCT in normal and fluocinolone actetonide implanted patients; scleral thickness measured at 3.5 mm posterior to sclera spur in four regions	Inferonasal 987 (770-1350) Inferotemporal 933 (630-1120) Superonasal 860 (660-1410) Superotemporal 881(670-1070)
Yoo <i>et al.</i> , (2010)	<i>In vivo</i> OCT in humans 2 mm posterior to the scleral spur in the temporal meridian	783.62 ± 57.03

Table 7.1 Previous measures of scleral thickness in humans by various investigators

In vivo studies: ^a distance of measurement unknown; ^b meridian of measurement unknown.

7.1.1 Anterior-Segment Optical Coherent tomography (AS-OCT)

Initially developed for assessing retinal structures *in vivo* (Huang *et al.*, 1991) OCT can also be used to evaluate the anterior segment structures of the eye (Izatt *et al.*, 1994). The basic principles of OCT are similar in concept to B-scan ultrasonography but instead of acoustic waves, light back reflected from ocular structures is utilized to form cross-sectional images of the ocular structures (van Velthoven *et al.*, 2007). The technique is based upon low coherent interferometry, where a light source is split into two beams, one a reference beam and the second reflected by the ocular structures (Ursea and Silverman, 2010). Coherent interference fringes are produced by varying the optical length of the reference beam and its interaction with the light reflected by the ocular tissues, to allow an image of the ocular structures to be produced (Wolffsohn and Peterson, 2006). Hoerauf *et al.*, (2000) first demonstrated the utility of a longer 1310 nm wavelength to provide images of the ciliary body and sclera with greater morphological detail than that of the 830 nm OCT systems. The hyper-reflectivity and light scattering within the sclera is a result of its variable refractive index due to the irregular collagen fibrils ($n=1.47$) and the ECM of mucopolysaccharides ($n=1.35$) (Maurice, 1962), which is intensified by the variation in the diameter of the collagen fibrils (Torczynski, 1988; Maurice, 1962; Müller *et al.*, 2007). Vogel *et al.*, (1991) reported that longer wavelengths of light improved scleral transmission, thus enabling enhanced transcleral imaging (Hoerauf *et al.*, 2002). Moreover

the ocular media absorbs 90% of the 1310 nm light before reaching the retina thus allowing the AS-OCT to use higher light intensities than retinal OCT hence reducing the signal-to-noise ratio and allowing the instrument to perform high speed image acquisition (Goldsmith *et al.*, 2005; Ursea and Silverman, 2010).

As a result of these findings the commercially available AS-OCT (*Visante*; Carl Zeiss Meditec, Dublin, California) uses a wavelength of 1310 nm, which allows improved penetration of the scleral tissue (Hoerauf *et al.*, 2000); however the iris blocks this wavelength thus restricting imaging behind the iris (Wolffsohn and Davies, 2007). The AS-OCT has been utilised in imaging various structures of the anterior segment: anterior chamber depth (ACD) and angle (Higashide *et al.*, 2009; Wang *et al.*, 2009), corneal thickness (CT) (Yazici *et al.*, 2010), ciliary body (Bailey *et al.*, 2008), iris and scleral spur characteristics (Piñero *et al.*, 2009; Sakata *et al.*, 2008; Liu *et al.*, 2010), lens thickness (Zeng *et al.*, 2009) and scleral thickness (Yoo *et al.*, 2010). The *Visante* AS-OCT produces cross-sectional images as either gray scale or false colour representation to depict differential backscattering contrast between the various components of the ocular tissue (Mohamed *et al.*, 2007). The instrument has an axial resolution of 18 μm and transverse resolution of 60 μm and offers a 16 mm x 6 mm scanning field (www.meditec.zeiss.com). The low-resolution images are generated from 256 A-scans in 125 ms and high-resolution images from 512 A-scans in 250 ms (*Visante* manual).

The imaging system of the AS-OCT is affected by variation in the refractive index and curvature of the eye (Izatt *et al.*, 1994; Radhakrishnan *et al.*, 2001). If the incident OCT beam is not perpendicular to the tissue over the whole area being scanned, refraction of the scanning beam occurs at the air-cornea and the cornea-aqueous interface (Radhakrishnan *et al.*, 2001; Goldsmith *et al.*, 2005). Therefore measurements are only accurate when the beam is perpendicular to the tissue and a correction factor is required during image processing for the off-axis distortion (see Appendix 12; Izatt *et al.*, 1994; Goldsmith *et al.*, 2005). In order to correct for this distortion, the *Visante* AS-OCT software attempts to identify the anterior and posterior corneal surfaces and applies a refractive index of 1.00 (air) to all structures in front of the anterior corneal surface, 1.388 (cornea) for all structures within the corneal section and 1.343 (aqueous) to all structures behind the back surface of the cornea (Richdale *et al.*, 2008; Lehman *et al.*, 2009). A recent study evaluated the accuracy of the *Visante* AS-OCT software and reported overestimation in the measurement of CT and ACD (Dunne *et al.*, 2007). The edge detection algorithms utilised

by the *Visante* are based on corneal parameters and can be manipulated to account for the refractive index changes of the ocular tissues as discussed later.

The *Visante* AS-OCT shows high levels of repeatability and reproducibility and compares well with other methods of imaging the anterior chamber dimensions (Wang *et al.*, 2009; Tan *et al.*, 2010), CT (Mohamed *et al.*, 2007, Wildner *et al.*, 2007) and lens thickness (Lehman *et al.*, 2009). In comparison to UBM the OCT has a number of advantages: OCT is a non-contact, non-invasive technique that offers superior spatial resolution than UBM (spatial resolution of 20-60 μm , with a depth penetration of 4 mm) (Radhakrishnan *et al.*, 2001). Additionally UBM is a contact technique that requires immersion of the eye and it is difficult to determine the exact location of the area being examined. Further, the requirement for contact may produce unknown distortion of the globe leading to inconsistency in the results (Baikoff *et al.*, 2004). The technique also requires a skilled examiner unlike the OCT, which utilises a simple PC-based operation system. Despite the many disadvantages of the UBM over the OCT its key advantage is its ability to image the ocular tissues behind the iris (Baikoff *et al.*, 2004; Garcia and Rosen, 2008).

AS-OCT has been used on the sclera by various investigators for a variety of purposes such as the imaging of scleral expansion bands for presbyopia (Wirbelauer *et al.*, 2003), assessing blebs in glaucoma patients (Singh *et al.*, 2007; Tominaga *et al.*, 2010), imaging foreign bodies (Garcia and Rosen, 2008), ocular trauma (Prakash *et al.*, 2009), assessment of sclerotomy sites (Guthoff *et al.*, 2010) and, more recently, for evaluating scleral thickness (Yoo *et al.*, 2010; Taban *et al.*, 2010).

7.2 Study objective

Due to the paucity of literature on scleral thickness, it is currently unknown whether anterior scleral thickness displays meridional differences. In light of the findings of Chapters 6, 8 and 10, regional variation in scleral resistance may be a correlate of differences in scleral thickness. The objective of the present study was to assess the reliability of the AS-OCT in measuring anterior scleral thickness and to evaluate scleral thickness in different meridians. As scleral biomechanics have been implicated in myopia development the present study also examines the variation in scleral thickness with refractive status.

7.3 Method

Seventy-five healthy individuals (150 eyes; 29 males and 46 females; 37 emmetropic and 38 myopic) aged between 18-40 years (27.8 ± 5.5) were assessed in the present study. Ethical approval and the exclusion/inclusion criteria followed those detailed in Chapter 6. The Zeiss *IOLMaster* and the Shin-Nippon auto-refractor were utilised as described in Chapter 6 to obtain ocular biometry and refractive error data for the present investigation.

7.3.1 Image acquisition

Scleral cross-sections were imaged in each subject using an AS-OCT (*Visante*; Carl Zeiss Meditec). Scleral images were acquired using the enhanced high-resolution corneal scan mode providing high transverse and axial imaging (transverse x axial) 10 x 3 mm cross-sectional images with a 512 x 1024 pixel resolution (Version 2) offered by the *Visante* software. Images were taken in 8 different meridians (superior (S); inferior (I), nasal (N), temporal (T), superior-temporal (ST), superior-nasal (SN), inferior-temporal (IT) and inferior nasal (IN)), which were imaged twice and acquired in a random order. To allow visualisation of the scleral sections, subjects were asked to look in eight different directions external to the instrument and maintain a steady gaze. The imaging plane was altered on the OCT depending on which meridian was being scanned. In the versional gazes where the lids impeded access to the sclera these were gently retracted by the patient to expose as much of the sclera as possible while ensuring that pressure was not exerted on the globe. Scleral sections up to approximately 7 mm from the limbus were accessed. In order to ensure optimal alignment between the image acquisition plane and the scleral section of interest, the *Visante* allows manipulation of the chin/headrest and image plane to ensure the anatomical features of interest were being imaged. The examiner observes a real-time image of the subject's eye on the video monitor, thus allowing easier manipulation and improved precision in alignment.

To obtain corneal pachymetry data from the *Visante* for subsequent comparison with the scleral thickness measurements, subjects were asked to fixate the instrument's internal fixation target. By manipulating the chin/headrest the reflex from the corneal apex was aligned with the centre of the measurement beam. On optimal alignment the subject was asked to keep his/her eyes wide open during the image capture. The global pachymetry scan protocol was chosen for assessment. The *Visante* system automatically processes 16

line scans and represents a map of the CT values. The average reading for the central 2 mm was taken for analysis.

7.3.2 Image processing

Due to the optical basis of the OCT technique, the images provided by the *Visante* are acquired in their raw state and are thus uncorrected for optical distortion produced by the respective refractive indices of tissues. Therefore to correct partially for this distortion, the *Visante* software applies a refractive index of 1.00 (air) to all structures before the anterior corneal surface, 1.388 (cornea) for all structures within the corneal section and 1.343 (aqueous) to all structures behind the back surface of the cornea (Richdale *et al.*, 2008; Lehman *et al.*, 2009). The *Visante* has a facility to change the refractive index in the ‘analysis’ mode. In this mode the correction lines applied by the software to the outer and inner surface of the image section can be seen. By dragging both lines to the bottom of the screen a refractive index of 1.00 is applied to the whole image, whereas dragging the anterior line to the top and the posterior line to the bottom applies a refractive index of 1.388 (Lehman *et al.*, 2009). In the present investigation two aspects of the images were being assessed: 1) scleral thickness changes along the length of the imaged section; 2) ciliary muscle thickness in the temporal and nasal meridians (see Chapter 13) (Figure 7.1). Therefore as the absolute refractive index of the sclera and ciliary muscle is unknown it was assumed that the 1.388 would provide a more optimised match than that using the refractive index of 1.00.

7.3.3 Scleral thickness measurements

Once the images were corrected for refractive index, the thickness measurements were performed in the ‘analysis’ mode. The *Visante* software provides seven callipers (with resolution increments of 10 μm) that can be used to measure the anatomical features imaged. These callipers can be freely moved over the screen and can be ‘hidden’ from view if required. All measurements were made manually by the same examiner (HP) using the protocol described below; the meridians were assessed in random order to avoid any order effects.

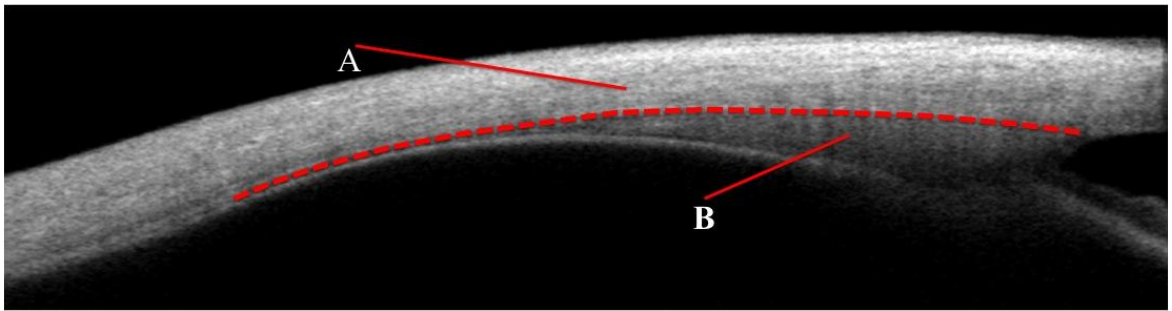


Figure 7.1 OCT image of temporal sclera and ciliary muscle. Dotted line delineates sclera (A) and ciliary muscle (B).

The scleral spur was initially identified as precisely as possible in each image to provide a reference point which appears as a prominent protrusion extending from the irido-scleral corneal junction (Liu *et al.*, 2010). In histological terms the scleral spur is located about 1.5 mm from the corneolimb junction but varies in its distance in different meridians (Hogan, 1971). Furthermore the location of the scleral spur varies between eyes and with refractive error being located more anterior in hypermetropes and more posterior in myopes (Spaeth, 2003). Hence for the purposes of comparison between meridians and individuals of varying refractive status, the scleral spur was assumed to be located 1 mm posterior to the corneolimb junction in all images assessed. Some variation was found between subjects in the quality of scleral spur visibility, therefore where images were unclear a mid point between the scleral spur was judged subjectively to be the reference point. Once the reference point was ascertained the calliper was extended perpendicularly to the outermost surface of the sclera and the lower section of the calliper moved to the innermost scleral surface independent of the respective curvature at the point of measurement (Figure 7.2). The interface between the hyper-reflective sclera and the less reflective episclera (i.e. the superficial hyporeflective layer constituting the conjunctiva, episclera and tenon's capsule) was considered to represent the outer surface and the delineation between the hyporeflective ciliary body considered to be the inner limit. The first scleral measurement (1 mm) was taken in this manner to avoid variability in judging the angle of the calliper relative to the local ocular surface. Thereafter another calliper was extended 1 mm along the scleral section and another measurement (i.e. designated the 2 mm measurement) was taken of the scleral thickness but with the calliper perpendicular to the scleral curvature. Using this method the 1 mm calliper was sequentially moved along the scleral section allowing scleral thickness measurements to be performed successively out to 7 mm from the scleral spur.

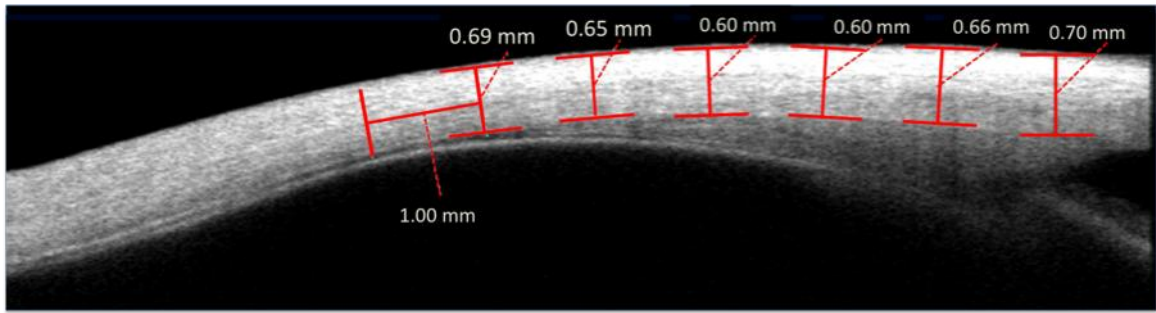


Figure 7.2 OCT image of the superior-temporal sclera; callipers (in red) shown for scleral thickness measurements for 6 mm along at 1 mm intervals.

The sclera appears as a hyper-reflective section in the OCT images and in turn the hypo-reflective ciliary muscle can be clearly defined below the sclera allowing ease of identification of their separate anatomical features (Figure 7.1). In the oblique scleral sections the extraocular muscle tendons were avoided; however in the cardinal directions these muscle tendons were occasionally visible. As the collagen characteristics of the muscle tendons is similar to that of the sclera (Hogan, 1971) and due to poor visibility and discrimination of the tendons in the posterior region of the scleral image sections, the full thickness of the scleral sections including the tendons were measured at these sites. Additionally, at times emissary blood vessels were observed in the scleral image sections; on these occasions the scleral thickness was not measured at those sites due to the effects of the blood vessels on the thickness measurement. Beyond approximately 7 mm the inner sections of scleral layer would show areas of inhomogeneous reflectivity, which may be due to the choroid and retinal pigment epithelium (Hoerauf *et al.*, 2002).

7.3.4 Intra- and inter-observer reliability of scleral thickness measurement

To assess the reliability and reproducibility of measuring scleral thickness with the AS-OCT, intraobserver and interobserver variability were examined. To assess the former, 7 images were taken of each of the 8 meridians for one subject. Implementing the above protocol for scleral thickness measurements, one examiner (HP) evaluated the images in a random order and was blind to the knowledge of which meridian was being evaluated.

Interobserver variability was evaluated by two examiners measuring the scleral thickness of 11 subjects. Two images were acquired for each of the 8 meridians, which were subsequently assessed by each examiner independently using the protocol described above.

Both examiners were masked to the results of the other tests and to which meridian were being measured.

7.4 Statistical procedures

Statistical evaluation was performed using *SPSS* version 15 for Windows (SPSS Inc, Chicago, IL) and Microsoft *Excel* (Microsoft Corporation, Redmond, Washington, USA). All data were initially examined for normal distribution using the Kolmogorov-Smirnov test.

To assess the intraobserver variability in scleral thickness measurements, the coefficient of variation (CoV) was calculated for each meridian and for each distance from the corneolimbic junction. CoV is an assessment of the proportional relationship between the standard deviation of the repeated measurements and the mean of these measurements (Campbell, 2007). A CoV of <10% is generally considered to represent good repeatability (Fleiss, 1981). In order to evaluate the interobserver variability the intraclass correlation coefficient (ICC) was evaluated for each meridian and distance. ICC was calculated using a two-way mixed ANOVA model, with a 95% confidence interval. *SPSS* calculates ICC as both single (i.e. only one examiner) and average (i.e. multiple examiners) values. In the present study only one examiner (HP) undertook the scleral thickness measurements, thus single ICC values were assessed. Additionally the ICC calculations can also be based on either absolute agreement or on a consistency measurement. Unlike absolute agreement, consistency measures of ICC do not take into account the systematic variability between examiners. In the present study the systematic variability due to the examiners was irrelevant hence the consistency measure was used.

To assess for differences in scleral thickness between meridians and distance from the corneolimbic junction two-way repeated measures ANOVAs were performed. Multiple three-way mixed repeated measures ANOVAs were performed with meridians and distance as the within-subject factor and between-subject factors as: refractive status, axial length, ethnicity, gender and age grouping. The influence of axial length on scleral thickness was assessed by splitting individuals into axial length (mm) subgroups: 1. (21.5 > - ≤ 23.5), 2. (23.5 > - ≤ 25.5), 3. (>25.5) and similarly the effect of age was evaluated by dividing the subjects into age (years) groups: (18 > - ≤ 29) and (29 > - ≤ 40). Pearson's product-moment correlation coefficient was used to test for relationships between scleral

thickness, CCT, refractive error and the ocular biometry parameters. For all statistical tests a p-value of <0.05 was taken as the criterion for statistical significance.

7.5 Results

7.5.1 Intraobserver variability

High levels of repeatability were found for all 8 meridians (superior (S), inferior (I), nasal (N), temporal (T), superior-temporal (ST), superior-nasal (SN), inferior-temporal (IT) and inferior nasal (IN)) and distances (1-7 mm) from the corneolimbic junction. For the meridians, lowest CoV% values were found for the T meridian and the highest values for IN and SN. In regards to distance from the limbus, greatest variability was found at the scleral spur (i.e. 1 mm distance) especially along meridian IT and least variability at 4 mm (Table 7.2).

Meridian	CoV (%) at distance from corneolimbic junction (mm)							Average CoV (%) for meridian
	1	2	3	4	5	6	7	
SN	6.69	5.21	7.89	4.03	4.20	3.77	6.06	5.41
S	3.86	3.75	4.69	4.22	2.13	2.93	3.62	3.60
ST	3.58	3.33	3.23	3.21	5.71	4.77	3.56	3.91
T	4.01	3.00	2.44	2.22	2.70	2.27	3.13	2.82
IT	7.93	3.20	3.15	2.30	3.77	2.79	3.11	3.75
I	4.83	4.34	3.79	5.81	5.86	6.18	2.65	4.78
IN	6.36	6.48	4.96	5.37	5.91	6.28	5.36	5.82
N	3.03	2.43	2.44	2.82	3.57	2.94	5.69	3.27
Average CoV (%) for distance	5.04	3.97	4.07	3.75	4.23	3.99	4.15	

Table 7.2 Intraobserver CoV (%) for the different meridians and distances from the corneolimbic junction.

A one-way repeated measures ANOVA with CoV% at the different distances as the within-subject factor revealed no significant difference between distances ($F(6, 42)=0.954$ ($p=0.468$)). A repeated measures ANOVA with meridional CoV% as the within-subject factors revealed a significant difference in CoV% between meridians ($F(3.036, 18.219)=5.494$ ($p=0.007$)) with a Bonferroni *post hoc* demonstrating the difference to be significant between IN and T; no other meridians were significantly different.

7.5.2 Interobserver variability

Single examiner ICC values for the interobserver variability demonstrated high levels of repeatability between examiners. Similar levels of repeatability were found for all meridians and distances, however the data indicated the scleral spur region to show the lowest levels of repeatability across all meridians. Similarly distances 4-5 mm along the nasal meridian showed lower levels of repeatability when compared to other meridians at the same distances.

Meridian	Distance from corneolimb junction (mm)						
	1	2	3	4	5	6	7
SN	0.820	0.954	0.913	0.904	0.900	0.891	0.960
S	0.865	0.941	0.967	0.986	0.927	0.954	0.854
ST	0.868	0.920	0.981	0.991	0.975	0.974	0.952
T	0.852	0.991	0.965	0.971	0.949	0.943	0.934
IT	0.870	0.980	0.968	0.939	0.917	0.927	0.822
I	0.921	0.897	0.926	0.966	0.934	0.934	0.923
IN	0.920	0.901	0.993	0.984	0.967	0.982	0.977
N	0.941	0.945	0.926	0.727	0.858	0.936	0.961

Table 7.3. ICC values for scleral thickness values.

A one-way repeated measures ANOVA with ICC at different distances as the within-subject factors revealed no significant differences between distances ($F(2.256, 15.792)=1.918$ ($p=0.177$)). Similarly a one-way repeated measures ANOVA with meridional ICC as the within-subject factors revealed no significant difference between meridians ($F(2.256, 13.536)=1.445$ ($p=0.272$)).

7.5.3 Differences in scleral thickness between meridians and location of measurement

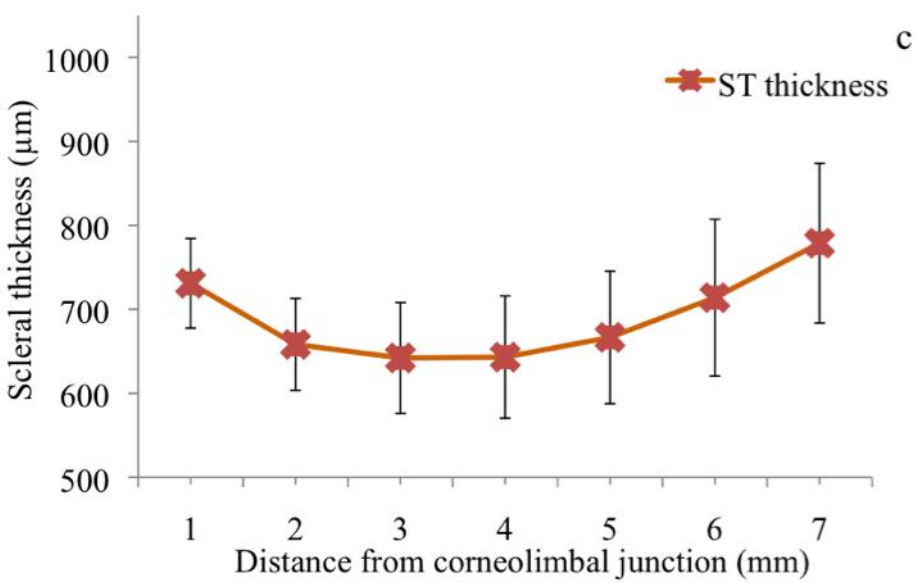
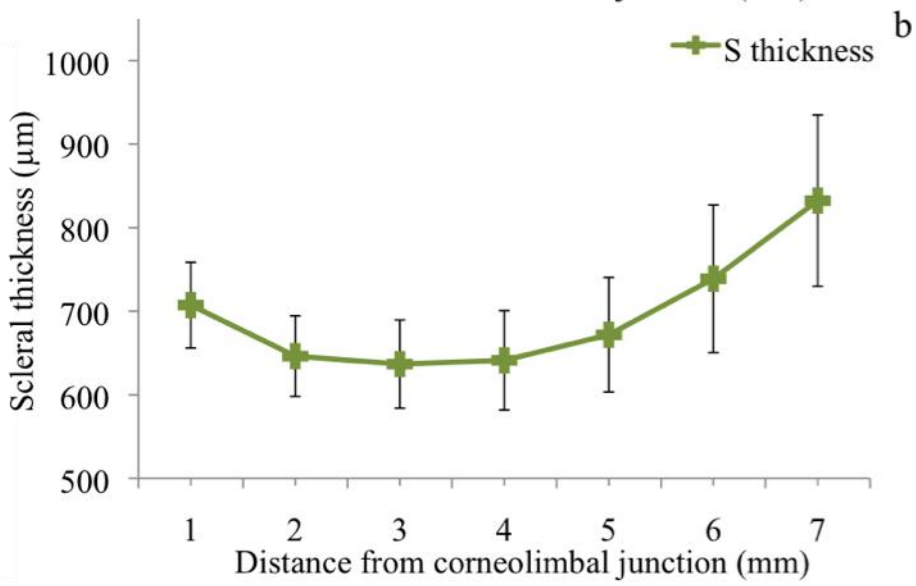
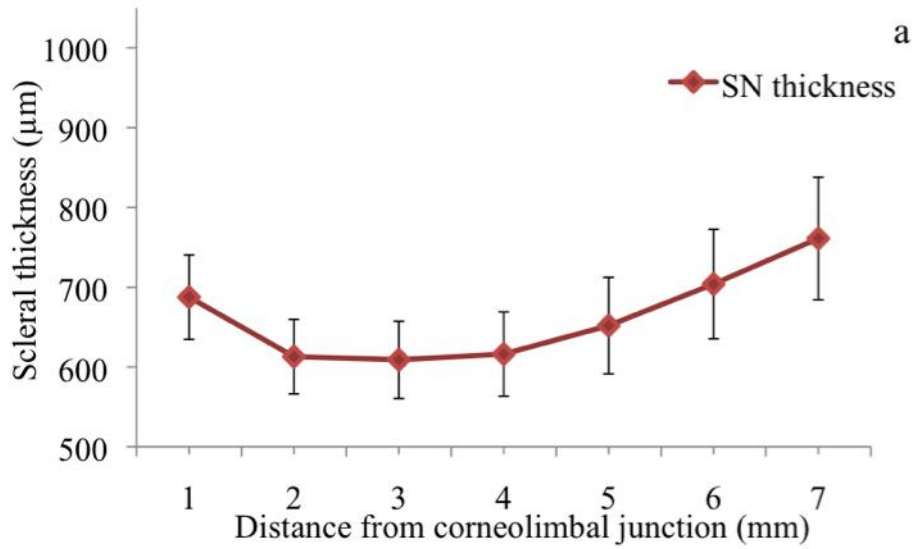
The data were analysed for non-myopic and myopic individuals [non-myopes (MSE ≥ -0.50) $n=37$ MSE (D) mean \pm SD (0.49 ± 1.08), range (-0.50 to +4.38), AL (mm) mean \pm SD (23.33 ± 0.72), range (21.61 - 24.74); myopes (MSE <0.50) $n=38$ MSE (D) mean \pm SD (-4.65 ± 4.09) range (-0.51 to -20.50), AL (mm) mean \pm SD (25.28 ± 1.28), range (23.33 - 28.32)].

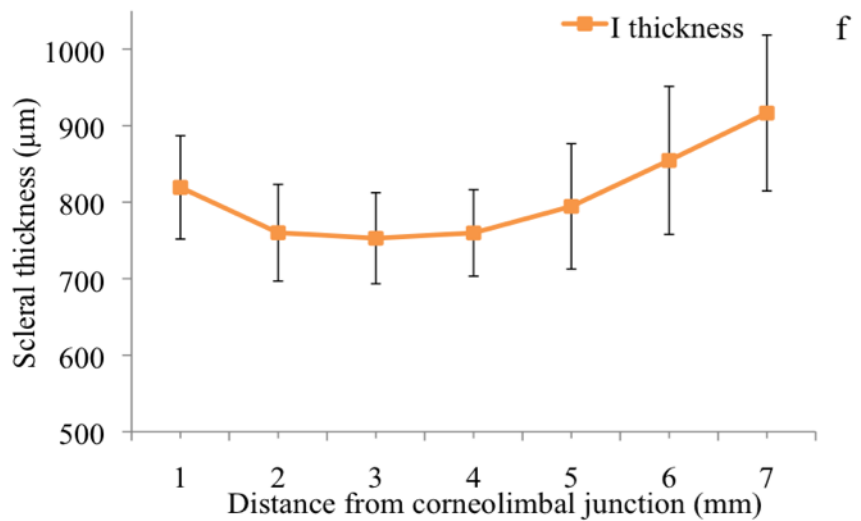
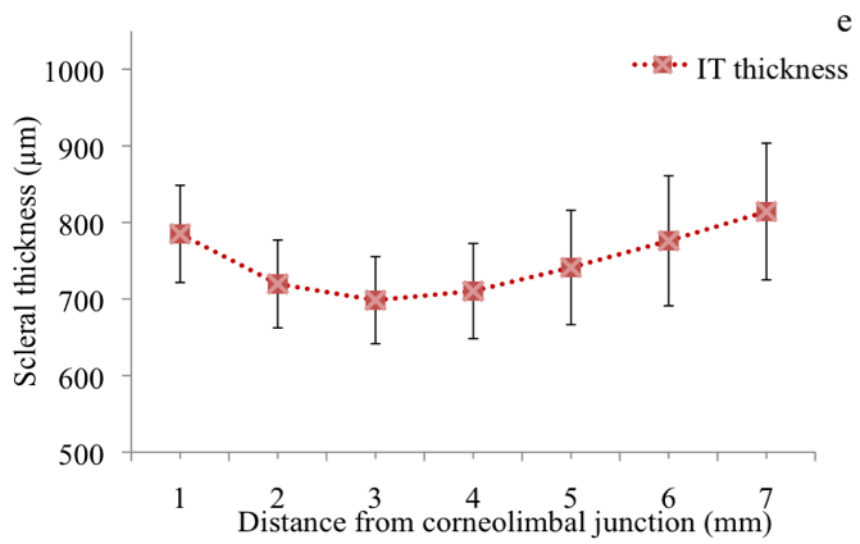
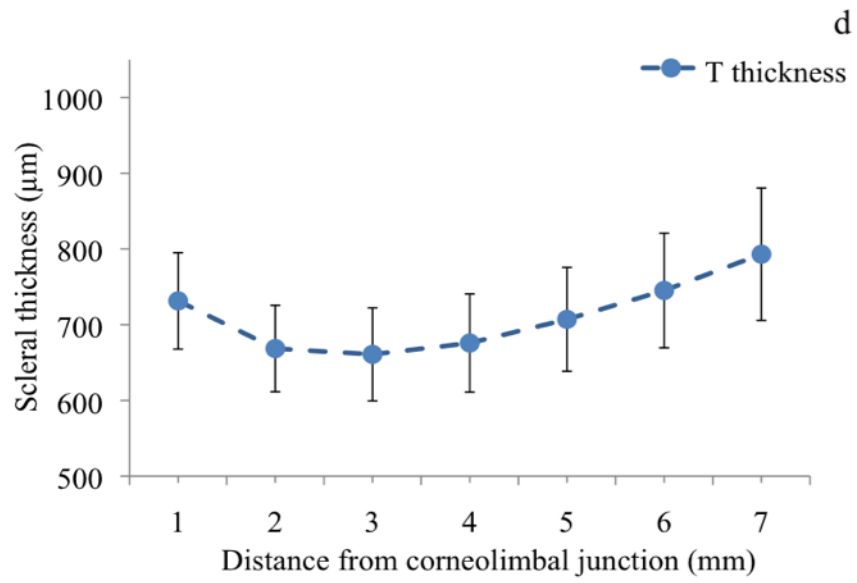
A two-way repeated measures ANOVA was performed to test the main effect of meridian and the distance (mm) of measurement on the scleral thickness. The analysis revealed a

significant effect for the main factor meridian ($F(5.581, 346.038)=125.275$, ($p<0.001$)), with a Bonferroni *post hoc* demonstrating a significant difference between all meridians except between S:ST, IT:IN, IT:N and IN:N. Additionally, a significant effect was also found with the distance of measurement ($F(1.682, 104.295)=177.988$ ($p<0.001$)), with a Bonferroni *post hoc* showing significant differences between all distances except between 1 mm and 6 mm and between 2 mm and 4 mm. Furthermore a significant interaction effect was found between meridians and distance of measurement ($F(11.877, 736.401)=15.403$ ($p<0.001$)), indicating that scleral thickness at any particular distance (1-7 mm) would vary with the meridian being examined (see Table 7.4 and Figures 7.3 (a-h) and 7.4).

Meridians	Distance from corneolimbic junction (mm)							Average thickness
	1	2	3	4	5	6	7	
SN	687 ± 52	613 ± 46	609 ± 48	616 ± 52	651 ± 60	704 ± 68	761 ± 76	663 ± 57
S	707 ± 51	646 ± 48	636 ± 52	641 ± 59	671 ± 68	738 ± 88	832 ± 103	696 ± 71
ST	731 ± 53	658 ± 54	642 ± 65	643 ± 72	666 ± 78	713 ± 93	778 ± 95	691 ± 52
T	731 ± 63	668 ± 57	660 ± 61	675 ± 64	707 ± 68	745 ± 75	793 ± 87	712 ± 48
IT	785 ± 63	719 ± 57	698 ± 56	710 ± 62	741 ± 74	776 ± 84	814 ± 89	749 ± 43
I	819 ± 67	760 ± 63	752 ± 59	759 ± 56	794 ± 81	854 ± 96	916 ± 101	808 ± 60
IN	781 ± 67	724 ± 63	717 ± 58	733 ± 65	768 ± 80	797 ± 88	825 ± 86	764 ± 41
N	699 ± 62	675 ± 62	691 ± 61	713 ± 56	746 ± 58	790 ± 69	846 ± 90	738 ± 62
Average thickness	743 ± 47	638 ± 48	676 ± 47	687 ± 51	719 ± 52	765 ± 50	821 ± 48	728 ± 47

Table 7.4 Measurements of scleral thickness for each meridian and distance from the corneolimbic junction (mean ± SD (µm)).





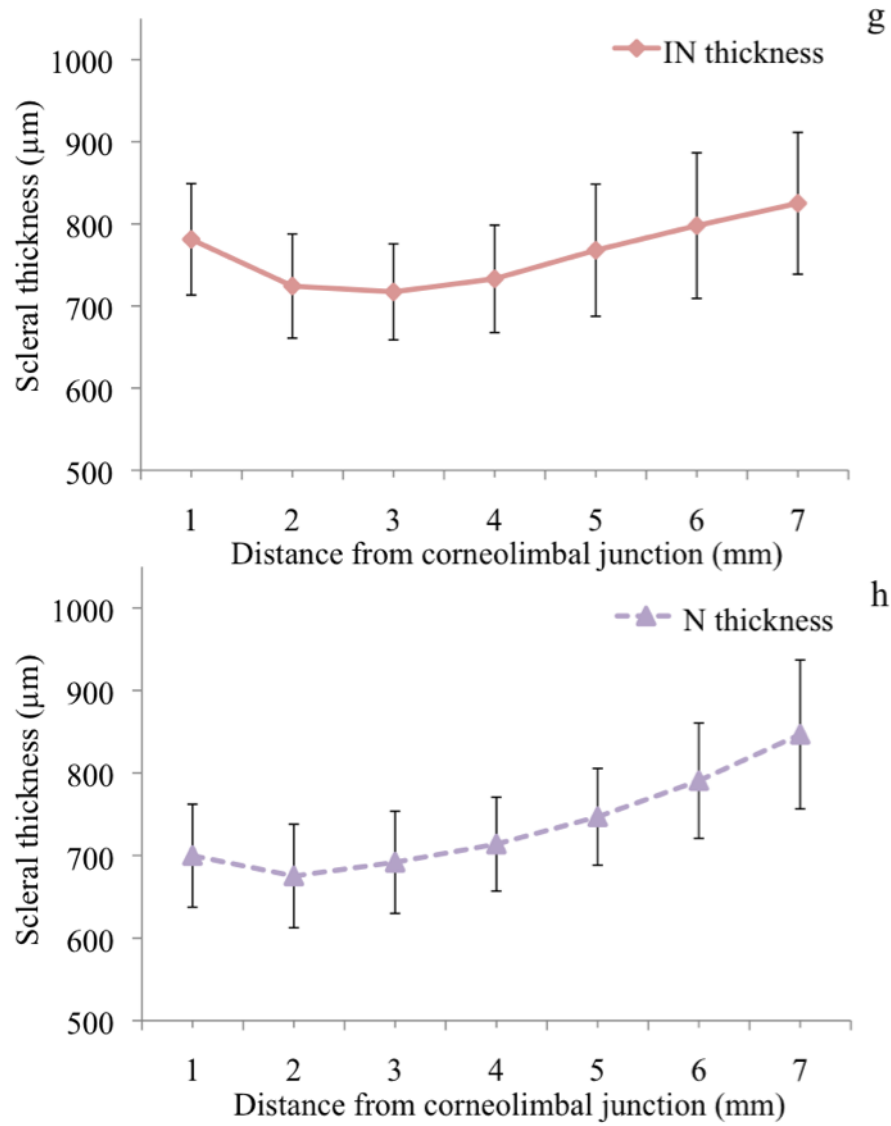


Figure 7.3 (a-h) Scleral thickness mean \pm SD (error bars) from 1-7 mm for meridians SN, S, ST, T, IT, I, IN and N.

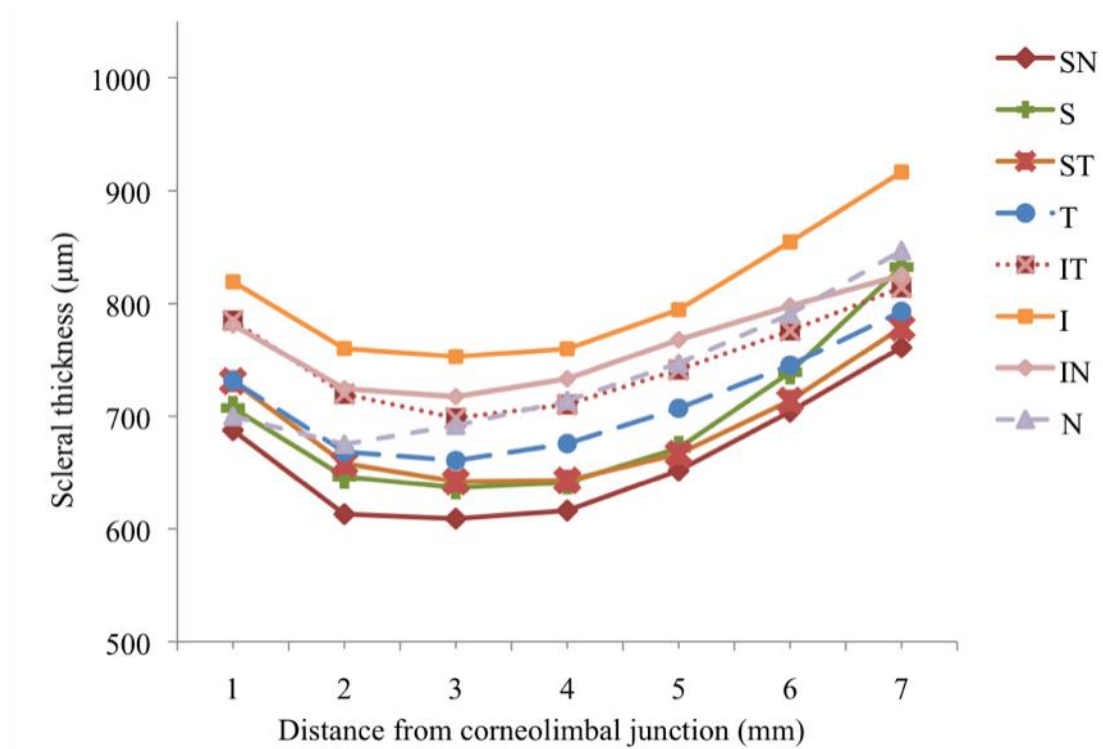


Figure 7.4. Scleral thickness for all 8 meridians from 1-7 mm.

7.5.4 The effect of various parameters on scleral thickness

7.5.4.1 Gender

In order to assess whether gender affects scleral thickness, a three-way mixed repeated measures ANOVA was performed with gender (males $n=23$, females $n=40$) as the between-subject factor and meridian and distances of measurement as within-subject factors. The analysis revealed a statistically significant difference between males and females ($F(1, 61)=15.311$ ($p<0.001$)), with males showing greater overall thickness than females (Figure 7.5 a-b). Additionally, significant differences between meridians ($F(5.551, 338.60)=116.503$ ($p<0.001$)) and distances of measurement ($F(1.659, 101.206)=170.964$ ($p<0.001$)) were still found, with a significant interaction between these two main factors. No significant interaction was found between the main factors gender and meridian; gender and distance of measurement; gender, meridian and distance of measurement.

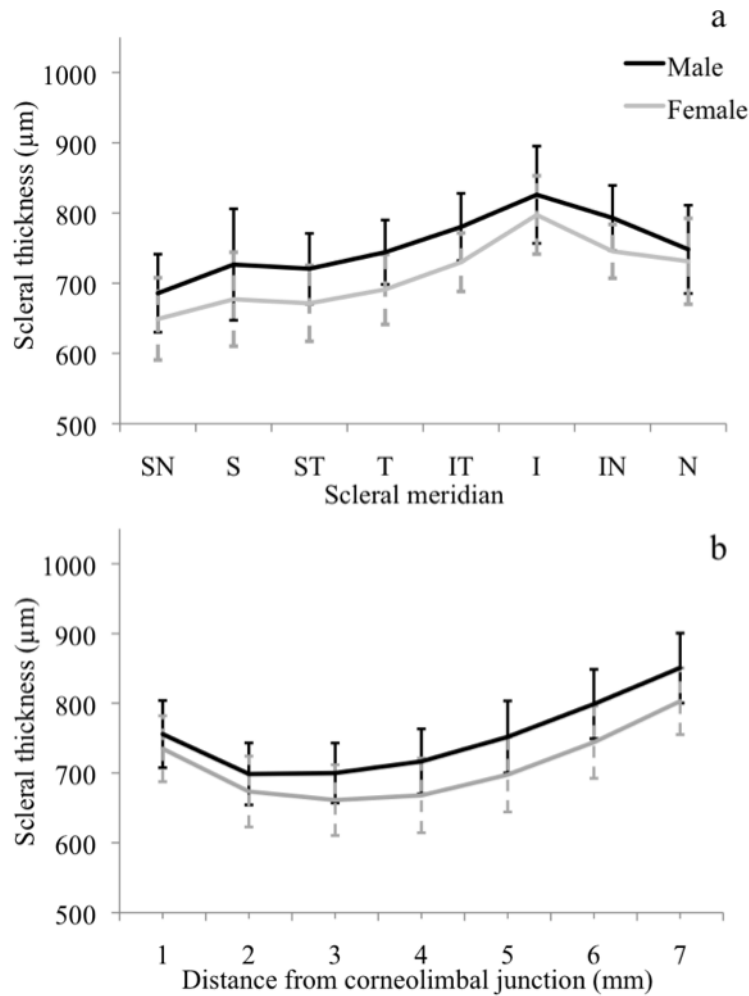


Figure 7.5 Scleral thickness changes in males and females **a)** with meridian and **b)** with distance from corneolimbic junction.

7.5.4.2 Refractive status

To test for the influence of refractive status on scleral thickness, a three-way mixed repeated measures ANOVA was performed with refractive status (myopes $n=32$, non myopes $n=31$) as the between-subject factor, whilst meridian and distance of scleral thickness measurement were within-subject variables. The analysis demonstrated a non-significant main effect of refractive status ($F(1, 61)=2.500$ ($p=0.119$)) on scleral thickness. A significant effect of meridian differences ($F(5.576, 340.145)=123.862$ ($p<0.001$)), and distance of measurement ($F(1.688, 102.975)=177.202$ ($p<0.001$)) was identified, with a significant interaction between the two variables ($F(12.070, 736.242)=15.495$ ($p<0.001$)). Refractive status failed to show any significant interaction with meridian, distance of measurement or with the combined effect of meridian and distance of measurement.

7.5.4.3 Axial length

A three-way mixed repeated measures ANOVA was performed to test the influence of axial length (mm) grouping (group 1 ($21.5 > - \leq 23.5$) $n=22$, group 2 ($23.5 > - \leq 25.5$) $n=28$, group 3 (>25.5) $n=12$) on scleral thickness; with axial length group as the between-subject factor and meridian and distance of measurement as the within-subject factors. No significant main effect was found for axial length grouping ($F(2, 59)=0.980$ ($p=0.907$)). A statistically significant effect persisted for both meridians ($F(5.603, 330.550)=107.010$ ($p<0.001$)) and distance of measurement ($F(1.675, 98.823)=154.000$ ($p<0.001$)) with a significant interaction between the two ($F(11.647, 687.145)=12.898$ ($p<0.001$)). Axial length showed no significant interaction with meridian or distance of measurement nor with the combined effect of meridian and distance of measurement.

7.5.4.4 Age grouping

To test for the influence of age on scleral thickness, a three way mixed repeated measures ANOVA was performed with age (years) group (group 1 ($18 > - \leq 29$) $n=44$, group 2 ($29 > - \leq 40$) $n=19$) as the between-subject factor and meridian and distance as the within-subject factors. No significant main effect was found for age grouping ($F(1, 61)=0.774$ ($p=0.382$)). Meridional differences ($F(5.601, 341.631)=102.904$ ($p<0.001$)) and distance of measurement ($F(1.663, 101.416)=144.774$ ($p<0.001$)) showed a significant effect on thickness measures, with a significant interaction between the two factors ($F(11.938, 728.213)=12.453$ ($p<0.001$)). Age grouping showed no significant interaction between the main factors of meridian and distance of measurement, or between the combined effect of meridian and distance of measurement.

7.5.4.5 Ethnicity

To test for an influence of ethnicity on scleral thickness, a three way mixed repeated measures ANOVA was performed with ethnicity (British White (BW) $n=40$, British South Asian (BSA) $n=23$) as the between-subject factor and meridian and distance of measurement as the within-subject factors. No significant main effect was found for ethnicity ($F(1, 61)=2.417$ ($p=0.125$)), however a weak trend for increased scleral thickness amongst the BSA individuals was noted. The main factors meridian ($F(5.585, 340.656)=117.894$ ($p<0.001$)) and distance of measurement ($F(1.661, 101.351)=166.930$ ($p<0.001$)), demonstrated a significant effect on scleral thickness measures with an

interaction effect between the two factors ($F(11.843, 722.412)=13.829$ ($p<0.001$)). Furthermore a significant interaction effect was noted between the main factors meridian and ethnicity ($F(5.585, 340.656)=3.489$ ($p=0.003$)), which on assessment of the interaction plot demonstrated meridians ST and T to behave differently between the BW and BSA individuals. No significant interaction was found between distance of measurement and ethnicity, however a significant interaction was found between ethnicity, meridian and distance ($F(11.843, 722.412)=2.601$ ($p=0.002$)).

7.5.5 Additional ocular biometric parameters

Independent Student *t test* analyses revealed no significant difference in ocular biometric parameters (i.e. refractive error, axial length, central corneal thickness (CCT), ACD and corneal curvature) between gender, age group and ethnicity. Only ACD was found to be affected by refractive status ($p<0.001$) with myopes showing deeper ACD than non-myopes. Similarly a one-way ANOVA revealed significant differences ($F(2, 73)=9.093$ ($p<0.001$)) in ACD between axial length groups 1 and 2 and groups 1 and 3.

7.5.5.1 Scleral thickness and additional ocular biometric parameters

Several correlations were observed between scleral thickness and axial length. In particular meridians S (3 mm), I (1 mm) and IT (3 mm) demonstrated significant positive correlations with axial length, whilst refractive error showed a negative association with scleral thickness along the S (3mm), ST (1-2 mm) and the I (1 mm) meridians. CCT also correlated negatively with scleral thickness along the SN (3-4 mm), S (4-6 mm), ST (4-6 mm), IT (4-5 mm) and I (5 mm) meridians. See Appendix 4 for further details.

7.6 Discussion

The present study evaluated the application of AS-OCT to measurement of anterior scleral thickness in different meridians *in vivo*. Intra- and inter-observer reliability for scleral thickness measurements was found to be excellent for all meridians and distances from the sclera spur. The investigation demonstrated the novel findings of significant differences in scleral thickness between different meridians except between S:ST, IT:IN, IT:N and IN:N. Furthermore the study showed substantial differences in scleral thickness between males and females with males showing significantly greater overall thickness than females. Ethnicity was also found to modulate differences in scleral thickness between meridians, with meridians ST and T demonstrating different behaviour between BSA and BW individuals. To date, as far as the author is aware this is the largest study to assess meridional variation in scleral thickness *in vivo*.

7.6.1 Reliability and reproducibility of measurement of scleral thickness

High levels of intra- and inter-observer repeatability were found in the scleral thickness measurements for the various meridians and distances from the corneolimbus junction. These results are concordant with the findings of a recent OCT study by Yoo *et al.*, (2010) who similarly evaluated the reliability of measuring scleral thickness *in vivo* along the temporal meridian. The investigators reported high interobserver ICC values of 0.902, which are consistent with the ICC value of 0.965 for the equivalent location in the current study. Furthermore the present study also demonstrated the reproducibility of scleral thickness measurements to fluctuate between meridians and distance of measurement from the corneolimbus junction. These differences were found to be significant for intraobserver variability between meridians IN and T; however no other significant differences were found for either intra- or inter-observer reliability.

The disparity in the reproducibility of scleral thickness measurement between different locations may be attributable to factors such as lid coverage in the various gazes. In particular, when imaging the gaze positions where lids had to be retracted, differences in lid position may have led to variation in the section of sclera imaged, which may have particularly affected the intra-observer reproducibility as multiple images were evaluated. In both OCT and UBM imaging the subjective nature of the calliper placement in manual measurement will inevitably produce some variability in the data acquired. Additionally

both techniques rely on location of the scleral spur as a reference point when taking measurements and hence discrepancy in scleral spur visibility may partly explain the inconsistency in measurements between meridians and distances. Pertinent to this, Sakata *et al.*, (2008) reported poor visibility of the scleral spur superiorly with successively increasing visibility for the inferior, nasal and temporal quadrants. Contrary to these findings Liu *et al.*, (2010) reported the inferior angle to show the worst visibility and the nasal to show the best. Despite these discrepancies, the studies demonstrate that anatomical differences in scleral spur location can affect image quality and may explain the decreased levels of repeatability found at the 1 mm (i.e. scleral spur) location. Moreover, it is also likely that localised scleral physiological changes such as fibrosis, thinning and contraction may affect the collagen fibril arrangement which would consequently affect the optical properties of the sclera and hence alter its image clarity (Hoerauf *et al.*, 2002).

The present values of inter-observer reproducibility compare well with other *in vivo* methods of measuring scleral thickness. In comparison to UBM for similar locations of measurement, the OCT shows improved repeatability with higher ICC values (Oliveira *et al.*, 2006; Tello *et al.*, 1994). This superior repeatability in the scleral thickness measurements in comparison to UBM is likely to be attributable to the improved image resolution provided by the OCT, thus allowing more consistent and reliable identification of ocular structures.

In regards to intra-observer reproducibility, Tello *et al.*, (1994) assessed UBM measures of scleral thickness at the scleral spur (meridian not identified) and reported higher levels of intraobserver reliability (i.e. CoV 1.1% to 2.2%) than those of the present study (i.e. 5.04%). The poorer level of repeatability is likely to be a result of differences in protocol. In the Tello *et al.*, (1994) study the same images were assessed on five occasions by three examiners to derive intraobserver reproducibility; in the present study, in order to assess both the variability in imaging as well as intra-observer reproducibility, seven images of the same meridian were taken and each assessed independently by one examiner. Therefore differences in physiological parameters (e.g. accommodation), differences in lid coverage, variation in gaze, and image acquisition plane may have contributed towards differences in the levels of repeatability and reproducibility of the scleral thickness measurements.

7.6.2 Comparison of present results to previous reports of scleral thickness

Due to technical limitations many of the previously published studies assessing scleral thickness *in vivo* have been restricted to examining a few specific locations along the temporal meridian (Oliveira *et al.*, 2006; Mohamed-Noor *et al.*, 2009) see Table 7.1. ***The results of the present study show some differences in the scleral thickness measurements when compared to these previous investigations.***

In regards to the temporal meridian, for values 1 mm posterior (i.e. the scleral spur) to the corneolimbic junction the present scleral thickness values are similar to those of Oliveira *et al.*, (2006), although lower than those of Pavlin *et al.*, (1992) (Figure 7.6). At the 2 mm site the Oliveira *et al.*, (2006) results are lower than those of the present study, whereas as at 3 mm (2 mm from scleral spur) the Oliveira *et al.*, (2006) values are considerably thinner than the present results and those of Mohamed-Noor *et al.*, (2009) and Yoo *et al.*, (2010). At 3.5 mm posterior to the scleral spur, Taban *et al.*, (2010) reported higher values of scleral thickness for the inferior-nasal, inferior-temporal, superior-nasal and superior-temporal regions when compared to the equivalent meridians and 3-4 mm distances in the present study. In contrast the average scleral thickness for 4 mm along the 12, 3, 6 and 9 o'clock meridians reported by Lam *et al.*, (2005) are substantially lower than those of the present study. In comparison to *in vitro* studies that have provided average measures of scleral thickness at the vicinity of the limbal region, Elsheikh *et al.*, (2010) demonstrated comparable values to the present study although both Norman *et al.*, (2009) and Olsen *et al.*, (1998) showed considerably lower values of thickness.

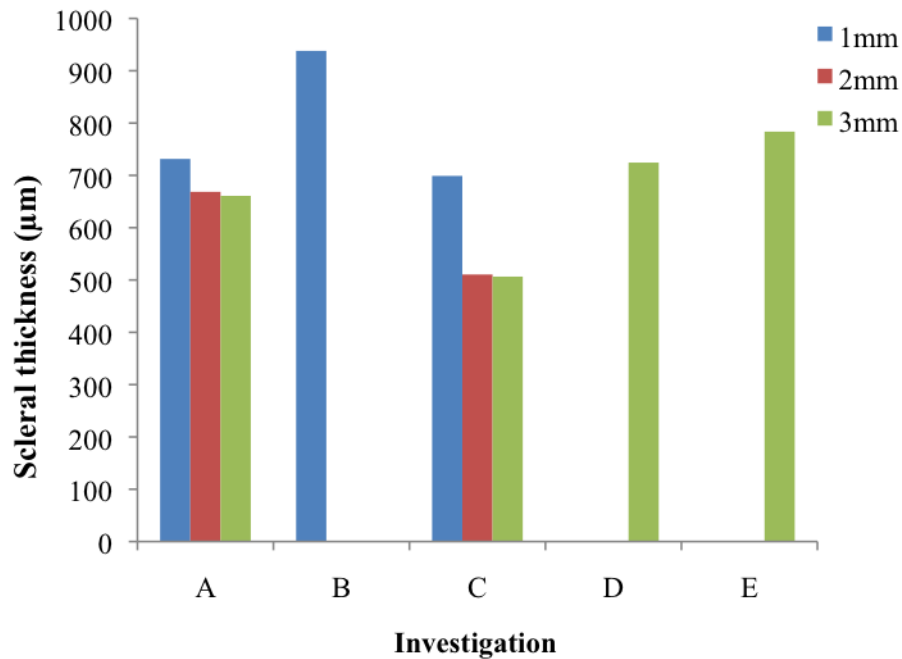


Figure 7.6 Comparison of present (A) measures of scleral thickness along the temporal meridian at 1-3 mm distance to previous studies; B (Pavlin *et al.*, 1996), C (Oliveira *et al.*, 2006), D (Mohammed-Noor *et al.*, 2009) and E (Yoo *et al.*, 2010). (Only studies with location and distances from corneolimbus junction equivalent to the present investigation are included).

On examination of Table 7.1 it is evident that substantial variation in scleral thickness exists between investigations. These discrepancies are likely to be a result of numerous factors. Inherent variations in the imaging devices are expected to introduce some discrepancies between studies. In UBM it is often difficult to know the exact location of the anatomy being imaged; therefore it is possible that slight deviations in location may contribute to the inconsistency between investigations (Pekmezci *et al.*, 2009; Baikoff *et al.*, 2004). Furthermore in UBM external compression due to the technique employed could produce slight distortion of the anterior segment (Baikoff *et al.*, 2004) and may thus be partly responsible for the variability in the results. In regards to the OCT, non-linear variations in refractive index across tissues may result in image warping. Despite the *Visante* software providing an approximate correction for this error, there is no set protocol for evaluating off-axis images and tissues other than the cornea (see Appendix 12). Hence differences in study protocol as to whether a correction factor was applied or not, may lead to significant differences in thickness measurements. Furthermore differences in the protocol for measurement of scleral thickness (e.g. whether the episclera was included in the measurement or not), could also affect the results. Previously, studies measuring

corneal thickness with OCT and ultrasound pachymetry have reported OCT to give lower pachymetry values than those of ultrasound (Ho *et al.*, 2007; Zhao *et al.*, 2007; Li *et al.*, 2007). Similarly when comparing UBM and OCT measures of anterior chamber angle the two techniques show significant correlation but poor agreement between their mean values (Mansouri *et al.*, 2010). Additionally, the use of ultrasound pachymetry *in vivo* to measure scleral thickness is likely to be affected by underlying structures such as the ciliary body and choroid, and is thus liable to provide erroneous measurements (Schmid *et al.*, 2003).

A significant limitation of all *in vitro* methods of assessing scleral thickness is the affect of autolysis (i.e. enzymatic digestion of cells by enzymes present within them) of tissue (Greene and McMahon, 1979). Since the objective of such experiments is to explore the properties of the ocular tissue material the affects of autolytic enzymes such as collagenase, which breaks down collagen fibres, needs to be considered. Furthermore, Gilger *et al.*, (2005) reported scleral thickness to be substantially affected by formalin fixation, with fixed tissues showing significantly thinner sclera when compared to fresh tissue. Moreover many such *in vitro* studies require sections of the ocular tissue to be cut from the globe following freezing or fixation, which may introduce further artefactual changes (Asejczyk-Widlicka *et al.*, 2008b).

7.6.3 Meridional variation in scleral thickness

The present study also assessed meridional differences in scleral thickness *in vivo*. As mentioned afore few studies have evaluated variation in scleral thickness in different meridians due to technical limitations (Lam *et al.*, 2005; Mohammed-Noor *et al.*, 2009). More recently in an OCT study, Taban *et al.*, (2010) assessed scleral thickness in patients implanted with fluocinolone acetonide steroid implants to treat chronic posterior uveitis. The study evaluated the effects of the implant on scleral thickness by measuring thickness at the implant site in four regions (ST, SN, IT and IN) in patients with uveitis and in healthy individuals. Interestingly, the study reported non-uniform scleral thickness with significantly increased thickness for the IN region in all subjects. Furthermore, a trend for decreasing scleral thickness from IN followed by IT, ST and SN was reported. These results support the present findings of heterogeneous scleral thickness across different locations on the globe. In the current study, although a difference in thickness between most meridians was demonstrated no significant distinction could be found between S:ST, IT:IN, IT:N and IN:N. The close proximity of each of these meridians and the

correspondence in structure between adjacent areas of sclera no doubt accounts, at least in part, for their similar thickness.

Furthermore, recently a number of investigators have measured scleral thickness *in vitro* in human eyes (see Table 7.1). Elsheikh *et al.*, (2010) measured scleral thickness using ultrasound pachymetry in eight different meridians (equivalent the meridians assessed in the present study) from the posterior pole to the limbus. The study demonstrated significant differences between anterior, equatorial and posterior scleral thickness but failed to find any significant differences between the 8 meridians. The results showed the oblique meridians (ST, SN, IT and IN) to exhibit greater thickness than the cardinal meridians (S, I, T and N) at 4-6 mm from the pole. As scleral thickness was found to vary significantly between the anterior, equatorial and posterior aspects of the globe, these larger changes in scleral thickness may have overshadowed the meridional differences in scleral thickness. As such the more subtle differences in scleral thickness between the meridians may not have been detected by the resolution offered by ultrasound pachymetry.

In an MRI study Norman *et al.*, (2009) measured scleral thickness *in vitro* in enucleated normal and ostensibly glaucomatous human eyes. The study reported significant intra- and inter- individual differences in scleral thickness and a non-significant trend for differences in thickness between the quadrants (S, I, T and N). In regards to the anterior scleral region (i.e. ~7 mm from the limbus) the results suggest that the I quadrant has the greatest thickness followed by the N, T and S quadrants. The investigators additionally reported the I scleral quadrant to exhibit, unlike the other regions, thickening near the equator.

In addition to the human *in vitro* studies, porcine scleral thickness has also been investigated previously, as porcine sclera has been found to be analogous to human sclera (Olsen *et al.*, 2002). In an OCT study, Asejczyk-Widlicka *et al.*, (2008b) reported *in vitro* porcine eyes to show greater variability in anterior scleral thickness in comparison to a more constant thickness for the posterior section; however the variability was found to be smaller than that following formaline fixation (Olsen *et al.*, 2002). ***Hence on reviewing the literature on scleral thickness, it is evident that many investigators have proposed meridional differences in anterior scleral thickness but due to differences in the study protocols i.e. in vitro conditions and location of scleral thickness measurements, these differences may not have been as discernible as in the present study.***

7.6.4 The effect of distance from the corneolimbic junction on the scleral thickness profile

In regards to changes in scleral thickness with distance from the limbus, numerous studies have found the scleral thickness to be greatest at the posterior pole, with a gradual reduction to a minimum close to the equator (i.e. 12-17 mm posterior to the limbus) followed by a steady increase towards the limbus (Elsheikh *et al.*, 2010; Norman *et al.*, 2009; Olsen *et al.*, 1998; Curtin, 1969). In the present study the changes in scleral thickness were measured between 1-7 mm from the corneolimbic junction. The general trend for all meridians indicates an initial decline from 1 to 2 mm and then a gradual increase from 3 mm onwards (Figure 7.4). Olsen *et al.*, (1998) demonstrated a similar trend with a gradual decline in scleral thickness from the limbus to approximately 6 mm, whereafter the thickness increased between 6-8 mm and but then continued to reduce towards the equator. Olsen *et al.*, (1998) suggested that a slight increase in scleral thickness in the 5-10 mm range might have been a result of insertion points of the recti muscles. Indeed this may account for the trend for increasing thickness from 3 mm onwards found in the present study although the vicinity of muscle insertion points does not affect all of the meridians assessed. Norman *et al.*, (2009) evaluated inter-quadrant differences in scleral thickness by assessing the average thickness for each quadrant from the limbus to the posterior pole. Inspecting their data for the anterior region pertinent to the present study demonstrates similar fluctuations in scleral thickness with increasing distance from the limbus. Hence it is envisaged that if each meridian had been assessed independently then the trend found in the present study may have been more evident.

As mentioned afore, in their *in vitro* study, Elsheikh *et al.*, (2010) reported significant differences in scleral thickness between the anterior, equatorial and posterior regions for all 8 meridians. The data from the Elsheikh *et al.*, (2010) study also suggests a trend for scleral thickness to reduce from the limbus to approximately 7 mm along the S, N, I and T meridians. Additionally, it is also apparent from their results that the gradient of decline in thickness up to 7 mm varies between meridians; the I and N meridians showed a similar decline in thickness, whereas the S meridian showed the greatest initial thickness and reached a minimum after 7 mm. In turn the T meridian failed to show as much thinning as the other meridians and actually showed an increase in thickness before 7 mm. In comparison, the oblique meridians (SN, IN, IT, ST) showed some fluctuation in their thickness up to 7 mm but appeared to behave in different ways; IT and ST appeared to

initially increase and then decline, whereas SN showed no thinning but a gradual increase in its thickness. In contrast IT showed a gradual decline to 7 mm and then increased in thickness. *These fluctuations and distinct differences in the profile of change in scleral thickness between the different meridians observed by Elsheikh et al., (2010) further support the present findings of meridional differences as well as significant variation in scleral thickness with distance from the limbus.*

7.6.5 The effect of axial length and refractive error on scleral thickness

In the present study no significant effect of axial length or refractive status was found on scleral thickness although numerous significant correlations of note were found. In particular axial length was positively correlated and refractive error negatively correlated with scleral thickness along the S meridian at 3 mm and with the I meridian at 1 mm. Additionally refractive error was found to correlate negatively with scleral thickness along ST (at 1 and 2 mm) meridian, whereas axial length was found to be positively correlated with thickness along IT (at 3 mm) meridian. In support of these findings Oliveira *et al.*, (2006) reported scleral thickness along the T meridian (at 1, 2 and 3 mm) to correlate positively with increasing axial length and with myopic refractive error. Contrary to these findings Yoo *et al.*, (2010) found no significant correlation between scleral thickness along the T meridian and axial length. These equivocal findings are contrary to the widely held supposition that the anterior sclera is independent of myopic growth. Indeed the finding of posterior scleral thinning in myopic eyes has been widely documented (Curtin, 1985; Guthoff *et al.*, 1987) although little is known of the affects on the anterior segment sclera.

The present study indicates that, as axial length increases, there is a concomitant increase in scleral thickness superiorly at 3 mm and inferiorly at 1 mm. In relation to ocular shape this may suggest greater resistance to stretching in the vertical meridian compared to the horizontal meridian in the anterior segment. Atchison *et al.*, (2005) reported most eyes to exhibit an oblate conformation, whilst myopic eyes show a greater tendency towards a relatively more prolate shape. These findings of structural differences between refractive status suggest that the ocular conformation may change with axial length expansion. In light of the present findings it may be possible to speculate that with increasing axial growth the greater scleral thickness at the superior and inferior meridians may provide an anchorage to the stretching mechanism, thus allowing the equatorial and posterior regions to stretch into a prolate conformation.

It is uncertain as to whether anterior segment changes contribute towards refractive error development (Mutti, 2010; Nomura *et al.*, 2004; Song *et al.*, 2008; McFadden *et al.*, 2010). Despite these equivocal reports, the results of Chapters 11, 13 and 14 present evidence for an association between axial length and anterior segment biomechanics. ***Therefore, considering the findings of the present study it seems justifiable to hypothesise that the anterior scleral thickness may influence the ocular conformation in refractive error development.***

7.6.6 Gender differences in scleral thickness

The present investigation showed significant differences in scleral thickness between males and females with males showing greater overall thickness in all meridians and at all distances. In support of these findings Mohamed-Noor *et al.*, (2009) reported CCT to be thicker in females than males, whereas scleral thickness was found to be thicker in males than females. Contrary to these findings, Yoo *et al.*, (2010) found no significant gender differences in scleral thickness. Reports of greater scleral thickness in males has been noted previously (Watson and Young, 2004) and may possibly be a consequence of their larger eyes which is generally linked to their greater stature (Atchinson *et al.*, 2005; Teikari, 1987; Johnson *et al.*, 1979). These findings corroborate with the gender differences found in Chapters 8 and 10 suggesting that the thicker sclera offers greater scleral resistance.

7.6.7 The effect of ethnicity on scleral thickness

A non-significant trend was found for greater scleral thickness in British South Asian (BSA) individuals when compared to British White (BW) individuals. Furthermore the study demonstrated a significant interaction between ethnicity and meridional differences in scleral thickness, which appeared to be attributable to the thickness profile for meridians ST and T. In comparison to scleral thickness measures amongst Asian Koreans (Yoo *et al.*, 2010), the present values of scleral thickness for the mixed BW-BSA group are notably lower. Ethnic differences were also noted by Oliveira *et al.*, (2006) who reported thickness at all locations along the temporal meridian to be thinner in Caucasian individuals when compared to non-Caucasian subjects. These findings of ethnic variation in scleral thickness support the findings of Chapter 8 where Hong Kong Chinese (HKC) individuals were found to have greater scleral resistance than the mixed BW-BSA group. Previously corneal thickness has been shown to vary with ethnicity: studies by Nemesure *et al.*, (2003),

Shimmyo *et al.*, (2003), Leite *et al.*, (2010) all reported black (African-Caribbean and African-American) individuals to have thinner corneas than white individuals. Furthermore, Aghaian *et al.*, (2004) reported CCT to vary significantly between Asian subpopulations with Japanese exhibiting thinner corneas than Chinese and Filipinos, whilst Caucasians, Chinese, Hispanics, and Filipinos demonstrated comparable CCT measurements, African Americans were found to have significantly thinner CCT than all other ethnicities. These distinct differences in corneal thickness between ethnicities support the supposition that scleral thickness is also likely to vary between ethnicities.

7.6.8 Corneal and scleral thickness

Due to the dearth of literature on scleral thickness there are no known studies that have measured scleral thickness in different meridians and evaluated their relationship with CCT. In the present study a number of significant negative correlations (see Appendix 4) were found between CCT and scleral thickness for SN (3-4 mm), S (4-6 mm), ST (4-6 mm), IT (4-5 mm) and I (5 mm). These results suggest that as CCT increases scleral thickness decreases. Contrary to these results, Oliveira *et al.*, (2006) noted a significant positive correlation between CCT and scleral thickness at the temporal scleral spur but not for scleral thickness at 2 and 3 mm posterior to the scleral spur. More recently, Yoo *et al.*, (2010) reported findings of thinner scleral thickness in NTG patients when compared to POAG and normal subjects. Furthermore the investigators also reported a significant correlation with CCT and scleral thickness in NTG subjects but not in POAG patients and normal subjects. Similarly, Mohamed-Noor *et al.*, (2009) found scleral thickness to be thicker in OHT subjects and noted a correlation between scleral thickness and CCT but only in NTG patients. It should be noted that all of these studies were limited to the temporal meridian for which the present study did not find any significant relationship between scleral thickness and CCT.

The importance of CCT has been widely studied owing to its importance in the accurate determination of IOP in glaucoma (Shah *et al.*, 1999; Doughty and Zaman, 2000; Herndon, 2006). The link between CCT and susceptibility to glaucoma is thought to be a tonometric artefact; such that a thick CCT leads to artificially higher IOPs and thin CCT lower IOPs, which has led to misclassification of individuals at risk of glaucoma. Contrary to this presumption a number of studies have recently demonstrated CCT to be an independent risk factor in the development of glaucoma (Gordon *et al.*, 2002; Miglior *et al.*, 2007;

Leske *et al.*, 2007). Of note the Ocular Hypertension treatment study demonstrated CCT to be the strongest predictor for progression from OHT to glaucoma (Gordon *et al.*, 2002), whilst the European Glaucoma Prevention study also reported CCT to be a significant predictor in glaucoma pathogenesis in OHT patients (Miglior *et al.*, 2007). In support of these findings the Early Manifest Glaucoma trial showed thinner CCT to be significantly related to visual field loss (Leske *et al.*, 2007). These findings of an association between CCT and glaucoma may be indicative of a mechanism relating the biomechanical properties of the anterior ocular tissues in the pathogenesis of glaucoma (Dimasi *et al.*, 2010).

A number of investigators have attempted to explain the relationship between CCT and glaucoma (Pakravan *et al.*, 2007; Cankaya *et al.*, 2008; Mohammed-Noor *et al.*, 2009; Jonas *et al.*, 2005) with equivocal reports. In a recent study Ren *et al.*, (2010) assessed susceptibility to glaucoma by evaluating the link between reduced CCT, a thin lamina cribrosa and peripapillary sclera in normal individuals. The investigators reported no significant association between these variables nor between a thin cornea and increased susceptibility to developing glaucoma.

Aside from corneal biomechanics, a growing body of literature suggests the mechanical properties of the sclera to have a significant role in the pathogenesis of glaucoma (Chapter 3; Bellezza *et al.*, 2000; Eligahi *et al.*, 2010a). Due to the lack of information on scleral biomechanics, few studies have assessed anterior scleral biomechanics as a risk factor in glaucoma (Sullivan-Mee *et al.*, IOVS 2010, 51: ARVO E-Abstract 5548). ***Considering the present findings of an inverse relationship between CCT and scleral thickness, the current investigation questions whether a thin CCT would indicate increased anterior sclera thickness and hence greater levels of stiffness.*** These findings of a possible inverse relationship between increasing scleral resistance and reducing corneal biomechanics are supported by the findings of Chapter 8 and 11. In Chapter 8 the HKC individuals were found to have increased scleral resistance when compared to the UK subjects, however in Chapter 11 the ORA parameters in these same individuals were found to show indications of ‘weaker’ corneal biomechanics. Furthermore, numerous studies have identified NTG patients to have thinner CCT than normals and OHT patients to have thicker CCT (Herman *et al.*, 2001; Brandt, 2004, Mohamed-Noor *et al.*, 2009; Yoo *et al.*, 2010). If a thinner CCT is linked to increased scleral thickness then NTG patients would be predisposed to increased anterior scleral thickness. A thicker CCT in OHT patients may serve as a

protective mechanism and thus explain the increased risk of glaucoma with reducing CCT. Individuals of African-Caribbean descent have often been found to have thinner corneas (Nemesure *et al.*, 2003, Shimmyo *et al.*, 2003, Leite *et al.*, 2010), which might suggest that these individuals are susceptible to increased scleral thickness and hence increased anterior scleral stiffness, a factor that may explain the greater risk of glaucoma amongst African-Caribbean individuals.

As the sclera covers 90% of the human globe (Oliveira *et al.*, 2006), increased thickness and stiffness of the anterior sclera may reduce its ability to absorb stress, which may consequently elevate stress levels at the posterior pole. Indeed increased posterior scleral stiffness has been previously suggested to be a significant factor in optic nerve head biomechanics (Sigal *et al.*, 2005b; 2009) but the findings of the present investigation propose that anterior scleral biomechanics may also have a significant role in the pathogenesis of glaucoma. Clearly more data are required to address the issues raised above.

7.7 Conclusion

In summary the key findings of the present study are:

- Measurements of scleral thickness with the OCT show high levels of intra- and interobserver repeatability.
- Significant differences in scleral thickness were found between meridians and also with progressing distance from the corneolimbus junction.
- Significant differences between males and females were found for scleral thickness, with males showing overall greater thickness than females.
- Scleral thickness was observed to be influenced by ethnicity (BW and BSA), with an interaction effect being demonstrated for meridians ST and T.
- The study demonstrated a significant correlation between axial length and anterior scleral thickness in the vertical meridians; suggesting a role for the anterior sclera in globe conformation.
- The findings of increased scleral thickness with reducing corneal thickness are suggestive of an inverse relationship between scleral and corneal biomechanics that may have a role in the pathogenesis of glaucoma.

8.0 THE USE OF REBOUND TONOMETRY TO ASSESS INTRAOCULAR PRESSURE AND REGIONAL VARIATIONS IN SCLERAL RESISTANCE

8.1 Introduction

The *iCare* tonometer determines the IOP by assessing the ballastic properties of a probe when it rebounds from the eye (Dekking and Coster, 1967; Kontiola, 2000). Considering this novel approach to measuring IOP, it can be speculated that RBT is less likely to suffer from the same fundamental assumptions that limit the reliability of applanation and non-contact tonometers (see Chapter 4; Chihara, 2008; Kniestedt *et al.*, 2008; Whitacre and Stein, 1993). Furthermore the *iCare* instrument utilises a small lightweight probe which is minimally affected by physiological variation in ocular parameters such as curvature and shape (Moreno-Montañés *et al.*, 2007) which are known to affect contact (Lamparter and Hoffmann, 2009; Elsheikh *et al.*, 2009) and non contact (Sánchez-Tocino *et al.*, 2005) tonometry.

Moreover it has been suggested that the rebound response of the probe might reflect the viscoelastic properties of the cornea (Chihara, 2008; Nakamura *et al.*, 2006). As is the case with all tonometers, variables such as corneal rigidity, oedema and thickness may potentially affect the probe's motion parameters on rebound (Nakamura *et al.*, 2006; Kontiola and Puska, 2004), which may indirectly provide an insight into the biomechanical properties of the ocular surfaces. Indeed various studies have reported an association between *iCare* readings and corneal thickness, with a trend to overestimate IOP with increasing CCT (Martinez-de-la-Casa *et al.*, 2005; Nakamura *et al.*, 2006). Furthermore, Chui *et al.*, (2008) reported *iCare* determined IOPs to be significantly influenced by corneal biomechanical parameters such as corneal hysteresis (CH) and corneal resistance factor (CRF), further signifying that RBT may be able to provide information on the viscoelastic and resistance properties of the cornea.

Tonometric measures of IOP are influenced by the biomechanical properties of the cornea and sclera and hence to attain accurate measures of IOP an assessment of the properties of ocular tissues is essential (Chihara, 2008; Whitacre and Stein, 1993). Furthermore the influence of corneal and scleral biomechanics in myopia (Rada *et al.*, 2006), AMD (Pallikaris *et al.*, 2006; Friedman, 2000) and glaucoma (Ebnetter *et al.*, 2009; Hommer *et*

al., 2008) has reconfirmed the need for accurate *in vivo* assessment of the mechanical properties of the ocular tissues. However evaluating the biomechanical characteristics of the individual ocular tissues *in vivo* is challenging, due to the complex interactions between the various ocular surfaces and components. As mentioned in Chapter 3, a number of investigators have also explored various *in vivo* methods of measuring ocular biomechanics (Pallikaris *et al.*, 2006; Hommer *et al.*, 2008) although these techniques are unable to discriminate between the corneal and scleral response to stress.

8.2 Study Objective

The objective of the present study was to evaluate the application of the *iCare* rebound tonometer to scleral measurement and to investigate whether regional variations exist in the biomechanical resistance of the sclera to deformation. Furthermore the study also examined the reliability and reproducibility of scleral and corneal *iCare* readings and evaluated the concordance of corneal measurements of IOP between the *iCare*, GAT and ORA. Furthermore, scleral measurements with the *iCare* and the Schiötz tonometer were correlated to assess the degree to which their respective measures of scleral resistance corroborated. As scleral resistance may be associated with scleral thickness, scleral *iCare* values were also correlated with measures of scleral thickness reported in Chapter 7. Corneal biomechanical parameters measured by the ORA (from Chapter 11) were also compared to *iCare* readings to investigate whether the *iCare* tonometer can be used effectively to evaluate the material properties of the cornea. Additionally as discussed in Chapter 2, due to the significantly higher prevalence levels of myopia in Chinese individuals (Lin *et al.*, 2001; Lam *et al.*, 2004; Fan *et al.*, 2004a; 2004b) when compared to Caucasian individuals (Grossniklaus and Green, 1992; Goldschmidt and Fledelius, 2005), the study also investigated scleral biomechanics in Hong Kong Chinese (HKC) subjects to assess whether ethnicity and refractive error influences the biomechanical properties of the anterior sclera.

Therefore the key objectives of the investigation were:

- Determining the intra- and inter-observer variation for both corneal and scleral *iCare* measurements;
- Evaluating the concordance between IOPs measured with the *iCare*, GAT and the ORA and assessing the relationship between *iCare* IOPs and the ORA biometrics (CH and CRF);

- Investigating the application of *iCare* tonometry to evaluate regional variation in scleral resistance in mixed British-White (BW) and British South Asian (BSA) (UK) subjects;
- Evaluating the agreement between the measures of scleral resistance with the *iCare* and Schiøtz tonometry;
- Assessing the relationship between scleral *iCare* values and scleral thickness measurements;
- Investigating the application of *iCare* tonometry to evaluate regional variation in scleral resistance in HKC subjects;
- Determining the influence of ethnicity (BW, BSA and HKC) on scleral resistance.

8.3 Methods

Ethical approval and the exclusion/inclusion criteria followed those detailed in Chapter 6. The following methods section details the general procedure for performing *iCare* tonometry on the cornea and the technique and adaptations implemented to allow the *iCare* to be applied to the sclera. The *Zeiss IOLMaster* and the Shin-Nippon auto-refractor were utilised as in Chapter 6 to obtain ocular biometry and refractive error data for all sections of the present investigation.

8.3.1 General measurement procedure with the *iCare* tonometer

The *iCare* tonometer measurement procedure is relatively simple and early reports of usage in clinical practice indicate that minimal experience is required to operate the device (Abraham *et al.*, 2008). The tonometer is self-calibrating and aside from regular cleaning and changing of the nozzle it requires very little additional maintenance. To take measurements with the instrument, a large grey button is depressed which activates a 'load' message on the LCD (Figure 8.2). While holding the tonometer horizontally a disposable probe is inserted into the collar of the instrument and then held upright. Pressing the button activates the solenoid and the probe is seen to visibly vibrate in the nozzle.

In order to take IOP measurements, the tonometer is held vertically in front of the eye at a distance of 4-8 mm. To aid stability when holding up the tonometer, the instrument has a variable length headrest, which can be supported against the subject's forehead. Once the

probe is aligned and perpendicular with the corneal apex, pressing the button fires the probe onto the eye, which is confirmed by a short auditory beep from the instrument. The manufacturers of the *iCare* tonometer recommend six such readings to be taken in order to obtain an accurate measurement of IOP. When these six readings are taken, the *iCare* software discards the highest and lowest readings and calculates the mean and standard deviation of the remaining four. The *iCare* software adopts this protocol for refinement of the results following evidence of more stable IOP measures when the two most extreme values were removed (Kontiola and Puska, 2004). The measurement range for the instrument is 7-50 mm Hg, but it displays estimated IOPs between 0-99 mm Hg (*iCare* tonometer manual).

The final mean value for the IOP is displayed in digital form as an integer next to a 'P' on the LCD display and a long auditory beep informs the examiner whether the results are valid or not. If the results are invalid or an error detected then an abrupt double beep is sounded. The *iCare* software also calculates the standard deviation of the readings taken and indicates the level of variance either by a means of a flashing 'P' indicating the standard deviation is greater than normal or by a bar to the left of the displayed IOP measurement (Fernandes *et al.*, 2005). If no line is present and the 'P' appears steady, the standard deviation is less than 1.8 mm Hg and the result is deemed reliable. If a low bar (_P) is displayed the standard deviation falls between 1.8 and 2.5 mm Hg and the results are considered to be unaffected by the variability; a bar in the middle of the screen (-P) indicates the standard deviation is 2.5 to 3.5 mm Hg, which is greater than deemed acceptable and a repeated measurement is recommended if the IOP is >19 mm Hg; and for higher than 3.5 mm Hg standard deviation, the bar appears at the top and a repeat measurement should be taken.

Additionally the *iCare* software is also programmed to detect erroneous results and indicates this by various error messages (*iCare* tonometer manual); E 01 *probe failed to move*, E 02 *the probe did not touch the eyes*, E 03 *probe speed too low* (measurement was taken from too far way or instrument tilted upwards), E 04 *probe speed too high* (the instrument maybe tilted downwards), E 05 *hit was too 'soft'* (probably hit the eyelids), E 06 *the hit was too hard* (probably made contact with the opening eyelid or calcification of the cornea) and E 07 *'bad hit'* (signal detected was unusual and the probe was probably twisted or inserted incorrectly or the probe made contact with the peripheral cornea). On

obtaining an error message realignment is recommended and another reading should be attempted.

8.3.2 Procedure for the use of the *iCare* tonometer on the sclera

In order for the *iCare* tonometer to be used on the cornea and sclera while controlling for variables such as eye-probe distance and angle, the tonometer was table mounted onto a custom designed and built movable base (Figure 8.1). Early studies with the prototype RBT tonometer showed the instrument to be tolerant to small variation in eye-probe distances (i.e. 3-5 mm on IOPs up to 36.8 mm Hg) and off-axis measurements (i.e. 25° off the corneal apex axis in the horizontal plane for IOPs between 6.3-24.8 mm Hg) (Kontiola *et al.*, 2001). Nevertheless, mounting the instrument was considered to be worthwhile as it has been shown to reduce the signal-to-noise ratio (Kontiola, 2000; Wang *et al.*, 2005) and also ensured the *iCare* probe housing was retained in its upright horizontal position. This also allowed the eye-probe distance to be kept constant (Pakrou *et al.*, 2008) throughout the measurement session by locking the instrument in place once the probe was aligned and perpendicular to the cornea.



Figure 8.1 *iCare* tonometry experimental setup side view. **A:** Custom-designed housing for the *iCare* tonometer, **B:** Graticule for estimating location of scleral measurement, **C:** *iCare* tonometer, **D:** Head rest for subject, **E:** Examiner ED.

To minimise head tilt and to further control probe-eye distance in different directions of gaze, subjects were asked to place their head against a forward headrest band; the head was

then strapped into a stable position with a rear *Velcro* belt to ensure stability. Care was taken to ensure that the restraint was not too tight so as not to exert any significant force on the head and neck that could artificially induce an increase in IOP. The tonometer was aligned with the tip of the probe 4-8 mm from the apex of the cornea in primary gaze and an IOP reading taken to ensure a valid reading could be obtained. Care was taken to ensure the probe was aligned perpendicular to the apex of the cornea as Wang *et al.*, (2005) reported that misalignment of the corneal apex may produce an artificially lower IOP. Once valid central corneal readings were obtained the instrument was locked into place for subsequent measurements on the sclera.

iCare tonometry was performed in eight scleral locations: nasal (N), temporal (T), superior (S), inferior (I), inferior nasal (IN), inferior temporal (IT), superior nasal (SN) and superior temporal (ST). In order to expose the sclera in these different locations the subjects were asked to follow a mobile fixation target and maintain their gaze steady. The distance of each fixation point was set by the examiner to produce an approximate displacement of the corneal apex of 10 mm after eye rotation (Figure 8.2). Keeping the *iCare* tonometer in one position and having the eye rotate in various different gazes ensured the probe was perpendicular to the ocular surface at all times; this technique is similar to that adopted by Jorge *et al.*, (2008) for taking peripheral corneal pachymetry readings. The *iCare* procedure was performed on the sclera approximately 4 mm from the limbus. The site of measurement was chosen to avoid areas of muscle insertion because it has been shown that scleral microstructure is affected by areas where extraocular muscles attach to the globe (Thale and Tillman, 1993). The 4 mm site also allows assessment of scleral biomechanics where scleral thickness changes in all meridians are relatively constant (Norman *et al.*, 2009). To aid location of the scleral site a custom-designed graticule was attached to the end of the *iCare* which allowed the examiner to judge distances approximately 4 mm from the limbus where the probe would make contact with the sclera horizontally, vertically, and in the oblique meridians.



Figure 8.2 Scleral measurement with *iCare* tonometry (graticule omitted for clarity).

Measurements were taken from both eyes in a random sequence. Additionally, to avoid any order effects and to minimise the possible effect of initial readings on subsequent readings, the order in which the eight regions were assessed was also randomised. Two readings (each reading averaged from the 6 measurements) were taken successively for each gaze position (before the direction of gaze was changed) to reduce the effect of localised massaging of the sclera. The procedure was repeated until at least four valid readings were recorded for each location on the sclera. Valid readings were either an IOP measurement with a steady 'P', without a bar or with a low bar. The data with high and mid bars were removed unless there were less than 2 results with no bars or low bar results, however this occurred rarely and in this situation the examiner would estimate a mean reading.

8.3.3 Determining the intra- and inter-observer variation for both corneal and scleral *iCare* measurements

Intraobserver variation of corneal and scleral measurements with the *iCare* were assessed by repeating *iCare* tonometry as described above five times on one subject (author HP on assistant ED (details below) and ED on HP) at the same time of day to control for diurnal variation in IOP (Read *et al.*, 2008). A period of two days to one week was left between readings to ensure results were not biased by previous results and the examiner was blind to the data from the previous sessions. Interobserver variability was evaluated by two

examiners (ED and HP) performing *iCare* tonometry on the cornea and sclera of 11 normal subjects. Subjects were seen at the same time of day on both occasions to control for the effect of diurnal variation and examiners were blind to each other's results.

8.3.4 Evaluating the concordance between IOPs measured with the *iCare*, GAT and the ORA and assessing the relationship between *iCare* IOPs and the ORA biometrics

The study assessed 75 healthy mixed British-White (BW) and British South-Asian (BSA) individuals (150 eyes; 29 males and 46 females) aged between 18-40 years (27.8 ± 5.5) who were recruited from the Aston University Optometry Department. IOP measurements were obtained with the *iCare*, GAT and ORA devices. The order of measurements with the different tonometers was not randomised to control for the effects of diurnal variation on IOP and to minimise the IOP lowering effect of contact tonometry on subsequent measures of IOP with the *iCare* and ORA. Hence *iCare* tonometry was always performed first followed by the ORA and then by GAT. *iCare* and ORA measurements were performed as described in Section 8.3.2 and 11.3 respectively. A 5-minute interval was allowed between each tonometric measurement to control for any massaging affect on subsequent measures. The study evaluated the effect of central corneal thickness (CCT) (data from Chapter 7) on the IOP measurements provided by the three tonometers. Furthermore, *iCare* results were also compared to the full range of ORA biomechanical metrics (e.g. corneal hysteresis (CH) and corneal resistance factor (CRF)) (see Chapter 11).

8.3.5 Investigating the application of *iCare* tonometry to evaluate regional variation in scleral resistance in mixed British White (BW) and British South Asian (BSA) (UK) subjects

iCare tonometry was applied to eight scleral regions (as described in Section 8.3.2) of the 75 healthy BW and BSA individuals who were also evaluated in Section 8.3.4.

8.3.6 Evaluating the agreement between the measures of scleral resistance with the *iCare* and Schiottz tonometry

Schiottz tonometry was performed on 65 healthy individuals (130 eyes; 23 males and 42 females) as described in Chapter 10. The scleral Schiottz indentation levels at 4 mm from the limbus for quadrants superior-temporal (ST), superior-nasal (SN), inferior-temporal (IT) and inferior-nasal (IN) were compared to the *iCare* values for the equivalent locations.

8.3.7 Assessing the relationship between scleral *iCare* values and scleral thickness measurements

To assess where the scleral thickness profile along each meridian affected the regional scleral resistance measures with the *iCare*, the scleral *iCare* values at 4 mm were correlated with thickness measurements from 1-7 mm from the corneolimbus junction (data from Chapter 7).

8.3.8 Application of the *iCare* tonometer for scleral measurement in Hong Kong Chinese (HKC) individuals

iCare tonometry was applied to eight scleral quadrants of 60 healthy HKC individuals (120 eyes; 31 males and 29 females) aged between 18-40 years (25.03 ± 4.75 years). HKC subjects were recruited from the Hong Kong Polytechnic University School of Optometry, Kowloon, Hong Kong. Ethical clearance was sought prior to experimental testing and approval obtained. The protocol for *iCare* scleral measurements on the HKC subjects followed the same format as that for the UK (BW-BSA) group. Furthermore, to assess whether scleral massaging affected IOP measurements in the HKC subjects, an additional corneal IOP reading with the *iCare* tonometer was taken before and after scleral measurements.

8.3.9 Determination of the influence of ethnicity and refractive error on scleral resistance

The investigation of differences in scleral biomechanics between ethnic groups comprised the following groups; BW (n=49), BSA (n=26) and HKC (n=60) young adults. *iCare* tonometry was applied to eight scleral quadrants of all individuals.

8.4 Statistical procedures

Statistical evaluation was performed using *SPSS* version 15 for Windows (*SPSS* Inc, Chicago, IL) and Microsoft *Excel* (Microsoft Corporation, Redmond, Washington, USA). All data were initially examined for normal distribution using the Kolmogorov-Smirnov test.

Inter eye and examiner (ED and HP) differences for the scleral and corneal *iCare* values were initially examined by performing Student's paired *t*-test. Intra- and interobserver variability was calculated using intraclass correlation coefficient (ICC). ICC was calculated using a two-way mixed ANOVA model, with a 95% confidence interval. *SPSS* calculates ICC as both single (i.e. only one examiner) and average (i.e. multiple examiners) repeatability values. In the present study, when assessing the intraobserver variability the results obtained by each examiner (HP and ED) were evaluated separately; hence the repeatability was assessed as single ICC values. As average ICC is a measure of the repeatability of multiple examiners and since both examiners participated in performing *iCare* tonometry on the BW-BSA and HKC subjects, the average ICC was the preferred measure of overall reliability and repeatability for the *iCare* on the cornea and sclera. As in Chapter 6 and 7 consistency measures of ICC were used. Coefficients of variation (CoV%) were also calculated for the intraobserver data.

Concordance between *iCare* tonometry, GAT and ORA was initially assessed using linear regression analysis. The coefficient of correlation is a measure of the relationship between the IOP readings and not an accurate determinant of the agreement between the results of the tests. Therefore as recommended by Bland and Altman (1986), the test for agreement was performed by plotting the mean IOP against the difference in IOP between the two instruments. Hence 95% limits of agreement (LoA) were calculated as mean difference between tonometers $\pm 1.96 \times$ Standard Deviation (SD) as recommended by (Bland and Altman, 1986; 1995). Pearson's correlation coefficient was calculated to indicate the relationship between IOP measurements and other ocular variables.

Multiple linear regression models were evaluated to test the relationship between ORA-derived corneal biometrics and *iCare* values. To test for differences in *iCare* readings between scleral regions, one-way repeated measures ANOVAs were conducted. Individuals were also split into axial length (mm) subgroups; 1. ($21.5 > - \leq 23.5$), 2. ($23.5 > - \leq 25.5$) and 3. (>25.5) to test the effect of axial length on scleral biomechanics. To assess the influence of age on scleral biomechanics, the subjects were divided into age (years) groups: ($18 > - \leq 29$) and ($29 > - \leq 40$). Multiple two-way mixed repeated measures ANOVAs were performed with sclera regions as within-subject factors and refractive status, axial length grouping, gender, age grouping and ethnic grouping as the between-subject factors. For all statistical tests a *p*-value of <0.05 was taken as the criterion for statistical significance.

8.5 Results

8.5.1 Determining the intra- and inter-observer variation for both corneal and scleral *iCare* measurements

No significant inter-ocular or examiner differences were found for the intraobserver *iCare* values; hence only RE data will be discussed (see Table 8.1). Intraobserver correlation coefficients for each individual observer were 0.909 for examiner ED and 0.886 for examiner HP. The CoV indicated the highest repeatability for the cornea (4.04%) and the least repeatability at the IN region (15.43%). Similarly, interobserver correlation coefficients also demonstrated highest repeatability for the cornea and the least repeatability for quadrants IT, I and N.

Examiner	ICC single	ICC average
ED	0.909	0.980
HP	0.886	0.975

Table 8.1 RE Intraobserver ICC for *iCare* tonometry on the cornea and sclera.

Location	Examiner ED CoV (%)	Examiner HP CoV (%)	Average CoV (%)
Cornea	2.84	5.24	4.04
SN	9.25	7.34	8.30
S	7.20	11.64	9.42
ST	6.10	11.10	8.60
T	8.63	10.97	9.80
IT	11.90	8.67	10.29
I	10.16	8.11	9.14
IN	16.68	14.18	15.43
N	8.59	6.14	7.37

Table 8.2 Intraobserver Coefficient of Variation (%) for *iCare* tonometry for the RE cornea and sclera.

Location	ICC Single measure	ICC average measure
Cornea	0.844	0.916
SN	0.766	0.868
S	0.756	0.861
ST	0.648	0.786
T	0.692	0.818
IT	0.431	0.602
I	0.179	0.303
IN	0.724	0.840
N	0.245	0.394

Table 8.3 Single and average ICC values for *iCare* tonometry for the RE cornea and sclera.

8.5.2 Concordance of *iCare* tonometry with GAT and the Reichert ORA

IOP data was collected on 75 individuals in the UK, and the data were analysed for non-myopic and myopic individuals [non-myopes (MSE \geq -0.50D) n=37, MSE (D) mean \pm SD (0.49 ± 1.08), range (-0.50 to +4.38), AL (mm) mean \pm SD (23.33 ± 0.72), range (21.61 - 24.74); myopes (MSE $<$ -0.50), n=38, MSE (D) mean \pm SD (-4.70 ± 4.14), range (-0.51 to -20.50), AL (mm) mean \pm SD (25.13 ± 1.28), range (22.81 - 28.12)]. Data obtained from both eyes were analysed and a strong correlation was found between the right and left eye IOP values obtained with all three tonometers. Paired *t*-tests showed no significant interocular differences in IOP determined by *iCare*, GAT and ORA, thus only RE results are discussed (Table 8.4). For determining the 95% confidence intervals (CIs), the critical value of 1.96 (df $>$ 30) was determined for df=75. The CIs were calculated as mean IOP \pm 1.96 x Standard Error (SE) and Table 8.5 shows the results from the three tests. No significant effect of gender or age was found.

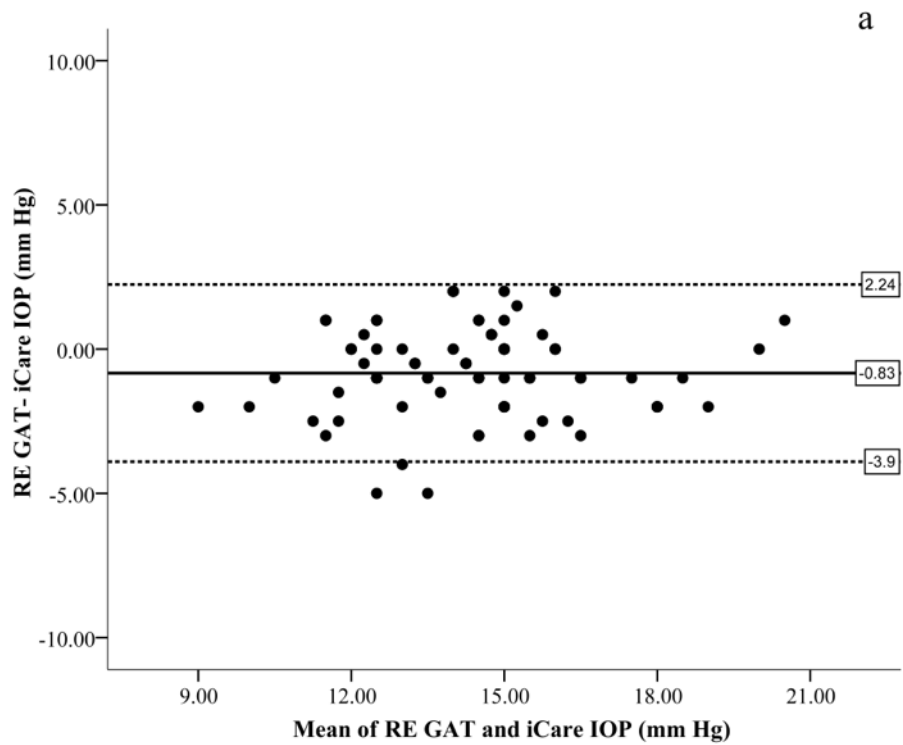
iCare tonometry correlated significantly with both GAT and ORA (IOPg and IOPcc) (Table 8.5). Paired *t*-tests revealed significant differences between *iCare* and GAT ($p < 0.001$), but no significant difference between *iCare* and ORA IOPg or IOPcc. Bland and Altman plots (Figure 8.3 a-c) showed *iCare* to overestimate GAT, with no systematic bias in overestimation, however the *iCare*-GAT difference was significantly greater when a higher IOP was measured by the *iCare* and GAT. 95% Limits of agreement (LoA) are shown in Table 8.5. No significant correlation was found between refractive error and *iCare*, GAT IOP, IOPcc and IOPg nor was any significant association found between *iCare*-GAT and *iCare*-ORA (IOPg and IOPcc) differences and refractive error. CCT correlated significantly with GAT, *iCare*, IOPg but not with IOPcc. CCT also correlated significantly with the IOP difference between *iCare* and IOPg, suggesting that as CCT increases the difference between IOPg and *iCare* also increases. *iCare* IOPs failed to correlated with axial length, corneal curvature and ACD. In regards to the ORA corneal biometrics, significant correlations were found between *iCare* and both CRF and CH. See Appendix 6 for full details on the statistical outcomes.

	Mean \pm SD	Min	Max	95% CI
<i>iCare</i>	14.72 \pm 2.36	10.00	20.00	14.18-15.26
GAT	13.93 \pm 2.43	8.00	21.00	13.37-14.49
ORA IOPg	14.77 \pm 3.16	7.23	24.17	14.04-15.50
ORA IOPcc	14.92 \pm 2.89	9.03	24.27	14.25-15.59

Table 8.4 RE measures of IOP (mm Hg) obtained with the *iCare*, GAT and ORA.

Comparison	Correlation/Sig	Mean Difference	95% LoA
GAT versus <i>iCare</i>	0.786 p<0.001	-0.83 \pm 1.57	-3.90 to +2.24
ORA IOPg versus <i>iCare</i>	0.718 p<0.001	0.03 \pm 2.20	-4.28 to +4.34
ORA IOPcc versus <i>iCare</i>	0.532 p<0.001	0.18 \pm 2.59	-4.90 to +5.26

Table 8.5 Correlations between different measures of RE IOP (mm Hg); mean IOP differences between tonometric tests; 95% LoA.



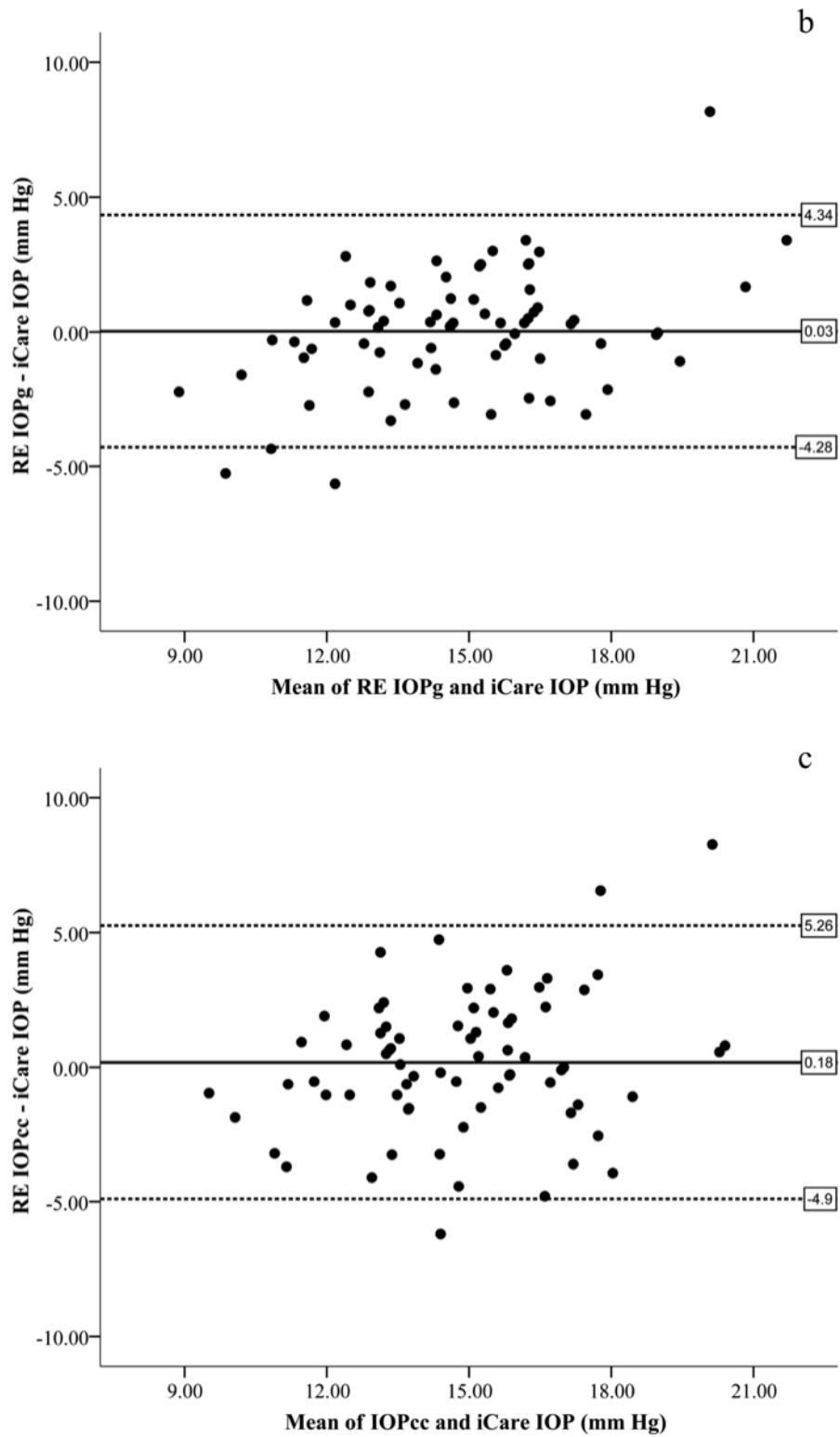


Figure 8.3 a) RE difference versus mean plot: GAT-*iCare* IOP, b) RE difference versus mean plot: IOPg-*iCare* IOP and c) RE difference versus mean plot: IOPcc-*iCare* IOP (Bold line denotes mean, dotted lines ± 1.96 SD).

A stepwise forward multiple linear regression model with corneal *iCare* values as the outcome variable and CCT, CH, CRF, refractive error, mean corneal curvature, axial

length, ACD, gender and age as predictor variables revealed CRF ($p<0.001$) and CH ($p<0.001$) to be significantly associated with *iCare* measures of IOP (Appendix 6). CCT was not significantly related to *iCare* IOPs when CH and CRF were included in the multiple regression model. The model revealed that when each of the other significant predictors variables were held constant, CRF accounted for 43.3% of the variability in *iCare* values, which was further increased by another 12.7% by adding CH. The results of the multiple regression indicated that for a 1 mm Hg increase in CRF, *iCare* values would increase by 1.72 mm Hg, and a 1 mm Hg increase in CH would lead to a 1.06 mm Hg reduction in *iCare* readings.

8.5.3 Application of the *iCare* tonometer to the sclera

Scleral *iCare* measurements were also obtained on 75 individuals assessed in section 8.5.2. A two-way mixed repeated measures ANOVA showed no significant difference in scleral values between myopes and non-myopes ($F(1, 73)=0.040$ ($p=0.841$)) hence the groups were combined. No significant difference was found between RE and LE scleral *iCare* values thus only RE data will be discussed. Table 8.6 and Figure 8.4 show a summary of the scleral *iCare* readings. A one-way repeated measures ANOVA revealed significant differences between regions ($F(5.28, 390.57)=94.53$ ($p<0.001$)), with a Bonferroni *post hoc* test showing the difference to be between all regions except IT:I, IT:N, I:N and T: I.

Multiple two-way mixed repeated measures ANOVAs were performed to examine the influence of axial length (mm) grouping (1. ($21.5>-\leq 23.5$) $n=26$, 2. ($23.5>-\leq 25.5$) $n=33$ and 3. (>25.5) $n=15$), ethnicity (BW $n=49$, BSA $n=26$), gender (males $n=29$, females $n=46$) and age (years) group ($(19> - \leq 29)$ $n=49$, $(29> - \leq 40)$ $n=26$). The analysis revealed a non-significant main effect of axial length grouping ($F(2, 71)=0.958$ ($p=0.389$)), ethnicity ($F(1, 73)=1.964$ ($p=0.165$)) and gender ($F(1, 73)=1.863$ ($p=0.176$)). Age grouping showed a significant ($F(1, 73)=8.923$ ($p=0.004$)) influence on scleral *iCare* readings with the older age group showing higher values for all regions than the younger group.

Location	Mean \pm SD <i>iCare</i> values	Minimum	Maximum
SN	30.34 \pm 9.41	15.75	54.00
S	26.73 \pm 8.55	14.50	50.50
ST	23.04 \pm 8.34	12.25	46.50
T	34.53 \pm 11.79	13.50	68.00
IT	39.36 \pm 11.50	21.60	69.75
I	38.68 \pm 14.59	9.33	70.00
IN	47.29 \pm 13.26	27.25	84.50
N	40.85 \pm 10.76	23.25	71.67

Table 8.6: RE scleral *iCare* (mm Hg) values for UK data set.

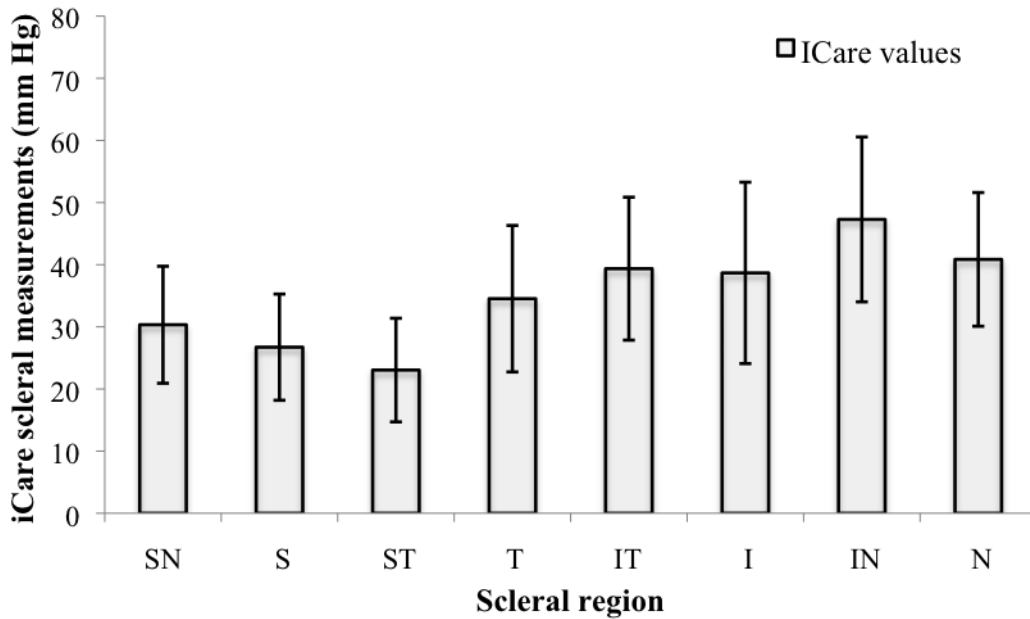


Figure 8.4 RE mean \pm SD (error bars) scleral *iCare* values at different regions for the UK data set.

No significant correlation was found between scleral *iCare* measures and CCT, refractive error, axial length and corneal IOPs. Refractive error was significantly negatively correlated with AL ($r=-0.859$, $p<0.001$). Performing a one-way ANOVA revealed no significant effect of gender, age group or ethnic differences on corneal *iCare* values and other biometric data (i.e. axial length, keratometry (K1: steep curve and K2: flat curve), ACD and CCT).

8.5.4 Comparison of regional scleral *iCare* values to Schiøtz scleral indentation for the 4 mm location from the limbus

Of the 75 healthy individuals assessed for the *iCare* study 65 also had scleral Schiøtz tonometry performed at four quadrants (ST, SN, IT, IN) 4 mm from the limbus. The subjects were aged between 19-40 years (27.66 ± 5.26) and the data were analysed for non-myopic and myopic individuals [non-myopes (MSE $\geq -0.50D$) $n=31$, MSE (D) mean \pm SD (0.50 ± 1.17), range (-0.50 to +4.38), AL (mm) mean \pm SD (23.38 ± 0.74), range (21.61 - 24.75); myopes (MSE $< -0.50D$) $n=34$, MSE (D) mean \pm SD (-4.40 ± 3.23), range (-10.56 to -0.51), AL (mm) mean \pm SD (25.30 ± 1.16), range (23.35 - 28.12)]. Several statistically significant correlations were noted between Schiøtz scale readings with different weights and the *iCare* values for the equivalent scleral locations (see Appendix 6 for further details).

8.5.5 Scleral *iCare* values and scleral thickness

For the 75 healthy individuals assessed in 8.5.2 and 8.5.3, scleral *iCare* values were correlated with scleral thickness measurements for the corresponding meridian. A number of significant correlations were found between *iCare* values for the S, ST and T regions and scleral thickness along the same meridians (see Appendix 6).

8.5.6 Assessment of regional variation in scleral *iCare* measurements in HKC subjects

60 HKC subjects were evaluated and the data were analysed for non-myopic and myopic individuals, [non-myopes (MSE $\geq -0.50D$) $n=11$, MSE (D) (mean \pm SD) (0.39 ± 0.66), range (-0.44 to +1.69), AL (mm) mean \pm SD (23.49 ± 0.37), range (22.90 - 24.00); myopes (MSE $< -0.50D$) $n=49$, MSE (D) mean \pm SD (-4.46 ± 2.70), range (-13.38 to -0.75), AL (mm) mean \pm SD (25.76 ± 1.12), range (23.83 - 29.78)]. No significant difference was found between RE and LE scleral *iCare* values thus only RE data will be discussed. Table 8.8 and Figure 8.5 summarize the scleral *iCare* readings.

Location	Mean \pm SD <i>iCare</i> values	Minimum	Maximum
SN	42.19 \pm 12.12	24.00	75.33
S	39.56 \pm 8.68	22.75	58.67
ST	29.75 \pm 8.21	13.25	48.00
T	40.75 \pm 10.85	22.67	75.50
IT	45.34 \pm 12.07	7.00	67.25
I	43.21 \pm 15.15	17.00	73.50
IN	55.53 \pm 14.00	30.50	96.00
N	48.41 \pm 12.17	23.50	80.25

Table 8.7 RE scleral *iCare* values (mm Hg) for the HKC individuals.

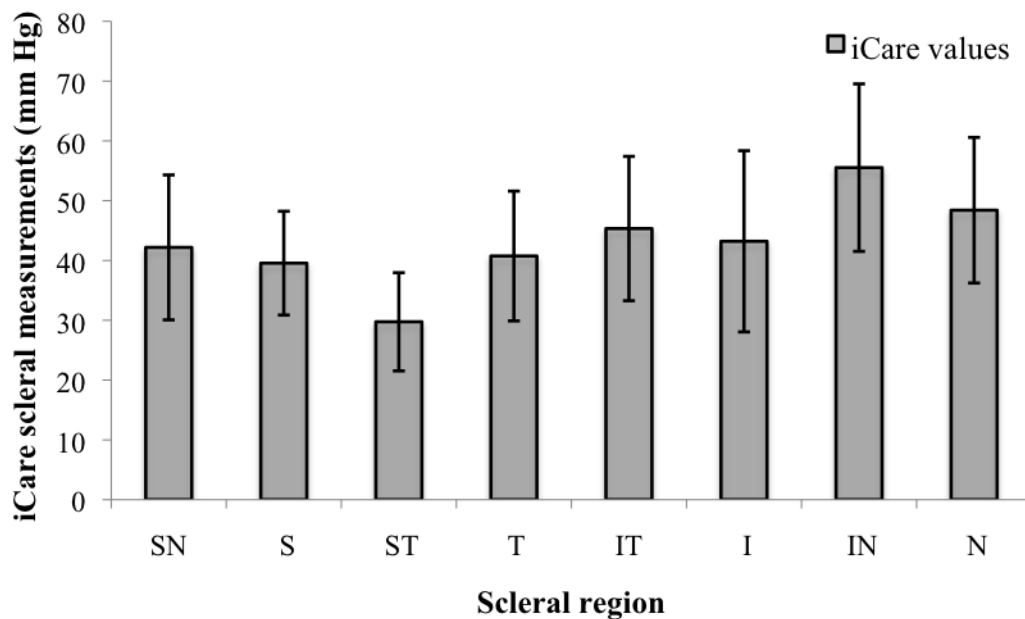


Figure 8.5 RE Mean \pm SD (error bars) scleral *iCare* values at different regions for the HKC data set.

No significant difference was found between myopes and non-myopes thus the data were combined. A one-way repeated measures ANOVA was performed to test for regional variation in scleral *iCare* readings. The analysis revealed a significant difference between regions ($F(4.647, 260.227)=46.180$ ($p<0.001$)); a Bonferroni *post hoc* test confirmed the difference to be between all regions except between regions SN:S, SN:T, SN:IT, SN:I, S:T, S:I, T:I, S:IT, IT:I, IT:N and I:N.

Multiple two-way mixed repeated measures ANOVAs were performed to test for an effect of axial length grouping (1. ($21.5 > \leq 23.5$) $n=4$, 2. ($23.5 > \leq 25.5$) $n=26$ and 3. (>25.5) $n=27$), gender (male $n=29$, female $n=28$) and age (years) grouping ($(19 > - \leq 29)$ $n=46$, ($29 > - \leq 40$) $n=11$). The analysis revealed no significant main effect of axial length grouping ($F(2, 54)=1.882$ ($p=0.162$)), but a significant influence of gender ($F(1, 55)=6.648$

($p=0.013$) on the scleral *iCare* readings with males showing higher values than females for all regions. Age group also demonstrated a significant effect on the scleral values ($F(1, 55)=8.518$ ($p=0.005$)) with the older age group showing higher values for all regions than the younger group.

Scleral *iCare* values for region ST correlated positively with axial length and negatively with refractive error (see Appendix 6). No other scleral or corneal *iCare* measurements showed significant correlations with refractive error, axial length, keratometry (K1: steep curve and K2: flat curve) and ACD.

One-way ANOVAs revealed a significant effect of gender on axial length ($F(1, 58)=5.282$ ($p=0.025$)) and K1 ($F(1, 58)=8.014$ ($p=0.006$)) and K2 ($F(1, 58)=7.038$ ($p=0.010$)), with males showing greater axial length and flatter corneal curvature. Testing for the effect of age on the biometric parameters revealed K1 ($F(1, 58)=9.191$ ($p=0.004$)) and K2 ($F(1, 58)=7.052$ ($p=0.010$)) to be significantly different between the younger and older group with the younger group showing flatter corneal curvature. No other effect of gender or age group was found on *iCare* values and other biometric data.

To test for a tonometric effect induced by multiple *iCare* readings on the sclera, a paired Student *t-test* was conducted on corneal IOP readings before and after the scleral measurements were taken. The analysis revealed no significant ($p=0.536$) effect of multiple scleral rebound tonometry on the corneal IOP measurements.

8.5.7 Comparison of BW-BSA (UK) and HKC (HK) scleral *iCare* measurements

A two-way mixed repeated measures ANOVA was performed to examine whether a significant difference existed between HK ($n=57$) and UK ($n=75$) scleral *iCare* values. The analysis revealed a significant difference ($F(1, 130)=24.073$ ($p<0.001$)), with the HK sample showing higher values than the UK data (Figure 8.6). Additionally a significant interaction effect ($F(5.257, 683.369)=5.030$ ($p<0.001$)) was also noted between regional variation and subject origin (i.e. HK or UK), which on examination of the plot was seen to be attributable to the behaviour of regions SN and S, in that they were clearly more similar to each other for the HK data than for the UK data. Additionally SN and S showed the largest difference in *iCare* values between the HK and UK data. The regional variation in

the scleral readings was still found to be significant ($F(5.257, 683.369)=127.522$ ($p<0.001$)). A Bonferroni *post hoc* test revealed statistically significant differences between all regions except between SN:T, T:I, IT:I and IT:N.

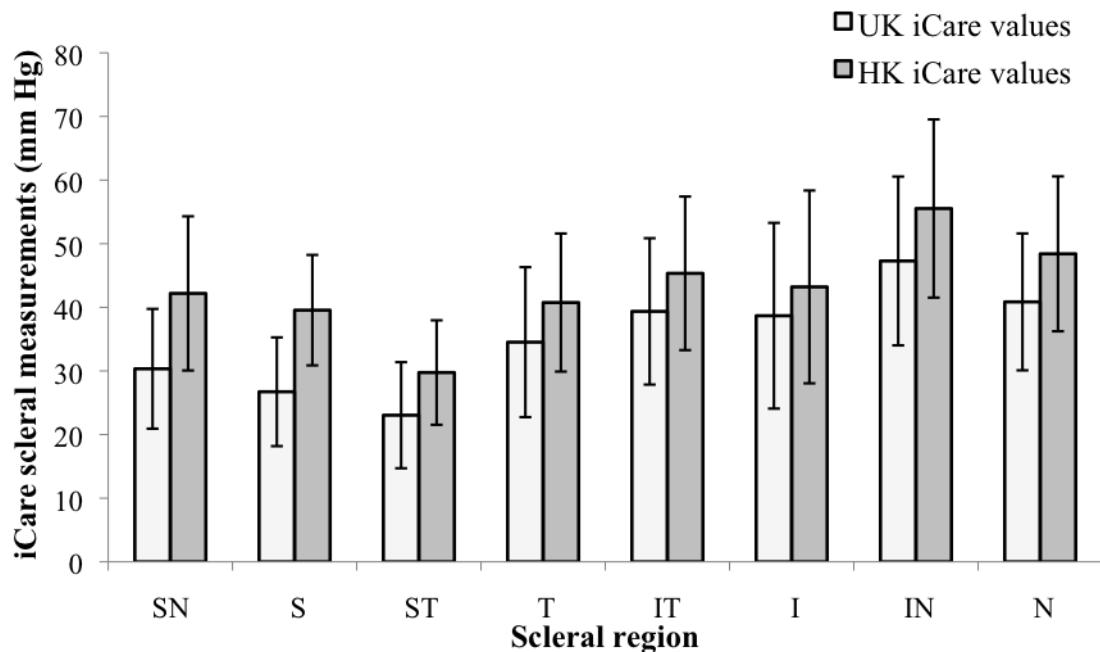


Figure 8.6 RE mean \pm SD (error bars) scleral *iCare* values for different regions in the UK and HK data set.

The data were further investigated for the effect of ethnicity. A two-way mixed repeated measures ANOVA revealed a significant influence of ethnicity (BW $n=49$, BSA $n=26$, HKC $n=60$) ($F(2, 129)=13.137$ ($p<0.001$)) on scleral *iCare* values (Figure 8.7). A Games Howells *post hoc* analysis revealed the difference to be between HKC individuals and both BW ($p<0.001$) and BSA ($p=0.023$). Additionally a significant ($F(10.487, 676.443)=2.715$ ($p=0.002$)) interaction effect was found between ethnicity and regional variation of the scleral *iCare* readings, which on examination of the interaction plot appeared to be attributable to regions SN and S, which behaved differently between the HKC and both BW and BSA data. The regional variation in scleral readings was still found ($F(5.244, 676.443)=117.929$ ($p<0.001$)). A Bonferroni *post hoc* test revealed statistically significant differences between all regions except between SN:T, T:I, IT:I, IT:N, I:N.

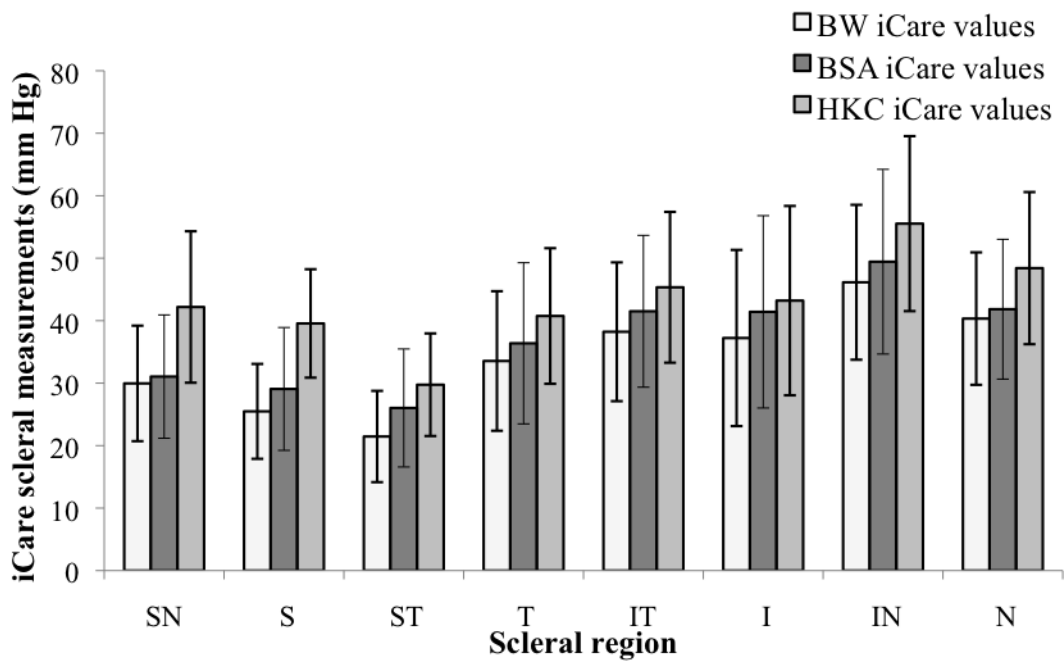


Figure 8.7 RE Mean \pm SD (error bars) scleral *iCare* values at different regions for the various ethnicities.

A one-way ANOVA revealed no significant effect of ethnicity on corneal *iCare* values, ACD and the steeper corneal curvature (i.e. K1). Significant differences were identified between axial length ($F(2, 130)=10.783$, ($p<0.001$)), with a Games Howells *post hoc* test revealing the difference to be between HKC and BW ($p<0.001$) and BSA ($p=0.010$) subjects. A significant difference was also seen for the flattest K value ($F(2, 129)=5.102$, ($p=0.007$)), with a *post hoc* test showing the difference to be between HKC and BW individuals ($p=0.024$). See Appendix 6 for further details.

8.6 Discussion

The objective of the present study was to demonstrate the novel application of the *iCare* rebound tonometer on the sclera to obtain an inferred measure of scleral resistance *in vivo*. The instrument was found to demonstrate high levels of intra- and interobserver repeatability when providing both corneal and scleral measurements. Furthermore the *iCare* showed high levels of correlation with GAT- and ORA-determined IOPs. The measures of scleral resistance from the present study are consistent with previous findings of regional variation in scleral biomechanics. In all ethnicities the superior regions showed the least tissue resistance with region ST displaying the lowest resistance. The scleral *iCare* values then sequentially increased in the inferior regions reaching a maximum in the IN region. Furthermore the study also investigated differences in scleral biomechanics between British-White (BW) and British South-Asian (BSA) individuals in the UK and, separately, Hong Kong Chinese (HKC) eyes as these are known to be associated with the greater susceptibility to higher levels of myopia. The data showed significantly higher scleral resistance in the predominantly myopic HKC sample compared to the other ethnicities.

8.6.1 Reliability and reproducibility of *iCare* tonometry for the cornea and sclera

The first phase of the present investigation assessed the reliability and reproducibility of the *iCare* tonometer. The study demonstrated high intraobserver correlation coefficients of 0.909 and 0.886 for both (ED and HP respectively) examiners, which were calculated as the repeatability between both cornea and the scleral regions. These findings are in agreement with previously reported values for the cornea (Martinez-de-la-Casa *et al.*, 2005; Detry-Morel *et al.*, 2006; Sahin *et al.*, 2007a). The intraobserver CoV was an average of 4% for the cornea and ranged between 7.37-15.43% for the various scleral regions. In comparison to previous reports lower values of CoV for the cornea were found which is likely to be the result of mounting the *iCare* instrument instead of using it in its handheld form (Sahin *et al.*, 2007a; *iCare* manual).

Reports of high levels of interobserver correlation coefficients of 0.820, 0.843, 0.798 have been reported for the *iCare* by Martinez-de-la-Casa *et al.*, (2005), Detry-Morel *et al.*, (2006), and Sahin *et al.*, (2007a) respectively. These results are consistent with the corneal interobserver correlation coefficient of 0.916 found in the present study. Furthermore

these levels of intra- and interobserver repeatability of the *iCare* tonometer compare well with other tonometers (Dielemans *et al.*, 1994; Aakre *et al.*, 2003; Kynigopoulos *et al.*, 2008; Moreno-Montañés *et al.*, 2008).

The assessment of the reliability and repeatability of applying the *iCare* tonometer to the sclera revealed good levels of repeatability which were under 10% CoV for all regions except the inferior nasal and temporal aspects. The interobserver results also show a similar trend with high repeatability in most areas apart from the nasal, inferior and inferior temporal regions. The regional difference in IOP reproducibility may be attributable to differences in anatomy and surface properties between the various locations.

In particular, factors such as the proximity of the site of measurement to muscle insertion points and tendons may have contributed to the discrepancies, as the local biomechanics of the tissues and collagen arrangement are likely to be altered in those regions (Thale and Tillmann, 1993; Greene, 1980). Additionally, conjunctival changes in certain locations, especially nasally and temporally where early pinguecula are commonly seen, may also explain the increased variability found in these areas. Also as mentioned afore, although the *iCare* tonometer is relatively tolerant to changes in probe-eye distances (i.e. within a range 3-5 mm) and angle of impact (up to 25 degrees from normal) (Kontiola *et al.*, 2001) several studies have reported that variation in impact points on the cornea may affect the IOP readings with lower readings found for the temporal (i.e. 2 mm from limbus) corneal regions (González-Méijome *et al.*, 2006; Queirós *et al.*, 2007). Therefore possible discrepancies in the location of the scleral measurements during the inter- and intra-observer reliability study may have contributed to the variability found.

Despite this inconsistency in repeatability across locations, the results indicate that the *iCare* tonometer is a viable method of assessing anterior scleral resistance. Furthermore the results of the study suggest that caution should be exercised when assessing the significance of data in regions of relatively high variability, notably the inferior and nasal regions.

8.6.2 Comparison between *iCare*, GAT and ORA tonometry

The study also demonstrated high levels of correlation between GAT and IOP determined by the *iCare*, which are similar to levels of correlation previously reported (Martinez-de-

la-Casa *et al.*, 2006; Davies *et al.*, 2006, Sahin *et al.*, 2007b; Munkwitz *et al.*, 2008). Moreover, concordant with the present study, various investigations have noted the *iCare* to overestimate IOPs when compared to GAT and have hence subsequently found significant differences between the measures of IOP between the two instruments (Díaz-Llopis *et al.*, 2007; Ruokonen *et al.*, 2007; Jorge *et al.*, 2010; Martinez-de-la-Casa *et al.*, 2009; López-Caballero *et al.*, 2007).

Despite the present findings of a significant difference between *iCare* and GAT IOPs, the levels of overestimation found with the *iCare* were lower than those of other studies (López-Caballero *et al.*, 2007; Diaz *et al.*, 2008; Martinez-de-la-Casa *et al.*, 2009). Possible reasons for this discrepancy may be related to the current investigation evaluating individuals with IOPs within the normal range (8-21 mm Hg), thus the smaller IOP range in comparison to previous studies could have affected the lower level of overestimation found. Other potential reasons for the lower levels of overestimation may be due to variation between study protocols, i.e. the *iCare* was table mounted in this study thus variability between GAT and *iCare* results would have been reduced compared to when it is used in its conventional handheld form. Additionally, the lower GAT readings may have been an artefact of a massaging effect on the IOP levels following multiple scleral *iCare* measurements taken prior to GAT. In support of this supposition, Schreiber *et al.*, (2007) and Jóhannesson *et al.*, (2008) noted a decline in IOPs after repeated corneal *iCare* measures. Contrary to these observations Wang *et al.*, (2005) showed no significant decline in IOPs following repeated *iCare* tonometry measurements (i.e. with up to 90 readings taken within several minutes) and suggested that, being minimal, the force of the probe is unlikely to affect IOP. Furthermore, as demonstrated in the present study, the variation in IOP pre- and post- scleral *iCare* tonometry measurements was not significantly different thus it is unlikely to have affected the subsequent GAT readings. Other reasons for relatively poor concordance between *iCare* and GAT IOPs could be linked to the use of topical anaesthesia in GAT, which has been reported to reduce the IOP (Almubrad and Ogbuehi., 2007; Montero *et al.*, 2008; Badouin and Gastaud, 1994).

Despite the overestimation of IOP measurements by the *iCare* tonometer, results of this study show that 83% of the IOP difference was within ± 2 mm Hg of the GAT results and 96% within ± 3 mm Hg. Similar levels of agreement between the two techniques have been noted by other investigators (Fernandes *et al.*, 2005; Iliev *et al.*, 2006; Jorge *et al.*, 2010) whilst others have found greater levels of discrepancy (López-Caballero *et al.*, 2007;

Martinez-de-la-Casa *et al.*, 2006a). These differences between studies may be a result of methodological differences such as the type of subjects assessed, the range of IOP measured and differences in experimental protocols.

The current study also evaluated the concordance between the ORA and the *iCare* IOPs and found no significant difference in measures between the two methods. These findings are in agreement with numerous studies that have evaluated both *iCare* tonometry and NCTs (Kontiola and Puska., 2004; Martinez-de-la-Casa *et al.*, 2009; Díaz-Llopis *et al.*, 2007). Additionally high levels of correlation were found between *iCare* and IOPg but lower levels with IOPcc. Interestingly, Jorge *et al.*, (2008) investigated corneal biomechanics using the *iCare* and ORA and reported lower correlation between IOPcc and *iCare*, concordant with the present findings. The investigators of the Jorge *et al.*, (2008) study hypothesised that the lower correlation values may be indicative of the *iCare* tonometer measuring corneal biomechanical properties and not just the IOP. Indeed in support of this, the present study and an investigation by Chui *et al.*, (2008) demonstrated a significant correlation between CH and CRF and *iCare* readings. The multiple regression analysis detailed earlier revealed that in comparison to CCT, CRF and CH were more strongly associated with the *iCare* values. The analysis demonstrated that as CRF increased so did *iCare* values but as CH increased *iCare* decreased. Similar findings were noted by Chui *et al.*, (2008), who also found a significant effect of CH and CRF on *iCare* values, but failed to show a correlation with CCT.

As in the present study numerous investigations have found significant correlation between CCT and GAT and *iCare* tonometry (Detry-Morel *et al.*, 2006; Iliev *et al.*, 2006; López-Caballero *et al.*, 2007). Martinez-de-la-Casa *et al.*, (2006a) reported that the difference in IOP between the thickest and thinnest CCT would produce a 2.5 mm Hg change with GAT and 3.6 mm Hg with *iCare*, whereas Brusini *et al.*, (2006) calculated that a CCT change of 10 μm resulted in a 0.7 mm Hg change in *iCare* IOP. In support of these findings, Poostchi *et al.*, (2009) found that a 10% increase in CCT translated to a 9.9% increase in *iCare* values, that is a 0.3 mm Hg change for every 10 μm CCT and additionally noted that the difference between *iCare* and GAT increased by 8.4% with a 10% increase in CCT. Similarly Pakrou *et al.*, (2008) reported that the difference between GAT and *iCare* increased with CCT, with every 100 μm increase in CCT increasing the difference by 1 mm Hg. Contrary to these findings the present study showed no significant correlation between CCT and the difference in *iCare* and GAT IOPs, although a significant trend was

found between ORA IOPg and *iCare* IOP and CCT. These results indicate that as CCT increases the difference between IOPg and the *iCare* increases, indicating that the biomaterial properties, in particular corneal thickness, contribute to the difference between the two measurements.

In summary the *iCare* tonometer shows high levels of correlation with the ‘gold standard’ GAT and the non-contact ORA tonometer. Nevertheless, the *iCare* tonometer does have a tendency to overestimate IOPs and is significantly affected by CCT and corneal biomechanical parameters (e.g. CH and CRF). Despite the various limitations of the *iCare* tonometer the instrument has been deemed to be suitable as a screening device (Jorge *et al.*, 2010) and its proposed application on the sclera in the present investigation has provided a useful insight into regional variation in scleral resistance as discussed below.

8.6.3 Measurement of scleral resistance with *iCare* tonometry

The assessment of the biomechanical properties of the sclera *in vivo* is challenging due to the complex inter-relationships of the various ocular surfaces and components. Literature on the scleral biomechanics has been limited to *in vitro* extensometry studies or invasive pressure- volume setups, which require a number of experimental assumptions. The current study assessed the viability of applying a tonometric device on the sclera to infer a measure of biomechanical properties. There are a number of examples in the literature where scleral measurements of IOP have been investigated for their reliability and validity as a surrogate for central measurement of IOP (Breitfeller and Krohn, 1980; Wilke, 1971; Khan *et al.*, 1991; Kolin *et al.*, 2003; Poostchi *et al.*, 2009). Of particular interest is an investigation by Kolin *et al.*, (2003) who applied the *Tono-Pen* to the inferior-nasal sclera and reported IOP values within the range of 4-99 mm Hg, with a mean \pm SD IOP of 40.2 ± 23 mm Hg and an average difference of 23.4 ± 22.4 mm Hg (mean \pm SD) between corneal and scleral readings. In comparison to the present study the IOP range for IN was 27.3-84.5 mm Hg, mean \pm SD 47.3 ± 13.3 mm Hg and the difference between corneal and scleral readings 32.6 ± 13.2 mm Hg, consistent with the Kolin *et al.*, (2003) study.

The application of RBT on the sclera is not new; in their first study assessing the validity of the prototype RBT, Kontiola, (1996) trialled the technique with a probe of the same weight and speed on the sclera and cornea of *in vitro* pig eyes with IOPs (0-60 mm Hg). Additionally the study also examined the validity of scleral RBT measurements on a series

of clinical patients using a faster (0.36m/s compared to 0.2m/s for the cornea) and heavier (1.5 g compared to 0.75 g for the cornea) probe, as slower and lighter probes failed to produce any reliable readings. Both aspects of the study reported maximum deceleration to be greater with the scleral measurements when compared to corneal readings at all IOPs. Furthermore scleral readings also characteristically had deceleration times that were shorter at all IOPs, with a trend to plateau after 30 mm Hg. More recently Poostchi *et al.*, (2009) investigated the *in vivo* application of *iCare* tonometry to the sclera to evaluate whether these readings could provide an inferred measure of IOP on the cornea. The investigation assessed the clinical significance of IOP measurements from the inferior sclera 4 mm from the limbus with the patient's gaze upwards and reported no significant correlation with corneal GAT readings.

In contrast to the studies mentioned afore the objective of the present investigation was to investigate whether *iCare* tonometry could be applied to assess regional differences in scleral resistance across the anterior globe. Previous studies by González-Méijome *et al.*, (2006), Queirós *et al.*, (2007) and Chui *et al.*, (2008) have assessed the application of the RBT principle to assess biomechanical characteristics of the cornea. Queirós *et al.*, (2007) evaluated central and peripheral corneal IOP measurements with the *iCare* tonometer. The study reported a trend for lower IOP readings at peripheral locations when compared to the central readings, particularly for the nasal periphery. Similarly González-Méijome *et al.*, (2006) reported significantly lower peripheral IOPs at both temporal and nasal locations with increasing age. Contrary to these findings Chui *et al.*, (2008) found no significant difference between the IOP measurements centrally and temporally, despite the peripheral cornea being significantly thicker than the central region.

The results from Queirós *et al.*, (2007) and González-Méijome *et al.*, (2006) are contrary to the expectation of higher resistance and hence higher IOPs in peripheral corneal regions due to the increased thickness. The investigators suggested that variation in corneal hydration between central and peripheral cornea could be attributed to the differences in IOP readings. Little is known about hydration and histological changes in different areas of the cornea but based on the findings of Boote *et al.*, (2003) if the stromal interfibrillar distance increases by 5-7% in the periphery compared to the central cornea, then it can be postulated that increased hydration may result due to the larger gaps between collagen fibrils, thus reducing the resistance of the material to deformation (Queirós *et al.*, 2007; González-Méijome *et al.*, 2006). Therefore despite the cornea being thinner centrally it

may still have greater resistance to tonometric deformation than the peripheral regions. Additionally the findings of significantly lower IOPs temporally with age may be a result of changes in the arrangement of stromal collagen with age (González-Méijome *et al.*, 2006). ***These findings suggest that the iCare is able to detect changes in ocular material properties and thus supports its application in determining scleral resistance.***

The characteristics of IOP measurement using the rebound tonometer are determined by both the IOP and the material properties of the tissue; therefore the regional differences found with the *iCare* are unlikely to be due to localized differences in IOP in the various scleral quadrants but are probably a consequence of biomechanical or localized geometric differences (e.g. shape, curvature and thickness) (see Chapters 7 and 14). As suggested by the *iCare* and corneal periphery studies (Queirós *et al.*, 2007; González-Méijome *et al.*, 2006) a possible explanation may be attributable to localized differences in collagen infrastructure. In their relaxed state or under low levels of stress the collagen fibrils in the sclera have a wavy formation (Siegwart and Norton, 1999). With increasing stress levels these fibrils straighten and become tense and an increasing number of collagen fibrils counteract the applied force thus inevitably causing the sclera to become stiff (Ku and Greene, 1981; Gathercole and Keller, 1991; Ker, 1992). Additionally it has been speculated that the biomechanical properties of the cornea may be a correlate of the density and geometric arrangement of its collagen fibrils, hence variation in the orientation of the lamellae may transmute into mechanical anisotropy (Pinsky *et al.*, 2005) and such differences may also affect the sclera. Indeed the scleral collagen fibre bundles are mainly orientated in the circumferential direction and are thus more resistant to variation in globe circumference than changes in radial thickness (Battagliolo and Kamm, 1984).

It has been postulated that as scleral stiffness changes, the level of deformation experienced by the sclera (at a given IOP) also changes (Sigal *et al.*, 2005b) thus intimating that the differences in scleral *iCare* values are a surrogate measure of regional scleral resistance. Furthermore, on comparing the findings of Chapter 10 numerous significant correlations were found between the Schiötz scale readings at different quadrants and the corresponding *iCare* values for the equivalent locations. The inconsistent relationship between the *iCare* and Schiötz indentation values for the different quadrants is presumably a consequence of the inherent variability in both techniques. ***Despite this, these results reaffirm that both the iCare and Schiötz tonometer are likely***

to be measuring the same biomechanical feature of the sclera, namely the resistance of the tissue to deformation.

8.6.4 Comparison of present findings to previous studies examining scleral biomechanics

There are few *in vivo* studies that have assessed regional variation in scleral biomechanics as measuring the different scleral locations represents a technical challenge. Over the years many investigators have attempted to quantify the biomechanical properties (see table 9.5 in Chapter 9) of the sclera via extensimetry experiments on human and animal scleral tissue (Elsheikh *et al.*, 2010; Downs *et al.*, 2003; Friberg and Lace, 1988, Gloster *et al.*, 1957, Battaglioli and Kamm, 1984). A key advantage of extensimetry studies over other methods is the ability to assess variation in the biomechanical properties of the sclera from different locations of the globe in different orientations (Curtin, 1969; Eilaghi *et al.*, 2010b; Elsheikh *et al.*, 2010). Results from such experiments generally reconfirm the nonlinear response of scleral tissue to stress with strips becoming less extensible at higher tension loads and reaching a plateau after a certain stress limit, indicating that the sclera becomes less distensible at elevated stress levels (Curtin, 1969, Gloster *et al.*, 1957, Schultz *et al.*, 2008).

A recent study by Elsheikh *et al.*, (2010) using uniaxial extensimetry evaluated scleral biomechanics in different regions (i.e. anterior, equatorial and posterior). The investigators reported a significant difference in elastic modulus between circumferential strips of sclera from the anterior, equatorial and posterior regions with the anterior region showing the highest levels of stress, followed by equatorial and posterior regions. These findings are supported by those of Curtin (1969) and Friberg and Lace, (1988) who both reported significant differences in distensibility with posterior scleral strips extending more than anterior sclera tissue strips. Elsheikh *et al.*, (2010) also reported that having high levels of stress (to a given strain level) in one region was usually indicative of high stress levels in other regions. In view of the present findings this supposition would suggest that the overall increased levels of anterior scleral resistance found in the HKC individuals might be indicative of greater scleral resistance in both equatorial and posterior regions of the globe.

In support of regional biomechanical differences, Downs *et al.*, (2003) found no significant variation in scleral stiffness between scleral strips from different quadrants of monkey (*Macaca mulatta* and *Macaca fascicularis*) eyes when subjected to 0-10% strain; however at strain levels $\geq 4\%$ they reported significant quadrant differences in rabbit peripapillary sclera with inferior quadrants displaying greater levels of stiffness (See Chapter 9 for further details). In contrast, in an *in vitro* study examining human scleral tissue, Eilaghi *et al.*, (2010b) demonstrated posterior scleral strips from four meridians (ST, SN, IT and IN) to exhibit isotropic behaviour when stretched in two directions [latitudinal (i.e. towards the poles) and longitudinal (i.e. circumferential)]. In support of these findings other studies have also found no significant difference between scleral strips from vertical and horizontal meridians of the posterior sclera, nor equatorial or meridional scleral tissue strips (Chen *et al.*, 2010a; Gloster *et al.*, 1957).

Numerous investigators have also attempted to investigate regional scleral biomechanics using variations of the extensimetry technique (Smolek, (1988), global inflation (Bisplinghoff *et al.*, 2009; 2008) and deformation testing (Avetisov *et al.*, 1978). Pertinent to the present findings, Smolek, (1988) noted significant differences in the coefficient of elasticity at different locations of the globe. Furthermore, Smolek, (1988) reported the superalateral region of the posterior globe to distend relatively more than the inframedial and median locations on the globe. Despite these findings being restricted to the posterior globe, the regional differences may remain the same and continue forward to the anterior segment and thus support the current findings of reduced scleral resistance at ST when compared to the IN and N regions. Avetisov *et al.*, (1978) also noted heterogeneity in scleral deformation and in particular noted differences in deformative properties along the equatorial belt and macula region to be unequal. The investigators found that despite the scleral thickness at the macula being the greatest, loading in the meridional direction showed more stretching than in the equatorial direction. More recently, Bisplinghoff *et al.*, (2009; 2008) in their global inflation studies reported significant differences in equatorial and meridional scleral stress-strain behaviour with the meridional direction showing greater strain levels than equatorial directions.

In support of the differences in strain levels and regional differences noted by Down *et al.*, (2003) mentioned afore, Elsheikh *et al.*, (2010) proposed that the scleral response to stress may be rate-dependent with faster strains showing higher stress levels. Hence it is plausible to assume that differences in study protocol, especially with regard to strain rates,

would affect the outcome of the investigation and presumably explain the discrepancies found in the literature. Additionally both Elsheikh *et al.*, (2010) and Eilaghi *et al.*, (2010b) reported significant inter-individual differences in scleral properties thus supporting the substantial variability in the anterior scleral resistance values found in the present study.

8.6.5 Scleral thickness and resistance

In parallel with the findings of regional biomechanical differences, the sclera has also been found to display considerable variation in thickness in different regions as seen in Chapter 7 and noted by previous investigators (Elsheikh *et al.*, 2010; Guthoff *et al.*, 1987; Olsen *et al.*, 1998; 2002; Norman *et al.*, 2009). Indeed the present findings of numerous significant correlations between scleral thickness and scleral *iCare* values suggest that tissue thickness may be a significant factor in scleral resistance. Although this relationship was not detected for all regions suggesting that inherent variability in both scleral *iCare* tonometry and thickness measurements may have been attributable to this discrepancy. On inspection of the regional thickness variation at the 4 mm location presently investigated, the change in thickness from thinnest to thickest shows a similar pattern of change as the scleral resistance with the *iCare*, with a notable difference between the inferior (thicker) and superior (thinner) regions. Previous studies examining scleral thickness have also reported large intra-individual and inter-individual differences in thickness values, which may translate into the variability of scleral resistance found in the present study (Norman *et al.*, 2009; Olsen *et al.*, 1998). ***Hence the reports of variation in scleral thickness are likely to affect the local stress-strain response to a constant IOP, thus supporting the present findings of regional differences in scleral biomechanics.***

8.6.6 Scleral curvature and shape

Scleral curvature has also been suggested as a factor that affects eye wall stress and hence resistance, with Friedman, (1966) proposing that the flatter the curvature of the globe, the greater the stress, resulting in localised differences in strain for a constant IOP level. Due to the technical limitations in assessing this feature *in vivo* there is inadequate data on this property of scleral tissue. Pierscioneck, *et al.*, (2007) assessed changes in scleral curvature with IOP changes using digital photographic profile images of porcine eye. The study reported that no significant change in corneal curvature occurred but that scleral curvature changed linearly with IOP. In the present study ethnicity and gender were found to have a

significant effect on the flattest corneal curvature and axial length. HKC individuals showed significantly flatter corneas and longer axial than BW subjects, whilst HKC male subjects showed longer axial length and flatter corneas than female subjects. The HKC *iCare* data showed a significant difference between gender, with higher scleral *iCare* readings in males than females. The UK data showed a similar trend although the difference was not significant. ***These observations of higher scleral iCare readings amongst individuals with longer axial length and flatter corneas suggest that such structural characteristics may have a significant influence on scleral biomechanics.***

Further support for regional variation in scleral biomechanics stems from studies investigating the internal dimensions of the anterior segment pertinent to intraocular lens sizing (Werner *et al.*, 2008; Rondeau *et al.*, 2004; Baikoff *et al.*, 2005). Such studies have reported that the anterior eye does not exhibit the commonly assumed geometrically round shape but in fact shows considerable anatomical variation in its conformation (Werner *et al.*, 2008; Rondeau *et al.*, 2004). Thus it is plausible to assume that the internal dimensions of the anterior eye are likely to affect the shape and physical parameters of the overlying sclera, which conceivably may translate into regional variation in scleral biomechanics.

8.6.7 Scleral resistance and Age

The present investigation showed age to modulate the scleral response to deformation in both the BW-BSA and HKC individuals, with higher scleral resistance seen in the older age group ($29 >$ to ≤ 40 years). Previously scleral rigidity has been found to increase with age due to increase in enzymatic and non-enzymatic cross-links between collagen as seen in other connective tissues (Keeley *et al.*, 1984, Watson and Young, 2004). In support of these findings, a recent study reported lower density of collagen in older human posterior sclera than porcine sclera; the human sclera showed greater rigidity as a result of increased non-enzymatic cross-links with age in contrast to the porcine sclera (Schultz *et al.*, 2008). These increased cross-links have also been suggested to be responsible for decreased solubility of collagen with age (Curtin, 1969). Age has not been found to affect the collagen content or type in either the anterior or posterior segments (Keeley *et al.*, 1984), although the fibres have been found to become thicker and less regular especially at the muscle insertion sites (Watson and Young, 2004). Increased irregularity may lead to accumulation of lipid and calcium deposits consequently causing yellowing of the sclera and the development of plaques (Bron, 1997; Avetisov *et al.*, 1983). Experimental studies

have similarly shown changes in mechanical behaviour of the sclera with age (Friberg and Lace, 1988; Perkins, 1981). Age has also been implicated as a factor in corneal rigidity, with numerous studies reporting increased rigidity with age (Friedenwald, 1937, Singh *et al.*, 1970; Wong *et al.*, 1991; Goodside, 1959; Lam *et al.*, 2003a; Pallikaris *et al.*, 2005).

8.6.8 Scleral resistance and its relation to myopia and ethnicity

Contrary to the present findings in Chapter 11 IOP was found to correlate significantly with axial length amongst the HKC individuals, whilst no such relation was found for the BW or BSA individuals. *It can be hypothesized from these findings that the HKC eyes may be under progressively higher stress as the axial length grows thus possibly increasing scleral resistance.* In experimental studies both Gloster and Perkins, (1957) and Ridley, (1930) reported reduced distensibility of ocular tissue after exposure to periods of elevated IOPs. Moreover scleral creep has also been noted in extensimetry studies, which is indicated by an initial rapid elongation followed by a relatively long period of time required by the scleral strips to reach a steady state during loading and unloading (Phillips *et al.*, 2000; Siegwart and Norton, 1999). Curtin, (1969) noted that the creep response constituted the greatest part of the overall response to scleral stress, with a relatively short initial change in length. Experimental studies assessing the pressure-volume relationships have also demonstrated a scleral creep rate when subjected to long periods of elevated IOP levels (Greene and McMahon, 1979; Mattson *et al.*, 2010).

The present study failed to show any significant difference in scleral resistance between myopes and non-myopes nor between axial length grouping. Myopic eyes have a greater posterior ocular volume than hypermetropic and emmetropic eyes (Gilmartin *et al.*, IOVS 2008, 49: ARVO E-Abstract 3582). Previously these larger myopic eyes have been shown to have statistically significant lower corneal rigidity than hypermetropic eyes (Friedenwald, 1937; Castrén and Pohjola, 1962; Goodside, 1959; Perkins, 1981, Ytteborg, 1960b), whilst others have found no significant difference in corneal rigidity between emmetropic and myopic individuals (Wong *et al.*, 1991; Zolog *et al.*, 1969). Considering the significant differences between corneal and scleral biochemical and biomechanical structure the response of these two tissues to deformation may vary.

Despite the findings of non-significant differences in scleral resistance between refractive status and axial length grouping, the investigation did identify significant differences in

scleral resistance between ethnicities. As discussed by Twelker *et al.*, (2009) ethnicity is a complex variable that defines individuals on the basis of genetic and environmental factors but also incorporates numerous additional variables such as nationality, physical appearance, language, religion and racial and cultural origin or background. Hence to assess whether ethnicity was a significant factor in scleral biomechanics, BW and BSA individuals were assessed in the UK (thus sharing a common environment) and HKC individuals in HK.

In the present study HKC individuals were found to have significantly higher scleral resistance in all regions when compared to BW and BSA subjects. Furthermore the HKC individuals were also found to have less regional differences than the individuals from the UK thus suggesting a more uniform globe than those of BW and BSA ethnicity. These differences may be attributable to variation in ocular architecture or biomechanical differences. When considering the higher prevalence levels of myopia in HK (Lin *et al.*, 2001; Lam *et al.*, 2004; Fan *et al.*, 2004a; 2004b) it can be speculated that an interaction effect between inherited structural and biomechanical characteristics coupled with environmental factors may explain the differences in the occurrence of myopia between populations.

Hereditary has long been suggested to be a significant risk factor in myopia development. In support of a genetic causative factor in myopia, numerous investigations have assessed family correlations where children of myopic parents have been found to be at greater risk of developing myopia than those with non-myopic parents (Jones *et al.*, 2007b, Guggenheim *et al.*, 2000; Baird *et al.*, 2010). Additionally reports from classic twin studies where environmental and genetic factors can be evaluated, have indicated heredity to be a significant factor in myopia (Tsai *et al.*, 2009; Teikari *et al.*, 1991; 1988; Lyhne *et al.*, 2001; Hammond *et al.*, 2001; Dirani *et al.*, 2006). Molecular genetics family linkage studies have also reported a number of myopia loci for different severity of myopia (Lam *et al.*, 2003b; Farbrother *et al.*, 2004a; Li *et al.*, 2009; Metlapally *et al.*, 2009; 2010). Despite a strong case for a genetic component in myopia development, no inherent difference in ocular biometry has been found between children of different ethnicities to explain a predisposition for some individuals to develop myopia, suggesting that an interaction between environmental and genetic risk factors may be more important in myopia pathogenesis (Twelker *et al.*, 2009; Morgan and Rose, 2005; Guggenheim, 2009).

The mechanism for myopia development is still elusive, however its aetiology is clearly linked to a failure of the mechanism that brings about emmetropization (Curtin, 1985). As shown by various investigators (Larsen, 1971; Zadnik *et al.*, 1993; 1995; Mutti *et al.*, 2005; Shih *et al.*, 2009) crystalline lens thinning occurs during infancy and continues to the age of puberty. The mechanism for the thinning of the lens has been postulated to occur due to the equatorial stretching caused by the enlarging globe in all radial directions (van Alphen and Graebel, 1991). This mechanism is thought to play a significant role in emmetropization in that it contributes to the equilibrium between axial length growth and ocular power that defines the emmetropic refractive state (Shih *et al.*, 2009; Mutti, 2010). More recently it has been suggested that a restrictive force to the normal thinning of the lens as ocular growth progresses may be a significant factor in the aetiology of myopia (Mutti, 2010). In particular thicker ciliary bodies have been found in myopic adults (Oliveira *et al.*, 2005) and children (Bailey *et al.*, 2008) and it has been suggested that these thicker ciliary muscles (Chapter 13) may perhaps have a biomechanical role in restricting the equatorial stretching required to progress successfully towards emmetropia (Mutti, 2010). ***In light of the findings of the present study the greater scleral resistance found amongst the predominantly myopic HKC group may suggest that a more rigid sclera is less likely to allow stretching for the purposes of lens thinning in emmetropization and would support the speculation of an anterior segment restriction promoting myopic growth.*** Furthermore the reduced levels of stretching may also additionally explain the lower levels of regional differences found in the HKC group when compared to the BW-BSA group.

In regards to ocular conformation and refractive status Atchison *et al.*, (2005) reported most eyes to conform to an oblate shape (i.e. peripheral retina flattens relative to the centre), whilst myopic eyes also demonstrate an oblate shape but have a greater tendency towards a less oblate and a more prolate conformation (i.e. retina steepens in the periphery relative to the centre). Previously a number of investigators have reported divergent findings; Chen *et al.*, (1992) employed MRI scanning to assess retinal contours and reported greater deviation from sphericity in myopic eyes when compared to hypermetropic and emmetropic eyes, whereas Cheng *et al.*, (1992) found myopic eyes not to show any significant difference in shape compared to hypermetropic and emmetropic eyes, and instead showed all eyes to demonstrate an oblate and spherical shape. Pertinent to the present study Zhou *et al.*, (1997) using CT scans showed 95.7% of Chinese myopic individuals to show a prolate shape and of the hypermetropic individuals 89.5% had an

oblate shape, whilst emmetropic individuals had either a oblate 43.4% or spherical shape 51.3%. In a peripheral refraction study assessing retinal contours in myopic and anisomyopic Caucasian and Taiwanese Chinese eyes, Logan *et al.*, (2004) reported myopic eyes to show a prolate shape in both ethnicities, however Caucasian subjects demonstrated a nasal-temporal asymmetry whilst the Chinese eyes showed a greater and more uniform relative expansion of the posterior retinal surface in their more myopic eyes. Additionally in comparison to the Caucasian eyes the Taiwanese-Chinese eyes showed a tendency for greater axial elongation in comparison to equatorial growth despite being matched for refractive error.

A number of reports have suggested significant inter-individual differences in ocular shape (Atchison *et al.*, 2004; Stone and Flitcroft, 2004), suggesting that if scleral biomechanics is linked to ocular conformation this may well also show significant individual variation. These divergent results in regards to ocular shape between investigations may be attributable to factors such as racial and demographics differences, levels of myopia or study methodology. Moreover what they identify is that there resides a significant difference in ocular shape between individuals and refractive status. In regards to the present study, the failure to detect scleral biomechanical differences between myopes and non-myopes could perhaps be ascribed to the significant inter-individual differences in globe conformation. ***In contrast the more note worthy findings of increased scleral resistance amongst the HKC individuals when compared to the BW-BSAs, may be indicative of ethnic differences in ocular tissue biomechanics.*** As Chinese eyes have a greater susceptibility to myopia these observations may suggest that the findings of higher scleral resistance in the HKC eyes is a structural correlate of myopia.

8.7 Conclusion

The key findings of the present study are:

- *iCare* rebound tonometry is a robust and viable technique for assessing anterior scleral resistance.
- The *iCare* tonometer was found to show high levels of agreement with ORA derived IOP measurements, whilst significant differences were found with GAT IOPs.
- Regional variation in scleral resistance exists with the ST region showing the least resistance and IN the most resistance.
- Scleral resistance may be a correlate of scleral thickness.
- Scleral resistance was found to increase with increasing age in both the UK and HKC subjects.
- Individuals of HKC descent show greater scleral resistance than individuals of BW-BSA origin.
- The increased scleral resistance in HKC individuals may be a correlate of the increased prevalence of myopia in East Asian populations.

Acknowledgements

College of Optometrist's Summer Scholarship (2009) for Elena Dold - Technical Assistant in the above study.

Graham Davies- construction of the custom designed housing for the *iCare* tonometer.

9.0 CALIBRATION OF MEASUREMENTS OF HUMAN SCLERAL RESISTANCE USING AGAROSE GELS

9.1 Introduction

In common with many connective tissues in the body the sclera displays viscoelastic properties (Downs *et al.*, 2005, van der Werff, 1981). A key characteristic of such tissues is the display of a biphasic response to strain: a rapid (elastic) response followed by a slower (i.e. creep) response (Edmund, 1988). Collagen fibre straightening and extension during the application of stress has been thought to produce this type of viscoelastic behaviour (Curtin, 1969). An assessment of the mechanical features of the scleral shell indicates that IOP, scleral curvature and thickness all contribute to the level of stress imposed on the ocular walls (Friedman, 1966). Furthermore, there appears to be disparity between studies as to whether the sclera exhibits a linear (Arciniegas *et al.*, 1980; Avezitsov *et al.*, 1983; Friberg and Lace, 1988) or non-linear (Eilaghi *et al.*, 2010b; Elsheikh *et al.*, 2010) stress-strain relationship. The difficulties posed by assessing such material properties *in vivo*, means there is a lack of research on the biomechanics of human scleral tissue.

The *in vitro* experimental assessment of biomechanical features of the sclera has been mainly via two modes; extensimetry (i.e. assessing change in length of strips of sclera following application of a predetermined force) (Chen *et al.*, 2010a; Eilaghi *et al.*, 2010b) or assessing the pressure-volume relationship of the ocular globe (i.e. increasing the volume of the eyes by known amounts and measuring the induced changes in curvature, thickness and pressure) (Mattson *et al.*, 2010; Bisplinghoff *et al.*, 2009). In recent years it has been proposed that the biomechanical features of the ocular coats should be described using engineering terms to facilitate understanding of what can be a confusing topic (White, 1990). The measures of stiffness of a given material vary with type and rate of force application as well as how deformation is measured (Stolz *et al.*, 2004). The term modulus is used to express the stiffness of a material and this expression is often modified (i.e. substituted by alternative terms) to define the type of force applied and how it varies with time to give expressions such as i.e. tensile, compression, shear, dynamic (de Freitas *et al.*, 2006).

The mechanical properties of soft materials such as gelatine have featured in research areas pertinent to the pharmaceutical and food industries (Fassihi and Parker, 1988; Watase and

Nishinari, 1980). The standard protocol as described in the British Pharmacopoeia (2007) for determining gelatine rigidity involves the assessment of the force required for a plunger of known diameter to indent a sample of gelatine to a predetermined depth. Similarly stiffness of articular cartilage and biological cells and tissues have been investigated on micro- and nanometer scales using indentation-type atomic force microscopy (IT AFM) (Julkunen *et al.*, 2008; Stolz *et al.*, 2004; Ebenstein and Pruitt, 2004; Lu *et al.*, 2006). In order to assess the biomechanics of biological materials, phantom materials, which exhibit mechanical properties similar to those of body tissues are generally required. As such hydrogels like agarose, alginate, chitosan, collagen, fibrin and hyaluronic acid (Ahearne *et al.*, 2005) have often been used for cartilage (Rahfoth *et al.*, 1998) and corneal (Minami *et al.*, 1993) models. A particular advantage of agarose gels is that at low concentrations (i.e. <2%) it can be used to produce relatively strong gels, which exhibit significant hysteresis on application of stress (Rakow *et al.*, 1995). Agarose is a complex mixture of polysaccharides derived from marine algae, which contains β -1,3 linked D-galactose and α -1,4 linked 3,6-anhydro- α L- galactose residues (Normand *et al.*, 2001).

Chapter 8 evaluated the utility of the *iCare* tonometer to assess regional variation in scleral resistance using the principle of rebound tonometry. In order to interpret the scleral *iCare* values as measures of scleral resistance the present investigation describes a calibration exercise using agarose gels of varying rigidity. The technique for assessing agarose rigidity was adapted from the British Pharmacopoeia protocol for assessing gelatine rigidity. Hence the objective of the investigation was to develop a method of calibration for the *iCare* tonometer to demonstrate its applicability in assessing the biomechanics of human sclera.

Mechanical Term	Mechanical definition	Expression/ Point of interest
Stress	Force applied to a material over a unit area assuming material is homogenous	Stress (Pa) =Force (Newton (N))/ Area (m ²)
Strain	Deformation (i.e. lengthening or shortening) caused by the stress	Strain (no units) = change in length/ initial length
Young's modulus (E)	Relation between stress and strain; assessment of a material's elastic properties	E= Stress/Strain Non-linear relation in most biological materials; units N/m ² ; the smaller the coefficient E the more elastic the material
Stiffness/rigidity	Relation between force and the resultant elastic deformation of a given material	Applied in extensimetry, pressure volume experiments and Schiotz tonometry
Tensile strength	Maximum stress when material	Assessed in stress-strain

	fails	experiments (Downs <i>et al.</i> , 2003)
Hysteresis	Difference in material behaviour to stress when loading and unloading	Evident as a hysteresis loop in stress-strain curves (Curtin, 1969)
Creep	Behaviour of materials to slowly deform permanently under the influence of stress over a period of time	Sclera has been found to demonstrate this type of behaviour as a result of the stress from the IOP (Ku and Green, 1981; Mattson <i>et al.</i> , 2010)

Table 9.1 A summary of biomechanical terminology commonly used to describe the physical properties of biological materials.

9.2 Materials and Methods

9.2.1 Agarose preparation

The form of agarose used in this study was Agarose Molecular Biology Reagent (Moisture<10; MB Biomedicals, LLC, California, USA). 2% w/v agarose solution was prepared by dispersing 8g of agarose powder making up to 400 ml with double distilled and filtered water. The solution was heated in a glass bottle (with cap secured to avoid evaporation) and stirred continuously for ~2 hours to disperse the agarose powder until the solution was clear. Eight concentrations (i.e. % w/v) were made in the following order using serial dilution: 2, 1.75, 1.5, 1.25, 1, 0.75, 0.50, and 0.25. When taken from the stock solution each concentration of the agarose solution was kept heated and 4 ml was pipetted out into glass vials (clear screw top, 14.75 mm diameter X 45 mm height; Kinesis, Cambridge, UK). 10 vials of each concentration were made and covered with parafilm to avoid any evaporation. The gels were left to cool overnight at room temperature (~20°C) before testing. Vials were assessed for any obvious bubbles or non-uniformity of the meniscus surface and if any anomalies were observed vials were removed from the study sample.

9.2.2 *iCare* tonometry and agarose gels

The vials were held horizontally with a retort stand/clamp fixture (Figure 9.1). Using an electronic calliper (Maplin Electronics, South Yorkshire, England) the *iCare* tonometer probe was set to be between 4-8 mm from the meniscus. A spirit level was used to ensure each vial was level and the *iCare* probe was aligned subjectively to provide approximately central readings. To comply with the scleral resistance study in humans four readings were taken and ensured to have reliability levels of; no bars, or low bars - mid bars and high bars were found to occur very infrequently.

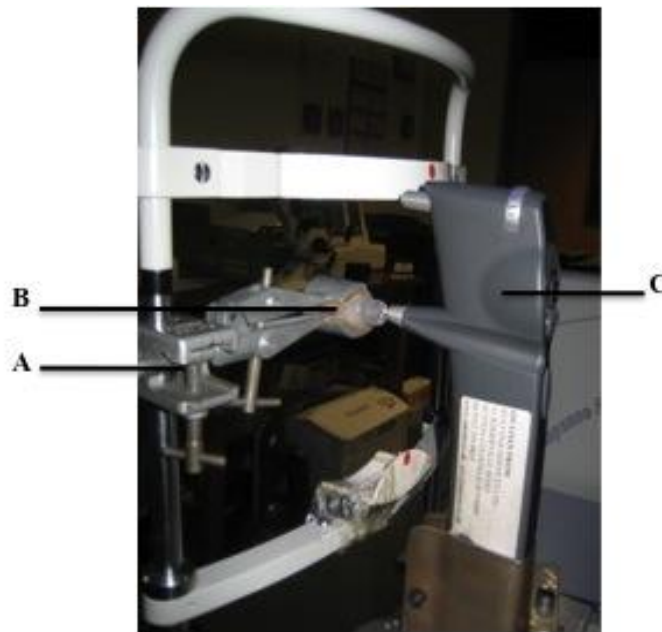


Figure 9.1 Experimental set-up for assessing *iCare* measurements of agarose gels of varying concentrations. **A:** clamp/stand, **B:** vial of agarose, **C:** *iCare* tonometer.

9.2.3 Hounsfield Tensometer

The Hounsfield tensometer (Tinius Olsen Ltd, UK) applies a controlled force to a sample of material and produces a force-displacement graph to display the characteristics of material behaviour. The tensometer applies the force at a constant rate and in turn readings of force and extension are recorded until the specimen sample breaks (i.e. rupturing of surface tension is evident). A load cell of 5N was used and a load range of up to 5N and displacement range (mm) of 0-2000 were set for the agarose indentation test. The machine crosshead was programmed to move down vertically at a speed of 2 mm/min.

In order to simulate the level of stress and strain applied during rebound tonometry, an *iCare* probe was used as the indenting probe (i.e. the ‘indenter’) for the present study. The *iCare* probe (11mg) is composed of a PMMA spherical head of 1.7 mm diameter, which is attached to a 24 mm long, 1 mm diameter stainless steel tube. The probe was attached to the Hounsfield 5N load cell via a screw (Figure 9.2). The diameter of the probe head is 1.7 mm and thus has a surface area of 9.07 mm² (i.e. cross-sectional indentation area of 4.54 mm²). The same probe was used for the duration of the study.

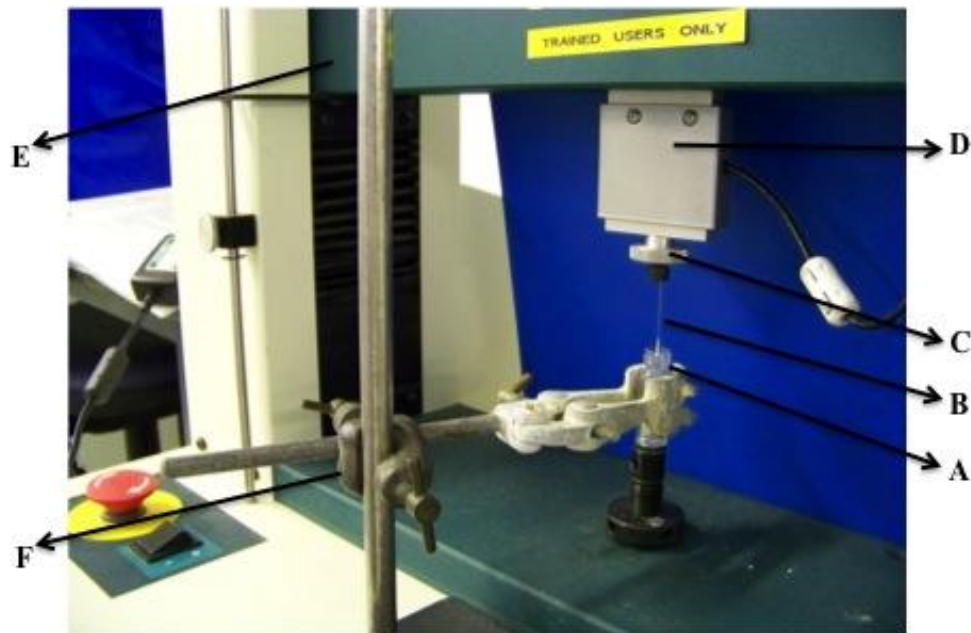


Figure 9.2 Experimental setup showing indentation of the agarose gel **A:** Vial of agarose **B:** *iCare* probe ‘indenter’ **C:** Screw attachment **D:** 5N load cell **E:** Hounsfield tensometer **F:** Retort stand/clamp.

To aid the stability of the agarose vials on indentation, the vials were held in a clamp below the indenter probe. As such the vials were aligned subjectively so that the indentation of the *iCare* probe would be as central as possible and match the approximate site where the *iCare* tonometer readings were taken beforehand. Each vial of agarose was only indented once and all testing was conducted at a constant room temperature of ~20°C. Testing with the indentation model assumes homogeneity of the sample material and negligible stress-strain effects in the indenter (Fischer-Cripps, 2003).

On press button initiation of the test sequence the machine moves the crosshead down at a constant speed of 2 mm/min. On detection of a load by the instrument load cell, an auditory beep is heard. The force-extension results are graphically displayed on a linked

PC monitor. The cross head was zeroed at the start of each test. The software was set to stop the crosshead movement once the surface tension was broken. The data were exported via the *QMAT (Questions MATerials*, Hounsfield Test Equipment Ltd, UK) graphical software into a Microsoft *Excel* (Microsoft Corporation, Redmond, Washington, USA) spreadsheet.

9.2.4 The conversion of force-extension data to stress-strain data

The force-extension graphs for each vial from the Hounsfield tensometer output were initially converted to stress-strain graphs. Stress and strain are calculated as:

$$\text{Engineering stress (Newton (N)/m}^2\text{)} = \text{Force (N)/cross-sectional area (m}^2\text{)} \quad \text{Eq 9.1}$$

$$\text{Engineering strain} = \text{Change in length/Original length} \quad \text{Eq 9.2}$$

Data from the loading portion of the stress-strain graphs were used to calculate Young's modulus (E). E provides a measure of the stiffness of a material with higher levels of E indicating greater stiffness than lower values. Thus stiffness is a measure of material resistance during stress application. An approximation of Hooke's law, where strain is proportional to stress, is used to calculate E:

$$E \text{ (Pascals (Pa))} = \text{Stress (Nm}^2\text{)/Strain} \quad \text{Eq 9.3}$$

On inspection of the multiple stress-strain curves, the level of variability was seen to be lower at initial sections of the curves for all concentrations (Figure 9.3). Bueckle, (1973) demonstrated that indentation strains of 10% or greater resulted in artificially elevated stiffness values due to stiffness of the surface supporting the specimen i.e. the walls of the glass vial, and hence recommended that stress-strain should be assessed below the 10% strain levels. In a recent study assessing pulsatile dynamic stiffness of agarose, the protocol implemented by the investigators when calculating E via stress-strain curves was to evaluate the initial 4-6.5% region of the loading curve and so fall within the limit recommended by Bueckle, (1973) (de Freitas *et al.*, 2006). Additionally de Freitas *et al.*, (2006) chose the 4-6.5% range to avoid non-linearities inherent at the start of the loading and at the point where the machine changes direction from loading to unloading. The investigators of the de Freitas *et al.*, (2006) study proposed that non-linearities at onset of

testing may be a result of a lack of parallelism of the indenter and the meniscus surface (i.e. off-angle indentation of the gel), whilst on reversal from loading to unloading the ‘lash’ in the motor system may further contribute towards the non-linearities near the breaking point. Therefore the approximately linear portion of the stress-strain curves (i.e. in the 4-6.5% strain range) was assessed in the present study.

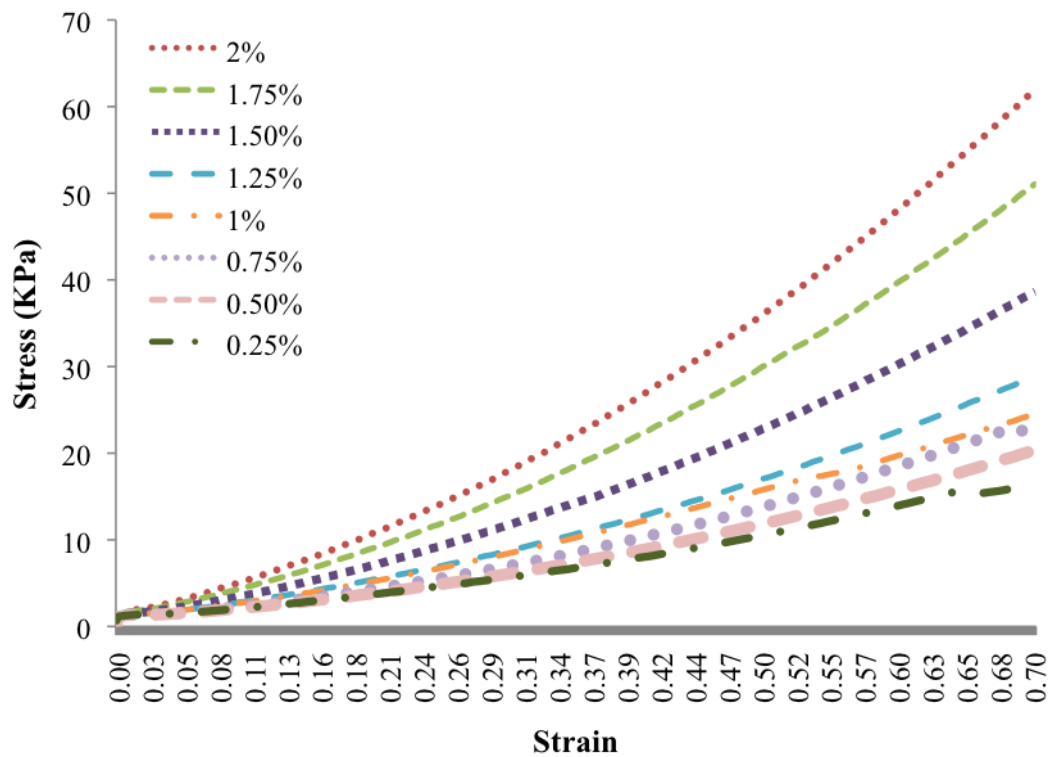


Figure 9.3 Average stress-strain curves for the multiple concentrations of agarose.

9.3 Statistical analysis

All statistical analysis was performed using *SPSS* Version 15 (SPSS, Inc., Chicago IL) and Microsoft *Excel* (Microsoft Corporation, Redmond, Washington, USA). The E data and *iCare* values for each concentration were checked and found to be normally distributed using the Kolmogorov-Smirnov test. One-way ANOVAs were conducted to test for differences in E and *iCare* readings between agarose concentrations. Following conversion of the human scleral *iCare* measurements (data from Chapter 8) to E values the data were assessed for a normal distribution using the Kolmogorov Smirnov test. To test for sample differences in E values between the UK and HK individuals, a two-way repeated measures ANOVA was performed with the within-subject factor as the E values for the 8 regions and the data origin (i.e. UK or HK) as the between-subject factor. Pearson's correlation coefficient was also performed to test for a relationship between human biometric data (axial length and refractive error) and E values. For all statistical tests a p-value of <0.05 was taken as the criterion for statistical significance.

9.4 Results

Due to significant non-uniformity of the agarose meniscus or the presence of large air bubbles near the meniscus, some vials were removed from the study (0.25% n=8; 0.50% n=10; 0.75% n=10; 1% n=6; 1.25% n=10; 1.5% n=10; 1.75% n=9; 2% n=9). A one-way ANOVA testing for the effect of agarose concentration on the E values, revealed significant differences ($F(7, 64)=52.51$ ($p<0.001$)) between the E value for the different concentrations. Games-Howell *post hoc* analysis revealed no significant difference between (0.25% and 0.5%, 0.75%); (0.50% and 0.75%); (1% and 1.25%, 1.5%); (1.25% and 1.5%); (1.75% and 2%). All other comparisons of E for different concentrations were significantly different. Figure 9.4 demonstrates a non-linear relationship between concentration of agarose and the corresponding E values. It is also evident from Figure 9.4 and Table 9.2 that as the concentration of agarose increased the variability of the E values also increased.

Table 9.2 shows *iCare* readings and the corresponding average E values for each concentration. A one-way ANOVA on the *iCare* data from agarose vials of each concentration revealed significant differences ($F(7, 70)=530.76$ ($p<0.001$)). A *post hoc* Games Howell test revealed no significant difference in *iCare* values between 0.25% and

0.50%; all other differences were significant. Figure 9.5 shows *iCare* values to increase progressively as the concentration of the agarose increased. A similar relationship was seen again between the *iCare* values and the rigidity of the agarose gels (i.e. E values) (see Figure 9.6) with a trend for increasing tonometric readings with progressively stiffer gels. A second order polynomial was fitted to evaluate the relationship between *iCare* values and agarose rigidity (Figure 9.7 and see Eq 9.4). The best fit for the polynomial was judged with reference to the r^2 value, with greater r^2 denoting improved fit.

$$\text{Young's modulus (E)} = 0.0048 * (\textit{iCare} \text{ values})^2 + (0.101 * \textit{iCare} \text{ values}) + 7.2362 \quad \text{Eq 9.4}$$

By implementing this polynomial, *iCare* values from Chapter 8 (UK and HK data) were converted to E values (Table 9.3 and Figure 9.8). A two-way mixed repeated measures ANOVA revealed significant regional variation (SN: superior-nasal; S: superior; ST: superior-temporal; T: temporal; IT: inferior-temporal; I: inferior; IN: inferior-nasal; N: nasal) in E values ($F(4.815, 640.404) = 106.918$ ($p < 0.001$)) and significant differences between the UK and HK E values ($F(1, 133) = 21.207$ ($p < 0.001$)). A Bonferroni *post hoc* demonstrated significant differences between all regions except between SN:T, IT:I, IT:N and I:N. Amongst the UK subjects only E values for region S showed a significant correlation with refractive error ($r = -0.235$ $p = 0.042$). For the HKC subjects E values for region ST correlated negatively with refractive error ($r = -0.267$ $p = 0.039$) and positively with axial length ($r = 0.277$ $p = 0.032$); E for region S also correlated with axial length ($r = 0.262$ $p = 0.043$).

Concentration (w/v %)	Average E (KPa)	E SD (KPa)	Average <i>iCare</i> reading (mm Hg)	<i>iCare</i> readings SD (mm Hg)
2	39.27	8.06	72.32	5.32
1.75	31.99	6.83	60.76	3.96
1.5	22.04	4.50	47.96	3.29
1.25	16.44	3.23	38.42	1.66
1	15.98	2.36	24.20	3.09
0.75	10.54	2.32	19.10	1.28
0.5	9.10	2.48	15.00	0.42
0.25	8.58	3.60	12.47	2.09

Table 9.2 *iCare* readings and E values for each concentration of agarose.

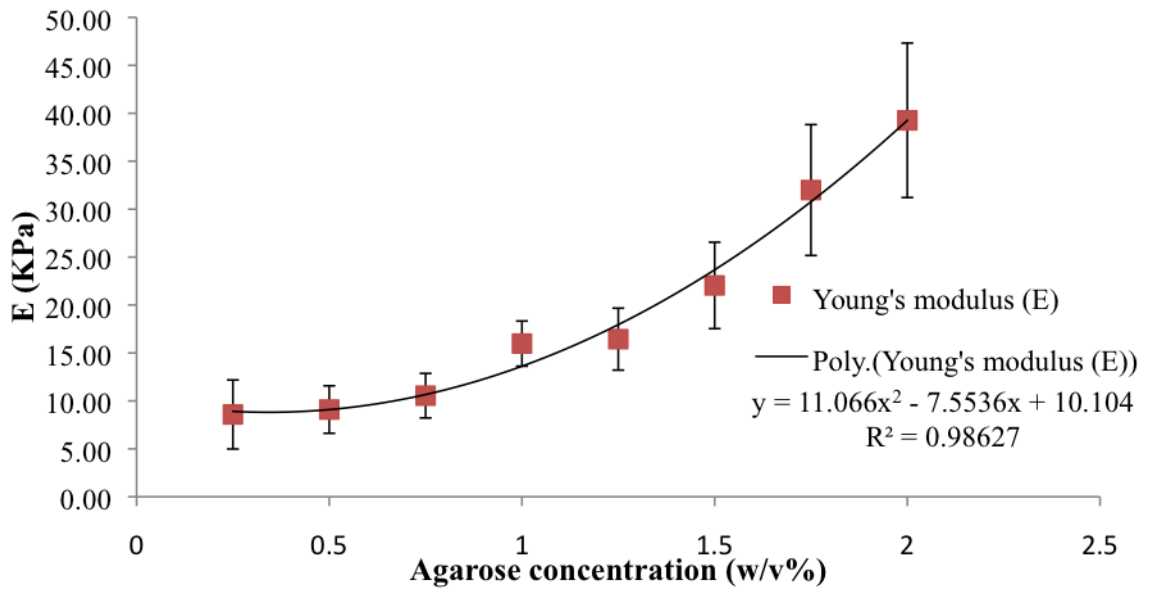


Figure 9.4 Agarose concentration versus mean E values \pm SD (error bars).

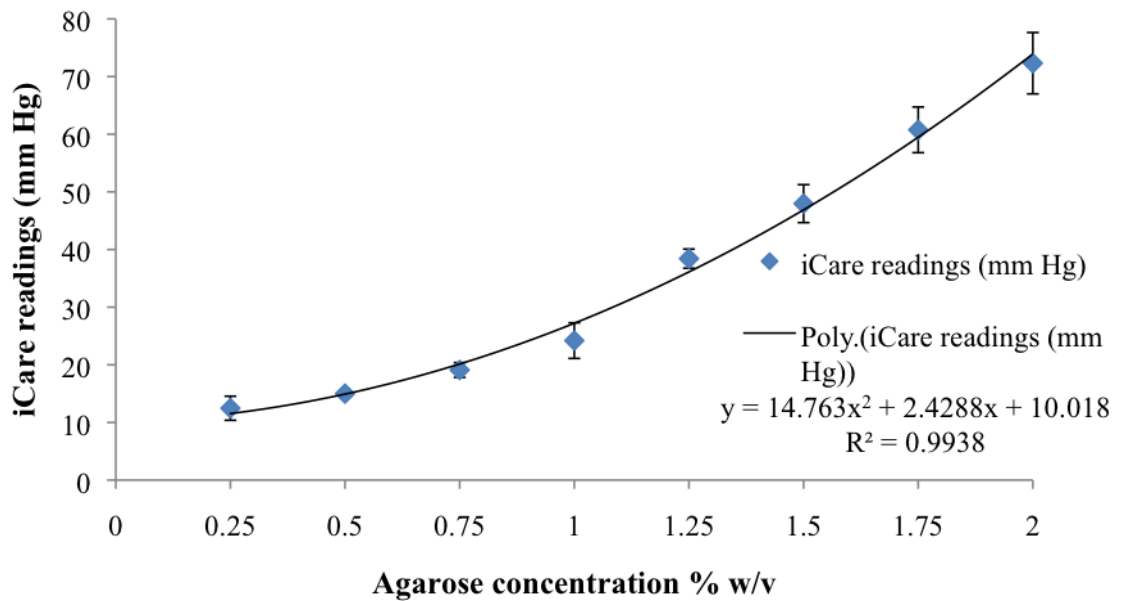


Figure 9.5 Agarose concentration versus mean *iCare* readings \pm SD (error bars).

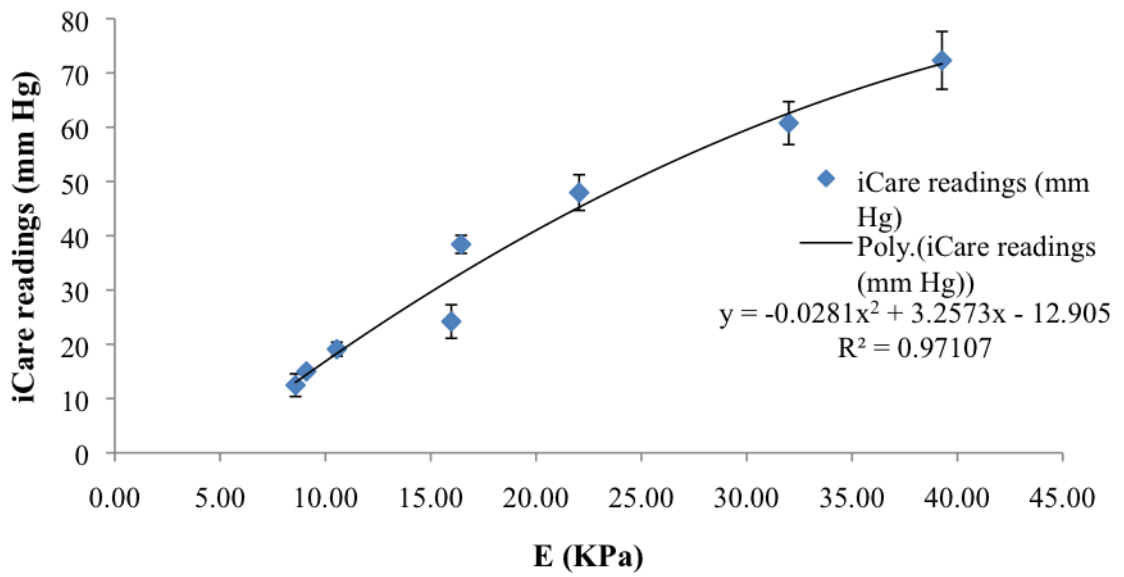


Figure 9.6 Agarose E values versus mean *iCare* readings \pm SD (error bars).

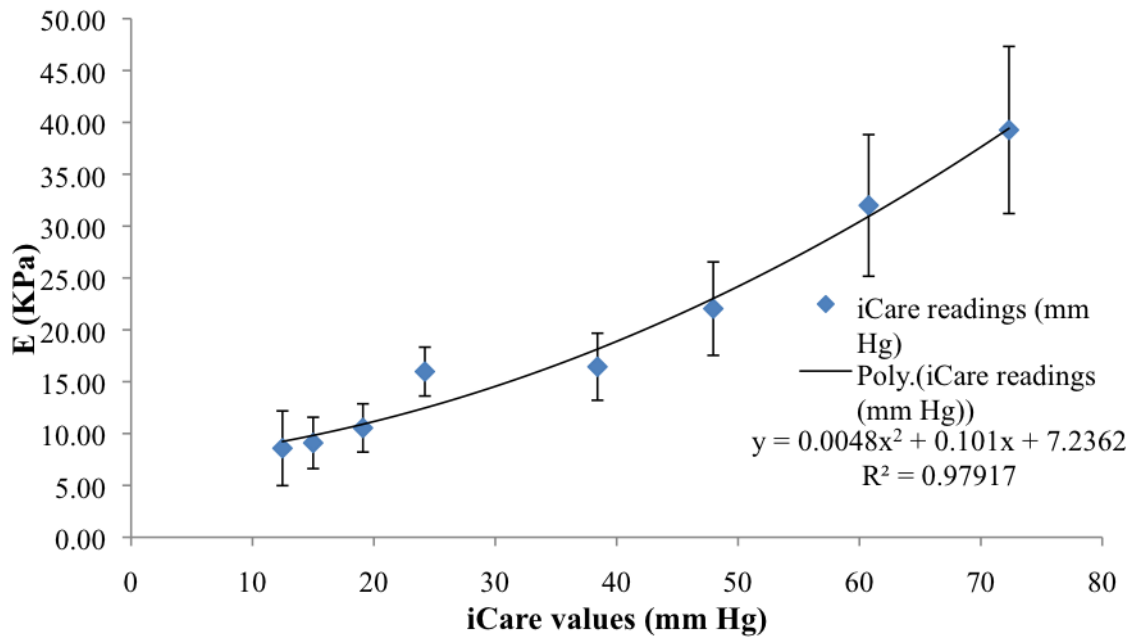


Figure 9.7 *iCare* values versus mean E values \pm SD (error bars).

Region	Mean UK <i>iCare</i> values (mm Hg)	Mean HK <i>iCare</i> values (mm Hg)	E values for UK (KPa) mean \pm SD	E values for HK (KPa) mean \pm SD	E difference HK-UK (KPa)
SN	30.34	42.19	15.14 \pm 4.04	20.51 \pm 6.80	5.37
S	26.73	39.56	13.71 \pm 3.35	18.70 \pm 4.76	4.99
ST	23.04	29.75	12.44 \pm 2.96	14.68 \pm 3.29	2.24
T	34.53	40.75	17.10 \pm 5.56	19.88 \pm 5.93	2.78
IT	39.36	45.34	19.27 \pm 5.84	22.37 \pm 6.15	3.10
I	38.68	43.21	19.33 \pm 7.26	21.41 \pm 8.35	2.07
IN	47.29	55.53	23.58 \pm 8.04	28.57 \pm 9.43	4.99
N	40.85	48.41	19.92 \pm 5.66	24.07 \pm 7.14	4.15

Table 9.3 RE mean regional *iCare* values converted to E values for both UK and HK data.

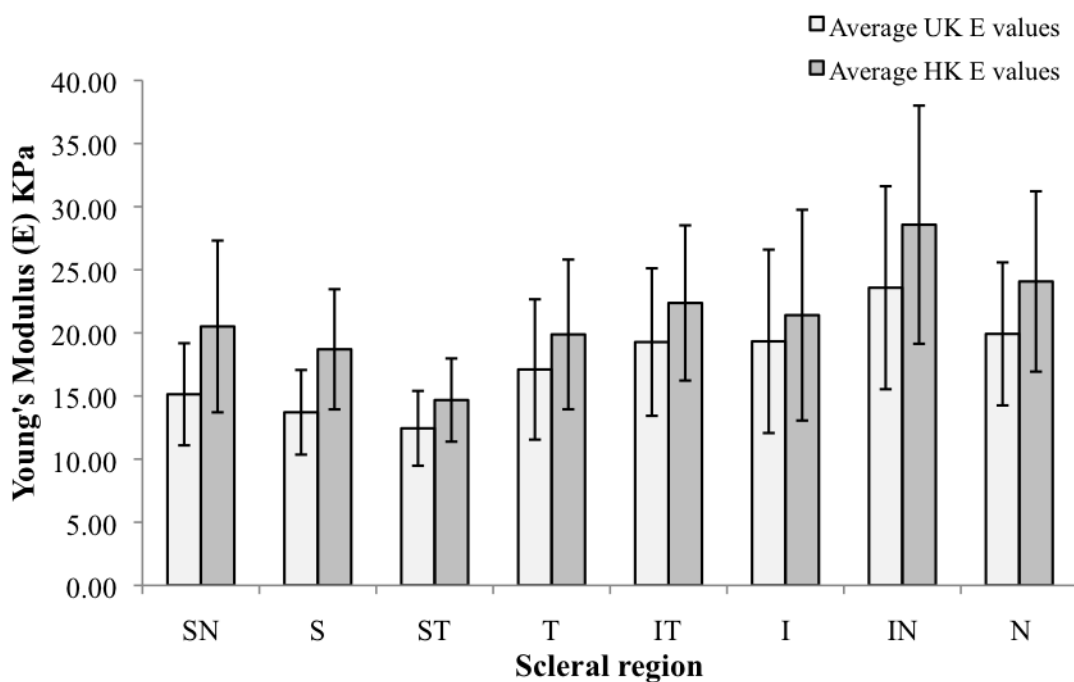


Figure 9.8 RE mean E \pm SD (error bars) for each region for both UK and HK groups.

9.5 Discussion

The principle objective of the present study was to assess whether the regional differences in scleral *iCare* measurements (Chapter 8) could be genuinely attributed to differences in stiffness of scleral material. The results of the investigation indicate that as the concentration of agarose increases, the stiffness of the gels also concurrently increases. Furthermore the study also confirmed the *iCare* values to be significantly influenced by the Young's modulus (E) of the agarose gels. These findings demonstrate that rebound tonometry is an effective method of assessing the mechanical properties of biological tissues as such as rigidity and hence support the findings of regional variation in scleral resistance in Chapter 8.

9.5.1 Agarose gels

The present findings of increased rigidity with progressively higher concentration of agarose gels are consistent with those found in previously published studies (Gu *et al.*, 2003; de Freitas *et al.*, 2006; Normand *et al.*, 2001; Stolz *et al.*, 2004; Ahearne *et al.*, 2005). Additionally the values of Young's modulus found for the different concentrations of agarose used are also concordant with those previously reported (Buckley *et al.*, 2009; Stolz *et al.*, 2004; Ross and Scanlon, 1999; Ahearne *et al.*, 2005) – see Table 9.4. Despite these encouraging results, inspection of Table 9.4 and reference to the comments de Freitas *et al.*, (2006), indicate that agarose gels can produce significant variation in results even with similar test methods (Rakow *et al.*, 1995). It is widely accepted that measures of Young's modulus are susceptible to significant variation due to discrepancies in composition of the sample and test method. In regards to agarose these variations may be attributable to differences in the composition of agarose used by different laboratories and inherent variation in the natural derivation of agarose from seaweed (Normand *et al.*, 2001). Furthermore, inconsistencies due to the test procedure (i.e. unconfined compression, cyclic or non cyclic indentation) may also contribute towards the variance seen in Table 9.4. In regards to the present study the Hounsfield tensometer has been shown to bias the measures of Young's modulus in the negative direction due to the relatively small levels of initial strain in the materials compared to relatively large movements of the machine; an optical encoder on the motor shaft determines the degree of crosshead movement and even though movement of the machine is absolute it is still relatively large in comparison to the sample strain values (<http://www.schooloftesting.com/askexpert/1-faq/5->

[extensometermeasure](#)). Therefore differences in test protocols are likely to significantly affect the consistency of the results found between investigations.

Additionally the use of the *iCare* probe may have affected the agreement of the present results to those previously reported as the indenter size has been shown to produce significant differences in Young's modulus values (Ross and Scanlon, 1999; Ebenstein and Pruitt, 2004; Costa *et al.*, 2003). Such discrepancies emanate from differences in the surface area of contact, with larger indenters providing a more overall assessment of the tissue whilst nano-indenters (i.e. radius ≤ 20 nm) measure only the material properties of the aggrecan molecules and the trapped water complex (de Freitas *et al.*, 2006). Spherical indenters have been found to be easier to model and to give more repeatable results than other types of indenters, thus justifying their use in assessing soft tissue materials (Stolz *et al.*, 2004).

The present study demonstrated a non-linear relationship between rigidity and agarose concentration (also found by Normand *et al.*, 2000; Gu *et al.*, 2003) whilst others have noted a linear relationship (found by Ahearne *et al.*, 2005; Buckley *et al.*, 2009). It is considered that the non-linear behaviour is a consequence of network-forming molecules like agarose escalating, with increasing concentration, their 3D junctions in a non-linear fashion (de Freitas *et al.*, 2006).

9.5.2 Agarose gels and *iCare* tonometry

The novel finding of increasing *iCare* values with progressively stiffer agarose gels is confirmation that the *iCare* tonometer can assess reliably surface material properties of ocular tissues. On converting the scleral *iCare* values to measures of Young's modulus it was evident that the difference in Young's modulus between the UK and HK group existed with the largest differences seen at regions S, SN, I and IN. Other than the two lowest concentrations (i.e. 0.25% and 0.5%) all *iCare* values were significantly different between the agarose concentrations; however it was evident that the Young's modulus values were not significantly different for a number of concentrations which suggests that the *iCare* tonometer can detect small changes in rigidity, a characteristic which may not be apparent in stress-strain experiments. As seen in Figure 9.4 and 9.5, it was evident that as the concentration of the agarose gels increased, the variability of both Young's modulus and *iCare* values also increased. These findings are likely to be due to the more viscous nature

of the higher concentration gels which would increase the likelihood of small bubbles being trapped within the gel matrix and thus producing greater heterogeneity (Ross and Scalon, 1999). Additionally it was noted that some vials exhibited a more irregular meniscus than others and this may have introduced some inconsistency in the *iCare* readings. In particular when assessing the reproducibility of the *iCare* tonometry in Chapter 8 it was noted that the least reliability was found at the inferior nasal and temporal scleral regions, which are possibly more predisposed to conjunctival changes, thus suggesting that surface irregularities may cause variability in the motion parameters of the probe on rebound.

Investigators	Technique	Agarose concentration (w/v %)	Compressive stiffness (mean KPa ± SD)
Ross and Scanlon, (1999)	Unconfined compression	3	52 ± 3.7
	Indentation testing	3	79
Normand <i>et al.</i> , (2001)	Unconfined compression	1	80
		2	240
		3	520
Costa <i>et al.</i> , (2003)	Unconfined compression	1.5	3.4
		3	24
	Cyclic Indentation IT AFM microsphere	1.5	3.7
		3	28
Gu <i>et al.</i> , (2003)	Confined compressive creep	2	1.5
		2.5	4.2
		3	10
Stolz <i>et al.</i> , (2004)	Unconfined compression	1.5	3
		2	14
		2.5	22
		3	31
		4	64
	Cyclic Indentation IT AFM microsphere	2.5	36
Ahearne <i>et al.</i> , (2005) ^a	Indentation testing	0.4	6
		0.6	8
		0.8	12
		1	15
		1.2	18
de Freitas <i>et al.</i> , (2006)	Cyclic pulsatile indentation	0.5	8.30 ± 1.89
		1.5	50.5 ± 1.60
		2.5	154 ± 4
Buckley <i>et al.</i> , (2009)	Unconfined compression	2	24.9 ± 1.7

Table 9.4 Previously reported Young's modulus values for different concentrations of agarose gels. ^a Estimated results from graphical representation of data.

9.5.3 Present findings in relation to scleral biomechanics

On reviewing the literature on scleral biomechanics, it is immediately apparent that there is significant disparity between investigations (See Table 9.5). These differences are presumably due to variations between studies in relation to differences in test protocols, sample preparation and how elasticity was calculated (Eilaghi *et al.*, 2010b). In particular it is interesting to note that some investigations have reported the sclera to exhibit a non-linear response (Woo *et al.*, 1972; Elsheikh *et al.*, 2010; Eilaghi *et al.*, 2010b) whilst others have reported elastic modulus values and assumed linear (Friberg and Lace, 1988; Downs *et al.*, 2003) or bilinear (Kobayashi *et al.*, 1971) elastic behaviour. ***The results found for Young's modulus from the present study are considerably lower than those previously reported in literature***- see Table 9.5.

Such discrepancies are likely to be due to a variety of differences between study protocols. In the present study the *iCare* readings were taken from small localised regions of the sclera. When considering the anisotropy of collagen fibres and the heterogeneity that is characteristically seen in scleral tissue (Hogan, 1971), it is likely that considerable differences in mechanical strength will be found if a small region of 4.54 mm² (i.e. the cross-sectional indentation area of the probe) is compared to scleral strips of significantly larger length and width (Curtin, 1969; Phillips and McBrien, 1995; Downs *et al.*, 2005; Eilaghi *et al.*, 2010b). Moreover the principle of rebound tonometry involves the assessment of the ballistic properties of the *iCare* probe on rebound, which occurs over a short 20 millisecond time period. This is unlike extensimetry or inflation testing where the stress is applied over a period of time and which may be cyclic (Schultz *et al.*, 2008; Ku and Greene, 1981) or non-cyclic (Chen *et al.*, 2010a; Mattson *et al.*, 2010). Furthermore such experiments may also assess scleral creep which is indicated by an initial rapid elongation followed by a relatively long period of time required by the scleral strips to reach a steady state during loading and unloading (Gloster *et al.*, 1957; Phillips *et al.*, 2000). Curtin, (1969) noted that the creep response constituted the greatest part of the overall response to stress, with a relatively short initial change in length. This delayed effect has been shown to last approximately 6 minutes depending on load (Curtin, 1969, Gloster *et al.*, 1957). Scleral creep has also been demonstrated in experiments assessing pressure-volume relationships and the affects of prolonged periods of elevated stress (Greene and McMahon, 1979; Mattson *et al.*, 2010). Hence due to the relatively short

measurement duration of the *iCare* tonometer it is unlikely to be measuring the same biomechanical features of the sclera as the experimental studies listed in Table 9.5.

There are several limitations to assessing the mechanical properties of tissues using extensometry and pressure-volume testing. The experiments involve scleral strips being cut from the ocular tissue and this procedure is likely to sever the collagen fibres and thus affect their physical characteristics (Duke-Elder, 1968, Greene, 1985). Also the scleral strips are initially curved and for such tests need to be straightened; this in itself may cause localised areas of stress-strain differences, which is unlike that found *in vivo* (Greene and McMahon, 1979). The assessment of scleral strips is dissimilar to the biaxial stress affecting the sclera *in situ*, since the strips are clamped and stretched in one particular direction; thus if the direction of stretch is along the same direction as the collagen fibre distribution, the levels of strain would be different to that should the stress be applied orthogonal to the collagen distribution (Gloster *et al.*, 1957). The stress imposed by IOP on the sclera is isotropic and unlike the uniaxial stretch the sclera is subjected to in extensometry. Furthermore factors relating to changes in hydration of the scleral strips during experiments, as well as the fixing chemicals causing collagen fibre dissociation and tissue swelling may also affect the mechanical properties of the sclera (Curtin, 1969, Olsen *et al.*, 1998; Gilger *et al.*, 2005).

Unlike the extensometry studies, pressure-volume investigations are unable to differentiate the response to stress of the cornea and the sclera. Therefore what is actually assessed is the overall composite response to pressure by the globe. Pressure-volume measurements do not take into account material and geometric factors (e.g. variation in thickness and shape of the sclera) but instead assume the eye to be a spherical vessel, with uniform thickness, that is small in comparison to the radius (Greene, 1985). Additionally viscoelastic properties are ignored and the tissue is assumed to be isotropic and homogenous (Purslow and Karwatowski, 1996). All these assumptions are invalid for the sclera as discussed earlier. Therefore caution must be exercised when comparing pressure-volume and extensometry data due to differences in how the stress is applied and the significant variations that can occur in the responses of the respective tissues (Gloster *et al.*, 1957; Eligahi *et al.*, 2010b). A limitation that applies to all such *in vitro* procedures is the possible effects of autolysis of tissue during experimentation (Greene and McMahon, 1979). Since the objective of such experiments is to explore the mechanical properties of the ocular tissue, the affects of autolytic enzymes such as collagenase, which break down

collagens fibres, needs to be considered and indicates further the need for improved methods of *in vivo* assessment.

Despite the poor concordance between the present measures of scleral elastic modulus and those in the literature, the present agarose study supports the proposal that rebound tonometry can reliably evaluate material properties of the ocular tissues. Additionally, the findings of increased *iCare* values with progressing agarose stiffness is consistent with the findings of regional variation in scleral biomechanics. These results would imply significant scope for the development of a validation system using biological materials such as agarose to allow a standardised procedure to quantify scleral biomechanics. Future studies will assess Young's modulus and *iCare* measurements with a material less variable than agarose and with a protocol that, unlike the Hounsfield tensometer, uses an extensometer that is able to detect smaller strain values.

9.6 Conclusion

The key findings from the present study were:

- As the concentration of agarose increases the stiffness of agarose gels also increases.
- The utility of rebound tonometry was demonstrated in measuring reliably mechanical properties of biogels such as agarose.
- Biogels provide scope for the development of validation models for rebound tonometry that may allow the *in vivo* assessment of scleral biomechanics.

Investigators	Measurement method/ species	Scleral biomechanics		
		Stress-strain relationship	Max strain (%)	Elastic modulus or material parameters/note of interest
Kobayashi <i>et al.</i> , (1971)	Finite element analysis using data on structural responses to IOP and tonometric loading	Linear	N/A	5.5 MPa
Woo <i>et al.</i> , 1972	Pressurization of human globe	Non-linear	13	2.3 MPa
Battaglioli and Kamm (1984)	Unconfined compression of human sclera	Non linear	15	$2.7 - 4.1 \times 10^{-2}$ MPa
Friberg and Lace, 1988	Uniaxial loading on human scleral strips	Linear	Until breaking point (~20)	0.29±0.14 MPa anterior sclera; 0.18±0.11 MPa posterior sclera
Smolek, 1988	Real time holographic interferometry on bovine sclera	Non-linear	N/A	3.9 – 9 MPa
Phillips and McBrien, 1995	Uniaxial loading on tree shrew (<i>Tupaia belangeri</i>) sclera	Non linear	Until failure	Secant modulus ^a (10^6 Pa) Posterior 2.28±1.25; anterior 3.44±1.23
Down <i>et al.</i> , 2003	Uniaxial testing on cynomolgous and rhesus monkey and New Zealand rabbit peripapillary sclera	Non linear at low stress values and linear at higher	20% and to failure	Rabbit instantaneous ^b : 11.6 MPa Rabbit equilibrium ^b : 0.786 MPa Monkey instantaneous ^b : 30.7 MPa Monkey equilibrium ^b : 4.10 MPa
Wollensak and Spoerl, 2004	Uniaxial loading on human sclera	Nonlinear	10-15	22.82 (at 8% strain) MPa
Down <i>et al.</i> , 2005	Uniaxial testing on cynomolgous and rhesus monkey sclera	Non linear at low stress values and linear at higher	20% and to failure	Instantaneous ^b 33.9±3.43 MPa Equilibrium ^b 4.94±1.22 MPa

Schultz <i>et al.</i> , 2008	Uniaxial loading on human and porcine sclera	Non linear	1%	Human 2.60±2.13 MPa Porcine 0.65±0.53 MPa
Asejczyk-Widlicka and Pierscionek, 2008	Pressure-volume experiment on porcine eyes	Non-linear	N/A	0.15 - 0.83 MPa
Wollensak and Iomdina, 2009	Uniaxial loading on rabbit sclera	N/A	Until rupture	Median (range): 9.8 (8.2 – 12)
Bisplinghoff <i>et al.</i> , 2009	High rate pressurization test on human globes	Non-linear	Until rupture (150%)	Maximum equatorial strain 0.041±0.014 and meridional strain 0.058±0.018
Mortazavi <i>et al.</i> , 2009	Unconfined compression (UCC) on human and porcine peripapillary sclera	Non-linear	5-15%	Drained secant modulus ^c (at 5% strain): Humans 1.1±0.08 KPa Porcine 3.9±0.57 KPa
Elsheikh <i>et al.</i> , 2010	Uniaxial testing on human sclera	Non linear	8% and 200%	Ratio between high and low stress application (MPa): 8% anterior 9.96±4.55, equatorial 12.96±4.96 and posterior 12.78±4.72; 200% anterior 7.27±3.03, equatorial 11.44±3.80, posterior 11.88±3.43
Chen <i>et al.</i> , 2010a	Uniaxial testing on porcine sclera	Non linear	N/A	Toe modulus ^d Vertical 70±87 KPa Horizontal 95±147 KPa Heel modulus ^e vertical 9428±3950 KPa Horizontal 11315±5297 KPa
Eilaghi <i>et al.</i> , 2010b	Biaxial testing on human sclera	Non linear	7%	Material parameters Latitudinal (towards poles) 2.9±2.0 MPa Longitudinal (circumferential) 2.8±1.9 MPa
Litwiller <i>et al.</i> , 2010	Magnetic resonance elastography on bovine eyes; pressure-volume experiment	Linear	N/A	1-7 MPa

Table 9.5 Previously reported values for human and animal sclera, and associated methodologies.

a Secant modulus of elasticity is stress divided by strain at any given value of stress or strain, **b** Equilibrium and instantaneous E are time dependent measures of E. **c** drained secant modulus refers to the compressive stiffness demonstrated by the sclera during a UCC test where fluid is free to escape laterally but not vertically, **d** toe modulus E values for the first two points of the elastic portion of the stress-strain graph, **e** heel modulus E values for the last two points of the elastic portion of the stress-strain graph

10.0 *IN VIVO* VARIATION IN SCLERAL RESISTANCE

10.1 Introduction

Despite the growing assertion of a significant influence of scleral biomechanics in ocular pathology, the ability to evaluate reliably the material properties of the sclera *in vivo* is limited. This is principally a result of the challenges posed by the complex inter-relationships between ocular tissues but also due to technological restrictions in evaluating biomechanical properties *in vivo*. Chapter 6 examined inter-quadrant variation in scleral resistance using the Schiötz indentation tonometer. The study demonstrated that, regardless of the inherent variability in the actual procedure, the Schiötz tonometer is a robust technique that can be applied to the anterior segment sclera to obtain an indirect measure of tissue resistance. The investigation demonstrated significant inter-quadrant variation, with the order of scleral resistance increasing progressively from the superior-temporal (ST) quadrant followed by the inferior-temporal (IT), superior-nasal (SN) and inferior-nasal (IN) quadrants. Despite previous reports of reduced corneal rigidity and differences in scleral biomechanics in myopes (Friedenwald, 1937; Castrén and Pohjola, 1961b; 1962) the study failed to reveal a significant difference between refractive groups.

A possible limitation of the previous study was the application of relatively low Schiötz weights (i.e. 5.5 g and 7.5 g). As demonstrated in Chapter 6, when Schiötz scale values were transformed to Friedenwald's scleral rigidity values, despite significant differences between the inter-quadrant indentation levels no significant difference was found between scleral rigidity values. This inconsistency may have been attributable to the low weights producing insufficient scleral indentation to induce a detectable change in ocular volume. Furthermore, Chapter 7 demonstrated scleral thickness to vary significantly between meridians and with distance from the corneolimb junction. These changes in tissue thickness would presumably contribute towards the characteristics of local scleral biomechanics.

The present study evaluates scleral resistance *in vivo* by the application of a heavier Schiötz weight (i.e. 10 g) and assesses variation in scleral biomechanics with distance from the corneolimb junction (i.e. 4 mm and 8 mm). The choice of these locations was based upon the outcome of Chapter 6 and the findings of Chapters 7, 8 and 13. In Chapter 8 the application of rebound tonometry to the sclera demonstrated regional variation in scleral

resistance at 4 mm from the limbus, whereas in Chapter 7 and 13, anterior sclera thickness was found to be related to axial length and ciliary muscle thickness (CMT) respectively. Regarding the latter, the positive association between scleral thickness and axial length was found to occur anterior to 4 mm from the limbus, whilst the affect of reducing scleral thickness with increasing CMT was found to be mainly posterior to 3 mm from the limbus. These findings of structural correlates for the anterior scleral thickness suggest that scleral biomechanics may also be altered at those sites where these effects were demonstrated.

10.2 Study objective

Therefore the aim of the present study was to evaluate scleral resistance using Schiötz tonometry at 4 mm from the limbus as this location was susceptible to the influences of both axial length and CMT changes. Scleral indention values at 4 mm were correlated with scleral thickness measures for the equivalent location (data from Chapter 7), to assess if tissue thickness influences scleral resistance. Additionally the study also furthers the initial findings of regional variation in scleral biomechanics found at the 8 mm (Chapter 6) site and assesses a larger range of refractive error to investigate the influence of ametropia on scleral and corneal biomechanics.

10.3 Method

Schiötz indentation tonometry was performed on healthy individuals between 18 - 40 years (mean 27.76 ± 5.26) at two locations; 4 mm (n=65) and 8 mm (n=68) from the corneolimbic junction. Ethical approval and the exclusion/inclusion criteria followed those detailed in Chapter 6. The *Zeiss IOLMaster* and the Shin-Nippon auto-refractor were utilised as in Chapter 6 to obtain ocular biometry and refractive error data for all sections of the present investigation.

The study protocol was based on that adopted in Chapter 6, with a few modifications as described below. All measurements were taken by a single investigator (HP) in one session. The Schiötz footplate (diameter 10 mm) was used as a reference gauge to allow measurements to be taken from each quadrant at approximately 4 mm and 8 mm from the corneolimbic junction. The order for assessing the specific location (i.e. 4 mm or 8 mm) was randomly chosen and evaluated separately with a 5-10 minute interval elapsing before the second site was measured. At each distance three plunger weights (i.e. 5.5 g, 7.5 g and 10 g) were used for the cornea ((CR) in primary gaze) and for four scleral quadrants:

superior temporal (ST), superior nasal (SN), inferior temporal (IT) and inferior nasal (IN). The scale reading recorded was again that estimated to be central to the range of pointer oscillation at measurement end point. The order of quadrants and eye measured was randomised for each subject. The lighter weights always preceded the heavier weights in order to minimise any massaging effect on the IOP and a 5-10 minute interval between each measurement cycle (4 mm or 8 mm) was designated as sufficient recovery time to pre-measurement IOP (Krakau and Wilke, 1971).

10.4 Statistical analysis

The Schiötz scale readings were assessed for normal distribution using the Kolmogorov-Smirnov test. The data for both 4 mm and 8 mm were initially found to exhibit a non-normal distribution, however when divided into age (years) groups ($18 > - \leq 29$ and $29 > - \leq 40$) and by refractive status (myopes (MSE < -0.50 D) and non-myopes (MSE ≥ -0.50 D)) the data were found to conform to a normal distribution. Separate two-way mixed repeated measures ANOVAs were performed with refractive error and age grouping as the between-subject factors and the Schiötz scale readings at each region the within-subject factor. The analysis revealed no significant difference between myopes and non-myopes nor between age groups and thus the data were merged for further analysis. No significant difference was found between RE and LE for both data sets (i.e. 8 mm and 4 mm), thus only RE data are evaluated.

Chapter 6 demonstrated that when scleral Schiötz scale readings were converted to Friedenwald's scleral rigidity values they were unable to show regional variation in scleral rigidity despite significant differences in the Schiötz indentation levels. In spite of this earlier finding, the efficacy of scleral rigidity values was reassessed due to the additional application of the heavier Schiötz weight (10 g). The transformation process applied followed that used in Chapter 6 with the additional conversion of the 10 g weight results. The scale readings were converted to corresponding Pt and Vc values for each weight and subsequently the paired readings (5.5 g-7.5 g and 5.5 g-10 g) were used to calculate two measures of corneal (Ko) and scleral rigidity (Ks). Rigidity data (Ko and Ks) were initially screened for any outliers and tested for normal distribution using the Kolmogorov-Smirnov test. The analysis demonstrated the data to be non-normal and this was presumed to be attributable to the logarithmic transformation process required when converting the Schiötz scale values to Friedenwald's rigidity values. As the Schiötz scale readings from which the Ko and Ks values were derived were normally distributed, normality was assumed *a priori*

thus allowing parametric statistical analysis to be carried out. No significant difference was found between the RE and LE data thus only RE data were evaluated.

One-way repeated measures ANOVAs were performed on scale readings for each weight and Ks values to test for regional differences in scleral resistance. A three-way mixed repeated measures ANOVA was performed to evaluate the effects of Schiotz weights and distance of measurement (4 mm or 8 mm) on the regional variation, with region and distance of measurement as the within-subject factors and weight as the between-subject factor. Multiple two-way mixed repeated measures ANOVAs were performed with refractive status, age (years) group ($18 > - \leq 29$; $29 > - \leq 40$), gender, ethnicity and axial length (AL) (mm) sub-grouping (1. $21.5 > - \leq 23.5$; 2. $23.5 > - \leq 25.5$; and 3. > 25.5) as the between-subject factors and the scale readings as the within-subject variable. Similarly the same two-way mixed repeated measures models were applied to the scleral rigidity values (5.5 g-7.5 g and 5.5 g-10 g) as the within-subject variable. To determine pairwise differences a Bonferroni *post hoc* was conducted when group were of equal sizes and a Games Howell *post hoc* test when the group sizes were unequal. For all statistical tests a p-value of < 0.05 was taken as the criterion for statistical significance.

10.5 Results

10.5.1 Schiötz scale readings: the effect of distance from limbus and Schiötz weights

See Appendix 7 for full details on statistical analysis with each distance of measurement and Schiötz weight. A two-way repeated measures ANOVA revealed Schiötz indentation data for both 8 mm ($F(2, 198)=171.715$ ($p<0.001$)) and 4 mm ($F(2, 190)=205.875$ ($p<0.001$)) to show a significant difference in mean values between all three Schiötz weights. Additionally, a three-way mixed repeated measures ANOVA with region and distance of measurement (i.e. 4 mm or 8 mm) as the within-subject factors and weight as the between-subject factor, revealed a significant effect of distance ($F(1, 187)=34.887$ ($p<0.001$)) and weights ($F(2, 187)=250.02$ ($p<0.001$)) on the scale values with a significant interaction between distance and regional variation ($F(2.840, 530.987)=51.189$ ($p<0.001$)). The results indicated overall lower Schiötz scale values for the 4 mm site when compared to the 8 mm site; on examination of the interaction plots, regions SN and IN were found to behave similarly between the 4 mm and 8 mm locations, whereas ST and IT showed greater levels of indentation at 8 mm than 4 mm. Hence, due to the difference in indentation levels between weights and measurement location the data were assessed separately for each distance and Schiötz weight.

10.5.2 Schiötz scale readings at 8 mm

The study assessed 68 healthy individuals (136 eyes; 24 males and 44 females) aged between 19-40 years (27.76 ± 5.26). The data were analysed for non-myopic and myopic individuals [non myopes (MSE $\geq -0.50D$), $n=33$, MSE (D) mean \pm SD (0.49 ± 1.14), range (-0.50 to +4.38), AL (mm) mean \pm SD (23.31 ± 0.73), range (21.61 - 24.75); myopes (MSE < -0.50), $n=35$, MSE (D) mean \pm SD (-4.36 ± 3.19), range (-10.56 to -0.51)), AL (mm) mean \pm SD (25.30 ± 1.15), range (23.35 - 28.12)].

A one-way repeated measures ANOVA for all three weights at 8 mm revealed a significant difference between all four quadrants ($p<0.001$), with a Bonferroni *post hoc* test demonstrating the difference to be for ST:SN, ST:IT, ST:IN, SN:IT, SN:IN and IT:IN ($p<0.001$). Table 10.1 and Figure 10.1 summarise the Schiötz scale values for the different weights.

Comparing scleral to corneal indentation values for all weights showed a significant difference between scleral quadrants and the cornea ($p < 0.001$), with the exception of CR:SN for all weights and CR:ST for the 5.5 g weight.

Schiotz weight	Location	Mean	SD	Min	Max
5.5 g	CR	6.42	1.27	4.00	10.00
	ST	7.08	1.98	3.00	12.00
	SN	6.03	1.94	3.00	11.00
	IT	5.15	1.67	3.00	10.00
	IN	3.97	1.64	1.00	9.00
7.5 g	CR	8.68	1.55	5.00	12.00
	ST	9.52	1.88	6.00	15.00
	SN	8.27	1.92	3.00	13.00
	IT	7.70	1.79	4.00	13.00
	IN	6.48	1.83	3.00	11.00
10 g	CR	11.49	1.77	8.00	16.00
	ST	12.28	2.12	6.00	17.00
	SN	11.46	2.07	7.00	16.00
	IT	10.32	2.11	6.00	15.00
	IN	9.02	1.82	5.00	14.00

Table 10.1: RE 8 mm Schiotz indentation scale readings.

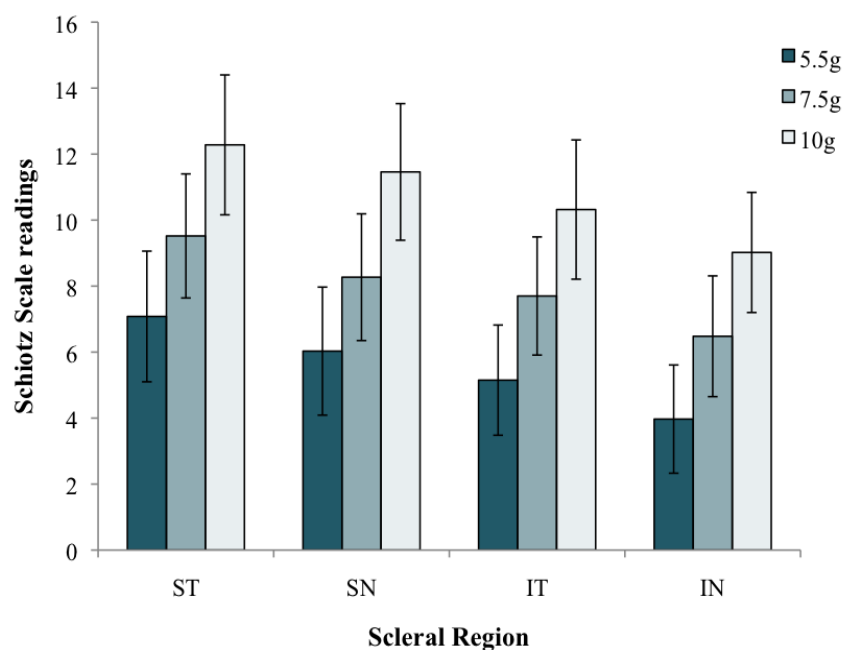


Figure 10.1 Regional mean \pm SD (error bars) Schiotz indentation scale values at 8 mm from the limbus.

10.5.2.1 Refractive status and axial length grouping

Statistical analysis revealed no significant main effect of refractive status (myopes n=35, non-myopes n=33) or axial length grouping (mm) (group 1 ($21.5 > - \leq 23.5$) n=23, group 2 ($23.5 > - \leq 25.5$) n=31, group 3 (>25.5) n= 14) on the Schiottz scale values of all 3 weights. Furthermore no interaction effect was found between regional differences and both refractive status and axial length grouping. See Table 10.2 for indentation values for myopes and non-myopes.

Schiottz weight	Location	Non- myopes				Myopes			
		Mean	SD	Min	Max	Mean	SD	Min	Max
5.5 g	CR	6.33	1.43	4.00	10.00	6.49	1.11	4.00	9.00
	ST	7.28	2.12	3.00	12.00	6.90	1.85	4.00	11.00
	SN	6.11	2.02	3.00	11.00	5.96	1.88	3.00	11.00
	IT	5.20	1.76	3.00	10.00	5.11	1.60	3.00	9.00
	IN	4.07	1.84	1.00	9.00	3.89	1.45	2.00	8.00
7.5 g	CR	8.56	1.74	5.00	12.00	8.79	1.37	6.00	12.00
	ST	9.66	1.94	6.00	15.00	9.39	1.84	6.00	14.50
	SN	8.49	2.06	3.00	12.00	8.06	1.79	5.00	13.00
	IT	7.65	1.75	4.00	11.00	7.74	1.85	5.00	13.00
	IN	6.38	2.09	3.00	11.00	6.57	1.58	4.00	10.00
10 g	CR	11.32	2.01	8.00	16.00	11.65	1.54	9.00	15.00
	ST	12.55	2.23	6.00	17.00	12.03	2.01	7.00	16.00
	SN	11.74	2.16	7.00	16.00	11.21	1.98	7.00	16.00
	IT	10.65	2.36	6.00	15.00	10.03	1.83	6.00	14.00
	IN	9.32	1.99	6.00	14.00	8.74	1.64	5.00	13.00

Table 10.2. RE 8 mm Schiottz indentation scale readings for non-myopes and myopes.

10.5.2.2. Age grouping and gender

Age (years) grouping ($(18 \geq - < 29)$ n=44, $(29 \geq - < 40)$ n=24) and gender (male n=24, females n=44) failed to show a main effect on the Schiottz scale values. No interaction effect was found between age grouping or gender and regional variation for any of the Schiottz weights.

10.5.2.3. Ethnicity

A two-way mixed repeated measures ANOVA tested the influence of ethnicity; British White (BW) n=44 and British South Asian (BSA) n=24 individuals on the Schiottz indentation levels. Schiottz 5.5 g showed no significant effect of ethnicity on the scleral scale readings however Schiottz 7.5 g ($p=0.028$) and Schiottz 10 g ($p=0.005$) demonstrated a significant effect of ethnicity with BW individuals showing higher Schiottz scale readings

in all quadrants than the BSAs. No interaction effect was seen between ethnicity and regions.

10.5.3 Schiøtz scale readings at 4 mm

Of the original 68 subjects, 65 individuals (130 eyes; 23 males and 42 females) also had Schiøtz tonometry performed at the 4 mm location from the corneolimbus junction. The subjects were aged between 19-40 years (27.66 ± 5.26) and data were analysed for non-myopic and myopic individuals [non myopes (MSE $\geq -0.50D$) $n=31$, MSE (D) mean \pm SD (0.50 ± 1.17), range (-0.50 to +4.38), AL (mm) mean \pm SD (23.38 ± 0.74), range (21.61 - 24.75); myopes (MSE $< -0.50D$) $n=34$, MSE (D) mean \pm SD (-4.40 ± 3.23), range (-10.56 to -0.51), AL (mm) mean \pm SD (25.30 ± 1.16), range (23.35-28.12)].

One way repeated measures ANOVA for all three weights revealed a significant difference between all four quadrants ST:IT, ST:IN, SN:IT and SN:IN ($p < 0.001$) except between ST:SN and between IN:IT. Table 10.3 and Figure 10.2 summarise the Schiøtz indentation values for the different weights at 4 mm.

Schiøtz weight	Location	Mean	SD	Min	Max
5.5 g	CR	6.20	1.03	4.00	8.00
	ST	5.62	1.50	2.00	9.00
	SN	5.92	1.49	3.00	10.00
	IT	4.02	1.49	2.00	8.00
	IN	4.23	1.36	2.00	8.00
7.5 g	CR	8.67	1.47	6.00	12.00
	ST	7.98	1.76	5.00	12.00
	SN	8.08	1.65	5.00	13.00
	IT	6.44	1.69	3.00	10.00
	IN	6.42	1.55	3.00	10.00
10 g	CR	11.40	1.43	9.00	15.00
	ST	10.84	2.01	7.00	15.00
	SN	10.92	1.84	7.00	15.00
	IT	9.00	2.01	5.00	13.00
	IN	8.81	1.61	6.00	13.00

Table 10.3 RE 4 mm Schiøtz indentation scale readings.

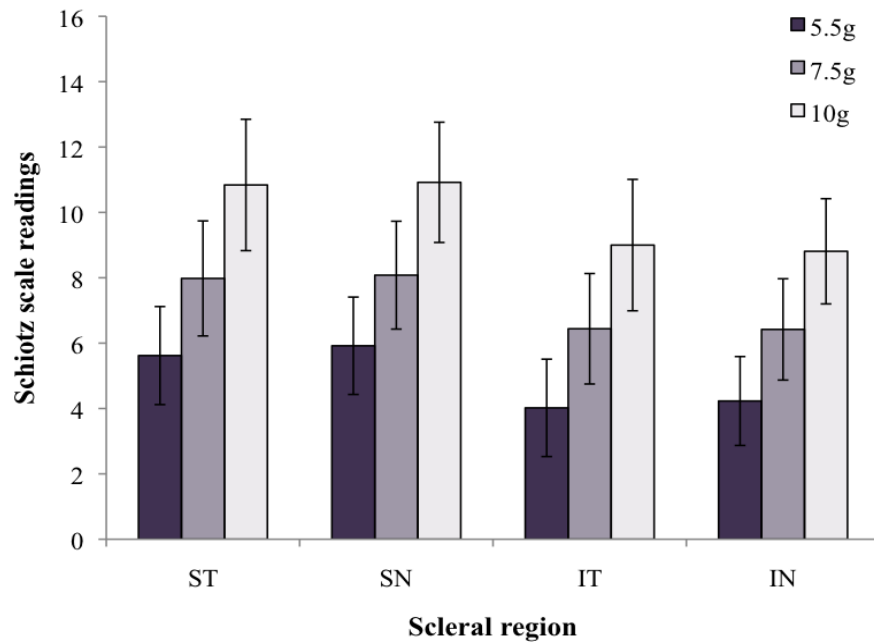


Figure 10.2 Regional mean \pm SD (error bars) Schiotz indentation scale values at 4 mm from the limbus.

All Schiotz weights showed a significant difference between scleral quadrants and the cornea ($p < 0.001$) except between CR:SN. A non-significant difference was also found between CR:ST for Schiotz 10 g.

10.5.3.1 Refractive status and axial length grouping

No significant influence of refractive status (myopes $n=34$ non-myopes $n=31$) was found for indentation values with all of the Schiotz weights. Table 10.4 shows Schiotz indentation values for myopes and non-myopes. Similarly on assessing for an influence of AL (mm) grouping (group 1 ($21.5 > - \leq 23.5$) $n=21$, group 2 ($23.5 > - \leq 25.5$) $n=30$, group 3 (>25.5) $n=14$) both Schiotz 5.5 g and 7.5 g failed to show a significant influence of AL grouping on the Schiotz scale readings, whilst Schiotz 7.5 g showed a significant interaction effect ($p=0.036$) between regional differences and AL grouping. On examination of the interaction graphs, quadrants ST and IT showed particularly higher indentation values amongst the shortest AL group (i.e. group 1) in comparison to the other two groups. Additionally, Schiotz 10g showed a significant effect of AL grouping on the Schiotz scale readings ($p=0.019$), with a Games-Howell *post hoc* test indicating that the difference was principally between groups 1 and 2. All Schiotz scale readings were significantly higher for group 1 than for group 2, yet no interaction effect was evident between regional differences and AL grouping.

Schiotz weight	Location	Non- myopes				Myopes			
		Mean	SD	Min	Max	Mean	SD	Min	Max
5.5 g	CR	6.10	0.91	4.00	8.00	6.30	1.13	5.00	8.00
	ST	5.87	1.50	3.00	9.00	5.38	1.48	2.00	8.00
	SN	6.13	1.61	3.00	10.00	5.74	1.38	3.00	8.00
	IT	3.94	1.69	2.00	8.00	4.09	1.31	2.00	7.00
	IN	4.35	1.40	2.00	8.00	4.12	1.32	2.00	7.00
7.5 g	CR	8.45	1.34	6.00	11.00	8.88	1.58	6.00	12.00
	ST	8.32	1.83	6.00	12.00	7.67	1.65	5.00	11.00
	SN	8.03	1.52	6.00	11.00	8.12	1.78	5.00	13.00
	IT	6.39	1.89	3.00	10.00	6.48	1.50	3.00	9.00
	IN	6.71	1.70	4.00	10.00	6.15	1.37	3.00	9.00
10 g	CR	11.03	1.11	9.00	14.00	11.75	1.63	9.00	15.00
	ST	11.10	2.31	7.00	15.00	10.61	1.68	8.00	15.00
	SN	11.32	2.17	7.00	15.00	10.55	1.39	7.00	13.00
	IT	8.97	2.26	5.00	13.00	9.03	1.78	6.00	12.00
	IN	9.19	1.92	6.00	13.00	8.45	1.18	7.00	11.00

Table 10.4 RE 4 mm Schiotz indentation scale readings for non-myopes and myopes.

10.5.3.2. Age and gender

No significant influence of age (years) grouping ($18 > - \leq 29$ $n=42$, $29 > - \leq 40$ $n=23$) was found for the Schiotz scale values with all 3 weights, however Schiotz 10 g showed a significant interaction effect ($p=0.022$) between age groups and regional variation. On examination of the interaction graph this interaction was observed to be attributable to quadrant IT, which appeared to reduce with increasing age.

On testing the influence of gender (male $n=23$, females $n=42$) Schiotz 5.5 g failed to show a significant effect on the scale readings, whilst both Schiotz 7.5 g ($p=0.011$) and 10 g ($p=0.005$) demonstrated a significant effect, with female subjects showing significantly higher scale readings than males. No interaction effect was found between regions and gender.

10.5.3.3. Ethnicity

Ethnicity (BW n=41, BSA n=24) demonstrated a significant effect on the scale readings with all 3 weights; Schiötz 5.5 g (p=0.003), 7.5 g (p=0.003), 10 g (p=0.001). With all weights the BW individuals showed higher scale readings than the BSAs. No significant interaction effect was present for regions and ethnicity.

10.5.3.4 Scleral thickness and Schiötz indentation values

Schiötz indentation values at 4 mm were correlated with scleral thickness measures for the equivalent meridian and distance from Chapter 7. Several significant correlations were observed (see Appendix 7); all showing a negative association between increasing thickness and reducing indentation values.

10.5.4 Corneal indentation

Independent samples *t tests* were performed to test for an effect of gender, age group, ethnicity and refractive status on the average corneal indentation values. The analysis revealed no significant effect of gender or age group for any of the Schiötz weights. With regard to refractive status no significant effect was found on the corneal indentation values with the 5.5 g and 7.5 g weights whereas a significant difference was found for 10 g (p=0.045) with myopes showing higher scale values than non-myopes. No significant effect of ethnicity was found on the corneal indentation values with the 5.5 g, and 7.5 g weights although a significant difference was found for 10 g (p=0.036) with BW individuals showing higher scale values than BSAs. A one-way ANOVA testing for the influence of AL grouping revealed no significant effect on the corneal indentation values with all Schiötz weights.

10.5.5 Conversion of Schiötz scale readings to Friedenwald's rigidity values

10.5.5.1 Friedenwald's Scleral rigidity (Ks)

Multiple one-way repeated measures ANOVAs were performed to assess for significant regional variation in rigidity between the four quadrants at the 4 and 8 mm locations. At both locations no significant regional differences were found for Ks 5.5 g-7.5 g and 5.5 g-10 g. A two-way repeated measures ANOVA showed no significant effect of location (i.e. 4 and 8 mm) on Ks 5.5 g-7.5 g and 5.5 g-10 g. Refractive status, axial length grouping,

gender, age grouping and ethnicity failed to demonstrate a significant influence on Ks (Ks 5.5 g-7.5 g and 5.5 g-10 g) at 4 and 8 mm. Table 10.5 summarises the Ko and Ks values for the 4 and 8 mm locations.

In regards to Ks values at 4 and 8 mm, neither 5.5 g-7.5 g nor 5.5 g-10 g showed any significant correlation with the ocular biometry parameters (axial length, ACD and corneal curvature). At 4 mm several significant inter-quadrant correlations were noted for Ks (Ks 5.5 g-7.5 g and 5.5 g-10 g) values, where as at 8 mm fewer inter-quadrant correlations were observed for both measures of Ks.

Location and rigidity measure	Mean	SD	Min	Max
Cornea				
5.5 g - 7.5 g	0.0211	0.0099	0.0060	0.0360
5.5 g - 10 g	0.0174	0.0070	0.0050	0.0330
8mm				
ST 5.5 g - 7.5 g	0.0161	0.0129	0.0020	0.0369
ST 5.5 g - 10 g	0.0204	0.0175	0.0008	0.0847
SN 5.5 g - 7.5 g	0.0183	0.0134	0.0008	0.0378
SN 5.5 g - 10 g	0.0186	0.0199	0.0014	0.0796
IT 5.5 g - 7.5 g	0.0157	0.0129	0.0012	0.0378
IT 5.5 g - 10 g	0.0222	0.0227	0.0008	0.0899
IN 5.5 g - 7.5 g	0.0217	0.0152	0.0012	0.0378
IN 5.5 g - 10 g	0.0253	0.0253	0.0014	0.0951
4mm				
ST 5.5 g - 7.5 g	0.0147	0.0117	0.0012	0.0357
ST 5.5 g - 10 g	0.0215	0.0230	0.0004	0.0796
SN 5.5 g - 7.5 g	0.0215	0.0138	0.0012	0.0369
SN 5.5 g - 10 g	0.0227	0.0191	0.0022	0.0847
IT 5.5 g - 7.5 g	0.0180	0.0145	0.0012	0.0378
IT 5.5 g - 10 g	0.0305	0.0308	0.0014	0.0951
IN 5.5 g - 7.5 g	0.0222	0.0152	0.0012	0.0378
IN 5.5 g - 10 g	0.0287	0.0250	0.0041	0.0899

Table 10.5 RE Schiott scale readings converted to Friedenwald's rigidity values ((mm³)⁻¹) for 4 and 8 mm from the limbus.

10.5.5.2 Friedenwald's Corneal Rigidity (Ko)

Independent *t tests* assessing for an influence of refractive status, gender and age grouping showed no significant influence on both measures of Ko (5.5 g-7.5 g and 5.5 g-10 g). Ethnicity demonstrated a significant influence on the 5.5 g-7.5 g Ko values ($p=0.036$), with BSA individuals showing significantly higher rigidity than BW individuals. A one way ANOVA testing for an influence of axial length grouping on the Ko values revealed no significant effect.

10.5.6 Ocular biometry

An independent *t test* showed no significant effect for gender differences on corneal curvature, axial length or ACD, however a significant difference between males and females was found for refractive error (8 mm $p=0.013$; 4 mm $p=0.018$), with females showing higher levels of myopia than males. No significant effect of ethnicity or age group was found on the biometric parameters (i.e. corneal curvature, axial length, refractive error and ACD)

10.6 Discussion

The results of the present study support the previous findings (reported in Chapters 6 and 8) of regional variation in scleral biomechanics across the anterior scleral quadrants. Furthermore the results also demonstrate scleral resistance to be significantly influenced by distance (i.e. 4 and 8 mm) from the limbus. Despite differences in the levels of indentation between the two locations, regional variations between the quadrants were still evident at both locations, although the inter-quadrant differences varied with the location of measurement. Additionally, in spite of the use of the heavier 10 g Schiottz weight the present results support the findings of Chapter 6 where transformed scleral rigidity values failed to show significant regional variation in scleral biomechanics.

10.6.1 Comparison of current results to findings of Chapter 6

Concordant with the findings of Chapter 6 and 8, the present study demonstrates further evidence of regional differences in scleral resistance to indentation. *These results suggest a general trend for increased scleral resistance amongst the inferior quadrants when compared to the superior regions.* In contrast to the findings of Chapter 6 the current results suggest that at the 8 mm site scleral quadrant SN offers lower levels of resistance

than quadrant IT. These differences may be attributable to shared biomechanical characteristics for these two regions. Indeed on examination of the LE (see Figure 6.2) data in Chapter 6, it is evident that the sequential change in indentation levels across the scleral quadrants conforms to that of the present study.

10.6.2 Regional variation in scleral resistance

The current study also investigated variation in scleral resistance at two locations; 4 mm and 8 mm from the limbus. Interestingly the 4 mm location showed significantly increased scleral resistance (i.e. low Schiøtz scale values) when compared to the 8 mm location. In particular quadrants SN and IN showed comparable behaviour between the 4 mm and 8 mm locations, whereas ST and IT showed greater levels of indentation at 8 mm than at 4 mm. *These findings would suggest that the resistance of the temporal scleral tissue reduces with increasing distance from the limbus.* Interestingly, the posterior temporal sclera has been consistently found to show initial rupturing in pressure-volume testing (Greene and McMahon, 1979). Furthermore it is usually the site of posterior myopic staphylomas (Greene, 1980) possibly indicating an inherent weakness in its biomechanical strength when compared to the nasal regions.

Moreover, the 4 mm location demonstrated fewer inter-quadrant differences than those at 8 mm, indicating that the sclera is more uniform in its biomechanical properties closer to the limbus than further away. These findings are consistent with increased variability in scleral thickness near the vicinity of the 8 mm location (Chapter 7) perhaps owing to its closer proximity to the equator and points of muscle insertion (Olsen *et al.*, 1998). *A particularly notable finding of the present study in regards to the 4 mm location was the absence of significant differences between the horizontal quadrants (SN:ST and IN:IT) in contrast to the vertical quadrants (ST:IT and SN:IN) implying that scleral biomechanics in the vertical meridian is distinct from that of the horizontal meridian.* These findings are unlike those for the 8 mm location where all scleral regions were found to differ from each other. Regarding scleral thickness measurements at the 4 mm location (from Chapter 7), differences in scleral thickness in the vertical meridian (SN-IN (117 μ m); ST:IT (67 μ m)) were found to be substantially greater than those between the horizontal meridian (SN-ST (27 μ m); IN:IT (23 μ m)). As the scleral thickness could not be measured at the 8 mm location, assessing values for the adjacent 7 mm location suggests a similar trend for larger differences along the vertical meridian (SN-IN (64 μ m); ST-IT (36 μ m)) than the

horizontally meridian (SN-ST (17 μm): IN-IT (11 μm)); however these vertical/horizontal thickness differences are not as notable for 7 mm as those for 4 mm from the limbus.

In regards to the inter-regional variation at the 8 mm and 4 mm sites, a similar order of change in tissue resistance was observed at both locations. Contrary to this consistency exhibited at both sites, ST demonstrated lower levels of resistance than SN at 8 mm but not at 4 mm. This discrepancy between the two locations may be a result of changes in scleral biomechanics with distance from the limbus. Furthermore inspection of scleral thickness results at 4 mm and 7 mm (measurements at 8 mm were not possible) from Chapter 7, reveals that the difference in scleral thickness between the SN and ST meridians declines from 27 μm at 4 mm to 17 μm at 7 mm. Therefore assuming that this trend continued to the 8 mm site the smaller difference in thickness between the quadrants may be a reason for the change in order of scleral resistance.

Moreover when comparing Schiøtz indentation values at 4 mm to the *iCare* results (also at 4 mm), the order of regional scleral resistance (i.e. low to high) is similar, except for the regions SN and ST. The *iCare* data suggest SN to show greater resistance than ST, which is contrary to the Schiøtz results. On evaluating their thickness profiles (see Chapter 7) it is evident that both SN and ST show a similar profile of thickness change with ST showing greater thickness than SN. It is also apparent that the difference between these two meridians becomes smaller as the distance from the limbus increases. Additionally, the difference in the *iCare* and Schiøtz results for SN and ST at 4 mm may be an artefact of the actual procedure as the smaller *iCare* probe (i.e. 1.7 mm diameter) is likely to provide greater accuracy and probably a more localised estimate of resistance than the larger footplate and plunger (i.e. 15 mm and 1.5 mm radius of curvature, respectively) of the Schiøtz tonometer (Schiøtz, 1905).

As discussed in Chapters 6 and 8, previous reports on regional variation in scleral biomechanics have been restricted to *in vitro* studies owing to the technical difficulties of *in vivo* measurement (Curtin, 1969; Elsheikh *et al.*, 2010; Friberg and Lace, 1988; Smolek, 1988; Bisplinghoff *et al.*, 2009; 2008). Furthermore meridional variations in scleral thickness found in Chapter 7 strongly support the present findings of regional differences in scleral resistance. ***In regards to the quadrants investigated the measures of scleral thickness at 4 mm demonstrated a progressive decrease in thickness from region IN followed by IT, ST and SN.*** This order of change in thickness reflects the general trend for

scleral resistance found at 4 mm for weights 7.5 g and 10 g. The 5.5 g weight failed to show the same order of effect perhaps as a result of the lighter weight not being able to discriminate between the less compliant scleral quadrants (IN and IT). Further support for thickness influencing the scleral indentation levels comes from a recent OCT study by Taban *et al.*, (2010) that assessed anterior scleral thickness at 3.5 mm from the limbus for the same quadrants evaluated in the present study. Taban *et al.*, (2010) reported variation in scleral thickness across the quadrants with significantly increased thickness at IN. Moreover, these results also show a trend for scleral thickness to decrease sequentially from IN followed by IT, ST and SN. Again this order of declining scleral thickness is analogous to the order of changes in scleral resistance at the 4 mm site for both the 7.5 g and 10 g weights.

The present study also provided evidence for scleral resistance to alter with distance from the limbus. In support of these findings Chapter 7 also confirmed the scleral thickness profile to change significantly between 1-7 mm from the corneolimbus junction. The general trend for all meridians indicates an initial decline from 1 to 2 mm and then a gradual increase after 3 mm onwards. Olsen *et al.*, (1998) demonstrated a similar trend with a gradual decline in scleral thickness from the limbus to approximately 6 mm, whereafter the thickness increased between 6 - 8 mm and but then continued to reduce towards the equator. In a recent *in vitro* study, Elsheikh *et al.*, (2010) reported significant differences in thickness between the anterior, equatorial and posterior regions across 8 meridians. It is apparent from their results that a general trend for reducing scleral thickness from the limbus to approximately 7 mm occurs for the superior, nasal, inferior and temporal meridians. Moreover it is also evident that the gradient of decline in thickness up to 7 mm varies between these meridians. Such fluctuation in scleral thickness with distance from the limbus and along the different meridians would presumably produce not only regional differences in scleral biomechanics but also changes in material properties with distance from the limbus as found in the present study.

The findings of reduced scleral resistance at 8 mm especially for ST and IT (compared to their values at 4 mm) do not match the findings of increasing scleral thickness from 1 to 7 mm reported in Chapter 7. One possible explanation for this could be the likelihood that the temporal readings may have been taken slightly further than at the 8 mm location. If so, reduced scleral resistance would have been found as a result of the scleral thinning reported in the vicinity of the equator (Olsen *et al.*, 1998). Another possibility may be that,

despite increased thickness in the vicinity of 8 mm, the actual mechanical resistance to indentation may be lower at 8 mm than at the 4 mm location. Indeed at the 4 mm site the underlying anterior segment structures such as the ciliary body (Hogan, 1971) may provide greater mechanical resistance than at the 8 mm location. Furthermore it has been proposed that variation in scleral curvature may affect eye wall stress and hence resistance (Phillips and Shaw, 1970). Friedman, (1966) proposed that the flatter the curvature of the globe, the greater the level of stress, resulting in localised differences in strain for a constant IOP level. Due to technical limitations in assessing scleral curvature *in vivo* there is insufficient data on this parameter in literature. *In vivo* MRI studies evaluating eye shape in ametropia (see Chapter 14) have reported the globe to exhibit a spherical-elliptical configuration with substantial inter-subject variation in globe conformation (Atchison *et al.*, 2004; 2005). Such findings would suggest that curvature variation may be present between the 4 mm and 8 mm location hence affecting the local scleral biomechanical properties (see Chapter 14).

The findings of a significant correlation between scleral thickness and the 4 mm Schiötz scale values supports the supposition that tissue thickness plays an important role in the scleral biomechanical properties. However the variability in the association between scleral thickness and the resistance levels is likely to be a consequence of the significant inherent inter-subject variability found for both parameters and the innate variability of the test methods used to evaluate them. These findings would strongly suggest that meridional differences in scleral thickness are closely associated with variation in scleral resistance. Besides tissue thickness affecting the compliance of the sclera on indentation it is also expected that variables such as curvature and proximity to ocular structures may also influence local scleral biomechanics.

Differential scleral resistance in the vertical and horizontal meridians at the 4 mm location might be a result of structural correlates of scleral thickness such as axial length and ciliary muscle thickness (CMT). In Chapter 7 axial length and myopic refractive error were found to be related to scleral thickness along the inferior (I) (1 mm from corneolimbic junction) and superior (S) (3 mm from corneolimbic junction) scleral meridians. Similarly in Chapter 13 CMT was found to be associated with reducing scleral thickness along several meridians particularly for the SN and I meridians, posterior to 3 mm (from corneolimbic junction). It is unclear why the scleral resistance should be similar horizontally but differ vertically at the 4 mm location. In regards to ocular shape differences between refractive

groups, the increased tendency for a less oblate and a relatively more prolate conformation in myopes (Atchison *et al.*, 2005) may be related to biomechanical resistance to stretching in the horizontal meridian and perhaps a susceptibility to expansion vertically. Interestingly in a 3-dimensional MRI study Nagra *et al* IOVS 2009, 50: ARVO E-Abstract 3941 evaluated meridional globe conformation in myopia between the nodal point to the 70% region of the axial length by assessing the maximum chord distance from the visual axis to the vitreous:retina interface. Their results suggest a trend for greater maximum chord distances in the vertical meridian when compared to the horizontal. These findings would suggest greater global expansion vertically than horizontally and could possibly imply regional variation in scleral biomechanics.

Significant differences between scleral and corneal indentation levels were found for all three Schiötz weights for each of the scleral quadrants at both 4 mm and 8 mm with the exception of cornea and quadrant SN. Further the cornea and quadrant ST were found to exhibit a similar indentation response with the 5.5 g weight at 8 mm and the 10 g weight at 4 mm. These results would suggest that despite significantly different collagen composition and presumably different biomechanical and biochemical characteristics (Komai and Ushiki, 1991; Hogan, 1971), the tissue resistance of the cornea and scleral quadrant SN might be comparable. The similarity in tissue resistance between the cornea and ST at both 4 mm and 8 mm but with different weights may be a reflection of the Schiötz weight failing to indent the less compliant scleral tissue to allow discrimination between the indentation levels. Alternatively the finding of the same levels of resistance as the cornea at 8 mm with the 5.5 g weight in comparison to the 10 g weight at 4 mm suggests that the biomechanical resistance offered by ST reduces with increasing distance from the limbus. As mentioned afore the temporal sclera has often been noted to show characteristics of weaker biomechanical strength than the nasal sclera and the findings of increased compliance at the 8 mm ST site may further support these findings (Greene and McMahon, 1979; Greene, 1980).

10.6.3 Friedenwald's rigidity values

In support of the findings of Chapter 6, Friedenwald's scleral rigidity values failed to show inter-quadrant differences in scleral biomechanics. These results are likely to be the consequence of corneal data used in the empirical transformation algorithm for Schiötz values instead of scleral biomechanical data (Friedenwald, 1937; 1957). These findings

question an early assumption that corneal rigidity is equivalent to scleral rigidity (Jackson *et al.*, 1965; Castrén and Pohjola, 1961b) and demonstrate the limited value of the Schiøtz tonometer in determining scleral rigidity data.

The corneal rigidity values of the current investigation match well to those of previously published studies (Lam *et al.*, 2003a; Wong *et al.*, 1991; Castrén and Pohjola, 1961b; Draeger, 1959; Friedenwald, 1937 see Table 6.5 in Chapter 6). The present values are higher than those of the preliminary investigation (Chapter 6) presumably due to the larger sample size and hence greater refractive error range. It is evident on inspection of the present results that the rigidity values differed with each pairing of the Schiøtz weights i.e. 5.5 g-7.5 g and 5.5 g-10 g. These findings are likely to be due to variation in indentation levels and hence volume changes with each of the weights. In particular this is notable for the 5.5 g-7.5 g rigidity values as the difference in volume between the two weights is likely to be small, thus resulting in higher estimates of rigidity when compared to the heavier weights.

10.6.4 Effect of refractive status and axial length on scleral resistance

No significant effect of refractive status was found on the Schiøtz indentation levels at the two locations (4 and 8 mm) with the three Schiøtz weights. Similarly no significant main effect of axial length was found for the 8 mm data and for the 5.5 g and 7.5 g indentation levels at 4 mm. Interestingly, at 4 mm the 7.5 g weight showed an interaction effect between axial length and regional variation, which appeared to be attributable to higher levels of indentation at quadrants ST and IT for the shortest axial length group ($21.5 > - \leq 23.5$ mm) when compared to the other two groups ($23.5 > - \leq 25.5$ mm and > 25.5 mm). These results would suggest increased scleral resistance for the ST and IT quadrants with increasing axial length. In support of these findings, the 10g weight at 4 mm showed a significant influence of axial length on the scale readings with individuals with the shortest ($21.5 > - \leq 23.5$ mm) axial length showing greater indentation than individuals with moderate axial lengths ($23.5 > - \leq 25.5$ mm). *These findings would imply that in comparison to the 8 mm site the more anterior 4 mm location might be more susceptible to the structural effects of axial length changes.* Additionally, these results support the findings of Chapter 7 where increasing scleral thicknesses in the vicinity of 4 mm along the superior and inferior meridians was associated with longer axial lengths. Moreover, Chapter 8 demonstrated greater levels of scleral resistance amongst the more myopic HK-

Chinese individuals when compared to the UK subjects, which supports the present findings of relatively increased levels of indentation in individuals with shortest axial length in comparison to eyes with moderate axial length.

Refractive status was also observed to significantly influence corneal indentation levels with the 10g weight with myopic individuals showing greater levels of indentation. These findings would support those of Chapter 11 where corneal biomechanical changes were noted with greater levels of myopia. In particular the investigation found reducing corneal hysteresis and corneal resistance factor with increasing axial length amongst the same cohort presently investigated. Corneal rigidity has been frequently found to be reduced in myopia (Friedenwald, 1937; Castrén and Pohjola, 1961b; 1962; Goodside, 1959; Perkins, 1981), however both the present and preliminary study (Chapter 6) failed to show an effect of refractive status on the corneal rigidity values.

10.6.5 The effect of age on scleral resistance

No significant effect of age grouping was found on the scale values at both 4 and 8 mm although a trend was noted for the older age group to show lower scale values than the younger group. Additionally an interaction effect was observed for the 10 g weight at 4 mm, which was identified as lower indentation levels for region IT with increasing age. A trend for lower scale values for the older age group would support the findings of increased scleral resistance with age found in Chapter 8. Indeed in regards to the sclera's ultrastructure, scleral rigidity has been shown to increase with age due to an increase in enzymatic and non-enzymatic cross-links between collagen as seen in other connective tissues (Keeley *et al.*, 1984, Watson and Young, 2004).

10.6.6 Scleral resistance and gender

In contrast to the 8 mm location, the 4 mm site showed significant gender differences for both 7.5 g and 10 g with females showing higher Schiotz indentation values than males. These gender differences match the findings of the *iCare* study where males were found to exhibit greater scleral resistance than females. Furthermore Chapter 7 demonstrated significant differences in scleral thickness between males and females with males showing greater overall thickness for all meridians and distances. In support of these findings Mohamed-Noor *et al.*, (2009) also reported scleral thickness to be greater in males than females.

It is likely that the thicker sclera in males may be a consequence of their larger eyes often linked to their greater stature (Wong *et al.*, 2001; Teikari, 1987; Johnson *et al.*, 1979). Recently retinal thickness was also shown to vary with gender with males showing greater foveal thickness than females (Kashani *et al.*, 2010). Since eye growth is a biological process involving tissues such as the retina, sclera and choroid (Bron, 1997), gender differences in tissue thickness may underpin the susceptibility of the eye to ocular pathology in males/females. Therefore gender differences in scleral biomechanics may contribute towards elucidating pathogenic associations in ocular diseases such as uveitis (Ayuso *et al.*, 2010) and AMD (Pokharel *et al.*, 2009), which have been shown to have a greater propensity in males and females respectively.

10.6.7 Scleral resistance and ethnicity

The present study demonstrated significant variation in scleral resistance between ethnic groups (British-White (BW) and British South-Asian (BSA)). At the 8 mm location both 7.5 g and 10 g showed a significant effect of ethnicity with BW individuals showing higher values than BSAs. Similarly at the 4 mm location indentation values with all Schiötz weights showed BWs to demonstrate higher levels of indentation than BSAs for all scleral quadrants. In regards to corneal values, only 10 g showed a significance difference in indentation levels with ethnicity, with BWs showing greater indentation levels than BSAs. These findings were further supported by significantly higher 5.5 g-7.5 g corneal rigidity amongst BSA individuals. The variation in the influence of ethnicity on the levels of indentation with the different Schiötz weights is likely to be attributable to the lighter weight (5.5 g), which is unlikely to produce sufficient scleral indentation to induce a detectable change in ocular volume that would allow discernable differences in scleral resistance between ethnic groups.

The results of the present study suggest that in comparison to BW individuals BSAs have greater scleral and corneal resistance. These findings support the observations of Chapter 8 where significant differences were found in scleral resistance between a mixed group of BW-BSAs and HK-Chinese individuals. Moreover Chapter 7 demonstrated a non-significant trend for greater scleral thickness in BSA individuals when compared to BW subjects. Oliveira *et al.*, (2006) also reported scleral thickness to be thinner in Caucasian individuals when compared to non-Caucasian subjects. Furthermore Singh and Jain, (1967)

reported average Ko (0.0223) values to be greater amongst South Asian individuals when compared to those of Caucasians (0.0215 found by Friedenwald, 1937).

In light of the findings of Chapter 8 where the predominantly myopic HK-Chinese individuals were found to exhibit greater scleral resistance, the present findings of increased scleral resistance amongst BSAs questions whether individuals of South Asian descent may also be predisposed to developing myopia. Interestingly in the UK, myopia prevalence has been shown to be greater in BSA children when compared to children of Caucasian and Black African-Caribbean descent (Rudnicka *et al.*, 2010; Logan *et al.*, IOVS 2008, 49: ARVO E-Abstract 2602). When considering the significant population differences in myopia prevalence, with comparatively low levels of myopia found amongst Caucasians (Ip *et al.*, 2008; Drover *et al.*, 2008; Goldschmidt and Fledelius, 2005) and highest levels in East Asians (Lin *et al.*, 2001; Lam *et al.*, 2004; Fan *et al.*, 2004a; 2004b; Edwards and Lam, 2004) the differential prevalence levels between populations may suggest a genetic predisposition to myopia development. Contrary to a genetic propensity for myopia development, environmental factors such as the ever increasing levels of urbanisation and pressure for higher levels of education have also been implicated as significant contributing factors in the elevated prevalence levels of myopia amongst East Asian populations (Morgan and Rose, 2005). Gilmartin, (2004) suggested that myopic eye growth might be a result of genetically determined inherited structural characteristics that are modulated by environmental and socio-economic factors. In the present study little was known about the parental socioeconomic background, but it may be assumed that the BW and BSA individuals come from a similar environment and socio-economic background. ***The findings of this study would suggest that structural correlates such as scleral biomechanics may perhaps be genetically governed and may influence the susceptibility to the onset and development of myopia.***

10.7 Conclusion

The key findings of the present study include:

- Regional differences in scleral biomechanics differ with the distance from the limbus.
- The more anterior 4 mm location from the limbus shows greater scleral resistance than the 8 mm site.
- Scleral thickness is likely to influence scleral resistance to indentation.
- Scleral resistance varies more in the vertical meridian than the horizontal meridian at the 4 mm location.
- Scleral resistance at 4 mm demonstrates a greater association with the effects of axial length changes.
- Males exhibit greater scleral resistance at the more anterior 4 mm site than females.
- BSA individuals exhibit overall greater scleral resistance than BW individuals.

11.0 STRUCTURAL CORRELATES OF CORNEAL BIOMECHANICS

11.1 Introduction

It has been suggested that myopia occurs when the refractive components of the anterior segment of the eye fail to compensate for the excessive growth of the posterior chamber (Zadnik *et al.*, 2003; Jones *et al.*, 2005). Considering the role of the anterior segment in the emmetropization process, it seems reasonable to question whether the biomechanical properties of these anterior components modulate the refractive changes that occur during myopia development (McFadden *et al.*, 2010). Indeed the findings of increased ciliary muscle thickness (Chapter 13; Bailey *et al.*, 2008) and the putative findings of increased anterior scleral resistance (Chapter 8) in myopic eyes would suggest that biomechanical factors may be involved in constraining the crystalline lens flattening that occurs during the emmetropization process (Mutti, 2010).

Furthermore, physiological variations such as increased anterior chamber depth (ACD) in myopic eyes (Uçakhan *et al.*, 2008; Carney *et al.*, 1997) suggest that axial length expansion influences the conformation of the anterior aspects of the globe (Park *et al.*, 2010). In regards to the role of the cornea in myopia, the literature is equivocal with several studies failing to find significant differences in central corneal thickness (CCT) between myopes and non-myopes or with levels of myopia (Pedersen *et al.*, 2005; Lim *et al.*, 2008; Shen *et al.*, 2008a; AlMahmoud *et al.*, 2010). However contrary to these reports others have observed differences in CCT and corneal curvature between refractive states (Chang *et al.*, 2001; Nomura *et al.*, 2004; Goss *et al.*, 1997). In terms of corneal biomechanics, corneal rigidity determined by Schiøtz tonometry has frequently been reported to be reduced in myopic eyes (Castrén and Pohjola, 1962; Drance, 1959; Goodside, 1959). More recently the introduction of the Reichert Ocular Response Analyser (ORA) has allowed *in vivo* non-contact assessment of corneal biomechanics. Several studies have explored a range of corneal biometrics (e.g. corneal hysteresis (CH) and corneal resistance factor (CRF)) provided by the ORA and their relationship to refractive error (Song *et al.*, 2008; Shen *et al.*, 2008; Chang *et al.*, 2009). The results of these studies are inconsistent with some investigators reporting reduced CH and CRF in myopic eyes (Shen *et al.*, 2008; Song *et al.*, 2008; Chang *et al.*, 2009), whilst other have found no significant differences between refractive status (Lim *et al.*, 2008).

11.2 Study Objective

The objective of the present study was to investigate whether differences in corneal biomechanics exist between refractive groups i.e. myopes (MSE <-0.50 D) and non-myopes (MSE ≥-0.50 D). Secondly, the study also assessed whether any differences in corneal biomechanics between refractive groups occur in mixed British White (BW) – British South Asian (BSA) individuals from the UK (data collected in the UK) and Hong Kong Chinese (HKC) individuals (data collected in Hong Kong). The prevalence of high myopia (i.e. -6.00 D to -15.00 D) in the general Caucasian population is approximately 2-3% (Grossniklaus and Green, 1992; Goldschmidt and Fledelius, 2005) whereas in comparison the prevalence among Chinese individuals is approximately 10% (Lin *et al.*, 2004; Wong *et al.*, 2000). Hence the objective of the study was to explore whether differences in corneal biomechanics exist between refractive groups and between ethnic groups, which may provide some insight into the pathogenesis of myopia and its higher prevalence in the Chinese population.

11.3 Methods

The study in the UK evaluated 74 healthy individuals (150 eyes; 29 males and 46 females) aged between 18-40 years (mean 27.8 ± 5.5). Ethical approval was obtained from Aston University and Hong Kong Polytechnic University School of Optometry, Kowloon, Hong Kong (HK); the exclusion/inclusion criteria followed those detailed in Chapter 6. The ORA is a table-mounted device that requires the patient to be in a seated position. The patient is asked to place his/her head against a movable headrest and to fixate on a red light target in the instrument nozzle. On pressing a button on the operation panel the examiner activates the instrument to search automatically for the eye/corneal reflex which, on alignment, fires a puff of air onto the eye. The results are displayed on the online PC as waveforms showing IOP, CH and CRF (see Section 4.6). To ensure valid and reliable results are obtained the ORA manufacturers recommend that the quality of the waveform should be assessed by identifying two well-defined peaks that are reasonably symmetrical and higher than the superimposed pressure curve. The evaluation of these waveforms is relatively subjective and dependent on examiner experience, therefore Reichert have recently launched a new version of the ORA software (i.e. version 2.04), which provides a score for each waveform to indicate its quality. The scale ranges from 0-10 with higher scores indicating greater reliability. The manufacturers recommend that four measurements

should be taken and any erroneous results deleted. The new software compares the four waveforms and selects the result with the highest score as the best signal value (BSV), which can be taken as the final result. Contrary to this recommendation, recent work by Lam *et al.*, (2010) investigated the use of waveform scoring and reported that, to optimize accuracy of measurements, an average value should be obtained from 3 readings with wave score values of ≥ 3.5 instead of the one BSV. As the wave scoring facility was being used in the current study, the protocol adopted followed that advocated by Lam *et al.*, (2010) and thus four readings were taken and three readings with the highest wave score (i.e. ≥ 3.5) were averaged.

GAT was also performed on all individuals, however the ORA was performed before GAT to avoid any effect of contact tonometry and its associated topical anaesthesia on corneal biometrics and IOP (Almubrad and Ogbuehi, 2007; Montero *et al.*, 2008; Dayanir *et al.*, 2004; Baudouin and Gastaud, 1994; Kotecha *et al.*, 2006). To minimise the effects of diurnal variation in IOP, all data were collected during office hours (i.e. 8am to 5pm) (Oncel *et al.*, 2009; González-Méijome *et al.*, 2008; Liu *et al.*, 2002). Ocular biometry data were collected using the *IOLMaster* (Carl Zeiss Meditec, AG, Oberkochen, Germany) and the Shin-Nippon auto-refractor (see Chapter 6); central corneal thickness (CCT) was measured using the *Visante AS-OCT* (see Chapter 7).

The investigation of corneal biomechanics across ethnic groups comprised two groups; BW-BSA young adults (n=74) and HKC (n=60) young adults. The BW and BSA subjects were recruited from the Aston University Department of Optometry, UK whilst the HKC subjects were recruited at the Hong Kong Polytechnic University School of Optometry, Kowloon, Hong Kong; this was the same cohort investigated in Chapter 8. The protocol for ORA and ocular biometry measurements on the HKC subjects was the same as that for the Aston University group; however due to logistical and time constraints, it was not possible to take GAT and CCT measurements on the HKC subjects.

11.4 Statistical Analysis

Initially the UK data and the HK data were evaluated separately. Data were analysed using the Kolmogorov-Smirnov test to ensure they conformed to a normal distribution. Concordance between the ORA and GAT measures of IOP was initially analysed using linear regression analysis. The coefficient of correlation is principally a measure of the

relationship between data and not an accurate determinant of agreement between data. Therefore as recommended by Bland and Altman (1986; 1995), the test for agreement was done by plotting mean IOP against the difference in IOP between the two instruments and hence the 95% limits of agreement (LoA) were calculated as mean difference between tonometers $\pm 1.96 \times$ Standard Deviation (SD).

Pearson's correlation coefficient was calculated to test the relationship between different ORA metrics and biometric parameters such as CCT and axial length. A stepwise-forward multiple linear regression was used as an exploratory test to determine which ocular biometric variables best explained the ORA values.

The influence of refractive error was initially assessed for myopes (MSE $< -0.50D$) and non-myopes (MSE $\geq -0.50D$). To determine whether a more structural categorisation of the ocular globe is pertinent to differences in corneal biomechanics, the eyes were also divided into three categories of axial length ($21.5 \geq - < 23.5$ mm), ($23.5 \geq - < 25.5$ mm) and (> 25.5 mm). A one-way ANOVA was conducted to test the influence of axial length on corneal biomechanics. Independent *t tests* were performed to test for refractive error (myopes vs. non-myopes) and gender differences within and between the population sample groups.

In regards to the additional waveform parameters (AWPs), one-way ANOVAs were performed on both the BW-BSA and HKC data to test differences in axial length grouping. Independent *Student's t tests* were performed to test refractive status (myopic vs. non-myopic) and gender differences. A two-way factorial ANOVA was performed to test the effect of ethnicity and refractive error on the AWP. A p-value of < 0.05 was taken as the criterion for statistical significance. See Appendix 8 for details on statistical analyses employed.

11.5 UK Results

11.5.1 IOP and corneal biometrics (corneal hysteresis (CH) and corneal resistance factor (CRF) for UK subjects

The study employed 72 healthy individuals (144 eyes; 26 males and 46 females) due to two individuals being removed as they each had astigmatism $> 1.75D$. The subjects were aged between 18-40 years (27.83 ± 5.41) and data were analysed for non-myopic and

myopic individuals [myopes (MSE <-0.50D), n=36, MSE (D) mean \pm SD (-4.62 \pm 4.09), range (-20.50 to -0.51), AL (mm) mean \pm SD (25.23 \pm 1.26), range (23.33 - 28.32); non myopes (MSE \geq -0.50D), n=36, MSE (D) mean \pm SD (0.41 \pm 0.97), range (-0.50 to +4.38), AL (mm) mean \pm SD (23.35 \pm 0.72), range (21.61 - 24.75)].

High levels of correlation were found between eyes for IOPg, IOPcc, CRF and CH. Paired *t tests* revealed no significant difference in the ORA parameters between RE and LE and thus only RE data were used. Table 11.1 displays data for parameters measured by the ORA. The mean \pm SD CCT was 532 \pm 30 μ m (range 470 - 597 μ m).

Variable	Mean \pm SD	Min	Max
GAT	13.85 \pm 2.50	8.00	21.00
IOPg	14.77 \pm 3.16	7.23	24.17
IOPcc	14.92 \pm 2.89	9.03	24.27
CRF	10.54 \pm 1.53	7.37	14.57
CH	10.81 \pm 1.28	7.60	14.40

Table 11.1 RE IOP (mm Hg) and ORA metrics (mm Hg) for the UK data.

Comparison	Correlation/Sig	Mean difference \pm SD	95% LoA
GAT versus IOPg	r=0.810 (p<0.001)	-0.87 \pm 1.85	(-4.50) to 2.76
GAT versus IOPcc	r=0.664 (p<0.001)	-1.02 \pm 2.21	(-5.35) to 3.31
IOPg versus IOPcc	r=0.881 (p<0.001)	-0.15 \pm 1.50	(-3.09) to 2.79

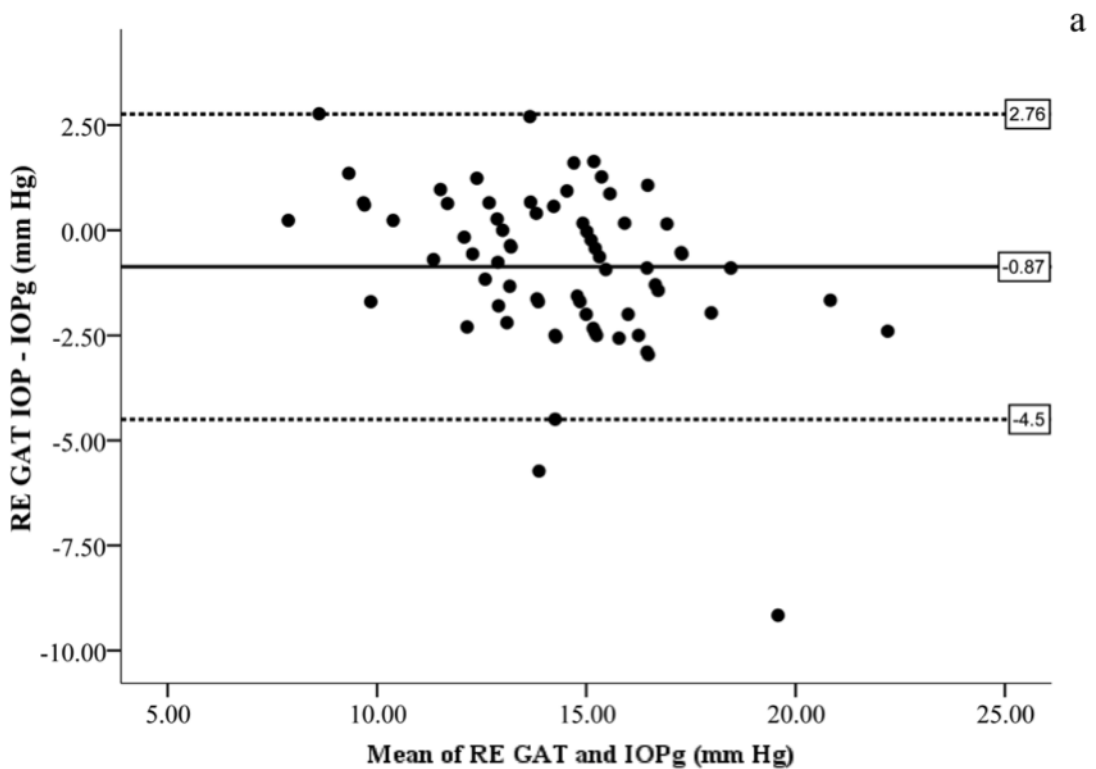
Table 11.2 Correlations and differences between RE IOP (mm Hg) measurement with GAT and ORA.

Both CH and CRF showed high levels of correlation. CH showed a weak negative correlation with IOPcc and no significant relationship with IOPg or GAT. In contrast CRF correlated significantly with IOPg, GAT and weakly with IOPcc. IOPg correlated significantly with IOPcc and GAT- see Table 11.2.

CCT correlated significantly with most measures of the ORA (i.e. IOPg, CH, CRF) except IOPcc. Additionally, CCT also correlated with GAT. Mean central corneal curvature showed a weak significant correlation with IOPcc and CH. Refractive error, axial length and ACD showed no significant relation with ORA metrics.

The difference in IOP measures between GAT-IOPg and GAT-IOPcc were tested statistically as the mean of the difference compared to zero. The hypothesis of zero bias was examined by a paired *t-test*. The test revealed significant differences in IOP measures between GAT-IOPg ($p < 0.001$) and GAT-IOPcc ($p < 0.001$) indicating that ORA measures of IOP are significantly overestimated. See Figure 11.1 (a, b and c) for mean versus difference plots for the various measures of IOP.

The difference between GAT-IOPg significantly correlated with CCT and CRF but no significant correlation was found with CH. The difference between GAT-IOPcc significantly correlated with CRF and CH but not CCT. Additionally the GAT-IOPcc difference showed a positive correlation with increasing levels of GAT measures of IOP, whilst the GAT-IOPg difference showed no such effect.



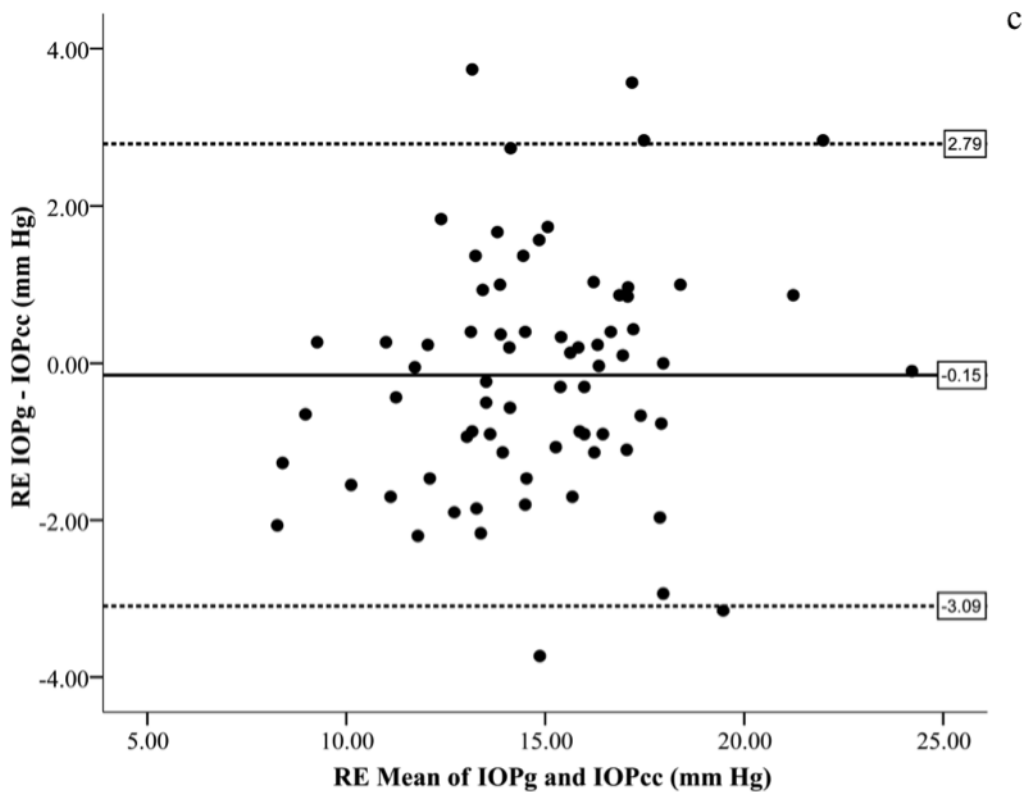
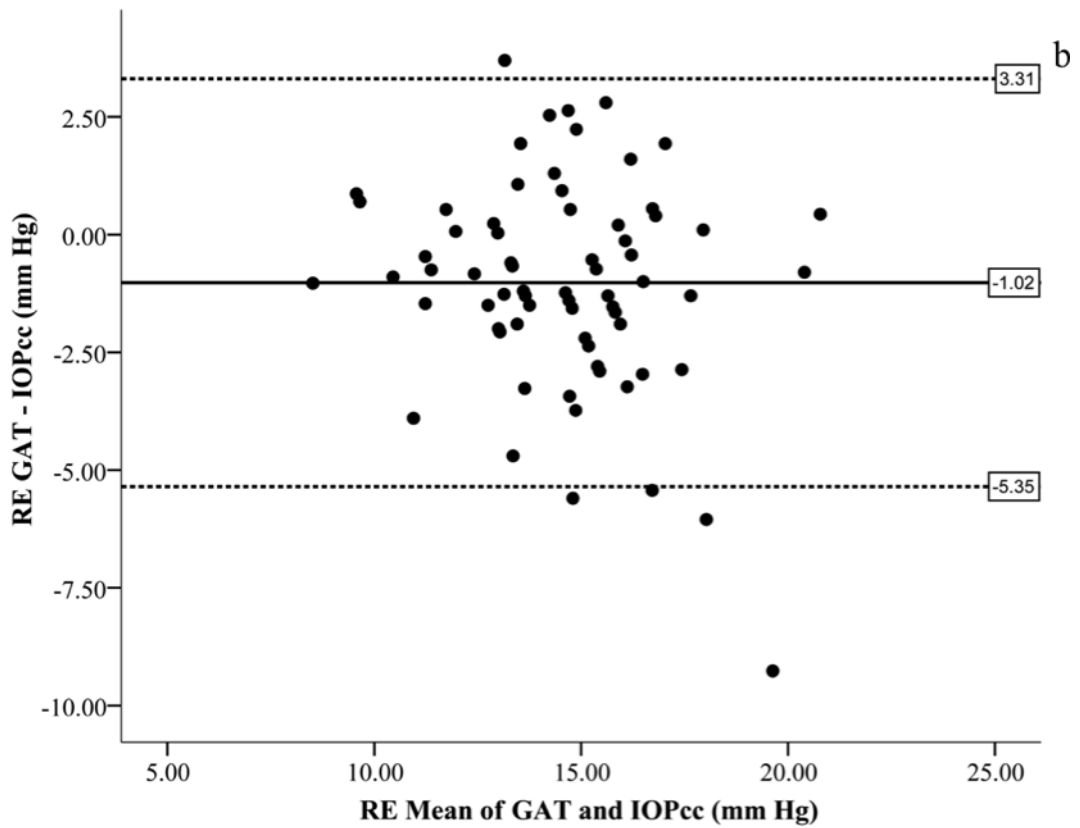


Figure 11.1 RE Bland Altman plots: a) GAT and IOPg difference as a function of their mean IOP, b) GAT and IOPcc difference as a function of their mean IOP and c) IOPg and IOPcc difference as a function of their mean IOP. Horizontal bold line denotes mean difference and dotted lines 95% LoA.

11.5.2 Corneal biomechanics and additional ocular biometrics for UK subjects

A stepwise forward multiple linear regression model with CH as the outcome variable and CCT, GAT, refractive error, mean corneal curvature, axial length, ACD, gender and age as predictor variables revealed CCT ($p<0.001$), mean corneal curvature ($p=0.003$) and axial length ($p=0.032$) to be significantly associated with CH (see Appendix 8 for more details). The model revealed that when the other significant predictor variables were held constant, CCT accounted for 27.7% of the variability in CH, which was further increased by another 9.4% by adding mean corneal curvature and a further 4.6% when accounting for axial length. The results of the multiple regression indicated that for a 100 μm increase in CCT, CH would increase by 2.30 mm Hg, and a 1 mm increase in corneal curvature would lead to a 1.59 mm Hg reduction in CH; for axial length a 1 mm increase was found to reduce CH by 0.20 mm Hg.

A similar multiple regression model was constructed for CRF with the same predictor variables as for CH. The results indicated that CCT ($p<0.001$), GAT ($p<0.001$), mean corneal curvature ($p=0.002$) and axial length ($p=0.015$) were significantly associated with CRF (see Appendix 8 for more details). The model revealed that CCT accounted for 45% of the CRF variability, which increased by 16.3% with the inclusion of GAT and a further 5.2% and 3.2% by adding mean corneal curvature and axial length respectively. The results indicate that for every 100 μm change in CCT, CRF would increase by 2.40 mm Hg, whilst a 1 mm Hg increase in GAT would result in a 0.34 mm Hg increase in CRF; a 1 mm increase in corneal curvature would produce a 1.56 mm Hg reduction in CRF whilst a 1 mm increase in axial length would cause a reduction in CRF of 0.21 mm Hg.

Multiple regression with IOPg as the outcome with the same predictors as for CH, revealed that only CCT was a significant predictor variable and accounted for 26.1% variability of IOPg, indicating that for every 100 μm change in CCT IOPg would increase by 5.1 mm Hg. In comparison, for IOPcc both mean corneal curvature ($p=0.007$) and axial length ($p=0.029$) were found to contribute significantly to the measurement. Mean corneal curvature explained 10.9% of the variability of IOPcc increasing the measurement by 3.67 mm Hg for every 1 mm increase in corneal curvature; axial length explained 6.6% of the IOPcc variance increasing IOPcc by 0.52 mm Hg for every 1 mm increase in axial length.

Independent *t tests* revealed no significant difference in CRF, CH, IOPg and IOPcc between myopes ($<-0.50D$) $n=36$ and non-myopes ($\geq-0.50D$) $n=36$. As the multiple regression analysis indicated that axial length was a significant predictor of CH and CRF, the subjects were split into axial length (mm) subgroups; 1: ($21.5 > - \leq 23.5$) $n=26$, 2: ($23.5 > - \leq 25.5$) $n=32$ and 3: (>25.5) $n=14$. A one-way ANOVA revealed no significant difference for CRF, CH, IOPg and IOPcc between these groups. See Figures 11.2 (a-d) for box and whiskers plots (i.e. median and interquartile range) for each ORA biometric (see Appendix 8). On inspection of box-plots a and b it can be noted that there is a weak trend for reduced CRF and CH with increasing axial length, whilst box plot c and d show a non-significant effect of increasing IOPg and IOPcc with higher axial length intervals.

In regards to the additional biometric variables (ACD, CCT and mean corneal curvature) a significant difference was found for axial length grouping for ACD ($p<0.001$) but not for corneal curvature or CCT. A Games-Howells *post hoc* analysis demonstrated the ACD difference to be between groups (1 and 2) and (1 and 3).

Independent *t tests* testing for an influence of age (years) grouping ($18 > - \leq 29$ $n=46$ and $29 > - \leq 40$ $n=26$) and gender (male $n=26$, female $n=46$) failed to show any significant affect on the ORA (CH, CRF, IOPg and IOPcc) and biometric (axial length, ACD, CCT and mean corneal curvature) parameters.

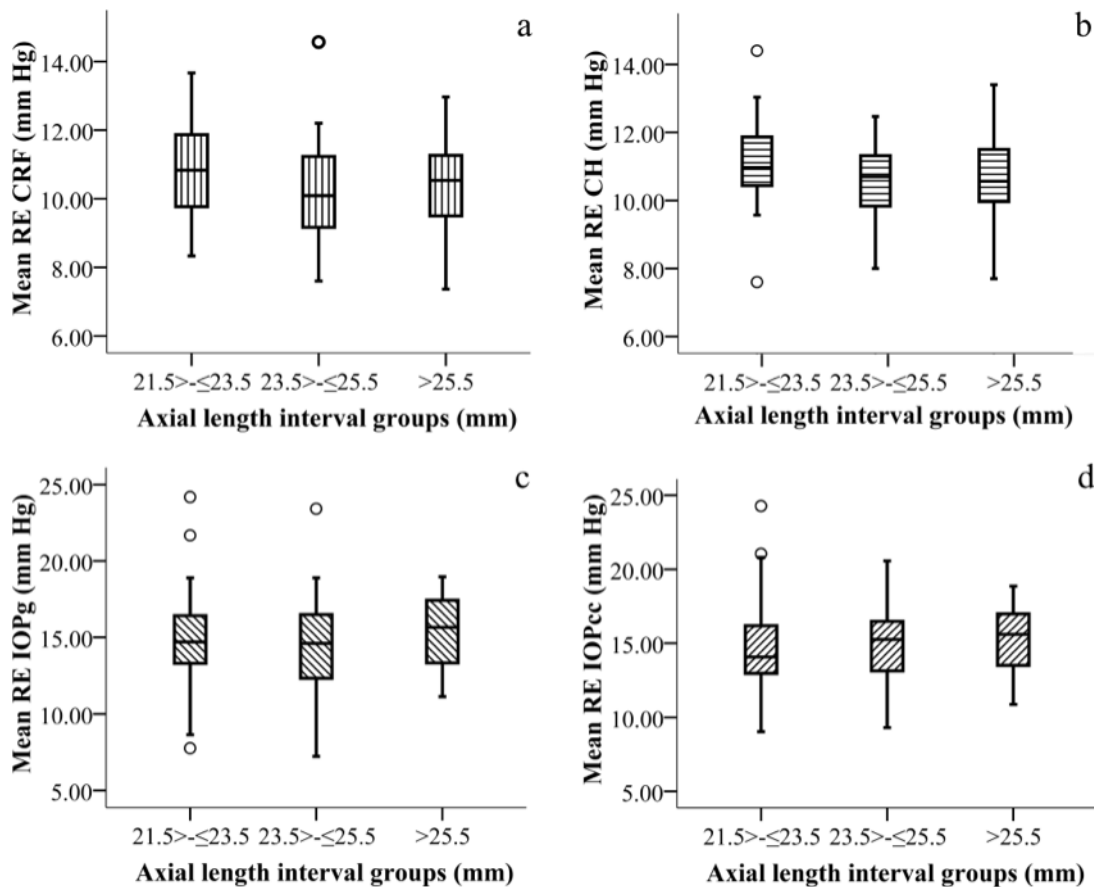


Figure 11.2 Box and whiskers plot (median and interquartile range) for a) CRF, b) CH, c) IOPg and d) IOPcc for three different intervals of axial length.

11.5.3 ORA Additional Waveform Parameters (AWPs) for UK subjects

No significant influence of axial length grouping was found for the AWP. On testing for an influence of refractive status on the AWP significant differences for p2area, aspect1, dslope1, w1, mslew1 and p2area1 ($p < 0.05$) were found. Gender was also found to have a significant affect on some AWP: path1, aplhf and path21 ($p < 0.05$). Several AWP were also influenced by age grouping (Appendix 8). Furthermore, there were numerous correlations between both ocular biometric parameters (refractive error, axial length, mean corneal curvature, CCT, ACD), age and the AWP. See Appendix 8 for further details.

A multiple linear regression analysis with refractive error as the dependent variable and aindex, bindex, p1area, p2area, aspect1, aspect2, w1, w2, dive1, dive2, path1, path2, mslew1, mslew2 and alphf as the predictor variables was carried out. The analysis revealed a significant association between refractive error and p2area ($p = 0.003$), w1 ($p = 0.008$) and mslew1 ($p = 0.025$). The model indicated that for every 1 unit change in p2area refractive

error would increase by 0.002, whereas a unit change in w1 would produce a 0.491 decrease in refractive error and a unit change in mslew1 would yet again reduce refractive error by 0.026.

The same model was applied with axial length as the dependent variable and the same predictor variables as before. The analysis revealed w1 (p=0.002) and path2 (p=0.012) to be significant predictor variables for axial length. The model indicated that a unit change in W1 would produce a 0.220 increase in axial length and a unit change in path2 would cause a 0.125 increase in axial length.

11.6 HK Results

11.6.1 IOP and corneal biometrics (CH and CRF) for HKC subjects

The study employed 56 healthy individuals (112 eyes; 30 males and 26 females) as 4 subjects were removed from the study as they presented with astigmatism >1.75D. The subjects were aged between 18-40 years (25 ± 4.74). The data were analysed for both non-myopic and myopic individuals [non myopes (MSE $\geq -0.50D$), n=11, MSE (D) mean \pm SD (0.39 ± 0.66), range (-0.44 to +1.69), AL (mm) mean \pm SD (23.49 ± 0.37), range (22.90 - 24.00); myopes (MSE $< -0.50D$), n=45, MSE (D) mean \pm SD (-4.16 ± 2.48), range (-13.38 to -0.75), AL (mm) mean \pm SD (25.70 ± 1.09), range (23.83-29.78)].

High levels of correlation between RE and LE were observed for all ORA biometrics (IOPg, IOPcc, CRF and CH). Paired *t test* revealed no significant difference between RE and LE thus only RE values will be discussed (Table 11.3).

Variable	Mean \pm SD	Min	Max
IOPg	14.63 \pm 2.99	7.37	20.93
IOPcc	14.88 \pm 2.38	9.93	21.57
CRF	10.44 \pm 1.73	6.30	14.43
CH	10.73 \pm 1.36	7.80	14.37

Table 11.3 RE ORA metrics (mm Hg) for the HK subjects.

CRF and CH were significantly correlated. CH correlated with IOPg but not IOPcc, whilst CRF correlated with both IOPg and IOPcc. IOPg also correlated significantly with IOPcc. Interestingly both IOPg and IOPcc correlated negatively with refractive error and positively with axial length. Both CH and CRF failed to correlate with either axial length

or refractive error. ACD and mean corneal curvature showed no relationship with the ORA parameters.

11.6.2 Corneal biomechanics and additional ocular biometrics for HKC subjects

The data were further explored with stepwise forward multiple linear regression models with CH and CRF as the dependent variables and age, gender, mean corneal curvature, ACD, refractive error and axial length as the predictor variables. The models revealed no significant association for both CH and CRF and the predictor variables.

Similar multiple linear regression models were also constructed for IOPg and IOPcc as the dependent variables and the same predictor variables as for CH and CRF. These models revealed axial length to be significantly associated with IOPg ($p=0.005$) and IOPcc ($p=0.001$) as they explained 13.9% and 19.3% of their variance, respectively. The model indicated that an axial length increase of 1 mm would produce a subsequent increase of 0.84 mm Hg in IOPg and 0.78 mm Hg in IOPcc. Similarly refractive error was also found to be associated with IOPg ($p=0.002$) and IOPcc ($p<0.001$) explaining 16.7% and 23.9% of the variance in these parameters, respectively. The results indicated that for every 1D increase in refractive error there would be a reduction in IOPg of 0.42 mm Hg and IOPcc of 0.40 mm Hg.

When testing for the effect of refractive status (myopes $n=45$ vs. non-myopes $n=11$) no significant difference was found for CH, CRF, IOPg but a significant difference was seen for IOPcc ($p=0.042$). As axial length was found to be a significant predictor for IOPg and IOPcc the data were assessed by dividing the sample into subgroups; 1: ($21.5 > - \leq 23.5$) $n=4$, 2: ($23.5 > - \leq 25.5$) $n=26$ and 3: (>25.5) $n=26$ as for the BW-BSA data. A one-way ANOVA revealed no significant differences in CH, CRF and IOPg. However a significant difference was noted between the subgroups for IOPcc ($p=0.020$), with a Bonferroni *post-hoc* test indicating that the difference was principally attributable to axial length groups 2 and 3. Figures 11.3 (a-d) show box and whiskers plot (median and interquartile range) for each ORA biometric parameter.

The additional biometric parameters (corneal curvature and ACD) showed a significant difference between axial length groups for flat corneal curvature ($p=0.031$) and steep

corneal curvature ($p=0.023$) and ACD ($p=0.008$). On performing a Bonferroni *post hoc* test these differences were found to be attributable to axial length groups 1 and 3.

Independent *t test* analysis revealed no significant influence of gender (male $n=28$, female $n=28$) and age (years) group ($19 > \leq 29$ $n=45$, $29 > \leq 40$ $n=11$) on the ORA parameters. A significant difference was found with regards to axial length ($p=0.027$) and mean corneal curvature ($p=0.012$) with male subjects showing longer axial length and flatter corneal curvature. Additionally none of the ORA or biometric variables were found be affected by age.

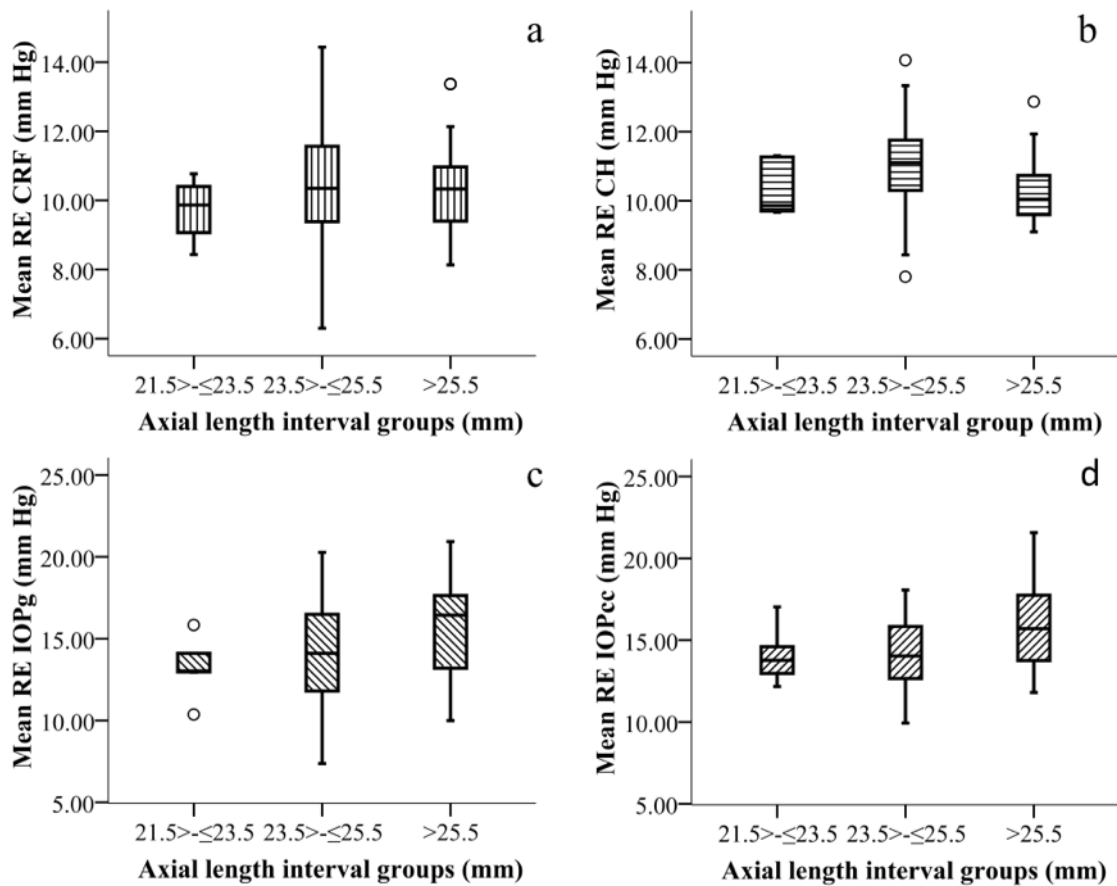


Figure 11.3 Box and whiskers plot (median and interquartile range) for a) CRF, b) CH, c) IOPg and d) IOPcc for three different intervals of axial length.

11.6.3 ORA Additional Waveform Parameters (AWPs) for HKC subjects

Statistical analysis revealed no significant effect of axial length grouping on the HK AWP data. Furthermore neither refractive error nor gender was found to significantly influence the AWP. There were fewer significant correlations amongst ocular biometric variables and the AWP, when compared to the UK data set. Unlike the UK data, refractive error and ACD failed to correlate with any of the AWP. Multiple linear regression revealed no significant association between refractive error, axial length and AWP. See Appendix 8 for further details.

11.7 Comparison of ORA metrics and ocular biometry between BW - BSA (UK) and HKC individuals

11.7.1 IOP and corneal biometrics (CH and CRF) for UK and HK subjects

Independent *t tests* revealed no significant difference between CH, CRF, IOPg and IOPcc between the UK and HK data and thus the data were combined to provide a larger range of refractive error.

A one-way ANOVA revealed no significant effect of ethnicity between the UK BW (n=48) - BSA (n=23) sample and the HKC (n=56) eyes for CH, CRF, IOPg and IOPcc. Other biometric data were also tested for differences between ethnic groups. Axial length was found to be significantly different, with a Bonferroni *post hoc* test indicating the difference to be between the BW and HKC subjects ($p < 0.001$), but not between the HKC and BSA individuals. Differences in corneal curvature when tested separately along the two principal meridians revealed the flattest meridian to be significantly different between the ethnic groups ($p = 0.007$), but no significant difference was found for the steeper curve. With Bonferroni *post hoc* analysis these ethnic differences for the flattest corneal meridian were found to be between the BW and HKC eyes. No significant difference was found for ACD between the ethnicities.

11.7.2 ORA Additional Waveform Parameters (AWPs) for UK and HK subjects

A two way factorial ANOVA was performed on each AWP to test for an influence and possible interaction between ethnicity and refractive status for the BW (n=48), BSA (n=23) and HKC (n=56) individuals.

A significant effect of ethnicity was found on a several AWP, with significant differences being identified between all ethnicities (BW, BSA and HKC). There were also a small number of AWP that were only significantly different between the BSA and HKC individuals. On findings of significant differences many of the AWP were lower amongst the HKC group when compared to the BW and BSA data. Refractive error also demonstrated a significant influence on the AWP with several AWP showing higher readings in non-myopic eyes when compared to myopic eyes. An interaction effect was also observed for refractive error and ethnicity for two AWP (P2 and mslew1). See Appendix 8 for further details.

11.8 Discussion

The findings indicate that geometric parameters such as axial length may play a determinant role in corneal biomechanics and IOP. Axial length was found to be a significant predictor of CH and CRF for the UK individuals but not for the HKC group. In contrast axial length and refractive error were found to be highly predictive of IOPg and IOPcc in the HKC group, which was not seen amongst the UK subjects. These differences in the inter-relationships between biomechanical and structural variables may signify fundamental variation in ocular structure between the two population samples. No significant influence of gender was found in either sample, however the HKC data showed male subjects to have greater axial length and flatter corneas. The main ORA biometrics (i.e. CH, CRF, IOPg and IOPcc) showed no significant difference between non-myopes and myopes nor between the different axial length grouping but there was a weak trend for a reduction in CH and CRF with increasing axial length. Refractive status was found to have a significant effect on various AWP with some parameters displaying an interaction with ethnicity. Furthermore significant differences were found between HKC and BW-BSA data for numerous AWP but no significant difference was found for the principal ORA metrics.

11.8.1 Comparison between measures of IOP with the ORA and GAT

Although it was not the primary objective of the study, a comparison was made between IOP measurements with GAT and the ORA (IOPg and IOPcc) to test their degree of concordance. *High levels of correlation were found between both GAT-IOPcc and GAT-IOPg although the ORA was found to consistently overestimate IOPs.* Similar levels of concordance and overestimation of IOP between the two techniques have been reported in several studies (PePOSE *et al.*, 2007; Martinez-de-la-Casa *et al.*, 2006b; Hager *et al.*, 2008; Kynigopoulos *et al.*, 2008). Furthermore the levels of overestimation with the ORA have been reported to increase with higher levels of IOPs (Martinez-de-la-Casa *et al.*, 2006b; Lam *et al.*, 2007); a trend that was noted (GAT-IOPcc) in the present study. Previously, it has been postulated that higher IOP may not only cause stretching of the cornea but could also affect its hydration properties hence influencing its biomechanical characteristics (Kamiya *et al.*, 2008). Such changes may partly explain the overestimation of IOP found with the ORA for higher levels of IOPs.

11.8.1.1 Measures of IOP with the ORA and GAT- the influence of ocular biometry

In the UK data all measures of ORA, except IOPcc, correlated with CCT, as previously reported in various studies (Hager *et al.*, 2008; Hager and Wiegand, 2008; Lim *et al.*, 2008; Franco and Lira, 2009). Moreover, the results of the multiple regression model demonstrated CCT to be a significant predictor variable for IOPg. Contrary to these results, IOPcc was found to be unaffected by CCT but was found to be significantly related to corneal curvature and axial length. *Similarly the HKC data also showed increasing axial length and myopic refractive error to be significantly associated with increasing IOPg and IOPcc.* These findings differ from other studies that have found no association between IOPcc and axial length and corneal curvature (Medeiros and Weinreb, 2006; Broman *et al.*, 2007). Corneal curvature has been previously implicated in measurement of IOP using GAT, with steeper curvature requiring greater force to applanate, thus artificially elevating IOP measurements (Whitacre and Stein, 1993). However the current findings are contrary to these observations as IOPcc increased as the cornea flattened. These opposing findings could be explained by reports of increased levels of stress on the ocular walls as the radius of curvature of the globe increases (Friedman, 1966). Both CH and CRF were also found to reduce as the cornea flattened but as IOPcc is independent of the effects of the material properties of the cornea it may be able to evaluate more accurately the increased levels of stress as the cornea flattens. Additionally it is likely that

the relation between axial length and IOPcc indicates that as ocular size increases the stress applied to the ocular walls also correspondingly increases (Sigal *et al.*, 2005b; Friedman, 1966) and thus the force required to applanate needs to be greater.

Moreover it has been hypothesised that the response of the eye may differ between static measures of IOP, as in GAT, and the more rapid application of ocular stress with the ORA (Hager *et al.*, 2007). The ‘rebound’ effect of the cornea during the ORA measurement may be related to the rate of change of the pressure-volume relationship that is, in turn, affected by the rate at which ocular stress is applied (Broman *et al.*, 2007). The behaviour of elastic materials are predictable as strain is proportional to stress and independent of the rate at which force is applied; however with viscous materials the stress/strain response is dependent on the rate of deformation (Hager *et al.*, 2007).

The results show that, in comparison to traditional methods of determining IOP with GAT, the IOPcc is less influenced by corneal biomechanical properties such as CCT. Furthermore IOPcc showed the weakest correlation with CRF compared to GAT and IOPg, which supports the findings of reduced influence of corneal properties on this aspect of IOP measurement. In their meta-analysis Doughty and Zaman, (2000) reported that a change of 10% in CCT would cause a change of 1.1 mm Hg in IOP in normal subjects thus inferring that instruments that are minimally affected by CCT will provide a more accurate determination of IOP. Despite the discrepancy between the ORA and GAT, ORA biomechanical metrics and IOP have been shown to have high repeatability and reproducibility in several studies (Moreno-Montañés *et al.*, 2008; Kynigopoulos *et al.*, 2008) thus supporting the efficacy of the ORA in clinical practice.

11.8.2 Structural correlates of corneal biomechanics

11.8.2.1 CCT and corneal biomechanics

The values for CH and CRF for both UK and HKC data sets are similar to those found in previous investigations (Shah *et al.*, 2006; 2007; Ortiz *et al.*, 2007; Montard *et al.*, 2007). *The UK data showed CH and CRF to correlate significantly with CCT indicating that the biomechanical metrics of the ORA are affected by physiological parameters of the cornea*; such findings have also been noted in various studies (Luce *et al.*, 2005; Carbonaro *et al.*, 2008; Strehlo *et al.*, 2008; Shen *et al.*, 2008). In particular Kamiya *et al.*,

(2008) reported CCT to be a significant factor in CH with thinner CCT showing reduced CH. Interestingly, many studies have reported changes in CH with various ocular conditions such as keratoconus (Shah *et al.*, 2007; Spörl *et al.*, 2009), Fuch's dystrophy (del Buey *et al.*, 2009), post laser *in situ* keratomileusis (LASIK) (Pepose *et al.*, 2007; Franco and Lira, 2009) and post clear corneal cataract surgery (Hager *et al.*, 2007). These findings would suggest that the associated changes in CCT in these ocular conditions may be a significant contributor to the reported CH changes. A low hysteresis indicates a cornea that quickly returns to its original shape after deformation, whilst a higher hysteresis indicates an eye that takes longer to return back to its original shape and thus indicates greater stiffness (Broman *et al.*, 2007). ***Therefore as CCT increases the overall resistance to deformation of the cornea may increase thus resulting in higher levels of CH.***

Despite the commonly reported association between CCT and CH, studies have highlighted that the moderate levels of correlation found between these two variables suggests that other unknown biomechanical factors must also contribute towards the characteristics of CH (Kirwan and O'Keefe, 2008; Kamiya *et al.*, 2008). Evidence for this conjecture stems from reports of lower CH following increased CCT as result of post-operative oedema (Hager *et al.*, 2007) and contact lens induced swelling (Lu *et al.*, 2007). Interestingly, Broman *et al.*, (2007) reported that eyes with the same CCT produced varying levels of CH, implying that other unidentified factors may be influencing corneal biomechanics.

11.8.2.2 Corneal ultrastructural changes and corneal biomechanics

Histopathological changes in various ocular pathologies such as Fuch's dystrophy (del Buey *et al.*, 2009; Shen *et al.*, 2008) and keratoconus (Chi *et al.*, 1956; Teng *et al.*, 1963; Gefen *et al.*, 2009) may also affect the biomechanical metrics measured by the ORA. Structural changes in the corneal matrix are likely to affect the cornea's biomechanical strength and various studies have reported reduced CH and CRF in Fuch's dystrophy and keratoconus (del Buey *et al.*, 2009; Shah *et al.*, 2007; 2009; Ortiz *et al.*, 2007; Spörl *et al.*, 2009; Saad *et al.*, 2009; Fontes *et al.*, 2010).

11.8.2.3 Corneal curvature and corneal biomechanics

In the present study corneal curvature was found to be significantly related to CH and CRF, with a flatter corneal curvature associated with reducing CH and CRF amongst the

UK subjects. Consistent with these findings Lim *et al.*, (2008) also reported decreasing levels of CH and CRF with increasingly flatter corneal curvatures. Contrary to these findings Broman *et al.*, (2007), Chang *et al.*, (2009) and Franco and Lira (2009) reported no association with central corneal curvature and CH or CRF. These divergent results could be explained by differences in study protocol; the Broman *et al.*, (2007) study employed individuals across a large age range (20-100 years) although 80% of the subjects were between the age of 40-80 years; Franco and Lira (2009) assessed subjects between the ages of 20-63 years; Chang *et al.*, (2009) assessed children between 7-18 years. In comparison to the present cohort (i.e. 18-40 years) and the Lim *et al.*, (2008) (12-15 years) study the age group and range for these previous studies was clearly significantly different. As age has been found to have a significant influence on corneal biomechanics (Daxer *et al.*, 1998; Malik *et al.*, 1992; Sherrard *et al.*, 1987; Lam *et al.*, 2003; Pallikaris *et al.*, 2005) and corneal curvature (Lim *et al.*, 2010; Lee *et al.*, 2010) the relationship between the two variables may also be altered.

11.8.3 Corneal biomechanics and glaucoma

Aside from a significant role of corneal morphology in the biomechanical properties of the cornea, there has been speculation that the ORA biometrics (e.g. CH and CRF) may also provide an inferred assessment of the mechanical characteristics of the whole globe (Kucumen *et al.*, 2008). The hypothesis originates from numerous reports of reduced CH in eyes with primary open angle (POAG), normal tension (NTG) and congenital glaucoma (CG) suggesting that pathological changes in the lamina cribrosa are linked to changes in anterior corneal biomechanics (Congdon *et al.*, 2006; Kirwan *et al.*, 2006; Strehlo *et al.*, 2008; Shah *et al.*, 2008). Moreover, reports of a hereditary influence on CH and ocular pulse amplitude (OPA) (Carbonaro *et al.*, 2008) and a significant association between OPA, CH and CRF indicate that the ORA biomechanical metrics may indeed be related to global biomechanics (Ehongo *et al.*, 2008).

These conjectures of interlinked anterior and posterior biomechanics would suggest that a more deformable cornea may somehow be linked to a greater susceptibility of the lamina cribrosa to changes in IOP (Song *et al.*, 2008). Kotecha *et al.*, (2006) suggests that viscoelastic materials show characteristic creep and stress relaxation and under constant high levels of IOP the cornea may remodel itself thus affecting its biomechanical characteristics. Indeed in support of this supposition, Kamiya *et al.*, (2008) reported high

IOP to be linked to reduced levels of CH. In a study assessing corneal biomechanics in glaucoma, Schroeder *et al.*, (2008) reported a significant correlation between CCT and CH in non-glaucomatous individuals but a reduced CH and no relation between CH and CCT in POAG subjects, suggesting altered biomechanics in glaucomatous eyes. However, such findings of corneal biomechanical changes in glaucoma are equivocal as various studies have failed to report significant difference in CH between normal and POAG subjects (Moreno-Montañés *et al.*, 2008; Hager and Wiegand, 2008). These disparate reports may be a result of the complex nature of global biomechanics, which is likely to be affected by physiological differences in ocular conformation, scleral thickness and haemodynamics.

11.8.4 Corneal biomechanics and myopia

There is a significant body of literature that links myopia and both glaucoma (POAG, LTG and NTG) and susceptibility to OHT (Podos *et al.*, 1966; Perkins and Phelps, 1982; Seddon *et al.*, 1983; Chihara and Honda, 1992; Chihara *et al.*, 1997; Mastropasqua *et al.*, 1992; Wu *et al.*, 1999; 2000; Mitchell *et al.*, 1999; Xu *et al.*, 2007). In relation to corneal biomechanics, Congdon *et al.*, (2006) first reported an association between CH and axial length and suggested that longer axial length may be a significant risk factor in glaucoma (POAG). It is debatable whether corneal changes occur in myopia with various studies reporting disparate results (Chang *et al.*, 2001; Cho and Lam, 1999; Fam *et al.*, 2006; Pedersen *et al.*, 2005; Goss *et al.*, 1997; Liu *et al.*, 1995; Nomura *et al.*, 2004; AlMahmoud *et al.*, 2010). In regards to an influence of refractive status on the cornea, some investigators have observed reduced CCT in myopia (Chang *et al.*, 2001), other have reported increased CCT (Nomura *et al.*, 2004), whilst a number have shown no difference in CCT between myopes and non-myopes or with levels of myopia (Cho and Lam, 1999; Pedersen *et al.*, 2005; Fam *et al.*, 2006; Lim *et al.*, 2008; Shen *et al.*, 2008; AlMahmoud *et al.*, 2010). Conversely, Goss *et al.*, (1997) noted myopic eyes to have significantly flatter corneas, whilst Liu *et al.*, (1995) reported increased corneal power in myopic eyes. Furthermore Farbrother *et al.*, (2004b) noted astigmatism axis to be influenced by spherical refractive error with low myopes showing a greater tendency for against-the-rule astigmatism. Additionally, animal models of myopia have also reported axial length growth to modulate corneal curvature and astigmatism (Kee *et al.*, 2005; Kee and Deng, 2008; Hayes *et al.*, 1986).

In relation to the present study, measures of CH and CRF were found to reduce with increasing axial length amongst the UK subjects. In support of these findings Song *et al.*, (2008) investigated corneal biomechanics in Chinese children and report a significant effect of reducing CH with increasing axial length. Interestingly, in a study assessing corneal biomechanics in high myopes (MSE <-9.00D) and a control group (MSE 0D - 3.00D) Shen *et al.*, (2008) reported no significant difference in CRF and CCT between the groups but significantly lower CH in the high myopia group. These investigators hypothesised that the higher the level of myopia, the greater the biomechanical changes to the cornea. Moreover, these findings of reduced levels of CH in the Shen *et al.*, (2008) study were not associated with any significant change in CCT, indicating that biomechanical changes in myopia may be attributable to microstructural changes in the cornea. In support of these findings, using univariate mixed modelling, Chang *et al.*, (2009) reported lower levels of CH to be associated with thinner CCT, deeper ACD and longer axial length, whilst CRF was found to be related to reduced CCT but not axial length or ACD. Additionally, the investigators also noted that in a multivariate mixed model, both CH and CRF were reduced with increasing axial length and reducing CCT. Furthermore, the study also provided substantive evidence for a role of axial length in CH and reported a significant correlation between the differences in axial length and CH between the two eyes.

In contrast to these findings, Lim *et al.*, (2008) found no effect of myopic status on CH or CRF, nor any correlation with axial length. Despite reports of axial length being associated with corneal biomechanics, refractive error has not been found to be similarly linked to CH and CRF, as is the case in the present study (Song *et al.*, 2008, Carbonaro *et al.*, 2008). These findings would indicate that the more global structural features such as axial length (also linked to ocular pathology such as retinal detachment and glaucoma) might be more important in predicting ocular biomechanics than refractive error.

These results also suggest that lower CH may perhaps be linked to a corneoscleral shell that is more predisposed to axial elongation (Song *et al.*, 2008). It is still unclear as to whether reduced CH is a precursor to, or a consequence of, axial length growth. For this issue to be resolved longitudinal studies would be required that monitor myopic growth and corneal biomechanics. As mentioned afore, reduced CH has been associated with glaucoma and OHT (Abitbol *et al.*, 2010; Mangouritsas *et al.*, 2009; Bochmann *et al.*, 2008), but when considering the lower CH found in myopic eyes, further support is found for

the link between myopia and glaucoma (Wu *et al.*, 1999; 2000; Mitchell *et al.*, 1999; Xu *et al.*, 2007). These findings suggest that the lower CH in myopes may indicate a more vulnerable ocular globe that is predisposed to the effects of changes in IOP.

11.8.5 IOP and myopia

When considering the higher prevalence of myopia in Chinese children compared with Caucasians (Park and Congdon, 2004; Ip *et al.*, 2008) lower CH may indicate an increased predisposition to myopic growth (Song *et al.*, 2008). Moreover, increased IOP may also play a role in the pathogenesis of myopia by promoting axial length elongation via the application of scleral stress (Pruett, 1988; Lee and Edwards, 2000). *Interestingly, in the present study the relationship between increasing axial length and reducing CH and CRF in the UK data was not found in the HKC subjects; instead axial length was found to correlate significantly with both IOPg and IOPcc in the HKC subjects, which was not seen in the UK data.* IOPcc was found to vary significantly between axial length (mm) ranges with differences seen particularly between ($23.5 > - \leq 25.5$) and (>25.5). These disparate findings between the two population samples may indicate important structural differences associated with ethnicity and its link to differential levels of myopia prevalence.

In support of a relationship between myopic status and increased IOP, Edwards and Brown (1993) and Quinn *et al.*, (1995) reported IOPs to be higher in myopic children when compared to non-myopes. Similarly, Jensen (1992) found high IOP to be a risk factor for higher levels of myopia in Danish children, which was recently supported by Shen *et al.*, (2008) who reported both IOPg and IOPcc to be significantly increased in highly myopic (MSE $< -9.00D$) children when compared to low level myopia (MSE $0D - 3.00D$). In a study assessing anisometric children Tomlinson and Phillips, (1972) reported higher IOP with greater axial and vitreous chamber length when both eyes were compared. Contrary to these findings Lee and Edwards (2000) failed to find any significant difference in IOP between refractive error and inter-eye axial length difference in anisomyopia.

Such findings of higher IOP with myopia have also been noted in adult populations (Tomlinson and Phillips, 1970; Abdalla and Hamdi, 1970; David *et al.*, 1985; Mitchell *et al.*, 1999; Wong *et al.*, 2003; Nomura *et al.*, 2004). In a more recent study Congdon *et al.*, (2006) noted an association between axial length specifically over 25 mm and high IOPs.

Interestingly, David *et al.*, (1985) reported a stronger relationship between refractive status and IOP among individuals who were born in North Africa or Asia when compared to individuals born in Europe or North America. In comparison a study in the UK failed to show any significant correlation between refractive status and IOP (Daub and Crick, 1981). These findings support the equivocal relationship between axial length and IOP found between the UK (BW-BSA) and HKC samples in the current study. Furthermore, Edwards *et al.*, (1993) found IOPs to be higher in children who had one myopic parent compared to no myopic parents, suggesting a genetic tendency for elevated IOPs with myopia. In view of the higher prevalence of myopia in HK compared to the UK, such genetic factors could further explain the discrepancies between the two samples. *These differences suggest that despite similar geometric conformation of the globe, the relationships between ocular parameters and the globe biomechanics differ between the two populations, which may be further affected by the level of myopia.*

The actual role of IOP in myopia development is still unclear in terms of whether IOP is a precursor to axial length growth or a consequence of increased globe size (Song *et al.*, 2008). In regards to this Edwards and Brown, (1996) found that myopic children had higher IOP following myopia development than subjects who did not develop myopia and concluded that IOP was not a contributory factor in myopic growth but was a consequence of myopia. In a similar study by Goss and Caffey (1999) the investigators failed to report high IOP before myopia onset but noted a non-significant trend for higher IOPs after myopia onset. Additionally, Edwards and Brown (1993) also found large variability in IOP amongst myopes when compared to non-myopes and concluded that IOP is unlikely to be a primary factor in myopigenesis.

11.8.6 Ocular wall stress and its relation to myopia and glaucoma

Despite these previous findings of a relation between IOP and myopic growth, Lee *et al.*, (2004) and Chang *et al.*, (2009) failed to show a correlation between axial length and IOP in children. These equivocal reports may be linked to the levels of myopia, ethnicity of the population and the technique used to measure IOP (Shen *et al.*, 2008; David *et al.*, 1985). Similarly, Lee and Edwards, (2000) found no significant difference in IOP between eyes in anisometric children but the investigators suggested that the application of Laplace's law would indicate the level of internal eye wall stress. Laplace' law expresses the relationship between stress-strain as:

$$\text{Stress} = Pr/2t$$

Eq 11.1

where P is the IOP, r is the radius of the particular eye (i.e. taken as approximately half the axial length) and t is the scleral thickness. Hence the greater the radius and the thinner the sclera the higher the level of stress produced. Therefore, regardless of differences in IOP between myopes and non-myopes and assuming a constant scleral thickness for all refractive groups, applying Laplace's equation to the longer myopic eyes reveals that scleral stress is greater with increased axial length (Lee and Edwards, 2000). Furthermore there are a number of reports of posterior scleral thinning in high myopia (Rada *et al.*, 2006; McBrien *et al.*, 2001a; Guthoff *et al.*, 1987) and therefore it is likely that eye wall stress would be even higher in the larger myopic eye. Friedman (1966) explored the use of Laplace's law for various ametropic states and reported that due to the combined effects of increased radius and thinner scleral thickness, small changes in IOP in highly myopic eyes would produce relatively large changes in stress. This proposal leads to what Curtin, (1970) considers to be an inexorable cycle where increased stress promotes axial length growth and consequent scleral thinning, which leads to increased stress even at constant IOP levels. ***Therefore in view of the current findings of increased IOP with axial length in the HK sample, this would indicate that HKC eyes are subjected to greater levels of stress at higher myopic levels in comparison to myopic eyes of BW-BSAs in the UK.***

Cahane and Bartov, (1992) implemented Laplace's law to assess the relationship between axial length and IOP and reported increased scleral tension across the lamina cribrosa in myopic eyes when compared to eyes with shorter axial length with the same IOP. Therefore in view of the higher IOP found with increased axial length it is reasonable that studies have often noted a correlation between myopia and glaucoma (POAG, NTG, LTG) and OHT (Abitbol *et al.*, 2010; Perkins and Phelps, 1982; Chihara and Honda, 1992; Mitchell *et al.*, 1999; Wong *et al.*, 2003). In fact, Wong *et al.*, (2003) reported a 60% increased risk of developing POAG in myopic individuals compared to emmetropic persons in a white Caucasian population.

Population differences in the association between myopia and POAG have been noted previously; the findings of the Blue Mountains Eye study (Mitchell *et al.*, 1999), which assessed a white Australian population showed a strong dose effect of increased level of myopia being associated with increasing odds-ratio of developing POAG. Other population

studies such as the Barbados Eye study that assessed African-Caribbean individuals in Barbados (Wu *et al.*, 1999; 2000) and the Beaver Dam study that evaluated white American individuals (Wong *et al.*, 2003) have also shown a relationship between myopia and POAG but one that was less marked than that found in the Blue Mountains Eye study (Mitchell *et al.*, 1999). Wong *et al.*, (2003) suggested that these differences could be ascribed to racial differences between the populations evaluated in each of the three studies. Furthermore, Xu *et al.*, (2007) reported no significant difference in IOP between low levels of myopia and marked or high levels of myopia in the Beijing Eye study but noted a significant increase in frequency of glaucomatous damage in the high levels of myopia.

The findings of the current study and reference to previous literature on refractive status and IOP indicate that myopic eyes may have a tendency for higher IOP especially at higher axial lengths (>25.5mm), however the relationship between these two factors maybe affected by racial differences. Furthermore, regardless of IOP levels high myopia may be linked to glaucomatous changes possibly due to the increased stress levels induce across the optic nerve head.

11.8.7 Ethnicity and corneal biomechanics

No significant difference was found in the current study between the corneal biomechanics in individuals from HK and the UK. In support of these findings Lim *et al.*, (2008) failed to find an effect of ethnicity on CH and CRF, whilst in contrast Song *et al.*, (2008) found CH to be significantly lower in Chinese children's eyes when compared to Irish children and Broman *et al.*, (2007) found individuals of African origin to show lower CH than individuals who were of European descent.

Recent work by Cabanaro and colleagues (2008) reported CH to be a strongly heritable characteristic, thus suggesting that corneal biomechanics may be genetically determined and may thus vary between ethnicities. Moreover, CCT has also been reported to have a strong genetic component (Alsbrink, 1978; Toh *et al.*, 2005; Zheng *et al.*, 2008), which would support the ethnic-related differences in CCT (Dimasi *et al.*, 2010) and possibly corneal biomechanics.

11.8.8 Age and corneal biomechanics

The findings of the present study indicate that the age range (19-40 years) investigated does not have a significant influence on ORA biometrics. Data from previous studies are equivocal with some studies noting no significant affect of age (Kirwan *et al.*, 2006; Shah *et al.*, 2007; Lim *et al.*, 2008), whilst others have shown reduced CH and CRF with progressing age (Kotecha *et al.*, 2006; Moreno-Montañés *et al.*, 2008; Kida *et al.*, 2008; Kamiya *et al.*, 2009; Carbonaro *et al.*, 2008; Franco and Lira, 2009; Fontes *et al.*, 2008). These discrepancies may potentially be associated with the age range assessed in the different investigations. In support of this, Ortiz *et al.*, (2007) reported a significant difference in CH only between the youngest (≤ 14 years) and oldest (> 60 years) individuals in their study but not for subjects in between these age ranges. Similarly in a study assessing individuals in the age range of 19-89 years, Kamiya *et al.*, (2009) suggested that CH and CRF decreased with age but more particularly over the age of 70 years. Moreover, studies have also reported higher values of CH and CRF in children than those reported for adults, suggesting a change in corneal biomechanics with age (Lim *et al.*, 2008; Kirwan and O'Keefe, 2008). Hence it is probable that the failure to detect an association between age and ORA biometrics in the present study maybe an artefact of the narrow age range of 18-40 years investigated.

11.8.9 Gender and corneal biomechanics

No significant differences in corneal biomechanics were found between males and females, which has been corroborated by numerous other studies (e.g. Shah *et al.*, 2007; Ortiz *et al.*, 2007; Montard *et al.*, 2007; Kamiya *et al.*, 2008; Lim *et al.*, 2008). Contrary to these reports Song *et al.*, (2008) reported a significant association between lower CH and male gender. These differences may be attributable to gender differences in ocular biometric parameters, since Song *et al.*, (2008) reported male gender to be associated with longer axial length and high IOPs. ***In the present study HKC male subjects were found to have greater axial length and flatter corneas when compared to females, however no gender differences in corneal biomechanics were found.*** Nevertheless the data suggested a non significant trend for higher CH ($p=0.277$) and CRF ($p=0.304$) amongst the HKC females. Observations of longer axial lengths and flatter corneas in males has been noted previously (Ip *et al.*, 2008; Wong *et al.*, 2001) and has been ascribed to larger body size for males in comparison to female subjects (Song *et al.*, 2008). Therefore if longer axial length is

related to reduced CH as discussed afore, then gender differences in corneal biomechanics may exist. The design of present study may not be sufficient to examine reliably whether gender differences in corneal biomechanics exist owing to the large inter-individual variation of CH and CRF in normal individuals and the considerable overlap in CH and CRF values for very short and very long axial lengths.

11.8.10 ORA Additional waveform parameters (AWPs)

As the amplitudes of the ORA waveform peaks are linked to the amount of light reflected back to the infrared detector during the applanation event (see Figures 4.3 and 4.4), it is presumed that the larger the applanation area the larger the peak amplitude and conversely the smaller the applanation area the lower the peak amplitude (Vinciguerra *et al.*, 2010). In the present study all measures of amplitude (H1,H2, H11, H21) for both peaks were lower in the HKC individuals than in the other ethnicities. ***These results would suggest that the HKC group presented a smaller or a more non-uniform area of applanation hence implying lower corneal stiffness in comparison to the other ethnicities.*** Additionally the HKC individuals also showed significantly lower peak areas (P1area, P2area, P1area1, P2area1) in comparison to (UK) BW and BSA individuals.

These findings are supported by recent investigations on the application of waveform morphology to corneal biomechanics (Vinciguerra *et al.*, 2010; Dauwe *et al.*, 2009; Kérautret *et al.*, 2008). In particular, a recent study assessed corneal biomechanics in keratoconic eyes pre- and post- implantation of intrastromal corneal ring segments; the investigators reported no significant difference in CH or CRF after surgery but a significant reduction in the amplitude of peak 2 and width of peak1 (Dauwe *et al.*, 2009). The study also noted that the amplitude of peak1 was higher with reduced severity of keratoconus, thus suggesting greater corneal stiffness.

In a case study, Kérautret *et al.*, (2008) reported no significant difference in CH and CRF between ectatic and nonectatic eyes, yet on analyses of the ORA waveform signals the amplitude of both peak 1 and 2 were significantly lower in the ectatic eye. Moreover, Kérautret *et al.*, (2008) analysed the ORA infrared signal using a specialised software program and reported that the width of the ORA peak reflected the speed of the corneal deformation; thus a wide peak would indicate a slow moving cornea on deformation whereas a narrow peak would indicate a cornea that easily deforms. In the present study

W1 and W11 were significantly higher in the HKC individuals than in the BW and BSA subjects suggesting a slower moving cornea (possibly suggesting greater inertia) for the HKC individuals. In turn the width of the second peak was lower for the HKC group compared to the other ethnicities, suggesting a faster recovery phase from concavity and thus implying lower corneal hysteresis. In support of these findings of a more elastic or 'weaker' cornea in the HKC subjects compared to the other ethnicities various other parameters were also lower (see Appendix 8). *These results may perhaps signify for HKC individuals a cornea with greater inertia that takes longer to pass through the distinct phases following deformation by the ORA pulse.*

Interesting many of the AWP's showed significant differences between the HKC and both BW and BSA individuals. Additionally there were some AWP's that were only different between the HKC and BSA. In these cases the AWP's were all lower amongst the HKC individuals when compared to the BSA group. These subsets of differences between the HKC and BSA individuals could suggest that the corneal biomechanics of these two ethnic groups may be more distinct (i.e. less variable) in contrast to the BW group, thus allowing greater discrimination of corneal biomechanical between ethnicity.

Refractive status also appeared to affect some of the AWP's with myopes showing lower values for several parameters but higher values for W1. As for the HKC individuals these lower values may signify a slower moving cornea and hence lower rates of increase and decrease in the various waveform characteristics. Furthermore both refractive error and axial length were found to be associated with numerous AWP's following analysis with multiple linear regression. An interaction effect between two AWP's (P2 and mslew1) and both refractive status and ethnicity suggested that corneal biomechanics may vary significantly between ethnicities but also between refractive states.

In support of the differences found in the present study Hongyok *et al.*, (2010) showed corneal scarring in ectatic corneas to affect significantly numerous AWP's including Aindex, Bindex, Aspect1, Aspect2, Uslope1, Uslope2, H1, H2, Dive1, Dive2, Mslew2, Slew2, Uslope21, Uslope11, Dslope21, H11, H21, W1, P1. Similarly, Sejjal, *et al*, IOVS 2010, 51: ARVO E-Abstract 4991 reported significant differences in p2area, CRF and aindex between keratoconic and non keratoconic individuals. In a study investigating corneal biomechanical changes in diabetes, Kondapalli *et al*, IOVS 2010, 51: ARVO E-Abstract 4631 reported amplitude of both peak1 and 2 to be significantly higher in diabetic

subjects when compared to non-diabetic individuals suggesting increased corneal stiffness in diabetes. Interestingly these differences were not detected by CH and CRF.

In the present study no significant difference in CH or CRF was found between ethnicities, yet on assessment of the AWP's numerous differences have been indicated. Similarly, in a study assessing corneal biomechanics pre- and post collagen crosslinkage (CXL) treatment Vinciguerra *et al.*, (2010) reported no significant difference in CH or CRF, yet on assessing the ORA waveforms following treatment they detected peak amplitudes to be significantly affected by corneal asymmetry and shape. The Vinciguerra *et al.*, (2010) study suggested that potential reasons for CH and CRF not detecting any treatment difference may be a result of the ORA not being able to discern the levels of stiffness changes produced by the CXL treatment. Alternatively the biomechanical changes produced by CXL may not be viscoelastic in nature and may thus not be detected by the ORA. In regards to the present study the application of the AWP's has provided a significant insight into the relationship between corneal biomechanics, ethnicity and refractive error, which the primary ORA metrics were unable to show.

11.9 Conclusion

The key findings of the present study were:

- Measures of IOP with the ORA correlate well with GAT IOPs despite a trend for overestimation.
- CCT and mean corneal curvature were found to be significantly related to measures of CH and CRF amongst the UK individuals.
- Axial length was found to significantly influence the ORA corneal biometrics amongst the UK subjects but not amongst the HKC individuals.
- IOPg and IOPcc were found to be significantly related to axial length and refractive error in the HKC individuals, although the association was not found for the UK subjects.
- Age and gender failed to show any influence on the ORA parameters.
- ORA-derived AWP's are able to provide a valuable insight into differences in corneal biomechanics between ethnicities and refractive states.

12.0 INVESTIGATION OF THE RELATIONSHIP BETWEEN ANTERIOR SEGMENT BIOMETRY AND CORNEAL BIOMECHANICS

12.1 Introduction

12.1.1 The relationship between anterior segment and refractive status

It is envisaged that structural characteristics of the anterior segment are likely to play an important role in modulating the biomechanical properties of the cornea and sclera (Yoo *et al.*, 2010; Leite *et al.*, 2010). As discussed in Chapter 11, myopia and longer axial lengths have frequently been reported to be associated with corneal biomechanical changes (Congdon *et al.*, 2006; Song *et al.*, 2008; Friedenwald, 1937). With reference to the findings of Chapter 11 where a relationship was demonstrated between axial length and corneal hysteresis (CH) and corneal resistance factor (CRF), it seems plausible to speculate that posterior axial expansion influences the biomechanics of the anterior segment structures. Furthermore, Chapter 11 also established several ORA additional waveform parameters (AWPs) to be significantly influenced by ethnicity and refractive status. These latter findings suggest a possible hereditary component in corneal biomechanics, which may be associated with the genetic influences known to contribute towards refractive error development (Baird *et al.*, 2010).

Changes in tissue biomechanics are usually allied with structural alterations (Vinciguerra *et al.*, 2010; Chen *et al.*, 2010b). Presumably then the observations of corneal biomechanical changes in myopia, discussed afore, may be coupled with corneal structural variations. However previous reports for such an association between anterior segment dimensions and refractive error are equivocal with some investigators reporting increased central corneal thickness (CCT) in myopia (Nomura *et al.*, 2004), others noting reduced CCT (Chang *et al.*, 2001) and some finding no differences between myopes and non-myopes (Pedersen *et al.*, 2005) or with levels of myopia (Cho and Lam, 1999; Fam *et al.*, 2006; Lim *et al.*, 2008; Shen *et al.*, 2008; AlMahmoud *et al.*, 2010). In regards to corneal curvature and refractive status, several investigators have identified an association: Liu *et al.*, (1995) observed increased corneal power in myopic eyes whilst contrary to these findings a number of studies have noted myopic eyes to have significantly flatter corneal curvatures (Park *et al.*, 2010; Fledelius and Goldschmidt, 2009; Chang *et al.*, 2001). Additionally spherical refractive error has also been implicated in influencing the axis of

astigmatism, with low myopes showing a greater tendency for against-the-rule astigmatism (Farbrother *et al.*, 2004b). In support of these findings, animal models of myopia have also reported corneal astigmatism and changes in corneal curvature with increasing axial length (Kee *et al.*, 2005; Kee and Deng, 2008; Hayes *et al.*, 1986).

Aside from the potential effect of myopia on corneal biometry, other anterior segment variations have also been noted in the literature. In particular, ciliary muscle thickness has been found to be greater (Bailey *et al.*, 2008, Chapter 13) and anterior chamber depth (ACD) deeper in myopic eyes (Park *et al.*, 2010; Uçakhan *et al.*, 2008; Hosny *et al.*, 2000). Park *et al.*, (2010) postulated that increased ACD coupled with findings of flatter corneal curvature in myopia (Chang *et al.*, 2001; Fledelius and Goldschmidt, 2009), may indicate that the ocular stretching during axial expansion occurs between the ciliary body and limbus; however such speculations still need be confirmed by histological and clinical studies. In view of these ambivalent findings of anterior segment structural changes in myopia and the previous findings of scleral and corneal biomechanical changes in Chapters 8, 11, 13 and 14 further investigations are required to elucidate the relationship between tissue biomechanics and biometry.

12.1.2 Evaluation of the anterior segment

Until relatively recently the evaluation of the anterior segment was limited to basic information such as anterior surface keratometry, CCT and ACD. In recent years the introduction of optical techniques using the Scheimpflug principle (*Pentacam*, Oculus, Wetzlar, Germany) has permitted imaging of the posterior corneal surface (Zhang and Wang, 2010; Dubbelman *et al.*, 2006). Such improvements in optical imaging now allow an assessment of changes in elevation of both the anterior and posterior surfaces with reference to three dimensional models of corneal tomography (Salouti *et al.*, 2009; Swartz *et al.*, 2007). Scheimpflug imaging also provides the facility to perform point-to-point pachymetry and in addition offers comprehensive information on anterior segment biometry from measurements of corneal power, curvature and shape; anterior chamber depth/volume and crystalline lens characteristics (Swartz *et al.*, 2007; Wegener and Laser-Junga, 2009).

12.1.3 Operational principles of the *Pentacam*

The *Pentacam* (Oculus, Wetzlar, Germany) is a non-contact anterior segment imaging device that is based on the principles of rotating Scheimpflug photography. The instrument uses a monochromatic slit light source (i.e. a blue LED at 475 nm) and a Scheimpflug camera, which together rotate around the optical axis of the eye (Lackner *et al.*, 2005a; 2005b). The principles of the imaging system are based on an intersection point between the illuminating slit beam and the imaging plane while the angles between the camera objective and the two planes are equal to each other (Masters, 1998). During its 180° rotation the *Pentacam* takes 25 or 50 slit images (depending on user settings) of the anterior segment in less than 2 seconds (Buehl *et al.*, 2006). Each slit image provides 500 measurement points on both the front and back corneal surface (Shankar *et al.*, 2008). The instrument also incorporates a second camera, which is able to monitor eye movement and thus allow for simultaneous correction for any such movement (Kopacz *et al.*, 2005).

On image acquisition, the software combines the multiple two-dimensional images to construct a three-dimensional model of the anterior segment by using edge detection in each slit image (Barkana *et al.*, 2005). Due to the rotational imaging procedure, each slit image scans the central cornea repeatedly thus providing highly precise measures of CCT and ACD (Buehl *et al.*, 2006). Optical distortion due to variation in refractive indices of tissue requires ray tracing algorithms to be implemented for accurate imaging of all surfaces posterior to the anterior corneal surface (Barkana *et al.*, 2005). The images provided by the system are of a high resolution (Dinc *et al.*, 2010) and as multiple scans are taken a single reading has been found to give highly reliable results (Al-Mezaine *et al.*, 2008; Falavarjani *et al.*, 2010; Barkana *et al.*, 2005). Furthermore the *Pentacam* has been found to be reliable and reproducible in measuring CCT and ACD in comparison to other anterior segment imaging devices (Lackner *et al.*, 2005a; 2005b; Rabsilber *et al.*, 2006; Reuland *et al.*, 2007; Bourges *et al.*, 2009). The main advantage of the *Pentacam* is its ability to provide large amounts of quantitative information (e.g. corneal topography, pachymetry (anterior and posterior surfaces), corneal aberrations, anterior chamber parameters (depth, angle and volume) and crystalline lens characteristics) within a relatively short imaging session (Konstantopoulos *et al.*, 2007).

12.2 Study objective

The objective of the present investigation was to evaluate whether information on anterior segment biometry provided by the *Pentacam* is a correlate of refractive error. Furthermore the study also tested the association between anterior segment morphology and information on corneal biomechanics obtained from the ORA (data from Chapter 11). Chapter 11 also demonstrated ethnicity and refractive status to significantly influence several additional waveform parameters (AWPs) and thus the present study also explores which anterior segment variables influence the outcome of the AWP. In addition, data on anterior segment biometry were also correlated with corneal rigidity measures obtained with the Schiotz tonometer (data from Chapter 10).

12.3 Method

The study assessed 42 healthy individuals (84 eyes; 17 males and 25 females) aged between 18-40 years (28.12 ± 6.04) of either British White (BW) or British South-Asian (BSA) ethnicity. Ethical approval and the exclusion/inclusion criteria followed those detailed in Chapter 6. The Zeiss *IOLMaster* and the Shin-Nippon auto-refractor were utilised as in Chapter 6 to obtain ocular biometry and refractive error data for the present investigation.

12.3.1 Image acquisition

The *Pentacam* (software version 1.16) is a table-mounted device that is connected to a PC. The patient is assessed in the seated position and asked to place his/her chin on a chin rest and to look at a red fixation light within the instrument. Once the patient details are entered and the option for a scan is selected, the software displays a screen where a real-time image of the patient's eye is visibly seen. By displaying arrows on the screen the software guides the examiner to move the instrument joystick to obtain correct alignment of the corneal apex. In the automatic release mode the software detects when optimal focus has been achieved and takes a scan automatically. In the current study the option for '25 images per scan' was chosen thus indicating that the camera takes 25 slit images in its rotational cycle (Chen and Lam, 2007). The software assesses each scan against set quality parameters and indicates the outcome on the screen as "OK" if these were met. If however the scan did not satisfy the quality checks then an error message is indicated and the scan is repeated until a high quality scan is obtained. All *Pentacam* scans were performed within a set time period

(i.e. office hours 9am -5pm) to control for the effects of diurnal variation on corneal shape and thickness (Read and Collins, 2009).

12.3.2 Pentacam image parameters

The *Pentacam* provides numerous topography maps (Figure 12.1). In the present study only the corneal thickness (CT), anterior best fit sphere (ABFS) and posterior best fit sphere (PBFS) maps were evaluated for the central 8 mm diameter. Both ABFS and PBFS are measures of corneal height that provide an estimate of the shape of the corneal surface that is independent of axis, orientation and position (*viz. Pentacam* instruction manual). Height data are displayed in relative terms, which is the difference in height between the corneal surface and a reference body. The *Pentacam* allows the reference body to be located at different settings, i.e. it can be centred at the apex of the cornea, or set as a ‘float map’. The float map provides a reference body that has no fixed centre but instead floats above the corneal surface ensuring that the distance between the cornea and the reference body is minimal. Furthermore the reference body can also provide the ‘Best Fit Sphere’ whereby calculations provide an approximation of a sphere that provides an optimal model of the true shape of the cornea and additionally facilitates comparison with other topographic systems. In the present study the measures of ABFS and PBFS were based on best-fit sphere float maps. (See glossary table 12.2 at end for abbreviations of all *Pentacam* parameters investigated)

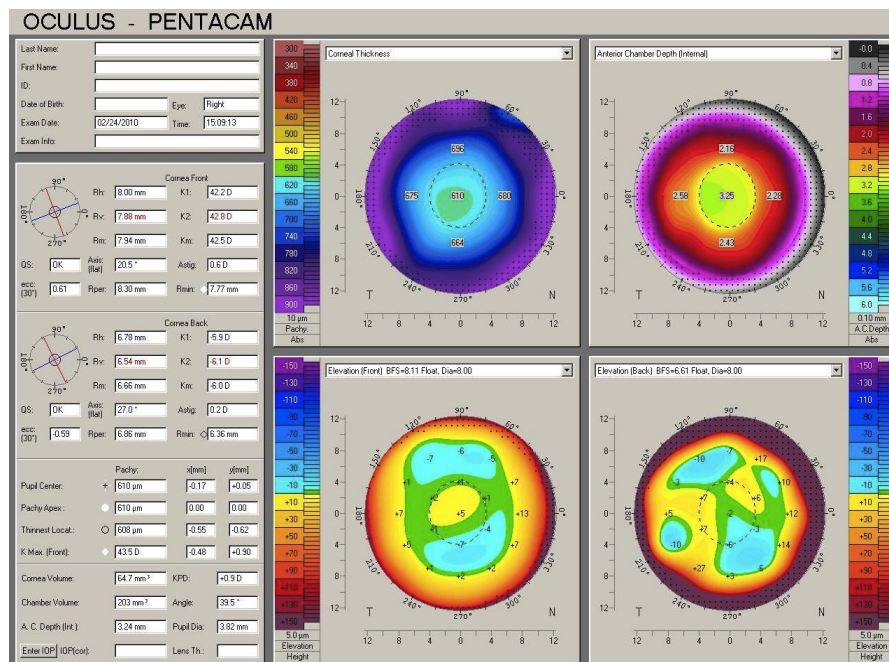


Figure 12.1 *Pentacam* topographical maps and numerical data.

Additional *Pentacam* parameters evaluated in the present study included minimum corneal thickness (CTmin); central corneal thickness (CCT; at pupil centre); peripheral corneal thickness 1.5 mm from pupil centre [superior (SCT), inferior (ICT), temporal (TCT) and nasal (NCT)]; total anterior chamber volume (ACV; calculated 12 mm around the corneal vertex for a volume generated between posterior corneal surface and the iris and lens); anterior chamber depth (ACD; from corneal endothelium along corneal vertex to anterior lens surface); corneal volume (CV; 10 mm diameter around the corneal vertex between anterior and posterior surfaces), CV at 3 mm (CV3), 5 mm (CV5), and 7 mm (CV7); front surface (FS) and back surface (BS) keratometry flat (Kf) and keratometry steep (Ks) (from central 3 mm zone) were all extracted from the data calculated by the *Pentacam* software (*Pentacam* instruction manual).

12.4 Statistical analysis

Data were initially assessed and confirmed to exhibit a normal distribution using the Kolmogorov-Smirnov test. Only RE data will be discussed. As axial length was found to be a significant predictor of CH and CRF in Chapter 11 the *Pentacam* data were divided into corresponding axial length (mm) subgroups; 1. ($21.5 < \leq 23.5$; n=14), 2. ($23.5 > - \leq 25.5$; n=16) and 3. (>25.5 ; n=12).

Student's independent *t* tests were conducted to test the effects of refractive error, age (years) group ($18 \geq - < 29$, $29 \geq - < 40$) ethnicity (British White and British South Asian) and gender. One-way ANOVAs were performed to test for differences in *Pentacam* parameters for axial length grouping. To determine pair-wise differences a Bonferroni *post hoc* was conducted when groups were of equal sizes and a Games Howell *post hoc* test when the group sizes were unequal. Pearson's correlation coefficient was calculated to test the relationship between different *Pentacam* parameters, ocular biometry, Schiottz corneal rigidity and ORA biometrics (CH, CRF and the AWP). A stepwise forward multiple linear regression was used as an exploratory test to determine which *Pentacam* variables were associated with the ORA values. A p-value of <0.05 was taken as the criterion for statistical significance.

12.5 Results

The study assessed 42 healthy individuals (84 eyes; 17 males and 25 females) aged between 18-40 years (28.12 ± 6.04). Data were assessed for non-myopic and myopic individuals; [non myopes (MSE ≥ -0.50 D) n=20 MSE (D) mean \pm SD (0.64 ± 1.38), range (-0.50 to +4.38), AL (mm) mean \pm SD (23.33 ± 0.67), range (mm) (21.75 - 24.45); myopes (MSE < -0.50 D) n=22 MSE (D) mean \pm SD (-6.24 ± 4.28), range (-20.50 to -0.75), AL (mm) mean \pm SD (25.69 ± 1.25) range (mm) (23.33 - 28.32)]. For full details of statistical tests and results see Appendix 9.

12.5.1 Structural correlates of anterior segment biometry

On a one-way ANOVA testing the effect of axial length grouping on all of the *Pentacam* parameters (see table 12.1) revealed only ACD to be significantly influenced by axial length grouping ($p=0.033$); Games Howell *post hoc* test revealed the difference to be between group 1 ($21.5 > - \leq 23.5$) and 3 (>25.5), with group 3 having deeper ACD values than group 1.

<i>Pentacam</i> parameter	Mean \pm SD	Range
CCT (μm)	550.02 ± 38.44	463 - 631
CTmin (μm)	547.02 ± 38.56	626 - 549
SCT (μm)	660.71 ± 47.50	566 - 784
ICT (μm)	614.31 ± 48.59	521 - 717
TCT (μm)	613.26 ± 38.16	533 - 689
NCT (μm)	632.02 ± 41.70	561 - 718
ACV (mm^3)	185.38 ± 29.91	125 - 265
ACD (mm)	3.15 ± 0.29	2.59 - 3.91
CV (mm^3)	60.57 ± 4.11	53 - 69.2
CV 3 (mm^3)	3.97 ± 0.27	3.4 - 4.6
CV5 (mm^3)	11.58 ± 0.80	9.90 - 13.3
CV7 (mm^3)	24.85 ± 1.69	21.4 - 28.5
Front Kf (mm)	42.96 ± 1.39	39.40 - 45.8
Front Ks (mm)	43.65 ± 1.41	41.50 - 47.60
Back Kf (mm)	-6.05 ± 0.23	-6.50 - (-5.40)
Back Ks (mm)	-6.34 ± 0.26	-6.80 - (-5.60)
ABFS (mm)	7.89 ± 0.26	7.31 - 8.47
PBFS (mm)	6.50 ± 0.25	6.09 - 7.17

Table 12.1. Overall mean \pm SD and range for the *Pentacam* parameters.

Student's independent *t tests* showed no significant effect of refractive status (myopic or non myopic), ethnicity (BW or BSA), age group ($19 > - \leq 29$; $29 > - \leq 40$ years) or gender on

any of the *Pentacam* variables assessed. A one-way repeated measures ANOVA revealed a significant difference between peripheral measures of CT ($p < 0.001$) with a Bonferroni *post hoc* analysis revealing the difference to be between all regions, except TCT:ICT.

Both FSKs and FSKf failed to correlate with any measures of CT, CV, ACD and ACV. Similarly BSKf showed no significant association with any of the *Pentacam* variables, whereas BSKs correlated significantly with measures of CV and several peripheral CT values. ACV correlated negatively with measures of CCT, peripheral CT and CV values. ABFS failed to correlate with any *Pentacam* variable whereas PBFS was associated with ACD and total CV. See Appendix 9.

12.5.2 Anterior segment biometry and corneal biomechanics

No significant correlations were found between *Pentacam* parameters and corneal rigidities determined with the Schiötz tonometer. No significant correlations were observed for either front and back Kf and Ks and the principle ORA metrics (CRF and CH). Both CRF and CH correlated with all measures of CT (central, minimum and peripheral) and CV. No measures of AC or ABFS and PBFS correlated with the ORA metrics. See Appendix 9.

Numerous AWP_s were found to correlate significantly with the *Pentacam* variables (See table A9.4 in Appendix 9). The correlation facilitated identification of which corneal and anterior chamber structural features may influence measures of corneal biomechanics. These anterior segment correlates were then tested for an association with ORA biometrics (CH, CRF and AWP_s) via multiple linear regression (see Appendix 9 for further details):

a. Corneal hysteresis (CH)

A stepwise forward multiple linear regression model with CH as the outcome variable and refractive error, mean corneal curvature (K) anterior and posterior, axial length, CV, ACD, ACV, gender and age as predictor variables was performed as an exploratory test. The model revealed only CV ($p = 0.006$) to be significantly associated with CH, explaining 17.7% of its variability. The model indicated that a 1 mm³ increase in CV would produce a 0.116 mm Hg increase in CH. When CV was replaced by CCT in the multiple regression model, it accounted for slightly lower CH variability (16.2%).

b. Corneal resistance factor (CRF)

A similar multiple linear regression model with the same predictor variables as for CH, showed CRF to be significantly related to CCT explaining 29.1% of the CRF variability. Furthermore the model predicted that a 100 μm increase in CCT would produce a 1.8 mm Hg increase in CRF. Replacing CCT with total CV in the predictive variables showed CV to be significantly related to CRF, however the r^2 was slightly lower explaining only 19.9% of the variability.

c. Additional Waveform parameters (AWPs)

Several *Pentacam* parameters were found to correlate with the AWP. To investigate which of the *Pentacam* parameters were the most significant predictors of the AWP, stepwise forward multiple linear regression analysis was performed as an exploratory test on each AWP and the related corneal variables. The results showed the anterior BFS to be the best predictor for P1area, P2area, Dive2 and P2area1. FSKf was found to be associated with H2, H21 and Path11, whilst FSKs was significantly related to H1, P1area1 and H11. ACD was found to influence aspect1, aspect2, aspect21, ulslope 11, dslope21, whereas ACV modulated dslope1. CCT was found to be the best predictor for Path1 and W21 whilst INCCT was found to be associated with Path2 and W11.

12.6 Discussion

The present investigation found no significant influence of axial length or refractive status on the corneal biometry parameters provided by the *Pentacam*. Contrary to these findings, ACD was found to be significantly deeper in individuals with the longest axial length when compared to those with the shortest axial lengths. With regards to corneal biomechanics, no significant correlation was found between corneal rigidity measured with Schiotz tonometry and the corneal biometric parameters assessed by the *Pentacam*. Conversely ORA metrics CH and CRF demonstrated significant correlations with corneal thickness and volume measurements. Moreover a number of AWP were found to show a significant association with various corneal and anterior chamber biometry parameters. In concordance with previous studies, all measures of the *Pentacam* parameters (Table 12.1) evaluated in the current investigation were comparable to results previously reported

(Falavarjani *et al.*, 2010; Aswhin *et al.*, 2009; Shankar *et al.*, 2008; Chen and Lam, 2007; Uçakhan *et al.*, 2008; Al-Mezaine *et al.*, 2008; Rosa *et al.*, 2007).

12.6.1 Corneal biometry and refractive status

The absence of a significant association between refractive status and the corneal parameters analysed would suggest that posterior ocular growth is independent of anterior segment dimensions. *Alternatively these results could suggest that in isolation corneal parameters may not identify differences between refractive groups, but when various structural characteristics are combined their synergistic effect may predispose the eye to myopic growth.*

As discussed afore, previous reports of an association between corneal biometry and refractive status have been equivocal (Chang *et al.*, 2001; Cho and Lam, 1999; Fam *et al.*, 2006; Goss *et al.*, 1997; Nomura *et al.*, 2004; AlMahmoud *et al.*, 2010). Pertinent to the present study, Uçakhan *et al.*, (2008) utilised the *Pentacam* to investigate corneal differences between refractive groups, and reported significantly reduced CT and CV amongst high myopes (i.e. MSE range -6D to -12.5D). Consistent with these findings Chang *et al.*, (2001) also found reduced CCT in myopic individuals, whilst Nomura *et al.*, (2004) reported increased CCT with myopia. A potential explanation for these discrepancies may stem from the significant differences in CCT between ethnicities (Doughty and Zaman, 2000). Ethnic-related differences in CCT are commonly reported in literature (Aghaian *et al.*, 2004; Landers *et al.*, 2007) and appear to be associated with a strong genetic component (Damasi *et al.*, 2010; Toh *et al.*, 2005). Therefore if CCT is a genetically determined trait then variation in CCT due to racial differences amongst the cohorts previously investigated may potentially confound the relationship between changes in corneal biometry and refractive status

Furthermore the present study failed to show any significant influence of refractive status on corneal curvature. Previously corneal curvature has been found to be flatter with longer axial lengths (Park *et al.*, 2010; Fledelius and Goldschmidt, 2009) and deeper vitreous chambers (Goss *et al.*, 1997; Yebra-Pimentel *et al.*, 2008). Contrary to these findings some investigators have also noted steeper corneal curvature in myopic eyes (Grosvenor and Scott, 1991; Liu *et al.*, 1995). Corneal shape as indexed by asphericity has also been associated with myopia development: Carney *et al.*, (1997) and Horner *et al.*,

(2000) demonstrated that as eyes became more myopic there was a significant reduction in rate of flattening in the peripheral cornea which was associated with increasing vitreous chamber depth and increasing axial length. Such divergent findings in regards to corneal curvature may be a result of differences in study protocol and levels of myopia assessed. In support of this supposition, Yebra-Pimentel *et al.*, (2008), suggested that characteristics of the inter-relationship between ocular components alter with axial length. Additionally the differences may also be attributable to significant inter-individual variation in globe conformation amongst myopic eyes (Atchison *et al.*, 2005; Chen *et al.*, 1992; Cheng *et al.*, 1992) as well as ethnic differences in the properties of the corneal material (Doughty and Zaman, 2000; Song *et al.*, 2008).

12.6.2 Regional differences in corneal thickness (CT)

The findings of the present study also indicated that significant regional variation existed amongst peripheral CT, with the temporal region showing the thinnest CT followed by ICT, NCT and SCT. In support of these findings both Rüfer *et al.*, (2005) and Khoramnia *et al.*, (2007) reported lower CT values in the temporal and inferior regions and thicker CT in the superior and nasal regions. Similarly both Ashwin *et al.*, (2009) and Uçakhan *et al.*, (2008) observed the inferotemporal region to be the thinnest corneal region. In agreement with these findings the location of the cone in keratoconus is commonly found in the inferotemporal sector (Demirbas and Pflugfelder, 1998) and it is rarely found superiorly (Ashwin *et al.*, 2009). Such findings would suggest that regional variation in corneal biomechanics may exist and if so may have implications for refractive surgery and keratoconus detection and management.

12.6.3 Anterior and posterior corneal surface curvature

Interestingly, both flat and steep FSK and ABFS failed to correlate with any corneal or anterior chamber parameters, whereas BSKs correlated significantly with CV, CV7 and peripheral measures of CT (SCT, INCT and NCT); PBFS was also found to correlate with both ACD and CV. These findings suggest that in comparison to the anterior corneal surface the posterior surface may play a more determinant role in the corneal structure. When compared to the anterior corneal surface the posterior surface provides little contribution to the overall refractive power of the eye, as result of the refractive index difference between the posterior corneal surface and the aqueous humour and hence until

relatively recently the posterior corneal surface had been considered as an insignificant refractive component of the cornea (Read and Scott, 2009). Contrary to this supposition, recent work has indicated that the posterior corneal surface may play a crucial function in astigmatism (Dubbelman *et al.*, 2006), spherical aberration (Sicam *et al.*, 2006), early screening of keratoconus (Belin and Khachikian, 2007; Schlegel *et al.*, 2008) and in detecting ectasia pre- and post- refractive surgery (Belin and Khachikian, 2007; Grzybowski *et al.*, 2005; Rao *et al.*, 2002). *In view of the present observation of a significant association between posterior corneal curvature and corneal volume and thickness, these results would imply a more significant role of the posterior corneal surface in corneal structure than that of the anterior corneal surface.*

12.6.4 Anterior chamber biometry and refractive status

In regards to the influence of myopic refraction on anterior segment biometry, the present study demonstrated ACD to be significantly deeper amongst individuals with the longest axial lengths when compared to those with the shortest axial lengths. Similar findings of deeper ACDs in myopes have been reported previously (Uçakhan *et al.*, 2008, Lo *et al.*, 1996; Carney *et al.*, 1997). However contrary to these findings some investigators have failed to find a significant correlation or difference in ACD between myopes and emmetropes but reported significantly shallower ACDs in hypermetropes (Utine *et al.*, 2009; Rabsilber *et al.*, 2003). Such discrepancies between studies may be linked to the findings of Yebra-Pimentel *et al.*, (2008) who reported a correlation between axial length and ACD up to axial lengths of 24 mm after which no significant correlation was found. Interestingly, Hosny *et al.*, (2000) found ACD to be influenced by axial length, corneal diameter, spherical equivalent refraction and patient age, indicating that the ACD may be vulnerable to greater inter-individual variation. In regards to the findings of increased ACD in myopia, Park *et al.*, (2010) hypothesized that if axial expansion occurred between the limbus and ciliary body this would lead to deeper ACD and corneal flattening thus explain the ACD changes found with longer axial lengths.

12.6.5 Corneal biomechanics and anterior segment biometry

In order to obtain a comprehensive understanding of corneal biomechanics an assessment of the corneal topography is vital. As Suzuki *et al.*, (2006) indicated given that the statistical analysis of corneal topography maps is difficult, corneal volume may provide a

suitable surrogate for surface topography. ***Indeed in support of this recommendation the present study demonstrated CV to be a slightly improved predictor for CH but not CRF, suggesting that CH may reflect a more composite effect of corneal thickness and contour variation.*** In contrast, as CRF assesses the overall resistance of the cornea it is less likely to be affected by corneal parameters such as, for example, curvature change (Shah *et al.*, 2006; Luce IOVS 2006, 47: ARVO E-Abstract 2266).

Moreover the present investigation also revealed numerous ORA AWP to be associated with anterior segment biometric parameters. As Reichert Inc recently introduced the assessment of AWP, little is known to date about which ocular feature is being assessed by the various aspects of the ORA waveform. Therefore the findings of the present study may help future interpretation of these AWP measures.

The results of the multiple regression analysis revealed that the anterior BFS, FSK1 and FSK2 were significant predictors of certain AWP. ***In Chapter 11 significant differences in AWP were observed between the predominantly myopic HK individuals and the UK subjects and in view of the present findings, the significant difference in the flattest corneal curvature between the two population samples may have contributed to the differences in the AWP.*** Furthermore the present study also indicated ACD and ACV to modulate various AWP. As in the present study the ORA investigation (Chapter 11) also demonstrated a significant effect of axial length on ACD. ***Therefore the significant differences in AWP observed between the refractive groups in Chapter 11 may have been a consequence of variation in ACD with axial length changes.***

12.7 Conclusion

The key findings of the present study are:

- No significant difference was found between refractive status and axial length grouping for the corneal biometry data provided by the *Pentacam*.
- ACD was shown to be significantly deeper amongst individuals with the longest axial length when compared to those with the shortest axial length.
- The presence of regional variation in peripheral CT was observed with the TCT showing the thinnest values followed by ICT, NCT and SCT.
- *Pentacam* parameters for the posterior corneal surface showed a greater number of significant correlations with other corneal and anterior chamber parameters

suggesting a more influential role in corneal structural characteristics (i.e. CT and CV) than the anterior corneal surface.

- Various corneal and anterior chamber parameters measured by the *Pentacam* were associated with the ORA AWP's providing an insight into which anterior segment structural features may be contributing to corneal biomechanics.

Abbreviations	Pentacam Parameters
AC	Anterior chamber
ACV	Anterior chamber volume
ACD	Anterior chamber depth
CT	Corneal thickness
CCT	Central corneal thickness
CTmin	Minimum corneal thickness
SCT	Superior corneal thickness
ICT	Inferior corneal thickness
TCT	Temporal corneal thickness
NCT	Nasal corneal thickness
CV	Corneal volume
CV3	Corneal volume around 3 mm diameter
CV5	Corneal volume around 5 mm diameter
CV7	Corneal volume around 7 mm diameter
FSKf	Front surface keratometry flat
FSKs	Front surface keratometry steep
BSKf	Back surface keratometry flat
BSKs	Back surface keratometry steep
ABFS	Anterior best fit sphere
PBFS	Posterior best fit sphere

Table 12.2 Glossary of the *Pentacam* parameters and their abbreviations.

13.0 STRUCTURAL CORRELATES OF THE HUMAN CILIARY MUSCLE

13.1 Introduction

As characteristically seen with various tissues in the human body the eye demonstrates a complex biomechanical and biochemical inter-relationship between its individual components (Davson, 1990). The anterior segment in particular demonstrates this relationship owing to its close structural and functional association with the iris, angle structures, ciliary body, cornea, and sclera (Chapter 1; Oyster, 1999). As discussed in Chapter 2 and 3, biomechanical properties of the sclera and cornea may influence refractive error development and additionally play a role in the pathogenesis of glaucoma and AMD (Rada *et al.*, 2006; Ebner *et al.*, 2009; Friedman, 2000). As well as their mechanical functions both the cornea and sclera have a significant role in ocular fluid dynamics. Similarly, the ciliary body has been widely studied over the years owing to its contribution to the accommodation mechanism and its association with the uveoscleral outflow (Charman, 2008; Tamm, 2009). Moreover, the ciliary muscle has been implicated in the aetiology of myopia. Contrary to Van Alphen's (1986) findings of a thinner ciliary muscle in myopic eyes recent *in vivo* imaging suggests that the ciliary muscle may in fact be thicker (Bailey *et al.*, 2008; Oliveira *et al.*, 2005) and longer in myopic eyes (Sheppard and Davies, 2010a).

It is unclear why myopes should have thicker ciliary muscles in comparison to non-myopes but it has been postulated that the difference may be related to the aetiology of myopia (Mutti, 2010). With the advent of improved MR imaging Atchison *et al.*, (2005) demonstrated that most eyes conform to an oblate shape, however in myopes the eye is less oblate than in emmetropes and hypermetropes. Additionally these investigators noted that there is considerable inter-individual variation in ocular conformation and that some eyes may show a prolate shape though this was not necessarily a specific characteristic of myopic eyes. Logan *et al.*, (2004) postulated that ocular growth patterns for the axial and transverse dimensions of the myopic eye may be regulated differently. Despite the findings of variation in the globe conformation with refractive status, the origin and aetiology of these changes is still unknown.

As shown by various investigators (Larsen, 1971; Zadnik *et al.*, 1993; 1995; Mutti *et al.*, 2005; Shih *et al.*, 2009) the process of emmetropization involves the thinning of the

crystalline lens during infancy and into early puberty. The occurrence of lens thinning has been postulated to be a result of equatorial stretching caused by the enlarging globe in all radial directions (van Alphen and Graebel, 1991). This mechanism is thought to play a significant role in emmetropization in that it contributes to the equilibrium attained between axial length growth and ocular power that defines the emmetropic refractive state (Shih *et al.*, 2009; Mutti, 2010). Recently it has been proposed that a restrictive force to the normal thinning of the lens as ocular growth progresses may be a significant component in the aetiology of myopia (Mutti, 2010). In particular the thicker ciliary bodies found in myopic adults (Oliveira *et al.*, 2005) and children (Bailey *et al.*, 2008), has led to the suggestion that thicker ciliary muscles (Mutti, 2010) may have a biomechanical role in restricting the equatorial stretching required for the eye to progress successfully towards emmetropia.

13.1.1 Functional and structural evaluation of the ciliary body

As the ciliary body is obscured by the iris and resides along the inside wall of the sclera, imaging this structure *in vivo* has been limited until relatively recently. Therefore much of the assessment of this structure, particularly in relation to its role in accommodation, has been based on histological studies (Wang *et al.*, 1999; Tamm *et al.*, 1991; Pardue and Sivak, 2000), animal models (Croft *et al.*, 1998; Glasser *et al.*, 2001) or by indirect measures of muscle contraction (Fisher, 1977; Swegmark, 1969). Rhesus monkeys (*Macaca mulatta*) have frequently been used in animal model studies owing to their accommodative system being analogous to that of humans and as they display comparable crystalline lens changes through life at a similar relative age course (Bito *et al.*, 1982; Neider *et al.*, 1990). In monkey animal models implantation of electrodes in the Edinger-Westphal nucleus allows artificial manipulation of the accommodative stimulus (Crawford *et al.*, 1989). Following iridectomy in monkey eyes, electrically stimulated changes in accommodation allow visualisation of the accommodative mechanism (Neider *et al.*, 1990; Wasilewski *et al.*, 2008; Ostrin *et al.*, 2007; Croft *et al.*, 2006). In addition to viewing the accommodative apparatus *in vivo*, ultrasound biomicroscopy (UBM) has been used to assess ciliary body biometry and morphology *in vivo* in its relaxed and accommodative state in both rhesus monkeys (*Macaca mulatta*) (Glasser *et al.*, 2001; Croft *et al.*, 2006) and humans (Wang *et al.*, 1999a; Kano *et al.*, 1999; Výborný *et al.*, 2007; Park *et al.*, 2008).

These studies have contributed significantly to the understanding of the accommodative system but more recently non-invasive *in vivo* MRI studies (Strenk *et al.*, 1999; 2006) examining ciliary body functionality have proposed that the human accommodation mechanism differs significantly from that of the rhesus monkey (Strenk *et al.*, 2005; 2010). The proposal may be attributable to histological differences in connective tissue distribution in primate and human ciliary muscle (Lütjen-Drecoll *et al.*, 1988; Pardue and Sivak, 2000). In view of these reports of potential differences in the accommodative mechanism of animal models and humans, there is an impetus for improved *in vivo* imaging of the human accommodative system.

13.1.2 Imaging the ciliary muscle body

As discussed in Chapter 7 accurate imaging of the internal anterior segment structures has been limited until relatively recently. UBM has been used traditionally to assess ciliary body parameters in humans (Oliveira *et al.*, 2005; Muftuoglu *et al.*, 2009), although this technique is often difficult to perform and suffers from the disadvantage of being a contact procedure. Furthermore the precise location of the anatomy being imaged with UBM is often difficult to interpret as distortion of the globe by the probe may cause artefacts (Pekmezci *et al.*, 2009; Baikoff *et al.*, 2004). In order to overcome some of the disadvantages of UBM, anterior segment optical coherent tomography (AS-OCT) has been implemented for imaging the ciliary body. In particular it has been utilised to evaluate the link between ciliary body morphology and refractive error (Bailey *et al.*, 2008; Sheppard and Davies, 2010a) and accommodative changes (Schultz *et al.*, 2009; Sheppard and Davies, 2010b). The AS-OCT is a non-contact, non-invasive technique that offers the unique facility to image the finer internal structures of the anterior segment *in vivo* (see Chapter 7 for further details).

13.2 Study objective

The objective of the present study was to assess the ciliary muscle body *in vivo* to demonstrate whether ciliary muscle morphology, in particular its thickness, is associated with other structural parameters such as axial length and ocular volume. Additionally the study also investigated the association between scleral and corneal thickness and ciliary muscle dimensions.

13.3 Method

Ciliary muscle thickness (CMT) was assessed in 63 subjects (26 male, 37 female) age 18-40 years (27.86 ± 5.44). Ethical approval and the exclusion/inclusion criteria followed those detailed in Chapter 6. The *Zeiss IOLMaster* and the Shin-Nippon auto-refractor were utilised as in Chapter 6 to obtain ocular biometry and refractive error data; scleral thickness and central corneal thickness (CCT) were measured using the *Visante AS-OCT* (see Chapter 7).

13.3.1 Image acquisition

OCT tomographs of both the nasal and temporal ciliary muscles of both eyes were obtained using an AS-OCT (*Visante*; Carl Zeiss Meditec). The images were captured using the *Visante* software's enhanced high-resolution corneal scan mode, which provides cross-sectional images of high transverse and axial resolution (transverse x axial) 10 x 3 mm with a 512 x 1024 pixel resolution (Version 2). The operational principles of the AS-OCT were discussed in Chapter 7. To allow imaging of the ciliary muscle, subjects were asked to fixate with the contralateral eye a target positioned on a wall located 3 meters away. The scanning acquisition plane was set horizontally for all images. Two good quality images (i.e. of sufficient quality to delineate both the ciliary muscle and scleral spur) were acquired for both the nasal and temporal ciliary muscle. The order of imaging of each region (i.e. nasal vs. temporal) was randomised to avoid order effects contaminating the data.

13.3.2 Image analysis

As discussed in Chapter 7 the *Visante* software allows modification of the refractive index applied to the OCT images to minimise the effects of optical distortion produced by variation in refractive indices of the tissues (Izatt *et al.*, 1994; Radhakrishnan *et al.*, 2001). As the ciliary body refractive index is unknown it was assumed that opting for a refractive index of 1.388 would provide a more realistic approximation to that for ocular tissue than that of air (refractive index of 1.00). As indicated in Chapter 7 once the images were corrected for the refractive index the thickness measurements were performed in the 'analysis' mode. CMT was measured in μm for both the temporal and nasal meridians. One examiner (HP) measured the CMT in all images. For comparison purposes the protocol adopted for CMT measurement and the distances of measurement (i.e. 1-3 mm from the

scleral spur) is similar to that employed by Bailey *et al.*, (2008) and Oliveira *et al.*, (2005). Once the scleral spur was identified and the reference point determined as described in Chapter 7 a 1 mm calliper (provided by the *Visante* software) was extended along the interface between the sclera and the ciliary muscle (Figure 13.1). To measure the CMT at 1 mm (from the scleral spur) another calliper was positioned perpendicular to the local scleral curvature, the measurement being taken from the anterior ciliary muscle- scleral boundary to the posterior ciliary pigment epithelial surface. To measure CMT at 2 mm and 3 mm, two more 1 mm callipers were placed sequentially along the ciliary muscle-scleral boundary and the CMT measured as indicated above.

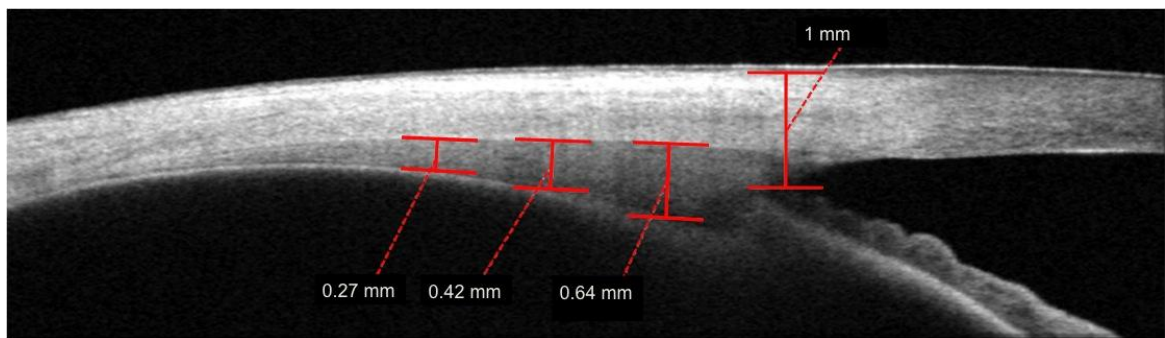


Figure 13.1 OCT image of the temporal ciliary muscle; callipers (in red) shown for the reference point and ciliary muscle thickness at 1, 2 and 3 mm from the scleral spur.

13.3.3 Calculation of ocular volume using 3-D MRI

MRI scans were performed on 32 of the original 63 subjects for whom CMT was assessed. The protocol for imaging and data analysis followed that outlined in Chapter 14. To extract ocular volume information from the MRI images additional analyses were required. In order to account for non-fluid structures such as the lens and errors in automatic shading, total ocular volume was determined by manually editing approximately 26 successive axial, sagittal and coronal image slices (Gilmartin *et al.*, IOVS 2008, 49: ARVO E-Abstract 3582). Since the anterior segment of the eye comprises all the structures situated between the front surface of the cornea and the front surface of the vitreous, anterior and posterior volumes of the fluid filled MR images were distinguished by gradually unshading coronal slices from the posterior corneal pole to the posterior lens pole.

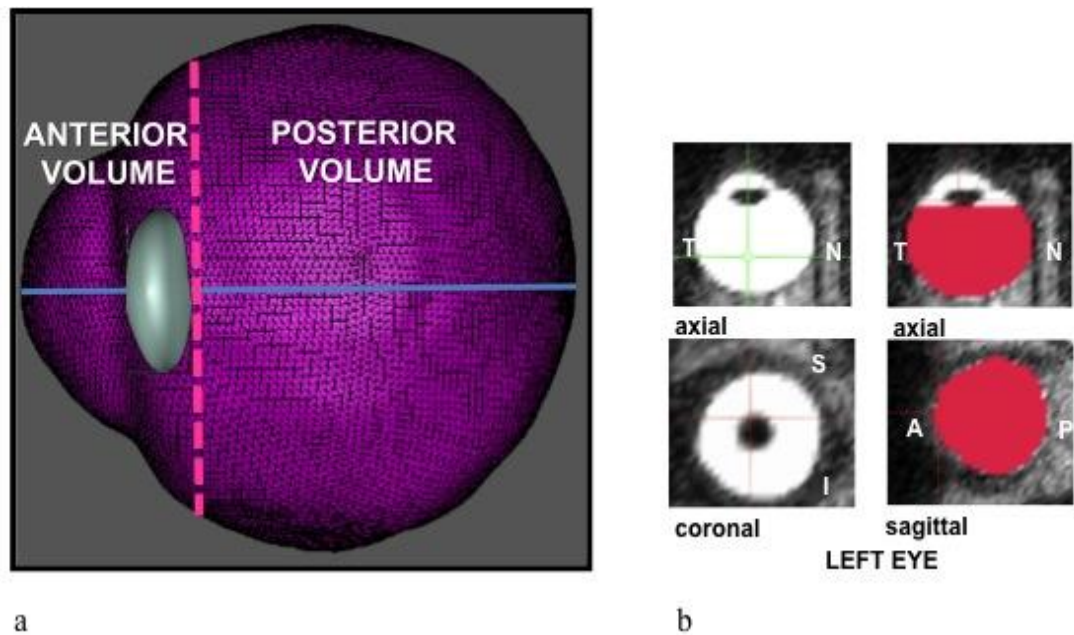


Figure 13.2 a) 3-D MRI depiction of the ocular globe, dotted line delineates the anterior and posterior ocular volume. **b)** Shading of the MRI images using the *mri3dX* program to derive ocular volumes (after Gilmartin *et al.*, 2008).

13.4 Statistical analysis

Data were shown to be normally distributed using the Kolmogorov Smirnov test. *SPSS* statistical software (Version 15, SPSS Inc., an IBM Company, Chicago, Illinois, USA) was used for statistical analysis. Two-way mixed repeated measures ANOVA were performed to test the difference in CMT between nasal (NCMT) and temporal (TCMT) measurements with region (i.e. nasal or temporal) as the between-subject variable and distance of CMT (i.e. 1-3 mm) as the within-subject variable. Multiple three-way mixed repeated measures ANOVAs were performed to test the influence of various different factors; between-subject variables factors were refractive status (myopes or non myopes), axial length (mm) grouping (1. ($21.5 > - \leq 23.5$), 2. ($23.5 > - \leq 25.5$), 3. (>25.5)), gender, age (years) grouping ($(18 > - \leq 29)$ and $(29 > - \leq 40)$) and ethnicity (British White (BW) or British South-Asian (BSA)); within-subject factors were region (nasal/temporal) and distance of CMT (1-3 mm; CMT1, -2, and -3 are 1, 2, and 3 mm). Additionally, Pearson's correlation coefficient was calculated to test the relationship between CMT measurements and both ocular biometry and scleral thickness. Furthermore a stepwise forward multiple linear regression was used as an exploratory test to determine which ocular biometric variables best explained the CMT values. For all statistical tests a p-value of <0.05 was taken as the criterion for statistical significance.

13.5 Results

13.5.1 Correlates of ciliary muscle thickness

CMT was measured in 63 healthy individuals (26 males and 37 females) aged between 18-40 years (27.85 ± 5.46). Data were analysed for non-myopic and myopic individuals [non-myopes (MSE $\geq -0.50D$) $n=31$, MSE(D) mean \pm SD (0.55 ± 1.17), range (-0.50 to +4.38), AL (mm) mean \pm SD (23.39 ± 0.74), range (mm) (21.61 - 24.75); myopes (MSE $< -0.50D$) $n=32$, MSE(D) mean \pm SD (-4.54 ± 4.20), range (-20.50 to -0.51), AL (mm) mean \pm SD (25.21 ± 1.22), range (mm) (23.33 - 28.32)]. For full details of statistical tests and results see Appendix 10.

As expected CMT1 was found to be thicker than CMT2 and CMT3, both nasally and temporally (Table 13.1). All CMT measurements both nasal and temporal correlated significantly with each other. Refractive error was found to correlate significantly with TCMT2, TCMT3 but not with TCMT1. Similarly axial length was significantly correlated with TCMT2, TCMT3, NCMT2 and NCMT3.

Interestingly various ciliary muscle measurements (e.g. TCMT2, TCMT3, NCMT2, NCMT3) were also positively correlated with ACD. Additionally, increasing age was significantly associated with reducing CMT (TCMT2 and NCMT1). Axial length correlated significantly with refractive error and ACD. Corneal thickness failed to correlate with any measures of CMT although a positive correlation was found between the flattest corneal curvature and TCMT1 and NCMT1.

CMT location	Mean \pm SD	Minimum	Maximum
Temporal CMT1	544.15 \pm 65.55	370.00	745.00
Temporal CMT2	341.16 \pm 57.65	175.00	450.00
Temporal CMT3	195.05 \pm 42.40	110.00	310.00
Nasal CMT1	556.91 \pm 69.36	350.00	690.00
Nasal CMT2	313.01 \pm 54.85	165.00	430.00
Nasal CMT3	171.69 \pm 37.31	75.00	245.00

Table 13.1 RE Ciliary muscle thickness (CMT) (μ m).

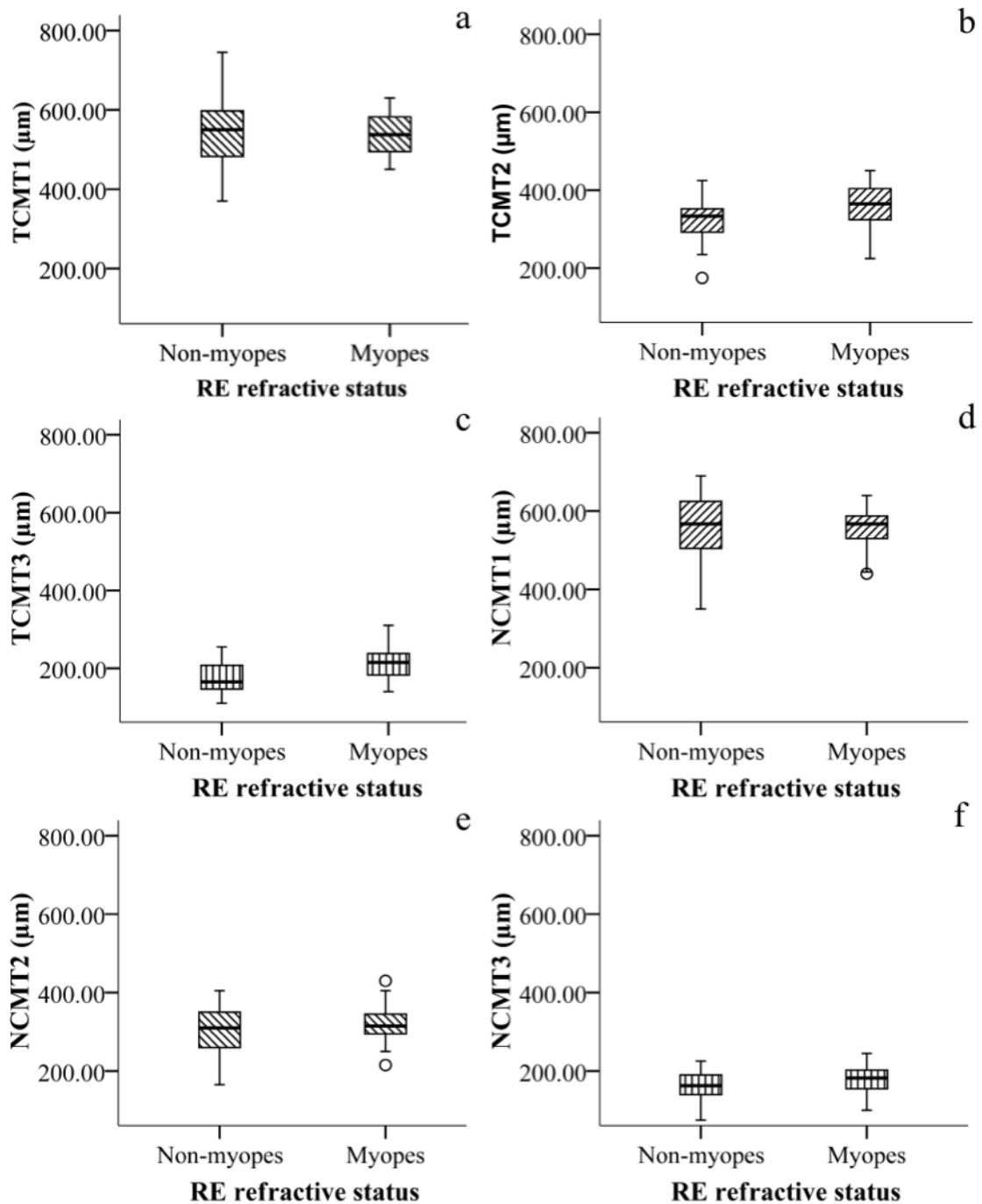
Statistical analysis revealed no significant difference between nasal and temporal CMT ($F(1, 122)=2.595$ ($p=0.110$)), however there was a trend for a thicker CM temporally than nasally for both CMT2 and CMT3 but not for CMT1. A significant difference was also seen with distance of CMT measurement ($F(1.45, 176.88)=3354.05$ ($p<0.001$)), with a

Bonferroni *post hoc* test identifying the difference to be between all (1, 2 and 3 mm) distances. Furthermore a significant interaction was found between region and distance of measurement ($F(1.45, 176.88)=11.91$ ($p<0.001$)); on inspection of the interaction graph this appeared to be attributable to CMT1 which failed to show greater thickness temporally in comparison to CMT2 and CMT3.

Refractive status (myopes $n=32$, non-myopes $n=31$) showed no significant effect on CMT ($F(1, 60)=1.690$ ($p=0.199$)) but demonstrated a second order interaction between the main factors of distance and refractive status ($F(1.44, 86.40)=7.80$ ($p=0.002$)). On inspection of the interaction plot the behaviour of CMT1 appeared to be the cause of the interaction effect, as both CMT2 and CMT3 were found to be greater in myopic subjects, whereas CMT1 failed to show this trend. Moreover a third order interaction demonstrated a significant effect of refractive status on the combined effect of the main factors region and distance ($F(1.643, 98.597)=6.212$ ($p=0.003$)); the results showed myopes to have thicker CM than non-myopes especially temporally, which was however slightly lower at CMT1 for myopes than non-myopes. Table 13.2 and Figure 13.3 summarise the CMT values for myopes and non-myopes.

Refractive status	Mean \pm SD CMT					
	TCMT1	TCMT2	TCMT3	NCMT1	NCMT2	NCMT3
Myopes	537.19 \pm 54.09	358.96 \pm 53.76	214.58 \pm 38.47	555.73 \pm 48.89	319.79 \pm 47.17	180.68 \pm 33.11
Non-myopes	551.34 \pm 75.83	324.25 \pm 56.24	174.89 \pm 36.87	558.17 \pm 86.95	305.78 \pm 62.00	162.11 \pm 39.65

Table 13.2 CMT (μm) for myopes and non-myopes.



Figures 13.3 (a-f) Box and whiskers plot (median and interquartile range) for temporal and nasal CMT (1, 2, and 3 mm).

On examination for an influence of axial length grouping (1.(21.5 > - \leq 23.5) n=19, 2.(23.5 > - \leq 25.5) n=30, 3.(> 25.5) n=12); no significant main effect was found on the CMT ($F(2, 58)=2.478$ ($p=0.093$)). A significant second order interaction was seen between axial length grouping and the main factor distance of measurement ($F(2.695, 78.149)=3.332$ ($p=0.028$)). On inspection of the interaction plot measures of CMT2 and CMT3 appear to show an increase with increasing axial length, which was not evident for CMT1.

Axial length group	Mean \pm SD CMT					
	TCMT1	TCMT2	TCMT3	NCMT1	NCMT2	NCMT3
1	535.53 \pm 78.14	317.37 \pm 63.32	179.74 \pm 35.76	552.71 \pm 88.96	302.72 \pm 59.91	163.51 \pm 33.84
2	552.89 \pm 61.72	343.17 \pm 53.79	191.89 \pm 40.05	556.78 \pm 68.45	306.00 \pm 49.82	167.50 \pm 38.02
3	537.92 \pm 65.61	379.86 \pm 40.55	232.22 \pm 41.31	562.78 \pm 35.87	351.67 \pm 44.86	195.28 \pm 35.56

Table 13.3 CMT (μm) between different axial length groups.

No significant influence of gender (males $n=26$, females $n=37$) ($F(1, 60)=0.005$ ($p=0.942$)) or ethnicity ($F(1, 60)=0.168$ ($p=0.684$)) was found for the CMT differences nor an interaction with region or distance of measurement. Similarly age (years) grouping ($(18 > - \leq 29)$ $n=43$, $(29 > - \leq 40)$ $n=19$) revealed no significant influence on the CMT differences ($F(1, 60)=3.363$ ($p=0.072$)) nor an interaction with region and distance, although there was a non-significant trend for thinner CMT in the older age group.

13.5.2 Ocular volume and ciliary muscle thickness

Ocular volumes (mm^3) were measured in 32 healthy individuals (14 males and 18 females) aged between 18-40 years (27.40 ± 6.20). Data were analysed for non-myopic and myopic individuals [non-myopes ($\text{MSE} \geq -0.50\text{D}$) $n=15$, MSE(D) mean \pm SD (0.73 ± 1.57), range (-0.50 to $+4.38$), AL (mm) mean \pm SD (23.43 ± 0.70), range (mm) ($21.75 - 24.45$); myopes ($\text{MSE} < -0.50\text{D}$) $n=17$, MSE(D) mean \pm SD (-6.76 ± 4.43), range (-20.50 to -0.81), AL (mm) mean \pm SD (25.80 ± 1.18), range (mm) ($23.33 - 28.32$)].

Both total and posterior volumes correlated positively with all measures of CMT (nasal and temporal). Furthermore, both total and posterior volumes also correlated with other biometric data: ACD, axial length and refractive error, whilst anterior volume failed to correlate with any measures of CMT or other biometric parameters.

Stepwise forward multiple linear regression models with the various measures of CMT as the outcome variable and CCT, mean corneal curvature, ocular volume (total, anterior and posterior), refractive error, axial length, ACD, gender and age as predictor variables were evaluated. Due to high levels of multicollinearity (>0.80) refractive error, axial length and

total, anterior and posterior ocular volume were assessed separately in the model. The analysis revealed:

- TCMT1 showed a significant association with mean corneal curvature ($p=0.009$), which explained 7.8% of the variability of TCMT1.
- TCMT2 was found to be associated with total ocular volume explaining 34.2% of the variability in TCMT2 measures. When assessed with the posterior ocular volume similar levels of association were noted, accounting for 34% of the TCMT2 variability. In contrast axial length explained only 12.8% of the variance in TCMT2 values.
- TCMT3 was found to be associated with total ocular volume, explaining 39.6% of the variability, whilst posterior volume was found to explain a greater proportion (42.2%) of the variance in TCMT3 measurements. In comparison axial length only accounted for 19.5% of the variability.
- NCMT1 failed to show any association with any of the parameters assessed in the model.
- NCMT2 showed an association with total ocular volume explaining 20.1% of the variability and posterior ocular volume accounting for a lower 16.7% of the measurement variance. Axial length explained a lower 9.4% of the NCMT2 variability.
- NCMT3 failed to show any relation with the ocular volumes and axial length, but showed an association with ACD explaining 19.3% of the thickness variability.

	Mean ± SD	Min	Min
Total volume	8193 ± 1079	5036	10291
Posterior volume	7093 ± 1079	4017	9081
Anterior volume	1100 ± 153	633	1414

Table 13.4 RE MRI Ocular volumes (mm³).

Independent *Student's t tests* revealed no significant difference in ocular volumes (total, anterior and posterior) between males and females, age groups or ethnicity. Refractive status demonstrated significant differences between myopes and non-myopes for total volume (p=0.001), posterior volume (p<0.001) and anterior volume (p=0.043). Similarly a one-way ANOVA with the axial length groups (1.<21.5>-≤ 23.5) n=9, 2.<23.5 > - ≤25.5) n=13, 3.>25.5) n=10) showed significant differences between groups for both the total and posterior ocular volumes (p<0.001) but not for anterior ocular volume; where significant differences were found, Games Howell *post hoc* test demonstrated significant differences between all three groups.

13.5.3 Ciliary muscle thickness and scleral thickness

Scleral thickness was also measured in all 63 individuals for whom CMT was considered (data from Chapter 7). Scleral thickness was measured at 1-7 mm from the corneolimbic junction in 8 meridians (superior (S), inferior (I), temporal (T), nasal (N), superior-nasal (SN), superior-temporal (ST), inferior-temporal (IT), inferior-nasal (IN) -see Chapter 7. Statistical analysis demonstrated a number of negative correlations, especially between temporal CMT and scleral thickness measurements along the superior (S, ST, SN) and inferior meridians. See Appendix 10.

13.6 Discussion

The findings of the present study suggest that axial length and refractive status modify ciliary muscle thickness (CMT) along its length, with myopes showing a trend for a thicker ciliary muscle profile when compared to non-myopes. Furthermore the study also established a significant association between ocular volume and CMT. In particular total and posterior ocular volumes were found to be more powerful predictors of CMT compared to axial length. Additionally the investigation also demonstrated an inverse relationship between increasing CMT and scleral thickness along various meridians. Together these observations provide substantial evidence for a significant role of ciliary muscle morphology in the determination of globe conformation.

13.6.1 Structural correlates of ciliary muscle thickness

The present findings of a significant influence of axial length and refractive error on the CMT across its length is consistent with the observations of Bailey *et al.*, (2008) who similarly reported a significant interaction between the location of the ciliary body measurement and both refractive error and axial length, noting that longer axial length was associated with increased ciliary body thickness (CBT). In another study assessing CBT, Oliveira *et al.*, (2005) also reported CBT at 2 and 3 mm from the scleral spur to be greater in myopic eyes than emmetropic and hyperopic eyes. In a more recent study Sheppard and Davies, (2010a) failed to show an effect of axial length on CMT but instead found the ciliary muscle to be longer with increasing axial length. Further confirmation for a role of CBT in refractive error stems from a study examining ciliary body dimensions in unilateral high axial myopes, where the investigators reported increased CBT in the myopic eye compared to the control fellow eye (Muftuoglu *et al.*, 2009). Interestingly, Muftuoglu *et al.*, (2009) noted that differences in CBT between myopic and non-myopic eyes was not wholly attributable to the corresponding differences in axial length, thus suggesting that the increased CBT in myopia is likely to be a result of a combination of factors and not solely dependent on axial length expansion.

Indeed in the present study ocular volume (total and posterior) was found to be a more powerful predictor of CMT (TCM2, TCM3 and NCM2) when compared to axial length. Moreover in contrast to the anterior ocular volume, both total and posterior ocular volumes correlated with all measures of CMT suggesting that the structural effects of CMT may be

related to expansion of the posterior globe. In support of these findings, Gilmartin *et al.*, IOVS 2008, 49: ARVO E-Abstract 3582 reported the anterior eye volume to be a non-significant structural correlate of refractive error. Furthermore their findings of a weaker correlation between posterior ocular volume and refractive error when compared to the longitudinal axial length suggested that the posterior ocular volume may reflect regional variation in the conformation of the posterior eye between refractive groups. ***The present findings of a stronger influence of the posterior volume on CMT when compared to the longitudinal axial length would imply that CMT might be associated in modulating the conformation of the posterior eye.***

The rising number of reports demonstrating increased CMT in myopia suggests that it is either a significant physiological factor in myopigenesis or a consequence of myopia. Interesting findings of the present study were the numerous correlations between scleral and ciliary muscle thickness. Of particular note was the inverse relationship found between increasing temporal CMT (CMT1, CMT2 and CMT3) and reducing scleral thickness 3 mm posterior to the scleral spur. This association was predominantly found for scleral thickness along the superior-nasal and inferior meridians. With reference to the findings of Chapter 7, the superior-nasal meridian was found to be the thinnest scleral meridian and the inferior meridian the thickest. These results would suggest that CMT influences scleral thickness particularly along these two meridians. ***Moreover, considering the association between increased CMT and longer axial length and increased ocular volume, these findings would indicate that scleral thickness along the superior nasal and inferior meridians shows more pronounced thinning posterior to 3 mm from the scleral spur with increasing levels of myopia.***

Furthermore refractive status demonstrated a significant interaction with the temporal CMT, with increasingly thicker CMT2 and CMT3 in myopic eyes. In contrast to the numerous associations between the temporal CMT and scleral thickness there were few correlations found for the nasal ciliary muscle parameters. Contrary to the present results, investigators (e.g. Sheppard and Davies, 2010a; Glasser *et al.*, 2001) have previously reported significant differences between the nasal and temporal CMT. In view of the differences in the association between the nasal/temporal CMT and both refractive status and scleral thickness, these findings may be indicative of structural asymmetry between the morphology of the nasal and temporal ciliary muscle.

These novel findings of a relationship between CMT and scleral thickness, when coupled with the observations of a strong association between CMT and posterior ocular volume, support the supposition of an important mediatory role for the ciliary muscle in determining globe conformation. A number of studies have demonstrated significant inter-subject variability in ocular shape in myopia (Chen *et al.*, 1992; Cheng *et al.*, 1992). Using *in vivo* 2-D measurements of the ocular globe via MR imaging Atchison *et al.*, (2005) demonstrated both myopic and non-myopic eyes on average to conform to an oblate shape and only infrequently to a prolate shape. Furthermore the investigators also noted that in myopic eyes the retinal contour moves towards a less oblate shape or a more prolate shape than in non-myopes although a prolate shape is not exclusive to myopia. Variation in retinal shape consequently affects peripheral refraction, with myopic eyes having relatively more hyperopic peripheral refractive errors than emmetropic eyes (Mutti *et al.*, 2000a; Logan *et al.*, 2004; Atchison *et al.*, 2006; Chen *et al.*, 2010c). Peripheral refraction studies have demonstrated asymmetry of globe shape with reference to a hypermetropic shift in the horizontal axis but a myopic shift vertically in myopic individuals (Chen *et al.*, 2010c; Millodot, 1981; Mutti *et al.*, 2000a). Interestingly, Seidemann *et al.*, (2002) reported increased levels of relative myopia in the inferior visual field (i.e. superior retina) when compared to the superior visual field (i.e. inferior retina) possibly suggesting asymmetric globe expansion in the vertical meridian. These meridional differences would suggest greater vertical chord height than horizontal chord width thus indicating a flatter contour vertically than horizontally (Atchinson *et al.*, 2004; 2005). ***The present findings of an association between CMT and scleral thickness particularly along the superior nasal and inferior meridians further supports the suggestion of meridional differences in ocular stretching and identifies a complex structural inter-relationship between the various ocular components.***

Furthermore, peripheral hyperopic defocus has been shown to be linked to the development of adult onset myopia but not yet for juvenile onset myopia (Hoogerheide *et al.*, 1971; Seidemann *et al.*, 2002; Mutti *et al.*, 2010). In regards to the mechanism by which this occurs Wallman and Winawer (2004) suggested that a relatively hyperopic periphery may stimulate myopic growth as a compensatory mechanism, whereby axial elongation allows the retinal and image plane to become conjugate. Indeed in partial support of this theory, a number of studies have reported myopic children to show accommodative deficits resulting in central (not peripheral) hyperopic retinal defocus (Mutti *et al.*, 2000b; 2006; Gwiazda *et al.*, 1993; 1999). In regards to the findings of increased ciliary muscle thickness, Bailey *et*

al., (2008) postulated that these physiological alterations may be due to hypertrophy which would presumably result in inadequate ciliary muscle contraction and hence explain the accommodative insufficiency found in myopic children.

Logan *et al.*, (2004) speculated that posterior segment myopic growth might display differential development along the axial and transverse dimensions of the eyes, with axial elongation being greater than transverse growth. Previously investigators have proposed that the change in ocular shape with myopic growth may be a result of either an internal mechanical restriction in the region of the ciliary body (Mutti *et al.*, 2007) or any external impedance to growth in certain directions (Atchison *et al.*, 2004). Atchison *et al.*, (2004) postulated that the altered shape in myopic eyes could be attributable to either anatomical restriction to growth from the bony orbital walls or as a result of regional variation in the ocular growth. In regards to meridional differences and propensity to expansion Atchison *et al.*, (2004) noted that all myopic eyes were vulnerable to axial elongation followed by the slightly greater susceptibility for expansion in the vertical than the horizontal meridians. Contrary to these findings, recently it has been suggested that a restrictive force to the normal thinning of the lens as ocular growth progresses may be a significant component in the aetiology of myopia (Mutti, 2010). Bailey *et al.*, (2008) proposed that the increased CBT could lead to hypertrophic changes and increased deposition of collagen, resulting in increased equatorial mechanical stiffness, which may hinder the normal thinning of the crystalline lens. Indeed, the present study demonstrated a significant interaction between the CMT profile and axial length but more importantly established a significant association between posterior globe expansion and thicker ciliary muscle. ***Hence the increased CMT and presumably greater mechanical resistance would lead to restricted ocular expansion in the horizontal plane. Furthermore the novel findings of a significant association between CMT and scleral thickness particularly along the superior nasal and inferior meridian are indicative of a link between reducing scleral thickness and increased CMT with longer axial length.***

13.6.2 Thickening of the ciliary muscle in myopia

Despite the mounting evidence for an association between myopic refractive error and greater CMT, it is unclear how the ciliary muscle structure alters with increasing axial length. Scleral remodelling in myopia animal models has identified matrix metalloproteinase (MMP-2) in scleral tissue to exhibit an active response to form vision

deprivation (Chapter 2; Guggenheim and McBrien, 1996). Interestingly, the ciliary body has also been shown to express MMP-1 and MMP-2 (Gaton *et al.*, 1999; Weinreb *et al.*, 2002). Consequently, prostaglandin-induced changes in ciliary body expression of MMP-2 have been found to result in extracellular remodelling of the ciliary muscle, iris root and sclera, which leads to an increase in the uveoscleral outflow (Marchini *et al.*, 2003; Weinreb *et al.*, 2002). Increased CBT is likely to provide larger spaces between the ciliary muscle fibers thus enhancing the ability of aqueous humour to flow through the ciliary body extracellular spaces (Lindsey *et al.*, 1997). The uveoscleral outflow passes from the anterior chamber through the extracellular spaces between the ciliary muscle fibre bundles to the suprachoroidal space towards the posterior globe exiting via the sclera (Weinreb *et al.*, 2002). As a result of the complex network of structures that partake in the uveoscleral outflow, it may be speculated that the retinal biochemical changes during form vision deprivation also influence the expression of MMP-2 in the ciliary body and hence stimulate biomechanical changes in the anterior segment. In regards to the role of the ciliary muscle in myopia, Fujikura *et al.*, (2002) suggested that the mechanical strains imposed by the ciliary muscle is likely to stimulate the activation of MMP-2 by the scleral fibroblasts. In support of these findings Shelton and Rada, (2007) also reported mechanical strain on the sclera to promote the activation of MMP-2. Therefore it may be postulated that increased CMT is likely to augment the levels of stress on the sclera, which may in turn promote extracellular matrix degradation and consequently accelerate myopic growth.

13.6.3 Ciliary muscle thickness and corneal biometry

In support of the present study Bailey *et al.*, (2008) found only CBT2 and CBT3 (equivalent to CMT2 and CMT3) to show an association with axial length and refractive error whilst CBT1 (equivalent to CMT1) was found to be independent of these variables. In contrast to the more stromal component of CBT1, it has been hypothesised that both CBT2 and CBT3 would primarily consist of ciliary muscle tissue (Bailey *et al.*, 2008) indicating that the more anterior areas of the ciliary body may differ in their material properties. *In the present study both nasal and temporal CMT1 demonstrated a significant positive correlation with corneal curvature indicating that the anterior portion of the ciliary muscle may be associated with biomechanical properties the cornea.* In support of a relationship between CMT and corneal parameters, Yasuda and Yamaguchi, (2005) reported increased central corneal refractive power as a result of increased steepness in corneal curvature after simulating accommodation by topical

instillation of pilocarpine in human volunteers. Since CMT reduces with accommodation (Pardue and Sivak, 2000), these findings would imply that steeping of the corneal curvature contributes to the increased refractive power obtained with accommodation (Yasuda and Yamaguchi, 2003).

13.6.4 Comparison to previous reports of ciliary muscle thickness

In reviewing the literature on ciliary muscle and body thickness it was evident that several investigators have measured ciliary muscle thickness and assumed it to represent ciliary body thickness (Oliveira *et al.*, 2005; Bailey *et al.*, 2008). Histological evidence would suggest that the *in vivo* ciliary images examined in these studies (Oliveira *et al.*, 2005; Bailey *et al.*, 2008) are in fact ciliary muscle rather than ciliary body sections (Hogan, 1971; Pardue and Sivak, 2000). In comparison to previous studies on CMT, the values found in the present study match well to those of Sheppard and Davies, (2010a) but are lower than those reported by Bailey *et al.*, (2008), Schultz *et al.*, (2009) and Oliveira *et al.*, (2005) - see Table 13.5. Differences in the OCT refractive index used in these studies are likely to explain some of the variability. For comparison purposes if the Bailey *et al.*, (2008) results are divided by the refractive index presently applied (i.e. 1.388) the average values (μm) would be lower (Bailey *et al.*, 2008 emmetropes (CBT1: 644.5, CBT2: 413.5, CBT3: 213.3), myopes (CBT1: 650.8, CBT2: 453.7, CBT3: 255.5)) but still greater than those of the current study. Additionally, variation in the protocol implemented to locate the CMT varied between the present study and previous OCT studies (Bailey *et al.*, 2008; Schultz *et al.*, 2009; Sheppard and Davies, 2010a). In the current investigation each measurement location was determined 1 mm posterior to the preceding measurement site thus minimising the effects of the local curvature of the ciliary muscle. In contrast, the Bailey *et al.*, (2008) study determined the location sites by extending callipers of 1, 2 and 3 mm from the scleral spur to identify their measurement point, thus failing to account for the curvature change in the ciliary muscle but maintaining a common point of origin for each location. Despite the discrepancy in the measurement protocol applied by the different studies, the findings of similar CMT2 values between the present study and that of Sheppard and Davies, (2010a), where the same protocol as the Bailey *et al.*, (2008) study was used, suggests that the differences in CMT values may be a result of some other unaccounted for factor.

Additionally differences in imaging techniques i.e. UBM vs. OCT may further explain the discrepancies in CMT values between investigations. OCT is an optical device that is affected by the distortion caused by changes in refractive index of the tissue, whereas UBM is unaffected by these changes but will be influenced by differences in the speed of sound between the structures being imaged (Pavlin *et al.*, 1992). In addition, UBM is a contact procedure that requires immersion of the anterior surface of the eye and hence it is difficult to determine the exact location of the area being examined (Pekmezci *et al.*, 2009; Baikoff *et al.*, 2004), which may further contribute to variability between investigations. Furthermore, the requirement for eye contact in UBM is likely to induce variable distortion of the globe leading to inconsistency in the results (Baikoff *et al.*, 2004). Variation in ciliary muscle dimensions may also be a consequence of the differences in the subject cohort assessed. Oliveira *et al.*, (2005) assessed a mixed group of normal and glaucoma (POAG and NTG) patients, and since narrow angles have been associated with thinner ciliary bodies (Gohdo *et al.*, 2000), this may partly explain the variation in reports of CBT between studies (Table 13.5).

Similarly, discrepancies between the studies (see Table 13.5) may potentially be related to the age of the study groups. Both the Bailey *et al.*, (2008) and Schultz *et al.*, (2009) investigations assessed children between the ages of 8-15 years whereas Sheppard and Davies (2010a) and the present study assessed young adults between the ages of 18-40 years. ***Indeed the present study demonstrated a weak non-significant trend for reducing TCMT2 and NCMT1 with age.*** In support of these findings Oliveira *et al.*, (2005) noted a non-significant negative association between age and CBT3, whilst Sheppard and Davies, 2010b reported temporal CMT at 50% and 75% of the of the total ciliary muscle length (posterior to the scleral spur) to reduce with age. Furthermore, histological (Pardue and Sivak, 2000; Tamm *et al.*, 1992) and clinical (Henzan *et al.*, 2010; Strenk *et al.*, 1999; Glasser *et al.*, 2001; Sheppard and Davies, 2010b) investigations have reported the ciliary muscle dimensions to become shorter and wider with age, with a move towards an anterior-inward position. More recently, both Sheppard and Davies, 2010b and Strenk *et al.*, (2010) reported an anterior displacement of the ciliary muscle apex with age implying that the reference points for the CMT measurements may vary between subjects and cohorts. Such anatomical changes would indicate that an alternative technique such as proportional measurements of the full length of the ciliary muscle, as advocated by Sheppard and Davies (2010a, b), might better control for variability in ciliary muscle

location. In view of the above findings it seems likely that CMT reduces with age but further studies assessing a larger age range would be required to verify the proposal.

The present study followed a protocol similar to that of Oliveira *et al.*, (2005) and hence accommodation was not eliminated by cycloplegia as was the case in studies examining ciliary body thickness in children (Bailey *et al.*, 2008; Schultz *et al.*, 2009). As the main objective of the present study was to assess differences in ciliary body conformation between myopes and non-myopes, the difference in accommodative response and the associated microfluctuations would be approximately $\pm 0.25D$ when viewing a high-contrast fixation target at 3 meters (Winn and Gilmartin, 1992). Therefore it is unlikely that differential accommodative responses between refractive groups would introduce significant variability to confound the present findings (Bullimore *et al.*, 1992; Krantz *et al.*, 2010).

Investigators	Study details	Results (μm)
Oliveira <i>et al.</i> , 2005	UBM measures of temporal CBT 2 and 3 mm from scleral spur Assessed adults (normal, OHT, suspect glaucoma and glaucoma (NTG, POAG, exfoliation syndrome and pigment dispersion syndrome) patients Mean age \pm SD 51.8 \pm 16.5 years	CBT 2 Myopes 490 \pm 115 Emmetropes 362 \pm 53 Hypermetropes 317 \pm 77 CBT3 Myopes 315 \pm 79 Emmetropes 247 \pm 49 Hypermetropes 224 \pm 53
Bailey <i>et al.</i> , (2008)	AS-OCT measures of nasal CBT 1, 2 and 3 mm from scleral spur Children age 8-15 years (cycloplegic)	CBT1 Myopes 903.3 \pm 119.1 Emmetropes 894.6 \pm 126.8 CBT2 Myopes 629.7 \pm 99.8 Emmetropes 573.9 \pm 100.4 CBT3 Myopes 354.7 \pm 68.1 Emmetropes 296.0 \pm 61
Schultz <i>et al.</i> , (2009)	AS-OCT measures of nasal CBT 2 mm from scleral spur Children age 8-15 years (cycloplegic)	Mean 604.06 \pm 104.28
Muftuoglu <i>et al.</i> , (2009)	UBM measures of temporal CBT and CMT at the limbus. Adults with unilateral high axial myopia aged 11-44 years	High myopic CBT 1350 \pm 34 CMT 698 \pm 57 Fellow eye CBT 1211 \pm 50 CMT 644 \pm 65

Sheppard and Davies, (2010a)	AS-OCT measures of temporal and nasal CMT 2 mm from the scleral spur Young adults aged 19-34 years	Nasal 347 ± 58 Temporal 405 ± 58
Sheppard and Davies, (2010b)	AS-OCT measures of temporal and nasal CMT 2 mm (CM2) from the scleral spur and at 25% (CM25), 50% (CM50) and 75% (CM75) of the total length posterior to the scleral spur Young adults aged 19-34 years Older adults aged 35-70 years	CM2 Myopes: nasal 372 ± 72 , temporal 419 ± 74 Emmetropes: nasal 327 ± 59 , temporal $434 - (2.079 \times \text{age})$ CM25 Myopes: nasal 541 ± 62 , temporal 546 ± 66 Emmetropes: nasal 528 ± 44 , temporal 541 ± 50 CM50 Myopes: nasal 304 ± 43 , temporal $581 - (3.810 \times \text{age})$ Emmetropes: nasal 284 ± 42 , temporal $383 - (1.940 \times \text{age})$ CM75 Myopes: nasal 157 ± 22 , temporal $276 - (1.26 \times \text{age})$ Emmetropes: nasal 143 ± 22 , temporal $184 - (0.760 \times \text{age})$
Present study	AS-OCT measures of temporal and nasal CMT 1, 2, 3 mm from the scleral spur Young adults aged 18-40 years	TCM1 544.15 ± 65.55 TCM2 341.16 ± 57.65 TCM3 195.05 ± 42.40 NCM1 556.91 ± 69.36 NCM2 313.01 ± 54.85 NCM3 171.69 ± 37.31

Table 13.5 Previously reported *in vivo* thickness measurements of human ciliary body/muscle.

13.7 Conclusion

In conclusion the key findings of the present study are:

- Refractive status and axial length showed an interaction effect with the location of CMT, demonstrating that the profile of change in thickness along the length of the ciliary muscle increased in thickness in myopic eyes when compared to non-myopic eyes.
- Posterior ocular volume was found to be a significant correlate of CMT and a more powerful predictor of CMT than axial length.
- Temporal CMT was found to be associated with reducing scleral thickness, particularly along the superior-nasal and inferior meridians.
- A non-significant trend for thinner CMT was found in the older age group

14.0 CONFORMATION OF THE ANTERIOR SEGMENT IN HUMAN MYOPIA

14.1 Introduction

It is widely accepted that the structural conformation of the globe governs the refractive status of the eye. There is now a significant body of literature that implies an important functional role of the sclera in governing the tissue biomechanical changes that occur during myopic growth (McBrien *et al.*, 2009; Jobling *et al.*, 2009; Shelton and Rada, 2007; Rada *et al.*, 2006; Guggenheim and McBrien, 1996). The evidence would suggest that the biomechanical and biochemical alterations in myopia are localised to the posterior regions of the globe and are independent of changes in the anterior segment (Avetisov *et al.*, 1983; Funata and Tokoro, 1990; Rada *et al.*, 2000; Norton and Rada, 1995; McBrien *et al.*, 2000; 2001a), although the findings from Chapters 7, 8, 10, 11 and 13 would refute this suggestion.

In Chapter 11 corneal biomechanics were shown to be significantly modulated by axial length amongst the UK subjects whilst in Chapter 8 the predominantly myopic HKC individuals exhibited higher levels of anterior scleral resistance than the UK subjects. Further, in Chapter 7 scleral thickness along the superior and inferior meridians was found to be associated with axial length changes, whereas in Chapter 13, ciliary muscle thickness was identified as a significant correlate of axial length and posterior ocular volume. Collectively these findings imply that myopic growth influences the anterior segment biomechanics and that the biophysical characteristics of the anterior segment have a significant role in the genesis of myopia.

In order to evaluate comprehensively the morphological features of the globe in myopia, an assessment of the three-dimensional (3-D) eye shape *in vivo* is crucial (Stone and Flitcroft, 2004). With this intention, several investigators have attempted to infer the conformation of the globe from the use of different methodologies; early determinations of posterior eye shape utilised x-ray techniques (Deller *et al.*, 1947) whilst more recently optical low coherent reflectometry (Schmid, 2003), peripheral refraction (Logan *et al.*, 2004), x-ray computed tomography (CT) (Zhou *et al.*, 1997) and magnetic resonance imaging (MRI) (Cheng *et al.*, 1992; Chen *et al.*, 1992; Atchison 2004; 2005; Chau *et al.*, 2004a; 2004b) have also been employed. Aside from MR and CT imaging these techniques are limited to

the assessment of a relatively small retinal field size (spanning the posterior fovea up to 10°) (Davson, 1976) and thus questions the validity of such methods of deducing overall globe conformation (Logan *et al.*, 2004).

Studies that have implemented the use of MRI have demonstrated its utility in evaluating ocular features such as retinal spherical radius, deviations from sphericity (Chen *et al.*, 1992), retinal shape (Atchison *et al.*, 2005) as well as linear dimensions of the globe (i.e. anterior-posterior, equatorial, and superior-inferior) using 2-D images (Cheng *et al.*, 1992; Atchison *et al.*, 2004). Furthermore several investigators have also applied MR imaging to measure ocular and orbital volumes, but failed to assess characteristics of the ocular shape pertinent to myopia (Chau *et al.*, 2004a; 2004b). These studies have provided vital information on the structural characteristics of the ocular globe for different refractive states but owing to signal-to-noise limitations they were unable to assess the eye wholly as a 3-D entity and hence inferred the globe's 3-D characteristics from a number of relatively coarse 2-D slices (Singh *et al.*, 2006).

Singh and colleagues (2006) subsequently demonstrated the use of MRI to depict the conformation of the globe in 3-D. This form of MR imaging allows an *in vivo* assessment of morphological characteristics such as, for example, ocular volume, surface area and surface curvature (Logan *et al.* IOVS 2005, 46: ARVO E-Abstract 4266). 3-D MRI offers an *in vivo* non-contact imaging technique that allows visualisation and assessment of the ocular globe from any angle in real time and has been used in humans (Singh *et al.*, 2006) and in evaluating animal models of myopia (Huang *et al.*, 2009; Smith *et al.*, 2009) and ocular development (Goodall *et al.*, 2009). The technique provides good correlation with partial coherence interferometry (PCI) measurement of axial length and repeatable and reproducible results (Singh *et al.*, 2006).

MR imaging is particularly suited to the eye owing to the eye's variable water content and due to the need for high spatial resolution over a small field of view (Langner *et al.*, 2010). Furthermore MR imaging is independent of the optical aberration and distortion caused by variations in refractive index of ocular tissues that often hampers optical imaging (Jones *et al.*, 2007a). Hence, MR imaging is frequently used in ophthalmology when assessing the posterior segment (Lam *et al.*, 2005; Trick *et al.*, 2008; Braun *et al.*, 2007), extraocular muscles (Kowal *et al.*, 1994; Krzizok and Schroeder, 2003), orbit (Georgouli *et al.*, 2008; Chau *et al.*, 2004a) and anterior segment structures (Strenk *et al.*, 1999; 2010; Jones *et al.*,

2007a). For the imaging of smaller ocular components, the presence of involuntary ocular saccades can hinder the quality of MR images (Patz *et al.*, 2007). In order to overcome this problem, several investigators have implemented various preparatory strategies and fixation techniques that allow enhanced imaging of the fine ocular structures (Patz *et al.*, 2007; Bert *et al.*, 2006). Furthermore, the introduction of 7.0 and 7.1 Tesla MR imaging has enabled imaging of the smaller structures such as the cornea, crystalline lens, anterior chamber, iris and ciliary body (Richdale *et al.*, 2009; Langner *et al.*, 2010).

14.1.1 Theoretical principles of MR imaging

MR imaging is a structural investigative technique that exploits the naturally occurring magnetic charge of commonly found hydrogen atoms in organic tissues (McRobbie, 2007). Hydrogen atoms characteristically have a positive charge due to the presence of a proton in the nucleus, which spins on its principle axis and consequently induces a magnetic charge (Hashemi, 2004). In the natural state, the orientation of these protons is random; however, if a large artificial magnetic force is introduced (e.g. in a MRI scanner), the protons align with the direction of the new magnetic field (McRobbie, 2007). The frequency at which these protons spin on their axis is known as the precessional (or Larmor) frequency (Mitchell, 2004).

The application of radio frequency (RF) waves provides the protons with an additional burst of energy, which causes them to change their orientation of spin to a higher state (i.e. in the opposite direction to the magnetic field); this only occurs when the RF is the same as the Larmor frequency of the particular proton (Papanicolaou, 1998). When the RF stops, these high-energy protons gradually lose their energy, returning to align with the magnetic field and consequently emitting RF energy, which is detected by the MR scanner (Jezzard, 2001). The change in the orientation of the protons is due to loss of energy from the RF but also due the inhomogeneity of the applied magnetic field (Papanicolaou, 1998). The inconsistency in the magnetic field leads to variation in the Larmor frequency throughout the ocular tissue, which subsequently leads to differences in the RF signals emitted (Hashemi, 2004). The technique enables the MR scanner to determine the density of each frequency, thus reflecting the amount of tissue at a given point (Jezzard, 2001). The time taken for the proton to return to the normal state determines whether the scan is termed T1 or T2 (Hashemi, 2004).

14.2 Study Objectives

It is generally accepted that myopia is a consequence of the optical facility provided by the anterior segment components failing to compensate for the concurrent growth of the posterior vitreous chamber (Zadnik *et al.*, 2003; Jones *et al.*, 2005). Despite several investigations into the gross morphological parameters of the eye and its internal structures (Atchison *et al.*, 2005; Singh *et al.*, 2006; Richdale *et al.*, 2009), few studies appear to have evaluated the structural characteristics of the anterior segment of the globe. As the scleral properties of the eye influence the conformation of the globe, an assessment of the 3-D depiction of the anterior segment is pertinent to the present investigation into human scleral biomechanics. Hence the objective of the present study was to evaluate the surface areas (SAs) and bulbosity of four anterior segment regions extending approximately 3.5-9 mm along the axial length and to determine whether these structural characteristics are affected by refractive status and associated axial length.

14.3 Method

Forty-three young adult subjects (mean 28.65 ± 6.2) were scanned using a whole body MRI scanner (3-Tesla Trio; Siemens, Erlangen, Germany). Ethical approval and the exclusion/inclusion criteria followed those detailed in Chapter 6. The Zeiss *IOLMaster* and the Shin-Nippon auto-refractor were utilised as in Chapter 6 to obtain ocular biometry and refractive error data for the present investigation.

14.3.1 Image acquisition

MR images were acquired using an eight-channel phased-array head coil, which allows simultaneous scanning of both eyes with a high signal-to-noise ratio. T2- weighted scans were obtained using an imaging protocol that allowed high definition delineation of the ocular surfaces. These scans were performed using a half-acquisition turbo spin echo sequence (HASTE) (Lagrèze *et al.*, 2009; Patel *et al.*, 1997) with the scanning parameters set as follows; 35 to 45 slices; 512 x 512 matrix; 256-mm field of view; 1 mm slice thickness; TR, 1240 ms; TE, 124 ms; flip angle, 150° ; 6 averages; 4/8 partial-phase acquisition; GRAPPA (generalised autocalibrating partially parallel acquisition) accelerator factor of 4. Subsequently the T2-weighted MR images (voxel thickness 1.0 x 1.0 x 1.0 mm) produced by this sequencing were optimised to allow discrimination of the eye's fluid-filled chambers from the rest of the head scan. During scanning, subjects were

asked to fixate on a distance target viewed through an angled mirror mounted on the head coil. Average scanning time was 5 minutes and 40 seconds.

14.3.2 Image analysis

The MR images were analysed using a specially modified version of freeware software, *mri3dX* (Singh *et al.*, 2006). The analysis initially involves labelling of the T2 weighted image voxels with the use of a 3-D flood-filling algorithm. This procedure known as shading, allows manual manipulation of the image to facilitate identification of geographic locations such as the anterior pole and differentiation of the anterior and posterior chambers for volume determination (Chapter 13). A spherical mesh comprising approximately 32K regularly spaced triangular polygons of equal area then encapsulates the shaded eye. A 3-D model of the globe is created by an automatic segmentation and meshing algorithm via an iterative shrink wrapping process centered about the geometrical centre of the initial sphere. Finally, the triangular polygon mesh is averaged locally to produce an improved 3-D depiction of eye shape (Figure 14.1; see Singh *et al.*, 2006).

To determine regional conformation of the globe, vector co-ordinates of the 3-D surface polygons were designated as superior-temporal (ST), superior-nasal (SN), inferior-temporal (IT) and inferior-nasal (IN). These divisions are based on a standardised co-ordinate system where the longitudinal axis of symmetry is projected from a line connecting the geometric centre of the eye to the anterior corneal pole. Whereas the procedure cannot account fully for the discrepancy between visual and optical axis (i.e. angle alpha) the discrepancy can be considered relatively small for anterior regions of the globe.

To illustrate morphological features of the globe, the 3-D array of polygons is then collapsed to provide a 2-D representation of each quadrant. The MRI data are initially represented along a percentage scale for the length of the given eye. By subsequently determining the length of the eye along each quadrant these percentage values can then be equated to distances (mm) along the axial length. Data were initially extracted for 15%-100% along the axial length for all quadrants. As the area of special interest for the anterior section lies between ~3.5-9 mm (equivalent to approximately 15%-40% along the axial length, Figure 14.1) a second order polynomial (Eq 14.1) was fitted to each quadrant for this range.

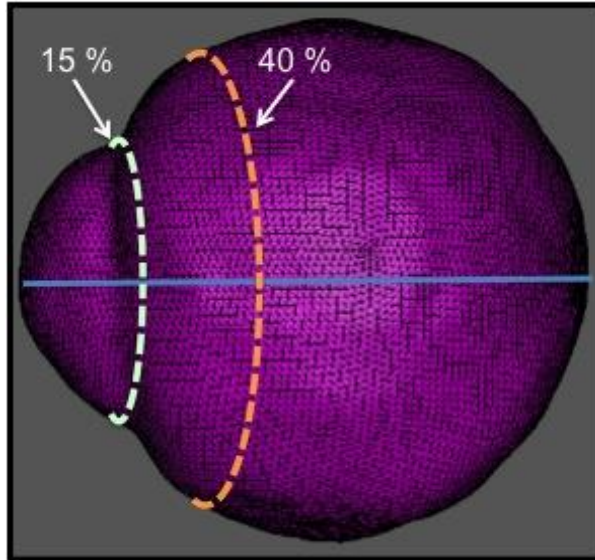


Figure 14.1 Diagrammatic depiction of the 15%-40% axial length range assessed.

Next, the second order polynomial was integrated and rotated about the x-axis to generate a surface area (SA) by rotation. By dividing the segment area by four a measure of the relative SA for each quadrant was determined (Eq 14.2). The coefficient of the x^2 polynomial provides a measure of the bulbosity of each respective quadrant.

$$y = ax^2 + bx + c \quad \text{Eq 14.1}$$

The values a, b, and c represent coefficient values for the polynomial.

SA calculations were made using a formula developed in collaboration Dr Bill Cox, Aston University.

$$S = \frac{\pi}{32a^2} \left[t\sqrt{1+t^2} (2t^2 + 4(4ac - b^2)) + (4(4ac - b^2) - 1) \ln(t + \sqrt{t^2 + 1}) \right]_{t_1}^{t_2} \quad \text{Eq 14.2}$$

Where $t_1 = b + 2al_1$ and $t_2 = b - 2al_2$ and SA represents surface area.

The values a, b and c correspond to the polynomial equation values of $y = ax^2 + bx + c$.

The values l_1 and l_2 (in mm) correspond to the respective 15% and 40% x-axis values.

As T2 weighted MR images were evaluated in the present study, both SA and bulbosity were measures of internal surface characteristics. These internal measures of the ocular conformation are likely to be representative of the external scleral shape and may thus provide an inferred assessment of the surface biomechanical properties.

14.4 Statistical analysis

Statistical evaluation was performed using *SPSS* version 15 for Windows (SPSS Inc, Chicago, IL) and Microsoft *Excel* (Microsoft Corporation, Redmond, Washington, USA). All data were initially examined for normal distribution using the Kolmogorov-Smirnov test.

As axial length is used as the reference for extracting the 15%-100% range of MRI data, inter-subject variability in axial length influences the width of this range and hence affect the size of the anterior region (15%-40%) of interest. The study protocol presently adopted controlled in part for this source of error: since the anterior 3.5 mm (15% along the axial length) is likely to vary with axial length, maintaining a constant end point at 9 mm (i.e. 40% along the axial length) ensured that the extent of the region assessed remained relatively constant between subjects.

Therefore to test initially for an effect of axial length on the SA and to assess for regional variation amongst the SAs, a one-way repeated measures ANCOVA was performed with quadrant SAs as the within-subject factor and axial length as the covariate. As a significant influence of axial length was demonstrated on the SAs (see below), multiple two-way mixed repeated measures ANCOVAs were performed to test for an effect of the between-subject factors: refractive status (myopes and non-myopes), gender, ethnicity (British White (BW) and British South-Asian (BSA)) and age (years) grouping ((18> - ≤29) (29> - ≤40)), on the within-subject factor SAs, whilst controlling for the effect of axial length.

In regards to bulbosity, a one-way repeated measures ANCOVA with quadrant bulbosity as the within-subject factor and axial length as the covariate failed to show a significant influence of axial length on bulbosity. In order to control for the possible artefactual effect of inter-subject axial length differences on the MRI measurements, multiple two-way repeated measures ANCOVAs were performed to test for the influence of the same between-subject factors as for SA (see above) on the within-subject factor bulbosity, whilst controlling for the axial length.

Each variable was assessed for the assumption of homogeneity of regression for individual quadrants before evaluation in the repeated measures ANCOVA models. On finding significant differences between SAs, a Bonferroni *post hoc* test was conducted to

determine pair-wise differences. Pearson's correlation coefficient was calculated to assess the relationship between SAs, bulbosity and ocular biometry parameters (i.e. axial length, ACD, corneal curvature). For all statistical tests a p-value of <0.05 was taken as the criterion for statistical significance.

14.5 Results

SA and bulbosity were assessed in 43 healthy individuals (16 males and 27 females) aged between 18-40 years (28.65 ± 6.20). Data were analysed for non-myopic and myopic individuals [non-myopes (MSE $\geq -0.50D$) n=20, MSE(D) mean \pm SD (0.57 ± 1.38) range (-0.50 to +4.38), AL (mm) mean \pm SD (23.37 ± 0.63), range (mm) (21.75 - 24.45); myopes (MSE $< -0.50D$) n=23, MSE(D) mean \pm SD (-6.37 ± 4.23) range (-20.50 to -0.75), AL (mm) mean \pm SD (25.77 ± 1.27), range (mm) (23.33 - 28.32)]. Only RE data will be discussed. For full details of statistical tests and results see Appendix 11.

14.5.1 Surface area

A one-way repeated measures ANCOVA demonstrated axial length to significantly influence SA ($F(1, 41)=4.962$ ($p=0.031$)). After controlling for the effects of axial length, significant differences were observed between quadrants ($F(2.314, 94.877)=12.493$ ($p<0.001$)), with the differences to lie between ST:IN, IN:IT and SN:IT.

Quadrant	Mean \pm SD	Min	Max
ST	106.07 \pm 5.70	93.50	115.78
IN	109.74 \pm 7.67	85.66	120.24
SN	108.46 \pm 5.63	91.04	121.09
IT	104.14 \pm 5.62	90.25	116.75

Table 14.1 RE surface areas of quadrants (mm²).

An ANCOVA testing for the effects of refractive status (myopes n= 23, non myopes n=20) revealed no significant effect for the axial length covariate ($F(1, 40)=0.845$ ($p=0.363$)) nor refractive status ($F(1, 40)=0.426$ ($p=0.518$)). However a significant interaction effect was noted between refractive status and regional differences ($F(2.412, 96.498)=4.269$ ($p=0.012$)) suggesting smaller temporal (ST and IT) and larger nasal (SN and IN) SAs in

myopes when compared to non-myopes. Regional differences were still found to be present ($F(2.412, 96.498)=15.093$ ($p<0.001$)) between ST:IN, IN:IT and SN:IT.

After controlling for the significant effect of axial length ($F(1, 40)=4.931$ ($p=0.032$)), no significant ($F(1, 40)=0.080$ ($p=0.779$)) influence of gender (male $n=16$, female $n=27$) was found on the measures of SA. Regional differences were still evident ($F(2.320, 92.802)=13.215$ ($p<0.001$)) however only between IN:IT and SN:IT. No interaction effect was observed between gender and regional differences.

Whilst controlling for a significant effect of axial length ($F(1, 40)=4.619$ ($p=0.038$)), ethnicity (BW $n=24$, BSA $n=19$) showed neither an influence ($F(1, 40)=0.057$ ($p=0.813$)) on SA nor an interaction with regional differences. The main effect of regional differences was still demonstrated ($F(2.310, 92.401)=13.349$ ($p<0.001$)) between ST:IN, IN:IT and SN:IT .

After accounting for a significant effect of axial length ($F(1, 40)=5.434$ ($p=0.025$)), age grouping ($(18>-\leq 29)$, $n=26$, $(29>-\leq 40)$ $n=17$) showed no significant effect on SA ($F(1, 40)=0.858$ ($p=0.360$)) nor an interaction effect with regional differences. Regional differences were still identified ($F(2.297, 91.890)=14.603$ ($p<0.001$)) however only between IN:IT and SN:IT.

Inter-quadrant SA correlations were evident, especially with quadrant IT. Axial length was found to correlate negatively and refractive error positively with SAs at IN, SN and IT. In regards to the keratometry measures, both flat and steep corneal curvatures were associated positively with SAs (IN, SN and IT). No relationship was found between ACD and SAs. See Appendix 11.

14.5.2 Quadrant bulbosity

The curvature for each region was represented as bulbosity and indexed by the x^2 coefficient of the second order polynomial for approx 3.5-9 mm section along the axial length.

Quadrant	Mean \pm SD	Min	Max
X^2 ST	0.075 \pm 0.022	0.036	0.120
X^2 IN	0.073 \pm 0.021	0.035	0.116
X^2 SN	0.083 \pm 0.024	0.037	0.146
X^2 IT	0.071 \pm 0.022	0.036	0.139

Table 14.2 RE bulbosity for the different quadrants.

A one-way repeated measures ANCOVA with axial length as the covariate, revealed no significant effect of axial length ($F(1, 41)=0.784$ ($p=0.381$)) on measures of bulbosity. Furthermore, no significant regional differences in bulbosity ($F(3, 123)=0.884$ ($p=0.451$)) were identified.

Refractive status (myopes $n= 23$, non myopes $n=20$), revealed no significant effect on bulbosity ($F(1, 40)=0.029$ ($p=0.866$)) nor an interaction effect while controlling for the non-significant effect of axial length ($F(1, 40)=0.479$ ($p=0.493$)). No significant regional differences in bulbosity were found ($F(3, 120)=2.619$ ($p=0.054$)).

After controlling for the axial length covariate ($F(1, 40)=0.483$ ($p=0.491$)), gender (male $n=16$ female $n=27$) showed no significant effect on quadrant bulbosity ($F(1, 40)=2.021$ ($p=0.163$)) nor an interaction effect. However males did show a non-significant trend for greater bulbosity for all quadrants than females. No significant regional differences in bulbosity were observed ($F(3, 120)=0.822$ ($p=0.484$)).

Similarly ethnicity (BW $n=24$, BSA $n=19$) demonstrated no significant effect ($F(1, 40)=0.032$ ($p=0.858$)) on bulbosity nor an interaction effect while controlling for the covariate of axial length ($F(1, 40)=0.795$ ($p=0.378$)). No significant regional differences in bulbosity were identified ($F(3, 120)=0.664$ ($p=0.576$)).

Age grouping ((18> - ≤29) n=26, (29> - ≤40) n=17) showed no significant effect on bulbosity ($F(1, 40)=0.703$ ($p=0.407$)) nor an interaction effect, whilst controlling for the axial length covariate ($F(1, 40)=0.573$ ($p=0.453$)). No significant regional differences in bulbosity were observed ($F(3, 120)=0.795$ ($p=0.499$)).

No significant correlations were found between both axial length and refractive error and the bulbosity values. Similarly neither corneal curvature nor ACD showed any relationship with the bulbosity measurements. Several inter-quadrant correlation were noted for bulbosity (see Appendix 11). Interestingly no correlation was found between SA and bulbosity measurements.

14.6 Discussion

Hitherto, no study is known to have examined scleral morphology of the human anterior segment *in vivo*. The data illustrate the novel findings of significant regional variation amongst the anterior segment (15%-40% along axial length) SAs with differences identified between quadrants ST:IN, IN:IT, SN:IT. Furthermore the study also established a significant interaction between SA and refractive error with myopic eyes showing reduced temporal (i.e. ST and IT) and increased nasal (i.e. SN and IN) SA when compared to non-myopic eyes. Additionally, increasing axial length and myopic refraction were associated with reducing SAs for IN, SN and IT. In spite of the regional differences between SAs, no significant variation was found between the bulbosity of the quadrants assessed.

14.6.1 Quadrant surface areas

The present findings of regional variation between SAs of the anterior segment quadrants further supports the previous observations of regional differences in scleral biomechanics (Chapters 6, 8 and 10). ***Despite the regional variation in SAs not corresponding exactly to the regional differences in scleral biomechanics, these findings are indicative of a contributory role of SA in the material properties of the ocular tissues.***

Additional support for SA variation amongst the quadrants can be found from studies investigating the internal dimensions of the anterior segment related to intraocular lens sizing (Werner *et al.*, 2008; Rondeau *et al.*, 2004; Baikoff *et al.*, 2005). Such studies have reported that the anterior eye fails to exhibit the commonly assumed geometrically

spherical shape but in fact shows considerable anatomical variation in its configuration (Werner *et al.*, 2008; Rondeau *et al.*, 2004). Thus the internal dimensions of the anterior eye are likely to affect the overall conformation of the anterior segment and may explain the variation in SAs presently found.

Aside from regional differences in SA, the present investigation also showed an inverse relationship between increasing axial length and reducing SA. These findings would imply a mechanism of structural remodeling by which the diameter of the anterior segment is constrained during myopic growth. In regards to myopigenesis, investigators have hypothesized that a restriction in the anterior region of the processes that govern crystalline lens flattening with axial length expansion may result in the failure to achieve an emmetropic state (Mutti, 2010). Considering this supposition, the present findings would indicate that anterior surface shrinkage and constraint, with axial length expansion provides greater resistance to the crystalline lens flattening hence stimulating myopic growth. Moreover the notable findings of reduced temporal and increased nasal SA in myopic eyes provides further evidence for a significant influence of refractive status on the anterior segment configuration. In a recent animal model study assessing anterior scleral cross-linking and exposure to form vision deprivation (FVD) in guinea pig eyes, McFadden *et al.*, (2010) reported cross-linkage treatment to the anterior 2/3 of the sclera to significantly alter the shape of the eye reducing the equatorial diameter but without affecting the normal growth of the posterior pole. In view of the present findings, these observations are suggestive of an important role of the anterior scleral biomechanics in modulating myopic growth.

14.6.1.1 Temporal/Nasal asymmetry of anterior SA and ocular globe conformation

It is unclear why the temporal region should show a marked reduction in SA with myopic growth. It may be that the smaller temporal SA is a consequence of reduced stretching along the temporal regions in myopic eyes; alternatively, and assuming a constant tissue volume, the smaller SA may be a subsequent effect of equatorial expansion which leads to reduced tissue mass in the more anterior and posterior regions which may be more notable.

In regards to the first explanation of a restriction to tissue expansion across the temporal regions, it is possible that these findings may be indicative of differential scleral biomechanics between the nasal and temporal regions seen in Chapters 6, 8 and 10. In

Chapter 10 the investigation demonstrated significantly reduced scleral resistance for the temporal region (ST and IT) at 8 mm from the limbus when compared to the 4 mm site. ***These findings would suggest increased scleral resistance at the more anterior 4 mm site hence presumably greater resistance to expansion.***

Furthermore in Chapter 13 myopes showed a significantly thicker ciliary muscle profile when compared to non-myopes though notably this structural variation was found to be greater temporally than nasally. These findings might indicate that the greater mass of the temporal ciliary muscle in myopic eyes provides a greater resistance to stretching during axial expansion. According to Park *et al.*, (2010) anterior segment changes in myopic eyes such as increased ACD and flatter corneal curvature would suggest that axial elongation affects the region between the limbus and the ciliary body. ***In fact the present study demonstrated a significant positive relation between both flat and steep corneal curvature and increasing SA; therefore differential resistance to tissue stretching may result in regional variation in SAs in myopic eyes.***

Regional differences in SA with increasing axial length might also be a consequence of anatomical differences between the medial and lateral orbital walls. The medial wall is the thinnest orbital wall (i.e. 0.2-0.4 mm) and is the only wall that is not obviously triangular in shape (Forrester, 2008; Bron, 1997). Being exposed to greater levels of stress, the lateral wall is the thickest orbital wall particularly at the orbital margin (Forrester, 2008; Snell and Lemp, 1997). Behind the orbital margin the lateral wall thins slightly, then thickens again and finally thins once more where it joins the middle cranial fossa at which point it is only 1 mm thick (Bron, 1997). Such structural differences between the orbital walls may transmute to an asymmetry in the resistance offered during ocular growth. ***Hence differential levels of anatomical restriction to ocular expansion anteriorly especially near the orbital margin, may explain the present findings of smaller temporal SAs in the larger myopic eyes.*** Interestingly in a MRI study Chau *et al.*, (2004b) failed to show an association between ocular and orbital volumes. Moreover in regards to orbit growth the same investigators noted that only the lateral orbital distance and the inter-temporal distance in the equatorial direction continue to increase in size throughout childhood. Such differential orbital growth rates may further explain the propensity for regional differences in ocular conformation in myopia.

Given the association between near work and myopia (Rosenfield and Gilmartin, 1998), it may be that increased levels of convergence in myopic eyes have a stretching effect on the nasal aspects of the anterior segment hence resulting in a larger SA. In fact the medial rectus muscle has a closer insertion to the cornea (5.5 mm) than the lateral rectus (6.9 mm) muscle (Bron, 1997) suggesting that its contraction on convergence may potentially bring about greater stresses on the anterior sclera thus promoting extension of the nasal SA.

The general consensus from human MRI studies examining ocular conformation in different refractive status indicates that all eyes generally exhibit a sphericoelliptical shape (Chen *et al.*, 1992; Cheng *et al.*, 1992), which is usually oblate in conformation (Atchison *et al.*, 2005). In myopia the eye shows a similar configuration although all dimensions of the globe are greater with a tendency towards a less oblate and a relatively more prolate shape (Atchison *et al.*, 2005). Similar findings have also been noted in MRI studies evaluating ocular shape in animal models (*Macaca Mulatta*) of myopia (Huang *et al.*, 2009; Smith *et al.*, 2009). Furthermore when considering the linear dimensions of the globe, most studies have reported the axial length to be a significant correlate of myopia when compared to the horizontal and vertical dimensions (Atchison *et al.*, 2005; Miller *et al.*, IOVS 2004, 45: ARVO E-Abstract 2388).

Contrary to these findings, when Cheng *et al.*, (1992) assessed their MRI images, they measured the ocular dimensions from outside the scleral boundary and reported that myopic eyes were longer horizontally than axially and longer axially than vertically. Interestingly in another MRI study Miller *et al.*, (2004) noted axial length to be the principal structural correlate in myopia but also found that in low to moderate myopia abnormal equatorial growth also occurred; equatorial expansion in myopic eyes has also been noted by other investigators (Singh *et al.*, 2006; Nagra *et al.*, IOVS 2009, 50: E-Abstract 3941).

In a study applying the same MR imaging protocol as that of the present investigation Singh *et al.*, (2006) reported some eyes to demonstrate nasal/temporal asymmetry in the equatorial region with the temporal regions showing increased bulging when compared to the nasal regions. Similarly in another study by the same group, Nagra *et al.*, (2009) assessed maximum distance (MD) from the visual axis to the inner aspect of the ocular surface from the nodal point to 70% along the axial length for quadrants (superior: S, inferior: I, temporal: T and nasal: N). Pertinent to the present study the investigation noted

increased MD for all quadrants in myopes when compared to emmetropes but especially marked expansion of the temporal region in myopic eyes. These reports of asymmetric growth at the equatorial region may be a result of differential scleral biomechanics in this region. In regards to scleral thickness and its probable affect on tissue biomechanics, Olsen *et al.*, (1998) reported a reduction in thickness near the equatorial region (12-17 mm from the limbus), which would correspond approximately with the site (50% along the axial length) of expansion noted by Nagra *et al.*, (2009). Moreover considering the results of Chapter 7, scleral thickness was found to be lower along the temporal meridian when compared to the nasal, further implying reduced resistance to growth along the temporal region. ***Considering these findings of equatorial expansion, which may be particularly biased to the temporal regions, it can be reasoned that, assuming a constant mass of scleral material, enlarging of the equatorial regions may result in remodeling of the anterior and posterior regions of the globe.*** This speculation would suggest reduced temporal SA at the anterior and posterior globe.

Nasal/temporal asymmetry along the posterior globe in humans has been noted previously. In a 3-D MRI study that scanned eyes over a wide range of refractive error, Logan *et al.*, IOVS 2005 46: E-Abstract 4266 reported an asymmetric configuration with the nasal vitreous chamber exhibiting greater steepness than the temporal region. Similarly in another MRI study assessing linear dimensions in emmetropic and myopic eyes, Atchison *et al.*, (2004) reported asymmetry in globe conformation to be common, with some eyes showing particularly steeper retinal boundaries especially on the nasal side. Furthermore peripheral refraction studies have also shown nasal/temporal asymmetry in myopic eyes (Chen *et al.*, 2010c; Taberner and Schaeffel, 2009; Seidemann *et al.*, 2002). In their study assessing peripheral refraction with a computer modeling program in iso- and anisomyopes of Caucasian and Taiwanese-Chinese ethnicity, Logan *et al.*, (2004) reported the more myopic eyes amongst Caucasians to show reduced expansion of the temporal retinal sector in comparison to the nasal regions. These findings further support the reports of nasal/temporal asymmetry in eye shape, but additionally suggest that the asymmetry in posterior ocular conformation may have a genetic component as the asymmetry was not observed amongst the Taiwanese-Chinese individuals (Logan *et al.*, 2004). ***These reports of an irregular configuration of the posterior segment suggest that the ocular globe may demonstrate differential growth rates along the nasal/temporal regions and that the properties of the sclera material and associated anatomical restrictions may dictate the shape of the globe both anteriorly and posteriorly.***

In regards to the cause of such differential growth patterns there is little literature in humans that would suggest a genetic or environment factor that may result in asymmetry of anterior segment SA with myopia. In animal myopia studies where part of the visual field is obscured in chick and tree shrew eyes (Hodos and Kuenzel, 1984; Wallman *et al.*, 1987; Gottlieb *et al.*, 1987; Norton and Siegart, 1991) the models have shown the eye to grow asymmetrically. In a more recent 3-D MRI study examining globe conformation *in vivo* Smith *et al.*, (2009) demonstrated rhesus monkeys (*Macaca Mulatta*) to also show differential ocular growth when subjected to hemiretinal form deprivation. Variation in the structure of the sclera in chicks and non-human primates (Norton, 1999), suggests that similar experimental manipulation of visual input may result in different ocular configuration (Smith *et al.*, 2009). In chicks the sclera has an additional cartilaginous layer, which is relatively rigid (Norton, 1999), and with vision deprivation causes a prominent bulge that corresponds to the area of deprivation (Troilo *et al.*, 1987; Wallman *et al.*, 1987). As the primate sclera is less rigid it has been hypothesized that the ocular expansion is likely to be more uniform and symmetrical thus leading to a more prolate shape (Smith *et al.*, 2009). In a recent study assessing the impact of short term monocular defocus in human eyes, Read *et al.*, (2010) demonstrated axial length changes modulated by choroidal thickness, that were comparable to those seen in animal models of myopia. These findings indicate that a vision-dependent feedback mechanism modulates ocular shape and refractive error development (Smith, 1998; Wallman and Winawer, 2004), although it is unclear how this may occur in long term myopia development in humans.

The link between the amount of time spend outdoors and the reduced risk of myopia (Jones-Jordan *et al.*, 2010; Rose *et al.*, 2008; Dirani *et al.*, 2009) would suggest that an environmental factor might be important in determining globe conformation. It is unclear as to why increased outdoor activities should act as a protective mechanism for myopia development (Mutti, 2010, Rose *et al.*, 2008). One theory suggests light intensity to be an important factor, in that the reduced pupil sizes outdoors would result in increased depth-of-field and hence subsequently reduce image blur. Since image blur in general has been postulated to stimulate myopic growth (Wallman and Winawer, 2004; Gwiadza *et al.*, 2005) time outdoors would hence serve as a protective mechanism (Rose *et al.*, 2008). Another theory relates light stimulated release of dopamine from the retina and the inhibitory effect of dopamine on ocular growth (McCarthy *et al.*, 2007). In regards to the latter theory it may be hypothesised that differential retinal exposure to light brings about

local differences in growth rates, which may result in regional variation in the posterior segment conformation; however, this hypothesis need clinical evidence and is difficult to confirm. In view of the present findings of variation in anterior segment SAs it may possible to question whether regional differences in posterior segment remodelling in myopia may also have a secondary affect on the anterior aspects of the globe.

14.6.2 Quadrant bulbosity

Despite the findings of regional variation in anterior segment SA, no significant difference was found between the bulbosity of different quadrants. These findings may be linked to the observations of Chapter 13 where anterior ocular volume was found to be independent of axial length and refractive status. These observations would imply that, despite the SA changing with myopia, the bulbosity and volume of the anterior segment are maintained constant irrespective of axial length expansion. In geometric terms the volume and surface area are not related i.e. volume may stay constant yet the surface area may change. Similarly bulbosity is an index of the degree of protrusion of a particular element of shape and hence is independent of SA and volume.

14.6.2.1 Quadrant Bulbosity and globe conformation

The anterior globe has previously been shown to have an approximate uniform geometric conformation. In an MRI study, Gilmartin *et al.*, IOVS 2007, 48: E-Abstract 1215 evaluated the globe conformation in myopia by measuring sphericity along the 2nd, 3rd and 4th quartile of the axial length. The study reported constant sphericity for the 2nd and 3rd quartile but a change in globe conformation at the 4th quartile. The investigators suggested that the differential structural conformation between the quartiles would indicate that the 2nd and 3rd quartile were a result of pre-programmed genetic growth process whilst the 4th quartile demonstrated visually modulated growth patterns. In a similar study Nagra *et al.*, (2009) assessed bulbosity of quadrants (S, T, I and N) between the nodal point (NP) and 70% along the axial length and from 70%-100%. The investigation showed no significant difference in bulbosity between quadrants in the NP-70% range but reported significant quadrant differences in bulbosity between 70%-100%. As mentioned afore the Nagra *et al.*, (2009) study also assessed globe conformation by measuring maximum distance (MD) from the visual axis to the inner aspect of the ocular surface at the equatorial region and found significant regional variations. Hence these findings would imply that despite

differential regional ocular expansion (equatorial and anterior) the actual surface curvature characteristics remain constant.

14.6.3 Ocular surface characteristic and scleral biomechanics

Intuitively, variation in curvature properties would be expected with regional variation in expansion and biomechanical properties (Chapters 6, 8 and 10). If the surface characteristics reflect the nature of scleral biomechanics these findings are contrary to the reports of increased scleral curvature with increasing internal stress (Asejczyk-Widlicka and Pierscionek, 2008a) as presumably when regions expand the stress they are subjected to increases concomitantly (Friedman, 1966). The present study did not assess curvature differences *per se* since bulbosity is a characteristic of curvature. Therefore in regards to bulbosity it is likely that anatomical constraints imposed by the surrounding tissue are likely to ensure uniformity between the different quadrants assessed. ***In view of the present findings these results suggest that the regional differences in scleral biomechanics and SA are unlikely to be related to the curvature characteristics of each of the different regions.*** Moreover in regards to structural changes with myopia these observations imply that despite the SA reducing with increasing axial length the actual bulbosity of the quadrant remains constant.

Neither ethnicity nor age grouping were found to have a significant influence on SA and bulbosity. Similarly no significant male/female differences were found for SA although a trend for increased bulbosity amongst male subjects was noted. Indeed gender differences have been noted previously with males showing larger eyes than females in all dimensions (i.e. length, height and width) (Atchison *et al.*, 2004), which may presumably affect the surface characteristics of the globe. However contrary to these observations Chapter 13 demonstrated no significant differences between male/female for either anterior or posterior ocular volumes. Moreover in Chapter 7 overall scleral thickness was found to be greater for males when compared to females. These inconsistent findings of gender differences between various structural features of the globe suggest that the surface characteristics i.e. ocular tissue biomechanics of the eye may be particularly influenced by gender and hence would support the findings of increased scleral resistance amongst male subjects in Chapter 10.

14.7 Conclusion

The key findings of the present study are:

- Anterior segment SAs for quadrants (ST, SN, IT and IN) between 15%-40% along the axial length demonstrated significant regional variation, with significant differences between quadrants ST:IN, IN:IT, SN:IT.
- Refractive status was found to have a significant interaction with quadrant differences with smaller temporal and larger nasal SAs in myopic eyes when compared to non-myopic eyes.
- Increasing axial length and myopic refractive error were found to be associated with reducing SA suggesting anterior segment constriction especially for quadrants IN, SN and IT.
- Despite significant differences between the regional SAs, no significant differences were found between the bulbosity of the various quadrants.

15.0 GENERAL DISCUSSION

15.1 Introduction

The biomechanical properties of the cornea and sclera are of increasing interest owing to their putative roles in myopia, glaucoma and age related macular degeneration (AMD). There is however a significant paucity of literature on the biomechanics of the human sclera. Such limited knowledge and understanding is attributable to the technical challenge posed in assessing the sclera's viscoelastic characteristics while accounting for its complex inter-relationships with other ocular components. Hitherto much of the literature on the material properties of the sclera has been limited to *in vitro* extensiometry studies or to assessment of the response of the sclera to induced changes in ocular pressure and volume. Whereas these investigations have provided valuable insight into scleral biomechanics they are subject to significant experimental assumptions. *Therefore the principal objective of the thesis was to address this deficit in the literature and to investigate the biomechanical properties of the anterior sclera and cornea in vivo, in the context of their possible association with myopia.*

15.2 The assessment of scleral biomechanics *in vivo*

As detailed in Chapter 9 there are several limitations to evaluating the biomechanical properties of the sclera *in vitro*. Therefore a primary aim of the thesis was to assess existing and new *in vivo* methods of inferring the properties of the scleral material. The Schiøtz tonometer has long been used for determining corneal rigidity and has been shown to have a possible application in assessing scleral biomechanics (Schmid *et al.*, 2003). *Chapters 6 and 10 confirmed the utility of the Schiøtz tonometer in examining scleral resistance;* although highlighted its limited applicability to the sclera due to the use of transformation algorithms based on empirical data taken from the cornea. *Therefore following a systematic calibration exercise with reference to agarose biogels of varying Young's moduli (Chapter 9), the novel application of rebound tonometry to the sclera demonstrates an alternative and viable method of determining scleral resistance (Chapter 8).*

On application of the Schiøtz and rebound tonometer to the sclera, it is important to note that the measure of scleral resistance determined by these instruments comprises the gross

mechanical resistance offered by a variety of ocular tissues and that identifying the contribution of specific tissues is restricted. However as the sclera constitutes the largest proportion of the ocular coat it can be reasonably presumed that the biomechanical resistance demonstrated is largely attributable to the sclera.

15.3 Regional variation in scleral biomechanics

Using both Schiötz and rebound tonometry to measure scleral resistance, the thesis demonstrates strong evidence for the presence of regional variation in scleral biomechanics. With both techniques scleral resistance was shown to be lowest in the superior regions and greatest in the inferior regions with a trend for the least resistance being in the superior temporal region and greatest resistance in the inferior nasal region. Furthermore Chapter 10 demonstrated the characteristics of the regional variation to differ with distance from the limbus implying significant heterogeneity in anterior scleral biomechanics.

Previous *in vitro* investigations into scleral biomechanics have reported regional (Smolek, 1988; Elsheikh *et al.*, 2010) and meridional differences (Bisplinghoff *et al.*, 2009; 2008) but these studies have been focused on either the posterior sclera or the whole globe. The significant meridional differences in scleral thickness observed in Chapter 7 and regional differences in surface area found in Chapter 14 provide additional support for the presence of regional variation in scleral resistance. ***Despite the differences in scleral thickness and surface area not corresponding precisely to the changes in scleral resistance, it can nevertheless be reasonably presumed that they are likely to be significant factors in governing tissue resistance.*** Discrepancies in regional variations of the different scleral parameters may be attributable to inter-subject variability coupled with the inherent variability of the measurement techniques employed.

Furthermore, variation in scleral resistance is likely to be affected by the internal shape and conformation of the anterior segment (Werner *et al.*, 2008; Rondeau *et al.*, 2004), ***although Chapter 14 failed to show any significant regional differences in scleral bulbosity.*** It is also likely that regional variation in the scleral collagen infrastructure (Thale and Tillman, 1993 Gathercole and Keller, 1991) may influence the local biomechanics, which may presumably lead to regional differences in scleral resistance.

15.4 Scleral biomechanics and myopia

Of relevance to the aetiology of myopia is whether regional variation in the biomechanical properties of the anterior sclera affects the conformation of the whole globe. Considering the role of the anterior segment in the emmetropization process, it seems plausible to question whether the biomechanical properties of anterior sclera modulate the refractive changes that occur during myopia development. *A particularly noteworthy finding from the Schiötz and rebound tonometry studies is the consistent findings of reduced resistance of the anterior temporal sclera compared to the anterior nasal sclera, suggesting an inherently weaker temporal sclera.* Of note is that the posterior temporal sclera is the first to rupture in pressure-volume tests (Greene and McMahon, 1979) and is often the site of myopic staphyloma (Curtin, 1985).

In Chapter 10 differential scleral resistance was demonstrated across the horizontal and vertical regions at the 4 mm location. *The data suggested the vertical regions to exhibit lower resistance than the horizontal regions.* Interestingly in Chapter 7 longer axial length and myopic refractive error were found to be related to increasing scleral thickness along the vertical meridians, anterior to 4 mm from the limbus. Moreover in Chapter 13 scleral thickness was negatively associated with increasing ciliary muscle thickness (which was found to be associated with increasing axial length) particularly along the superior-nasal and inferior meridians, but posterior to 3 mm from the limbus. *Together these findings of changes in scleral material with axial expansion and refractive status suggest that the anterior ocular conformation may be susceptible to alteration with myopic growth.*

Furthermore, in regards to ocular shape differences between refractive groups, the increased tendency for a less oblate and a relatively more prolate conformation in myopes (Atchison *et al.*, 2005) may be related to differential biomechanical resistance to stretching along the vertical/horizontal meridians. The present findings suggest that an increase in scleral thickness along the vertical meridians with longer axial length may provide an anchorage to the stretching mechanism during ocular growth, thus allowing the equatorial and posterior regions to stretch into a prolate conformation. Further evidence for the influence of the anterior segment in myopia was observed in Chapter 14 where surface area exhibited a nasal/temporal asymmetry with myopic growth. The data demonstrated smaller temporal and larger nasal surface area in myopic eyes when compared to non-myopic eyes. It was speculated that differential levels of anatomical restriction to ocular expansion

anteriorly especially near the orbital margin, may explain the asymmetry between the nasal/temporal surface areas.

Nevertheless, there is uncertainty as to whether anterior scleral biomechanics contributes to refractive error development since much of the literature has concerned posterior scleral biomechanics. In a recent animal model study assessing anterior scleral cross-linking and exposure to form vision deprivation in guinea pig eyes, McFadden *et al.*, (2010) reported cross-linkage treatment to the anterior 2/3 of the sclera to significantly influence the equatorial expansion characteristically observed in myopic growth. In spite of these supportive findings for a role of the anterior segment biomechanics in myopic growth, there is a particular challenge in discerning the biomechanical differences between myopes and non-myopes. A number of reports have suggested significant inter-individual differences in ocular shape (Atchison *et al.*, 2004; Stone and Flitcroft, 2004) implying that if scleral biomechanics is linked to ocular conformation this may well also show significant individual variation. Therefore to partly account for such inherent variability in the population, the thesis examined two subgroups of subjects; a mixed British White (BW)-British South Asian group in the UK with a wide range of refractive error and a group of Hong Kong Chinese (HKC) individuals in HK who were predominantly myopic. ***By comparing the homogenous myopic HKC individuals to the mixed BW-BSAs, it was envisaged that scleral biomechanical differences between the two population samples would provide an insight into the structural correlates of the higher prevalence of myopia amongst Chinese individuals.***

Interestingly, with rebound tonometry the mean scleral resistance for the HKC subjects was significantly greater for all regions when compared to the BW-BSAs. In regards to the aetiology of myopia, these findings of increased anterior scleral stiffness in the predominantly myopic HKC group may suggest that a more rigid sclera is less likely to allow stretching for the purposes of lens thinning during emmetropization; thus supporting the hypothesis that anterior segment restriction promotes myopic growth (Mutti, 2010). In regards to causes of the increased anterior scleral resistance, Chapter 14 demonstrated increasing axial length and myopic refractive error to be associated with reducing anterior surface area, which may consequently lead to greater levels of tissue resistance.

Furthermore, in comparison to the BW-BSAs, the HKC subjects demonstrated fewer regional differences in scleral resistance, hence implying their anterior scleral

biomechanics to be more uniform than that of the BW-BSAs. Assuming that regional differences in scleral biomechanics produce local variation in ocular conformation, the posterior conformation of Chinese-Taiwanese individuals has been previously found to be more uniform than that of Caucasian subjects (Logan *et al.*, 2004). ***These findings would suggest that the more homogenous anterior scleral resistance present in the HKC individuals might be consistent with a more regular posterior segment configuration.***

15.5 Corneal biomechanics and myopia

In contrast to scleral biomechanics, the material properties of the cornea have been widely studied owing to their affect on measurement of IOP (Doughty and Zaman, 2000; Liu and Roberts, 2005). Reduced corneal rigidity has frequently been associated with myopic refractive status. Contrary to these findings, ***corneal rigidities determined with the Schiøtz tonometer failed to show an association with refractive error in Chapters 6 and 10.*** Similar findings have been noted by previous investigators (Wong *et al.*, 1991; Zolog *et al.*, 1969), but the failure to detect a relationship between refractive error and corneal rigidity may also be a consequence of significant inter-subject and instrument variability.

Corneal biomechanics were also evaluated with the Ocular Response Analyser (ORA) providing measures of corneal hysteresis (CH) and corneal resistance factor (CRF). ***In Chapter 11, both CH and CRF were found to be negatively associated with increasing axial length amongst the BW-BSA individuals.*** These findings suggest that lower CH and CRF may perhaps be linked to a corneoscleral shell that is more predisposed to axial elongation. Despite these suggestions for an association between corneal biomechanics and myopia, a similar relationship was not evident for the predominantly myopic HKC group. These disparate findings between the two population samples perhaps indicate important structural differences associated with ethnicity that may be linked to the different levels of myopia prevalence.

Additional inter-ethnic differences were noted in Chapter 11 such that ***HKC subjects showed increasing IOP with progressively longer axial length, a relationship not observed in the BW-BSA group.*** Several investigators have reported increased IOP with myopia (Wong *et al.*, 2003; Nomura *et al.*, 2004) although the literature is equivocal as to whether this is a precursor to axial length growth or a consequence of increased globe size. However on application of Laplace's Law to the myopic eye (as advocated by Lee and

Edwards, (2000)), these findings would suggest that the HKC eyes are subjected to greater levels of stress with increasing axial expansion, thus possibly explaining the increased anterior scleral resistance identified in Chapter 8.

The increasing levels of eye wall stress with axial expansion may potentially contribute in the pathogenesis of myopia. Furthermore the frequently reported association between myopia and glaucoma may also be associated with the greater levels of stress with increasing axial length and higher levels of IOP (Cahane and Bartov, 1992). Posterior scleral biomechanics have been widely implicated in the pathogenesis of glaucoma (Eilaghi *et al.*, 2010), but the findings of Chapter 7 also suggest a role for the anterior scleral biomechanics. ***Chapter 7 suggested reduced CCT to be related to increased anterior scleral thickness.*** Since reduced CCT has been found to be a significant risk factor in the aetiology of glaucoma, a concomitant increase in scleral thickness may result in greater anterior scleral stiffness. As such it may be speculated that the increased anterior scleral resistance may reduce its ability to absorb the stress of the IOP, hence increasing the mechanical stress imposed on the optic nerve head.

The main ORA corneal biometrics were unable to demonstrate significant differences between ethnicity and refractive status, although on assessment of the additional waveform parameters (AWPs) significant differences were identified for several parameters. These findings suggest that anterior segment biomechanical differences are likely to be present between refractive groups and ethnicities but that these changes may not be discernable using the techniques presently available. However the findings of Chapter 11 suggest that by assessing the waveform morphology of the ORA corneal response, may provide scope for better understanding of these biomechanical differences. On examination of the anterior segment structures most likely to have contributed to the AWP differences found between refractive groups and ethnicities, several structural features such as anterior and posterior curvature, anterior chamber depth/volume and corneal thickness were identified. These findings would suggest that myopia may be related to specific alterations in anterior segment structure, which may occur independently, or in association with other structural changes.

15.6 Ciliary muscle thickness and myopia

Another anterior segment structure that has been recently implicated in the aetiology of myopia is the ciliary muscle. Reports of increased ciliary muscle thickness (CMT) in myopic adults (Oliveira *et al.*, 2005) and children (Bailey *et al.*, 2008) have generated the notion that greater CMT may have a role in the restriction of the equatorial expansion associated with the crystalline lens flattening during emmetropization (Mutti, 2010). In support of these findings, *Chapter 13 demonstrated refractive status and axial length to be associated with the location of CMT with myopes showing a trend for a thicker ciliary muscle profile when compared to non-myopes. Furthermore posterior ocular volume was found to be a more powerful predictor of CMT than axial length.* In regards to the mechanical affects of the ciliary muscle, Fujikura *et al.*, (2002) suggested that the mechanical strain imposed by the ciliary muscle during accommodation is likely to stimulate the activation of MMP-2 by the scleral fibroblasts. Hence presumably the greater CMT in myopic eyes would augment the levels of stress imposed on the sclera, which may subsequently promote extracellular matrix degradation and thus accelerate myopic growth. *These findings would imply that the morphological characteristics of the ciliary muscle may influence the conformation of the globe during myopic growth.*

15.7 The effect of ethnicity and myopia on scleral and corneal biomechanics

The thesis provides evidence for a significant influence of ethnicity on scleral and corneal biomechanics. In Chapter 10 scleral resistance was found to be significantly higher amongst the BSAs when compared to the BW individuals, whilst in Chapter 8 the HKC group demonstrated significantly higher scleral resistance when compared to the BW-BSA group. Moreover in Chapter 7 BSAs showed a non-significant trend for thicker sclera when compared to the BW individuals. Similar ethnic differences in scleral thickness were also observed by Oliveira *et al.*, (2006) who reported scleral thickness to be thinner in Caucasians when compared to non-Caucasian subjects. In regards to the cornea, ethnic differences in CCT have frequently been reported (Aghaian *et al.*, 2004; Nemesure *et al.*, 2003) but the ORA AWP's demonstrated corneal biomechanics to also vary with ethnicity. Together these findings imply that scleral and corneal biomechanics may be heritable traits that could potentially be associated with the genetic component known to influence refractive error development.

Indeed the findings of greater scleral resistance amongst the predominantly myopic HKC individuals provide compelling evidence for a genetic component in scleral biomechanics. Additionally, reports of increased prevalence of myopia amongst BSAs in the UK (Rudnicka *et al.*, 2010; Logan *et al.*, IOVS 2008, 49: ARVO E-Abstract 2602) further suggest that the greater scleral resistance identified in the BSAs may be a correlate of their refractive status. Gilmartin, (2004) suggested that myopic growth might be a result of genetically determined inherited structural characteristics that are modulated by environmental and socio-economic factors. *Therefore the findings of the thesis suggest that biomechanical characteristics of the sclera and cornea may be genetically governed and would consequently influence susceptibility to the onset and development of myopia.*

15.8 Limitations of present investigations and proposals for future work

15.8.1 Scleral biomechanics and myopia

The significant differences in scleral resistance found between ethnic groups were not evident for the refractive groups examined. Throughout the thesis, several studies indicated a significant influence of gender and age on the biomechanics of ocular tissue. Therefore the variability introduced by these factors may have confounded the differences in scleral biomechanics between myopes and non-myopes. To overcome this limitation future studies should aim to evaluate individuals matched for age, gender and refractive error to effectively control and assess the influence of these variables on scleral and corneal biomechanics. Furthermore, to determine conclusively the role of ocular biomechanics in myopia, evaluation of substantially anisomyopic individuals (i.e. $\geq 2D$) is likely to provide valuable information as to whether scleral and corneal material properties are altered with refractive status.

15.8.2 Regional variation in scleral biomechanics and gaze dependent IOP

A potential confounding factor when assessing scleral resistance with both the Schiötz and rebound tonometer is the possible influence of gaze-dependent changes in IOP. As discussed in Chapter 6 it is generally assumed that the changes in IOP with gaze in normal healthy individuals are significantly less than in individuals with thyroid eye disease or restricted ocular motility. Despite the significant evidence in literature to support this assumption, confirmation of regional variation in scleral resistance should be investigated

in primary gaze with rebound tonometry being performed at the 4 mm site without version movement of the eyes.

15.8.3 Rebound tonometry and scleral resistance

Chapters 8 and 9 demonstrated the utility of the rebound tonometer in the measurement of scleral resistance. Despite the significant variability in the values of Young's modulus for the different concentrations of agarose, agarose gels provided a convenient material for assessing the ability of the *iCare* to discriminate differences in scleral rigidity. A particular constraint of the validation experiment was the inability of the Hounsfield tensometer to detect the small strain values during the initial stress application, which may have led to artificially low values of Young's modulus. Therefore future studies will assess Young's modulus and corresponding *iCare* measurements with a material less variable than agarose and with a protocol that, unlike the Hounsfield tensometer, uses an extensometer that is able to detect smaller strain values.

15.8.4 Scleral biomechanics and conformation of the anterior segment

The use of T2 weighted MR images in Chapter 14 provided an inferred measure of scleral surface characteristics. T2 MR imaging allows an evaluation of the internal fluid filled conformation of the eye and the reliability to extrapolate these measurements as scleral surface characteristics needs to be confirmed. T1 ocular images with 7 Tesla scanners have been found to provide high quality images of the fine structures of the anterior eye (Richdale *et al.*, 2009). Further studies need to evaluate differences in external and internal ocular conformation by using a combination of T1 and T2 MR imaging.

15.8.5 Corneal biomechanics and myopia

As discussed in Chapter 11, corneal biomechanical changes are likely to occur with myopic growth. Indeed several studies have shown CH and CRF to reduce in myopic eyes (Song *et al.*, 2008; Shen *et al.*, 2008) however it is unclear as to whether these changes are a precursor to, or a consequence of axial growth. For this question to be addressed longitudinal studies that monitor both myopic growth and corneal biomechanics need to be conducted.

15.8.6 Scleral and ciliary muscle thickness and AS-OCT off-axis distortion

The use of the AS-OCT to measure ciliary muscle and scleral thickness has provided valuable information on the morphological features of these structures. The AS-OCT was primarily designed for assessing anterior segment structures such as the cornea, anterior angle structures and the crystalline lens. Off-axis distortions are known to occur in OCT imaging and is therefore of particular interest when imaging structures such as the ciliary muscle and sclera. An investigation is presently being conducted to evaluate the potential levels of off-axis distortion during anterior segment imaging with the *Visante* AS-OCT (see Appendix 12 for further details). Furthermore the utility of the AS-OCT to determine scleral thickness needs to be verified by comparing scleral image measurements with ultrasound biometry which is unaffected by optical distortion.

15.8.7 Scleral biomechanics and pulsatile ocular blood flow

Pathological changes of the sclera have been implicated in the aetiology of AMD (Friedman, 2000). Such changes have been found to be affected by the hemodynamic changes in the choroid along with the reduced compliance of the scleral tissue (Friedman, 1997). The Ocular blood flow analyser (OBF, Paradigm Medical Industries, Salt Lake City, UT) assesses the choroidal vasculature by measuring the pulsatile blood flow while assuming a stable venous outflow and a constant corneal rigidity for all eyes (Lam *et al.*, 2003). The OBF is a non-invasive tonometric method of measuring the pulsatile ocular blood flow (POBF). The OBF records the IOP at a frequency of 200 Hz, thus obtaining a pressure profile over a given time frame. This profile is then converted to volume data by using the well-known Friedenwald equation (see Chapter 4) assuming an average corneal rigidity value of 0.0215. As the OBF is based upon the principles of the pressure-volume relationship (Silver and Geyer, 2000), changes in corneal rigidity are likely to affect its measurement of POBF and therefore caution must be exercised as these assumptions are unsubstantiated and may lead to misleading results. It has been speculated that changes in corneal rigidity with age may alter the response of the choroidal blood vessels to the expansion force during vessel filling, consequently directing the force towards the retinal tissue (Lam *et al.*, 2003a). Such changes may contribute to the pathogenesis of conditions such as AMD. Future work will explore the utility of the POBF in determining the relationship between corneal and scleral rigidity and OBF in AMD and other ischaemic conditions such as glaucoma.

15.8.8 Biomechanics of the limbus

The biomechanical properties of the cornea, sclera and limbus are likely to be important in influencing the optics of the eye. In particular the limbal region has been suggested to form a rigid ring that maintains corneal curvature during stress application (Maurice, 1988) and has thus been implicated in the maintenance of retinal image quality (Asejczyk-Wildlicka *et al.*, 2004). At present there is no viable *in vivo* method of assessing the biomechanical properties of the limbal region. Using the concepts utilised by the ORA, the *Pulsair EasyEye* tonometer (Keeler, Windsor, UK) has been adapted to provide a morphological waveform signature (see Appendix 12 for further details). As the ORA is unable to take off- axis measurements, it is envisaged that the hand held *Pulsair* instrument will provide further understanding of limbal biomechanics.

15.9 Conclusion

The biomechanical properties of the anterior segment tissues are likely to be important determinants in ocular growth and in the aetiology of certain types of ocular pathology. The thesis contributes to an area of research that has previously received little attention and in presenting new data on the biomechanical properties of the anterior segment provides further understanding of the structural changes associated with the onset and development of myopia.

REFERENCES

- Aakre, B.M, Doughty, M.J., Dalane, O.V., Berg, A., Aamodt, Ø. and Gangstad, H. (2003). Assessment of reproducibility of measures of intraocular pressure and central corneal thickness in young white adults over a 16-h time period. *Ophthalmic Physiol Opt*, **23**, 271-283.
- Abdalla, M.I. and Hamdi, M. (1970). Applanation ocular tension in myopia and emmetropia. *Br J Ophthalmol*. **54**, 122-125.
- Abitbol, O., Bouden, J, Doan, S., Hoang-Xuan, T. and Gatinel, D. (2010). Corneal hysteresis measured with the Ocular Response Analyzer in normal and glaucomatous eyes. *Acta ophthalmologica*. **88**, 116-119.
- Adler, D. and Millodot, M. (2006). The possible effect of undercorrection on myopic progression in children. *Clin Exp Optom*. **89**, 315-331.
- Aghaian, E., Choe, J.E., Lin, S. and Stamper, R.L. (2004). Central corneal thickness of Caucasians, Chinese, Hispanics, Filipinos, African Americans, and Japanese in a glaucoma clinic. *Ophthalmology*. **111**, 2211-2219.
- Ahearne, M., Yang, Y., El Haj, A.J., Then, K.Y. and Liu, K.K. (2005). Characterizing the viscoelastic properties of thin hydrogel-based constructs for tissue engineering applications. *J R Soc Interface*. **2**, 455-463.
- Al-Mezaine, H.S., Al-Amro, S.A., Kangave, D., Sadaawy, A., Wehaib, T.A. and Al-Obeidan, S. (2008). Comparison between central corneal thickness measurements by oculus pentacam and ultrasonic pachymetry. *Int Ophthalmol*. **28**, 333-338.
- Alastrué, V., Calvo, B., Peña, E. and Doblaré, M. (2006). Biomechanical modeling of refractive corneal surgery. *J Biomech Eng*. **128**, 150-160.
- Albon, J., Karwatowski, W.S., Avery, N., Easty, D.L. and Duance, V.C. (1995). Changes in the collagenous matrix of the aging human lamina cribrosa. *Br J Ophthalmol*. **79**, 368-375.
- Albon, J., Karwatowski, W.S., Easty, D.L., Sims, T.J. and Duance, V.C. (2000). Age related changes in the non-collagenous components of the extracellular matrix of the human lamina cribrosa. *Br J Ophthalmol*. **84**, 311-317.
- Allen, M.J. and Wertheim, G.J. (1963a). Schiotz tonometer plunger retractor. *J. Amer. Optom. Assn*. **34**, 616-617.
- Allen M.J. and Wertheim, G.J. (1963b). A technique for the use of the Schiotz tonometer on the sclera. *J Amer Optom Assoc*. **34**, 956-960.
- Allen M.J. and Wertheim, G.J. (1964). Calibration of the Schiotz tonometer. *Am J Optom Arch Am Acad Optom*. **41**, 476-480.
- AlMahmoud, T., Priest, D., Munger, R. and Jackson, B.W. (2010). Correlation between refractive error, corneal power and thickness in a large population with a wide range of ametropia. *Invest Ophthalmol Vis Sci*. Papers in Press. Published on Nov 4, 2010 as Manuscript iovs.10-5449.
- Almubrad, T.M. and Ogbuehi, K.C. (2007). Clinical investigation of the effect of topical anesthesia on intraocular pressure. *Clin Ophthalmol*. **1**, 305-309.

- Alsbirk, P.H. (1978). Corneal thickness. II. Environmental and genetic factors. *Acta ophthalmologica*. **56**, 105-113.
- Ambati, J., Canakis, C.S., Miller, J.W., Gragoudas, E.S., Edwards, A., Weissgold, D.J., Kim, I., Delori, F.C. and Adamis, A.P. (2000). Diffusion of high molecular weight compounds through sclera. *Invest Ophthalmol Vis Sci*. **41**, 1181-1185.
- Anderson, D. and Grant, W. (1970). Re-evaluation of the Schiøtz tonometer calibration. *Invest Ophthalmol Vis Sci*. **9**, 430-446.
- Arciniegas, A. and Amaya, L.E. (1980). Bio-structural model of the human eye. *Ophthalmologica*. **180**, 207-211.
- Arciniegas, A. and Amaya, L.E. (1986). Mechanical behaviour of the sclera. *Ophthalmologica*. **193**, 45-55.
- Armaly, M.F. (1959). The consistency of the 1955 calibration for various tonometer weights. *Am J Ophthalmol*. **48**, 602-611.
- Asejczyk-Widlicka, M., Srodka, W., Kasprzak, H. and Iskander, R.D. (2004). Influence of IOP on geometrical properties of a linear model of the eyeball. Effect of optical self-adjustment. *Optics*. **115**, 517-524.
- Asejczyk-Widlicka, M., Sródka, D.W., Kasprzak, H., Pierscionek, B.K. (2007). Modelling the elastic properties of the anterior eye and their contribution to maintenance of image quality: the role of the limbus. *Eye*. **21**, 1087-1094.
- Asejczyk-Widlicka, M. and Pierscionek, B.K. (2008a). The elasticity and rigidity of the outer coats of the eye. *Br J Ophthalmol*. **92**, 1415-1418.
- Asejczyk-Widlicka, M., Schachar, R.A. and Pierscionek, B.K. (2008b). Optical coherence tomography measurements of the fresh porcine eye and response of the outer coats of the eye to volume increase. *J Biomed Opt*. **13**, 024002-024006.
- Ashwin, P.T., Shah, S., Pushpoth, S., Wehbeh, L. and Ilango, B. (2009). The relationship of Central Corneal Thickness (CCT) to Thinnest Central Cornea (TCC) in healthy adults. *Cont Lens Anterior Eye*. **32**, 64-67.
- Atchison, D.A., Jones, C.E., Schmid, K.L., Pritchard, N., Pope, J.M., Strugnell, W.E. and Riley, R.A. (2004). Eye shape in emmetropia and myopia. *Invest Ophthalmol Vis Sci*. **45**, 3380-3386.
- Atchison, D.A., Pritchard, N., Schmid, K.L., Scott, D.H., Jones, C.E. and Pope, J.M. (2005). Shape of the retinal surface in emmetropia and myopia. *Invest Ophthalmol Vis Sci*. **46**, 2698-2707.
- Atchison, D.A., Pritchard, N. and Schmid, K.L. (2006). Peripheral refraction along the horizontal and vertical visual fields in myopia. *Vision Res*. **46**, 1450-1458.
- Avetisov, E.S., Saulgozis, I.Z. and Volkolokova, R.I. (1978). Heterogeneity of deformative properties of human sclera. *Vestn Oftalmol*. **6**, 35-38.
- Avetisov, E.S., Savitskaya, N.F., Vinetskaya, M.I. and Iomdina, E.N. (1983). A study of biochemical and biomechanical qualities of normal and myopic eye sclera in humans of different age groups. *Metab Pediatr Syst Ophthalmol*. **7**, 183-188.

- Ayuso, V.K., Cate, H.A.T.T., van der Does, P., Rothova, A. and de Boer, J.H. (2010). Male gender as a risk factor for complications in uveitis associated with juvenile idiopathic arthritis. *Am J Ophthalmol.* **149**, 994-999.
- Backhouse, S. and Phillips, J.R. (2010). Effect of Induced Myopia on Scleral Myofibroblasts and in vivo Ocular Biomechanical Compliance in the Guinea Pig. *Invest Ophthalmol Vis Sci.* **51**, 6162-6171.
- Baikoff, G., Lutun, E., Ferraz, C. and Wei, J. (2004). Static and dynamic analysis of the anterior segment with optical coherence tomography. *J Cataract Refract Surg.* **30**, 1843-1850.
- Baikoff, G., Jodai, H.J. and Bourgeon, G. (2005). Measurement of the internal diameter and depth of the anterior chamber: IOLMaster versus anterior chamber optical coherence tomographer. *J Cataract Refract Surg.* **31**, 1722-1728.
- Bailey, M.D., Sinnott, L.T. and Mutti, D.O. (2008). Ciliary body thickness and refractive error in children. *Invest Ophthalmol Vis Sci.* **49**, 4353-4360.
- Baird, P.N, Schäche, M. and Dirani, M. (2010). The GENes in Myopia (GEM) study in understanding the aetiology of refractive errors. *Prog Retin Eye Res.* **6**, 520-542.
- Barkana, Y., Gerber, Y., Elbaz, U., Schwartz, S., Ken-Dror, G., Avni, I. and Zadok, D. (2005). Central corneal thickness measurement with the Pentacam Scheimpflug system, optical low-coherence reflectometry pachymeter, and ultrasound pachymetry. *J Cataract Refract Surg.* **31**, 1729-1735.
- Battaglioli, J.L. and Kamm, R.D. (1984). Measurements of the compressive properties of scleral tissue. *Invest Ophthalmol Vis Sci.* **25**, 59-65.
- Baudouin, C. and Gastaud, P. (1994). Influence of topical anesthesia on tonometric values of intraocular pressure. *Ophthalmologica.* **208**, 309-313.
- Bayerle-Eder, M., Kolodjaschna, J., Wolzt, M., Polska, E., Gasic, S. and Schmetterer, L. (2005). Effect of a nifedipine induced reduction in blood pressure on the association between ocular pulse amplitude and ocular fundus pulsation amplitude in systemic hypertension. *Br J Ophthalmol.* **89**, 704-708.
- Belin, M.W. and Khachikian, S.S. (2007). Keratoconus: it is hard to define, but. *Am J Ophthalmol.* **143**, 500-503.
- Bellezza, A.J., Hart, R.T. and Burgoyne, C.F. (2000). The optic nerve head as a biomechanical structure: initial finite element modelling. *Invest Ophthalmol Vis Sci.* **41**, 2991-3000.
- Bert, R.J., Patz, S., Ossiani, M., Caruthers, S.D., Jara, H., Krejza, J. and Freddo, T. (2006). High-resolution MR imaging of the human eye 2005. *Acad Radiol.* **13**, 368-378.
- Bisplinghoff, J.A., McNally, C., Brozoski, F.T. and Duma, S.M. (2008). Dynamic material property measurements of human eyes. *Biomed Sci Instrum.* **44**, 177-182.
- Bisplinghoff, J.A., McNally, C., Manoogian, S.J. and Duma, S.M. (2009). Dynamic material properties of the human sclera. *J Biomech.* **42**, 1493-1497.
- Bito, L.Z., DeRousseau, C.J., Kaufman, P.L., Bito, J.W. (1982). Age-dependent loss of accommodative amplitude in rhesus monkeys: an animal model for presbyopia. *Invest Ophthalmol Vis Sci.* **23**, 23-31.

- Bland, J.M. and Altman, D.G. (1986). Statistical methods for assessing agreement between two methods of clinical measurement. *Lancet*. **1**, 307-310.
- Bland, J.M. and Altman, D.G. (1995). Comparing methods of measurement: why plotting difference against standard method is misleading. *Lancet*. **346**, 1085-1087.
- Bochmann, F., Ang, G.S. and Azuara-Blanco, A. (2008). Lower corneal hysteresis in glaucoma patients with acquired pit of the optic nerve (APON). *Graefes Arch Clin Exp Ophthalmol*. **246**, 735-738.
- Boote, C., Dennis, S., Newton, R.H., Puri, H. and Meek, K.M. (2003). Collagen fibrils appear more closely packed in the prepupillary cornea: optical and biomechanical implications. *Invest Ophthalmol Vis Sci*. **44**, 2941-2948.
- Boubriak, O.A., Urban, J.P. and Bron, A.J. (2003). Differential effects of aging on transport properties of anterior and posterior human sclera. *Exp Eye Res*, **76**, 701-713.
- Bourges, J.L., Alfonsi, N., Laliberté, J.F., Chagnon, M., Renard, G., Legeais, J.M. and Brunette, I. (2009). Average 3-dimensional models for the comparison of Orbscan II and Pentacam pachymetry maps in normal corneas. *Ophthalmology*. **116**, 2064-2071.
- Brandt, J.D. (2004). Corneal thickness in glaucoma screening, diagnosis, and management. *Curr Opin Ophthalmol*. **15**, 85-89.
- Braun, R.D., Gadianu, M., Vistisen, K.S., Roberts, R.L. and Berkowitz, B.A. (2007). Manganese-enhanced MRI of human choroidal melanoma xenografts. *Invest Ophthalmol Vis Sci*. **48**, 963-967.
- Breitfeller, J.M. and Krohn, D.L. (1980). Limbal pneumatonometry. *Am J Ophthalmol*. **89**, 344-352.
- Briesen, S., Schwering, M.S., Roberts, H., Kollmann, M., Stachs, O., Behrend, D., Schäfer, S. and Guthoff, R. (2009). Minimal cross-infection risk through Icare rebound tonometer probes: a useful tool for IOP-screenings in developing countries. *Eye (Lond)*. **24**, 1279-1283.
- British Pharmacopoeia. Volume 1 (2007). London : The Stationary Office. 944-945.
- Broman, A.T., Congdon, N.G., Bandeen-Roche, K. and Quigley, H.A. (2007). Influence of corneal structure, corneal responsiveness, and other ocular parameters on tonometric measurement of intraocular pressure. *J Glaucoma*. **16**, 581-588.
- Bron, A.J., Tripathi, R.C., Tripathi, B.J (1997). *Wolff's Anatomy of the Eye and Orbit*. 8th Edition. London: Chapman and Hall Medical. 5-370.
- Brunner, H.G., van Beersum, S.E., Warman, M.L., Olsen, B.R., Ropers, H.H. and Mariman, E.C. (1994). A Stickler syndrome gene is linked to chromosome 6 near the COL11A2 gene. *Hum Mol Genet*. **3**, 1561-1564.
- Brusini, P., Salvetat, M.L., Zeppieri, M., Tosoni, C. and Parisi, L. (2006). Comparison of iCare tonometer with Goldmann applanation tonometer in glaucoma patients. *J Glaucoma*. **15**, 213-217.
- Buckley, C.T., Thorpe, S.D., O'Brien, F.J., Robinson, A.J. and Kelly, D.J. (2009). The effect of concentration, thermal history and cell seeding density on the initial mechanical properties of agarose hydrogels. *J Mech Behav Biomed Mater*. **2**, 512-521.

- Bueckle, H. (1973). Use of hardness to determine other material properties. In *The Science of Hardness Testing and Its Research Applications*. Editors J. W. Westbrook and H. Conrad. American Society for Metals, Materials Park, OH.
- Buehl, W., Stojanac, D., Sacu, S., Drexler, W. and Findl, O. (2006). Comparison of three methods of measuring corneal thickness and anterior chamber depth. *Am J Ophthalmol.* **141**, 7-12.
- Bullimore, M.A., Gilmartin, B. and Royston, J.M. (1992). Steady-state accommodation and ocular biometry in late-onset myopia. *Doc Ophthalmol.* **80**, 143-155.
- Burgoyne, C.F., Downs, J.C., Bellezza, A.J., Suh, J.K.F. and Hart, R.T. (2005). The optic nerve head as a biomechanical structure: a new paradigm for understanding the role of IOP-related stress and strain in the pathophysiology of glaucomatous optic nerve head damage. *Prog Retin Eye Res.* **24**, 39-73.
- Cahane, M. and Bartov, E. (1992). Axial length and scleral thickness effect on susceptibility to glaucomatous damage: a theoretical model implementing Laplace's law. *Ophthalmic research.* **24**, 280-284.
- Campbell, M.J., Machin, D., Walters, S.J. (2007). *Medical Statistics, A textbook for the Health Sciences*. Chichester: Wiley. 201-215.
- Cankaya, A.B., Elgin, U., Batman, A. and Acaroglu, G. (2008). Relationship between central corneal thickness and parameters of optic nerve head topography in healthy subjects. *European J Ophthalmology.* **18**, 32-38.
- Carbonaro, F., Andrew, T., Mackey, D.A., Spector, T.D. and Hammond, C.J. (2008). The heritability of corneal hysteresis and ocular pulse amplitude: a twin study. *Ophthalmology.* **115**, 1545-1549.
- Carney, L.G., Mainstone, J.C. and Henderson, B.A. (1997). Corneal topography and myopia. A cross-sectional study. *Invest Ophthalmol Vis Sci.* **38**, 311-320.
- Castrén, J.A and Pohjola, S. (1961a). Scleral rigidity at puberty. *Acta ophthalmologica.* **39**, 1015-1019.
- Castrén, J. and Pohjola, S. (1961b). Refraction and scleral rigidity. *Acta ophthalmologica.* **39**, 1011-1014.
- Castrén, J. and Pohjola, S. (1962). Myopia and scleral rigidity. *Acta ophthalmologica.* **40**, 33-36.
- Celorio, J.M. and Pruett, R.C. (1991). Prevalence of lattice degeneration and its relation to axial length in severe myopia. *Am J Ophthalmol.* **111**, 20-23.
- Cervino, A. (2006). Rebound tonometry: new opportunities and limitations of non-invasive determination of intraocular pressure. *Br J Ophthalmol.* **90**, 1444-1446.
- Chang, P.Y., Chang, S.W. and Wang, J.Y. (2009). Assessment of corneal biomechanical properties and intraocular pressure with Ocular Response Analyzer in childhood myopia. *Br J Ophthalmol.* **94**, 877-881.
- Chang, S.W., Tsai, I.L., Hu, F.R., Lin, L.L. and Shih, Y.F. (2001). The cornea in young myopic adults. *Br J Ophthalmol.* **85**, 916-920.
- Charman, W.N. (2008). The eye in focus: accommodation and presbyopia. *Clin Exp Optom.* **91**, 207-225.

- Chau, A., Fung, K., Pak, K. and Yap, M. (2004a). Is eye size related to orbit size in human subjects? *Ophthalmic Physiol Opt.* **24**, 35-40.
- Chau, A., Fung, K., Yip, L. and Yap, M. (2004b). Orbital development in Hong Kong Chinese subjects. *Ophthalmic Physiol Opt.* **24**, 436-439.
- Chen, D. and Lam, A.K.C. (2007). Intrasession and intersession repeatability of the Pentacam system on posterior corneal assessment in the normal human eye. *J Cataract Refract Surg.* **33**, 448-454.
- Chen, D., Lam, A.K.C. (2009). Reliability and repeatability of the Pentacam on corneal curvatures. *Clin Exp Optom.* **92**, 110-118.
- Chen, J.F., Elsner, A.E. and Burns, S.A. (1992). The effect of eye shape on retinal responses. *Clin Vision Sci.* **7**, 521-530.
- Chen, K., Rowley, A.P. and Weiland, J.D. (2010a). Elastic properties of porcine ocular posterior soft tissues. *J Biomed Mater Res A.* **93**, 634-645.
- Chen, S., Chen, D., Wang, J., Lu, F., Wang, Q. and Qu, J. (2010b). Changes in ocular response analyzer parameters after LASIK. *J Refract Surg.* **26**, 279-288.
- Chen, S.J., Cheng, C.Y., Lee, A.F., Lee, F.L., Chou, J.C., Hsu, W.M. and Liu, J.H. (2001). Pulsatile ocular blood flow in asymmetric exudative age related macular degeneration. *Br J Ophthalmol.* **85**, 1411-1415.
- Chen, X., Sankaridurg, P., Donovan, L., Lin, Z., Li, L., Martinez, A., Holden, B. and Ge, J. (2010c). Characteristics of peripheral refractive errors of myopic and non-myopic Chinese eyes. *Vision Res.* **50**, 31-35.
- Cheng, D., Schmid, K.L. and Woo, G.C. (2007). Myopia prevalence in Chinese-Canadian children in an optometric practice. *Optom Vis Sci.* **84**, 21-32.
- Cheng, H.M., Singh, O.S., Kwong, K.K., Xiong, J., Woods, B.T. and Brady, T.J. (1992). Shape of the myopic eye as seen with high-resolution magnetic resonance imaging. *Optom Vis Sci.* **69**, 698-701.
- Chi, H.H., Katzin, H.M. and Teng, C.C. (1956). Histopathology of keratoconus. *Am J Ophthalmol.* **42**, 847-860.
- Chiara, G.F., Semes, L.P., Potter, J.W., Cutter, G.R and Tucker, W.R. (1989). Portable tonometers: a clinical comparison of applanation and indentation devices. *J Am Optom Assoc.* **60**, 105-110.
- Chihara, E. (2008). Assessment of true intraocular pressure: the gap between theory and practical data. *Surv Ophthalmol.* **53**, 203-218.
- Chihara, E. and Honda, Y. (1992). Multiple defects in the retinal nerve fiber layer in glaucoma. *Graefes Arch Clin Exp Ophthalmol.* **230**, 201-205.
- Chihara, E., Liu, X., Dong, J., Takashima, Y., Akimoto, M., Hangai, M., Kuriyama, S., Tanihara, H., Hosoda, M. and Tsukahara, S. (1997). Severe myopia as a risk factor for progressive visual field loss in primary open-angle glaucoma. *Ophthalmologica.* **211**, 66-71.
- Cho, P. and Lam, C. (1999). Factors affecting the central corneal thickness of Hong Kong-Chinese. *Curr Eye Res.* **18**, 368-374.

- Chui, W., Lam, A., Chen, D. and Chiu, R. (2008). The influence of corneal properties on rebound tonometry. *Ophthalmology*. **115**, 80-84.
- Chung, K., Mohidin, N. and O'Leary, D.J. (2002). Undercorrection of myopia enhances rather than inhibits myopia progression. *Vision Res.* **42**, 2555-2559.
- Ciulla, T., Harris, A. and Martin, B. (2001). Ocular perfusion and age-related macular degeneration. *Acta Ophthalmol. Scand.* **79**, 108-115.
- Clark, J.H. (1932). A method for measuring elasticity in vivo and results obtained on the eyeball at different intraocular pressure. *Am J Physiol.* **101**, 474.
- Coleman, H.R., Chan, C.C., Ferris, F.L. and Chew, E.Y. (2008). Age-related macular degeneration. *Lancet.* **372**, 1835-1845.
- College of Optometrists. (2009). Guidance on the Re-Use of Contact Lenses and Ophthalmic Devices. http://www.college-optometrists.org/coo/download.cfm?uuid=C0AD0CD9-91F8-4872-A73036813DDB6C60&type=public_guidance. (accessed 30 September 2010).
- Congdon, N.G., Youlin, Q., Quigley, H., Hung, P.T., Wang, T.H., Ho, T.C. and Tielsch, J.M. (1997). Biometry and primary angle-closure glaucoma among Chinese, white, and black populations. *Ophthalmology*. **104**, 1489-1495.
- Congdon, N., O'Colmain, B., Klaver, C.C., Klein, R., Munoz, B., Friedman, D.S., Kempen, J., Taylor, H.R. and Mitchell, P. (2004). Causes and prevalence of visual impairment among adults in the United States. *Arch Ophthalmol.* **122**, 477-485.
- Congdon, N.G., Broman, A.T., Bandeen-Roche, K., Grover, D. and Quigley, H.A. (2006). Central corneal thickness and corneal hysteresis associated with glaucoma damage. *Am J Ophthalmol.* **141**, 868-875.
- Copt, R.P., Thomas, R. and Mermoud, A. (1999). Corneal thickness in ocular hypertension, primary open-angle glaucoma, and normal tension glaucoma. *Arch Ophthalmol.* **117**, 14-16.
- Cordain, L., Eaton, S.E., Miller, J.B., Lindeberg, S. and Jensen, C. (2002). An evolutionary analysis of the aetiology and pathogenesis of juvenile-onset myopia. *Acta Ophthalmol Scand.* **80**, 125-135.
- Costa, K.D., Ho, M.M.Y. and Hung, C.T. (2003). Multi-scale measurements of mechanical properties of soft samples with atomic force microscopy. In: *Summer Bioengineering Conference*, June 25-29, Sonesta Beach Resort in Key Biscayne, Florida.
- Crawford, K., Terasawa, E. and Kaufman, P.L. (1989). Reproducible stimulation of ciliary muscle contraction in the cynomolgus monkey via a permanent indwelling midbrain electrode. *Brain Res.* **503**, 265-272.
- Croft, M.A., Kaufman, P.L., Crawford, K.S., Neider, M.W., Glasser, A. and Bito, L.Z. (1998). Accommodation dynamics in aging rhesus monkeys. *Am J Physiol.* **275**, 1885-1897.
- Croft, M.A., Glasser, A. and Kaufman, P.L. (2001). Accommodation and presbyopia. *Int Ophthalmol Clin.* **41**, 33-46.
- Croft, M.A., Glasser, A., Heatley, G., McDonald, J., Ebbert, T., Dahl, D.B., Nadkarni, N.V. and Kaufman, P.L. (2006). Accommodative ciliary body and lens function in rhesus monkeys, I: normal lens, zonule and ciliary process configuration in the iridectomized eye. *Invest Ophthalmol Vis Sci.* **47**, 1076-1086.

- Curtin, B.J. (1969). Physiopathologic aspects of scleral stress-strain. *Trans Am Ophthalmol Soc.* **67**, 417-461.
- Curtin, B.J. (1970). Myopia: a review of its etiology, pathogenesis and treatment. *Surv Ophthalmol.* **15**, 1-17.
- Curtin, B.J., Iwamoto, T. and Renaldo, D.P. (1979). Normal and staphylomatous sclera of high myopia. An electron microscopic study. *Arch Ophthalmol.* **97**, 912-915.
- Curtin, B.J. (1985). *The Myopias, Basic Science and Clinical Management*. Cambridge: Harper & Row. 200-285.
- Danias, J., Kontiola, A.I., Filippopoulos, T. and Mittag, T. (2003). Method for the noninvasive measurement of intraocular pressure in mice. *Invest Ophthalmol Vis Sci.* **44**, 1138-1141.
- Dastiridou, A.I., Ginis, H.S., Brouwere, D.D, Tsilimbaris, M.K., Pallikaris, I.G. (2009). Ocular rigidity, ocular pulse amplitude, and pulsatile ocular blood flow: the effect of intraocular pressure. *Invest Ophthalmol Vis Sci.* **50**, 5718-5722.
- Daubs, J.G. and Crick, R.P. (1981). Effect of refractive error on the risk of ocular hypertension and open angle glaucoma. *Trans Ophthalmol Soc U K.* **101**, 121-126.
- Dauwe, C., Touboul, D., Roberts, C.J., Mahmoud, A.M., Kérautret, J., Fournier, P., Malecaze, F. and Colin, J. (2009). Biomechanical and morphological corneal response to placement of intrastromal corneal ring segments for keratoconus. *J Cataract Refract Surg.* **35**, 1761-1767.
- David, R., Zangwill, L.M., Tessler, Z. and Yassur, Y. (1985). The correlation between intraocular pressure and refractive status. *Arch Ophthalmol.* **103**, 1812-1815.
- Davies, L.N., Bartlett, H., Mallen, E.A. and Wolffsohn, J.S. (2006). Clinical evaluation of rebound tonometer. *Acta Ophthalmol Scand.* **84**, 206-209.
- Davson, H. (1976). *The Physiology of the Eye. 3rd ed.* New York & San Francisco: Academic Press. Section II:126–127.
- Davson, H. (1990). *Davson's Physiology of the Eye*. London: Macmillian Press. 211-394.
- Daxer, A., Misof, K., Grabner, B., Ettl, A. and Fratzl, P. (1998). Collagen fibrils in the human corneal stroma: structure and aging. *Invest Ophthalmol Vis Sci.* **39**, 644-648.
- Dayanir, V., Sakarya, R., Ozcura, F., Kir, E., Aktunç, T., Ozkan, B.S. and Pinar Okyay, P. (2004). Effect of corneal drying on central corneal thickness. *J Glaucoma.* **13**, 6-8.
- de Freitas, P.S., Wirz, D., Stolz, M., Göpfert, B., Friederich, N.F. and A U Daniels, A.U. (2006). Pulsatile dynamic stiffness of cartilage-like materials and use of agarose gels to validate mechanical methods and models. *J Biomed Mater Res Part B Appl Biomater.* **78**, 347-357.
- Dekking, H.M. and Coster, H.D. (1967). Dynamic tonometry. *Ophthalmologica.* **154**, 59-74.
- del Buey, M.A., Cristóbal, J.A., Ascaso, F.J., Lavilla, L. and Lanchares, E. (2009). Biomechanical properties of the cornea in Fuchs' corneal dystrophy. *Invest Ophthalmol Vis Sci.* **50**, 3199-3202.
- Deller, J.F.P., O'Connor, A.D. and Sorsby, A. (1947). X-ray measurements of the diameters of the living eye. *Proc R Soc Lond B Biol Sci.* **134**, 456-467.

- Demirbas, N.H. and Pflugfelder, S.C. (1998). Topographic pattern and apex location of keratoconus on elevation topography maps. *Cornea*. **17**, 476-484.
- Detry-Morel, M., Jamart, J., Detry, M.B., Pourjavan, S., Charlier, L., Dethinne, B., Huges, L. and Ledoux, A. (2006). Clinical evaluation of the dynamic rebound tonometer Icare. *J Fr Ophthalmol*. **29**, 1119-1127.
- Di Girolamo, N. Lloyd, A., McCluskey, P., Filipic, M. and Wakefield, D. (1997). Increased expression of matrix metalloproteinases in vivo in scleritis tissue and in vitro in cultured human scleral fibroblasts. *Am J Pathol*. **150**, 653-666.
- Díaz-Llopis, M., García-Delpech, S. and Udaondo, P. (2007). Rebound tonometry vs Goldmann vs Neumotonometer. *Arch Soc Esp Ophthalmol*. **82**, 607-608.
- Diaz, A., Yebra-Pimentel, E., García Resua, C., Gilino, J., Jesus Giraldez, M. (2008). Accuracy of the ICare rebound tonometer in glaucomatous eyes with topical ocular hypotensive medication. *Ophthalmic Physiol Opt*. **28**, 29-34.
- Dielemans, I., Vingerling, J.R., Hofman, A., Grobbee, D.E. and Jong, P.T. (1994). Reliability of intraocular pressure measurement with the Goldmann applanation tonometer in epidemiological studies. *Graefes Arch Clin Exp Ophthalmol*. **232**, 141-144.
- Diether, S. and Schaeffel, F. (1997). Local changes in eye growth induced by imposed local refractive error despite active accommodation. *Vision Res*. **37**, 659-668.
- Dietz, H.C., Cutting, G.R., Pyeritz, R.E., Maslen, C.L., Sakai, L.Y., Corson, G.M., Puffenberger, E.G., Hamosh, A., Nanthakumar, E.J., Curren, S.M. (1991). Marfan syndrome caused by a recurrent de novo missense mutation in the fibrillin gene. *Nature*. **352**, 337-339.
- Dimasi, D.P., Burdon, K.P. and Craig, J.E. (2010). The genetics of central corneal thickness. *Br J Ophthalmol*. **94**, 971-976.
- Dinc, U.A., Gorgun, E., Oncel, B., Yenerel, M.N. and Alimgil, L. (2010). Assessment of Anterior Chamber Depth Using Visante Optical Coherence Tomography, Slitlamp Optical Coherence Tomography, IOL Master, Pentacam and Orbscan IIz. *Ophthalmologica*. **224**, 341-346.
- Dirani, M., Chamberlain, M., Shekar, S.N., Islam, A.F.M., Garoufalidis, P., Chen, C.Y., Guymer, R.H. and Baird, P.N. (2006). Heritability of refractive error and ocular biometrics: the Genes in Myopia (GEM) twin study. *Invest Ophthalmol Vis Sci*. **47**, 4756-4761.
- Dirani, M., Tong, L., Gazzard, G., Zhang, X., Chia, A., Young, T.L., Rose, K.A., Mitchell, P. and Saw, S.M. (2009). Outdoor activity and myopia in Singapore teenage children. *Br J Ophthalmol*. **93**, 997-1000.
- Dorairaj, S., Liebmann, J.M. and Ritch, R. (2007) Quantitative evaluation of anterior segment parameters in the era of imaging. *Trans Am Ophthalmol Soc*. **105**, 99-110.
- Doughty, M.J. and Zaman, M.L. (2000). Human corneal thickness and its impact on intraocular pressure measures: a review and meta-analysis approach. *Surv Ophthalmol*. **44**, 367-408.
- Doughty, M.J., Laiquzzaman, M., Müller, A., Oblak, E. and Button, N.F. (2002). Central corneal thickness in European (white) individuals, especially children and the elderly, and assessment of its possible importance in clinical measures of intra-ocular pressure. *Ophthalmic Physiol Opt*. **22**, 491-504.

- Downs, J.C., Blidner, R.A., Bellezza, A.J., Thompson, H.W., Hart, R.T., Burgoyne, C.F. (2002). Peripapillary scleral thickness in perfusion-fixed normal monkey eyes. *Invest Ophthalmol Vis Sci.* **43**, 2229-2235.
- Downs, J.C., Suh, J.K.F., Thomas, K.A., Bellezza, A.J., Burgoyne, C.F. and Hart, R.T. (2003). Viscoelastic characterization of peripapillary sclera: material properties by quadrant in rabbit and monkey eyes. *J Biomech Eng.* **125** 124-131.
- Downs, J.C., Suh, J.K.F., Thomas, K.A., Bellezza, A.J., Hart, R.T. and Burgoyne, C.F. (2005). Viscoelastic material properties of the peripapillary sclera in normal and early-glaucoma monkey eye. *Invest Ophthalmol Vis Sci.* **46**, 540-546.
- Draeger, J. (1959). Studies on the rigidity coefficient. *Doc Ophthalmol.* **13**, 431-486.
- Draeger, J. (1966). *Tonometry, Physical Fundamentals Development of Methods and Clinical Application*. Basel: S. Karger. 34-71.
- Drance, S.M. (1960). The coefficient of scleral rigidity in normal and glaucomatous eyes. *Arch Ophthalmol.* **63**, 668-674.
- Drover, J.R., Kean, P.G., Courage, M.L. and Adams, R.J. (2008). Prevalence of amblyopia and other vision disorders in young Newfoundland and Labrador children. *Can J Ophthalmol.* **43**, 89-94.
- Dubbelman, M., Sicam, V.A.D.P. and Van der Heijde, G.L. (2006). The shape of the anterior and posterior surface of the aging human cornea. *Vision Res.* **46**, 993-1001.
- Duke-Elder, S. (1968). *System of Ophthalmology Volume IV*. London: Henry Kimpton. 262-271.
- Dunne, M.C.M., Davies, L.N. and Wolffsohn, J.S. (2007). Accuracy of cornea and lens biometry using anterior segment optical coherence tomography. *J Biomed Opt.* **12**, 064023-4.
- Dupps, W.J. (2007). Hysteresis: new mechanospeak for the ophthalmologist. *J Cataract Refract Surg.* **33**, 1499-1501.
- Ebenstein, D.M. and Pruitt, L.A. (2004). Nanoindentation of soft hydrated materials for application to vascular tissues. *Journal of biomedical materials research Part A.* **69**, 222-232.
- Eberly, D.W. (1967) Plunger lifter modified Schiottz tonometer used on the cornea: a population study. *Am J Optom Arch Am Acad Optom.* **44**, 374-378.
- Ebnetter, A., Wagels, B. and Zinkernagel, M.S. (2009). Non-invasive biometric assessment of ocular rigidity in glaucoma patients and controls. *Eye (Lond).* **23**, 606-611.
- Edmund, C. (1988). Corneal elasticity and ocular rigidity in normal and keratoconic eyes. *Acta Ophthalmol Scand.* **66**, 134-140.
- Edwards, K., Llwellyn, R (1988). *Optometry*. London: Butterworths - Heinemann. 380-393.
- Edwards, M.H. (1996). Animal models of myopia. A review. *Acta Ophthalmol Scand.* **74**, 213-219.
- Edwards, M.H. and Brown, B. (1993). Intraocular pressure in a selected sample of myopic and nonmyopic Chinese children. *Optom Vis Sci.* **70**, 15-17.

- Edwards, M.H. and Brown, B. (1996). IOP in myopic children: the relationship between increases in IOP and the development of myopia. *Ophthalmic Physiol Opt.* **16**, 243-246.
- Edwards, M.H., Chun, C.Y. and Leung, S.S. (1993). Intraocular pressure in an unselected sample of 6- to 7-year-old Chinese children. *Optom Vis Sci.* **70**, 198-200.
- Edwards, M.H. and Lam, C.S.Y. (2004). The epidemiology of myopia in Hong Kong. *Ann Acad Med Singap.* **33**, 34-38.
- Ehongo, A., Maertelaer, V.D, Cullus, P. and Pourjavan, S. (2008). Correlation between corneal hysteresis, corneal resistance factor, and ocular pulse amplitude in healthy subjects. *J Fr Ophthalmol.* **31**, 999-1005.
- Eilaghi, A., Flanagan, J.G., Simmons, C.A. and Ethier, C.R. (2010a). Effects of scleral stiffness properties on optic nerve head biomechanics. *Ann Biomed Eng.* **38**, 1586-1592.
- Eilaghi, A., Flanagan, J.G., Tertinegg, I., Simmons, C.A., Brodland, G.W., Ethier, C.R. (2010b). Biaxial mechanical testing of human sclera. *J Biomech.* **43**, 1696-1701.
- Eisenlohr, J.E., Langham, M.E., Maumenee, A.E. (1962). Manometric studies of the pressure-volume relationship in living and enucleated eyes of individual human subjects. *Br J Ophthalmol.* **46**, 536-548.
- ElMallah, M.K. and Asrani, S.G. (2008). New ways to measure intraocular pressure. *Curr Opin Ophthalmol.* **19**, 122-126.
- Elsheikh, A. and Wang, D. (2007). Numerical modelling of corneal biomechanical behaviour. *Comput Methods Biomech Biomed Engin.* **10**, 85-95.
- Elsheikh, A., Alhasso, D. and Pye, D. (2009). Goldmann tonometry correction factors based on numerical analysis. *J Biomech Eng.* **131**, 111-113.
- Elsheikh, A., Geraghty, B., Alhasso, D., Knappett, J., Campanelli, M. and Rama, P. (2010). Regional variation in the biomechanical properties of the human sclera. *Exp Eye Res.* **90**, 624-633.
- Ethier, C.R. (2006). Scleral biomechanics and glaucoma--a connection? *Can J Ophthalmol*, **41**, 9-12.
- Falavarjani, K.G., Modarres, M., Joshaghani, M., Azadi, P., Afshar, A.E. and Hodjat, P. (2010). Interocular differences of the Pentacam measurements in normal subjects. *Clin Exp Optom.* **93**, 26-30.
- Fam, H.B, How, A.C.S., Baskaran, M., Lim, K.L., Chan, Y.H. and Aung, T. (2006). Central corneal thickness and its relationship to myopia in Chinese adults. *Br J Ophthalmol.* **90**, 1451-1453.
- Fan, D.S.P., Lam, D.S.C., Lam, R.F., Lau, J.T.F., Chong, K.S., Cheung, E.Y.Y., Lai, R.Y.K. and Chew, S.J. (2004a). Prevalence, incidence, and progression of myopia of school children in Hong Kong. *Invest Ophthalmol Vis Sci.* **45**, 1071-1075.
- Fan, D.S.P., Cheung, E.Y.Y, Lai, R.Y.K., Kwok, A.K.H. and Lam, D.S.C. (2004b). Myopia progression among preschool Chinese children in Hong Kong. *Ann Acad Med Singap.* **33**, 39-43.
- Farbrother, J.E., Kirov, G., Owen, M.J., Pong-Wong, R., Haley, C.S. and Guggenheim, J.A. (2004a). Linkage analysis of the genetic loci for high myopia on 18p, 12q, and 17q in 51 U.K. families. *Invest Ophthalmol Vis Sci.* **45**, 2879-2885.

- Farbrother, J.E, Welsby, J.W. and Guggenheim, J.A. (2004b). Astigmatic axis is related to the level of spherical ametropia. *Optom Vis Sci.* **81**, 18-26.
- Feltgen, N., Leifert, D. and Funk, J. (2001). Correlation between central corneal thickness, applanation tonometry, and direct intracameral IOP readings. *Br J Ophthalmol.* **85**, 85-87.
- Fernandes, P., Diaz-Rey, J.A., Queiros, A., Gonzalez-Mejome, J.M. and Jorge, J. (2005). Comparison of the ICare rebound tonometer with the Goldmann tonometer in a normal population. *Ophthalmic Physiol Opt.* **25**, 436-440.
- Fischer-Cripps, A.C. (2003). Analysis of instrumented indentation test data for functionally graded materials. *Surface and Coatings Technology.* **168**, 136–141.
- Fisher, R.F. (1977). The force of contraction of the human ciliary muscle during accommodation. *J Physiol (Lond).* **270**, 51-74.
- Fishman, D.R. and Benes, S.C. (1991). Upgaze intraocular pressure changes and strabismus in Graves' ophthalmopathy. *J Clin Neuroophthalmol.* **11**, 162-165.
- Fledelius, H.C. and Goldschmidt, E. (2009). Oculometry findings in high myopia at adult age: considerations based on oculometric follow-up data over 28 years in a cohort-based Danish high-myopia series. *Acta ophthalmologica.* **88**, 472-478.
- Fleiss J.L. (1981). *Statistical Methods for Rates and Proportions.* New York: John Wiley. 38-46.
- Fontes, B.M, Ambrósio, R., Velarde, G.C. and Nosé, W. (2010). Ocular Response Analyzer Measurements in Keratoconus with Normal Central Corneal Thickness Compared with Matched Normal Control Eyes. *J Refract Surg.* May 19:1-7. [Epub ahead of print]
- Fontes, B.M., Ambrósio, R., Alonso, R.S., Jardim, D., Velarde, G.C. and Nosé, W. (2008). Corneal biomechanical metrics in eyes with refraction of -19.00 to +9.00 D in healthy Brazilian patients. *J Refract Surg.* **24**, 941-945.
- Forrester, J.V., Dick, A.D., McMenamin, P.G. and Roberts, F. (2008). *The Eye, Basic sciences in practice.* Philadelphia: Elsevier. 1-108.
- Foster, C.S. and Sainz de la Maza, M. (1994). *The Sclera.* New York: Springer-Verlag. 1-32
- Foster, P.J., Wong, J.S., Wong, E., Chen, F.G., Machin, D. and Chew, P.T. (2000). Accuracy of clinical estimates of intraocular pressure in Chinese eyes. *Ophthalmology.* **107**, 1816-1821.
- Franco, S. and Lira, M. (2009). Biomechanical properties of the cornea measured by the Ocular Response Analyzer and their association with intraocular pressure and the central corneal curvature. *Clin Exp Optom.* **92**, 469-475.
- Friberg, T.R. and Lace, J.W. (1988). A comparison of the elastic properties of human choroid and sclera. *Exp Eye Res,* **47**, 429-436.
- Fridenwald, J.S. (1937). Contribution to the theory and practice of tonometry. *Am J Ophthalmol.* **20**, 985-1024.
- Friedenwald, J.S. (1947). Some problems in the calibration of tonometers. *Trans Am Acad Ophthalmol Otolaryngol.* **45**, 355-375.

- Friedenwald J.S. (1957). Tonometer Calibration: An attempt to remove discrepancies found in the 1954 calibration scale for Schiottz tonometers. *Trans Am Acad Ophthalmol Otolaryngol.* **61**, 108-123.
- Friedman, B. (1966). Stress upon the ocular coats: effects of scleral curvature scleral thickness, and intra-ocular pressure. *Eye Ear Nose Throat Mon.* **45**, 59-66.
- Friedman, E. (1997). A hemodynamic model of the pathogenesis of age-related macular degeneration. *Am J Ophthalmol.* **124**, 677-682.
- Friedman, E. (2000). The Role of the Atherosclerotic Process in the Pathogenesis of Age-related Macular Degeneration. *Am J Ophthalmol.* **130**, 658-663.
- Friedman, E. (2004). Update of the vascular model of AMD. *Br J Ophthalmol.* **88**, 161-163.
- Friedman, E., Ivry, M., Ebert, E., Glynn, R., Gragoudas, E. and Seddon, J. (1989). Increased scleral rigidity and age-related macular degeneration. *Ophthalmology.* **96**, 104-108.
- Fujikura, H., Seko, Y., Tokoro, T., Mochizuki, M. and Shimokawa, H. (2002). Involvement of mechanical stretch in the gelatinolytic activity of the fibrous sclera of chicks, in vitro. *Jpn J Ophthalmol.* **46**, 24-30.
- Funata, M. and Tokoro, T. (1990). Scleral change in experimentally myopic monkeys. *Graefes Arch Clin Exp Ophthalmol.* **228**, 174-179.
- Gabbiani, G. (2003). The myofibroblast in wound healing and fibrocontractive diseases. *J Pathol.* **200**, 500-503.
- Gamblin, G.T., Harper, D.G., Galentine, P., Buck, D.R., Chernow, B. and Eil, C. (1983). Prevalence of increased intraocular pressure in Graves' disease--evidence of frequent subclinical ophthalmopathy. *N Engl J Med.* **308**, 420-424.
- Garcia-Resua, C., Gonzalez-Meijome, J.M., Gilino, J., Yebra-Pimentel, E. (2006). Accuracy of the new ICare rebound tonometer vs. other portable tonometers in healthy eyes. *Optom Vis Sci.* **83**, 102-107.
- Garcia, J.P.S. and Rosen, R.B. (2008). Anterior segment imaging: optical coherence tomography versus ultrasound biomicroscopy. *Ophthalmic Surg Lasers Imaging.* **39**, 476-484.
- Gathercole, L.J. and Keller, A. (1991). Crimp morphology in the fibre-forming collagens. *Matrix.* **11**, 214-434.
- Gaton, D.D., Sagara, T., Lindsey, J.D. and Weinreb, R.N. (1999). Matrix metalloproteinase-1 localization in the normal human uveoscleral outflow pathway. *Invest Ophthalmol Vis Sci.* **40**, 363-369.
- Gefen, A., Shalom, R., Elad, D and Mandel, Y. (2009). Biomechanical analysis of the keratoconic cornea. *J Mech Behav Biomed Mater.* **2**, 224-236.
- Gensler, H.M. (1967). An evaluation of the Schiottz tonometer in glaucoma screening programs. *Am J Optom Arch Am Acad Optom.* **44**, 634-641.
- Gentle, A., Liu, Y., Martin, J.E., Conti, G.L. and McBrien, N.A. (2003). Collagen gene expression and the altered accumulation of scleral collagen during the development of high myopia. *J Biol Chem.* **278**, 16587-16594.

- Georgouli, T., Chang, B., Nelson, M., James, T., Tanner, S., Shelley, D., Saldana, M. and McGonagle, D. (2008). Use of high-resolution microscopy coil MRI for depicting orbital anatomy. *Orbit*. **27**, 107-114.
- Gilger, B.C., Reeves, K.A. and Salmon, J.H. (2005). Ocular parameters related to drug delivery in the canine and equine eye: aqueous and vitreous humor volume and scleral surface area and thickness. *Vet Ophthalmol*. **8**, 265-269.
- Gilmartin, B. (2004). Myopia: precedents for research in the twenty-first century. *Clin Experiment Ophthalmol*. **32**, 305-324.
- Gilmartin, B., Logan, N.S. and Singh, K.D. (2007). Determining regional variations in globe conformation using 3-D ocular MRI. *Invest Ophthalmol Vis Sci*. E-Abstract:1215: 48.
- Gilmartin, B., Logan, N.S. and Singh, K.D. (2008). *In vivo* comparison of anterior and posterior ocular volume in human ametropia. *Invest Ophthalmol Vis Sci*. E-Abstract 3582: 49.
- Girard, M.J.A., Downs, J.C., Burgoyne, C.F. and Suh, J.K.F. (2008). Experimental surface strain mapping of porcine peripapillary sclera due to elevations of intraocular pressure. *J Biomech Eng*. **130**, 041017.
- Girard, M.J.A., Downs, J.C., Bottlang, M., Burgoyne, C.F. and Suh, J.K.F. (2009a). Peripapillary and posterior scleral mechanics--part II: experimental and inverse finite element characterization. *J Biomech Eng*. **131**, 051012.
- Girard, M.J.A., Suh, J.K.F., Bottlang, M., Burgoyne, C.F. and Downs, J.C. (2009b). Scleral biomechanics in the aging monkey eye. *Invest Ophthalmol Vis Sci*. **50**, 5226-5237.
- Glasser, A. and Kaufman, P.L. (1999). The mechanism of accommodation in primates. *Ophthalmology*. **106**, 863-872.
- Glasser, A., Croft, M.A., Brumback, L. and Kaufman, P.L. (2001). Ultrasound biomicroscopy of the aging rhesus monkey ciliary region. *Optom Vis Sci*. **78**, 417-424.
- Gloster, J. and Perkins, E.S. (1957). Distensibility of the eye. *Br J Ophthalmol*, **41**, 93-102.
- Gloster, J., Perkins, E.S., and Pommier, M.L. (1957). Extensibility of strips of sclera and cornea. *Br J Ophthalmol*, **41**, 103-110.
- Goh, P.P., Abqariyah, Y., Pokharel, G.P. and Ellwein, L.B. (2005). Refractive error and visual impairment in school-age children in Gombak District, Malaysia. *Ophthalmology*. **112**, 678-685.
- Gohdo, T., Tsumura, T., Iijima, H., Kashiwagi, K. and Tsukahara, S. (2000). Ultrasound biomicroscopic study of ciliary body thickness in eyes with narrow angles. *Am J Ophthalmol*. **129**, 342-346.
- Goldblum, D., Kontiola, A.I., Mittag, T., Chen, B., Danias, J. (2002). Non-invasive determination of intraocular pressure in the rat eye. Comparison of an electronic tonometer (TonoPen), and a rebound (impact probe) tonometer. *Graefes Arch Clin Exp Ophthalmol*. **240**, 942-946.
- Goldmann, H. and Schmidt, T. (1957). Applanation tonometry. *Ophthalmologica*. **134**, 221-242.
- Goldschmidt, E. (1968). On the etiology of myopia. *Acta Ophthalmol*. (Suppl) 98.
- Goldschmidt, E. and Fledelius, H.C. (2005). High myopia progression and visual impairment in a nonselected group of Danish 14-year-olds followed over 40 years. *Optom Vis Sci*. **82**, 239-243.

- Goldsmith, J.A., Li, Y., Chalita, M.R., Westphal, V., Patil, C.A., Rollins, A.M., Izatt, J.A. and Huang, D. (2005). Anterior chamber width measurement by high-speed optical coherence tomography. *Ophthalmology*. **112**, 238-244.
- Gomi, C.F., Yates, B., Kikkawa, D.O., Levi, L., Weinreb, R.N. and Granet, D.B. (2007). Effect on intraocular pressure of extraocular muscle surgery for thyroid-associated ophthalmopathy. *Am J Ophthalmol*. **144**, 654-657.
- González-Méijome, J.M., Jorge, J., Queirós, A., Fernandes, P., Montés-Micó, R., Almeida, J.B. and Parafita, M.A. (2006). Age differences in central and peripheral intraocular pressure using a rebound tonometer. *Br J Ophthalmol* **90**, 1495-1500.
- González-Méijome, J.M., Queirós, A., Jorge, J., Díaz-Rey, A. and Parafita, M.A. (2008). Intraoffice variability of corneal biomechanical parameters and intraocular pressure (IOP). *Optom Vis Sci*. **85**, 457-462.
- Goodall, N., Kisiswa, L., Prashar, A., Faulkner, S., Tokarczuk, P., Singh, K., Erichsen, J.T., Guggenheim, J., Halfter, W. and Wride, M.A. (2009). 3-Dimensional modelling of chick embryo eye development and growth using high resolution magnetic resonance imaging. *Exp Eye Res*. **89**, 511-521.
- Goodside, V. (1959). Ocular rigidity. *A.M.A. Archives of Ophthalmology*. **62**, 839-841.
- Gordon, M.O., Beiser, J.A., Brandt, J.D., Heuer, D.K., Higginbotham, E.J., Johnson, C.A., Keltner, J.L., J. Philip Miller, AB; Richard K. Parrish II; M. Roy Wilson, MD; Michael A. Kass. (2002). The Ocular Hypertension Treatment Study: baseline factors that predict the onset of primary open-angle glaucoma. *Arch Ophthalmol*. **120**, 714-720.
- Goss, D.A. and Caffey, T.W. (1999). Clinical findings before the onset of myopia in youth: 5. Intraocular pressure. *Optom Vis Sci*. **76**, 286-291.
- Goss, D.A., Cox, V.D., Herrin-Lawson, G.A., Nielsen, E.D. and Dolton, W.A. (1990). Refractive error, axial length, and height as a function of age in young myopes. *Optom Vis Sci*. **67**, 332-338.
- Goss, D.A., Veen, H.G.V., Rainey, B.B. and Feng, B. (1997). Ocular components measured by keratometry, phakometry, and ultrasonography in emmetropic and myopic optometry students. *Optom Vis Sci*. **74**, 489-495.
- Gottlieb, M.D., Fugate-Wentzek, L.A. and Wallman, J. (1987). Different visual deprivations produce different ametropias and different eye shapes. *Invest Ophthalmol Vis Sci*. **28**, 1225-1235.
- Grabner, G., Eilmsteiner, R., Steindl, C., Ruckhofer, J, Mattioli, R. and Husinsky, W. (2005). Dynamic corneal imaging. *J Cataract Refract Surg*. **31**, 163-174.
- Greene, P.R. (1980). Mechanical considerations in myopia: relative effects of accommodation, convergence, intraocular pressure, and the extraocular muscles. *Am J Optom Physiol Opt*. **57**, 902-914.
- Greene, P.R. (1985). Closed-form ametropic pressure-volume and ocular rigidity solutions. *Am J Optom Physiol Opt*. **62**, 870-878.
- Greene, P.R. and McMahon, T.A. (1979). Scleral creep vs. temperature and pressure in vitro. *Exp Eye Res*, **29**, 527-537.

- Grossniklaus, H.E. and Green, W.R. (1992). Pathologic findings in pathologic myopia. *Retina (Philadelphia, Pa)*. **12**, 127-133.
- Grosvenor, T. (1987). A review and a suggested classification system for myopia on the basis of age-related prevalence and age of onset. *Am J Optom Physiol Opt*. **64**, 545-554.
- Grosvenor, T. and Scott, R. (1991). Comparison of refractive components in youth-onset and early adult-onset myopia. *Optom Vis Sci*. **68**, 204-209.
- Grunwald, J.E., Hariprasad, S.M. and DuPont, J. (1998). Foveolar choroidal blood flow in age-related macular degeneration. *Invest Ophthalmol Vis Sci*. **39**, 385-390.
- Grzybowski, D.M., Roberts, C.J., Mahmoud, A.M. and Chang, J.S. (2005). Model for nonectatic increase in posterior corneal elevation after ablative procedures. *J Cataract Refract Surg*. **31**, 72-81.
- Gu, W.Y., Yao, H., Huang, C.Y. and Cheung, H.S. (2003). New insight into deformation-dependent hydraulic permeability of gels and cartilage, and dynamic behavior of agarose gels in confined compression. *J Biomech*. **36**, 593-598.
- Gueta, R., Barlam, D., Shneck, R.Z. and Rousso, I. (2006). Measurement of the mechanical properties of isolated tectorial membrane using atomic force microscopy. *Proc Natl Acad Sci USA*. **103**, 14790-14795.
- Guggenheim, J. (2009). Myopia - Theories, controversies and attempts to slow its progression. In: *Lectures from Optometry Tomorrow 2009*. College of Optometrist, Brighton. UK.
- Guggenheim, J.A. and McBrien, N.A. (1996). Form-deprivation myopia induces activation of scleral matrix metalloproteinase-2 in tree shrew. *Invest Ophthalmol Vis Sci*. **37**, 1380-1395.
- Guggenheim, J.A., Kirov, G. and Hodson, S.A. (2000). The heritability of high myopia: a reanalysis of Goldschmidt's data. *J Med Genet*. **37**, 227-231.
- Guthoff, R., Berger, R.W. and Draeger, J. (1987). Ultrasonographic measurement of the posterior coats of the eye and their relation to axial length. *Graefes Arch Clin Exp Ophthalmol*. **225**, 374-376.
- Guthoff, R., Riederle, H., Meinhardt, B. and Goebel, W. (2010). Subclinical Choroidal Detachment at Sclerotomy Sites after 23-Gauge Vitrectomy: Analysis by Anterior Segment Optical Coherence Tomography. *Ophthalmologica*. **224**, 301-307.
- Gwiazda, J., Grice, K. and Thorn, F. (1999). Response AC/A ratios are elevated in myopic children. *Ophthalmic Physiol Opt*. **19**, 173-179.
- Gwiazda, J., Thorn, F. and Held, R. (2005). Accommodation, accommodative convergence, and response AC/A ratios before and at the onset of myopia in children. *Optom Vis Sci*. **82**, 273-278.
- Gwiazda, J., Thorn, F., Bauer, J. and Held, R. (1993). Myopic children show insufficient accommodative response to blur. *Invest Ophthalmol Vis Sci*. **34**, 690-694.
- Hager, A. and Wiegand, W. (2008). Methods of measuring intraocular pressure independently of central corneal thickness. *Ophthalmologe*. **105**, 840-844.
- Hager, A., Loge, K., Schroeder, B., Füllhas, M.O. and Wiegand, W. (2008). Effect of central corneal thickness and corneal hysteresis on tonometry as measured by dynamic contour tonometry,

- ocular response analyzer, and Goldmann tonometry in glaucomatous eyes. *J Glaucoma*. **17**, 361-365.
- Hager, A., Loge, K., Füllhas, M.O., Schroeder, B., Grossherr, M. and Wiegand, W. (2007). Changes in corneal hysteresis after clear corneal cataract surgery. *Am J Ophthalmol*. **144**, 341-346.
- Hammond, C.J., Snieder, H., Gilbert, C.E. and Spector, T.D. (2001). Genes and environment in refractive error: the twin eye study. *Invest Ophthalmol Vis Sci*. **42**, 1232-1236.
- Hanna, C.L., Roberts, R.T., Hwang, S.J. and Wilhelmus, K.R. (2004). Pachymetry of donor corneas: effect of ethnicity and gender on central corneal thickness. *Cornea*. **23**, 701-703.
- Harrington, D.O. and Parsons, A.H. (1941). Tonometric standardization: a method of increasing the accuracy of tonometry. *Arch Ophth*. **26**, 859-885.
- Harvey, B. (2003). Examination of intraocular pressure. In: *Investigative Techniques and Ocular Examination*. Eds. Doshi, S. and Harvey, W. Edinburgh: Butterworth - Heinemann. 61-67.
- Hashemi, R.H., Bradley, W.G. and Lisanti, C.J. (2004). *MRI The Basics*. Philadelphia: Lippincott Williams & Wilkins. 3-41.
- Hayes, B.P., Fitzke, F.W., Hodos, W. and Holden, A.L. (1986). A morphological analysis of experimental myopia in young chickens. *Invest Ophthalmol Vis Sci*. **27**, 981-991.
- He, M., Zheng, Y. and Xiang, F. (2009). Prevalence of myopia in urban and rural children in mainland China. *Optom Vis Sci*. **86**, 40-44.
- He, M., Zeng, J., Liu, Y., Xu, J., Pokharel, G.P. and Ellwein, L.B. (2004). Refractive error and visual impairment in urban children in southern china. *Invest Ophthalmol Vis Sci*. **45**, 793-799.
- Heinzen, H., Luder, P., & Muller, A. (1958). Examination of rigidity factor. *Ophthalmologica*, **135**, 649-655.
- Helmhotz, H. (1855). Uber die akkommodation des auges. *Arch Ophthalmol*. **1**, 1-74.
- Helveston, E.M., Bick, S.E. and Ellis, F.D. (1980). Differential intraocular pressure as an indirect measure of generated muscle force. *Ophthalmic Surg*. **11**, 386-391.
- Henzan, I.M., Tomidokoro, A., Uejo, C., Sakai, H., Sawaguchi, S., Iwase, A. and Araie, M. (2010). Ultrasound Biomicroscopic Configurations of the Anterior Ocular Segment in a Population-Based Study The Kumejima Study. *Ophthalmology*. **117**, 1720-1728.
- Herman, D.C., Hodge, D.O. and Bourne, W.M. (2001). Increased corneal thickness in patients with ocular hypertension. *Arch Ophthalmol*. **119**, 334-336.
- Herndon, L.W. (2006). Measuring intraocular pressure-adjustments for corneal thickness and new technologies. *Curr Opin Ophthalmol*. **17**, 115-119.
- Herndon, L.W., Choudhri, S.A., Cox, T., Damji, K.F., Shields, M.B. and Allingham, R.R. (1997). Central corneal thickness in normal, glaucomatous, and ocular hypertensive eyes. *Arch Ophthalmol*. **115**, 1137-1141.
- Herzog, D., Hoffmann, R., Schmidtman, I., Pfeiffer, N., Preussner, P.R. and Pitz, S. (2008). Is gaze-dependent tonometry a useful tool in the differential diagnosis of Graves' ophthalmopathy? *Graefes Arch Clin Exp Ophthalmol*. **246**, 1737-1741.

- Hetland-Eriksen, J. (1966). On tonometry. 9. The pressure-volume relationship by Schiötz tonometry. Concluding observations. *Acta Ophthalmol (Copenh)*. **44**, 893-900.
- Higashide, T., Shimizu, F., Nishimura, A. and Sugiyama, K. (2009). Anterior segment optical coherence tomography findings of reverse pupillary block after scleral-fixated sutured posterior chamber intraocular lens implantation. *J Cataract Refract Surg*. **35**, 1540-1547.
- Hine, M.L. (1916). Some observations with the Schiötz tonometer on the normal eye. *Transactions of the Ophthalmological Society of the UK*, **36**, 226-234.
- Hitzenberger, C.K. (1991). Optical measurement of the axial eye length by laser Doppler interferometry. *Invest Ophthalmol Vis Sci*, **32**. 616-624.
- Hjortdal, J.O. (1996). Regional elastic performance of the human cornea. *J Biomech*. **29**, 931-942.
- Ho, T., Cheng, A.C.K., Rao, S.K., Lau, S. Leung, C.K.S. and Lam, D.S.C. (2007). Central corneal thickness measurements using Orbscan II, Visante, ultrasound, and Pentacam pachymetry after laser in situ keratomileusis for myopia. *J Cataract Refract Surg*. **33**, 1177-1182.
- Hodos, W. and Kuenzel, W.J. (1984). Retinal-image degradation produces ocular enlargement in chicks. *Invest Ophthalmol Vis Sci*. **25**, 652-659.
- Hoerauf, H., Gordes, R.S., Scholz, C., Wirbelauer, C., Koch, P., Engelhardt, R., Winkler, J., Laqua, H. and Birngruber, R. (2000). First experimental and clinical results with transscleral optical coherence tomography. *Ophthalmic Surg Lasers*. **31**, 218-222.
- Hoerauf, H., Winkler, J., Scholz, C., Wirbelauer, C., Gordes, R.S., Koch, P., Engelhardt, R., Laqua, H. and Birngruber, R. (2002). Transscleral optical coherence tomography--an experimental study in ex-vivo human eyes. *Lasers Surg Med*. **30**, 209-215.
- Hogan, M.J., Alvarado, J.A. and Weddell, J.E. (1971). *Histology of the Human Eye*. Philadelphia: Saunders Company. 55-200.
- Hommer, A., Fuchsjager-Mayrl, G., Resch, H., Vass, C., Garhofer, G. and Schmetterer, L. (2008). Estimation of ocular rigidity based on measurement of pulse amplitude using pneumotometry and fundus pulse using laser interferometry in glaucoma. *Invest Ophthalmol Vis Sci*. **49**, 4046-4050.
- Hongyok, T., Cohen, E.J., Hammersmith, K.M., Laibson, P.R. and Rapuano, C.J. (2010). Ocular Response Analyzer Waveform Analysis in the Ectatic Corneas: Correlation of the New Corneal Biomechanics Parameters and Severity of Keratoconus. In: *World Cornea Congress VI*, April 7-9. Boston, MA, USA.
- Hoogerheide, J., Rempt, F. and Hoogenboom, W.P. (1971). Acquired myopia in young pilots. *Ophthalmologica*. **163**, 209-215.
- Hornbeak, D.M. and Young, T.L. (2009). Myopia genetics: a review of current research and emerging trends. *Curr Opin Ophthalmol*. **20**, 356-362.
- Horner, D.G., Soni, P.S., Vyas, N. and Himebaugh, N.L. (2000). Longitudinal changes in corneal asphericity in myopia. *Optom Vis Sci*. **77**, 198-203.
- Hosny, M., Alio, J.L., Claramonte, P., Attia, W.H. and Perez-Santonja, J.J. (2000). Relationship between anterior chamber depth, refractive state, corneal diameter, and axial length. *J Refract Surg*. **16**, 336-340.

- Huang, D., Swanson, E.A. and Lin, C.P. (1991). Optical coherence tomography. *Science*. **254**, 1178-1181.
- Huang, J., Hung, L.F., Ramamirtham, R., Blasdel, T.L., Humbird, T.L., Bockhorst, K.H. and Smith, E.L. (2009). Effects of form deprivation on peripheral refractions and ocular shape in infant rhesus monkeys (*Macaca mulatta*). *Invest Ophthalmol Vis Sci*. **50**, 4033-4044
- Hysi, P.G., Young, T.L., Mackey, D.A., Andrew, T., Fernández-Medarde, A., Solouki, A.M., Hewitt, A.W., Macgregor, S., Vingerling, J.R., Li, Y.J., Ikram, M.K., Fai, L.Y., Sham, P.C., Manyes, L., Porteros, A., Lopes, M.C., Carbonaro, F., Fahy, S.J., Martin, N.G., van Duijn, C.M., Spector, T.D., Rahi, J.S., Santos, E., Klaver, C.C.W. and Hammond, C.J. (2010). A genome-wide association study for myopia and refractive error identifies a susceptibility locus at 15q25. *Nat Genet*. **42**, 902-905.
- Iliev, M.E., Goldblum, D., Katsoulis, K., Amstutz, C. and Frueh, B. (2006). Comparison of rebound tonometry with Goldmann applanation tonometry and correlation with central corneal thickness. *Br J Ophthalmol*. **90**, 833-835.
- Ip, J.M., Huynh, S.C., Robaei, D., Kifley, A., Rose, K.A., Morgan, I.G., Wang, J.J. and Mitchell, P. (2008). Ethnic differences in refraction and ocular biometry in a population-based sample of 11-15-year-old Australian children. *Eye (London)*. **22**, 649-656.
- Irving, E.L., Sivak, J.G. and Callender, M.G. (1992). Refractive plasticity of the developing chick eye. *Ophthalmic Physiol Opt*. **12**, 448-456.
- Ishikawa, T. (1962). Fine structure of the human ciliary muscle. *Invest Ophthalmol*. **1**, 587-608.
- Izatt, J.A., Hee, M.R., Swanson, E.A., Lin, C.P., Huang, D., Schuman, J.S., Puliafito, C.A. and Fujimoto, J.G. (1994). Micrometer-scale resolution imaging of the anterior eye in vivo with optical coherence tomography. *Arch Ophthalmol*. **112**, 1584-1589.
- Jackson, C.R. (1965). Schiötz tonometers. An assessment of their usefulness. *Br J Ophthalmol*. **49**, 478-484.
- Jackson, T.L., Hussain, A., Hodgetts, A., Morley, A.M.S., Hillenkamp, J., Sullivan, P.M. and Marshall, J. (2006). Human scleral hydraulic conductivity: age-related changes, topographical variation, and potential scleral outflow facility. *Invest Ophthalmol Vis Sci*. **47**, 4942-4946.
- Jaén-Díaz, J.I., Cordero-García, B., López-de-Castro, F., de-Castro-Mesa, C., Castilla-López-Madrudejos, F. and Berciano-Martínez, F. (2007). Diurnal variability of intraocular pressure. *Arch Soc Esp Oftalmol*. **82**, 675-679.
- Jain, I. and Singh, K. (1967) A clinical study of myopia scleral rigidity III. *Orient Arch Ophthalmol*. **5**, 81-84.
- Jensen, H. (1992). Myopia progression in young school children and intraocular pressure. *Doc Ophthalmol*. **82**, 249-255.
- Jezzard, P., Matthews, P.M., Smith, S.M. (2001). *Functional MRI: An introduction to Methods*. Oxford: Oxford University Press. 3-34.
- Jobling, A.I., Gentle, A., Metlapally, R., McGowan, B.J. and McBrien, N.A. (2009). Regulation of scleral cell contraction by transforming growth factor-beta and stress: competing roles in myopic eye growth. *J Biol Chem*. **284**, 2072-2079.

- Jóhannesson, G., Hallberg, P., Eklund, A. and Lindén, C. (2008). Pascal, ICare and Goldmann applanation tonometry--a comparative study. *Acta ophthalmologica*. **86**, 614-621.
- Johnson, G.J., Matthews, A. and Perkins, E.S. (1979). Survey of ophthalmic conditions in a Labrador community. I. Refractive errors. *Br J Ophthalmol*. **63**, 440-448.
- Johnson, J.M., Young, T.L. and Rada, J.A.S. (2006). Small leucine rich repeat proteoglycans (SLRPs) in the human sclera: identification of abundant levels of PRELP. *Mol Vis*. **12**, 1057-1066.
- Jonas, J.B., Stroux, A., Velten, I., Juenemann, A., Martus, P. and Budde, W.M. (2005). Central corneal thickness correlated with glaucoma damage and rate of progression. *Invest Ophthalmol Vis Sci*. **46**, 1269-1274.
- Jones, C.E., Atchison, D.A. and Pope, J.M. (2007a). Changes in lens dimensions and refractive index with age and accommodation. *Optom Vis Sci*. **84**, 990-995
- Jones, L.A., Mitchell, G.L., Mutti, D.O., Hayes, J.R., Moeschberger, M.L. and Zadnik, K. (2005). Comparison of ocular component growth curves among refractive error groups in children. *Invest Ophthalmol Vis Sci*. **46**, 2317-2327.
- Jones, L.A., Sinnott, L.T., Mutti, D.O., Mitchell, G.L., Moeschberger, M.L. and Zadnik, K. (2007b). Parental history of myopia, sports and outdoor activities, and future myopia. *Invest Ophthalmol Vis Sci*. **48**, 3524-3532.
- Jones-Jordan, L.A., Mitchell, G.L., Cotter, S.A., Kleinstein, R.N., Manny, R.E., Mutti, D.O., Twelker, J.D., Sims, J.R. and Zadnik, K. (2010). Visual Activity Prior to and Following the Onset of Juvenile Myopia. *Invest Ophthalmol Vis Sci*. Papers in Press. Published on Oct 6, 2010 as Manuscript iovs.09-4997.
- Jorge, J., Fernandes, P., Queirós, A., Ribeiro, P., Garces, C. and González-Méijome, J.M. (2010). Comparison of the IOPen and iCare rebound tonometers with the Goldmann tonometer in a normal population. *Ophthalm. Physiol. Opt.* **30**, 108-112.
- Jorge, J.M.M., González-Méijome, J.M., Queirós, A., Fernandes, P., Parafita, M.A. (2008). Correlations between corneal biomechanical properties measured with the ocular response analyzer and ICare rebound tonometry. *J Glaucoma*. **17**, 442-448.
- Julkunen, P., Korhonen, R.K., Herzog, W. and Jurvelin, J.S.(2008). Uncertainties in indentation testing of articular cartilage: a fibril-reinforced poroviscoelastic study. *Med Eng Phys*. **30**, 506-515.
- Kaiser-Kupfer, M.I., Podgor, M.J., McCain, L., Kupfer, C. and Shapiro, J.R. (1985). Correlation of ocular rigidity and blue sclerae in osteogenesis imperfecta. *Trans Ophthalmol Soc U K*. **104**, 191-195.
- Kamiya, K., Shimizu, K and Ohmoto, F. (2009). Effect of aging on corneal biomechanical parameters using the ocular response analyzer. *J Refract Surg*. **25**, 888-893.
- Kamiya, K., Hagishima, M., Fujimura, F. and Shimizu, K. (2008). Factors affecting corneal hysteresis in normal eyes. *Graefes Arch Clin Exp Ophthalmol*. **246**, 1491-1494.
- Kano, K., Kuwayama, Y., Mizoue, S., Hashitani, T., Sasamoto, Y., Horimoto, K. and Okamoto, H. (1999). Observation of physiological change in the human ciliary body using an ultrasound biomicroscope during accommodation. *Nippon Ganka Gakkai Zasshi*. **103**, 297-300.

- Karwatowski, W.S., Jeffries, T.E., Duance, V.C., Albon, J., Bailey, A.J. and Easty, D.L. (1991). Collagen and ageing in Bruch's membrane. *Biochem Soc Trans.* **19**, 349S.
- Karwatowski, W.S., Jeffries, T.E., Duance, V.C., Albon, J., Bailey, A.J. and Easty, D.L. (1995). Preparation of Bruch's membrane and analysis of the age-related changes in the structural collagens. *Br J Ophthalmol*, **79**, 944-952.
- Kashani, A.H., Zimmer-Galler, I.E., Shah, S.M., Dustin, L., Do, D.V., Elliott, D., Haller, J.A., Nguyen, Q.D. (2010). Retinal thickness analysis by race, gender, and age using Stratus OCT. *Am J Ophthalmol*. **149**, 496-502.
- Katz, J., Tielsch, J.M. and Sommer, A. (1997). Prevalence and risk factors for refractive errors in an adult inner city population. *Invest Ophthalmol Vis Sci*. **38**, 334-340.
- Kee, C.S. and Deng, L. (2008). Astigmatism associated with experimentally induced myopia or hyperopia in chickens. *Invest Ophthalmol Vis Sci*. **49**, 858-867.
- Kee, C.S., Hung, L.F., Qiao-Grider, Y., Ramamirtham, R., Smith, E.L. (2005). Astigmatism in monkeys with experimentally induced myopia or hyperopia. *Optom Vis Sci*. **82**, 248-260.
- Keeley, F.W., Morin, J.D. and Vesely, S. (1984). Characterization of collagen from normal human sclera. *Exp Eye Res*. **39**, 533-542.
- Kempen, J.H, Mitchell, P., Lee, K.E., Tielsch, J.M., Broman, A.T., Taylor, H.R., Ikram, M.K., Congdon, N.G. and O'Colmain, B.J. (2004). The prevalence of refractive errors among adults in the United States, Western Europe, and Australia. *Arch Ophthalmol*. **122**, 495-505.
- Ker, R. F. (1992). Tensile fibres: strings and straps. In J. F. V. Vincent, *Biomechanics materials- a practical approach*. New York: Oxford University Press. 75-97.
- Kerautret, J., Colin, J., Touboul, D. and Roberts, C. (2008). Biomechanical characteristics of the ectatic cornea. *J Cataract Refract Surg*. **34**, 510-513.
- Khan, J.A., Davis, M., Graham, C.E., Trank, J., Whitacre, M.M. (1991). Comparison of Oculab Tono-Pen readings obtained from various corneal and scleral locations. *Arch Ophthalmol*. **109**, 1444-1446.
- Khoramnia, R., Rabsilber, T.M. and Auffarth, G.U. (2007). Central and peripheral pachymetry measurements according to age using the Pentacam rotating Scheimpflug camera. *J Cataract Refract Surg*. **33**, 830-836
- Kida, T., Liu, J.H.K. and Weinreb, R.N. (2008). Effects of aging on corneal biomechanical properties and their impact on 24-hour measurement of intraocular pressure. *Am J Ophthalmol*. **146**, 567-572.
- Kirwan, C. and O'Keefe, M. (2008). Corneal hysteresis using the Reichert ocular response analyser: findings pre- and post-LASIK and LASEK. *Acta ophthalmologica*. **86**, 215-218.
- Kirwan, C., O'Keefe, M. and Lanigan, B. (2006). Corneal hysteresis and intraocular pressure measurement in children using the reichert ocular response analyzer. *Am J Ophthalmol*. **142**, 990-992.
- Kleinstein, R.N., Jones, L.A., Hullett, S., Kwon, S., Lee, R.J., Friedman, N.E., Manny, R.E., Mutti, D.O., Yu, J.A. and Zadnik, K. (2003). Refractive error and ethnicity in children. *Arch Ophthalmol*. **121**, 1141-1147.

- Kniestedt, C., Punjabi, O., Lin, S. and Stamper, R.L. (2008). Tonometry through the ages. *Surv Ophthalmol.* **53**, 568-591.
- Kobayashi, A.S., Woo, S.L., Lawrence, C. and Schlegel, W.A. (1971). Analysis of the corneo-scleral shell by the method of direct stiffness. *J Biomech.* **4**, 323-330.
- Kokott, W. (1938). Uber mechanisch-funktionelle Strukturen des Auges. *A von Graefes Arch Ophthalmol.* **138**, 424-485.
- Kolin, T., Wedemeyer, L.L., Kolin, E. and Braun, Y. (2003). Comparison of scleral and corneal Tono-Pen readings. *J AAPOS.* **7**, 291-292.
- Komai, Y. and Ushiki, T. (1991). The three-dimensional organization of collagen fibrils in the human cornea and sclera. *Invest Ophthalmol Vis Sci.* **32**, 2244-2258.
- Kondapalli, S.A., Roberts, C.J., Mahmoud, A., Weber, P.A. and Peterson, J. (2010). The effect of diabetes on biomechanical properties of the cornea. *Invest Ophthalmol Vis Sci.* ARVO E-Abstract 4631: 51.
- Konomi, H., Hayashi, T., Sano, J., Terato, K., Nagai, Y., Arima, M., Nakayasu, K., Tanaka, M. and Nakajima, A. (1983). Immunohistochemical localization of type I, III and IV collagens in the sclera and choroids of bovine, rat, and normal and pathological human eyes. *Biomed. Res.* **4**, 451 - 458.
- Konstantopoulos, A., Hossain, P. and Anderson, D.F. (2007). Recent advances in ophthalmic anterior segment imaging: a new era for ophthalmic diagnosis? *Br J Ophthalmol.* **91**, 551-557.
- Kontiola, A. (1996). A method and a device for measuring intraocular pressure. Patent no: WO 96/06560.
- Kontiola, A. (1997). A new electromechanical method for measuring intraocular pressure. *Doc Ophthalmol.* **93**, 265-276.
- Kontiola, A.I. (2000). A new induction-based impact method for measuring intraocular pressure. *Acta Ophthalmol Scand.* **78**, 142-145.
- Kontiola, A.I., Goldblum, D., Mittag, T. and Danias, J. (2001). The induction/impact tonometer: a new instrument to measure intraocular pressure in the rat. *Exp Eye Res.* **73**, 781-785.
- Kontiola, A. and Puska, P. (2004). Measuring intraocular pressure with the Pulsair 3000 and Rebound tonometers in elderly patients without an anesthetic. *Graefes Arch Clin Exp Ophthalmol.* **242**, 3-7.
- Kopacz, D., Maciejewicz, P. and Kecik, D. (2005). Pentacam--the new way for anterior eye segment imaging and mapping. *Klin Oczna.* **107**, 728-731.
- Koster, W. (1895). Beitrage zur Tonometric und Manometric des Auges. *von Graefes Arch. Ophth.* **41**, 113. Cited in Fridenwald, J.S. (1937). Contribution to the theory and practice of tonometry. *Am J Ophthalmol.* **20**, 985-1024.
- Kotecha, A., Elsheikh, A., Roberts, C.R., Zhu, H. and Garway-Heath, D.F. (2006). Corneal thickness- and age-related biomechanical properties of the cornea measured with the ocular response analyzer. *Invest Ophthalmol Vis Sci.* **47**, 5337-5347.
- Kowal, L., Troski, M. and Gilford, E. (1994). MRI in the heavy eye phenomenon. *Aust N Z J Ophthalmol.* **22**, 125-226

- Krachmer, J.H., Mannis, M.J. and Holland, E.J. (2005). *Cornea, Volume 1, Fundamental, diagnosis and management*. Philadelphia: Elsevier Mosby, 27-33.
- Krakau, C.E. (1969). On the regulation of the intraocular pressure. *Acta Ophthalmol (Copenh)*. **47**, 1069-1088.
- Krakau, C.E. (1971). On vibration tonometry. *Exp Eye Res*. **11**, 140.
- Krakau, C.E. and Wilke, K. (1971). On repeated tonometry. *Acta ophthalmologica*. **49**, 611-4.
- Krantz, E.M., Cruickshanks, K.J., Klein, B.E.K., Klein, R., Huang, G.H. and Nieto, F.J. (2010). Measuring refraction in adults in epidemiological studies. *Arch Ophthalmol*. **128**, 88-92.
- Kronfeld, P.C. (1959). The clinical estimation of the ocular rigidity. *Am J Ophthalmol*, **47**, 147-154.
- Krzizok, T. and Schroeder, B. (2003). Quantification of recti eye muscle paths in high myopia. *Strabismus*. **11**, 213-220.
- Ku, D.N. and Greene, P.R. (1981). Scleral creep in vitro resulting from cyclic pressure pulses: applications to myopia. *Am J Optom Physiol Opt*. **58**, 528-535.
- Kuc, I.M. and Scott, P.G. (1997). Increased diameters of collagen fibrils precipitated in vitro in the presence of decorin from various connective tissues. *Connect Tissue Res*. **36**, 287-296.
- Kucumen, R.B., Yenerel, N.M., Gorgun, E., Kulacoglu, D.N., Oncel, B., Kohen, M.C., Alimgil, M.L. (2008). Corneal biomechanical properties and intraocular pressure changes after phacoemulsification and intraocular lens implantation. *J Cataract Refract Surg*. **34**, 2096-2098.
- Kynigopoulos, M., Schlote, T., Kotecha, A., Tzamalis, A., Pajic, B. and Haefliger, I. (2008). Repeatability of intraocular pressure and corneal biomechanical properties measurements by the ocular response analyser. *Klin Monbl Augenheilkd*. **225**, 357-360.
- Lackner, B., Schmidinger, G. and Skorpik, C. (2005a). Validity and repeatability of anterior chamber depth measurements with Pentacam and Orbscan. *Optom Vis Sci*. **82**, 858-861.
- Lackner, B., Schmidinger, G., Pieh, S., Funovics, M.A. and Skorpik, C. (2005b). Repeatability and reproducibility of central corneal thickness measurement with Pentacam, Orbscan, and ultrasound. *Optom Vis Sci*. **82**, 892-899.
- Lagrèze, W.A., Gaggl, M., Weigel, M., Schulte-Mönting, J., Bühler, A., Bach, M., Munk, R.D., Bley, T.A. (2009). Retrobulbar optic nerve diameter measured by high-speed magnetic resonance imaging as a biomarker for axonal loss in glaucomatous optic atrophy. *Invest Ophthalmol Vis Sci*. **50**, 4223-4228
- Laiquzzaman, M., Bhojwani, R., Cunliffe, I. and Shah, S. (2006). Diurnal variation of ocular hysteresis in normal subjects: relevance in clinical context. *Clin Experiment Ophthalmol*. **34**, 114-118.
- Lam, A., Chen, D., Chiu, R., Chui, W.S. (2007). Comparison of IOP measurements between ORA and GAT in normal Chinese. *Optom Vis Sci*. **84**, 909-914
- Lam, A., Sambursky, R.P. and Maguire, J.I. (2005). Measurement of scleral thickness in uveal effusion syndrome. *Am J Ophthalmol*. **140**, 329-331.

- Lam, A.K., Chan, R. and Pang, P.C. (2001). The repeatability and accuracy of axial length and anterior chamber depth measurements from the IOLMaster. *Ophthalmic Physiol Opt.* **21**, 477-483.
- Lam, A.K., Chan, S.T., Chan, H. and Chan, B. (2003a). The effect of age on ocular blood supply determined by pulsatile ocular blood flow and color Doppler ultrasonography. *Optom Vis Sci*, **80**, 305-311.
- Lam, A.K.C., Chen, D. and Tse, J. (2010). The Usefulness of Waveform Score from the Ocular Response Analyzer. *Optom Vis Sci*. Jan 30. [Epub ahead of print]
- Lam, C.S.Y., Goldschmidt, E. and Edwards, M.H. (2004). Prevalence of myopia in local and international schools in Hong Kong. *Optom Vis Sci*. **81**, 317-322.
- Lam, D.S.C., Tam, P.O.S., Fan, D.S.P., Baum, L., Leung, Y., Pang, C.P. (2003b). Familial high myopia linkage to chromosome 18p. *Ophthalmologica*. **217**, 115-118.
- Lamparter, J. and Hoffmann, E.M. (2009). Measuring intraocular pressure by different methods. *Ophthalmologie*. **106**, 676-682.
- Landers, J.A., Billing, K.J., Mills, R.A., Henderson, T.R. and Craig, J.E. (2007). Central corneal thickness of indigenous Australians within Central Australia. *Am J Ophthalmol*. **143**, 360-362.
- Langner, S., Martin, H., Terwee, T., Koopmans, S.A., Krüger, P.C., Hosten, N., Schmitz, K.P., Guthoff, R.F. and Stachs, O. (2010). 7.1T MRI to Assess the Anterior Segment of the Eye. *Invest Ophthalmol Vis Sci*. **51**, 6575-6581.
- Lanza, M., Borrelli, M., Bernardo, M.D., Filosa, M.L. and Rosa, N. (2008). Corneal parameters and difference between goldmann applanation tonometry and dynamic contour tonometry in normal eyes. *J Glaucoma*. **17**, 460-464.
- Larsen, J.S. (1971). The sagittal growth of the eye. II. Ultrasonic measurement of the axial diameter of the lens and the anterior segment from birth to puberty. *Acta ophthalmologica*. **49**, 427-440.
- Lee, A.J., Saw, S.M., Gazzard, G., Cheng, A., Tan, D.T.H. (2004). Intraocular pressure associations with refractive error and axial length in children. *Br J Ophthalmol*. **88**, 5-7.
- Lee, D.W., Kim, J.M., Choi, C.Y., Shin, D., Park, K.H. and Cho, J.G. (2010). Age-related changes of ocular parameters in Korean subjects. *Clin Ophthalmol*. **4**, 725-730.
- Lee, S.B., Geroski, D.H., Prausnitz, M.R. and Edelhauser, H.F. (2004). Drug delivery through the sclera: effects of thickness, hydration, and sustained release systems. *Exp Eye Res*. **78**, 599-607.
- Lee, S.M. and Edwards, M.H. (2000). Intraocular pressure in anisometric children. *Optom Vis Sci*. **77**, 675-679.
- Lehman, B.M., Berntsen, D.A., Bailey, M.D. and Zadnik, K. (2009). Validation of optical coherence tomography-based crystalline lens thickness measurements in children. *Optom Vis Sci*. **86**, 181-187.
- Leighton, D.A. and Tomlinson, A. (1973). Ocular tension and axial length of the eyeball in open-angle glaucoma and low tension glaucoma. *Br J Ophthalmol*. **57**, 499-502.
- Leite, M.T., Alencar, L.M., Gore, C., Weinreb, R.N., Sample, P.A., Zangwill, L.M. and Medeiros, F.A. (2010). Comparison of corneal biomechanical properties between healthy blacks and whites using the Ocular Response Analyzer. *Am J Ophthalmol*. **150**, 163-168.

- Leske, M.C., Heijl, A., Hyman, L., Bengtsson, B., Dong, L.M. and Yang, Z. (2007). Predictors of long-term progression in the early manifest glaucoma trial. *Ophthalmology*. **114**, 1965-1972.
- Leydhecker, W. The difficulties of rigidity determination with the Schiøtz tonometer. *Klin Monbl Augenheilkd Augenarztl Fortbild*. **135**, 669-678.
- Li, E.Y.M., Mohamed, S., Leung, C.K.S., Rao, S.K., Cheng, A.C.K., Cheung, C.Y.L., Lam, D.S.C. (2007). Agreement among 3 methods to measure corneal thickness: ultrasound pachymetry, Orbscan II, and Visante anterior segment optical coherence tomography. *Ophthalmology*. **114**, 1842-1847.
- Li, L. and Tighe, B. (2007). Nonlinear analysis of static axisymmetric deformation of the human cornea. *Computational Materials Science*. **38**, 618-624.
- Li, Y.J., Guggenheim, J.A., Bulusu, A., Metlapally, R., Abbott, D., Malecaze, F., Calvas, P., Rosenberg, T., Paget, S., Creer, R.C., Kirov, G., Owen, M.J., Zhao, B., White, T., Mackey, D.A. and Young, T.L. (2009). An international collaborative family-based whole-genome linkage scan for high-grade myopia. *Invest Ophthalmol Vis Sci*. **50**, 3116-3127.
- Lim, L., Gazzard, G., Chan, Y.H., Fong, A., Kotecha, A., Sim, E.L., Tan, D., Tong, L. and Saw, S.M. (2008). Cornea biomechanical characteristics and their correlates with refractive error in Singaporean children. *Invest Ophthalmol Vis Sci*. **49**, 3852-3857.
- Lim, L.S., Saw, S.M., Jeganathan, V.S.E, Tay, W.T., Aung, T., Tong, L., Mitchell, P. and Wong, T.Y. (2010). Distribution and determinants of ocular biometric parameters in an Asian population: the Singapore Malay eye study. *Invest Ophthalmol Vis Sci*. **51**, 103-109.
- Lin, L.L., Shih, Y.F., Hsiao, C.K., Chen, C.J., Lee, L.A. and Hung, P.T. (2001). Epidemiologic study of the prevalence and severity of myopia among schoolchildren in Taiwan in 2000. *J Formos Med Assoc*. **100**, 684-691.
- Lin, L.L.K., Shih, Y.F., Hsiao, C.K. and Chen, C.J. (2004). Prevalence of myopia in Taiwanese schoolchildren: 1983 to 2000. *Ann Acad Med Singap*. **33**, 27-33.
- Lindsey, J.D., Kashiwagi, K., Kashiwagi, F. and Weinreb, R.N. (1997). Prostaglandin action on ciliary smooth muscle extracellular matrix metabolism: implications for uveoscleral outflow. *Surv Ophthalmol*. **41**, 53-59.
- Litwiller, D.V., Lee, S.J., Kolipaka, A., Mariappan, Y.K., Glaser, K.J., Pulido, J.S. and Ehman, R.L. (2010). MR elastography of the ex vivo bovine globe. *J Magn Reson Imaging*. **32**, 44-51.
- Liu, J. and Roberts, C.J. (2005). Influence of corneal biomechanical properties on intraocular pressure measurement: quantitative analysis. *J Cataract Refract Surg*. **3**, 146-155.
- Liu, J.H.K, Kripke, D.F., Twa, M.D., Gokhale, P.A., Jones, E.I., Park, E.H., Meehan, J.E. and Weinreb, R.N. (2002). Twenty-four-hour pattern of intraocular pressure in young adults with moderate to severe myopia. *Invest Ophthalmol Vis Sci*. **43**, 2351-2355.
- Liu, J.H.K., Sit, A.J. and Weinreb, R.N. (2005). Variation of 24-hour intraocular pressure in healthy individuals: right eye versus left eye. *Ophthalmology*. **112**, 1670-1675.
- Liu, S., Li, H., Dorairaj, S., Cheung, C.Y.L., Rousso, J., Liebmann, J., Ritch, R., Lam, D.S.C. and Leung, C.K.S. (2010). Assessment of scleral spur visibility with anterior segment optical coherence tomography. *Journal of glaucoma*. **19**, 132-135.

- Liu, Z., Chen, J. and Li, S. (1995). The differences in corneal shape between myopic and normal eyes. *Zhonghua Yan Ke Za Zhi*. **31**, 282-284.
- Lo, P.I., Ho, P.C., Lau, J.T., Cheung, A.Y., Goldschmidt, E. and Tso, M.O. (1996). Relationship between myopia and optical components--a study among Chinese Hong Kong student population. *Yan Ke Xue Bao*. **12**, 121-125.
- Logan, N.S., Gilmartin, B., Wildsoet, C.F. and Dunne, M.C.M. (2004). Posterior retinal contour in adult human anisomyopia. *Invest Ophthalmol Vis Sci*. **45**, 2152-2162.
- Logan, N.S., Singh, K.D. and Gilmartin, B. (2005). 3D conformation of human eye shape using MRI. *Invest Ophthalmol Vis Sci*. E-Abstract 4266: 46.
- López-Caballero, C., Contreras, I., Muñoz-Negrete, F.J., Rebolleda, G., Cabrejas, L. and Marcelo, P. (2007). Rebound tonometry in a clinical setting. Comparison with applanation tonometry. *Arch Soc Esp Oftalmol*. **82**, 273-278.
- Lu, F., Xu, S., Qu, J., Shen, M., Wang, X., Fang, H. and Wang, J. (2007). Central corneal thickness and corneal hysteresis during corneal swelling induced by contact lens wear with eye closure. *Am J Ophthalmol*. **143**, 616-622.
- Lu, Y.B., Franze, K., Seifert, G., Steinhäuser, C., Kirchhoff, F., Wolburg, H., Guck, J., Janmey, P., Wei, E.Q., Käs, J. and Reichenbach, A. (2006). Viscoelastic properties of individual glial cells and neurons in the CNS. *Proc Natl Acad Sci USA*. **103**, 17759-17764.
- Luce, D.A. (2005a). Duel Mode Non-Contact Tonometer. Patent no:US 6,875,175 B2.
- Luce, D.A. (2005b). Determining in vivo biomechanical properties of the cornea with an ocular response analyzer. *J Cataract Refract Surg*. **31**, 156-162.
- Luce D and Taylor D. 2006. Reichert Ocular Response Analyzer Measures Corneal Biomechanical Properties and IOP Provides New Indicators for Corneal Specialties and Glaucoma Management. White paper.
- Luce, D. (2006). Methodology for cornea compensated IOP and corneal resistance factor for Reichert ocular response analyzer. *Invest Ophthalmol Vis Sci*. ARVO E-Abstract 2266; 47.
- Lütjen-Drecoll, E., Tamm, E. and Kaufman, P.L. (1988). Age-related loss of morphologic responses to pilocarpine in rhesus monkey ciliary muscle. *Arch Ophthalmol*. **106**, 1591-1598.
- Luyckx, J. (1967). Relationship between the rigidity coefficient and the length of the eye, measured by ultrasonic echography. *Ophthalmologica*. **153**, 355-366.
- Lyhne, N., Sjølie, A.K., Kyvik, K.O. and Green, A. (2001). The importance of genes and environment for ocular refraction and its determiners: a population based study among 20-45 year old twins. *Br J Ophthalmol*. **85**, 1470-1476.
- Maino, A.P., Uddin, H.J. and Tullo, A.B. (2006). A comparison of clinical performance between disposable and Goldmann tonometers. *Eye (Lond)*. **20**, 574-578.
- Malik, N.S., Moss, S.J., Ahmed, N., Furth, A.J., Wall, R.S. and Meek, K.M. (1992). Ageing of the human corneal stroma: structural and biochemical changes. *Biochim Biophys Acta*. **1138**, 222-228.
- Mallen, E.A., Wolffsohn, J.S., Gilmartin, B. and Tsujimura, S. (2001). Clinical evaluation of the Shin-Nippon SRW-5000 autorefractor in adults. *Ophthalmic Physiol Opt*. **21**, 101-107.

- Mangouritsas, G., Morphis, G., Mourtzoukos, S. and Feretis, E. (2009). Association between corneal hysteresis and central corneal thickness in glaucomatous and non-glaucomatous eyes. *Acta ophthalmologica*. **87**, 901-905.
- Mansouri, K., Sommerhalder, J. and Shaarawy, T. (2010). Prospective comparison of ultrasound biomicroscopy and anterior segment optical coherence tomography for evaluation of anterior chamber dimensions in European eyes with primary angle closure. *Eye (Lond)*. **24**, 233-239.
- Marchini, G., Ghilotti, G., Bonadimani, M. and Babighian, S. (2003). Effects of 0.005% latanoprost on ocular anterior structures and ciliary body thickness. *J Glaucoma*. **12**, 295-300.
- Marr, J.E., Halliwell-Ewen, J., Fisher, B., Soler, L. and Ainsworth, J.R. (2001). Associations of high myopia in childhood. *Eye (Lond)*. **15**, 70-74.
- Marshall, G.E. (1995). Human scleral elastic system: an immunoelectron microscopic study. *Br. J. Ophthalmol*. **79**, 57-64.
- Marshall, G.E., Konstas, A.G. and Lee, W.R. (1993). Collagens in the aged human macular sclera. *Curr Eye Res*. **12**, 143-153.
- Martinez-de-la-Casa, J.M., Garcia-Feijoo, J., Castillo, A. and Garcia-Sanchez, J. (2005). Reproducibility and clinical evaluation of rebound tonometry. *Invest Ophthalmol Vis Sci*. **46**, 4578-4580.
- Martinez-de-la-Casa, J.M., Garcia-Feijoo, J., Fernandez-Vidal, A., Mendez-Hernandez, C. and Garcia-Sanchez, J. (2006b). Ocular response analyzer versus Goldmann applanation tonometry for intraocular pressure measurements. *Invest Ophthalmol Vis Sci*. **47**, 4410-4414.
- Martinez-de-la-Casa, J.M., Garcia-Feijoo, J., Vico, E., Fernandez-Vidal, A., Benitez del Castillo, J.M., Wasfi, M. and Garcia-Sanchez, J. (2006a). Effect of corneal thickness on dynamic contour, rebound, and goldmann tonometry. *Ophthalmology*. **113**, 2156-2162.
- Martinez-de-la-Casa, J.M., Jimenez-Santos, M., Saenz-Frances, F., Matilla-Rodero, M., Mendez-Hernandez, C., Herrero-Vanrell, R., Garcia-Feijoo, J. (2009). Performance of the rebound, noncontact and Goldmann applanation tonometers in routine clinical practice. *Acta ophthalmologica*. no. doi: 10.1111/j.1755-3768.2009.01774.x [Epub ahead of print].
- Masters, B. (1998). Three-dimensional microscopic tomographic imagings of the cataract in a human lens in vivo. *Opt Express*. **3**, 332-338.
- Mastropasqua, L., Lobefalo, L., Mancini, A., Ciancaglini, M. and Palma, S. (1992). Prevalence of myopia in open angle glaucoma. *Eur J Ophthalmol*. **2**, 33-35.
- Mattson, M.S., Huynh, J., Wiseman, M., Coassin, M., Kornfield, J.A. and Schwartz, D.M. (2010). An in vitro intact globe expansion method for evaluation of cross-linking treatments. *Invest Ophthalmol Vis Sci* **51**, 3120-3128.
- Mauger, R.R., Likens, C.P. and Applebaum, M. (1984). Effects of accommodation and repeated applanation tonometry on intraocular pressure. *Am J Optom Physiol Opt*. **61**, 28-30.
- Maurice, D.M. (1957). The structure and transparency of the cornea. *J Physiol (Lond)*. **136**, 263-286.
- Maurice, D.M. (1962). The cornea and sclera, In: Davson H, editor. *The Eye, Vol. 1*. New York: Academic Press, 289-368.

- Maurice, D.M. (1988). Mechanics of the cornea. In: Cavanagh H.D. editor. *The Cornea*. New York : Raven Press, 187–193.
- McAllister, J.A. and Wilson, R.P. (1986). *Glaucoma*. Oxford: Butterworth: Heinemann. 229-254.
- McBrien, N.A. and Adams, D.W. (1997). A longitudinal investigation of adult-onset and adult-progression of myopia in an occupational group. Refractive and biometric findings. *Invest Ophthalmol Vis Sci*. **38**, 321-333.
- McBrien, N.A. and Gentle, A. (2003). Role of the sclera in the development and pathological complications of myopia. *Prog Retin Eye Res*. **22**, 307-338.
- McBrien, N.A. and Norton, T.T. (1992). The development of experimental myopia and ocular component dimensions in monocularly lid-sutured tree shrews (*Tupaia belangeri*). *Vision Res*. **32**, 843-852.
- McBrien, N.A., Cornell, L.M. and Gentle, A. (2001a). Structural and ultrastructural changes to the sclera in a mammalian model of high myopia. *Invest Ophthalmol Vis Sci*. **42**, 2179-2187.
- McBrien, N.A., Gentle, A. and Anastasopoulos, F.A., (2001b). TIMP-2 regulation of MMP-2 activity during visually guided remodelling of the tree shrew sclera in lens-induced myopia. *Invest. Ophthalmol. Vis. Sci*. **42**, S56.
- McBrien, N.A., Jobling, A.I. and Gentle, A. (2009). Biomechanics of the sclera in myopia: extracellular and cellular factors. *Optom Vis Sci*. **86**, 23-30.
- McBrien, N.A., Lawlor, P. and Gentle, A. (2000). Scleral remodeling during the development of and recovery from axial myopia in the tree shrew. *Invest Ophthalmol Vis Sci*. **41**, 3713-3719.
- McBrien, N.A., Metlapally, R., Jobling, A.I. and Gentle, A. (2006). Expression of collagen-binding integrin receptors in the mammalian sclera and their regulation during the development of myopia. *Invest Ophthalmol Vis Sci*. **47**, 4674-4682.
- McCarthy, C.S., Megaw, P., Devadas, M. and Morgan, I.G. (2007). Dopaminergic agents affect the ability of brief periods of normal vision to prevent form-deprivation myopia. *Exp Eye Res*. **84**, 100-107.
- McFadden, S.A., Howlett, M.H.C. and Mertz, J.R. (2004). Retinoic acid signals the direction of ocular elongation in the guinea pig eye. *Vision Res*. **44**, 643-653.
- McFadden, S.A., Coassin, M., Mattson, M.S., Howlett, M.H., Kornfield, J.A., and Schwartz, D.M. (2010). The effect of scleral cross-linking on emmetropisation and eye shape. In: *International Myopia Conference*, 26-29 July 2010 Tübingen, Germany.
- McRobbie, D.W., Moore, E.A., Graves, M.J. and Prince, M.R. (2007). *MRI From Picture to Proton*. Cambridge: Cambridge University Press. 30-46.
- Medeiros, F.A. and Weinreb, R.N. (2006). Evaluation of the influence of corneal biomechanical properties on intraocular pressure measurements using the ocular response analyzer. *J Glaucoma*. **15**, 364-370.
- Meek, K.M. and Fullwood, N.J. (2001). Corneal and scleral collagens--a microscopist's perspective. *Micron*. **32**, 261-272.

- Mertz, J.R. and Wallman, J. (2000). Choroidal retinoic acid synthesis: a possible mediator between refractive error and compensatory eye growth. *Exp Eye Res.* **70**, 519-527.
- Metlapally, R., Ki, C.S., Li, Y.J., Tran-Viet, K.N., Abbott, D., Malecaze, F., Calvas, P., Mackey, D.A., Rosenberg, T., Paget, S., Guggenheim, J.A. and Young, T.L. (2010). Genetic association of insulin-like growth factor-1 polymorphisms with high-grade myopia in an international family cohort. *Invest Ophthalmol Vis Sci.* **51**, 4476-4479.
- Metlapally, R., Li, Y.J., Tran-Viet, K.N., Abbott, D., Czaja, G.R., Malecaze, F., Calvas, P., Mackey, D., Rosenberg, T., Paget, S., Zayats, T., Owen, M.J., Guggenheim, J.A. and Young, T.L. (2009). COL1A1 and COL2A1 genes and myopia susceptibility: evidence of association and suggestive linkage to the COL2A1 locus. *Invest Ophthalmol Vis Sci.* **50**, 4080-4086.
- Metlapally, S. and McBrien, N.A., (2008). The effect of positive lens defocus on ocular growth and emmetropization in the tree shrew. *J. Vis.* **8**, 1-12.
- Miglior, S., Pfeiffer, N., Torri, V., Zeyen, T., Cunha-Vaz, J. and Adamsons, I. (2007). Predictive factors for open-angle glaucoma among patients with ocular hypertension in the European Glaucoma Prevention Study. *Ophthalmology.* **114**, 3-9.
- Miller, J.M., Wildsoet, C.F., Guan, H., Limbo, M. and Demer, J.L. (2004). Refractive error and eye shape by MRI. *Invest Ophthalmol Vis Sci.* E-Abstract 2388: 45.
- Millodot, M. (1981). Effect of ametropia on peripheral refraction. *Am J Optom Physiol Opt.* **58**, 691-695.
- Minami, Y., Sugihara, H. and Oono, S. (1993). Reconstruction of cornea in three-dimensional collagen gel matrix culture. *Invest. Ophthalmol. Vis. Sci.* **34**, 2316–2324.
- Mitchell, D.G. and Cohen, M.S. (2004). *MRI Principles*. Philadelphia: Elsevier.1-20.
- Mitchell, P., Hourihan, F., Sandbach, J., Wang, J.J. (1999). The relationship between glaucoma and myopia: the Blue Mountains Eye Study. *Ophthalmology.* **106**, 2010-2015.
- Mohamed-Noor, J., Bochmann, F., Siddiqui, M.A.R., Atta, H.R., Leslie, T., Maharajan, P., Wong, Y.M. and Azuara-Blanco, A. (2009). Correlation between corneal and scleral thickness in glaucoma. *J Glaucoma.* **18**, 32-36.
- Mohamed, S., Lee, G.K.Y., Rao, S.K., Wong, A.L., Cheng, A.C.K., Li, E.Y.M., Chi, S.C.C. and Lam, D.S.C. (2007). Repeatability and reproducibility of pachymetric mapping with Visante anterior segment-optical coherence tomography. *Invest Ophthalmol Vis Sci.* **48**, 5499-5504.
- Montard, R., Kopito, R., Touzeau, O., Allouch, C., Letaief, I., Borderie, V. and Laroche, L. (2007). Ocular response analyzer: feasibility study and correlation with normal eyes. *J Fr Ophthalmol.* **30**, 978-984.
- Montero, J.A., Ruiz-Moreno, J.M., Fernandez-Munoz, M. and Rodriguez-Palacios, M.I. (2008). Effect of topical anesthetics on intraocular pressure and pachymetry. *Eur J Ophthalmol.* **18**, 748-750.
- Moreno-Montañés, J., García, N., Fernández-Hortelano, A. and García-Layana, A. (2007). Rebound tonometer compared with goldmann tonometer in normal and pathologic corneas. *Cornea.* **26**, 427-430.
- Moreno-Montañés, J., Maldonado, M.J., García, N., Mendiluce, L., García-Gómez, P.J. and Seguí-Gómez, M. (2008). Reproducibility and clinical relevance of the ocular response analyzer in

- nonoperated eyes: corneal biomechanical and tonometric implications. *Invest Ophthalmol Vis Sci.* **49**, 968-974.
- Morgan, I. and Rose, K. (2005). How genetic is school myopia? *Prog Retin Eye Res.* **24**, 1-38.
- Mortazavi, A.M., Simon, B.R., Stamer, W.D. and Geest, J.P.V. (2009). Drained secant modulus for human and porcine peripapillary sclera using unconfined compression testing. *Exp Eye Res.* **89**, 892-897.
- Moses, R.A. (1971). Theory of the Schiøtz tonometer and its empirical calibration. *Trans Am Ophthalmol Soc.* **69**, 494-562
- Moses, R.A., Grodzki, W.J., Starcher, B.C. and Galione, M.J. (1978). Elastin content of the scleral spur, trabecular mesh, and sclera. *Invest Ophthalmol Vis Sci.* **17**, 817-818.
- Moses, R.A., Lurie, P. and Wette, R. (1982). Horizontal gaze position effect on intraocular pressure. *Invest Ophthalmol Vis Sci.* **22**, 551-553.
- Motolko, M.A., Feldman, F., Hyde, M. and Hudy, D. (1982). Sources of variability in the results of applanation tonometry. *Can J Ophthalmol.* **17**, 93-95.
- Muhtuoglu, O., Hosal, B.M., Zilelioglu, G. (2009). Ciliary body thickness in unilateral high axial myopia. *Eye (Lond).* **23**, 1176-1181.
- Müller, M., Winter, C., Hüttmann, G., Laqua, H. and Hoerauf, H. (2007). Evaluation of cyclophotocoagulation effects with 1310-nm contact optical coherence tomography. *Curr Eye Res.* **32**, 171-176.
- Munkwitz, S., Elkarmouty, A., Hoffmann, E.M., Pfeiffer, N. and Thieme, H. (2008). Comparison of the iCare rebound tonometer and the Goldmann applanation tonometer over a wide IOP range. *Graefes Arch Clin Exp Ophthalmol.* **246**, 875-879.
- Mutti, D.O. and Zadnik, K. (1996). Is computer use a risk factor for myopia? *J Am Optom Assoc.* **67**, 521-530.
- Mutti, D.O., Sholtz, R.I., Friedman, N.E. and Zadnik, K. (2000a). Peripheral refraction and ocular shape in children. *Invest Ophthalmol Vis Sci.* **41**, 1022-1030.
- Mutti, D.O., Jones, L.A., Moeschberger, M.L. and Zadnik, K. (2000b). AC/A ratio, age, and refractive error in children. *Invest Ophthalmol Vis Sci.* **41**, 2469-2478.
- Mutti, D.O., Mitchell, G.L., Moeschberger, M.L., Jones, L.A. and Zadnik, K. (2002). Parental myopia, near work, school achievement, and children's refractive error. *Invest Ophthalmol Vis Sci.* **43**, 3633-3640.
- Mutti, D.O., Mitchell, G.L., Jones, L.A., Friedman, N.E., Frane, S.L., Lin, W.K., Moeschberger, M.L. and Zadnik, K. (2005). Axial growth and changes in lenticular and corneal power during emmetropization in infants. *Invest Ophthalmol Vis Sci.* **46**, 3074-3080.
- Mutti, D.O., Mitchell, G.L., Hayes, J.R., Jones, L.A., Moeschberger, M.L., Cotter, S.A., Kleinstein, R.N., Manny, R.E., Twelker, J.D. and Zadnik, K. (2006). CLEERE Study Group. Accommodative lag before and after the onset of myopia. *Invest Ophthalmol Vis Sci.* **47**, 837-846.
- Mutti, D.O., Hayes, J.R., Mitchell, G.L., Jones, L.A., Moeschberger, M.L., Cotter, S.A., Kleinstein, R.N., Manny, R.E., Twelker, J.D. and Zadnik, K. (2007). Refractive error, axial length,

- and relative peripheral refractive error before and after the onset of myopia. *Invest Ophthalmol Vis Sci.* **48**, 2510-2519.
- Mutti, D.O. (2010). Hereditary and environmental contributions to emmetropization and myopia. *Optom Vis Sci.* **87**, 255-259.
- Mutti, D.O., Sinnott, L.T., Mitchell, G.L., Jones-Jordan, L.A., Moeschberger, M.L., Cotter, S., Kleinstein, R.N., Manny, R.E., Twelker, D. and Zadnik, K. (2010). Relative peripheral refractive error and the risk of onset and progression of myopia in children. *Invest Ophthalmol Vis Sci.* Papers in Press. Published on August 25, 2010 as Manuscript iovs.09-4826.
- Nagra, M., Gilmartin, B., Logan, N.S., Furlong, P. and Wilkinson, E. (2009). Conformation of sagittal and axial meridians in human myopia. *Invest Ophthalmol Vis Sci.* ARVO E-Abstract 3941: 50.
- Nakamura, M., Darhad, U., Tatsumi, Y., Fujioka, M., Kusuhara, A., Maeda, H. and Negi, A. (2006). Agreement of rebound tonometer in measuring intraocular pressure with three types of applanation tonometers. *Am J Ophthalmol.* **142**, 332-334.
- Nardi, M., Bartolomei, M.P., Romani, A. and Barca, L. (1988). Intraocular pressure changes in secondary positions of gaze in normal subjects and in restrictive ocular motility disorders. *Graefes Arch Clin Exp Ophthalmol.* **226**, 8-10.
- Neider, M.W., Crawford, K., Kaufman, P.L. and Bito, L.Z. (1990). *In vivo* videography of the rhesus monkey accommodative apparatus. Age-related loss of ciliary muscle response to central stimulation. *Arch Ophthalmol.* **108**, 69-74.
- Nemesure, B., Wu, S.Y., Hennis, A. and Leske, M.C., (2003). Corneal thickness and intraocular pressure in the Barbados eye studies. *Arch Ophthalmol.* **121**, 240-244.
- Nickla, D.L. and Wallman, J. (2010). The multifunctional choroid. *Prog Retin Eye Res.* **29**, 144-168.
- Nickla, D.L., Wildsoet, C. and Wallman, J. (1997). Compensation for spectacle lenses involves changes in proteoglycan synthesis in both the sclera and choroid. *Curr Eye Res.* **16**, 320-326.
- Nolan, W. (2008). Anterior segment imaging: ultrasound biomicroscopy and anterior segment optical coherence tomography. *Current Opinion in Ophthalmology.* **19**, 115–121.
- Nomura, H., Ando, F., Niino, N., Shimokata, H. and Miyake, Y. (2004). The relationship between intraocular pressure and refractive error adjusting for age and central corneal thickness. *Ophthalmic Physiol Opt.* **24**, 41-45.
- Norman, R.E., Flanagan, J.G., Rausch, S.M.K., Sigal, I.A., Tertinegg, I., Eilaghi, A., Portnoy, S., Sled, J.G. and Ethier, C.R. (2009). Dimensions of the human sclera: Thickness measurement and regional changes with axial length. *Exp Eye Res.* **90**, 277-284.
- Normand, V., Lootens, D.L., Amici, E., Plucknett, K.P. and Aymard, P. (2001). New insight into agarose gel mechanical properties. *Biomacromolecules.* **1**, 730-738.
- Norton, T.T. (1999). Animal Models of Myopia: Learning How Vision Controls the Size of the Eye. *ILAR J.* **40**, 59-77.
- Norton, T.T. and Siegart, J.T. (1991). Local myopia produced by partial visual- field deprivation in tree shrew. *Soc Neurosci Abstr.* **17**, 558.

- Norton, T.T. and Rada, J.A. (1995). Reduced extracellular matrix in mammalian sclera with induced myopia. *Vision Res.* **35**, 1271-1281.
- Norton, T.T., Essinger, J.A. and McBrien, N.A. (1994). Lid-suture myopia in tree shrews with retinal ganglion cell blockade. *Vis Neurosci.* **11**, 143-153.
- Obbink, J. (1931). Onderzoek naar het verband tusschen inwendigen oogdruk en ballistische reacties. Thesis, Utrecht.
- Ojaimi, E., Rose, K.A., Morgan, I.G., Smith, W., Martin, F.J., Kifley, A., Robaei, D. and Mitchell, P. (2005). Distribution of ocular biometric parameters and refraction in a population-based study of Australian children. *Invest Ophthalmol Vis Sci.* **46**, 2748-2754.
- Oliveira, C., Tello, C., Liebmann, J. and Ritch, R. (2006). Central corneal thickness is not related to anterior scleral thickness or axial length. *J Glaucoma.* **15**, 190-194.
- Oliveira, C., Tello, C., Liebmann, J.M. and Ritch, R. (2005). Ciliary body thickness increases with increasing axial myopia. *Am J Ophthalmol.* **140**, 324-325.
- Olsen, T.W., Aaberg, S.Y., Geroski, D.H. and Edelhauser, H.F. (1998). Human sclera: thickness and surface area. *Am J Ophthalmol.* **125**, 237-241.
- Olsen, T.W., Edelhauser, H.F., Lim, J.I. and Geroski, D.H. (1995). Human scleral permeability. Effects of age, cryotherapy, transscleral diode laser, and surgical thinning. *Invest Ophthalmol Vis Sci.* **36**, 1893-1903.
- Olsen, T.W., Sanderson, S., Feng, X. and Hubbard, W.C. (2002). Porcine sclera: thickness and surface area. *Invest Ophthalmol Vis Sci.* **43**, 2529-2532.
- Oncel, B., Dinc, U.A., Gorgun, E., Yalvaç, B.I. (2009). Diurnal variation of corneal biomechanics and intraocular pressure in normal subjects. *Eur J Ophthalmol.* **19**, 798-803.
- Ortiz, D., Piñero, D., Shabayek, M.H., Arnalich-Montiel, F. and Alió, J.L. (2007). Corneal biomechanical properties in normal, post-laser in situ keratomileusis, and keratoconic eyes. *J Cataract Refract Surg.* **33**, 1371-1375.
- Ortiz, S., Siedlecki, D., Remon, L. and Marcos, S. (2009). Optical coherence tomography for quantitative surface topography. *Applied Optics.* **48**, 6708-6715.
- Ortiz, S., Siedlecki, D., Grulkowski, I., Remon, L., Pascual, D., Wojtkowski, M. and Marcos, S. (2010). Optical distortion correction in Optical Coherence Tomography for quantitative ocular anterior segment by three-dimensional imaging. *Optics Express.* **18**, 2782- 2796.
- Ostrin, L.A. and Glasser, A. (2007). Effects of pharmacologically manipulated amplitude and starting point on edinger-westphal-stimulated accommodative dynamics in rhesus monkeys. *Invest Ophthalmol Vis Sci.* **48**, 313-320.
- Oyster, C.W. (1999). *The Human Eye, Structure and Fuction*. Massachusetts: Sinauer Associates, Inc. 323-410.
- Pakravan, M., Parsa, A., Sanagou, M. and Parsa, C.F. (2007). Central corneal thickness and correlation to optic disc size: a potential link for susceptibility to glaucoma. *Br J Ophthalmol.* **91**, 26-28.
- Pakrou, N., Gray, T., Mills, R., Landers, J. and Craig, J. (2008). Clinical comparison of the Icare tonometer and Goldmann applanation tonometry. *J Glaucoma.* **17**, 43-47.

- Pallikaris, I.G., Kymionis, G.D., Ginis, H.S., Kounis, G.A., Christodoulakis, E. and Tsilimbaris, M.K. (2006). Ocular rigidity in patients with age-related macular degeneration. *Am J Ophthalmol.* **141**, 611-615.
- Pallikaris, I.G., Kymionis, G.D., Ginis, H.S., Kounis, G.A., Tsilimbaris, M.K. (2005). Ocular rigidity in living human eyes. *Invest Ophthalmol Vis Sci.* **46**, 409-414.
- Papanicolaou, A.C. (1998). *Fundamentals of Functional Brain Images: A Guide to the Methods and their applications to Psychology and Behavioural Neuroscience*. Abingdon: Swets & Zeitlinger. 10-30.
- Pardue, M.T. and Sivak, J.G. (2000). Age-related changes in human ciliary muscle. *Optom Vis Sci.* **77**, 204-210.
- Park, D.J.J. and Congdon, N.G. (2004). Evidence for an "epidemic" of myopia. *Ann Acad Med Singap.* **33**, 21-26.
- Park, K.A., Yun, J.H. and Kee, C. (2008). The effect of cataract extraction on the contractility of ciliary muscle. *Am J Ophthalmol.* **146**, 8-14.
- Park, S.H., Park, K.H., Kim, J.M. and Choi, C.Y. (2010). Relation between axial length and ocular parameters. *Ophthalmologica.* **224**, 188-193.
- Patel, H., Gilmartin, B., Cubbidge, R., Logan, N. (2009). *In vivo* measurement of regional variation in scleral rigidity on humans. *Invest Ophthalmol Vis Sci.* ARVO E-Abstract 3947; 50.
- Patel, M.R., Klufas, R.A., Alberico, R.A. and Edelman, R.R. (1997). Half-fourier acquisition single-shot turbo spin-echo (HASTE) MR: comparison with fast spin-echo MR in diseases of the brain. *AJNR Am J Neuroradiol.* 1997 **18**, 1635-1640.
- Patz, S., Bert, R.J., Frederick, E. and Freddo, T.F. (2007). T(1) and T(2) measurements of the fine structures of the in vivo and enucleated human eye. *J Magn Reson Imaging.* **26**, 510-518.
- Pavlin, C.J., Harasiewicz, K. and Foster, F.S. (1992). Ultrasound biomicroscopy of anterior segment structures in normal and glaucomatous eyes. *Am J Ophthalmol.* **113**, 381-389.
- Pedersen, L., Hjortdal, J. and Ehlers, N. (2005). Central corneal thickness in high myopia. *Acta Ophthalmol Scand.* **83**, 539-542.
- Pekmezci, M., Porco, T.C. and Lin, S.C. (2009). Anterior segment optical coherence tomography as a screening tool for the assessment of the anterior segment angle. *Ophthalmic Surg Lasers Imaging.* **40**, 389-398.
- Pepose, J.S., Feigenbaum, S.K., Qazi, M.A., Sanderson, J.P. and Roberts, C.J. (2007). Changes in corneal biomechanics and intraocular pressure following LASIK using static, dynamic, and noncontact tonometry. *Am J Ophthalmol.* **143**, 39-47.
- Perkins, E.S. (1981). Ocular volume and ocular rigidity. *Exp Eye Res.* **33**, 141-145.
- Perkins, E.S. and Phelps, C.D. (1982). Open angle glaucoma, ocular hypertension, low-tension glaucoma, and refraction. *Arch Ophthalmol.* **100**, 1464-1467.
- Pervite, L.R., Burris, J.E. and Carter, V. (1974). Halberg hand applanation tonometer: statistical analysis of tonometry with Goldmann, Halberg and Schiottz tonometry on 2000 eyes. *Ann Ophthalmol.* **6**, 567-570.

- Phillips, C.I. and Shaw, T.L. (1970). Model analysis of impression tonometry and tonography. *Exp Eye Res.* **10**, 161-182.
- Phillips, J.R. and McBrien, N.A. (1995). Form deprivation myopia: elastic properties of sclera. *Ophthalmic Physiol Opt*, **15**, 357-362.
- Phillips, J.R. and McBrien, N.A. (2004). Pressure-induced changes in axial eye length of chick and tree shrew: significance of myofibroblasts in the sclera. *Invest Ophthalmol Vis Sci.* **45**, 758-763.
- Phillips, J.R., Khalaj, M. and McBrien, N.A. (2000). Induced myopia associated with increased scleral creep in chick and tree shrew eyes. *Invest Ophthalmol Vis Sci.* **41**, 2028-2034.
- Pierscionek, B.K., Asejczyk-Widlicka, M. and Schachar, R.A. (2007). The effect of changing intraocular pressure on the corneal and scleral curvatures in the fresh porcine eye. *Br J Ophthalmol.* **91**, 801-803.
- Piñero, D.P., Puche, A.B.P. and Alió, J.L. (2009). Ciliary sulcus diameter and two anterior chamber parameters measured by optical coherence tomography and VHF ultrasound. *J Refract Surg.* **25**, 1017-1025.
- Pinsky, P.M., van der Heide, D. and Chernyak, D. (2005). Computational modeling of mechanical anisotropy in the cornea and sclera. *J Cataract Refract Surg.* **31**, 136-145.
- Podoleanu, A., Charalambous, I., Plesea, L., Dogariu, A., and Rosen, R. (2004). Correction of distortions in optical coherence tomography imaging of the eye. *Phys. Med. Biol.* **49**, 1277-1294.
- Podos, S.M., Becker, B. and Morton, W.R. (1966). High myopia and primary open-angle glaucoma. *Am J Ophthalmol.* **62**, 1038-1043.
- Pokharel, S., Malla, O.K., Pradhananga, C.L. and Joshi, S.N. (2009). A pattern of age-related macular degeneration. *JNMA J Nepal Med Assoc.* **48**, 217-220.
- Poostchi, A., Mitchell, R., Nicholas, S., Purdie, G. and Wells, A. (2009). The iCare rebound tonometer: comparisons with Goldmann tonometry, and influence of central corneal thickness. *Clin Experiment Ophthalmol.* **37**, 687-691.
- Poukens, V., Glasgow, B.J. and Demer, J.L. (1998). Nonvascular contractile cells in sclera and choroid of humans and monkeys. *Invest Ophthalmol Vis Sci.* **39**, 1765-1774.
- Prakash, G., Ashokumar, D., Jacob, S., Kumar, K.S., Agarwal, A. and Agarwal, A. (2009). Anterior segment optical coherence tomography-aided diagnosis and primary posterior chamber intraocular lens implantation with fibrin glue in traumatic phacocoele with scleral perforation. *J Cataract Refract Surg.* **35**, 782-784.
- Pruett, R.C. (1988). Progressive myopia and intraocular pressure: what is the linkage? A literature review. *Acta Ophthalmol Suppl.* **185**, 117-127.
- Purslow, P.P. and Karwatowski, W.S. (1996). Ocular elasticity. Is engineering stiffness a more useful characterization parameter than ocular rigidity? *Ophthalmology.* **103**, 1686-1692.
- Qiao-Grider, Y., Hung, L., Kee, C. and Ramamirtham, R. (2010). Nature of the Refractive Errors in Rhesus Monkeys (*Macaca mulatta*) with Experimentally Induced Ametropias. *Vision Research.* **50**, 1867-1881.
- Qiao-Grider, Y., Hung, L.F., Kee, C.S., Ramamirtham, R. and Smith, E.L. (2004). Recovery from form-deprivation myopia in rhesus monkeys. *Invest Ophthalmol Vis Sci.* **45**, 3361-3372.

- Queirós, A., González-Méijome, J.M., Fernandes, P., Jorge, J., Montés-Micó, R., Almeida, J.B., Parafita, M.A. (2007) Technical note: a comparison of central and peripheral intraocular pressure using rebound tonometry. *Ophthalmic Physiol Opt.* **27**, 506-511.
- Quinn, G.E., Berlin, J.A., Young, T.L., Ziylan, S. and Stone, R.A. (1995). Association of intraocular pressure and myopia in children. *Ophthalmology.* **102**, 180-185.
- Quinn, G.E., Shin, C.H., Maguire, M.G. and Stone, R.A. (1999). Myopia and ambient lighting at night. *Nature.* **399**, 113-114.
- Quinn, G.E., Dobson, V., Davitt, B.V., Hardy, R.J., Tung, B., Pedroza, C. and Good, W.V. (2008). Progression of myopia and high myopia in the early treatment for retinopathy of prematurity study: findings to 3 years of age. *Ophthalmology.* **115**, 1058-1064.
- Rabsilber, T.M., Becker, K.A., Frisch, I.B. and Auffarth, G.U. (2003). Anterior chamber depth in relation to refractive status measured with the Orbscan II Topography System. *J Cataract Refract Surg.* **29**, 2115-2121.
- Rabsilber, T.M., Khoramnia, R. and Auffarth, G.U. (2006). Anterior chamber measurements using Pentacam rotating Scheimpflug camera. *J Cataract Refract Surg.* **32**, 456-459.
- Rada, J.A., Achen, V.R., Perry, C.A. and Fox, P.W. (1997). Proteoglycans in the human sclera. Evidence for the presence of aggrecan. *Invest Ophthalmol Vis Sci.* **38**, 1740-1751.
- Rada, J.A., Nickla, D.L. and Troilo, D. (2000). Decreased proteoglycan synthesis associated with form deprivation myopia in mature primate eyes. *Invest Ophthalmol Vis Sci.* **41**, 2050-2058.
- Rada, J.A., Shelton, S. and Norton, T.T. (2006). The sclera and myopia. *Exp Eye Res.* **82**, 185-200.
- Rada, J.A.S. and Wiechmann, A.F. (2009). Ocular expression of avian thymic hormone: changes during the recovery from induced myopia. *Mol Vis.* **15**, 778-92.
- Radhakrishnan, S., Rollins, A.M., Roth, J.E., Yazdanfar, S., Westphal, V., Bardenstein, D.S. and Izatt, J.A. (2001). Real-time optical coherence tomography of the anterior segment at 1310 nm. *Arch Ophthalmol.* **119**, 1179-1185.
- Rahfoth, B., Weisser, J., Sternkopf, F., Aigner, T., Von Der Mark, K. and Brauer, R., (1998). Transplantation of allograft chondrocytes embedded in agarose gel into cartilage defects of rabbits. *Osteoarthritis and Cartilage.* **6**, 50-65.
- Rai, G.K., Gilmartin, B., Wolffsohn, J.S. and Cervino, A. (2006). The effect of accommodation on IOP: evidence for dose dependency. *Invest Ophthalmol Vis Sci.* ARVO E-Abstract 5859; 47.
- Rai, G.K. (2007). Accommodation and intraocular pressure. PhD thesis. Aston University.
- Rakow, A. and Belfiore, L. (1995). Extrusion effects on the Mechanical properties of agar. *J Appl Polymer Sci.* **57**, 139-143.
- Rao, S.N., Raviv, T., Majmudar, P.A. and Epstein, R.J. (2002). Role of Orbscan II in screening keratoconus suspects before refractive corneal surgery. *Ophthalmology.* **109**, 1642-1646.
- Raviola, E., and Wiesel, T.N. (1985). An animal model of myopia. *N Engl J Med.* **312**, 1609-1615
- Read, S.A, Collins, M.J. and Iskander, D.R. (2008). Diurnal variation of axial length, intraocular pressure, and anterior eye biometrics. *Invest Ophthalmol Vis Sci.* **49**, 2911-2918.

- Read, S.A. and Collins, M.J. (2009). Diurnal variation of corneal shape and thickness. *Optom Vis Sci.* **86**, 170-180.
- Read, S.A., Collins, M.J. and Sander, B. (2010). Human optical axial length changes in response to defocus. *Invest Ophthalmol Vis Sci.* **51**, 6262-6269.
- Reader, A.L. (1982). Normal variations of intraocular pressure on vertical gaze. *Ophthalmology.* **89**, 1084-1087.
- Ren, R., Li, B., Gao, F., Li, L., Xu, X., Wang, N. and Jonas, J.B. (2010). Central corneal thickness, lamina cribrosa and peripapillary scleral histomorphometry in non-glaucomatous chinese eyes. *Graefes Arch Clin Exp Ophthalmol.* **248**, 1579–1585.
- Reuland, M.S., Reuland, A.J., Nishi, Y. and Auffarth, G.U. (2007). Corneal radii and anterior chamber depth measurements using the IOLmaster versus the Pentacam. *J Refract Surg.* **23**, 368-373.
- Richdale, K., Bullimore, M.A. and Zadnik, K. (2008). Lens thickness with age and accommodation by optical coherence tomography. *Ophthalmic Physiol Opt.* **28**, 441-447
- Richdale, K., Wassenaar, P., Bluestein, K.T., Abduljalil, A., Christoforidis, J.A., Lanz, T., Knopp, M.V. and Schmalbrock, P. (2009). 7 Tesla MR imaging of the human eye in vivo. *J Magn Reson Imaging.* **30**, 924-932.
- Ridley, F. (1930). The Intraocular Pressure and Drainage of the Aqueous Humour. *Br. J. Exper. Path.* **11**, 215.
- Rivara, A. and Zingirian, M. (1968). Volume of the bulb and scleral rigidity. *Ophthalmologica.* **156**, 394-398.
- Roberts, M.D., Sigal, I.A., Liang, Y., Burgoyne, C.F. and J Downs, J.C. (2010). Changes in the Biomechanical Response of the Optic Nerve Head in Early Experimental Glaucoma. *Invest Ophthalmol Vis Sci.* **51**, 5675-5684.
- Roberts, W. and Rogers, J.W. (1964). Postural Effects On Pressure and Ocular rigidity measurements. *Am J Ophthalmol.* **57**, 111-118.
- Rohen, J.W. (1979) Scanning electron microscopic studies of the zonular apparatus in human and monkey eyes. *Invest Ophthalmol Vis Sci.* **18**, 133–144.
- Rohrer, B. and Stell, W.K. (1994). Basic fibroblast growth factor (bFGF) and transforming growth factor beta (TGF-beta) act as stop and go signals to modulate postnatal ocular growth in the chick. *Exp Eye Res.* **58**, 553-561.
- Rondeau, M.J., Barcsay, G., Silverman, R.H., Reinstein, D.Z., Krishnamurthy, R., Chabi, A., Du, T. and Coleman, D.J. (2004). Very high frequency ultrasound biometry of the anterior and posterior chamber diameter. *J Refract Surg.* **20**, 454-464.
- Rosa, N., Lanza, M., Borrelli, M., Polito, B., Filosa, M.L. and Bernardo, M.D. (2007). Comparison of central corneal thickness measured with Orbscan and Pentacam. *J Refract Surg.* **23**, 895-899.
- Rosa, N., Lanza, M., Cennamo, G. and Capasso, L. (2008). Accuracy of Schiottz Tonometry in Measuring the Intraocular Pressure After Corneal Refractive Surgery. *J Optom.* **1**, 59-64.

- Rose, K.A., Morgan, I.G., Ip, J., Kifley, A., Huynh, S., Smith, W. and Mitchell, P. (2008). Outdoor activity reduces the prevalence of myopia in children. *Ophthalmology*. **115**, 1279-1285.
- Rosenfield, M. and Gilmartin, B. (1998). Myopia and near work: causation or merely association? In *Myopia and Nearwork*. Eds Rosenfield, M. and Gilmartin, B. Oxford: Butterworth-Heinemann, 193-206.
- Ross, K.A. and Scanlon, M.G. (1999) Analysis of the elastic modulus of agar gel by indentation. *J Texture Studies*. **30**, 17-27.
- Roy, A.S. and Dupps, W.J. (2009). Effects of altered corneal stiffness on native and postoperative LASIK corneal biomechanical behaviour: A whole-eye finite element analysis. *J Refract Surg*. **25**, 875-887.
- Royal College of Ophthalmologist. (2009) Guide for intravitreal injections procedure.
- Rudnicka, A.R., Owen, C.G., Nightingale, C.M., Cook, D. and Whincup, P. (2010). Ethnic differences in the prevalence of myopia and ocular biometry in 10-11 year old children: the Child Heart And Health Study in England (CHASE). *Invest Ophthalmol Vis Sci*. **51**, 6270-6276.
- Rüfer, F., Schröder, A., Arvani, M.K. and Erb, C. (2005). Central and peripheral corneal pachymetry--standard evaluation with the Pentacam system. *Klin Monbl Augenheilkd*. **222**, 117-122.
- Ruokonen, P.C., Schwentek, T. and Draeger, J. (2007). Evaluation of the impedance tonometers TGDc-01 and iCare according to the international ocular tonometer standards ISO 8612. *Graefes Arch Clin Exp Ophthalmol*. **245**, 1259-1265.
- Saad, A., Lteif, Y., Azan, E. and Gatinel, D. (2009). Biomechanical properties of keratoconus suspect eyes. *Invest Ophthalmol Vis Sci*. **51**, 2912-2916.
- Saeteren, T. (1960). Scleral rigidity in normal human eyes. *Acta Ophthalmol (Copenh)*. **38**, 303-311.
- Sahin, A., Basmak, H., Niyaz, L. and Yildirim, N. (2007a). Reproducibility and tolerability of the ICare rebound tonometer in school children. *J Glaucoma*. **16**, 185-188.
- Sahin, A., Niyaz, L. and Yildirim, N. (2007b). Comparison of the rebound tonometer with the Goldmann applanation tonometer in glaucoma patients. *Clin Experiment Ophthalmol*. **35**, 335-339.
- Sakata, L.M, Lavanya, R., Friedman, D.S., Aung, H.T., Seah, S.K., Foster, P.J. and Aung, T. (2008). Assessment of the scleral spur in anterior segment optical coherence tomography images. *Arch Ophthalmol*. **126**, 181-185.
- Salouti, R., Nowroozadeh, M.H., Zamani, M., Fard, A.H. and Niknam, S. (2009). Comparison of anterior and posterior elevation map measurements between 2 Scheimpflug imaging systems. *J Cataract Refract Surg*. **35**, 856-862.
- Sánchez-Tocino, H., Bringas-Calvo, R. and Iglesias-Cortiñas, D. (2005). Comparative study between the non-contact pneumotonometer Canon TX10 and the Goldmann tonometer. *Arch Soc Esp Oftalmol*. **80**, 643-649.
- Sandberg-Lall, M., Hägg, P.O., Wahlström, I. and Pihlajaniemi, T. (2000). Type XIII collagen is widely expressed in the adult and developing human eye and accentuated in the ciliary muscle, the optic nerve and the neural retina. *Exp Eye Res*. **70**, 401-410.

- Santodomingo-Rubido, J., Mallen, E.A., Gilmartin, B. and Wolffsohn, J.S. (2002). A new non-contact optical device for ocular biometry. *Br J Ophthalmol.* **86**, 458-462.
- Saunders, R.A., Helveston, E.M. and Ellis, F.D. (1981). Differential intraocular pressure in strabismus diagnosis. *Ophthalmology.* **88**, 59-70.
- Saw, S.M. (2003). A synopsis of the prevalence rates and environmental risk factors for myopia. *Clin Exp Optom.* **86**, 289-294.
- Saw, S.M., Carkeet, A., Chia, K.S., Stone, R.A., Tan, D.T.H. (2002a). Component dependent risk factors for ocular parameters in Singapore Chinese children. *Ophthalmology.* **109**, 2065-2071.
- Saw, S.M., Chua, W.H., Hong, C.Y., Wu, H.M., Chan, W.Y., Chia, K.S., Stone, R.A. and Tan, D. (2002b). Nearwork in early-onset myopia. *Invest Ophthalmol Vis Sci.* **43**, 332-339.
- Saw, S.M., Nieto, F.J., Katz, J., Schein, O.D., Levy, B. and Chew, S.J. (2001). Familial clustering and myopia progression in Singapore school children. *Ophthalmic Epidemiol.* **8**, 227-236.
- Saw, S.M., Tan, S.B., Fung, D., Chia, K.S., Koh, D., Tan, D.T.H. and Stone, R.A. (2004). IQ and the association with myopia in children. *Invest Ophthalmol Vis Sci.* **45**, 2943-2948.
- Schaeffel, F., Glasser, A. and Howland, H.C. (1988). Accommodation, refractive error and eye growth in chickens. *Vision Res.* **28**, 639-657.
- Schaeffel, F., Simon, P., Feldkaemper, M., Ohngemach, S. and Williams, R.W. (2003). Molecular biology of myopia. *Clin Exp Optom.* **86**, 295-307.
- Schiötz, H. (1920). Tonometry. *Br J Ophthalmol.* **4**, 201-210.
- Schiötz, H.J. (1905). A new tonometer- Tonometry. *Archiv Augenheilkunde.* **52**, 401-424.
- Schlegel, Z., Hoang-Xuan, T. and Gatinel, D. (2008). Comparison of and correlation between anterior and posterior corneal elevation maps in normal eyes and keratoconus-suspect eyes. *J Cataract Refract Surg.* **34**, 789-795.
- Schmid, G.F. (2003). Variability of retinal steepness at the posterior pole in children 7-15 years of age. *Curr Eye Res.* **27**, 61-68.
- Schmid, K., Li, R. and Edwards, M. (2003). The expandability of the eye in childhood myopia. *Curr Eye Res.* **26**, 65-71.
- Schmidt, T. (1957). The differential value as a measure for the rigidity of the eyeball. *Klin Monatsblätter Augenheilkd Augenarztl Fortbil.* **131**, 195-202.
- Schmidt, T. (1959). The use of the Goldmann applanation tonometer. *Trans Ophthalmol Soc U K.* **79**, 637-650.
- Schmidt, T.A. (1960). The clinical application of the Goldmann applanation tonometer. *Am J Ophthalmol.* **49**, 967-978.
- Schreiber, W., Vorwerk, C.K., Langenbucher, A., Behrens-Baumann, W. and Viestenz, A. (2007). A comparison of rebound tonometry (ICare) with TonoPenXL and Goldmann applanation tonometry. *Ophthalmologie.* **104**, 299-304.

- Schroeder, B., Hager, A., Kutschan, A. and Wiegand, W. (2008). Measurement of viscoelastic corneal parameters (corneal hysteresis) in patients with primary open angle glaucoma. *Ophthalmologie*. **105**, 916-920.
- Schubert, H. (1996). Postsurgical hypotony: relationship to fistulization, inflammation, chorioretinal lesions, and the vitreous. *Surv Ophthalmol*. **41**, 97-125.
- Schulman, P.F. (1963). An evaluation of the Schiotz Sklar Corneal tonometer used on the sclera. *Am J Optom Arch Am Acad Optom*. **40**, 133-139.
- Schulten, M.W. (1884). Experimentelle Untersuchungen über die Circulationsverhältnisse des Auges. *Von Graefes Arch. Ophth.* **30**, 6. Cited in Fridenwald, J.S. (1937). Contribution to the theory and practice of tonometry. *Am J Ophthalmol*. **20**, 985-1024.
- Schultz, D.S., Lotz, J.C., Lee, S.M., Trinidad, M.L. and Stewart, J.M. (2008). Structural factors that mediate scleral stiffness. *Invest Ophthalmol Vis Sci*. **49**, 4232-4236.
- Schultz, K.E., Sinnott, L.T., Mutti, D.O. and Bailey, M.D. (2009). Accommodative fluctuations, lens tension, and ciliary body thickness in children. *Optom Vis Sci*. **86**, 677-684.
- Seddon, J.M., Schwartz, B. and Flowerdew, G. (1983). Case-control study of ocular hypertension. *Arch Ophthalmol*. **101**, 891-894.
- Seidemann, A., Schaeffel, F., Guirao, A., Lopez-Gil, N. and Artal, P. (2002). Peripheral refractive errors in myopic, emmetropic, and hyperopic young subjects. *J Opt Soc Am A Opt Image Sci Vis*. **19**, 2363-2373.
- Sejpal, K.D., Johnson, D., Yu, F. and Hamilton, D.R. (2010). Advanced assessment of corneal biomechanical properties in normal and keratoconic eyes using the Ocular Response Analyzer. *Invest Ophthalmol Vis Sci*. ARVO E-Abstract 4991: 51.
- Serini, G. and Gabbiani, G. (1999). Mechanisms of myofibroblast activity and phenotypic modulation. *Exp Cell Res*. **250**, 273-283.
- Shah, S., Chatterjee, A., Mathai, M., Kelly, S.P., Kwartz, J., Henson, D. and McLeod, D. (1999). Relationship between corneal thickness and measured intraocular pressure in a general ophthalmology clinic. *Ophthalmology*. **106**, 2154-2160.
- Shah, S. (2000). Accurate intraocular pressure measurement-the myth of modern ophthalmology? *Ophthalmology*. **107**, 1805-1807.
- Shah, S., Laiquzzaman, M., Cunliffe, I. and Mantry, S. (2006). The use of the Reichert ocular response analyser to establish the relationship between ocular hysteresis, corneal resistance factor and central corneal thickness in normal eyes. *Cont Lens Anterior Eye*. **29**, 257-262.
- Shah, S., Laiquzzaman, M., Bhojwani, R., Mantry, S. and Cunliffe, I. (2007). Assessment of the biomechanical properties of the cornea with the ocular response analyzer in normal and keratoconic eyes. *Invest Ophthalmol Vis Sci*. **48**, 3026-3031.
- Shah, S., Laiquzzaman, M., Mantry, S. and Cunliffe, I. (2008). Ocular response analyser to assess hysteresis and corneal resistance factor in low tension, open angle glaucoma and ocular hypertension. *Clin Experiment Ophthalmol*. **36**, 508-513.
- Shah, S. and Laiquzzaman, M. (2009). Comparison of corneal biomechanics in pre and post-refractive surgery and keratoconic eyes by Ocular Response Analyser. *Cont Lens Anterior Eye*. **32**, 129-132.

- Shankar, H., Taranath, D., Santhirathelagan, C.T. and Pesudovs, K. (2008). Anterior segment biometry with the Pentacam: comprehensive assessment of repeatability of automated measurements. *J Cataract Refract Surg.* **34**, 103-113.
- Shelton, L. and Rada, J.S. (2007). Effects of cyclic mechanical stretch on extracellular matrix synthesis by human scleral fibroblasts. *Exp Eye Res.* **84**, 314-322.
- Shen, M., Fan, F., Xue, A., Wang, J., Zhou, X. and Lu, F. (2008a). Biomechanical properties of the cornea in high myopia. *Vision Res.* **48**, 2167-2171.
- Shen, M., Wang, J., Qu, J., Xu, S., Wang, X., Fang, H. and Lu, F. (2008b). Diurnal variation of ocular hysteresis, corneal thickness, and intraocular pressure. *Optom Vis Sci.* **85**, 1185-1192.
- Sheppard, A.L. and Davies, L.N. (2010a). *In vivo* analysis of ciliary muscle morphologic changes with accommodation and axial ametropia. *Invest Ophthalmol Vis Sci.* **51**, 6882-6889.
- Sheppard, A.L. and Davies, L.N. (2010b). The effect of ageing on *in vivo* human ciliary muscle morphology and contractility. *Invest Ophthalmol Vis Sci.* Papers in Press. Published on Nov 2011, as Manuscript iovs. 10-6447.
- Sherrard, E.S., Novakovic, P., Speedwell, L. (1987). Age-related changes of the corneal endothelium and stroma as seen *in vivo* by specular microscopy. *Eye (Lond).* **1**, 197-203.
- Shih, Y.F., Chiang, T.H. and Lin, L.L.K. (2009). Lens thickness changes among schoolchildren in Taiwan. *Invest Ophthalmol Vis Sci.* **50**, 2637-2644.
- Shimmyo, M., Ross, A.J., Moy, A. and Mostafavi, R. (2003). Intraocular pressure, Goldmann applanation tension, corneal thickness, and corneal curvature in Caucasians, Asians, Hispanics, and African Americans. *Am J Ophthalmol.* **136**, 603-613.
- Sicam, V.A.D.P., Dubbelman, M. and van der Heijde, R.G.L. (2006). Spherical aberration of the anterior and posterior surfaces of the human cornea. *J Opt Soc Am A Opt Image Sci Vis.* **23**, 544-549.
- Sieglwart, J.T. and Norton, T.T. (1998). The susceptible period for deprivation-induced myopia in tree shrew. *Vision Res.* **38**, 3505-3515.
- Sieglwart, J.T. and Norton, T.T. (1999). Regulation of the mechanical properties of tree shrew sclera by the visual environment. *Vision Res.* **39**, 387-407.
- Sieglwart, J.T. and Norton, T.T. (2001). Steady state mRNA levels in tree shrew sclera with form-deprivation myopia and during recovery. *Invest Ophthalmol Vis Sci.* **42**, 1153-1159.
- Sieglwart, J.T. and Norton, T.T. (2010). Binocular lens treatment in tree shrews: Effect of age and comparison of plus lens wear with recovery from minus lens-induced myopia. *Exp Eye Res.* doi:10.1016/j.exer.2010.08.010. [Epub ahead of print].
- Sigal, I.A., Flanagan, J.G., Tertinegg, I., Ethier, C.R. (2004). Finite element modeling of optic nerve head biomechanics. *Invest Ophthalmol Vis Sci.* **45**, 4378-4387.
- Sigal, I.A., Flanagan, J.G., Tertinegg, I. and Ethier, C.R. (2005a). Reconstruction of human optic nerve heads for finite element modelling. *Technol Health Care.* **13**, 313-329.
- Sigal, I.A., Flanagan, J.G. and Ethier, C.R. (2005b) Factors influencing optic nerve head biomechanics. *Invest Ophthalmol Vis Sci.* **46**, 4189-4199.

- Sigal, I.A. (2009). Interactions between geometry and mechanical properties on the optic nerve head. *Invest Ophthalmol Vis Sci.* **50**, 2785-2795.
- Sigal, I.A., Flanagan, J.G., Tertinegg, I. and Ethier, C.R. (2009). Modeling individual-specific human optic nerve head biomechanics. Part II: influence of material properties. *Biomech Model Mechanobiol.* **8**, 99-109.
- Singh, K.D., Logan, N.S. and Gilmartin, B. (2006). Three-dimensional modeling of the human eye based on magnetic resonance imaging. *Invest Ophthalmol Vis Sci.* **47**, 2272-2279.
- Singh, M., Chew, P.T.W., Friedman, D.S., Nolan, W.P., See, J.L., Smith, S.D., Zheng, C., Foster, P.J. and Aung, T. (2007). Imaging of trabeculectomy blebs using anterior segment optical coherence tomography. *Ophthalmology.* **114**, 47-53.
- Singh, Y.P., Goel, S.K. and Misra, R.N. (1970). Scleral rigidity in emmetropes. *J All India Ophthalmol Soc.* **18**, 167-169.
- Smith, E.L. (1998). Environmentally induced refractive errors in animals. In: *Myopia and Nearwork*, Edts M. Rosenfield, and B. Gilmartin. Oxford: Butterworth-Heinemann, 57-90.
- Smith, E.L. and Hung, L.F. (1999). The role of optical defocus in regulating refractive development in infant monkeys. *Vision Res.* **39**, 1415-1435.
- Smith, E.L., Huang, J., Hung, L.F., Blasdel, T.L., Humbird, T.L. and Bockhorst, K.H. (2009). Hemiretinal form deprivation: evidence for local control of eye growth and refractive development in infant monkeys. *Invest Ophthalmol Vis Sci.* **50**, 5057-5069.
- Smolek, M. (1988). Elasticity of the bovine sclera measured with real-time holographic interferometry. *Am J Optom Physiol Opt.* **65**, 653-660.
- Snell, R.S. and Lemp, M.A. (1998). *Clinical Anatomy of the Eye*. Washington, D.C.: Blackwell Science. 132-207.
- Solouki, A.M., Verhoeven, V.J.M., van Duijn, C.M., Verkerk, A.J.M.H., Ikram, M.K., Hysi, P.G., Despriet, D.D.G., van Koolwijk, L.M., Ho, L., Ramdas, W.D., Czudowska, M., Kuijpers, R.W.A.M., Amin, N., Struchalin, M., Aulchenko, Y.S., van Rij, G., Riemslag, F.C.C., Young, T.L., Mackey, D.A., Spector, T.D., Gorgels, T.G.M.F., Willemse-Assink, J.J.M., Isaacs, A., Kramer, R., Swagemakers, S.M.A., Bergen, A.A.B., van Oosterhout, A.A.L.J., Oostra, B.A., Rivadeneira, F., Uitterlinden, A.G., Hofman, A., de Jong, P.T.V.M., Hammond, C.J., Vingerling, J.R. and Klaver, C.C.W. (2010). A genome-wide association study identifies a susceptibility locus for refractive errors and myopia at 15q14. *Nat Genet.* **42**, 897-901.
- Song, Y., Congdon, N., Li, L., Zhou, Z., Choi, K., Lam, D.S.C., Pang, C.P., Xie, Z., Liu, X., Sharma, A., Chen, W. and Zhang, M. (2008). Corneal hysteresis and axial length among Chinese secondary school children: the Xichang Pediatric Refractive Error Study (X-PRES) report no. 4. *Am J Ophthalmol.* **145**, 819-826.
- Spaeth, G. (2003). Indications for Surgery In: *Ophthalmic Surgery Principles and Practice 3rd ed.* Editor Spaeth G. Philadelphia: Saunders. 211-221.
- Spieler, A. and Eisenstein, Z. (1991). The role of increased intraocular pressure on upgaze in the assessment of Graves ophthalmopathy. *Ophthalmology.* **98**, 1491-1494.
- Spitznas, M. (1971). The fine structure of human scleral collagen. *Am J Ophthalmol.* **71**, 68.

- Spörl, E., Terai, N., Haustein, M., Böhm, A.G., Raiskup-Wolf, F. and L E Pillunat, L.E. (2009). Biomechanical condition of the cornea as a new indicator for pathological and structural changes. *Ophthalmologie*. **106**, 512-520.
- Stewart, J.M., Schultz, D.S., Lee, O.T. and Trinidad, M.L. (2009). Exogenous collagen cross-linking reduces scleral permeability: modeling the effects of age-related cross-link accumulation. *Invest Ophthalmol Vis Sci*. **50**, 352-357.
- Stolz, M., Raiteri, R., Daniels, A.U., VanLandingham, M.R., Baschong, W. and Aebi, U. (2004). Dynamic elastic modulus of porcine articular cartilage determined at two different levels of tissue organization by indentation-type atomic force microscopy. *Biophys J*. **86**, 3269-3283.
- Stone, R.A. and Flitcroft, D.I. (2004). Ocular shape and myopia. *Ann Acad Med*. **33**, 7–15. Stone, R.A., Wilson, L.B., Ying, G.S., Liu, C., Criss, J.S., Orlow, J., Lindstrom, J.M. and Quinn, G.E. (2006). Associations between childhood refraction and parental smoking. *Invest Ophthalmol Vis Sci*. **47**, 4277-4287.
- Streho, M., Dariel, R., Giraud, J.M., Verret, C., Fenolland, J.R., Crochelet, O., May, F., Maurin, J.F. and Renard, J.P. (2008). Evaluation of the Ocular Response Analyzer in ocular hypertension, glaucoma, and normal populations. Prospective study on 329 eyes. *J Fr Ophthalmol*. **31**, 953-960.
- Strenk, S.A., Semmlow, J.L., Strenk, L.M., Munoz, P., Gronlund-Jacob, J. and DeMarco, J.K. (1999). Age-related changes in human ciliary muscle and lens: a magnetic resonance imaging study. *Invest Ophthalmol Vis Sci*. **40**, 1162-1169.
- Strenk, S.A., Strenk, L.M. and Guo, S. (2006). Magnetic resonance imaging of aging, accommodating, phakic, and pseudophakic ciliary muscle diameters. *J Cataract Refract Surg*. **32**, 1792-1798.
- Strenk, S.A., Strenk, L.M. and Guo, S. (2010). Magnetic resonance imaging of the anteroposterior position and thickness of the aging, accommodating, phakic, and pseudophakic ciliary muscle. *J Cataract Refract Surg*. **36**, 235-241.
- Strenk, S.A., Strenk, L.M. and Koretz, J.F. (2005). The mechanism of presbyopia. *Prog Retin Eye Res*. **24**, 379-393.
- Sullivan-Mee, M., Halverson, K., Pensyl, D., Colonna, K., Gerhardt, G. and Chavez, C. (2010). Anterior Scleral Rigidity in Primary Open-Angle Glaucoma. *Invest Ophthalmol Vis Sci*. ARVO E-Abstract 5548; 51.
- Suzuki, H., Takahashi, H., Hori, J., Hiraoka, M., Igarashi, T. and Shiwa, T. (2006). Phacoemulsification associated corneal damage evaluated by corneal volume. *Am J Ophthalmol*. **142**, 525-528.
- Swartz, T., Marten, L. and Wang, M. (2007). Measuring the cornea: the latest developments in corneal topography. *Curr Opin Ophthalmol*. **18**, 325-333.
- Swegmark, G. (1969). Studies with impedance cyclography on human ocular accommodation at different ages. *Acta ophthalmologica*. **47**, 1186-1206.
- Taban, M., Lowder, C.Y., Ventura, A.A.C.M., Sharma, S., Nutter, B., Hayden, B.C., Dupps, W.J. and Kaiser, P.K. (2010). Scleral Thickness following Fluocinolone Acetonide Implant (Retisert). *Ocul Immunol Inflamm*. **18**, 255-263.
- Taberner, J. and Schaeffel, F. (2009). More irregular eye shape in low myopia than in emmetropia. *Invest Ophthalmol Vis Sci*. **50**, 4516-4522

- Tamm, E., Lütjen-Drecoll, E., Jungkunz, W. and Rohen, J.W. (1991). Posterior attachment of ciliary muscle in young, accommodating old, presbyopic monkeys. *Invest Ophthalmol Vis Sci.* **32**, 1678-1692.
- Tamm, S., Tamm, E. and Rohen, J.W. (1992). Age-related changes of the human ciliary muscle. A quantitative morphometric study. *Mech Ageing Dev.* **62**, 209-221.
- Tamm, E.R. and Lütjen-Drecoll, E. (1996). Ciliary body. *Microsc Res Tech.* **33**, 390-439.
- Tamm, E.R. (2009). The trabecular meshwork outflow pathways: structural and functional aspects. *Exp Eye Res.* **88**, 648-655.
- Tan, A.N., Sauren, L.D., de Brabander, J., Berendschot, T.T., Passos, V.L., Webers, C.A., Nuijts, R.M. and Beckers, H.J. (2010). Reproducibility of anterior chamber angle measurements with Anterior Segment Optical Coherence Tomography. *Invest Ophthalmol Vis Sci.* Papers in Press. Published on September 29, as Manuscript iovs.10-5872.
- Teikari, J.M. (1987). Myopia and stature. *Acta ophthalmologica.* **65**, 673-676.
- Teikari, J.M., Kaprio, J., Koskenvuo, M.K. and Vannas, A. (1988). Heritability estimate for refractive errors--a population-based sample of adult twins. *Genet Epidemiol.* **5**, 171-181.
- Teikari, J.M., O'Donnell, J., Kaprio, J. and Koskenvuo, M. (1991). Impact of heredity in myopia. *Hum Hered.* **41**, 151-156.
- Tello, C., Liebmann, J., Potash, S.D., Cohen, H. and Ritch, R. (1994). Measurement of ultrasound biomicroscopy images: intraobserver and interobserver reliability. *Invest Ophthalmol Vis Sci.* **35**, 3549-3552.
- Teng, C. (1963). Electron microscope study of the pathology of keratoconus. *Am J Ophthalmol.* **55**, 18-47.
- Tengroth, B. and Ammitzbøll, T. (1984). Changes in the content and composition of collagen in the glaucomatous eye--basis for a new hypothesis for the genesis of chronic open angle glaucoma--a preliminary report. *Acta ophthalmologica.* **62**, 999-1008.
- Kida, T., Liu, J.H.K. and Weinreb, R.N. (2006). Effect of 24-hour corneal biomechanical changes on intraocular pressure measurement. *Invest Ophthalmol Vis Sci.* **47**, 4422-4426.
- Thale, A. and Tillmann, B. (1993). The collagen architecture of the sclera--SEM and immunohistochemical studies. *Ann Anat.* **175**, 215-220.
- Thale, A., Tillmann, B. and Rochels, R., (1996a). Scanning electron microscopic studies of the collagen architecture of the human sclera--normal and pathological findings. *Ophthalmologica* **210**, 137-141.
- Thale, A., Tillmann, B., and Rochels, R. (1996b). SEM studies of the collagen architecture of the human lamina cribrosa: normal and pathological findings. *Ophthalmologica*, **210**, 142-147.
- Thale, A.B., Gordes, R.S., Rochels, R. and Tillmann, B. (1996c). Changes in extracellular matrix in the lamina cribrosa of patients with secondary glaucoma. *Ophthalmologie*, **93**, 586-591.
- Ting, P.W.K., Lam, C.S.Y., Edwards, M.H. and Schmid, K.L. (2004). Prevalence of myopia in a group of Hong Kong microscopists. *Optom Vis Sci.* **81**, 88-93.

- Tinius Olsen, 2010, Testing in Education. Available through <http://www.schooloftesting.com/askexpert/1-faq/5-extensometermeasure> [accessed 2nd October 2010].
- Toh, T.Y., Liew, S.H.M, MacKinnon, J.R., Hewitt, A.W., Poulsen, J.L., Spector, T.D., Gilbert, C.E., Craig, J.E., Hammond, C.J. and Mackey, D.A. (2005). Central corneal thickness is highly heritable: the twin eye studies. *Invest Ophthalmol Vis Sci.* **46**, 3718-3722.
- Tominaga, A., Miki, A., Yamazaki, Y., Matsushita, K. and Otori, Y. (2010). The Assessment of the Filtering Bleb Function With Anterior Segment Optical Coherence Tomography. *J Glaucoma.* **19**, 551-555.
- Tomlinson, A., and Phillips, C.I. (1970). Applanation tension and axial length of the eyeball. *Br J Ophthalmol.* **54**, 548-553.
- Torcynski, E.. Sclera. (1988). In: *Biomedical foundations of Ophthalmology Vol I.* Edts Duane, T.D. and Jaeger E.A.. Philadelphia: J.B. Lippincott Company. 1-23.
- Trick, G.L., Edwards, P.A., Desai, U., Morton, P.E., Latif, Z. and Berkowitz, B.A. (2008). MRI retinovascular studies in humans: research in patients with diabetes. *NMR Biomed.* **21**, 1003-1012.
- Trier, K. (2005). The Sclera. *Advances in Organ Biology.* **10**, 353-373.
- Trier, K., Olsen, E.B. and Ammitzbøll, T. (1990). Regional glycosaminoglycans composition of the human sclera. *Acta ophthalmologica.* **68**, 304-306.
- Troilo, D., Gottlieb, M.D. and Wallman, J. (1987). Visual deprivation causes myopia in chicks with optic nerve section. *Curr Eye Res.* **6**, 993-999.
- Troilo, D., Nickla, D.L. and Wildsoet, C.F. (2000). Choroidal thickness changes during altered eye growth and refractive state in a primate. *Invest Ophthalmol Vis Sci.* **41**, 1249-1258.
- Troilo, D., Nickla, D.L. and Wildsoet, C.F. (2000). Form deprivation myopia in mature common marmosets (*Callithrix jacchus*). *Invest Ophthalmol Vis Sci.* **41**, 2043-2049.
- Tsai, M.Y., Lin, L.L.K., Lee, V., Chen, C.J., Shih, Y.F. (2009). Estimation of heritability in myopic twin studies. *Jpn J Ophthalmol.* **53**, 615-622.
- Tscherning, M. (1882). Studier oven myopiens aetiology. *Kobenhavn.* Cited in Curtin, B.J. (1985). *The Myopias, Basic Science and Clinical Management.* Cambridge: Harper & Row.
- Twelker, J.D., Mitchell, G.L., Messer, D.H., Bhakta, R., Jones, L.A., Mutti, D.O., Cotter, S.A., Klenstein, R.N., Manny, R.E. and Zadnik, K. (2009). Children's Ocular Components and Age, Gender, and Ethnicity. *Optom Vis Sci.* **86**, 918-935.
- Uçakhan, U.O., Gesoğlu, P., Ozkan, M. and Kanpolat, A. (2008). Corneal elevation and thickness in relation to the refractive status measured with the Pentacam Scheimpflug system. *J Cataract Refract Surg.* **34**, 1900-1905.
- Uchio, E., Ohno, S., Kudoh, J., Aoki, K. and Kisielwicz, L.T. (1999). Simulation model of an eyeball based on finite element analysis on a supercomputer. *Br J Ophthalmol.* **83**, 1106-1011.
- Ursea, R. and Silverman, R.H. (2010). Anterior-segment imaging for assessment of glaucoma. *Expert review of ophthalmology.* **5**, 59-74.

- Utine, C.A., Altin, F., Cakir, H. and Perente, I. (2009). Comparison of anterior chamber depth measurements taken with the Pentacam, Orbscan IIz and IOLMaster in myopic and emmetropic eyes. *Acta ophthalmologica*. **87**, 386-391.
- van Alphen, G.W. (1986). Choroidal stress and emmetropization. *Vision Res.* **26**, 723-734.
- van Alphen, G.W. and Graebel, W.P. (1991). Elasticity of tissues involved in accommodation. *Vision Res.* **31**, 1417-1438.
- van der Jagt, L.H. and Jansonius, N.M. (2005). Three portable tonometers, the TGDc-01, the ICARE and the Tonopen XL, compared with each other and with Goldmann applanation tonometry. *Ophthalmic Physiol Optics*. **25**, 429-435.
- van Velthoven, M.E.J., Faber, D.J., Verbraak, F.D., van Leeuwen, T.G. and de Smet, M.D. (2007). Recent developments in optical coherence tomography for imaging the retina. *Prog Retin Eye Res.* **26**, 57-77.
- van der Werff, T.J. (1981). A new single-parameter ocular rigidity function. *Am J Ophthalmol.* **92**, 391-395.
- Villarreal, M.G., Ohlsson, J., Abrahamsson, M., Sjöstrom, A. and Sjöstrand, J. (2000). Myopisation: the refractive tendency in teenagers. Prevalence of myopia among young teenagers in Sweden. *Acta Ophthalmol Scand.* **78**, 177-181.
- Vinciguerra, P., Albè, E., Mahmoud, A.M., Trazza, S., Hafezi, F. and Roberts, C.J. (2010). Intra- and Postoperative Variation in Ocular Response Analyzer Parameters in Keratoconic Eyes After Corneal Cross-Linking. *J Refract Surg.* doi: 10.3928/1081597X-20100331-01. [Epub ahead of print].
- Vitale, S., Sperduto, R.D. and Ferris, F.L. 3rd. (2009). Increased prevalence of myopia in the United States between 1971-1972 and 1999-2004. *Arch Ophthalmol.* **127**, 1632-1639.
- Vogel, A., Dlugos, C., Nuffer, R. and Birngruber, R. (1991). Optical properties of human sclera, and their consequences for transscleral laser applications. *Lasers Surg Med.* **11**, 331-340.
- Výborný, P., Hejsek, L., Sicáková, S. and Pasta, J. (2007). Changes of the thickness of the ciliary body after the latanoprost 0.005 % application. *Cesk Slov Oftalmol.* **63**, 418-421.
- Walia, J.S. and Chronister, C.L. (2001). Possible iatrogenic transmission of Creutzfeldt-Jakob disease via tonometer tips: a review of the literature. *Optometry.* **72**, 649-652.
- Wallman, J. and Adams, J.I. (1987). Developmental aspects of experimental myopia in chicks: susceptibility, recovery and relation to emmetropization. *Vision Res.* **27**, 1139-1163.
- Wallman, J., Gottlieb, M.D., Rajaram, V. and Fugate-Wentzek, L.A. (1987). Local retinal regions control local eye growth and myopia. *Science.* **237**, 73-77.
- Wallman, J., Wildsoet, C., Xu, A., Gottlieb, M.D., Nickla, D.L., Marran, L., Krebs, W., and Christensen, A.M. (1995). Moving the retina: choroidal modulation of refractive state. *Vision Res.* **35**, 37-50.
- Wallman, J. and Winawer, J. (2004). Homeostasis of eye growth and the question of myopia. *Neuron.* **43**, 447-468.

- Wang, D., Pekmezci, M., Basham, R.P, He, M., Seider, M.I. and Lin, S.C. (2009). Comparison of different modes in optical coherence tomography and ultrasound biomicroscopy in anterior chamber angle assessment. *J Glaucoma*. **18**, 472-478.
- Wang, T., Liu, L., Li, Z., Hu, S., Yang, W., Zhu, X. (1999b). Ultrasound biomicroscopic study on changes of ocular anterior segment structure after topical application of cycloplegia. *Chin Med J*. **112**, 217-220.
- Wang, W.H., Millar, J.C., Pang, I.H., Wax, M.B. and Clark, A.F. (2005). Noninvasive measurement of rodent intraocular pressure with a rebound tonometer. *Invest Ophthalmol Vis Sci*. **46**, 4617-4621.
- Wang, Y.D., Chen, H.B., Jin, M., Ou, B., Kashiwagi, K. and Tsukahara, S. (1999a). Three-dimensional arrangement of collagen fibrils in human ciliary body. *Ophthalmic Res*. **31**, 378-386.
- Wasilewski, R., McDonald, J.P., Heatley, G., Lütjen-Drecoll, E., Kaufman, P.L. and Croft, M.A. (2008). Surgical intervention and accommodative responses, II: forward ciliary body accommodative movement is facilitated by zonular attachments to the lens capsule. *Invest Ophthalmol Vis Sci*. **49**, 5495-5502.
- Watase, M. and Nishinari, K. (1980). Rheological properties of agarose-gelatine gels. *Rheologica Acta*. **19**, 220-225.
- Watson, P.G., and Young, R.D. (2004). Scleral structure, organisation and disease. A review. *Exp Eye Res*. **78**, 609-623.
- Weale, R.A. (2003). Epidemiology of refractive errors and presbyopia. *Surv Ophthalmol*. **48**, 515-543.
- Wegener, A. and Laser-Junga, H. (2009). Photography of the anterior eye segment according to Scheimpflug's principle: options and limitations - a review. *Clin Experiment Ophthalmol*. **37**, 144-154.
- Weinreb, R.N. and Lindsey, J.D. (2002). Metalloproteinase gene transcription in human ciliary muscle cells with latanoprost. *Invest Ophthalmol Vis Sci*. **43**, 716-722.
- Weinreb, R.N., Toris, C.B., Gabelt, B.A.T., Lindsey, J.D. and Kaufman, P.L. (2002). Effects of prostaglandins on the aqueous humor outflow pathways. *Surv Ophthalmol*. **47**, 53-64.
- Wensor, M., McCarty, C.A. and Taylor, H.R. (1999). Prevalence and risk factors of myopia in Victoria, Australia. *Arch Ophthalmol*. **117**, 658-663.
- Werner, L., Lovisolo, C., Chew, J., Tetz, M. and Müller, M. (2008). Meridional differences in internal dimensions of the anterior segment in human eyes evaluated with 2 imaging systems. *J Cataract Refract Surg*. **34**, 1125-1132.
- Westphal, V., Rollins, A.M., Radhakrishnan, S., and Izatt, J.A. (2002). Correction of geometric and refractive image distortions in optical coherence tomography applying Fermat's principle. *Opt. Express*. **10**, 397-404.
- Wessel, H., Anderson, S., Fite, D., Halvas, E., Hempel, J. and SundarRaj, N. (1997). Type XII collagen contributes to diversities in human corneal and limbal extracellular matrices. *Invest Ophthalmol Vis Sci*. **38**, 2408-2422.

- Weymouth, F.W. and Hirsch, M.J. (1991). Theories, Definitions, and Classifications of Refractive Errors. In *Refractive Anomalies*, Editors Grosvenor, T. and Flom, M.C. Stoneham: Butterworth-Heinemann, 1-14.
- Whitacre, M.M and Stein, R. (1993). Sources of error with use of Goldmann-type tonometers. *Surv Ophthalmol.* **38**, 1-30.
- Whitacre, M.M, Stein, R.A. and Hassanein, K. (1993). The effect of corneal thickness on applanation tonometry. *Am J Ophthalmol.* **115**, 592-596.
- White, O.W. (1990). Ocular elasticity? *Ophthalmology.* **97**, 1092-1094.
- Wiesel, T.N. and Raviola, E. (1977). Myopia and eye enlargement after neonatal lid fusion in monkeys. *Nature.* **266**, 66-68.
- Wildner, K., Müller, M., Dawczynski, J. and Strobel, J. (2007). Comparison of the corneal thickness as measured by Visante anterior segment OCT versus ultrasound technique. *Klin Monbl Augenheilkd.* **224**, 832-836.
- Wildsoet, C. and Pettigrew, J.D. (1988). Experimental myopia and anomalous eye growth patterns unaffected by optic nerve section in chickens: evidence for local control of eye growth. *Clin Vision Sci.* **3**, 99 –107.
- Wildsoet, C. and Wallman, J. (1995). Choroidal and scleral mechanisms of compensation for spectacle lenses in chicks. *Vision Res.* **35**, 1175-1194.
- Wildsoet, C.F. (1997). Active emmetropization--evidence for its existence and ramifications for clinical practice. *Ophthalmic Physiol Opt.* **17**, 279-290.
- Wilke, K. (1971). Intraocular pressure measurement on various parts of the cornea. *Acta ophthalmologica.* **49**, 545-551.
- Wilson, J.R. and Sherman, S.M. (1977). Differential effects of early monocular deprivation on binocular and monocular segments of cat striate cortex. *J Neurophysiol.* **40**, 891-903.
- Winn, B. and Gilmartin, B. (1992). Current perspective on microfluctuations of accommodation. *Ophthalmic Physiol Opt.* **12**, 252-256.
- Wirbelauer, C., Karandish, A., Aurich, H. and Pham, D.T. (2003). Imaging scleral expansion bands for presbyopia with optical coherence tomography. *J Cataract Refract Surg.* **29**, 2435-2438.
- Wolffsohn, J.S. and Davies, L.N. (2007). Advances in anterior segment imaging. *Curr Opin Ophthalmol.* **18**, 32-38.
- Wolffsohn, J.S. and Peterson, R.C. (2006). Anterior ophthalmic imaging. *Clin Exp Optom.* **89**, 205-214.
- Wollensak, G. and Iomdina, E. (2009). Long-term biomechanical properties of rabbit sclera after collagen crosslinking using riboflavin and ultraviolet A (UVA). *Acta ophthalmologica.* **87**, 193-198.
- Wollensak, G. and Spoerl, E. (2004). Collagen crosslinking of human and porcine sclera. *J Cataract Refract Surg.* **30**, 689-695.
- Wong, E. and Maurice, K.H. (1991). Factors affecting ocular rigidity in the Chinese. *Clin Exp Optom.* **74**, 156-159.

- Wong, T.Y., Foster, P.J., Hee, J., Ng, T.P., Tielsch, J.M., Chew, S.J., Johnson, G.J. and Seah, S.K. (2000). Prevalence and risk factors for refractive errors in adult Chinese in Singapore. *Invest Ophthalmol Vis Sci.* **41**, 2486-2494.
- Wong, T.Y., Foster, P.J., Ng, T.P., Tielsch, J.M., Johnson, G.J. and Seah, S.K. (2001). Variations in ocular biometry in an adult Chinese population in Singapore: the Tanjong Pagar Survey. *Invest Ophthalmol Vis Sci.* **42**, 73-80.
- Wong, T.Y., Klein, B.E.K., Klein, R., Knudtson, M. and Lee, K.E. (2003). Refractive errors, intraocular pressure, and glaucoma in a white population. *Ophthalmology.* **110**, 211-217.
- Woo, S.L., Kobayashi, A.S., Schlegel, W.A., Lawrence, C., 1972. Nonlinear material properties of intact cornea and sclera. *Exp Eye Res.* **1**, 29-39.
- Wu, H.M., Seet, B., Yap, E.P., Saw, S.M., Lim, T.H. and Chia, K.S. (2001). Does education explain ethnic differences in myopia prevalence? A population-based study of young adult males in Singapore. *Optom Vis Sci.* **78**, 234-239.
- Wu, S., Nemesure, B. and Leske, M. (1999). Refractive errors in a black adult population: the barbados eye study. *Invest Ophthalmol Vis Sci.* **40**, 2179-2184.
- Wu, S., Nemesure, B. and Leske, M. (2000). Glaucoma and myopia. *Ophthalmology.* **107**, 1026-1027.
- Xu, L., Wang, Y., Wang, S., Wang, Y. and Jonas, J.B. (2007). High myopia and glaucoma susceptibility the Beijing Eye Study. *Ophthalmology.* **114**, 216-220.
- Yasuda, A. and Yamaguchi, T. (2005). Steepening of corneal curvature with contraction of the ciliary muscle. *J Cataract Refract Surg.* **31**, 1177-1181.
- Yasuda, A., Yamaguchi, T. and Ohkoshi, K. (2003). Changes in corneal curvature in accommodation. *J Cataract Refract Surg.* **29**, 1297-1301.
- Yazici, A.T., Bozkurt, E., Alagoz, C., Alagoz, N., Pekel, G., Kaya, V. and Yilmaz, O.F. (2010). Central corneal thickness, anterior chamber depth, and pupil diameter measurements using Visante OCT, Orbscan, and Pentacam. *J Refract Surg.* **26**, 127-133.
- Yebra-Pimentel, E., González-Méijome, J.M., García-Resúa, C. and Giráldez-Fernández, M.J. (2008). The relationships between ocular optical components and implications in the process of emmetropization. *Arch Soc Esp Oftalmol.* **83**, 307-316.
- Yoo, C., Eom, Y.S., Suh, Y.W. and Kim, Y.Y. (2010). Central Corneal Thickness and Anterior Scleral Thickness in Korean Patients With Open-angle Glaucoma: An Anterior Segment Optical Coherence Tomography Study. *J Glaucoma.* doi:10.1097/IJG.0b013e3181dde051 [Epub ahead of print].
- Ytteborg, J. (1960a). The effect of intraocular pressure on rigidity coefficient in the human eye. *Acta Ophthalmol (Copenh).* **38**, 548-561.
- Ytteborg, J. (1960b). Further investigations of factors influencing size of rigidity coefficient. *Acta Ophthalmol (Copenh),* **38**, 643-657.
- Ytteborg, J. (1960c). The role of intraocular blood volume in rigidity measurements on human eyes. *Acta Ophthalmol (Copenh),* **38**, 410-436.

- Yu, .W, Cao, G., Qiu, J., Liu, X., Ma, J., Li, N., Yu, M., Yan, N., Chen, L. and Pang, I.H. (2009). Evaluation of monkey intraocular pressure by rebound tonometer. *Mol Vis.* **15**, 2196-2201.
- Zadnik, K., and Mutti, D.O. (1995). How applicable are animal myopia models to human juvenile onset myopia? *Vision Res.* **35**, 1283-1288.
- Zadnik, K., Manny, R.E., Yu, J.A., Mitchell, G.L., Cotter, S.A., Quiralte, J.C., Shipp, M., Friedman, N.E., Kleinstein, R.N., Walker, T.W., Jones, L.A., Moeschberger, M.L. and Mutti, D.O. (2003). Ocular component data in schoolchildren as a function of age and gender. *Optom Vis Sci.* **80**, 226-236.
- Zadnik, K., Mutti, D.O., Friedman, N.E. and Adams, A.J. (1993). Initial cross-sectional results from the Orinda Longitudinal Study of Myopia. *Optom Vis Sci.* **70**, 750-758.
- Zadnik, K., Mutti, D.O., Fusaro, R.E. and Adams, A.J. (1995). Longitudinal evidence of crystalline lens thinning in children. *Invest Ophthalmol Vis Sci.* **36**, 1581-1587.
- Zappia, R.J., Winkelman, J.Z. and Gay, A.J. (1971). Intraocular pressure changes in normal subjects and the adhesive muscle syndrome. *Am J Ophthalmol.* **71**, 880-883.
- Zeng, Y., Liu, Y., Liu, X., Chen, C., Xia, Y., Lu, M. and He, M. (2009). Comparison of lens thickness measurements using the anterior segment optical coherence tomography and A-scan ultrasonography. *Invest Ophthalmol Vis Sci.* **50**, 290-294.
- Zhang, L. and Wang, Y. (2010). The Shape of Posterior Corneal Surface in Normal, Post-LASIK, and Post-Epi-LASIK Eyes. *Invest Ophthalmol Vis Sci.* **51**, 3468-3475.
- Zhao, P.S., Wong, T.Y., Wong, W.L., Saw, S.M. and Aung, T. (2007). Comparison of central corneal thickness measurements by visante anterior segment optical coherence tomography with ultrasound pachymetry. *Am J Ophthalmol.* **143**, 1047-1049
- Zheng, Y., Ge, J., Huang, G., Zhang, J., Liu, B., Hur, Y.M. and He, M. (2008). Heritability of central corneal thickness in Chinese: the Guangzhou Twin Eye Study. *Invest Ophthalmol Vis Sci.* **49**, 4303-4307.
- Zhou. X.D., Wang, F.R., Zhou, S.Z. and Shi, J.S. (1997). A computed tomographic study of the relation between ocular axial biometry and refraction. In: *Myopia Updates: Proceedings of the 6th International Conference on Myopia*. Ed. Tokoro, T. New York: Springer. 112– 115.
- Zolog, N., Chercota, G. and Koos, D. (1969). Scleral rigidity in myopia forte. *Oftalmologica (Buc).* **13**, 123-125.

APPENDIX 1

ETHICAL APPROVAL



Aston University

MEMORANDUM **REGISTRY & PLANNING SERVICES**

DATE: 22 April 2008

TO: Dr Nicola Logan,
Life & Health Sciences

FROM: John Walter,
Academic Registrar

SUBJECT: **Project 08/5: Investigation of ocular and scleral rigidity in human subjects**

I am writing to inform you that a Sub-Group of the University's Ethics Committee has, on behalf of the Ethics Committee, approved the above-mentioned project.

The details of the investigation will be placed on file. You should notify me of any difficulties experienced by the volunteer subjects, and any significant changes which may be planned for this project in the future.

Best wishes,

A handwritten signature in black ink that reads "J. G. Walter".

Secretary to the Ethics Committee

APPENDIX 2

SUBJECT GROUPS FOR EACH STUDY

Subjects included in each study throughout the thesis.

Note the same 60 Hong Kong Chinese individuals were evaluated in Chapters 8 and 11.

Subject no	Chp 6	Chp 7	Chp 8	Chp 10		Chp 11	Chp 12	Chp 13	Chp 14
				4 mm	8 mm				
1	X	X	X	X	X	X	X	X	X
2	X	X	X	X	X	X	X	X	X
3	X	X	X	X	X	X	X		X
4	X	X	X	X	X	X	X		X
5	X	X	X	X	X	X	X	X	X
6	X	X	X		X	X			
7	X	X	X		X	X	X		X
8	X	X	X	X	X	X		X	X
9	X	X	X	X	X	X	X		X
10	X	X	X	X	X	X	X		X
11	X	X	X	X	X	X	X		X
12	X	X	X			X	X	X	X
13	X	X	X	X	X	X	X	X	X
14	X	X	X		X	X	X		X
15	X	X	X	X	X	X	X	X	X
16	X	X	X	X	X	X	X	X	X
17	X	X	X	X	X	X	X		X
18	X	X	X	X	X	X		X	
19	X	X	X	X	X	X		X	
20	X	X	X	X	X	X		X	
21		X	X	X	X	X		X	
22	X	X	X	X	X	X	X	X	X
23		X	X	X	X	X		X	
24	X	X	X	X	X	X	X	X	X
25		X	X			X		X	
26		X	X	X	X	X	X	X	X
27		X	X	X	X	X		X	
28	X	X	X	X	X	X	X	X	X
29		X	X	X	X	X		X	
30		X	X	X	X	X	X		X
31		X	X	X	X	X		X	
32		X	X	X	X	X		X	
33		X	X			X		X	
34		X	X	X	X	X		X	
35		X	X	X	X	X	X	X	X
36		X	X		X	X		X	
37		X	X	X	X	X		X	
38		X	X	X	X	X		X	
39		X	X	X	X	X		X	
40		X	X	X	X	X		X	
41		X	X	X	X	X		X	
42		X	X	X	X	X	X	X	X
43		X	X	X	X	X	X	X	X
44		X	X	X	X	X		X	

45		X	X	X	X	X		X	
46		X	X	X	X	X		X	
47		X	X	X	X	X		X	
48		X	X	X	X	X		X	
49		X	X	X	X	X		X	
50		X	X	X	X	X		X	
51		X	X	X	X	X		X	
52		X	X	X	X	X		X	
53		X	X	X	X	X		X	
54		X	X			X	X	X	X
55		X	X	X	X	X		X	
56		X	X	X	X	X		X	
57		X	X	X	X	X		X	
58		X	X			X	X	X	X
59		X	X	X	X	X	X	X	X
60	X	X	X	X	X	X	X	X	X
61	X	X	X	X	X	X	X	X	X
62		X	X	X	X	X	X	X	X
63	X	X	X	X	X	X	X		X
64		X	X	X	X	X	X	X	X
65		X	X	X	X	X	X	X	X
66		X	X	X	X	X	X	X	X
67		X	X	X		X	X	X	X
68		X	X			X	X	X	X
69		X	X	X	X	X	X	X	X
70		X	X	X	X	X	X	X	X
71		X	X	X	X	X	X	X	X
72		X	X	X	X	X	X	X	X
73		X	X	X	X		X		X
74		X	X	X	X	X	X	X	X
75		X	X	X	X	X	X	X	X

Table A2.1 Subjects included in each chapter throughout the thesis.

APPENDIX 3

STATISTICAL APPENDIX FOR CHAPTER 6

The study employed 26 healthy individuals (52 eyes; 10 males and 16 females) aged between 18-40 years (mean 29.48 ± 5.9). The data were analysed for non-myopic and myopic individuals [MSE (D) 14 non-myopes (≥ -0.50) $+0.48 \pm 1.22$, range (-0.50 to +4.38); 12 myopes (< -0.50) -4.44 ± 3.35 , range (-0.75 to -10.56)].

Section 6.5.1 Schiötz Indentation: raw data

5.5 g Scale readings:

Two way repeated measures ANOVA testing for the influence of refractive status revealed no significant effect ($F(24, 1)=0.016$ ($p=0.900$)), however Schiötz scale readings showed significant regional differences ($F(3, 72)=18.97$ ($p<0.001$)), with a Bonferroni *post hoc* test showing differences between ST:SN, ST:IT, ST:IN.

7.5 g Scale readings:

Two way repeated measures ANOVA testing for the effect of refractive status revealed no significant effect ($F(24, 1)=0.693$ ($p=0.413$)), however Schiötz scale readings showed significant regional differences ($F(3, 72)=18.29$ ($p<0.001$)), with a Bonferroni *post hoc* test showing differences between ST:SN, ST:IT, ST:IN.

Section 6.5.4 Intra- and interobserver variability using Schiötz tonometry.

Region	Mean	SD	CoV (%)
CR	4.8	0.5	10.5
ST	6.2	2.3	36.8
SN	6.6	2.1	31.4
IT	5.6	1.8	32.5
IN	4.8	1.3	27.1

Table A3.1 RE Scale readings and CoV for observer LD for the 5.5 g weight.

Region	Mean	SD	CoV (%)
CR	7.0	0.8	11.7
ST	8.8	1.1	12.4
SN	9.2	2.4	26.0
IT	8.2	1.6	20.0
IN	8.2	1.9	23.4

Table A3.2 RE Scale readings and CoV for observer LD for the 7.5 g weight.

Region	Mean	SD	CoV (%)
CR	6.8	0.6	8.2
ST	7.2	1.3	18.1
SN	4.2	0.5	10.6
IT	8.6	2.4	27.9
IN	8.0	1.9	23.4

Table A3.3 RE Scale readings and CoV for observer HP for the 5.5 g weight.

Region	Mean	SD	CoV (%)
CR	9.0	1.2	13.6
ST	10.2	3.8	37.0
SN	8.4	1.5	18.1
IT	9.6	2.5	26.2
IN	9.6	3.2	33.4

Table A3.4 RE Scale readings and CoV for observer HP for the 7.5 g weight.

Region	ICC RE Single	ICC RE Average	ICC LE Single	ICC LE Average
CR	0.682	0.811	0.643	0.783
ST	0.574	0.729	0.356	0.525
SN	0.425	0.596	0.188	0.317
IT	0.432	0.603	0.524	0.688
IN	0.342	0.510	0.431	0.603

Table A3.5 Schiotz 5.5 g single and average ICC.

Region	ICC RE Single	ICC RE Average	ICC LE Single	ICC LE Average
CR	0.388	0.559	0.548	0.708
ST	0.600	0.750	0.466	0.636
SN	0.386	0.557	0.245	0.394
IT	0.344	0.512	0.647	0.785
IN	0.187	0.316	0.561	0.719

Table A3.6 Schiotz 7.5 g single and average ICC.

Region	% Absolute Error	% Error SD	95% CI
RE CR	16.86	10.00	36.80 - (-3.14)
RE ST	17.87	15.33	48.53 - (-12.79)
RE SN	20.12	11.94	44.00 - (-3.76)
RE IT	29.71	22.86	75.43 - (-16.01)
RE IN	25.18	20.21	65.60 - (-15.24)

Table A3.7 Schiotz 5.5 g average PE.

Region	% Absolute Error	% Error SD	95% CI
RE CR	14.33	12.27	38.87 - (-10.21)
RE ST	15.52	9.88	35.28 - (-4.24)
RE SN	13.89	7.33	28.55 - (-0.77)
RE IT	25.26	18.64	62.54 - (-12.02)
RE IN	24.21	21.99	68.19 - (-19.77)

Table A3.8 Schiotz 7.5 g average PE.

APPENDIX 4

STATISTICAL APPENDIX FOR CHAPTER 7

The scleral thickness of 75 healthy individuals (150 eyes; 29 males and 46 females; 37 non-myopic and 38 myopic) aged between 18-40 years (27.8 ± 5.5) was assessed. The data were analysed for non-myopic and myopic individuals [non-myopes (MSE ≥ -0.50 D), n=37 MSE (D) mean \pm SD (0.49 ± 1.08), range (-0.50 to +4.38), AL (mm) mean \pm SD (23.33 ± 0.72), range (21.61 - 24.74); myopes (MSE < -0.50 D), n=38 MSE (D) mean \pm SD (-4.65 ± 4.09), range (-0.51 to -20.50), AL (mm) mean \pm SD (25.28 ± 1.28), range (23.33 - 28.32)].

Section 7.5.5.1 Scleral thickness and additional ocular biometric parameters

Scleral thickness measurements for the 8 meridians from 1-7 mm were correlated with various ocular biometry parameters (axial length, refractive error, ACD, corneal curvature and CCT). Note - only significant correlations discussed:

Axial length and scleral thickness at meridian IT at 3 mm ($r=0.261$, $p=0.025$), S at 3 mm ($r=0.257$, $p=0.027$) and I at 1 mm ($r=0.258$, $p=0.026$) showed significant positive correlations.

Refraction and scleral thickness at meridian S at 3 mm ($r=-0.253$, $p=0.028$), ST at 1 mm ($r=-0.233$, $p=0.045$), ST at 2 mm ($r=-0.235$, $p=0.043$) and I at 1 mm ($r=-0.228$, $p=0.049$) showed significant negative correlations.

CCT and scleral thickness at meridians SN at 3 mm ($r=-0.266$, $p=0.036$), SN at 4 mm ($r=-0.274$, $p=0.031$), S at 4 mm ($r=-0.351$, $p=0.005$), S at 5 mm ($r=-0.402$, $p=0.001$), S at 6 mm ($r=-0.292$, $p=0.021$), ST at 4 mm ($r=-0.280$, $p=0.028$), ST at 5 mm ($r=-0.300$, $p=0.018$), ST at 6 mm ($r=-0.289$, $p=0.022$), IT at 4 mm ($r=-0.317$, $p=0.012$), IT at 5 mm ($r=-0.267$, $p=0.036$) and I at 5 mm ($r=-0.251$, $p=0.049$) showed significant negative correlations.

APPENDIX 5

HIGH SPEED PHOTOGRAPHY OF REBOUND TONOMETRY ON THE CORNEA AND SCLERA

CD ROM contents:

5.1A High speed photography of rebound tonometry being performed on the cornea

5.1B High speed photography of rebound tonometry being performed on the sclera

See end of thesis for CD.

APPENDIX 6

STATISTICAL APPENDIX FOR CHAPTER 8

Section 8.5.2 Concordance of *iCare* tonometry with GAT and the Reichert ORA

IOP was measured in 75 individuals (150 eyes; 29 males and 46 females; 37 non-myopic and 38 myopic) aged between 18-40 years (27.8 ± 5.5). The data were analysed for non-myopic and myopic individuals [non-myopes (MSE $\geq -0.50D$), $n=37$, MSE (D) mean \pm SD (0.49 ± 1.08), range (-0.50 to +4.38), AL (mm) mean \pm SD (23.33 ± 0.72), range (21.61 - 24.74); myopes (MSE $< -0.50D$), $n=38$ MSE (D) mean \pm SD (-4.70 ± 4.14), range (-0.51 to -20.50), AL (mm) mean \pm SD (25.13 ± 1.28), range (mm) (22.81 - 28.12)].

Correlation between RE and LE for various tonometric tests:

RE and LE IOP *iCare*: ($r= 0.682$, $p<0.001$); RE and LE GAT: ($r=0.924$, $p<0.001$); RE and LE IOPg: ($r=0.835$, $p<0.001$); RE and LE IOPcc ($r=0.700$, $p<0.001$).

Bland and Altman plots showed *iCare* to overestimate GAT, with no systematic bias in overestimation, however the *iCare*-GAT difference was significantly greater when a higher IOP was measured by the *iCare* ($r=0.276$, $p=0.019$) and GAT ($r=0.378$, $p=0.001$).

Correlations between ocular variables and IOP:

CCT correlated significantly with GAT ($r=0.415$, $p=0.001$), *iCare* ($r=0.320$, $p=0.009$), IOPg ($r=0.511$, $p<0.001$) but not with IOPcc. CCT also correlated significantly with IOP difference between *iCare* and IOPg ($r=0.396$, $p=0.001$).

Significant correlations were found between *iCare* and CRF ($r=0.659$, $p<0.001$) and CH ($r=0.299$, $p=0.011$).

Stepwise forward multiple linear regression:

Model 1: Outcome variable *iCare* (mm Hg)

Predictor variables: CCT (μ m), CH (mm Hg), CRF (mm Hg), refractive error (D), mean corneal curvature (K (mm)), axial length (mm), ACD (mm), gender and age (years). (Note: where variables were found to have high (>0.8) multicollinearity they were assessed separately).

Parameter	R	R ²	Adjusted R ²	SE of the Estimate	Change statistics					
					R ²	F	df1	df2	Sig. F Change	Durbin Watson
CRF	0.659	0.434	0.426	1.792	0.434	53.742	1	70	<0.001	2.571
CRF CH	0.749	0.561	0.548	1.590	0.127	19.942	1	69	<0.001	

Table A6.1 Model summary for outcome variable corneal *iCare* measurements.

Model parameters	Unstandardized Coefficients		Standardized Coefficient	t	Sig.
	B	Std. Error	Beta		
1. Constant	3.995	1.481		2.697	0.009
CRF	1.020	0.139	0.659	7.331	<0.001
2. Constant	8.089	1.602		5.048	<0.001
CRF	1.723	0.200	1.113	8.613	<0.001
CH	-1.064	0.238	-0.577	-4.466	<0.001

Table A6.2 Multiple linear regression outcome table for corneal *iCare* measurements.

Result: CRF ($t(70)=8.613$, ($p < 0.001$)) and CH ($t(69) = -4.466$, ($p < 0.001$)) are significant predictors for corneal *iCare* values.

Section 8.5.3 Application of the *iCare* tonometer to the sclera

Scleral *iCare* measures were also obtained on the individuals assessed in Section 8.5.2. The scleral *iCare* data were initially checked to be normally distributed using the Kolmogorov Smirnov test. The UK data (mixed BW-BSA; $n=75$) failed to show a normal distribution when the whole sample was assessed but when divided into myopes and non-myopes the distributions were found to be normal. A two-way mixed repeated measures ANOVA showed no significant difference in scleral values between myopes and non-myopes ($F(1, 73)=0.040$ ($p=0.841$)) hence the groups were combined.

Section 8.5.4 Comparison of regional scleral *iCare* values (mm Hg) to Schiottz scleral indentation values for the 4 mm location from the limbus

65 healthy individuals also had scleral Schiottz tonometry performed at four quadrants (ST, SN, IT, IN) 4 mm from the limbus. The subjects were aged between 19-40 years (27.66 ± 5.26) and the data was analysed for non-myopic and myopic individuals [non-myopes (MSE $\geq -0.50D$) $n=31$, MSE (D) mean \pm SD (0.50 ± 1.17), range (-0.50 to +4.38), AL (mm) mean \pm SD (23.38 ± 0.74), range (21.61 - 24.75); myopes (MSE $< -0.50D$) $n=34$, MSE (D) mean \pm SD (-4.40 ± 3.23), range (-10.56 to -0.51), AL (mm) mean \pm SD (25.30 ± 1.16), range (23.35 - 28.12)].

Schiottz weight	Regions	Scleral <i>iCare</i>			
		ST	IT	SN	IN
5.5 g	ST	$r=-0.311$			
	IT	$r=-0.345$			$r=-0.247$
	SN				
	IN				
7.5 g	ST				
	IT	$r=-0.377$ p	$r=-0.294$	$r=-0.268$	$r=-0.387$
	SN				
	IN		$r=-0.248$	$r=-0.298$	$r=-0.314$,
10 g	ST				
	IT	$r=-0.467$	$r=-0.402$		$r=-0.301$
	SN				
	IN	$r=-0.257$	$r=-0.265$		$r=-0.273$

Table A6.3 Pearson's correlation coefficients for scleral *iCare* values and Schiottz indentation readings at 4 mm from the limbus. (Note only significant correlations shown).

Section 8.5.5 Scleral *iCare* values and scleral thickness

Scleral <i>iCare</i> readings	Scleral thickness at various distances (mm) from the corneo-limbal junction				
	2	3	4	5	6
SN					
S				$r=0.278$ $p=0.016$	
ST	$r=0.278$ $p=0.016$	$r=0.302$ $p=0.008$	$r=0.279$ $p=0.026$		
T		$r=0.321$ $p=0.005$	$r=0.379$ $p=0.001$	$r=0.325$ $p=0.004$	$r=0.240$ $p=0.038$

IT					
I					
IN					
N					

Table A6.4 Pearson's correlation coefficients for scleral *iCare* values and scleral thickness along the same meridians at different distances from the limbus. (Note only significant correlations shown).

Section 8.5.6 Assessment of regional variation in scleral measurements in the HKC individuals

Scleral region ST was found to correlate significantly with refractive error ($r=-0.264$, $p=0.043$), axial length ($r=0.289$, $p=0.026$) and corneal *iCare* readings ($r=0.283$, $p=0.031$). Axial length correlated significantly with refractive error ($r=-0.870$, $p<0.001$).

APPENDIX 7

STATISTICAL APPENDIX FOR CHAPTER 10

Scleral Schiötz tonometry was performed at the 8 mm locations on 68 healthy individuals (136 eyes; 24 males and 44 females) who were aged between 19-40 years (27.76 ± 5.26). The data was analysed for non-myopes and myopes [non myopes ($\geq -0.50D$) $n=33$ MSE (D) mean \pm SD (0.49 ± 1.14), range (-0.50 to +4.38), AL (mm) mean \pm SD (23.31 ± 0.73), range (21.61-24.75); myopes ($< -0.50D$) $n=35$ MSE (D) mean \pm SD (-4.36 ± 3.19), range (-10.56 to -0.51), AL (mm) mean \pm SD (25.30 ± 1.15), range (23.35-28.12)].

Of the original 68 subjects, 65 individuals (130 eyes; 23 males and 42 females) also had Schiötz tonometry performed at the 4 mm location from the corneolimbus junction. The subjects were aged between 19-40 years (27.66 ± 5.26) and data were assessed for non-myopes and myopes [non myopes ($\geq -0.50D$) $n=31$ MSE (D) mean \pm SD (0.50 ± 1.17), range (-0.50 to +4.38), AL (mm) mean \pm SD (23.38 ± 0.74), range (21.61-24.75); myopes ($< -0.50D$) $n=34$ MSE (D) mean \pm SD (-4.40 ± 3.23), range (-10.56 to -0.51), AL (mm) mean \pm SD (25.30 ± 1.16), range (23.35-28.12)].

Section 10.5.1 Schiötz scale readings: the effect of distance from limbus and Schiötz weights

8 mm and Schiötz weights

Two-way repeated measures ANOVA (Regional scale values x Schiötz weights) showed significant difference between all three weights ($F(2, 198)=171.715$ ($p<0.001$)), significant difference between all four quadrants ($F(2.874, 569.142)=269.810$ ($p<0.001$)) and no interaction effect between weights and regions ($F(5.749, 569.142)=1.078$ ($p=0.374$)).

4 mm and Schiötz weights

Two-way repeated measures ANOVA (Regional scale values x Schiötz weights) showed significant difference between all three weights ($F(2, 190)=205.875$ ($p<0.001$)), significant difference between all four quadrants ($F(3, 570)=167.048$ ($p<0.001$)) and no interaction effect between weights and regions ($F(6, 570)=1.291$ ($p=0.259$)).

4 and 8 mm and Schiötz weights

Three way mixed repeated measures ANOVA (distance (4 or 8 mm) x Schiötz weights x Regional scale values) revealed a significant effect for distance ($F(1, 187)=34.887$ ($p<0.001$)), weight ($F(2, 187)=250.02$ ($p<0.001$)) with a significant interaction effect for distance and regional variation ($F(2.840, 530.987)=51.189$ ($p<0.001$)). On inspection of the interaction plot regions ST and IT appeared to behave differently between the 4 and 8 mm sites. No significant effect of weights was found on the regional variation ($F(6, 539)=1.442$ ($p=0.204$)). Furthermore no interaction effect was found for the factors weight and distance ($F(2, 187)=0.577$ ($p=0.563$)) or regions, distance and weights ($F(5.679, 530.987)=0.660$ ($p=0.673$)).

Section 10.5.2 Schiötz scale readings at 8 mm

Regional variations for each weight was assessed by performing a one-way repeated measures ANOVA. The results showed:

- Schiötz 5.5 g: a significant difference was found between all four quadrants ($F(2.70, 180.62)=111.38$, ($p<0.001$)) with differences between ST:SN, ST:IT, ST:IN, SN:IT, SN:IN and IT:IN ($p<0.001$).
- Schiötz 7.5 g: a significant difference was also found between all four quadrants ($F(3, 201)=78.72$, ($p<0.001$)) with differences between ST:SN, ST:IT, ST:IN, SN:IT, SN:IN and IT:IN ($p<0.05$).

- Schiötz 10 g: a significant difference was found between all four quadrants ($F(3, 192)=86.10$, ($p<0.001$)), with differences between ST:SN, ST:IT, ST:IN, SN:IT, SN:IN ($p<0.001$).

Comparing scleral and corneal (CR) indentations:

- Schiötz 5.5 g showed a significant difference between scleral quadrants and corneal indentation values ($F(3.32, 222.44)=75.73$, ($p<0.001$)); no difference was found between CR:ST and CR:SN.
- Schiötz 7.5 g showed significant differences between scleral and corneal indentation values ($F(4, 268)=60.18$, ($p<0.001$)) except between CR:SN and SN:IT.
- Schiötz 10 g concurred the results of the other two weights and showed a significant difference between scleral and corneal scale values ($F(4, 256)=61.24$, ($p<0.001$)) except between CR:SN.

ANOVA	Weights	Treatment effect		Regional Variation		Interaction	
		F	p	F	p	F	p
Refractive status X RSV	5.5 g	0.266	0.607	110.266	<0.001	0.265	0.851
	7.5 g	1.744	0.191	79.146	<0.001	1.069	0.363
	10 g	0.076	0.784	84.507	<0.001	0.021	0.996
Axial length group X RSV	5.5 g	1.621	0.206	94.637	<0.001	0.687	0.660
	7.5 g	0.650	0.526	65.920	<0.001	1.062	0.387
	10 g	2.160	0.124	76.186	<0.001	1.950	0.075
Age group X RSV	5.5 g	0.937	0.337	100.566	<0.001	0.043	0.983
	7.5 g	0.896	0.347	75.043	<0.001	0.658	0.579
	10 g	2.506	0.118	77.595	<0.001	0.344	0.794
Gender X RSV	5.5 g	2.804	0.099	101.493	<0.001	0.135	0.925
	7.5 g	1.862	0.177	75.679	<0.001	0.772	0.511
	10 g	1.249	0.268	79.652	<0.001	0.241	0.868
Ethnicity X RSV	5.5 g	3.367	0.071	97.600	<0.001	0.400	0.732
	7.5 g	5.052	0.028	74.985	<0.001	1.484	0.220
	10 g	8.536	0.005	78.073	<0.001	1.555	0.202

Table A7.1 Multiple two-way repeated measures ANOVAs assessing for the effect of different variables (treatment effect) on regional Schiötz scale values (RSV) at 8 mm.

Section 10.5.3 Schiötz scale readings at 4 mm

Regional variations for each weight was assessed by performing a one-way repeated measures ANOVA. The results showed:

- Schiötz 5.5 g: a significant difference was found between all four quadrants ($F(3, 192)=62.427$, ($p<0.001$)), ST:IT, ST:IN, SN:IT and SN:IN ($p<0.001$) except between ST:SN and IN:IT.
- Schiötz 7.5 g: a significant difference was found between all four quadrants ($F(3, 189)=39.878$, ($p<0.001$)), except between ST:SN and IN:IT.
- Schiötz 10 g: a significant difference was found between all four quadrants ($F(3, 189)=70.885$, ($p<0.001$)), except between ST:SN and IN:IT.

Comparing scleral and corneal indentations:

- Schiötz 5.5 g: a significant difference was found between scleral quadrants and CR ($F(4, 252)=66.351$, ($p<0.001$)) except between CR:SN, ST:SN and IT:IN.
- Schiötz 7.5 g: a significant difference was found between scleral quadrants and CR ($F(4, 248)=46.621$, ($p<0.001$)) except between CR:SN, ST:SN and IT:IN.

- Schiötz 10 g: a significant difference was found between scleral quadrants and CR (F(3.393, 210.340)=58.639, (p<0.001)) except between CR:SN, CR:ST, ST:SN and IT:IN.

ANOVA	Weight	Treatment effect		Regional Variation		Interaction	
		F	p	F	p	F	p
Refractive status X RSV	5.5 g	0.668	0.417	63.349	<0.001	1.350	0.260
	7.5 g	0.604	0.440	40.463	<0.001	1.949	0.123
	10 g	1.449	0.233	72.309	<0.001	2.061	0.107
Axial length group X RSV	5.5 g	0.240	0.787	52.461	<0.001	1.842	0.093
	7.5 g	1.757	0.181	34.786	<0.001	2.403	0.036
	10 g	4.230	0.019	65.008	<0.001	1.465	0.193
Age group X RSV	5.5 g	1.190	0.279	55.857	<0.001	0.063	0.979
	7.5 g	0.686	0.411	40.670	<0.001	1.440	0.233
	10 g	0.001	0.978	74.064	<0.001	3.282	0.022
Gender X RSV	5.5 g	1.598	0.211	60.318	<0.001	0.698	0.555
	7.5 g	6.900	0.011	39.353	<0.001	0.934	0.425
	10 g	8.459	0.005	71.688	<0.001	2.820	0.040
Ethnicity X RSV	5.5 g	9.214	0.003	59.008	<0.001	1.391	0.247
	7.5 g	9.534	0.003	34.750	<0.001	1.586	0.194
	10 g	11.527	0.001	66.619	<0.001	2.622	0.051

Table A7.2 Multiple two-way repeated measures ANOVAs assessing for the effect of different variables (treatment effect) on regional Schiötz scale values (RSV) at 4 mm.

Quadrant	Schiötz weight	Distance from limbus (mm)						
		1	2	3	4	5	6	7
SN	5.5 g							
	7.5 g			r=- 0.260 p=0.038	r=- 0.295 p=0.018	r=- 0.321 p=0.010	r=- 0.259 p=0.039	r=- 0.309 p=0.013
	10 g							
ST	5.5 g			r=- 0.259 p=0.037				
	7.5 g		r=- 0.306 p=0.014	r=- 0.380 p=0.002	r=- 0.327 p=0.008			
	10 g			r=- 0.296 p=0.018				
IT	5.5 g		r=- 0.251 p=0.044	r=- 0.341 p=0.005	r=- 0.400 p=0.001	r=- 0.435 p<0.001	r=- 0.379 p=0.002	r=- 0.307 p=0.013
	7.5 g			r=- 0.280 p=0.025	r=- 0.401 p=0.001	r=- 0.327 p=0.008	r=- 0.252 p=0.044	
	10 g			r=- 0.280 p=0.025	r=- 0.378 p=0.002	r=- 0.375 p=0.002	r=- 0.299 p=0.017	

IN	5.5 g							r=- 0.266 p=0.032
	7.5 g					r=- 0.318 p=0.010	r=- 0.331 p=0.008	r=- 0.321 p=0.010
	10 g				r=- 0.263 p=0.036	r=- 0.330 p=0.008	r=- 0.353 p=0.004	r=- 0.390 p=0.001

Table A7.3 Pearson's correlations coefficients for meridional scleral thickness at various distances and regional Schiottz scale readings with different weights at 4 mm from the limbus (Note only significant results shown).

Section 10.5.4 Corneal indentation

Variable	Schiottz weights		
	5.5 g	7.5 g	10 g
Gender	0.239	0.514	0.155
Age group	0.603	0.317	0.287
Refractive status	0.423	0.256	0.045
Ethnicity	0.334	0.113	0.036

Table A7.4 Independent samples *t tests* assessing for an effect of different variables upon corneal scale values with different weights (only p values given).

A one-way ANOVA assessing for the influence of axial length grouping revealed no significant effect on the corneal indentation values with 5.5 g (p=0.994), 7.5 g (p=0.662) and 10 g (p=0.550).

Section 10.5.5.1 Friedenwald's Scleral rigidity (Ks)

ANOVA	Ks at 4 mm				Ks at 8 mm			
	5.5 g-7.5 g		5.5 g-10 g		5.5 g-7.5 g		5.5 g-10 g	
	F	p	F	p	F	p	F	p
One-way repeated: Regional Ks	0.516	0.672	2.205	0.101	0.742	0.532	0.532	0.661
Two-way mixed repeated: refractive status X Regional Ks	0.108	0.745	0.039	0.845	1.462	0.245	0.425	0.517
Two-way mixed repeated: Axial length subgroup X Regional Ks	0.335	0.730	1.106	0.340	0.071	0.931	0.519	0.598
Two-way mixed repeated: Age grouping X Regional Ks	0.760	0.300	0.670	0.440	0.850	0.427	0.973	0.337
Two-way mixed repeated: Gender X Regional Ks	0.207	0.660	0.050	0.875	0.800	0.450	0.780	0.575

Table A7.5 ANOVAs on Friedenwald's scleral rigidity (Ks) values at 4 and 8 mm.

Comparing rigidity values between 4 and 8 mm (two-way repeated measures ANOVA: Distance of measurement X Regional Ks) :

- Ks 5.5 g-7.5 g values showed no significant (F(1, 23)=0.318, (p=0.578)) differences between the two locations.
- Ks 5.5 g-10 g values showed no significant (F(1,101)=1.565, (p=0.214)) differences between the two locations.

Pearson's correlation coefficients for the various Ks values revealed:

at 4 mm:

- Ks 5.5 g-7.5 g for ST and IT correlated significantly ($r=0.374$, $p=0.035$).
- Ks 5.5 g-10 g for ST and IT ($r=0.444$, $p=0.001$); IT and SN ($r=0.436$, $p=0.001$); ST and SN ($r=0.332$, $p=0.013$); IT and IN ($r=0.399$, $p=0.003$) correlated significantly.

at 8 mm:

- Ks 5.5 g-10 g for IT and IN correlated significantly ($r=0.325$, $p=0.013$).

Section 10.5.5.2 Friedenwald's corneal rigidity (Ko)

Variable	Ks 5.5 g-7.5 g	Ks 5.5 g-10 g
Gender	0.970	0.880
Age group	0.070	0.089
Refractive status	0.839	0.097
Ethnicity	0.036	0.057

Table A7.6 Independent samples *t* tests assessing for an effect of different variables upon corneal rigidity values (only p values given).

A one-way ANOVA assessing for the influence of axial length grouping revealed no significant effect on Ko 5.5 g-7.5 g ($p=0.945$) or Ko 5.5 g-10 g ($p=0.506$).

APPENDIX 8

STATISTICAL APPENDIX FOR CHAPTER 11

Section 11.5.1 IOP and corneal biometrics (CH and CRF) for UK subjects

The study employed 72 healthy individuals (144 eyes; 26 males and 46 females) due to two individuals being removed as they each had astigmatism $>1.75D$. The subjects were aged between 18-40 years (27.83 ± 5.41) and data were analysed for non-myopic and myopic individuals [non myopes (MSE $\geq -0.50D$), $n=36$, MSE (D) mean \pm SD (0.41 ± 0.97), range (-0.50 to +4.38), AL (mm) mean \pm SD (23.35 ± 0.72), range (21.61 - 24.75); myopes (MSE $< -0.50D$), $n=36$, MSE (D) mean \pm SD (-4.62 ± 4.09), range (-20.50 to -0.51), AL (mm) mean \pm SD (25.23 ± 1.26), range (23.33 - 28.32)].

High levels of correlation were found between RE and LE: IOPg ($r=0.835$, $p<0.001$), IOPcc ($r=0.700$, $p<0.001$), CRF ($r=0.869$, $p<0.001$), CH ($r=0.705$, $p<0.001$).

	CH	CRF	IOPg	IOPcc	GAT	CCT
CH		$r=0.787$ $p<0.001$		$r=-0.361$ $p=0.002$		$r=0.526$ $p<0.001$
CRF	$r=0.787$ $p<0.001$		$r=0.708$ $p<0.001$	$r=0.291$ $p=0.013$	$r=0.647$ $p<0.001$	$r=0.671$ $p<0.001$
IOPg		$r=0.708$ $p<0.001$		$r=0.881$ $p<0.001$	$r=0.810$ $p<0.001$	$r=0.511$ $p<0.001$
IOPcc	$r=-0.361$ $p=0.002$	$r=0.291$ $p=0.013$	$r=0.881$ $p<0.001$			
GAT		$r=0.647$ $p<0.001$	$r=0.810$ $p<0.001$			$r=0.404$ $p=0.001$
CCT	$r=0.526$ $p<0.001$	$r=0.671$ $p<0.001$	$r=0.511$ $p<0.001$		$r=0.404$ $p=0.001$	
Mean corneal curvature	$r=-0.250$ $p=0.035$			$r=0.273$ $p=0.021$		

Table A8.1 Correlation matrix for various measures of IOP (mm Hg) and ORA biometrics (mm Hg).

- The average difference between GAT-IOPg ($M= -0.87$ $SE= 0.22$) was significantly greater than the hypothesis of a zero bias ($t(70) = 3.942$, ($p<0.001$)).
- The average difference between GAT-IOPcc ($M= -1.02$ $SE= 0.26$) was significantly greater than the hypothesis of a zero bias ($t(70) = 3.878$, ($p<0.001$)).
- GAT-IOPg difference correlated significantly with CCT ($r=-0.320$, $p=0.009$) and CRF ($r=-0.359$, $p=0.002$).
- GAT-IOPcc difference correlated significantly with CRF ($r=0.336$, $p=0.004$) and CH ($r=0.689$, $p<0.001$). The GAT-IOPcc difference showed a positive correlation ($r=0.239$, $p=0.044$) with increasing levels of GAT measures of IOP.

Section 11.5.2 Corneal biomechanics and additional ocular biometrics for UK subjects

Stepwise forward multiple linear regression:

All forward stepwise linear regression models were examined for high multicollinearity. Assessing the Durbin Watson test ensured the independence of error assumption. An assumption for no multicollinearity was assessed by variance inflation factor (VIF) and tolerance statistics. Residuals were ensured to be normally distributed. All data were found to exhibit homoscedasticity by

assessing plots of standardized predicted values versus Studentized residuals; presence of any significantly influential cases was assessed by Cook's and Mahalanobis distances.

Model 1: Outcome variable CH (mm Hg)

Predictive variables: GAT (mm Hg), CCT (μm), axial length ((mm); AL), refractive error ((D); Rx), ACD (mm), age (years), gender and mean corneal curvature (K (mm)). Note AL and Rx were not input together due to high levels of collinearity ($r = >0.80$).

Parameter	R	R ²	Adjusted R ²	SE of the Estimate	Change statistics					
					R ²	F	df1	df2	Sig. F Change	Durbin Watson
CCT	0.526	0.277	0.266	1.06	0.277	24.121	1	63	0.000	1.644
CCT K	0.609	0.371	0.351	1.00	0.094	9.280	1	62	0.003	
CCT K AL	0.646	0.417	0.388	0.97	0.046	4.810	1	61	0.032	

Table A8.2 Model summary for outcome variable CH.

Model parameters	Unstandardized Coefficients		Standardized Coefficient	t	Sig.
	B	Std. Error	Beta		
Constant	-.616	2.314		-.266	0.791
CCT	0.021	0.004	0.526	4.911	<0.001
Constant	10.834	4.343		2.495	0.015
CCT	0.023	0.004	0.570	5.599	<0.001
K	-1.602	0.526	-0.310	-3.046	0.003
Constant	15.456	4.712		3.280	0.002
CCT	0.023	0.004	0.575	5.822	<0.001
K	-1.588	0.510	-0.307	-3.110	0.003
AL	-0.200	0.091	-0.215	-2.193	0.032

Table A8.3 Multiple linear regression outcome table for CH.

Result: CCT ($t(61) = 5.82$, ($p < 0.001$)), mean corneal curvature ($t(61) = -3.11$, ($p = 0.003$)) and axial length ($t(61) = -2.193$, ($p = 0.032$)) were all significant predictors for CH.

Model 2: Outcome variable CRF (mm Hg) ; predictive variables as for CH (see above)

Model parameter	R	R ²	Adjusted R ²	SE of the Estimate	Change statistics					
					R ² change	F change	Df1	Df2	Sig. F Change	Durbin Watson
CCT	0.671	0.450	0.441	1.135	0.450	51.508	1	63	<0.001	1.744
CCT GAT	0.783	0.613	0.601	0.959	0.164	26.251	1	62	<0.001	
CCT GAT K	0.816	0.665	0.649	0.900	0.052	9.396	1	61	0.003	
CCT GAT K AL	0.835	0.697	0.677	0.863	0.032	6.304	1	60	0.015	

Table A8.4 Model summary for outcome variable CRF.

Model parameters	Unstandardized Coefficients		Standardized Coefficient	t	Sig.
	B	Std. Error	Beta		
Constant	-7.252	2.469		-2.937	0.005
CCT	0.033	0.005	0.671	7.177	<0.001
Constant	-6.148	2.097		-2.932	0.005
CCT	0.024	0.004	0.487	5.610	<0.001
GAT	0.270	0.053	0.444	5.124	<0.001
Constant	4.710	4.052		1.162	0.250
CCT	0.024	0.004	0.493	6.059	<0.001
GAT	0.309	0.051	0.508	6.047	<0.001
K	-1.497	0.488	-0.237	-3.065	0.003
Constant	10.245	4.468		2.293	0.025
CCT	0.024	0.004	0.478	6.100	<0.001
GAT	0.341	0.051	0.561	6.734	<0.001
K	-1.558	0.469	-0.246	-3.321	0.002
AL	-0.211	0.084	-0.185	-2.511	0.015

Table A8.5 Multiple linear regression outcome table for CRF.

Result: CCT (t (60)= 6.100, (p <0.001)), GAT (t (60) = 6.734, (p<0.001)), mean corneal curvature (t (60)=-3.321, (p=0.002)) and axial length (t (60) = -2.511, (p=0.015)) were all significant predictors for CRF.

Model 3: outcome variable IOPg (mm Hg)

Predictive variables: CCT (μm), AL (mm), ACD (mm), age (years) , gender and mean corneal curvature (K (mm)). Note AL and RX are not inputted together due to high levels of collinearity (r= >0.8).

Parameter	R	R ²	Adjusted R ²	SE of the Estimate	Change statistics					
					R ²	F	df1	df2	Sig. F Change	Durbin Watson
CCT	0.511	0.261	0.249	2.63	0.261	22.245	1	63	<0.001	1.769

Table A8.6 model summary for outcome variable IOPg.

Model parameters	Unstandardized Coefficients		Standardized Coefficient	t	Sig.
	B	Std. Error	Beta		
Constant	-12.301	5.727			
CCT	0.051	0.011	0.511	4.716	<0.001

Table A8.7 Multiple linear regression outcome table for IOPg.

Results: CCT (t (63)= 4.716, (p <0.001)) was a significant predictor for IOPg.

Model 4: outcome variable IOPcc (mm Hg); predictor variables as for IOPg.

Model parameter	R	R ²	Adjusted R ²	SE of the Estimate	Change statistics					
					R ² change	F change	Df1	Df2	Sig. F Change	Durbin Watson
K	0.331	0.109	0.095	2.570	0.109	7.731	1	63	0.007	1.977
K AL	0.419	0.175	0.149	2.492	0.066	4.972	1	62	0.029	

Table A8.8 model summary for outcome variable IOPcc.

Model parameters	Unstandardized Coefficients		Standardized Coefficient	t	Sig.
	B	Std. Error	Beta		
Constant	-13.844	10.347			
K	3.720	1.338	0.331	2.780	0.007
Constant	-26.135	11.450			
K	3.672	1.298	0.326	2.829	0.006
AL	0.522	0.234	0.257	2.230	0.029

Table A8.9 Multiple linear regression outcome table for IOPcc.

Results: mean corneal curvature ($t(63)=2.829$, ($p=0.006$)) and axial length ($t(62)=2.230$, ($p=0.029$)) are significant predictors of IOPcc.

Independent <i>t</i> tests	Degrees of freedom	t value	p value
Effect of refractive status on:			
CH	70	0.821	0.414
CRF	70	0.664	0.509
IOPg	56.85	0.096	0.924
IOPcc	70	-0.306	0.760
CCT	66	0.065	0.948
Mean corneal curvature	72	1.862	0.067
ACD	72	-4.467	<0.001
Effect of gender on:			
CH	70	-0.695	0.489
CRF	70	-0.268	0.789
IOPg	35.48	0.294	0.770
IOPcc	70	-0.646	0.520
Axial length	72	-1.100	0.275
CCT	66	-0.774	0.442
Mean corneal curvature	72	1.076	0.285
ACD	72	-1.075	0.286
Effect of age grouping on:			
CH	70	-0.853	0.397
CRF	70	0.029	0.977
IOPg	70	1.061	0.292
IOPcc	70	1.421	0.160
Axial length	72	1.531	0.130
CCT	66	0.072	0.943
Mean corneal curvature	72	0.896	0.373
ACD	72	1.189	0.055

Table A8.10 Independent *t* tests assessing the effect of refractive error, gender and age grouping on the ORA and biometric parameters.

A one-way ANOVA exploring the influence of axial length subgroups on ORA parameters, revealed no significant influence on: CH ($F(2, 68)=1.212$, ($p=0.304$)), CRF ($F(2, 68)=0.921$, ($p=0.403$)), IOPg ($F(2, 68)=0.278$, ($p=0.758$)) and IOPcc ($F(2, 68)=0.328$, ($p=0.722$)).

A one-way ANOVA exploring the influence of axial length subgroups on the biometric parameters revealed significant differences for ACD ($F(2, 73)=9.093$, ($p<0.001$)) but no significant influence on CCT ($F(2, 67)=0.424$, ($p=0.656$)) and mean corneal curvature ($F(2, 73)=1.545$, ($p=0.220$)).

Construction of Box- Whiskers plots

Figures 11.2 and 11.3 represent box and whiskers plots (median and interquartile range) for each ORA biometric. The top of the box represents the 75th percentile, the bottom of the box represents the 25th percentile, and the line in the middle represents the 50th percentile. The whiskers

represent the highest and lowest values that are not outliers or extreme values. Outliers (values that are between 1.5 and 3 times the interquartile range) and extreme values (values that are more than 3 times the interquartile range) are represented by circles beyond the whiskers.

Section 11.5.3 ORA Additional Waveform Parameters (AWPs) for UK subjects

Independent <i>t</i> test	Degrees of freedom	t value	p value
Effect of refractive status on:			
P2area	72	2.367	0.021
Aspect1	72	2.912	0.005
Dslope1	72	3.198	0.002
W1	72	-3.324	0.001
Mslew1	72	2.498	0.015
P2area1	72	2.287	0.025
Effect of gender			
Path1	72	2.262	0.027
Aplhf	72	2.669	0.009
Path21	72	2.913	0.005
Effect of age group			
Aspect1	72	-3.212	0.002
Uslope1	72	-3.453	0.001
Dslope1	72	-2.420	0.018
W1	72	2.433	0.017
H1	72	-2.134	0.036
Dive1	72	-2.168	0.033
Path1	72	-2.239	0.028
Mslew1	72	-2.536	0.013
Slew1	72	-3.174	0.002
Aspect11	72	-3.325	0.001
Uslope11	72	-3.135	0.002
W11	72	2.324	0.023
H11	72	-2.134	0.036

Table A8.11 Independent *t* tests assessing the effect of refractive status, gender and age (years) grouping on the AWP (Note: only significant outcomes shown).

Model 5: outcome variable refractive error (Rx)

Predictor variables: aindex, bindex, p1area, p2area, aspect1, aspect2, w1, w2, dive1, dive 2, path1, path2, mslew1, mslew2 and alphf (predictor variable selection was based on Pearson's correlation coefficients shown in Table 8.16 a and b).

Model parameter	R	R²	Adjusted R²	SE of the Estimate	Change statistics					
					R² change	F change	Df 1	Df2	Sig. F Change	Durbin Watson
P2area	0.255	0.065	0.052	3.822	0.065	5.017	1	72	0.028	1.636
P2area W1	0.365	0.133	0.109	3.706	0.068	5.567	1	71	0.021	
P2area W1 Mslew2	0.440	0.194	0.159	3.599	0.061	5.276	1	70	0.025	

Table A8.12 Model summary for outcome variable Rx.

Model parameters	Unstandardized Coefficients		Standardized Coefficient	t	Sig.
	B	Std. Error	Beta		
Constant	-7.660	2.482		-3.087	0.003
P2area	0.002	0.001	0.255	2.240	0.028
Constant	0.338	4.157		0.081	0.935
P2area	0.002	0.001	0.312	2.762	0.007
W1	-0.431	0.183	-0.267	-2.360	0.021
Constant	5.151	5.549		1.132	0.261
P2area	0.002	0.001	0.344	3.105	0.003
W1	-0.491	0.179	-0.303	-2.734	0.008
Mslew2	-0.026	0.011	-0.250	-2.297	0.025

Table A8.13 Multiple linear regression outcome table for Rx.

Results: P2area (t (72)= 3.105, (p=0.003)), W1 (t (71) = -2.734, (p=0.008)) and mslew2 (t (70)=-2.297, (p=0.025)) are significant predictors of refractive error.

Model 6: outcome variable axial length (AL); predictor variables as for Model 5.

Model parameter	R	R ²	Adjusted R ²	SE of the Estimate	Change statistics					
					R ² change	F change	Df1	Df2	Sig. F Change	Durbin Watson
W1	0.275	0.076	0.063	1.381	0.076	5.819	1	71	0.018	1.658
W1 Path2	0.396	0.157	0.133	1.328	0.081	6.719	1	70	0.012	

Table A8.14 Model summary for outcome variable AL.

Model parameters	Unstandardized Coefficients		Standardized Coefficient	t	Sig.
	B	Std. Error	Beta		
Constant	20.916	1.436		14.566	<0.001
W1	0.161	0.067	0.275	2.412	0.018
Constant	16.589	2.167		7.656	<0.001
W1	0.220	0.068	0.377	3.232	0.002
Path2	0.125	0.048	0.302	2.592	0.012

Table A8.15 Multiple linear regression outcome table for AL.

Results: W1 (t (71)= 3.232, (p=0.002)) and Path2 (t (70)= 2.592, (p=0.012)) are significant predictors of axial length.

Biometric variable	Bindex	P1area	P2 area	Aspect 1	Uslope 1	Dslope 1	W1	H1	H2	Dive1	Dive2	Path1	Path2	Mslw 1	Slew1	Alphf
Rx			0.255			0.249							-0.236			
AL						-0.232	0.275									
K		0.343	0.367					0.349	0.272							
CCT	0.256	0.453	0.601			0.269		0.352	0.420		0.457	-0.490	-0.301			-0.270
ACD				-0.287		-0.344	-0.328									
Age				0.350	0.339	0.271	-0.266	0.233		0.237		0.256		0.285	0.299	

Table A8.16a Correlations (only r values shown) between ocular biometric data and the AWP for the UK data ($p < 0.05$). AWP from upper 75% of the applanation peak.

Biometric variable	P1area 1	P2area 2	Aspect 11	Uslope 11	Dslope 11	W11	W21	H11	H21	Path11	Path21
Rx							0.261				
AL							-0.244				
K	0.288	0.311						0.349	0.272		
CCT	0.440	0.584				0.291	0.371	0.352	0.420	-0.502	-0.262
ACD											
Age			0.424	0.322	0.344	-0.282		0.233			

Table A8.16b Correlations (only r values shown) between ocular biometric data and the AWP for the UK data ($p < 0.05$). AWP from the upper 50% of the applanation peak.

Section 11.6.1 IOP and corneal biometrics (CH and CRF) for HKC subjects

The study assessed 56 healthy HKC individuals (112 eyes; 30 males and 26 females) as 4 subjects were removed from the study as they presented with astigmatism >1.75D. The subjects were aged between 18-40 years (25 ± 4.74). The data were analysed for both non-myopic and myopic individuals [non myopes (MSE ≥ -0.50 D), n=11, MSE (D) mean \pm SD (0.39 ± 0.66), range (-0.44 to +1.69), AL (mm) mean \pm SD (23.49 ± 0.37), range (22.90 - 24.00); myopes (MSE <-0.50D), n=45, MSE (D) mean \pm SD (-4.16 ± 2.48), range (-13.38 to -0.75), AL (mm) mean \pm SD (25.70 ± 1.09), range (23.83-29.78)].

High levels of correlation were found between RE and LE: IOPg ($r=0.847$, $p<0.001$), IOPcc ($r=0.750$, $p<0.001$), CRF ($r=0.787$, $p<0.001$) and CH ($r=0.667$, $p<0.001$).

	CH	CRF	IOPg	IOPcc	Refractive error	Axial length
CH		$r=0.881$ $p<0.001$	$r=0.410$ $p=0.002$			
CRF	$r=0.881$ $p<0.001$		$r=0.793$ $p<0.001$	$r=0.316$ $p=0.019$		
IOPg	$r=0.410$ $p=0.002$	$r=0.793$ $p<0.001$		$r=0.829$ $p<0.001$	$r=-0.409$ $p=0.002$	$r=0.373$ $p=0.005$
IOPcc		$r=0.316$ $p=0.019$	$r=0.829$ $p<0.001$		$r=-0.489$ $p<0.001$	$r=0.440$ $p=0.001$

Table A8.17 Correlation matrix for various measures of ORA biometrics (mm Hg) and ocular variables for the HKC subjects.

Section 11.6.2 Corneal biomechanics and additional ocular biometrics for HKC subjects

Stepwise forward multiple linear regression:

Model 7a: Outcome variable IOPg (mm Hg)

Predictive variables: **axial length** (AL (mm)), ACD (mm), age (years), gender and mean corneal curvature (K (mm)). Note AL and Rx could not be inputted together due to high levels of collinearity ($r > 0.8$).

Model parameter	R	R ²	Adjusted R ²	SE of the Estimate	Change statistics					
					R ² change	F change	Df1	Df2	Sig. F Change	Durbin Watson
AL	0.373	0.139	0.123	2.803	0.139	8.576	1	53	0.005	2.163

Table A8.18 Model summary for outcome variable IOPg.

Model parameters	Unstandardized Coefficients		Standardized Coefficient	t	Sig.
	B	Std. Error	Beta		
Constant	-6.471	7.216		-0.897	0.374
AL	0.836	0.285	0.373	2.929	0.005

Table A8.19 Multiple linear regression outcome table for IOPg.

Results: Axial length ($t(53) = 2.929$, ($p=0.005$)) is a significant predictor of IOPg.

Model 7b: Outcome variable IOPg (mm Hg).

Predictive variables: **refractive error** ((Rx) D), ACD (mm), age (years), gender and mean corneal curvature (K (mm)).

Model parameter	R	R ²	Adjusted R ²	SE of the Estimate	Change statistics					
					R ² change	F change	Df1	Df2	Sig. F Change	Durbin Watson
Rx	0.409	0.167	0.151	2.757	0.167	10.632	1	53	0.002	2.080

Table A8.20 Model summary for outcome variable IOPg.

Model parameters	Unstandardized Coefficients		Standardized Coefficient	t	Sig.
	B	Std. Error	Beta		
Constant	13.260	0.562		23.601	<0.001
Rx	-0.420	0.129	-0.409	-3.261	0.002

Table A8.21 Multiple linear regression outcome table for IOPg.

Results: Refractive error (t (53)= -3.261, (p=0.002)) is a significant predictor of IOPg.

Model 8a Outcome variable IOPcc (mm Hg).

Predictive variables: **axial length** (AL (mm)), ACD (mm), age (years), gender and mean corneal curvature (K (mm)). Note AL and Rx could not be inputted together due to high levels of collinearity (r= >0.8).

Model parameter	R	R ²	Adjusted R ²	SE of the Estimate	Change statistics					
					R ² change	F change	Df1	Df2	Sig. F Change	Durbin Watson
AL	0.440	0.193	0.178	2.161	0.193	12.699	1	53	0.001	1.966

Table A8.22 model summary for outcome variable IOPcc.

Model parameters	Unstandardized Coefficients		Standardized Coefficient	t	Sig.
	B	Std. Error	Beta		
Constant	-4.924	5.564		-0.885	0.380
AL	0.784	0.220	0.440	3.564	0.001

Table A8.23 Multiple linear regression outcome table for IOPcc.

Results: Axial length (t (53)= 3.564, (p=0.001)) is a significant predictor of IOPcc.

Model 8b Outcome variable IOPcc (mm Hg).

Predictive variables: **refractive error** ((Rx) D), ACD (mm), age (years), gender and mean corneal curvature (K (mm)).

Model parameter	R	R ²	Adjusted R ²	SE of the Estimate	Change statistics					
					R ² change	F change	Df1	Df2	Sig. F Change	Durbin Watson
Rx	0.489	0.239	0.225	2.099	0.239	16.635	1	53	<0.001	1.897

Table A8.24 Model summary for outcome variable IOPcc.

Model parameters	Unstandardized Coefficients		Standardized Coefficient	t	Sig.
	B	Std. Error	Beta		
Constant	13.568	-0.428		31.720	<0.001
Rx	-0.400	0.098	-0.489	-4.079	<0.001

Table A8.25 Multiple linear regression outcome table for IOPcc.

Results: Refractive error ($t(53) = -4.079, (p < 0.001)$) is a significant predictor of IOPcc.

Independent <i>t</i> tests	Degrees of freedom	t value	p value
Effect of gender on:			
CH	53	-1.100	0.277
CRF	53	-1.038	0.304
IOPg	53	-0.584	0.561
IOPcc	53	0.036	0.972
Axial length	54	2.270	0.027
Mean corneal curvature	54	2.590	0.012
ACD	54	1.471	0.147
Effect of refractive status on:			
CH	53	0.458	0.649
CRF	53	-0.544	0.588
IOPg	53	-1.652	0.104
IOPcc	53	-2.087	0.042
Mean corneal curvature	54	-1.310	0.196

Table A8.26 Independent *t* tests assessing the influence of refractive status and gender on the ORA and ocular biometry parameters for the HKC subjects.

A one-way ANOVA exploring whether ORA biometry differences existed between axial length subgroups revealed no significant difference for CH ($F(2, 52) = 1.243, (p = 0.297)$), CRF ($F(2, 52) = 0.485, (p = 0.619)$), IOPg ($F(2, 52) = 2.011, (p = 0.144)$) but a significant difference for IOPcc ($F(2, 52) = 4.206, (p = 0.020)$).

A one-way ANOVA exploring whether ocular biometry differences existed between axial length subgroups revealed significant difference for flat corneal curvature ($F(2, 53) = 3.730, (p = 0.031)$), steep corneal curvature ($F(2, 53) = 4.072, (p = 0.023)$) and ACD ($F(2, 53) = 5.307, (p = 0.008)$).

Section 11.6.3 ORA Additional Waveform Parameters (AWPs) for HKC subjects

Biometry	P2area	Uslope1	Slew1	Slew2	Dslope21	Uslope11
Axial Length		0.271		0.271	0.275	
Mean k	0.280					
Age		0.282	0.287			0.293

Table A8.27 Correlations between ocular biometric data and the AWP ($p < 0.05$).

Section 11.7 Comparison of ORA metrics and ocular biometry between BW-BSA (UK) and Hong-Kong Chinese (HKC) individuals

Independent <i>t</i> tests	Degrees of freedom	t value	p value
Effect of group (HK or UK) on:			
CH	125	0.328	0.744
CRF	125	0.358	0.721
IOPg	125	0.249	0.804
IOPcc	125	0.089	0.930

Table A8.28 Independent *t* tests assessing the effect of data origin (UK or HK) on ORA biometrics.

A one way ANOVA was performed to assess for an effect for ethnicity (BW-BSA and HKC) on the ORA parameters. No significant difference was found CH ($F(2, 124) = 0.634, (p = 0.532)$), CRF ($F(2, 124) = 0.485, (p = 0.617)$), IOPg ($F(2, 124) = 0.106, (p = 0.900)$), and IOPcc ($F(2, 124) = 0.103, (p = 0.902)$).

A one way ANOVA was performed to assess for an effect for ethnicity (BW-BSA and HKC) on the biometric parameters. A significant difference was found for AL ($F(2, 127)=8.082, (p<0.001)$), flat corneal curvature ($F(2, 127)=5.226, (p=0.007)$) but not for steep corneal curvature ($F(2, 127)=0.937, (p=0.395)$) and ACD ($F(2, 127)= 0.258, (p=0.773)$).

Section 11.7.2 ORA Additional Waveform Parameters (AWPs) for UK and HK subjects

A two-way factorial ANOVA was performed on each AWP to test for an effect and possible interaction between ethnicity and refractive status for the combined BW-BSA and HKC data:

- A significant effect of ethnicity was found for BW-BSA and HKC individuals for the following AWP ($p<0.05$): Bindex, P1area, P2area, Aspect1, Uslope1, Dslope1, W1, W2, H1, H2, Dive, Dive2, Path1, Mslew1, Mslew2, Slew1, P1area1, P2 area1, Aspect11, Uslope11, Dslope11, W11, H11, H21. The following AWP ($p<0.05$): Uslope2, Slew 2, Aspect21, Uslope21, Path11 showed a significant difference only between individuals of BSA and HKC origin.
- The results of the current study indicate that the HKC eyes have lower values of P1area, P2area, Aspect1, Uslope1, Dslope1, W2, H1, H2, Dive1, Dive2, P1, Mslew1, Mslew2, Slew1, P1Area, P2Area, Aspect11, Uslope11, Dslope11, H11, H21 and higher values for Bindex, W1 and W11 when compared to both BW and BSA eyes. Further ethnic differences demonstrated Uslope2, Slew 2, Aspect21, Uslope21 and Path11 to be significantly lower in HKC subjects in comparison to only BSA eyes.
- The statistical analysis also revealed a significant effect of refractive status ($p<0.05$) on P2area, Aspect1, Dslope1, W1, Dive2 and P2 area1. Refractive status appeared to affect some of the AWP with P2area, Aspect1, Dslope1, Dive2, P2 area to be higher in non-myopic individuals when compared to myopes. However W1 was found to be higher in myopic eyes when compared to non-myopic eyes.
- An interaction was found between ethnicity and refractive status ($p<0.05$) for Mslew1 and P2. Mslew1 and P2 demonstrated a significant interaction between ethnicity and refractive state. Both BW and BSA showed Mslew1 to be higher for non-myopes than myopes, whereas HKC individuals showed myopic individuals to have higher Mslew1 than non-myopic. For P2, both HKC and BSA myopic individuals had higher values than non-myopes subjects, whereas BW non-myopes had higher P2 for than myopes.

APPENDIX 9

STATISTICAL APPENDIX FOR CHAPTER 12

The study assessed 42 healthy individuals (84 eyes; 17 males and 25 females) aged between 18-40 years (28.12 ± 6.04). Data were assessed for non-myopic and myopic individuals; [non myopes (MSE $\geq -0.50D$) n=20 MSE (D) mean \pm SD (0.64 ± 1.38), range (-0.50 to +4.38), AL (mm) mean \pm SD (23.33 ± 0.67), range (21.75-24.45); myopes (MSE $< -0.50D$) n=22 MSE (D) mean \pm SD (-6.24 ± 4.28), range (-20.50 to -0.75), AL (mm) mean \pm SD (25.69 ± 1.25) range (23.33 - 28.32)].

Section 12.5.1 Structural correlates of anterior segment biometry

A one-way repeated measures ANOVA testing the influence of axial length sub-grouping on the *Pentacam* parameters revealed no significant effect on CT (CCT, CT min, SCT, ICT, TCT, NCT), CV (CV3, CV5, CV7), ACV, FS (Kf and Ks), BS (Kf and Ks), ABFS and PBFS ($p > 0.05$).

A one way repeated measures ANOVA between regional (central, superior, inferior, temporal and nasal) CT measures revealed significant differences ($F(2.521, 103.38) = 93.86$, ($p < 0.001$)).

Variable	Mean \pm SD	Minimum	Maximum
Rigidity 5.5 g-7.5 g	0.0224 ± 0.0091	0.0066	0.0357
Rigidity 5.5 g-10 g	0.0197 ± 0.0072	0.0086	0.0329
CRF	10.21 ± 1.28	7.37	12.97
CH	10.52 ± 1.15	7.60	13.40
IOPg	14.49 ± 2.91	7.23	21.67
IOPcc	14.99 ± 2.83	9.13	21.05

Table A9.1 RE Schiotz corneal rigidity (mm^3)⁻¹ and ORA biometrics (mm Hg).

Pentacam parameter	CCT	CTmin	SCT	ICT	TCT	NCT	ACD	CV	CV3	CV5	CV7
ACV	r=-0.342 p=0.019		r=0.383 p=0.012	r=-0.361 p=0.019	r=-0.339 p=0.028	r=-0.379 p=0.013			r=-0.367 p=0.018	r=-0.372 p=0.017	r=-0.367 p=0.018
Back Ks			r=-0.385 p=0.012	r=-0.393 p=0.010		r=-0.309 p=0.047		r=-0.514 p=0.001			r=-0.363 p=0.020
PBFS							r=-0.312 p=0.047	r=-0.359 p=0.021			

Table A9.2 Significant correlations between *Pentacam* parameters.

Section 12.5.2 Anterior segment biometry and corneal biomechanics

ORA parameter	CCT	CTmin	SCT	ICT	TCT	NCT	CV	CV3	CV5	CV7
CH	r=0.403 p=0.009	r=0.404 p=0.009	r=0.375 p=0.016	r=0.342 p=0.028	r=0.386 p=0.013	r=0.340 p=0.030	r=0.420 p=0.006	r=0.400 p=0.011	r=0.401 p=0.010	r=0.402 p=0.010
CRF	r=0.540 p<0.001	r=0.551 p<0.001	r=0.445 p=0.004	r=0.479 p=0.002	r=0.482 p=0.001	r=0.411 p=0.008	r=0.436 p=0.004	r=0.507 p=0.001	r=0.511 p=0.001	r=0.495 p=0.001

Table A9.3 Significant correlations between *Pentacam* parameters and the main ORA biometrics (CH and CRF).

Parameter	ORA AWP's																							
	P1area	P2 area	Aspect1	Aspect2	Dslope1	H1	H2	Dive2	Path1	Path2	Slew1	P1area1	P2area2	Aspect21	U1slope1	U1slope21	D1slope21	W11	W21	H11	H21	Path 11		
CCT	r=-0.392 p=0.010	r=-0.451 p=0.003							r=-0.436 p=0.004	r=-0.394 p=0.011		r=-0.402 p=0.009	r=-0.456 p=0.003					r=-0.356 p=0.023	r=-0.383 p=0.013					
CTmin	r=-0.392 p=0.011	r=-0.453 p=0.003							r=-0.434 p=0.005	r=-0.387 p=0.012		r=-0.402 p=0.009	r=-0.462 p=0.002					r=-0.356 p=0.022	r=-0.382 p=0.014					
SCT	r=-0.322 p=0.040	r=-0.403 p=0.009										r=-0.342 p=0.028	r=-0.399 p=0.010											
ICT	r=-0.389 p=0.012	r=-0.448 p=0.003							r=-0.428 p=0.005	r=-0.419 p=0.006		r=-0.414 p=0.007	r=-0.426 p=0.005					r=-0.372 p=0.017	r=-0.373 p=0.016				r=-0.333 p=0.033	
TCT		r=-0.337 p=0.031							r=-0.320 p=0.042			r=-0.365 p=0.019							r=-0.330 p=0.035					
NCT	r=-0.363 p=0.020	r=-0.421 p=0.006							r=-0.383 p=0.013	r=-0.400 p=0.010		r=-0.380 p=0.014	r=-0.420 p=0.006					r=-0.322 p=0.040	r=-0.384 p=0.013					
ACV			r=-0.391 p=0.010		r=-0.379 p=0.015	r=-0.317 p=0.043	r=-0.312 p=0.047							r=-0.328 p=0.036						r=-0.317 p=0.043	r=-0.312 p=0.047			
ACD			r=-0.399 p=0.010	r=-0.313 p=0.046	r=-0.371 p=0.017	r=-0.333 p=0.033	r=-0.350 p=0.025				r=-0.339 p=0.030		r=-0.357 p=0.018	r=-0.369 p=0.018		r=-0.377 p=0.015	r=-0.323 p=0.040	r=-0.346 p=0.027	r=-0.338 p=0.031		r=-0.333 p=0.033	r=-0.350 p=0.025		
CV		r=-0.359 p=0.021							r=-0.367 p=0.018	r=-0.369 p=0.018									r=-0.362 p=0.020					

CV3	r=0.36 5 p=0.0 21	r=0.41 8 p=0.0 07						r=- 0.424 p=0.0 06	r=- 0.379 p=0.0 16		r=0.38 5 p=0.0 14	r=0.42 1 p=0.0 07					r=0.34 7 p=0.0 28	r=0.35 7 p=0.0 24			
CV5	r=0.37 8 p=0.0 16	r=0.43 1 p=0.0 05						r=- 0.403 p=0.0 10	r=- 0.368 p=0.0 20		r=0.39 2 p=0.0 2	r=0.42 6 p=0.0 06					r=0.31 8 p=0.0 45	r=0.36 5 p=0.0 21			
CV7	r=0.35 0 p=0.0 27	r=0.41 5 p=0.0 08						r=- 0.381 p=0.0 15	r=- 0.364 p=0.0 21		r=0.36 8 p=0.0 20	r=0.40 5 p=0.0 10						r=0.35 9 p=0.0 23			
FKf		r=- 0.484 p=0.0 01					r=- 0.454 p=0.0 03	r=- 0.377 p=0.0 15			r=0.40 3 p=0.0 09	r=- 0.461 p=0.0 02								r=- 0.454 p=0.0 03	r=0.35 0 p=0.0 23
FKs	r=- 0.436 p=0.0 04	r=- 0.420 p=0.0 06					r=- 0.391 p=0.0 11	r=- 0.353 p=0.0 23	r=- 0.361 p=0.0 20		r=- 0.420 p=0.0 06	r=- 0.400 p=0.0 10							r=- 0.391 p=0.0 11	r=- 0.353 p=0.0 23	r=0.32 2 p=0.0 40
BKf	r=0.33 7 p=0.0 31	r=0.44 9 p=0.0 03						r=0.36 3 p=0.0 20	r=0.32 2 p=0.0 40			r=0.39 9 p=0.0 10								r=0.36 3 p=0.0 20	
ABF S	r=0.45 6 p=0.0 03	r=0.50 8 p=0.0 01					r=0.32 1 p=0.0 41	r=0.42 3 p=0.0 06	r=0.38 4 p=0.0 13		r=0.42 5 p=0.0 06	r=0.48 1 p=0.0 01							r=0.32 1 p=0.0 41	r=0.42 3 p=0.0 06	r=- 0.349 p=0.0 25
PBFS	r=0.34 4 p=0.0 30	r=0.31 3 p=0.0 49						r=0.32 8 p=0.0 39				r=0.31 5 p=0.0 47								r=0.32 8 p=0.0 39	

Table A9.4 Significant correlations between *Pentacam* parameters and the AWP.

Stepwise forward multiple linear regression:

Model 1: outcome variable corneal hysteresis (CH (mm Hg))

Predictive variables: refractive error (D), mean anterior K (mm), mean posterior K (mm), axial length (mm), CCT (μm), CV (mm^3), ACD (mm), ACV (mm^3), gender and age (years). (CCT and CV), (ACD and ACV) (mean anterior and posterior K) and (refractive error and axial length) were not included in the model simultaneously due to high levels of multicollinearity ($r > 0.8$).

Parameter	R	R ²	Adjusted R ²	SE of the Estimate	Change statistics					
					R ²	F	df1	df2	Sig. F Change	Durbin Watson
Total CV	0.420	0.177	0.156	1.05	0.177	8.366	1	39	0.006	1.815

Table A9.5 Model summary for outcome variable CH.

Model	Unstandardized Coefficients		Standardized Coefficient	t	Sig.
	B	Std. Error	Beta		
Constant	3.514	2.428	0.420	1.447	0.156
Total CV	0.116	0.040		2.892	0.006

Table A9.6 Multiple linear regression outcome table for CH.

Result: total CV ($t(39) = 2.89$, $p = 0.006$) is a significant predictor of CH.

Model 2: outcome variable corneal resistance factor (CRF); predictor variables as for CH (see above)

Parameter	R	R ²	Adjusted R ²	SE of the Estimate	Change statistics					
					R ²	F	df1	df2	Sig. F Change	Durbin Watson
CCT	0.540	0.291	0.273	1.09	0.291	16.013	1	39	<0.001	1.373

Table A9.7 Model summary for outcome variable CRF.

Model	Unstandardized Coefficients		Standardized Coefficient	t	Sig.
	B	Std. Error	Beta		
Constant	0.463	2.442	0.540	0.189	0.851
CCT	0.018	0.004		4.002	<0.000

Table A9.8 Multiple linear regression outcome table for CRF.

Result: CCT ($t(39) = 4.00$, $p < 0.001$) is a significant predictor of CRF

Stepwise forward multiple linear regression analysis were performed for each AWP as the outcome variable and its associated *Pentacam* parameters (from the significant correlations found in Table 9.4) as the predictor variables. Table 9.9 summaries the best anterior segment biometry predictors for the various AWPs.

ORA AWP	Best <i>Pentacam</i> predictors
P1area	Anterior BFS $r^2 = 0.191$, $p = 0.005$
P2area	Anterior BFS $r^2 = 0.258$ $p = 0.001$
Aspect1	ACD $r^2 = 0.159$ $p = 0.010$
Aspect2	ACD $r^2 = 0.098$ $p = 0.046$

Aspect21	ACD $r^2=0.142$ $p=0.015$
Dslope1	ACV $r^2=0.143$ $p=0.015$
H1	FSK2 $r^2=0.153$ $p=0.011$
H2	FSK1 $r^2=0.190$ $p=0.005$
Dive2	Anterior BFS $r^2=0.136$ $p=0.019$
Path1	CCT $r^2=0.190$ $p=0.004$
Path2	INCT $r^2=0.179$ $p=0.007$
P1area1	FSK2 $r^2=0.177$ $p=0.006$
P2area1	Anterior BFS $r^2=0.231$ $p=0.001$
Uslope11	ACD $r^2=0.104$ $p=0.040$
Dslope21	ACD $r^2=0.114$ $p=0.031$
W11	INCT $r^2=0.138$ $p=0.017$
W21	CCT $r^2=0.155$ $p=0.012$
H11	FSK2 $r^2=0.153$ $p=0.011$
H21	FSK1 $r^2 = 0.186$ $p=0.003$
Path11	FSK1 $r^2=0.122$ $p=0.025$

Table A9.9 Best *Pentacam* predictor variables for ORA AWP.

APPENDIX 10

STATISTICAL APPENDIX FOR CHAPTER 13

Ciliary muscle thickness (CMT) was measured in 63 healthy individuals (26 males and 37 females) aged between 18-40 years (27.85 ± 5.46). Data were analysed for non-myopic and myopic individuals [non-myopes (MSE $\geq -0.50D$) $n=31$, MSE(D) mean \pm SD (0.55 ± 1.17), range (-0.50 to +4.38), AL (mm) mean \pm SD (23.39 ± 0.74), range (mm) (21.61 - 24.75); myopes (MSE < -0.50) $n=32$, MSE(D) mean \pm SD (-4.54 ± 4.20), range (-20.50 to -0.51), AL (mm) mean \pm SD (25.21 ± 1.22), range (mm) (23.33 - 28.32)].

Section 13.5.1 Correlates of ciliary muscle thickness

Construction of Box- Whiskers plots

Figures 13.3 (a-f) box and whiskers plot (median and interquartile range) for each CMT measurement. The top of the box represents the 75th percentile, the bottom of the box represents the 25th percentile, and the line in the middle represents the 50th percentile. The whiskers represent the highest and lowest values that are not outliers or extreme values. Outliers (values that are between 1.5 and 3 times the interquartile range) and extreme values (values that are more than 3 times the interquartile range) are represented by circles beyond the whiskers.

	TCMT1	TCMT2	TCMT3	NCMT1	NCMT2	NCMT3
TCMT1		$r=0.688$ $p<0.001$	$r=0.398$ $p=0.001$	$r=0.737$ $p<0.001$	$r=0.558$ $p<0.001$	$r=0.278$ $p=0.029$
TCMT2	$r=0.688$ $p<0.001$		$r=0.820$ $p<0.001$	$r=0.618$ $p<0.001$	$r=0.728$ $p<0.001$	$r=0.505$ $p<0.001$
TCMT3	$r=0.398$ $p=0.001$	$r=0.820$ $p<0.001$		$r=0.386$ $p=0.002$	$r=0.601$ $p<0.001$	$r=0.540$ $p<0.001$
NCMT1	$r=0.737$ $p<0.001$	$r=0.618$ $p<0.001$	$r=0.386$ $p=0.002$		$r=0.718$ $p<0.001$	$r=0.421$ $p=0.001$
NCMT2	$r=0.558$ $p<0.001$	$r=0.728$ $p<0.001$	$r=0.601$ $p<0.001$	$r=0.718$ $p<0.001$		$r=0.721$ $p<0.001$
NCMT3	$r=0.278$ $p=0.029$	$r=0.505$ $p<0.001$	$r=0.540$ $p<0.001$	$r=0.421$ $p=0.001$	$r=0.721$ $p<0.001$	
Refractive error		$r=-0.338$ $p=0.007$	$r=-0.362$ $p=0.004$			
Axial length		$r=0.456$ $p<0.001$	$r=0.472$ $p<0.001$		$r=0.348$ $p=0.006$	$r=0.258$ $p=0.045$
ACD		$r=0.314$ $p=0.013$	$r=0.357$ $p=0.004$		$r=0.276$ $p=0.031$	$r=0.332$ $p=0.009$
Age		$r=-0.265$ $p=0.036$		$r=-0.324$ $p=0.010$		
Flattest corneal curvature	$r=0.318$ $p=0.012$			$r=0.269$ $p=0.036$		
Total volume	$r=0.392$ $p=0.027$	$r=0.684$ $p<0.001$	$r=0.627$ $p<0.001$	$r=0.393$ $p=0.029$	$r=0.561$ $p=0.001$	$r=0.395$ $p=0.028$
Posterior volume	$r=0.366$ $p=0.039$	$R=0.691$ $p<0.001$	$r=0.647$ $p<0.001$	$r=0.362$ $p=0.046$	$r=0.540$ $P=0.002$	$r=0.387$ $p=0.031$

Table A10.1 Pearson's correlation coefficient matrix for temporal and nasal CMT, age and ocular biometry variables.

- Axial length correlated significantly with refractive error ($r=-0.856$, $p<0.001$) and ACD ($r=0.369$, $p=0.003$).

Section 13.5.2 Ocular volume and ciliary muscle thickness

- Total volume correlated with other biometric data: ACD ($r=0.377$, $p=0.013$), axial length ($r=0.843$, $p<0.001$) and refractive error ($r=-0.671$, $p<0.001$).
- Posterior volume also correlated with other biometric data: ACD ($r=0.378$, $p=0.013$), axial length ($r=0.858$, $p<0.001$) and refractive error ($r=-0.688$, $p<0.001$).

Scleral meridian	Distance (mm)	TCMT1	TCMT2	TCMT3	NCMT1	NCMT2	NCMT3
SN	5	$r=-0.381$ $p=0.002$	$r=-0.338$ $p=0.007$	$r=-0.332$ $p=0.008$	$r=-0.250$ $p=0.050$		
	6	$r=-0.433$ $p<0.001$	$r=-0.418$ $p=0.001$	$r=-0.366$ $p=0.003$	$r=-0.321$ $p=0.011$	$r=-0.277$ $p=0.029$	
	7	$r=-0.353$ $p=0.005$	$r=-0.348$ $p=0.005$	$r=-0.284$ $p=0.024$			
S	7		$r=-0.315$ $p=0.012$	$r=-0.338$ $p=0.007$			
ST	5			$r=-0.292$ $p=0.020$			
	6			$r=-0.287$ $p=0.023$			
	7			$r=-0.295$ $p=0.019$			
I	5		$r=-0.263$ $p=0.037$	$r=-0.293$ $p=0.020$			
	6	$r=-0.308$ $p=0.015$	$r=-0.287$ $p=0.024$	$r=-0.286$ $p=0.024$			
	7		$r=-0.331$ $p=0.014$	$r=-0.378$ $p=0.004$			
IN	4			$r=-0.308$ $p=0.014$			
	5			$r=-0.315$ $p=0.012$			
	6			$r=-0.276$ $p=0.028$			
N	1				$r=0.280$ $p=0.027$	$r=0.333$ $p=0.008$	$r=0.375$ $p=0.003$
	2				$r=0.250$ $p=0.050$		
	4			$r=-0.300$ $p=0.017$			
	5			$r=-0.261$ $p=0.039$			
	6			$r=-0.302$ $p=0.016$			

Table A10.2 Pearson's correlation coefficient matrix for scleral thickness along various meridians/distances from the corneolimbus junction and CMT (temporal and nasal) Note: only significant correlations are shown.

APPENDIX 11

STATISTICAL APPENDIX FOR CHAPTER 14

Surface area and bulbosity were assessed in 43 healthy individuals (16 males and 27 females) aged between 18-40 years (28.65 ± 6.20). Data were analysed for non-myopic and myopic individuals [non-myopes (MSE $\geq -0.50D$) $n=20$, MSE(D) mean \pm SD (0.57 ± 1.38) range (-0.50 to +4.38), AL (mm) mean \pm SD (23.37 ± 0.63), range (mm) (21.75 - 24.45); myopes (MSE $< -0.50D$) $n=23$ MSE(D) mean \pm SD (-6.37 ± 4.23) range (-20.50 to -0.75), AL (mm) mean \pm SD (25.77 ± 1.27), range (mm) (23.33 - 28.32)].

Section 14.5.1 Surface area (SA)

Inter-quadrant correlations were evident between SAs for ST:IT ($r=0.408$, $p=0.007$), IN:SN ($r=0.665$, $p<0.001$), IN:IT ($r=0.735$, $p<0.001$), SN:IT ($r=0.588$, $p<0.001$).

	ST SA	SN SA	IT SA	IN SA
Axial length		$r=-0.327$ $p=0.032$	$r=-0.309$ $p=0.044$	$r=-0.517$ $p<0.001$
Refractive error		$r=0.393$ $p=0.009$	$r=0.460$ $p=0.002$	$r=0.633$ $p<0.001$
Flat corneal curvature		$r=0.359$ $p=0.018$	$r=0.505$ $p=0.001$	$r=0.370$ $p=0.015$
Steep corneal curvature		$r=0.322$ $p=0.035$	$r=0.465$ $p=0.002$	$r=0.403$ $p=0.007$

Table A11.1 Pearson's correlation coefficient matrix for quadrant SAs and ocular biometry variables.

Section 14.5.2 Quadrant Bulbosity

Inter-quadrant correlations for bulbosity were evident between quadrants ST:IN ($r=0.333$, $p=0.029$), ST:SN ($r=0.317$, $p=0.038$), IN:SN ($r=0.591$, $p<0.001$), IN:IT ($r=0.568$, $p<0.001$) and SN:IT ($r=0.441$, $p=0.003$).

APPENDIX 12

EVALUATION OF OFF-AXIS DISTORTION IN IMAGES PRODUCED BY ANTERIOR SEGMENT OPTICAL COHERENT TOMOGRAPHY (AS-OCT)

The AS-OCT has been widely utilized in the thesis and as discussed in Chapter 7 the instrument provides a useful means of evaluating the anterior segment structures *in vivo*. The following section details current and future work that aims to address the issues of off-axis distortion associated with the AS-OCT.

The AS-OCT was primarily designed for assessing anterior segment structures such as the cornea, the anterior chamber angle and crystalline lens. Off-axis distortions are known to occur in OCT imaging and are therefore of particular interest when imaging structures such as the ciliary muscle and sclera which require off-axis imaging (Chapter 7 and 13). Optical distortion with off-axis imaging occurs as a result of the combined effect of the corneal curvature and differences in refractive indices of ocular tissue (Izatt *et al.*, 1994; Radhakrishnan *et al.*, 2001). As the cornea is curved the OCT beam fails to be perpendicular to the corneal surface over the whole scanning field which results in refraction of the scanning beam at the air-cornea interface (Radhakrishnan *et al.*, 2001). Therefore corneal measurements are only accurate at points where the incident beam is perpendicular to the corneal surface; for all other points accurate measurements require software to implement appropriate correction factors (Izatt *et al.*, 1994; Goldsmith *et al.*, 2005).

The OCT is subject to two main types of distortion: fan and optical distortion (Dorairaj *et al.*, 2007). Fan (i.e. field) distortion is a set of aberrations related to the rastering of the surfaces being imaged with optical scanners (Ortiz *et al.*, 2010). Fan distortion results in poor imaging of the first surface and causes flat surfaces to appear curved; although correction algorithms are able to correct for this type of distortion (Ortiz *et al.*, 2009). Optical distortion due to refraction by the ocular tissues degrades the geometrical features of the observed surfaces and therefore physical parameters, such as curvature and thickness cannot be accurately measured directly from the images (Ortiz *et al.*, 2010). To partly correct for this distortion the AS-OCT software applies a correction for the different refractive indices of the anterior segment structures by dividing the OCT optical distances by the refractive index (Chapter 7; Nolan, 2008); however imaging the inner structures of the eye is likely to be subject to optical distortion as each layer differs in shape, structure and refractive index. Few studies have evaluated the problem of optical distortion with OCT imaging of the eye and those that have, suggest the implementation of 2-D corrections for OCT images (Podoleanu *et al.*, 2004; Westphal *et al.*, 2002). However, due to the rotational asymmetry of the eye and its failure to demonstrate homocentricity about the optical axis, correction algorithms based on 2-D ray tracing have been found to be inadequate and a 3-D approach has been advocated (Ortiz *et al.*, 2010).

In collaboration with the Aston University Electronic Engineering and Applied Physics Department (the Photonics Research Group) the investigation proposes to evaluate off-axis distortion that may affect imaging of internal ocular anatomy with the AS-OCT. Using femtosecond inscription, highly repeatable 3-D structures have been created within a transparent silica media. These 3-D calibration slides incorporate equally spaced lines running parallel to the surface at various depths within the fused silica. 2-D OCT images will be acquired at different locations to create a 3-D depiction of the phantom slides.



Figure A12.1 Experimental setup- **A**: rotatory table, **B**: custom designed slide holder, **C**: silica slide (with femtosecond inscription) **D**: *Visante* AS-OCT.

Images will be acquired at 2° intervals to assess off-axis imaging. Standard OCT signal processing applied by the *Visante* software will be applied to reduce the signal-to-noise ratio (Figure A12.1). A custom written program in MATLAB and C will be used to construct 3-D images. Using prior knowledge of the phantom slide dimensions will allow measurement of off-axis distortion. It is envisaged that the procedure will allow specification of a single correction factor for distortion, and subsequently a map of correction factors for different sections of the OCT image. Once experimentally verified, the distortion and correction factors will be incorporated into numerical algorithms that can be applied to OCT images.

Acknowledgements

Graham Davies for the design and construction of the off-axis mounting described in Figure A12.1

APPENDIX 13

INVESTIGATING HUMAN LIMBAL BIOMECHANICS USING THE PULSAIR EASYEYE TONOMETER (KEELER, WINDSOR, UK)

The *Pulsair EasyEye* tonometer is a non-contact portable device that has been utilised in previous work by our laboratory in Aston University to assess the fluctuations in IOP with accommodation (Rai *et al.*, 2006). In collaboration with its manufacturer, modification of the instrument and the implementation of a custom written program allowed an *in vivo* evaluation of the corneal response and the IOP changes over a 19 ms cycle (Rai, 2007). By connecting the instrument to a PC, a recording and analysis software 'Puff-Retrieve' provided a means of analysing the IOP changes with accommodation using *Microsoft Excel* (Rai, 2007). This section describes how the measurement technique was extended to non-contact measurement of responses from limbal regions.

The operational principles of the *Pulsair* are comparable to those of the Reichert ORA (Chapter 11). Hence the *Pulsair* obtains a morphological waveform signal from the central cornea and provides a graphical representation of a pressure-response relationship over a 19 ms pressure output cycle (Figure 13.1).

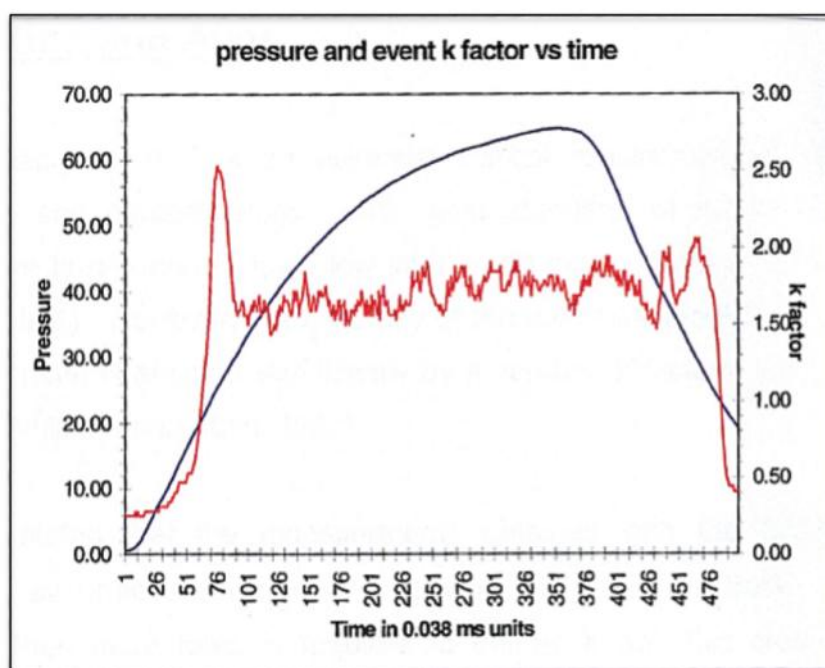


Figure A13.1 Pressure-response graph from the *Pulsair* (after Rai, 2007).

The *Pulsair* uses a rapid bolus of air to produce a localised area of appplanation on the cornea (Figure 13.1- blue curve). Data from three photodiodes, which detect light reflected via three LEDs from the corneal surface is used to formulate a 'k factor' (Figure 13.1- red curve). The k factor is calculated as:

$$k = (S1 - S2)/(S1 + S2) \quad \text{Eq 13.1}$$

Where S1 is the mean signal from the outer two photodiodes and S2 is the signal from the inner photodiode. When the cornea is in its normal convex form, minimum light is reflected and detected by the photoreceptors. However, when the ocular tissue is applated, the flattened corneal surface reflects the maximum intensity of light, which is detected by the photodiodes.

The point at which the photodiodes detect maximum light is referred to as ‘contrast reversal’. The pressure (y-axis Fig 13.1) at the applanation point is sampled and, following a calibration procedure, provides a measure of the IOP. The tonometer results are fed into an *Excel* spreadsheet, where a visual basic macro is used to process the data and provide a calculated value for IOP. Examination of the pressure-response graph shows that the cornea goes through two applanation phases (seen as the two peaks on the red graph); the first when it changes from its convex shape and moves inwards, the second when it returns from slight concavity to its original shape.

As demonstrated in Chapter 11 the ORA allows an *in vivo* evaluation of the biomechanical properties of the cornea. However measurements with the ORA are limited to the central corneal region and assessing the paracentral or limbal areas is not feasible owing to the fixed table-mounted design of the ORA. The biomechanical properties of the cornea, sclera and limbus are likely to be important in influencing the optics of the eye. In particular these ocular tissues are vital in resisting the stresses of accommodation, ocular eye movement and fluctuations in IOP, while maintaining optical image quality (Asejczyk-Wildlicka *et al.*, 2007). The limbal region has been suggested to form a rigid ring that maintains corneal curvature during stress application (Maurice, 1988) and has thus been implicated in the maintenance of image quality on the retina (Asejczyk-Wildlicka *et al.*, 2004). Indeed stress-strain experiments have shown the cornea to demonstrate significant regional variation in its biomechanical properties; the paracentral and peripheral parts of the cornea deform less in the meridional directions when compared to the central corneal and limbal regions, whilst circumferentially the paracentral corneal region deforms the most (Hjortdal, 1996). It is anticipated that greater understanding of the anisotropy of the biomechanical characteristics of the cornea and limbus may be important in refractive eye surgery and collagen cross-linking in keratoconus (Roy and Dupps, 2009).

In order to assess peripheral corneal biomechanics, a preliminary investigation utilised the modified *Pulsair* (described above) to obtain waveform signals from the paracentral regions of the cornea. Custom designed software (Keeler Ltd) allows a PC interface to control the firing of the instrument thus allowing off-centre measures of IOP and corneal responses to be assessed. In particular nasal and temporal signals were obtained from the corneal regions 3 mm from the limbus (Figure A13.2).

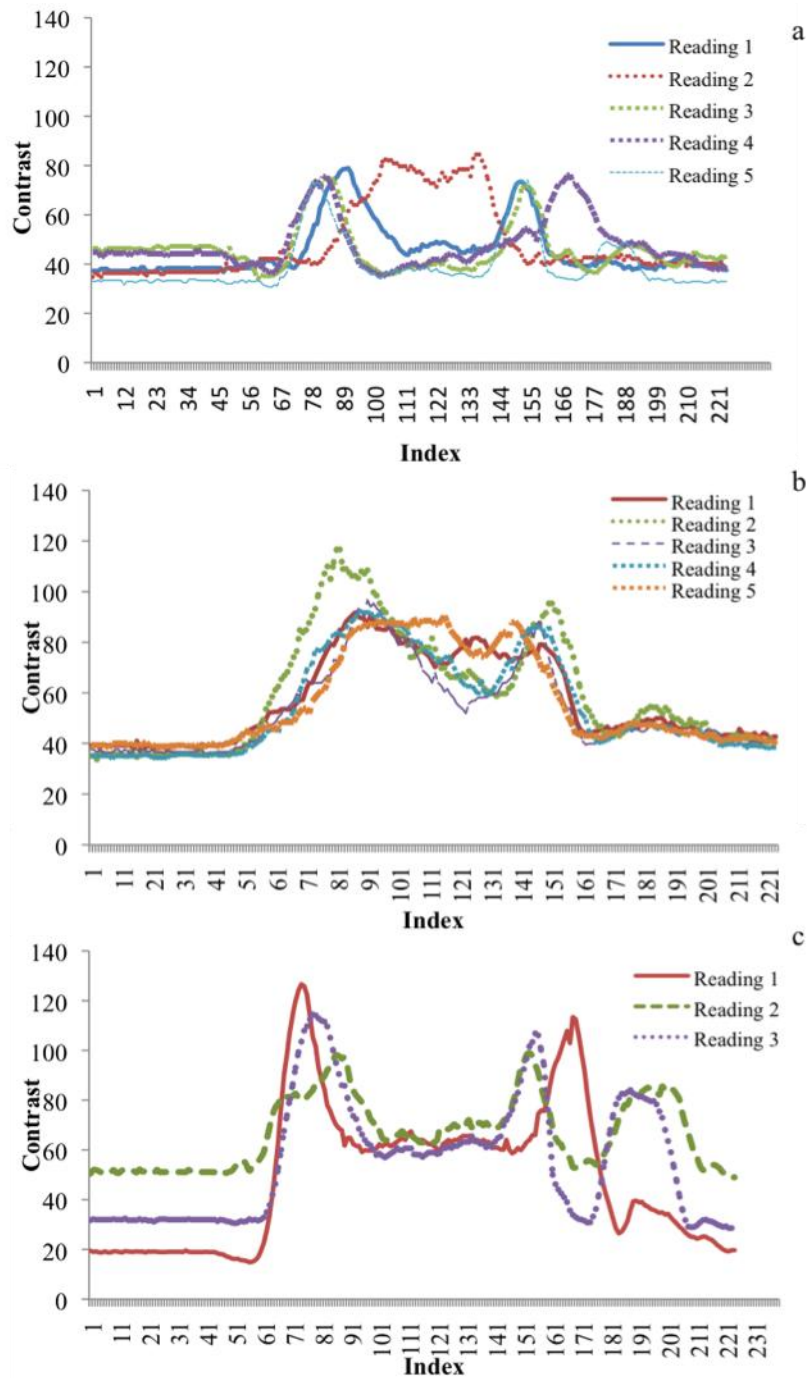


Figure A13.2 Pulsair waveforms from a) temporal paracentral region b) nasal paracentral region c) central corneal. Subject RC RE +4.00D.

Due to the variability of the peripheral corneal curvatures, reliable and consistent measurements have so far been limited, however the technique provides scope for a means of examining the biomechanical properties of the paracentral cornea and limbal areas. To take account of the reduced intensity and asymmetry of light reflected from peripheral corneal surfaces future work will reset the criteria for firing of *Pulsair* photoreceptors with reference to their relative placement and spatial separation.

SUPPORTING PUBLICATIONS

COLLEGE OF OPTOMETRIST'S CONFERENCE ABSTRACT, March 2009

Intraobserver and interobserver regional variations in Schiøtz tonometry measurements

Hetal Patel, Robert Cubbidge, Bernard Gilmartin, Nicola Logan, Larisa Dorochtchak
Ophthalmic Research Group, School of Life and Health Sciences, Aston University Birmingham,
B4 7ET

Background: The magnitude and variation of scleral and ocular (measured on the cornea) rigidity is relevant to our understanding of the development of myopia and ocular pathology such as glaucoma and age-related macular degeneration. To date, the principal method of measuring rigidity *in vivo* has been to employ the Schiøtz indentation tonometer despite its inherent variability, technical limitations and reliance on data transformation. We examine whether data provided by the Schiøtz tonometer are sufficiently robust to assess reliably regional variations in scleral and ocular rigidity.

Objective: To determine the effects of intra- and inter-observer variation on the precision of Schiøtz tonometer readings.

Method: Schiøtz tonometry was performed on both eyes of 25 normal young adult subjects by two independent observers on two occasions using 5.5g and 7.5g plunger loads on the cornea and four scleral quadrants; superior temporal (ST) and nasal (SN), inferior temporal (IT) and nasal (IN). In addition each observer measured one subject five times at different occasions. Data were analysed using coefficient of variation (CV) and percentage error (PE) for intraobserver variation. Inter-observer concordance was evaluated by intra-class correlation coefficient (ICC) and PE.

Results: Intraobserver CV varied with site of measurement, with highest repeatability on the cornea (5.5g: 9.37%; 7.5g: 12.63%) and lowest at IT (5.5g: 30.2%) and IN (7.5g: 28.4%). Intraobserver differences in PE were not significant. The 5.5g and 7.5g readings showed the cornea to have the least PE (5.5g $20.39 \pm 22.32\%$, 7.5g $14.92 \pm 10.53\%$) but no significant difference was found between the cornea and the scleral quadrants. Interobserver concordance showed 5.5g to have the highest ICC 0.682 for cornea and lowest ICC 0.342 at IN, whereas 7.5g had lower values of ICC 0.388 for cornea and 0.187 for IN. No significant difference was found for PE between quadrants; however lower values were obtained for cornea (5.5g, $16.86 \pm 10\%$, 7.5g $14.33 \pm 12.27\%$) and higher values for IT (5.5g, $29.71 \pm 22.86\%$, 7.5g, $25.26 \pm 18.64\%$).

Conclusion: Despite relatively high levels of intra- and interobserver variance the data are sufficiently robust to utilise the Schiøtz tonometer for measurement of regional variations in ocular and scleral rigidity.

ARVO CONFERENCE ABSTRACT, May 2009, 3947- A58

In vivo Measurement of Regional Variations in Scleral Rigidity in Humans

H. D. Patel, B. Gilmartin, R. P. Cubbidge and N. S. Logan
School of Life and Health Sciences, Aston University, Birmingham, United Kingdom

Purpose

The principal method of measuring ocular rigidity (K_0) *in vivo* has been via corneal indentation using the Schiøtz tonometer. We estimate via scleral indentation, regional variations in scleral rigidity (K_s) using raw data from Schiøtz scale readings and their transformation using algorithms employed to calculate K_0 . Given the relevance of scleral biomechanics to the aetiology of myopia, variation in K_s is compared for subjects with and without myopia.

Methods

Data were collected from both eyes of 26 normal young adult subjects [MSE (D) 14 without myopia (-0.50) $+0.48 \pm 1.22$, range (-0.50:+4.38), 12 with myopia (<-0.50) -4.44 ± 3.35 , range (-0.75:-10.56)]. IOPs were determined using Schiøtz and Goldmann tonometry. Schiøtz tonometry (5.5g & 7.5g loads) was randomly assigned to four scleral quadrants (approx 8mm from limbus); supero temporal (ST) and nasal (SN), infero temporal (IT) and nasal (IN) and the scale readings used to calculate K_s using Friedenwald's tables. Biometric data (refraction, corneal radius, anterior chamber depth and axial length) were compiled using autorefractometry and the Zeiss IOLMaster.

Results

Data for RE only are presented. Values of K_0 were consistent with those previously reported (mean 0.0101 ± 0.0082 , range 0.0019-0.0304) and within- and between- observer repeatability ($n=2$) was robust with typical coefficients of variation of 9% and intra-class correlation coefficients of 0.682. Goldmann and Schiøtz measures of IOP were significantly correlated. For K_s differences in refractive error, quadrants and post-hoc contrasts were non-significant. As calculation of K_0 uses empirical corneal data regional variations were examined for raw scale data. Mean refractive group differences were insignificant. Mean scale readings were 5.5g: cornea 5.93 ± 1.14 , ST 8.05 ± 1.58 , IT 7.03 ± 1.86 , SN 6.25 ± 1.10 , IN 6.02 ± 1.49 ; 7.5g: cornea 9.26 ± 1.27 , ST 11.56 ± 1.65 , IT 10.31 ± 1.74 , SN 9.91 ± 1.20 , IN 9.50 ± 1.56 . There were significant differences ($p < 0.0001$) for both weights between means for the cornea and ST; ST and SN; ST and IT, ST and IN. These differences were concordant with the LE data.

Conclusions

There is scope for the use of Schiøtz tonometry in estimating relative regional variations in K_s but no evidence for characteristic variations occurring in the myopic eye.